

Matagorda Bay Ecosystem Assessment Technical Report

Submitted to the Texas Comptroller of Public Accounts

May 31, 2023

Principal Investigators:

Gregory W. Stunz, Ph.D.	<i>Texas A&M University- Corpus Christi</i>
James C. Gibeaut, Ph.D.	<i>Texas A&M University- Corpus Christi</i>
Edmund L. Oborny Jr., M.S.	<i>BIO-WEST, Inc.</i>
Pamela T. Plotkin, Ph.D.	<i>Texas A&M University/Texas Sea Grant</i>
Jennifer Beseres Pollack, Ph.D.	<i>Texas A&M University- Corpus Christi</i>
Jay R. Rooker, Ph.D.	<i>Texas A&M University- Galveston</i>
R.J. David Wells, Ph.D.	<i>Texas A&M University- Galveston</i>
Michael S. Wetz, Ph.D.	<i>Texas A&M University- Corpus Christi</i>

Table of Contents

Acknowledgments	6
Project Background and Introduction	8
Project Goals:	9
Research Objectives:	10
Habitat Mapping for Evaluation of Habitat Change	10
Bathymetric Mapping	10
Overview	10
Methods	11
Results	16
High Resolution Habitat Map	20
Methods	20
Results	31
Mapping Land Cover Through Time	34
Methods	34
Results	41
Historic Wetlands Trends	55
Background	55
Methods	55
Results	58
Modeling Landscape Change Under Varying SLR Scenarios	62
General Overview	62
Methods	62
Results	64
Habitat Vulnerability	69
General Overview	69
Methods	69
Results	71
Discussion	79
Literature Cited	80
Appendix A: WV-2 Land Cover Classifications Through Time	83
Appendix B: Imagery Comparisons Along with Classified Land Covers	87
Appendix C: Digitized Land Cover Classifications Through Time	91

Appendix D: Land cover transitions	97
Appendix E: Historic Wetland Trends Through Time	103
Appendix F: Extent of habitats lost under low and high RSLR scenarios by 2100	106
Seagrass Habitat	118
Methods	118
Results	120
Literature Cited	123
Sea Turtle Movement and Ecosystem Connectivity	124
Overview	124
Introduction	125
Goals	125
Objectives	125
Prior Research	125
Species of Interest	126
Methods	129
Permits	129
Study area	130
Historical sea turtle captures	131
Sea turtle sampling plan	131
Sea turtle capture and handling	132
Satellite and Acoustic Transmitters	134
Data analysis	138
Outreach	142
Results	143
Historical distribution of sea turtle captures	143
Sampling distribution and effort	145
Sea turtle demographics and body condition index	148
<i>Sea turtle home ranges and high use areas derived from satellite tracking data</i>	153
Sea turtle home ranges derived from acoustic tracking data	169
Outreach and engagement	186
Preliminary Conclusions	188
Future Management Recommendations	195
Literature Cited	197

Appendix A: List of project collaborators and supporters	209
Appendix B: Comparison of potential satellite transmitter models to deploy on sea turtles in Matagorda Bay.	211
Appendix C: Outreach material	212
Appendix D: Satellite locations of sea turtles received during day (orange) and night (purple) hours.	219
Appendix E: Photo of a loggerhead turtle sighted and reported by an iSeaTurtle user. Photo credits: Captain Kenneth Gregory.	220
Appendix F: Data management	220
Appendix G: Sample Sea Turtle Data Collection Sheet	222
Appendix H: Transmitter Attachment Protocol	223
Appendix I: Research permits	223
Biological Sampling Across Habitats	224
Introduction and Project Goals	224
Methods	226
Results	232
Discussion	255
Conclusions	262
Literature Cited	264
Marsh Ecosystem Sampling for Flooding/Sea Level Rise Assessment	274
Introduction	274
Marsh Vegetation Assessment	275
Site Selection	275
Methods	277
Results	281
Appendix	285
Summary/Discussion	288
Appendix	291
Avian Assessment	297
Introduction	297
Literature Review: Species of Interest	298
Methods	301
Data Analysis	304
Results	305
Literature Cited	310

Trophic Ecology and Food Web Analysis	316
Introduction	316
Sample Collection and Isotope Processing Methods	316
Results	320
Continued Work	328
Literature Cited	329
Habitat and Resource Use Across the Matagorda Bay Ecosystem	330
Overview	330
Oyster Reefs	331
Wind-tidal Flats	343
Ecosystem Scale Resource Use	349
Literature Cited	357
Water Quality and Plankton Monitoring using Historical and Ongoing Datasets	365
Water Quality and Plankton Monitoring	365
Overview	365
Methods	365
Results and Discussion	368
Summary and recommendations	375
Literature Cited	376
Influence of freshwater inflow from the Colorado River on nutrients and phytoplankton in Matagorda Bay	378
Overview	378
Site Description	378
Methods	379
Results	380
Discussion	407
Future implications and recommendations	410
Literature Cited	411
Moving Forward	417
Project Findings Summary	417
Key Deliverables and Takeaways:	417

Acknowledgments

A project of this magnitude could not be completed without the help of so many outstanding researchers and other team members. The countless hours spent in the field collecting samples, sorting, measuring, analyzing, and final compilation of these data into one report speaks volumes regarding the dedication the team put toward this study. This included completing these deliverables during a worldwide pandemic.

We would like to thank the Texas Comptroller of Public Accounts for providing the funding for this study. The foresight to see the importance of doing an ecosystem assessment on Matagorda Bay using a multitude of researchers with various expertise was unprecedented. This project created an incredible collaborative opportunity to look at everything from water quality and flow, habitat, invertebrates, and vertebrates (fish, turtles, and birds), and then examine how these pieces fit together to create such a unique habitat. Specifically, this project would not have been possible without the help of Meghan Hope, Chelsea Jones, and Lauren Borland, along with key administration support from Melissa Salmon. The TX CPA team was always available to provide guidance and help when asked.

We would particularly like to thank Quentin Hall for being the lead Coordinator, who helped forge a timeline and ensured tasks were completed in a timely manner. He was not only heavily involved in conducting and coordinating the fieldwork, but also in running stakeholder workshops, countless researcher meetings, and the initial compilation of the final report. Tara Topping also played a key role in project administration and the final compilation of the report, which was certainly no small undertaking.

In addition, we would like to thank the many dedicated BIO-WEST scientists who contributed to this amazing ecological endeavor. The extensive benthic mapping portion of this project was labor intensive and involved numerous hours in the field. In addition, they provided both the avian and salt marsh assessments, from which this report was able to connect habitat use with higher order species.

We'd also like to thank Jessica Magolan, Dr. Lihong Su, Mukesh Subedee, and Brach Lupher of the Coastal and Marine Geospatial Lab at the Harte Research Institute, Texas A&M University – Corpus Christi who compiled mapping data, conducted various geospatial analyses, and prepared many data visualization graphics for this report. Jessica Magolan led the analysis of historical and future coastal change as well as authored and organized the data and report. Dr. Su conducted the remote sensing analysis resulting in the land cover map. Mukesh Subedee created the habitat vulnerability map, and Branch Lupher provided GIS support.

The sea turtle movement and ecosystem connectivity team would like to thank Dr. Natalie Wildermann for the hours spent tagging turtles, collecting specimens that resulted from the freeze, and then analyzing and writing this section of the report. This portion of the project would not have been possible without her dedication and hard work. We'd also like to thank Dr. Danny Coffey for his movement analysis and written contributions to this report. His additional expertise created a more complete picture of how sea turtles use Matagorda Bay and the surrounding areas. We'd like to thank Quentin Hall and Jason Williams for their help tagging sea

turtles. There was a steep learning curve, and with Dr. Wildermann's help and guidance were able to tag an incredible number of turtles. We would also like to acknowledge all of the people who assisted us with the project (referenced in Appendix A, page 210), the NOAA Fisheries Office of Protected Resources who issued Permits #18029 and #22822-02, and the Texas Parks and Wildlife for issuing Scientific Research Permit #SPR-0219-021.

For the marsh ecosystem, biological sampling, and trophic ecology teams, we'd like to thank the members and volunteers of the TAMUG Shark Biology and Fisheries Science Lab and the TAMUG Fisheries Ecology Lab. Specifically, Emily Meese who helped quantify and describe the food web of Matagorda Bay using stable isotope work and Liam Batchelder whose work involved countless benthic sled samples and the analysis of nekton and invertebrates within the seagrass bed nursery habitat. We'd also like to thank the Texas A&M University and University of California Santa Cruz Stable Isotope Labs for their help with some of the isotope processing. Collectively, these analyses helped to build a large-scale view of the habitat and the various relationships among the species residing in it. We'd like to thank the HRI Coastal Conservation and Restoration Ecology Lab. Alyssa Outhwaite for coordinating fieldwork and leading efforts in sample processing and interpretation as well as all of those who contributed to field and laboratory work: Dr. Terry Palmer, Hannah Bueltel, Daphne White, Abigail Shulz, Mackenzie de los Santos, Natasha Breaux, Jennifer Gilmore, Danielle Downey, Devin Comba, Alexis Neffinger, Abraham Margo, and Auria Avalos. In addition, we'd like to thank HRI's Center for Sportfish Science and Conservation, specifically Jeff Kaiser and the lab personnel for their time sorting the hundreds of samples collected throughout this project. Finally, we would like to thank Dr. Benoit Lebreton for his guidance on stable isotope analyses and Dr. Kim Withers for her helpful knowledge and direction with the investigation of tidal flats.

The water quality team would like to thank Dr. Amie West for her statistical analysis of the historic water quality data. Analyzing such a comprehensive dataset is no small feat and her work helped provide a bigger picture view of the change in water quality throughout time. We also thank the following individuals for their hard work and dedication with field sampling and sample processing: Laura Beecraft, Dominic Burch, Tiffany Chin, Jordana Cutajar, Elani Morgan-Eckert, Ken Hayes, Sankar Sasidharan, Sarah Tominack, and Lily Walker. We are especially grateful to Mr. James Gann and Mr. Buzzy Romine, who volunteered their time and resources to help us get the data that were collected as part of this study. We would also like to thank these boat captains that were gracious enough to volunteer their time and knowledge to help us collect these samples.

The dedication and hard work from everyone on this incredible team above is greatly appreciated!

Project Background and Introduction

Spanning over 400 square miles of the Central Texas coast, Matagorda Bay serves as a rich resource for numerous industries including commercial and recreational fishing, farming and agriculture, and tourism. Just as impressive as the fishing grounds in Matagorda Bay, the system also boasts impressive avian biodiversity and productivity. Unlike the industrial bays and ports to the north and south, Matagorda Bay is surrounded by a relatively small human population. Thus, extensive and relatively undeveloped, Matagorda Bay is frequently dubbed ‘pristine’ by those who live and work around the water’s edge. In fact, Matagorda Bay does not have the same sources of environmental degradation that compromise the natural resources of bays to the north and south. However, given the complexity of factors that influence the bay, from economic development to hurricanes, the ‘pristine’ status of Matagorda Bay is not certain. With the aid of stakeholder engagement, this study sought to develop science-based solutions that balance economic activity and the sustainable use of environmental resources in Matagorda Bay.

The bay supports a wide diversity of fish, endangered and threatened sea turtles, and a diversity of waterfowl. The last wild migrating flock of endangered whooping cranes is expanding east from the neighboring San Antonio Bay, and it is thought that Matagorda Bay could potentially become part of their habitat range. Several species of imperiled shorebirds, including the black skimmer and American oystercatcher, may be seen foraging and resting among intact oyster reefs and shallow waters. Despite the ecological and economic value of the area, little research has been conducted on the distribution and health of the many important habitats in the bay and their value to the overall ecosystem health. Thus, The Texas Comptroller of Public Accounts (CPA) partnered with the Harte Research Institute for Gulf of Mexico Studies at Texas A&M University – Corpus Christi in 2019 to conduct research to:

- (1) inform the development of effective conservation strategies for endangered sea turtles; and
- (2) explore opportunities for avian conservation relative to potential impacts from flooding and sea rise by implementing a multi-disciplinary ecosystem assessment of Matagorda Bay.

This assessment of West Matagorda Bay was unique in that it was the first study to integrate a broad ecosystem-based management approach to a major estuarine system. Traditional studies in this region and others have generally focused on the role single species play in ecosystem food webs, habitat, and water quality. While managing species on an individual basis can provide valuable biological information, to fully understand ecosystems, it is important to gain an in-depth understanding of the fundamental underlying ecological processes and stressors (e.g., flooding and sea level rise) that interact to support a resilient ecosystem. This could not be more relevant than when managing endangered species - knowing their biology is important, but

understanding the ecosystem that supports these fragile populations is paramount. Sea turtles and endangered bird populations in Texas' estuaries are a perfect example of where robust science on the estuarine ecosystem that supports these endangered species can greatly enhance recovery and long-term sustainability of their populations. Data generated from an ecosystem-based approach such as this study will be crucial to developing effective restoration and conservation strategies, and they can be used to identify and prioritize areas for long-term protection of sea turtles and many other species. Moreover, this study generated key baseline information that will be essential to gauge progress and make predictions about future change.

This study was multifaceted and complex and comprehensive in scope. However, the underpinning focus was to apply robust science on the estuarine ecosystem to better understand how this bay supports endangered species, promotes/enhances recovery, and develop long-term scientific recommendations for sustaining and enhancing their populations. Thus, a major focus was on iconic sea turtle populations that occur in the area. Matagorda Bay hosts several species of endangered and threatened sea turtles that forage on crabs and seagrasses sheltered in its shallow waters. Researchers captured, tagged, and tracked sea turtle movement to determine how they utilize available resources. Tissue samples were used to incorporate sea turtles into the context of a larger food web analysis. By collecting sea turtle, fish, and plant tissues, researchers evaluated energy flow pathways within the bay ecosystem. Finally, researchers collected data necessary to establish baseline conditions of marsh productivity. Marshes play a fundamental role in the bay's health. The productivity of these habitats influences the abundance and diversity of the marine and avian life that enrich the bay ecosystem. Researchers also compiled, collected, and analyzed abiotic and biotic data to provide comprehensive results to Matagorda Bay stakeholders. Benthic mapping along segments of open water delineated key estuarine habitats, including oyster reefs and seagrass beds, and established a baseline habitat condition for fishes and other estuarine species. The mapping was also closely linked with water quality and biological sampling to gather insight on the ecological processes occurring in the ecosystem.

Along with their respective research teams, this team of expert scientists addressed the most pressing issues in endangered species conservation for sea turtles and other endangered or threatened species (e.g., coastal birds) that rely upon these ecosystems. This Overview and Synopsis along with the comprehensive technical report will help to better understand the suite of imperiled, threatened, and endangered sea turtle and bird species, as well as the potential impacts of evolving environmental factors.

Project Goals:

- Inform the development of effective restoration and conservation strategies for endangered sea turtles;
- Explore opportunities for mitigation and restoration activities to inform priority areas for conservation relative to potential impacts from flooding and sea rise with regard to bird

species of interest by implementing a multi-disciplinary ecosystem assessment for West Matagorda Bay;

- Inform the viability of future habitat restoration efforts in the Colorado River Delta particularly for critical nursery habitat.

Research Objectives:

- Develop detailed habitat maps forming the basis for the study. As the primary function of an estuary stems from foundational habitats, this mapping will allow assessments and visualization of biological and physical characteristics of the estuary on a spatial and temporal (seasonal) basis.
- Establish an extensive animal tracking component for key species of interest. This will allow an understanding of distribution, migration, and movement patterns.
- Perform detailed ecological assessments of specific habitat communities that will allow us to assess macrofaunal density, bird abundance, richness, community composition, food base, and habitat trends on a seasonal basis to make predictions about temporal changes and ecological hotspots of productivity.
- Perform strategic water quality monitoring to establish baselines and better understand changing environmental conditions on nutrients, plankton and other food base factors as a measure of productivity.
- Conduct detailed food web evaluations using isotopic and amino acid analyses to determine key ecological interactions among species of interest and their habitats.
- Evaluate the influence of habitat arrangement and dynamic changes in water quality and quantity on a monthly basis to understand changes to habitat suitability for species of interest.
- Engage the Matagorda Bay scientific, management, and policy communities and other stakeholders in the process to gather feedback and give updates as to the status of this project.
- Perform a detailed benthic habitat characterization of the Colorado River Delta study area to provide an updated habitat baseline.
- Conduct a comprehensive ecological assessment linking the distribution of species and their habitats spatially within the Colorado River Delta study area.
- Complete a hydrological assessment to better understand water availability, flow paths, and topography in the Colorado River Delta.

Habitat Mapping for Evaluation of Habitat Change

Bathymetric Mapping

Overview

A comprehensive acoustic remote sensing survey was conducted to map the benthic marine resources within the designated area of Matagorda Bay. As part of this comprehensive effort, both side-scan sonar (SSS) and bathymetric surveying of approximately 56,000 acres were completed and compiled to create a benthic habitat map (e.g., oyster reefs, seagrasses and open bay bottom) with water depths.

Methods

Side Scan Sonar and Bathymetry

Equipment for this survey consisted of a Hemisphere® VS110 differentially corrected global positioning system (DGPS) receiver; an EdgeTech® 4125 Chirp 400/900 kilohertz (kHz) side-scan sonar (SSS) sensor (towfish) and topside processor with DISCOVER acquisition software; and a Teledyne Odom Hydrographic, Inc. Hydrotrac™ 200 kHz single beam echo sounder with 10° transducer. Vessel guidance, position, and data logging were accomplished with a navigation processor utilizing Trimble® HYDROpro™ Navigation software. Positional information for the survey vessel and each instrument sensor, via layback calculations, was stored in the navigation processor at a rate of one reading per second. Echo sounder depth data was also recorded in the navigation processor at one reading per second. Vessel speed during the survey averaged 4.0 knots (4.6 miles per hour; 7.4 kilometers per hour), providing in-line data spacing of approximately 6.8 feet (2.1 meters). A minimum water depth of 2.5 feet (0.76 meters) was required to provide adequate depth for the SSS towfish and draft for the navigation vessels. To ensure imagery for 150+ percent coverage of the project area with appropriate depths, survey transects were spaced between 40- and 60-meter intervals, depending on the location in the bay, weather patterns, reference landmarks, and transducer range settings.

For SSS data processing, Chesapeake Technology's SonarWiz© V7.05 was utilized. The typical project workflow included data collection, download and correction, and post-processing through the respective programs. For SSS, the raw files (e.g., .jsf for Edgetech Technology equipment) were downloaded to a processing computer and imported using a variety of settings specific to each project, including scalar factor, compression rate, and soundwave velocity. Once imported, each file was bottom-tracked to correct for anomalies and interference. To determine the appropriate gain settings based on project specific constraints, one or two test files were selected to run through each setting and analyzed the results. Once a specific gain setting was selected for a group of files, it was applied to all files to produce a final mosaic. Final editing included color palette selection, file ordering, organization, and export. The sonar imagery was designed to depict any features located on the surface of the bay bottom or substrate (Figure 1). Once processed, this geo-rectified imagery was used to help identify marine natural resources as well as other anthropogenic features found of the bottom.

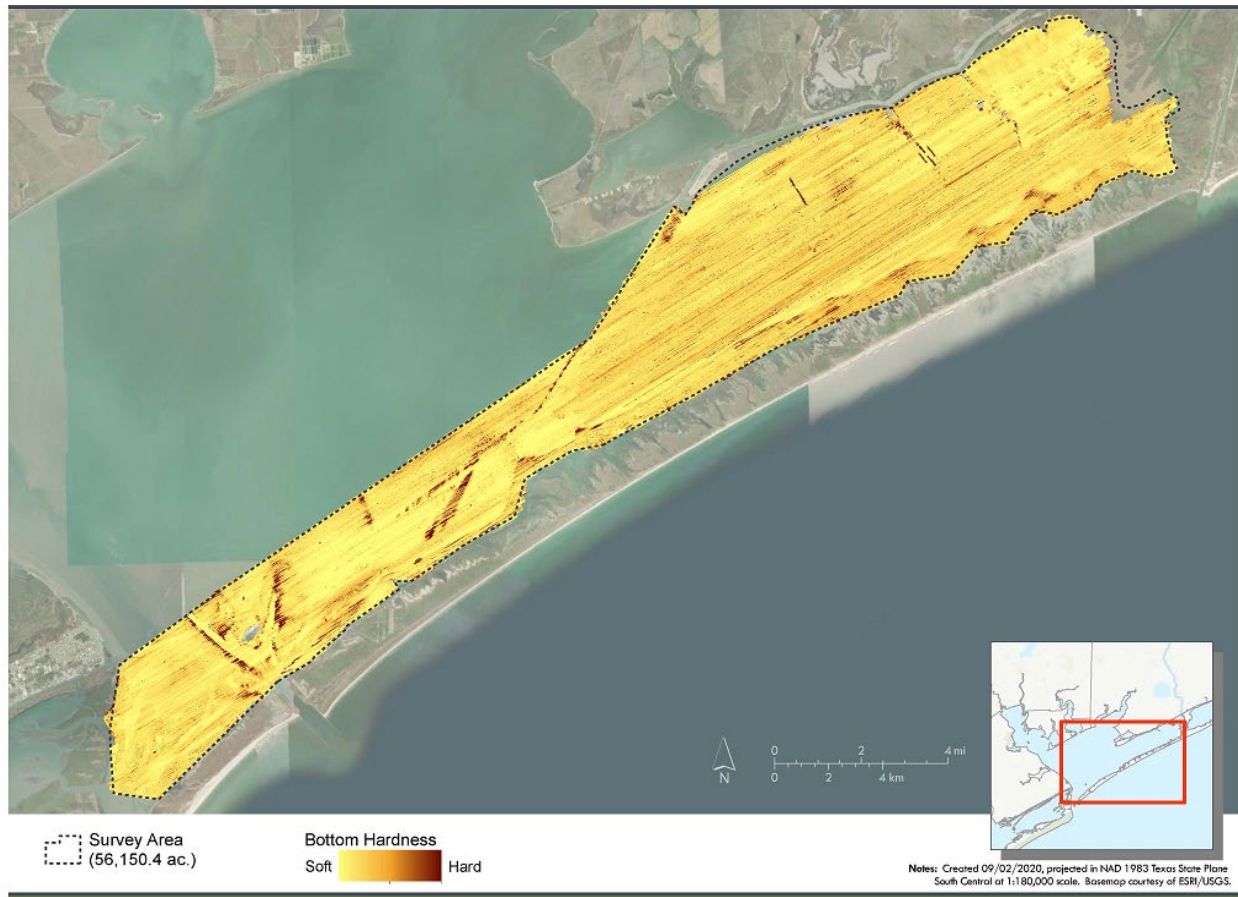


Figure 1. Side Scan Sonar Imagery for Project Area.

For bathymetry, raw x,y,z data was exported via Trimble Hydropro© V2.3 to either excel or .csv file types for processing and correction in ESRI ArcGIS 10.7©. The bathymetry dataset was tidally corrected via the closest tidal station. The data can be exported into a GIS format for projection (Figure 2) via hillshade, contour lines, or other formats as needed for Task 2.



Figure 2. Bathymetry Imagery for Project Area.

To determine potential oyster habitat, the side scan sonar was processed during and after completion of the remote sensing phase of the survey, and a high-resolution mosaic was created to guide field verification sampling. A draft map of potential oyster habitat was compiled through geospatial imagery classification of the SSS imagery using training samples of known oyster reefs (Figure 3), as well as heads-up digitization of known reef areas, resulting in approximately 4,000 acres of potential oyster reef habitat. While high reflectance values in the imagery may indicate hard substrates such as oyster reef and shell hash, similar reflectance values are also generated by rock, dredged channel and pipeline reinforcements and pilings, compact sandstone, shipwrecks, and other materials which are less likely to foster oyster growth, so systematic field verification was required to distinguish regions of potential habitat from less hospitable oyster zones.

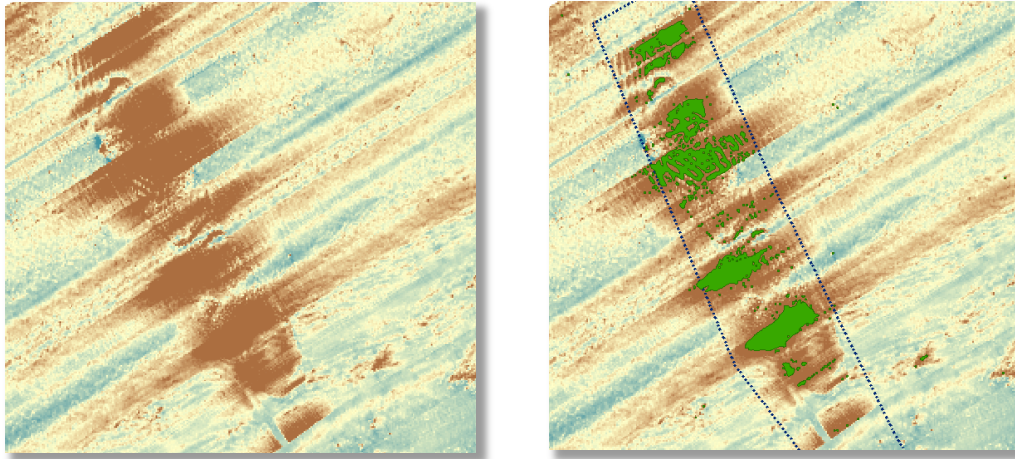


Figure 3. High reflectance bottom scans from side scan sonar (left) and isolated through imagery classification (right).

Oyster Field Verification Sampling

The projected area was divided into uniform 10-acre hexagonal polygons, and 61 hexagons (610 acres, or 15% of potential oyster habitat) were randomly selected for sampling. An additional 10 hexagons of “open” areas containing no delineated reef habitat were also sampled to verify absence of reef habitat for a total of 71 sampled sites containing 710 acres (Figure 4).

In the week of August 3 through 7, biologists conducted oyster dredge tows across the survey area at the targeted 10-acre hexagon locations identified in the side-scan imagery as potential reef habitat or open locations. The sample site hexagons were loaded onto a GPS-enabled tablet which uses real time data to show current position in relation to the proposed sample hexagons. At each sample location, a custom oyster dredge was towed along random linear transects for approximately 30 seconds and retrieved (Figure 5). The dimensions of the dredge are 33 in (80 cm) long by 18 in (47 cm) wide by 11 in (29 cm) deep with a 0.5-in (1.3 cm) wire mesh lined collection basket to retain small shell hash and bivalve/benthic species.

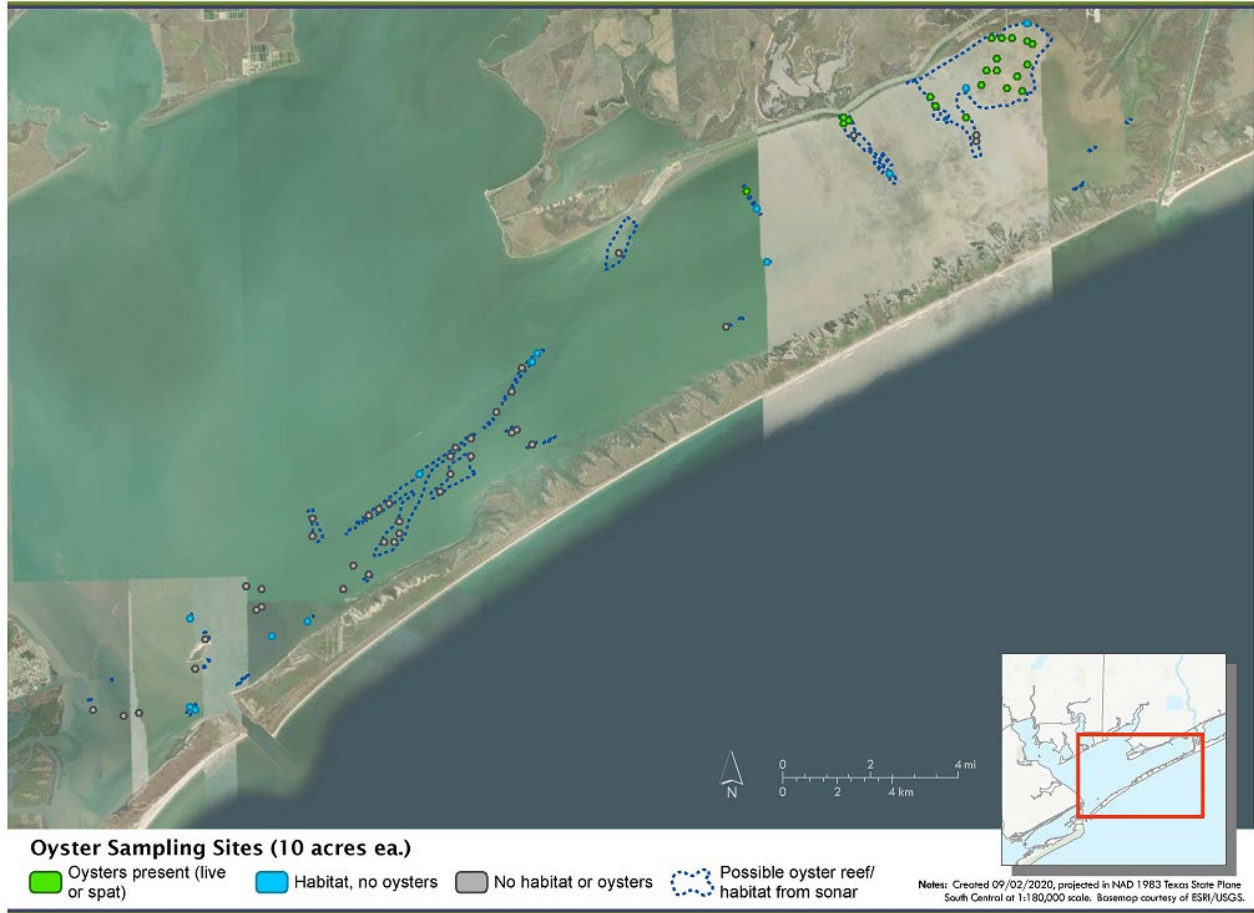


Figure 4. Oyster Reef Field Verification Sampling Locations.

The collected contents were photo-documented (pre- and post-rinse) and described. Live oysters, oyster shell, shell hash, and reef material were noted to determine potential presence or absence of oyster reefs and suitable substrate. Also, any additional finds were noted including but not limited to rangia shells, barnacles, hook mussels, and worms.



Figure 5. Custom oyster dredge (left) and collected materials being rinsed (right).

At each hexagon that had oysters or reef material, biologists also documented water quality parameters to characterize ambient water conditions over potential reef locations using a YSI® 6920 multi-parameter water quality data sonde. The parameters measured included temperature (°C), specific conductivity (mS/cm³), salinity (‰), dissolved oxygen (DO) (mg/L), and pH (su). Additionally, live oysters were collected from 21 sample sites used in stable isotope analysis (discussed below).

Results

Live oysters or spat were found at 21 sampling sites during field verification, all in the northeast corner of Matagorda Bay. An additional 12 locations contained dead oysters, broken shells, shell hash, or other indicators of possible reef habitat. These sites are more uniformly dispersed across Matagorda Bay, from the northeastern corner down to the southwestern end of the bay. No oysters or possible habitat were detected at 38 sample sites, 10 of which were open sites not expected to contain reef or habitat. Within the 28 sites where reef habitat was delineated but not detected, six had hard sandstone or rocky substrates with similar reflectance to reef, while the remaining 22 sites had mud substrate with little or no shell. The following examples are provided to show the classification process from imagery to dredge haul.

Category 1: Living Oyster Reef

(Reference Sample Site S-12)



According to various state agencies such as Texas Parks and Wildlife Department (TPWD, 2020a and 2020b), and Louisiana Department of Wildlife and Fisheries (LDWF, 2012), living oyster reefs were characterized by dense, clustered, or semi-aggregated of living oysters, regardless of size class, over suitable hard or firm substrates. For the purpose of this classification, if appropriate substrate and attachment material and at least one live oyster were observed, the sample area was classified as Category 1.

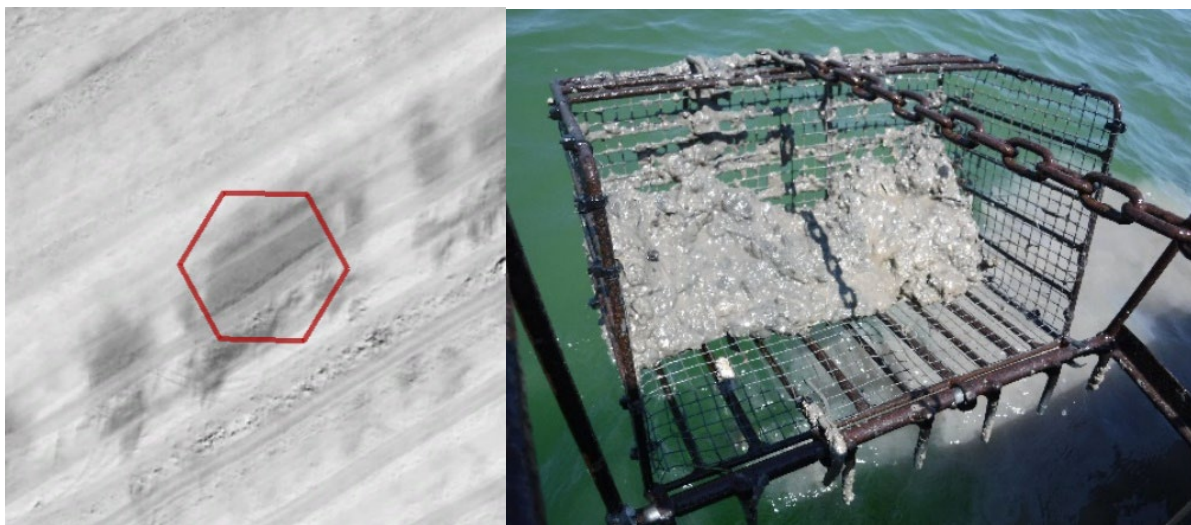
Category 2: Viable Oyster Habitat
(Reference Sample Site S-31)



According to the same agencies, this category exhibits a wider range of conditions and a variety of potential habitat structures and types, including the presence of live or dead shell greater than 25 mm in size on firm, hard, consolidated substrates; suitable buried, partially buried or exposed calcium-rich shell or other material (i.e. limestone, concrete, clam shell, etc.); or even

historical or dead reef or reef clusters. Additionally, all of these potential habitat types would be considered viable habitat, regardless of the presence of live oysters, due to the reproductive cycle of the Eastern oyster. Outside enhancement and expansion of living reef areas, this category could potentially demonstrate the highest probability for oyster reef restoration and creation activities.

Category 3: Interspersed Firm Mud and Sand
(Reference Sample Site S-43)



During the last century, a host of projects and anthropogenic influences have shaped and altered the substrate and bay bottom of various portions of Matagorda Bay. These projects have included the historical Intracoastal Waterway (prior to its current alignment) and multiple dredged ship and barge channels to access both Matagorda Island and shallower portions of Matagorda Bay. During these events, dredged spoil material was generally side-cast, resulting in changes to the natural bay bottom habitats and a range of material classifications, including firm and soft muds and a general lack of large sandy areas. Additionally, buried and/or black shell and other similarly stained substrate was observed in this category. This category would potentially represent low to moderate success probability for oyster reef restoration and creation activities and would need to be analyzed further for suitability.

Category 4: Open Bay Bottom
(Reference Sample Site S-02)



Devoid of oysters, viable habitat, or potentially favorable materials for reef establishment, the majority of Matagorda Bay was classified as Category 4. While dredge tows, sampling efforts, and sonar analysis in this category revealed no oysters or suitable substrate, it did reveal the presence of various other bay features including underwater sand waves and ripples in the southern portion of the survey area, open bay flats and seagrass beds along the central portion, and unconsolidated silts/clays, especially around the Diversion Cut and near the lower Colorado River delta in the northeast. This category would potentially represent lowest probability of success for oyster reef restoration and creation activities.

The resulting map from this classification approach and subsequently applied analysis is presented in Figure 6. As we only performed limited verification sampling in open bay habitat, we did not classify the remainder of the bay as that particular habitat type (Category 4).

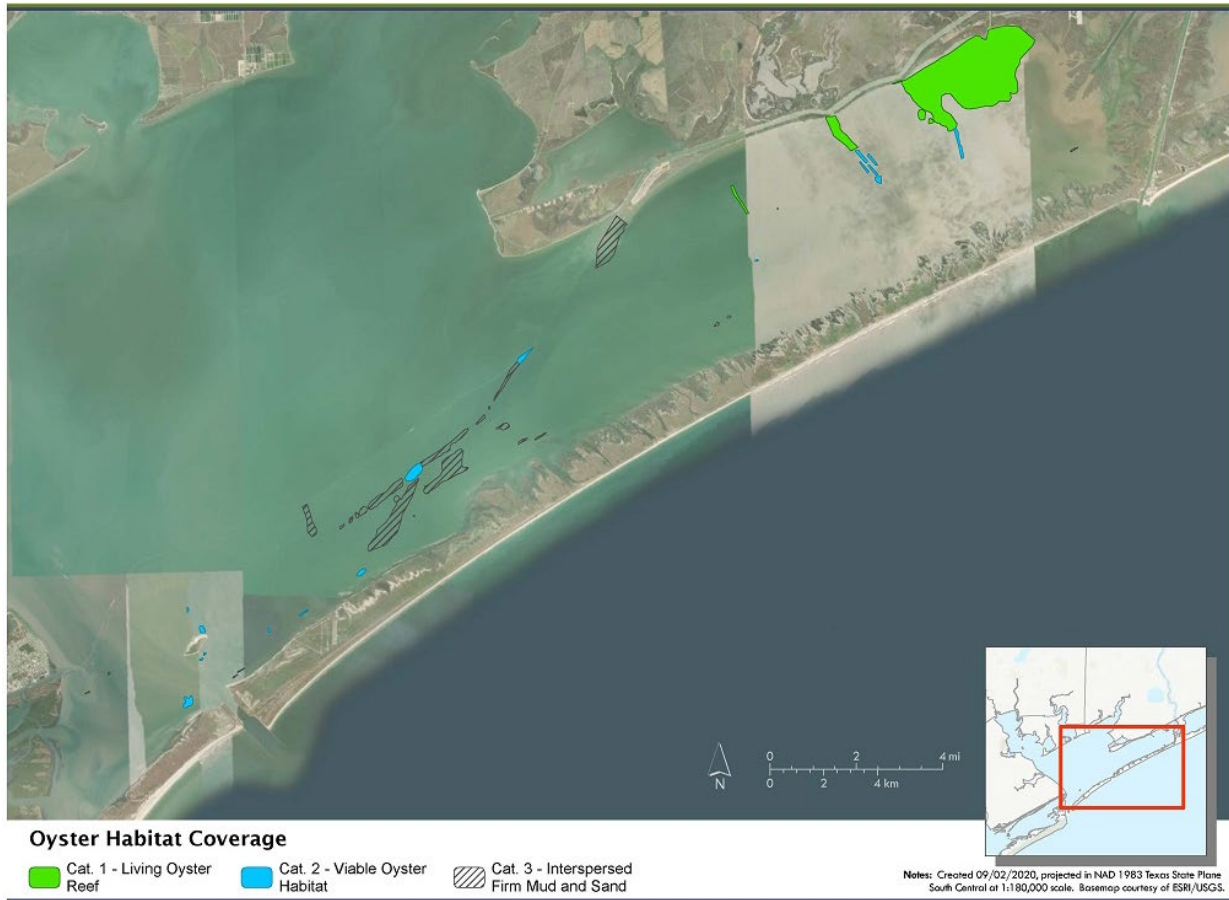


Figure 6. Oyster Reef and Viable Habitat Coverage.

High Resolution Habitat Map

Methods

General Overview

High-resolution multi-spectral satellite imagery such as WorldView-2 (WV-2) is suitable for separating water, land, and vegetation. WV-2 is advantageous over other satellites due to its high spatial and spectral resolution and 8 bands, which exploit additional wavelengths of the electromagnetic spectrum not available in other satellites (Table 1). However, spectral data can misclassify 1) algal flat and marsh, and 2) forest and grass due to their similar chlorophyll absorption of radiation. This confusion can be alleviated through the incorporation of a lidar point cloud. Similarly, water can be misclassified on both the spectral imagery and lidar point clouds. For example, a spectral classifier may classify spilling and plunging breakers as land due to the white foam of the breaking waves which is not a typical spectral response of water while a point cloud classifier may classify these waters as low vegetation due to elevation changes of the waves. Water with breaking waves misclassified as low vegetation, however, can be corrected using a rule-based filter by considering the context of neighboring environments and how they are classified.

Table 1. WV-2 spectral bands and their wavelengths.

Spectral Band	Wavelength (nm)
Coastal	400 – 450
Blue	450 – 510
Green	510 – 580
Yellow	585 – 625
Red	630 – 690
Red Edge	705 – 745
Near-IR1	770 – 895
Near-IR2	860 – 1040

This study incorporated WV-2 and lidar to obtain a 2-m resolution habitat map for the entire study area. A novel stacked classification approach was developed to take advantage of high-resolution satellite imagery and airborne lidar point clouds. Ultimately, a rule-based classifier was stacked on a group of machine learning classifiers for multispectral images and a filter classifier for lidar point clouds.

The methodology used to classify WV-2 data can be separated into nine parts which are described in greater detail in following sections. Figure 10 depicts the workflow of the nine sections to obtain the final habitat map.

- 1) Preprocessing
- 2) Create Training Data
- 3) Band Indices & Classification Methods
- 4) Water Classification
- 5) Agriculture Classification
- 6) Lidar Classification
- 7) Marsh, Algal Flat, Grass, Forest Classification
- 8) Final Combination
- 9) Accuracy Assessment

Data Sources

- 1) 26 WV-2 tiles, with acquisition dates of 11/17/2012, 5/5/2013, and 12/16/2013, were needed to cover the study area. The imagery had 8 spectral bands with a 2-m spatial resolution.
- 2) Two lidar datasets were needed to cover the entire study area and were downloaded from the Texas Natural Resources Information System (TNRIS). Acquisition dates ranged from 1/4/2018 – 2/23/2018 (USGS, 2018) and 1/24/2019 – 1/29/2019 (USGS, 2019).
- 3) NOAA’s 2016 Coastal Change Analysis Program (CCAP) Regional Land Cover dataset (NOAA, 2016) assisted in classifying the WV-2 imagery. C-CAP uses data from the

National Land Cover Dataset (NLCD) to classify 25 landcover types with a spatial resolution of 30 x 30 m.

Figure 7 illustrates the 1) location, acquisition date, and overlap of WV-2 tiles, and 2) the extent of coverage for the two lidar sources.

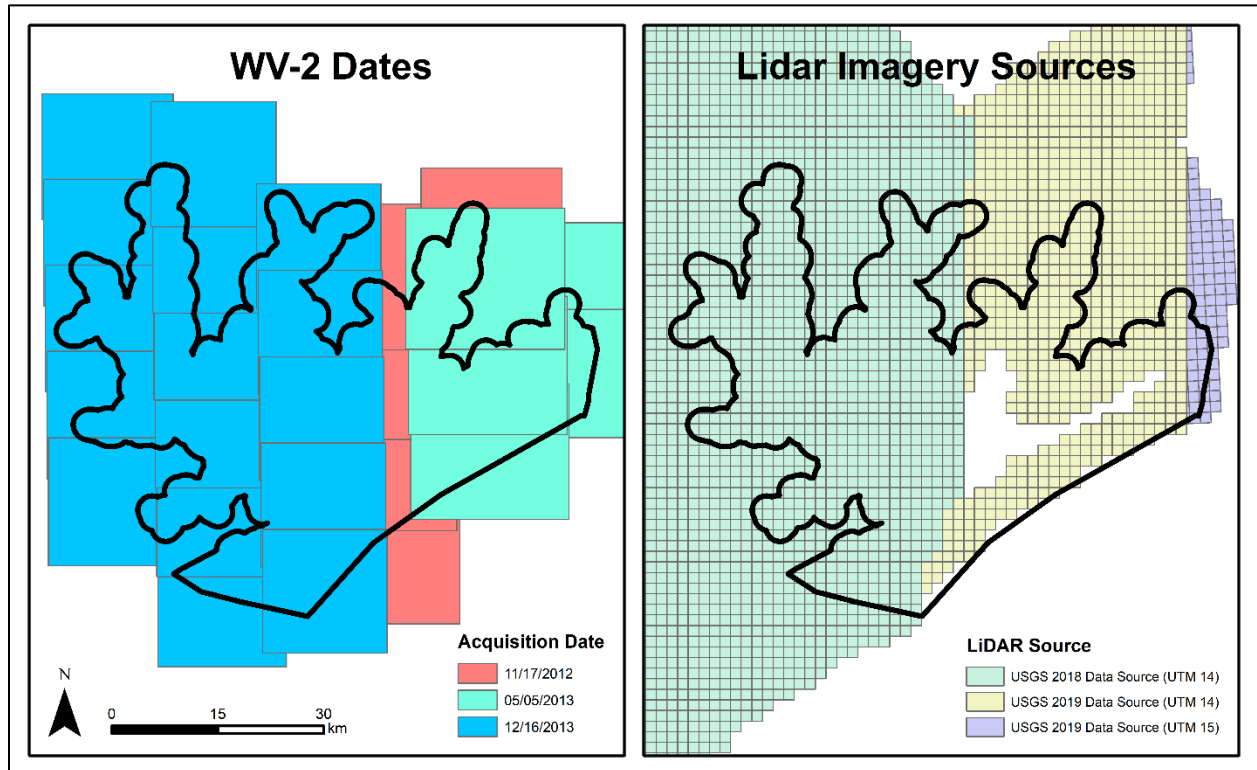


Figure 7. WV-2 and lidar tile locations, acquisition dates, and overlap.

Preprocessing

Each WV-2 image was corrected for terrain displacement and radiometric settings by the Polar Geospatial Center (PGC) at the University of Minnesota. The original image data and orthorectification parameters came stored in *.ntf files. NTF is an image file format created by the National Imagery Transmission Format Standard (NITFS). An ArcGIS python script was developed to convert the *.ntf files to geotiff *.tif files. Then, University of South Florida's MATLAB code was used to:

- 1) Radiometrically calibrate digital count data,
- 2) Atmospherically correct images by subtracting Rayleigh Path Radiance, and
- 3) Convert images to surface reflectance by accounting for Earth-Sun distance, solar zenith angle, and average spectral irradiance.

Create Training Data

ENVI software's Feature Extraction was used to generate segments based on similar spectral signatures. Segments were then manually classified into three land covers: 1) bare soil, 2) shrub/tree/grass, and 3) marsh/algal flat (Figure 8).

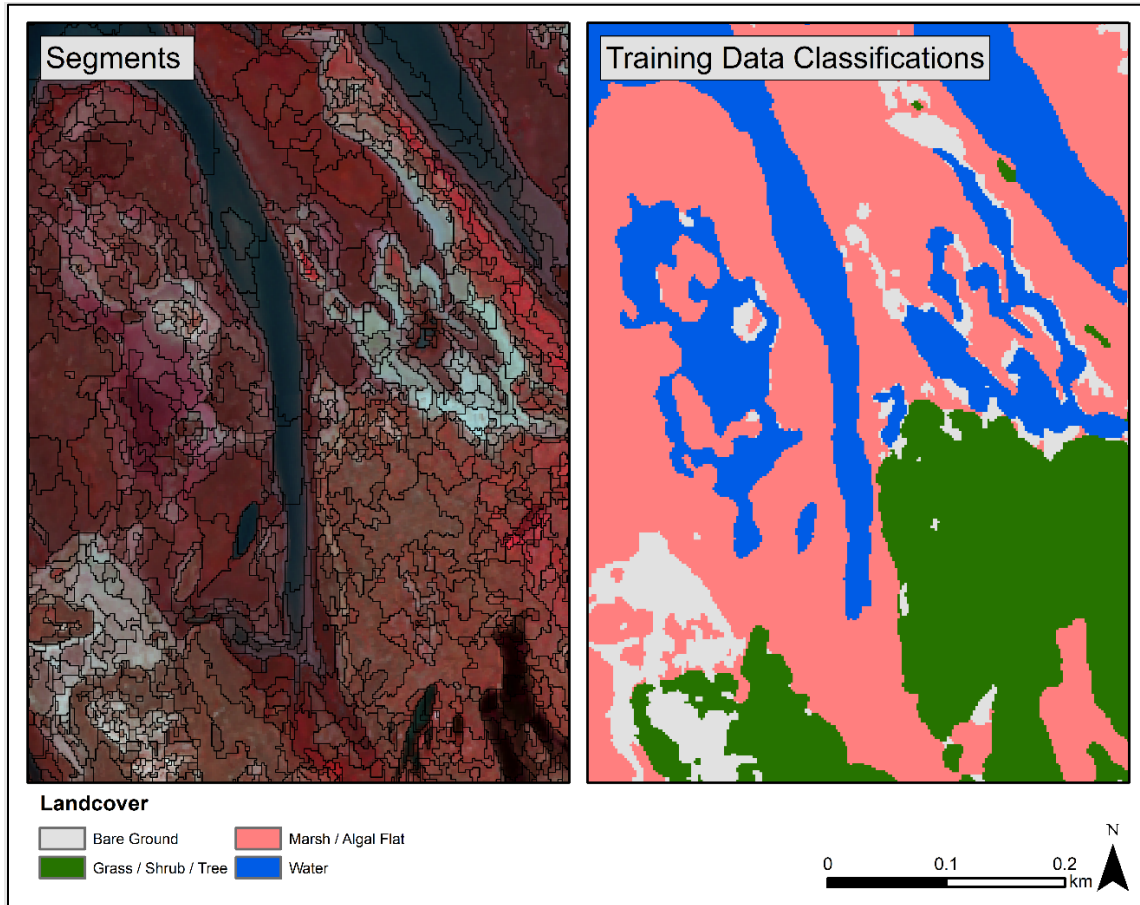


Figure 8. Segments created using ENVI software's feature extraction shown overlaid on WV-2 imagery (left) and their land cover classifications (right).

Band Indices & Classification Methods

Three band indices were used to classify the land cover. Structure Insensitive Pigment Index (SIPI) (Equation 1) is useful for identifying vegetation health and identifying vegetation with varying canopy structures by determining the ratio of carotenoids to chlorophyll. Shadow Index (SI) (Equation 2) is used to distinguish shadows from other features. Modified Soil Adjusted Vegetation Index (MSAVI) (Equation 3) is used to mitigate soil effects on agriculture monitoring by reducing the effect of soil on the calculation of vegetation density. MSAVI can identify vegetation with low chlorophyll (ex: during seed germination and leaf development there is a lot of bare soil present).

$$SIPI = \frac{(NIR1 - Blue)}{(NIR1 - Red)} \quad (\text{Equation 1})$$

$$SI = \sqrt{(1.0 - Blue) * (1.0 - Green)} \quad (\text{Equation 2})$$

$$MSAVI = \frac{2 * NIR + 1 - \sqrt{(2 * NIR + 1)^2 - 8 * (NIR1 - Red)}}{2} \quad (\text{Equation 3})$$

The training data classifications in combination with the three band indices (SIPI, SI, and MSAVI) were ran through five pixel-based classification methods (Random Forest, Support Vector Machine, Multilayer Perceptron, Maximum Likelihood, Gradient Boosting Machine) to classify each pixel into three land covers (bare ground, upland grass/forest, and marsh/algal flat).

- 1) Random Forest (RF) classifier is an ensemble learning method for classification by constructing a multitude of decision trees at training time. For classification tasks, the output of the random forest is the class selected by most trees.
- 2) Support-Vector Machine (SVM) classifier is a supervised learning model for classification. SVMs are one of the most robust prediction methods, being based on statistical learning frameworks. Given a set of training examples, SVM maps train examples to points in space to maximize the width of the gap between the two categories. New examples are then mapped into that same space and predicted to belong to a category based on which side of the gap they fall.
- 3) Multilayer Perceptron (MLP) is a fully connected class of a feedforward artificial neural network. A MLP consists of at least three layers of nodes: an input layer, a hidden layer, and an output layer. Except for the input nodes, each node is a neuron that uses a nonlinear activation function. MLP utilizes a supervised learning technique called backpropagation for training. It can distinguish data that is not linearly separable.
- 4) The main idea of Maximum Likelihood Classification (MLC) is to predict the class label y that maximizes the likelihood of our observed data x . Here, we assume the distribution of x (usually a Gaussian distribution). The Gaussian distribution has 2 parameters: the mean, μ , and the standard deviation, σ . We calculated the 2 parameters from training datasets.
- 5) Gradient Boosting (GBM) classification is a machine learning technique. It gives a prediction model in the form of an ensemble of weak prediction models, which are typically decision trees. Boosting is a method of converting weak learners into strong learners. Gradient Boosting trains many models in a gradual, additive, and sequential manner.

For each pixel, the results from the five pixel-based classification methods were combined (based on how consistently each land cover class was classified in each method) to obtain final, more accurate land cover designations. For example, if a pixel was classified as

“marsh” using RF, SVM, and MP, but “grass” using ML and GBM, the pixel would be classified as “marsh”. Figure 9 illustrates the difference between the five classification methods.

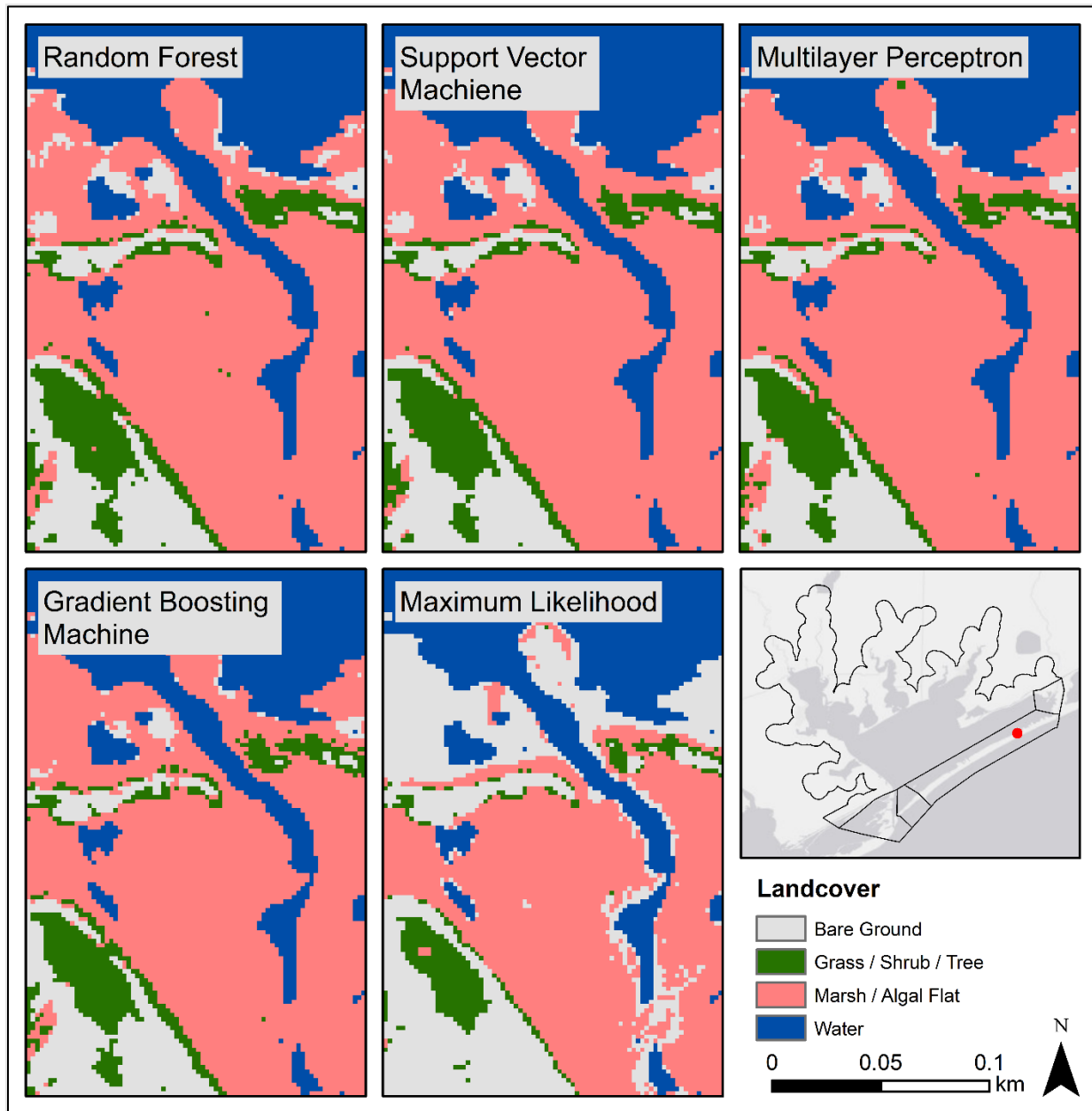


Figure 9. Example illustrating how the five classification methods (Random Forest, Support Vector Machine, Multilayer Perceptron, Gradient Boosting Machine, and Maximum Likelihood) classify land covers slightly differently.

Water Classification

WV-2 was used to create a Normalized Difference Water Index (NDWI) (Equation 4). NDWI outputs values from -1 to 1 and is useful in distinguishing water from any other land cover.

$$NDWI = \frac{(Green - NIR2)}{(Green + NIR2)} \quad (\text{Equation 4})$$

Creating a NDWI resulted in a continuous water body (gulf and bay) plus numerous isolated water bodies (lakes). Due to presence of multiple water bodies, the Connected Components Labeling (CCL) algorithm was used to group water pixels together. CCL is an algorithm that is used to connect regions of an image based on similarity between adjacent pixel values. CCL works by scanning an image from left to right and top to bottom, assessing similarity between adjacent pixels, and labeling them accordingly. Ultimately, all the pixels within a connected component are in some way connected to each other.

Following the execution of the CCL algorithm, water was extracted from 2016 CCAP data. However, CCAP has a coarser spatial resolution than WV-2 (30 x 30 m), which could exaggerate the water extent and ultimately classify some land as water. To overcome this, the water extent was reduced by 60 m. Next, the CCL algorithm was used to group pixels together based on similar elevation values.

Then the CCL results from WV-2 water and CCAP water were intersected to check for 1) complete, 2) partial, and 3) no overlap between water bodies.

- 1) When the WV-2 water was completely inside the CCAP water, this typically represented water within the gulf or bay. Then, the CCL algorithm was used to generate a 60 m buffer. The elevation for each CCL block was then obtained. If the elevation of a CCL block was less than the average, the WV-2 was classified as water, otherwise the WV-2 water classification was removed.
- 2) If the WV-2 water partially overlapped the CCAP water, the WV-2 area that did not overlap was further processed. Areas that had this partial overlap consisted of upriver extents where CCAP did not classify the water, but WV-2's smaller spatial resolution allowed for the classification of water. First, the WV-2's neighboring water blocks elevation was obtained. Then the CCL algorithm was used for the non-overlapped areas and the elevation was obtained. If the non-overlapped area's elevation was less than the average of the neighboring waters elevation, the WV-2 was classified as water, otherwise the WV-2 water classification was removed.
- 3) If the WV-2 water did not overlap the CCAP water, we kept the WV-2 water classification as these could represent smaller lakes and ponds.

Agriculture Classification

First, "Cultivated Crops" were extracted from the CCAP data and shrank by 60 m. Then, three steps were taken to clean up the CCAP agriculture classification:

- 1) Agricultural features < 10,000 m² were removed since agricultural areas are typically large.

- 2) Agricultural features where the LiDAR was classified as “medium vegetation” or “high vegetation” were removed.
- 3) Any area previously classified as water (details in “Water Classification” section) were removed.

Next, training pixels were randomly selected using the WV-2 spectral indices (SIPI, SI, MSAVI) outputs that were created previously (details in “Band Indices and Classification Methods” section). Using the training pixels, the random forest classifier was used to classify agriculture. Lastly, the WV-2 classification pixels were grouped together using the CCL algorithm and the WV-2 agriculture classification was overlapped with the CCAP “Cultivated Crops” classification. If the WV-2 agricultural classification block overlapped the CCAP “Cultivated Crops”, the WV-2 agricultural area was kept. If no overlap occurred, the WV-2 agriculture classification was removed.

Lidar Classification

First, holes were filled in the data. Then, the following were created: 1) a digital elevation model (DEM) from "Bare Ground" returns, 2) a digital surface model (DSM) from all returns, and 3) a normalized digital surface model (nDSM) calculated as $DSM - DEM$. Next, all unclassified Lidar points were used to create CCL. Based on the CCL values, buildings and vegetation were separated. Lastly, vegetation was separated into three classes based on their values:

- 1) low vegetation (CCL < 0.75 m),
- 2) medium vegetation (CCL 0.75 – 2 m), and
- 3) high vegetation (CCL > 2 m).

Marsh, Algal Flat, Grass, Forest Classification

After the initial classification of bare ground, grass/tree, and marsh/algal flat from the three WV-2 derived band indices and five pixel-based classification methods (details provided in section "Band Indices & Classification Methods"), additional steps were needed to separate 1) upland grass from trees, 2) marsh from algal flat, and 3) any other misclassified pixels. A complex decision tree incorporating the lidar low, medium, and high vegetation returns and the original landcover designations from "Band Indices & Classification Methods" was developed to fix the aforementioned issues. The decision tree is illustrated in Figure 10.

Final Combination

After all classifications were complete, the individual classification rasters were combined to get one raster for each WV-2 image. The order of raster combination/overlap was crucial to obtaining the most accurate classification and was overlapped as follows:

- 1) Marsh, Algal Flat, Upland Grass, and Upland Forest Classification,
- 2) Agriculture Classification,
- 3) Water Classification, and

4) Culvert, Bridge Deck, and Building Classification.

Once the classifications were combined into one raster for each WV-2 image, salt-and-pepper artifacts that arise when conducting pixel-based classifications were eliminated. Specifically, small features ≤ 9 pixels (36 m^2) were removed from water bodies. Lastly, after executing the above processing steps and getting final classifications for the 26 WV-2 images, the 26 final classification outputs were mosaicked together by giving preference to the newer imagery dates in overlap areas.

Accuracy Assessment

Lastly, a classification accuracy assessment was conducted to assess the accuracy of the WV-2 classifications. A 50 m buffer was generated around the CMGL’s most recent ESI shoreline and validation points were created with at least 50 m between points using ArcGIS’ “Create Random Points” tool. Ultimately 493 randomly located points were created. **Table 2** indicates the number of validation points per study area section. Then the 493 points were manually classified by referencing the WV-2 imagery and Pictometry’s oblique imagery (EagleView, 2022). **Table 3** lists the number of points that were correctly and incorrectly classified indicating a 79% accuracy. Lastly, “User’s Accuracy” (the probability that a certain land cover on the ground is classified correctly) and “Producer’s Accuracy” (the probability the class on the map will actually be present on the ground) were calculated and values varied from 0–100% with culverts being the worst and buildings being the best (**Table 3**).

Table 2. Number of accuracy assessment points per study area.

Section	Total Validation Points
Colorado River Delta	46
Matagorda Peninsula	55
Pass Cavallo to Matagorda Shipping Channel	15
Matagorda Island	32
Inland Matagorda	345
Total	493

Table 3. Classification error matrix indicating the number of correctly and incorrectly classified points.

		Validation Data											
		Water	Bare Ground	Forest	Grass	Marsh	Algal Flat	Building	Culvert	Bridge	Agriculture	Grand Total	Producer's Accuracy
WV-2 Classified Data	Water	46	1		1	1					0	49	81%
	Bare Ground	2	20		6	3				4	1	36	95%
	Forest			73	23	7					0	103	83%
	Grass	3		11	113					3	7	137	77%
	Marsh	1		2	2	70	2				0	77	79%
	Algal Flat	3				8	2				0	13	50%
	Building							10			0	10	100%
	Culvert	2			1					0	5	8	0%
	Bridge			1						2	2	5	14%
	Agriculture			1							54	55	87%
	Grand Total	57	21	88	146	89	4	10	2	14	62	493	
User's Accuracy	94%	56%	71%	82%	91%	15%	100%	0%	40%	98%			

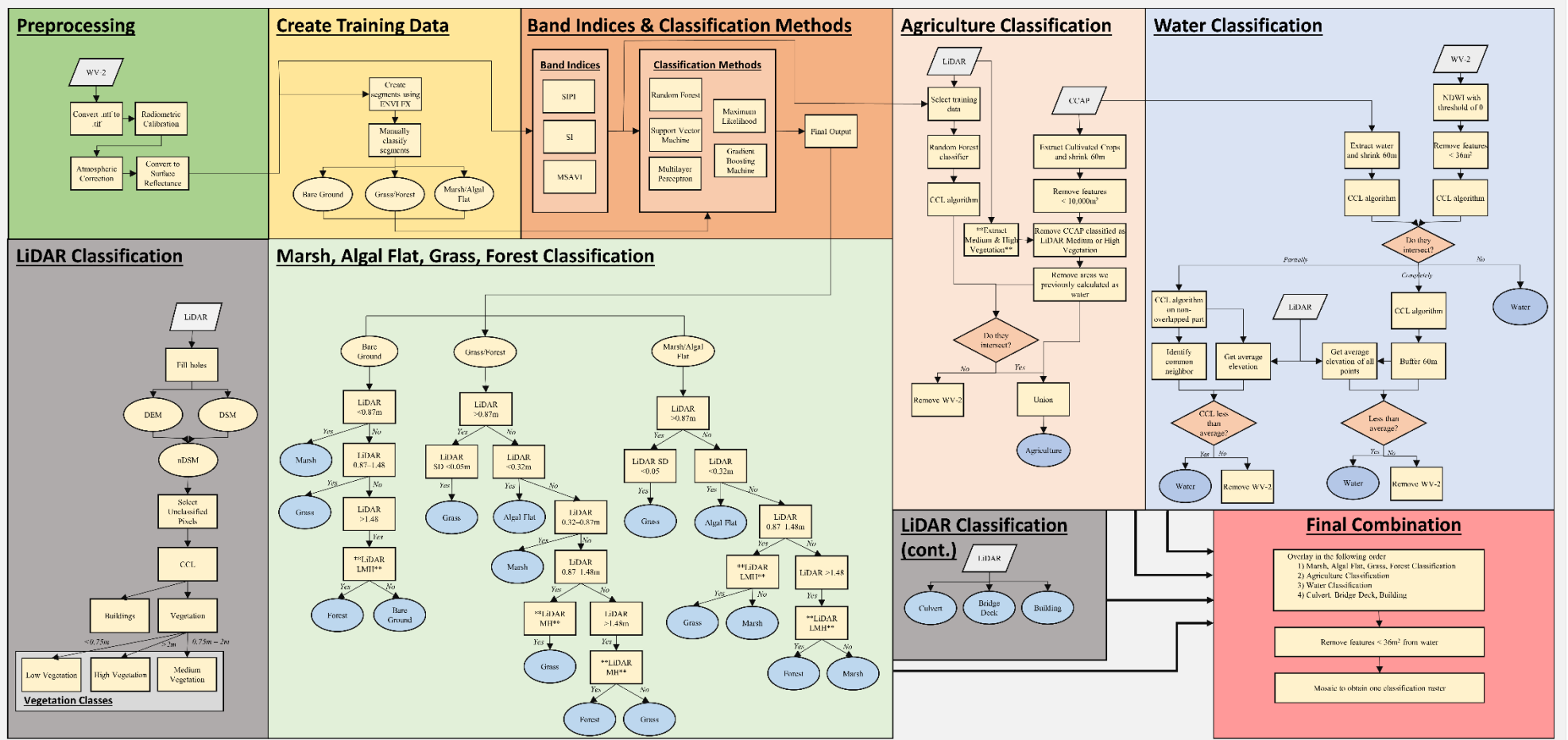


Figure 10. Methodology used to classify the WV-2 imagery including 1) Preprocessing, 2) Creating Training Data, 3) RENAME, 4) Water Classification, 5) Agriculture Classification, 6) Lidar Classification, 7) Marsh, Algal Flat, Grass, and Forest Classification. Each section is presented in greater detail in the text. Boxes containing a double asterisk reference the “Vegetation Classes” with “Lidar Classification”.

Results

The high-resolution habitat map for the entire study area is depicted in Figure 11 while Appendix A: WV-2 Land Cover Classifications Through Time contains maps zoomed in to each section, allowing for more details to be observed. Throughout the entire study area, the order of land cover dominance was: 1) Water, 3) Upland Grass, 3) Upland Forest, 4) Agricultural Crops, 5) Marsh, 6) Bare Ground, 7) Algal Flats, 8) Buildings, 9) Bridge Decks, and 10) Culverts (Figure 12). However, calculating the areal extent for the five sections separately resulted in slightly different trends (Figure 13). For all sections, the areal coverage of water was the greatest due to encompassing West Matagorda Bay and the Gulf of Mexico. Excluding water, the greatest coverage within the Colorado River Delta and Matagorda Island was marsh followed by upland forests and grasses (Figure 13). Conversely, for Matagorda Peninsula and Pass Cavallo to Matagorda Ship Channel, the greatest coverage was upland grass followed by bare ground (sand) and marsh (Figure 13). Inland Matagorda was dominated by upland grass, forests, and agricultural crops (Figure 13), however, there was still 85 km² of marsh surrounding the rivers feeding into West Matagorda Bay (Lavaca River and Colorado River being the most prominent).

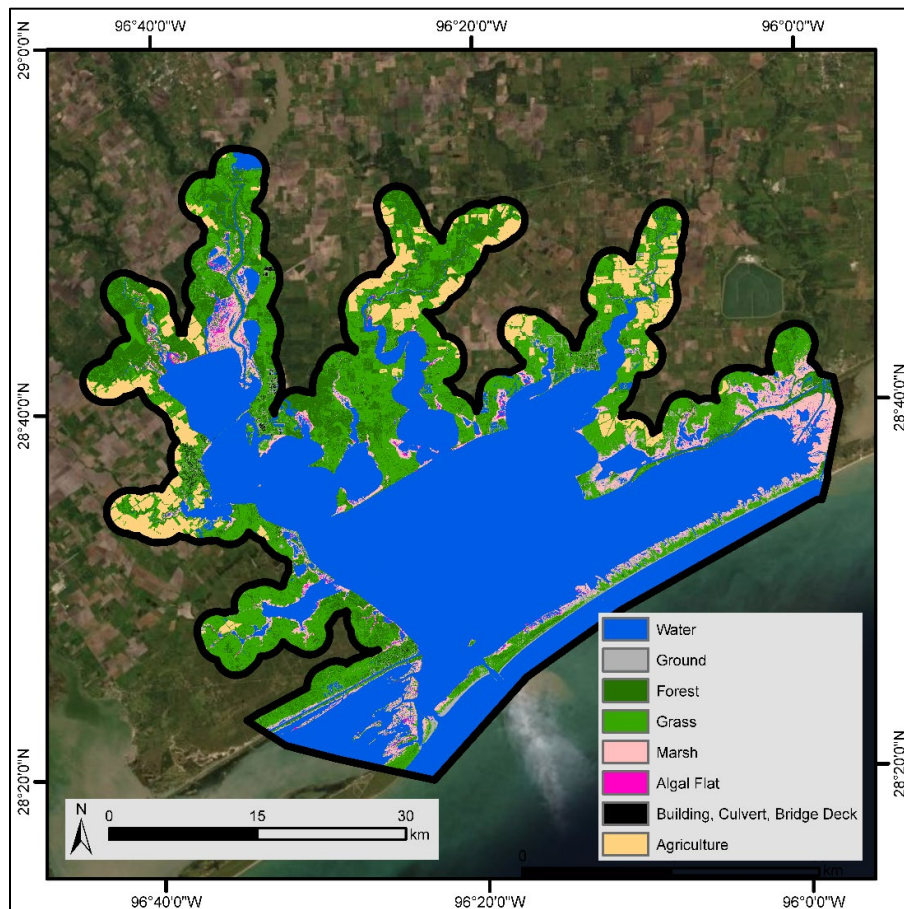


Figure 11. WV-2 Habitat Classifications. Buildings, Culverts, and Bridge Decks were combined into one class due to their small areal extent.

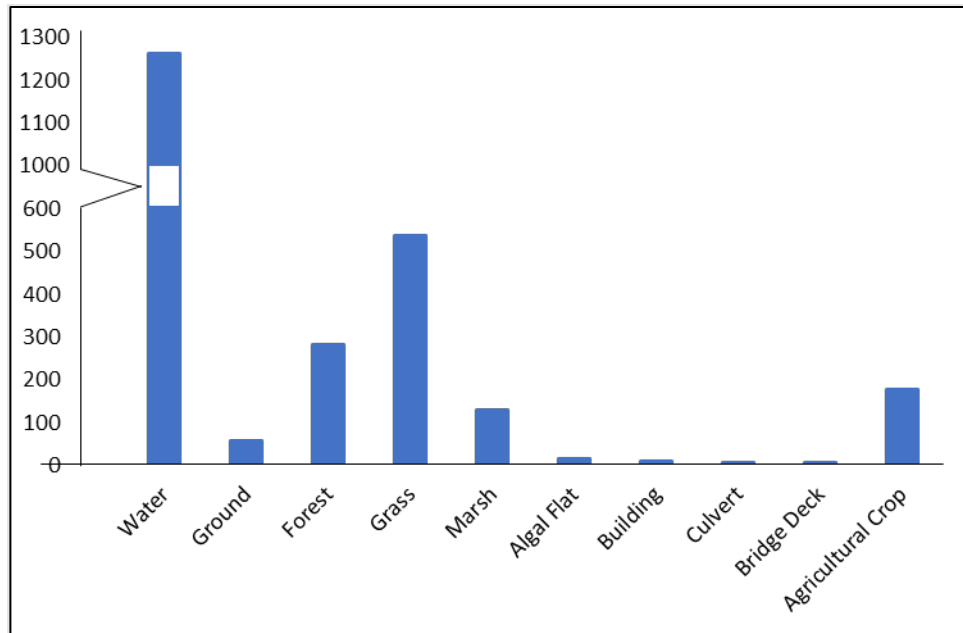


Figure 12. Area (km²) land cover extent for WV-2 imagery classifications for the entire study area.

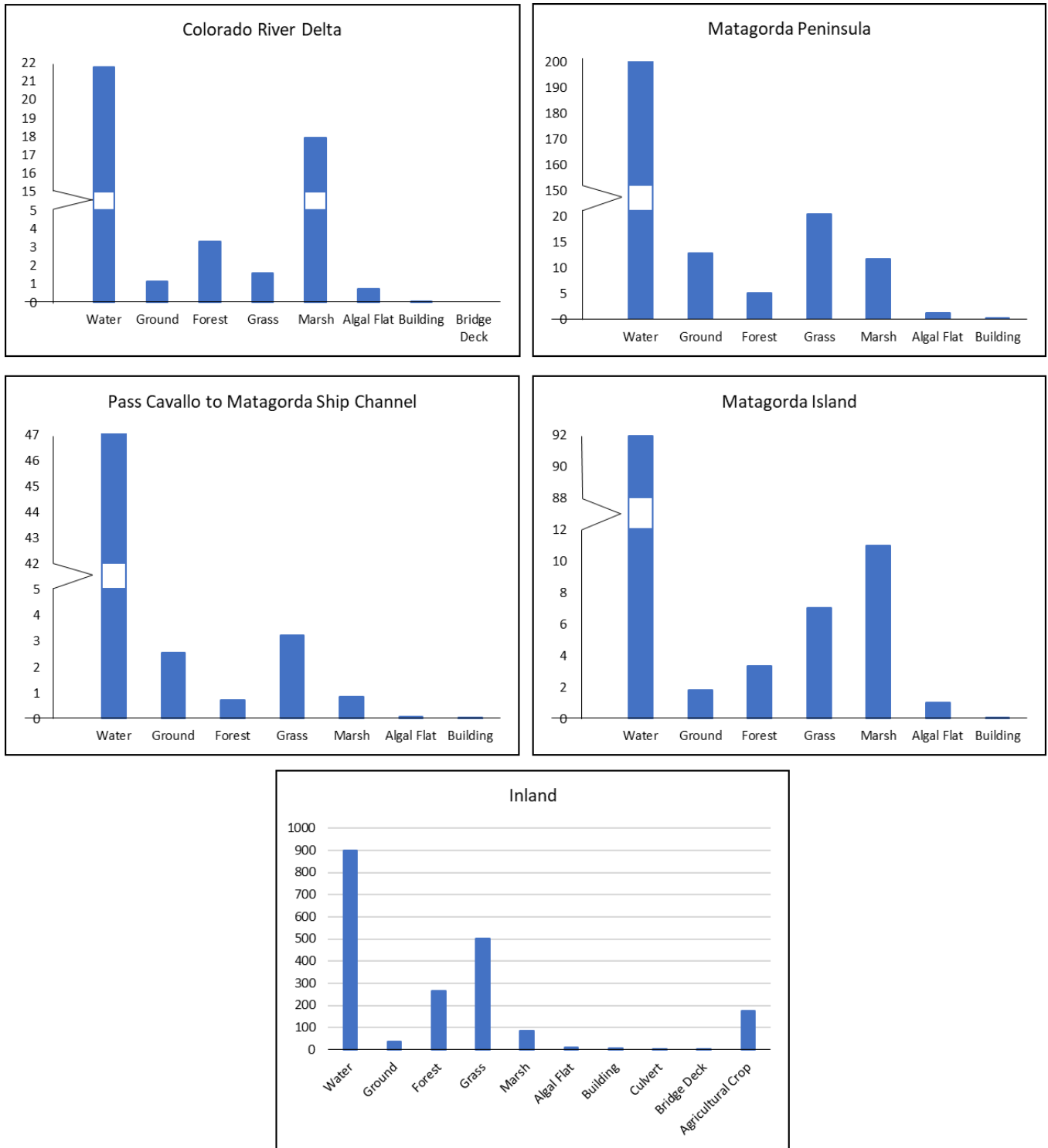


Figure 13. Area (km²) land cover extent for WV-2 imagery classifications for the Colorado River Delta, Matagorda Peninsula, Pass Cavallo to Matagorda Ship Channel, Matagorda Island, and Inland Matagorda County.

Mapping Land Cover Through Time

Methods

General Overview

This study analyzed land cover dynamics for the coastal region of the study area (Colorado River Delta through Matagorda Island) over fourteen imagery dates (1850's, 1930's, 1943, 1953, 1972, 1981, 1995, 2001, 2004, 2009, 2012, 2015, 2018, 2020) spanning 170 years. Due to the long linear coast (~53 km), the coastal region was separated into four sections to conduct analysis based on natural breaks such as Pass Cavallo and the Matagorda Ship Channel (Figure 14). However, due to historical imagery availability, there were some data gaps throughout the study area (Figure 14).

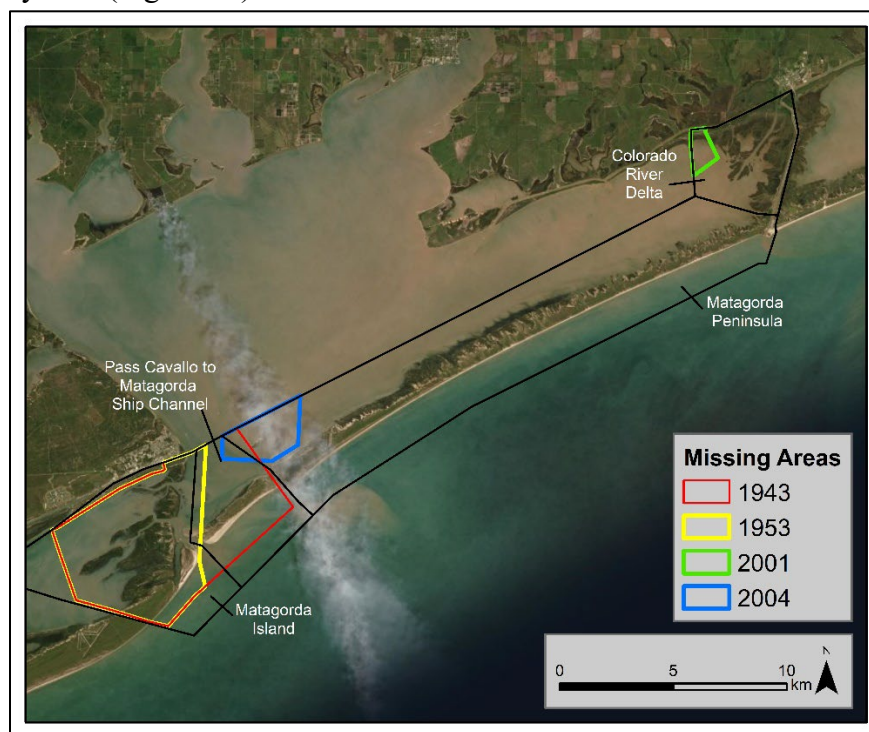


Figure 14. Study area boundaries for the coastal region as well as locations of imagery data gaps.

Various metrics for the five sections were calculated including:

- 1) **Area Through Time:** Total land area; Area sand; Area vegetation
- 2) **Rate of Area Change Through Time:** Total land area rate of change; Rate of sand change; Rate of vegetation change
- 3) **Change Analysis:** Area of transition between landcovers through time
- 4) **Width Through Time:** Gulf beach width; Vegetation width; Total land width (Gulf beach and vegetation combined)
- 5) **Positional Changes of the Gulf Shoreline, Gulf Vegetation Line, and Bay Shoreline**

Figure 15 represents a general workflow of the processes required to calculate the above metrics. Additionally, due to the aforementioned data gaps, not all five metrics were able to be calculated for the various timeframes or study area sections. **Table 4** summarizes the five metrics by timeframe and study area and whether the metric was able to be calculated. All metrics in Figure 15 are indicated by a dark blue oval and labeled 1–5; similarly, all metrics are labeled 1–5 in **Table 4** which correlate to the metric numbers above.

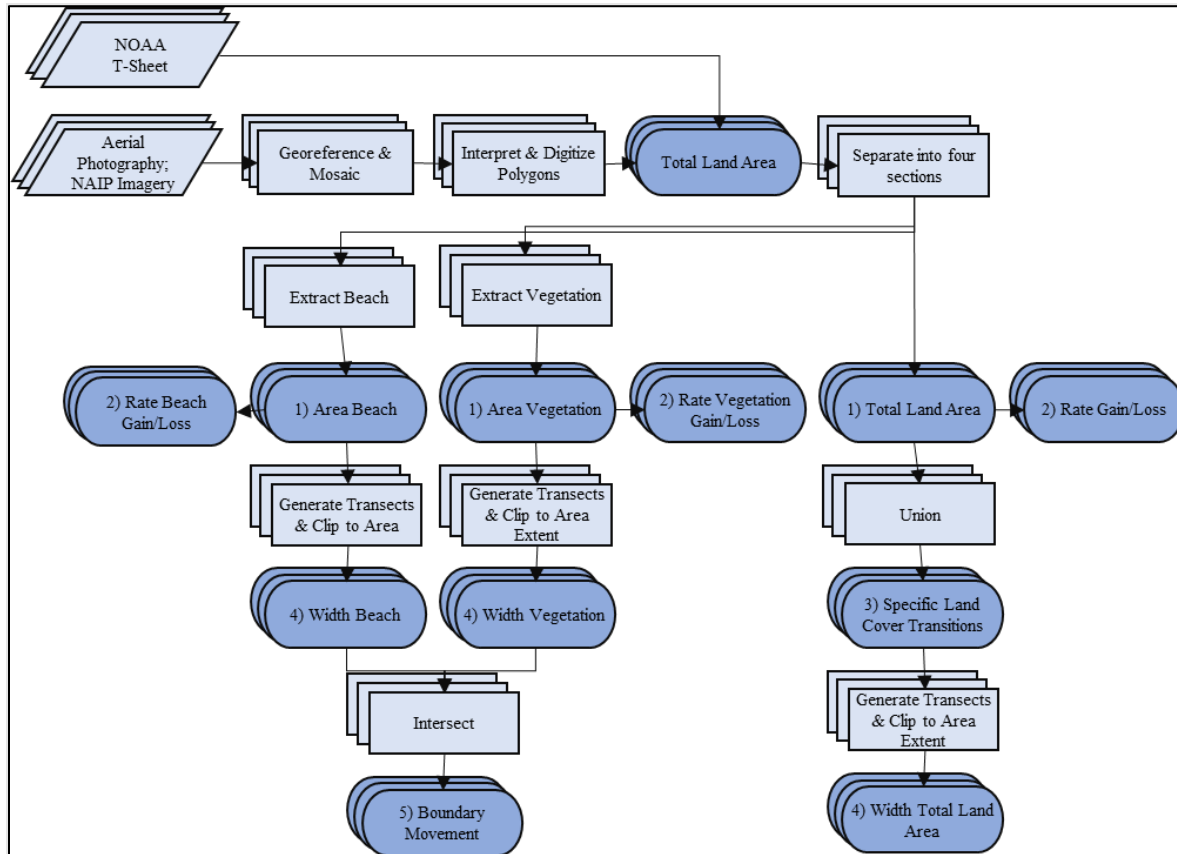


Figure 15. Generalized workflow for analyzing historical land cover dynamics. Numbers 1–5 correlate to the numbers listed above for the various metrics calculated.

Table 4. Summary by timeframe of the usability of the five metrics we calculated. Numbers 1 through 4 in the first-row correlate to the study area (1 = Colorado River Delta, 2 = Matagorda Peninsula, 3 = Pass Cavallo to Matagorda Ship Channel, 4 = Matagorda Island). Y = metric was calculated, N = value was unable to be calculated. The section numbers are labeled 1 through 5 and correlate to Figure 15.

Section	Subsection	1				2				3				4				1				2				3				4								
		1850's	1933	1943	1953	1972	1981	1995	2001	2004	2009	2012	2015	2018	2020	1850's-1933	1933-1943	1943-1953	1953-1972	1972-1981	1981-1995	1995-2001	2001-2004	2004-2009	2009-2012	2012-2015	2015-2018	2018-2020										
Area	1) Area Through Time	All Land Extent Through Time	Y	Y	Y	Y	Y	Y	Y	Y	Y	Y	Y	Y	Y	Y	Y	Y	Y	Y	Y	Y	Y	Y	Y	Y	Y	Y	Y	Y	Y	Y	Y	Y	Y	Y	Y	Y
		Vegetation and Sand Through Time	Y	Y	Y	N	Y	Y	Y	N	Y	Y	Y	N	Y	Y	Y	N	Y	Y	Y	N	Y	Y	Y	N	Y	Y	Y	N	Y	Y	Y	N	Y	Y	Y	N
	2) Rate of Change Through Time	All Land Extent Rate of Change	Y	Y	Y	Y	Y	Y	N	N	Y	Y	N	N	Y	Y	N	N	Y	Y	N	N	Y	Y	N	N	Y	Y	N	N	Y	Y	N	N	Y	Y	N	N
		Vegetation and Sand Rate of Change	Y	Y	Y	N	Y	Y	N	N	Y	Y	N	N	Y	Y	N	N	Y	Y	N	N	Y	Y	N	N	Y	Y	N	N	Y	Y	N	N	Y	Y	N	N
	3) Change Analysis	Land Cover Transitions Through Time	Y	Y	Y	N	Y	Y	N	N	Y	Y	N	N	Y	Y	N	N	Y	Y	N	N	Y	Y	N	N	Y	Y	N	N	Y	Y	N	N	Y	Y	N	N
			Y	Y	Y	N	Y	Y	N	N	Y	Y	N	N	Y	Y	N	N	Y	Y	N	N	Y	Y	N	N	Y	Y	N	N	Y	Y	N	N	Y	Y	N	N
Width	4) Width Through Time	All Land Width Through Time	N	Y	Y	N	N	Y	Y	N	N	Y	Y	N	N	Y	Y	N	N	Y	Y	N	N	Y	Y	N	N	Y	Y	N	N	Y	Y	N	N	Y	Y	N
		Vegetation Width Through Time	N	Y	Y	N	N	Y	Y	N	N	Y	Y	N	N	Y	Y	N	N	Y	Y	N	N	Y	Y	N	N	Y	Y	N	N	Y	Y	N	N	Y	Y	N
		Gulf Beach Width Through Time	N	Y	Y	N	N	Y	Y	N	N	Y	Y	N	N	Y	Y	N	N	Y	Y	N	N	Y	Y	N	N	Y	Y	N	N	Y	Y	N	N	Y	Y	N
	5) Positional Changes of Gulf Shoreline, Gulf Vegetation Line, and Bay Shoreline	Gulf Shoreline, Gulf Vegetation Line, and Bay Shoreline		1				2				3				4																						
				N				Y				Y				Y																						
				N				Y				Y				Y																						
		N				Y				Y				N																								

Data Sources Compilation & Preparation

Fourteen imagery dates (1850's, 1930's, 1943, 1953, 1972, 1981, 1995, 2001, 2004, 2009, 2012, 2015, 2018, 2020), originating from a variety of sources (NOAA T-Sheets, Aerial Photo Single Frames (ASPF), National High-Altitude Photography (NHAP), Texas Orthoimagery Program (TOP), and National Agriculture Imagery Program (NAIP)), with varying spatial and spectral characteristics were used to map land cover (Table 5). Twelve of the sources (1943–2020) consisted of aerial photography while 1850's and 1930's were NOAA T-Sheets. Imagery from 1943–2001 required rectification while 2004–2020 came rectified (Table 5). The six unrectified aerial photography sources were rectified in ArcMap 10.8 to 2016 National Agriculture Imagery Program (NAIP) orthorectified aerial photography (using Universal Transverse Mercator (UTM) coordinate system, North American Datum (NAD) 83). Additionally, to cover the entire study area, multiple images for each timeframe were required, and after rectification images were mosaicked together. For the 1850's and 1930's NOAA T-Sheets, each T-Sheet consisted of a compilation of years and resultingly the 1850's data is from 1855–1859 while the 1933 data is from 1933, 1934, and 1939. The georeferenced T-Sheets as well as their vectorized shoreline were downloaded from the NOAA Shoreline Website (U.S. DOC, NOAA, NESDIS, and NOS., 2016). Appendix B: Imagery Comparisons Along with Classified Land Covers illustrates the difference between sources.

Table 5. All imagery dates that were used for historical analysis. *1850's data is from 1855–1859 while 1930's data is from 1933, 1934, 1939.

Data Source	Download Location	Year	Imagery Type	Spectral Resolution	Spatial Resolution (m)
(U.S. DOC, NOAA, NESDIS, and NOS., 2016)	NOAA	*1850's	NOAA T – Sheet	BW	N/A
(U.S. DOC, NOAA, NESDIS, and NOS., 2016)	NOAA	*1930's	NOAA T – Sheet	BW	N/A
(Research and Distribution Center, 1943)	TNRIS	1943		BW	1
(USDA, 1953)	TNRIS	1953		BW	2
(USGS, 1972)	USGS EE	1972	APSF	CIR	3.25
(USGS, 1981)	USGS EE	1981	NHAP	CIR	1.6
(Strategic Mapping Program, 1996)	TNRIS	1995	TOP	CIR	1
(Texas General Land Office, 2001)	GLO	2001		CIR	1
(USDA, 2004)	TNRIS	2004	NAIP	CIR	1
(Strategic Mapping Program, 2009)	TNRIS	2009	NAIP/TOP	CIR	0.5
(USDA, 2012)	TNRIS	2012	NAIP	RGBN	1
(TNRIS, 2015)	TNRIS	2015	TOP	RGBN	0.5
(USDA, 2018)	TNRIS	2018	NAIP	RGBN	0.6
(USDA, 2020)	TNRIS	2020	NAIP	RGBN	0.6

Area Through Time

After rectifying and mosaicking imagery together, all twelve years of imagery (1943 through 2020) were manually digitized in ArcMap 10.8 and then classified using visual inspection. The map scale of digitization varied depending on the spatial resolution (Table 5). Digitized polygons were classified into three land covers: vegetation, sand, and water (Appendix C: Digitized Land Cover Classifications Through Time). After digitization and classification were complete, the data were 1) smoothed using the "Smooth" tool with 2 m Peak to get rid of jagged edges, and 2) checked for topological errors to ensure there were no overlapping features or gaps in the data.

The 1850's and 1930's NOAA T-Sheets required a slightly different workflow. The vectorized shoreline delineated the land/water boundary rather than differentiating vegetation, water and sand. However, the georeferenced T-Sheet distinguished vegetation, water, and sand

based on textural differences (Figure 16). Both files were used concurrently to digitize the sand/vegetation boundary (essentially the Gulf vegetation line) and the boundary was incorporated into the vectorized shoreline. This ultimately allowed for the same land cover classifications (vegetation, sand, water) that were obtained from the aerial photography.

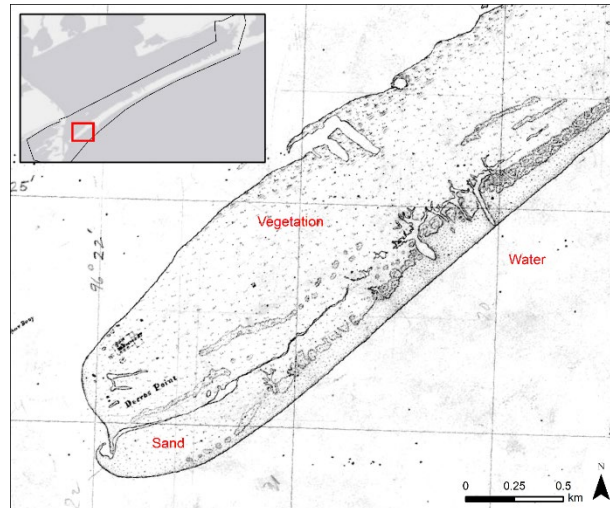


Figure 16. 1850's NOAA T – Sheet.

Rate of Area Change Through Time

Due to differing time lapses between sequential imagery dates from 1850–2020, the rate of land cover change between the thirteen sequential timeframes (1850's–1930's, 1930's–1943, 1943–1953, 1953–1972, 1972–1981, 1981–1995, 1995–2001, 2001–2004, 2004–2009, 2009–2012, 2012–2015, 2015–2018, 2018–2020) was calculated to show short-term and long-term trends in land cover prevalence.

Change Analysis

After all fourteen years were digitized and classified, the “Union” tool was used to combine sequential years together, allowing for investigation of specific landcover transitions over thirteen transition periods (1850's–1930's, 1930's–1943, 1943–1953, 1953–1972, 1972–1981, 1981–1995, 1995–2001, 2001–2004, 2004–2009, 2009–2012, 2012–2015, 2015–2018, 2018–2020) for each study area section (Appendix D: Land cover transitions illustrates specific land cover transitions). Since vegetation, sand, and water were digitized, nine land cover transitions were possible: 1) Vegetation to Water, 2) Vegetation to Vegetation, 3) Vegetation to Sand, 4) Water to Water, 5) Water to Vegetation, 6) Water to Sand, 7) Sand to Water, 8) Sand to Vegetation, and 9) Sand to Sand. Due to the apparent changes between landcovers (ex: vegetation being converted to sand and sand being converted to vegetation throughout the same timeframe), the net change between the following land cover were further analyzed: 1) Sand and Water (primarily representing the change between Gulf beach and the Gulf of Mexico), 2) Sand

and Vegetation (representing changes along the Gulf vegetation line), and 3) Vegetation and Water (representing changes to the bay shoreline).

Width Through Time

While quantifying the area of land cover change over time can provide insight into the processes driving the change, it is still necessary to analyze the spatial patterns associated with those changes. Spatial patterns were analyzed in terms of width at the transect level. First, the Digital Shoreline Analysis System (DSAS) was used to generate a baseline parallel to the coastline and transects were generated every 20 m perpendicular to the baseline resulting in over 2,500 transects. The transects were then clipped to the vegetation, Gulf beach, and land extents. If vegetation patches were present within the Gulf beach, they were included in the Gulf beach width. Non-Gulf beach sand which was primarily found along the bay shoreline was included within the vegetation width. Land width consisted of the total width of the island (Gulf beach width and vegetation width combined). Lastly, the transects were summarized by study area for all fourteen dates. However, due to expansive marsh presence in the Matagorda Island study area where marsh coverage extends from Matagorda Island to Port O'Connor, the vegetation width and total land width was not calculated through time for that area. Figure 17 portrays an example of the beach width transects for 1972 and 2001.

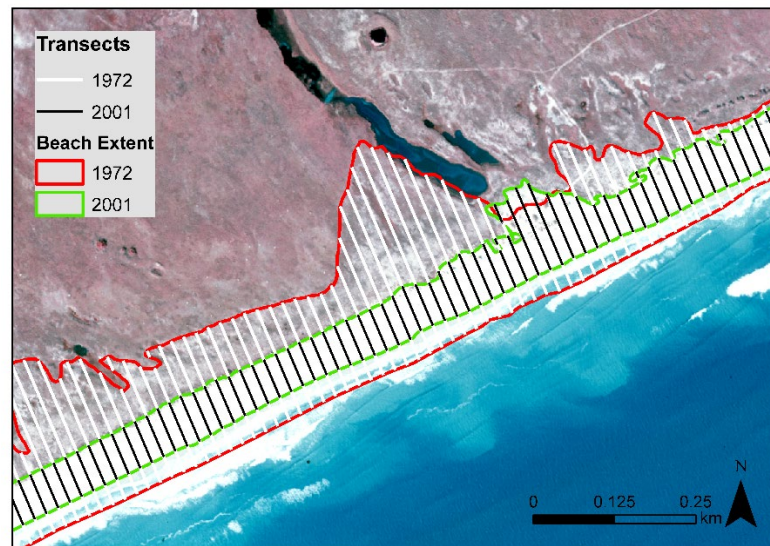


Figure 17. Example of transects showing the beach width for 1972 and 2001.

Positional Changes of Gulf Shoreline, Gulf Vegetation Line, and Bay Shoreline

Knowing the width through time gives a general picture of where the coast is changing, however does not give insight onto how the changes are occurring. Therefore, in addition to measuring the width of the coast over time to analyze spatial patterns of change, a transect analysis was conducted to understand the types of land cover changes occurring across the study area. For example: 1) beach width may be decreasing, but it is unknown if the beach is being lost to open water (erosion) or sand; 2) vegetation width may be decreasing, but it is unknown if

vegetation is being lost to water on the bay side or undergoing a rollback of barrier islands and being converted to sand. To investigate this, the previously clipped transects were intersected for: 1) sand and vegetation (Gulf vegetation line), 2) sand and water (Gulf shoreline), and 3) vegetation and water (bay shoreline) for all thirteen transitions periods, and the net change per transect per timeframe was calculated. Then, the net change from 1850–2020 was calculated.

Results

Area Through Time

The area of total land cover for the entire study (all four sections combined) from 1850–2020 fluctuated between 95.1 km² and 102.7 km² (Figure 18). From 1850–1933 the area saw a 3.9 km² decrease, followed by a 7.5 km² increase from 1972–2015, after which the area decreased 2.6 km² from 2015–2020.

However, when looking at each section individually, it becomes evident that these changes are not uniformly distributed throughout the entire study area (Figure 19). The Colorado River Delta increased 21.22 km² over time, from 1.59 km² in 1850 to 22.81 km² in 2020. This area experienced a substantial increase from 1850–1943 (16.18 km²) followed by a much smaller increase from 1943–2020 (5.04 km²). Additionally, the greatest increase (9.55 km²) occurred from 1933–1943. Matagorda Peninsula experienced a 7.91 km² decrease over time, from 56.34 km² in 1850 to 48.43 km² in 2020. However, Matagorda Peninsula experienced multiple fluctuations of increases and decreases. For example, area decreased 8.03 km² from 1850–1943, increased 3.1 km² from 1943–1972, remained stable from 1972–2015, then experienced a rapid decline of 2.28 km² from 2015–2020. Pass Cavallo to Matagorda Ship Channel only decreased 0.54 km² from 1850–2020. However, area decreased 1.99 km² from 1850–1953 and then increased 1.45 km² from 1953–2020. Matagorda Island decreased 11.34 km² over time, from 33 km² in 1850 to 21.66 km² in 2020. This area experienced a decrease from 1850–1973 (11.06 km²) and then remained stable from 1972–2020, only experiencing a 0.28 km² loss.

When separating vegetation from sand, it becomes clear that transitions between vegetation and sand are occurring due to increased periods of vegetation growth occurring when sand decreases and increased periods of sand growth occurring when vegetation decreases (Figure 19). The Colorado River Delta does not have a Gulf facing shoreline resulting in little to no sand throughout the study area. This area experienced high vegetation growth from 1850–1933 (6.63 km²) and 1933–1943 (9.31 km²) followed by much smaller periods of growth from 1943–2020 (5.26 km²). Opposite from the Colorado River Delta's increase in vegetation from 1850–1943, Matagorda Peninsula experienced high vegetation loss from 1850–1933 (7.62 km²) and 1933–1943 (6.1 km²). From 1943–1995, vegetation increased (7.52 km²), then remained stable (0.61 km² loss). Conversely, sand increased from 1850–1953 (6.71) then decreased from 1953–2020 (7.79 km²). For Pass Cavallo to the Matagorda Ship Channel, vegetation decreased from 1850–1972 (2.98 km²), then increased from 1972–2020 (1.9 km²). Conversely, sand increased from 1850–1972 (1.42 km²), rapidly decreased from 1972–1981 (0.91 km²), and then remained stable from 1981–2020 (0.3 km² decrease). Lastly, for Matagorda Island, vegetation increased 1.08 km² while sand decreased 1.36 km² from 1972–2020.

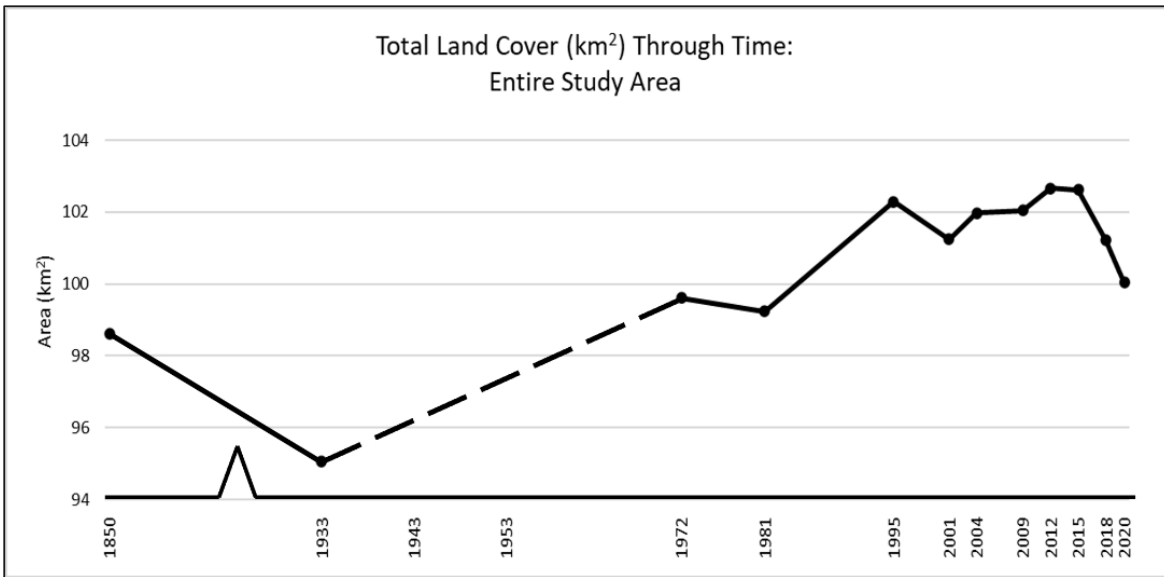


Figure 18. Area (km²) land cover through time through time for the entire study area. The dashed line represents inferred transitions due to data gaps.

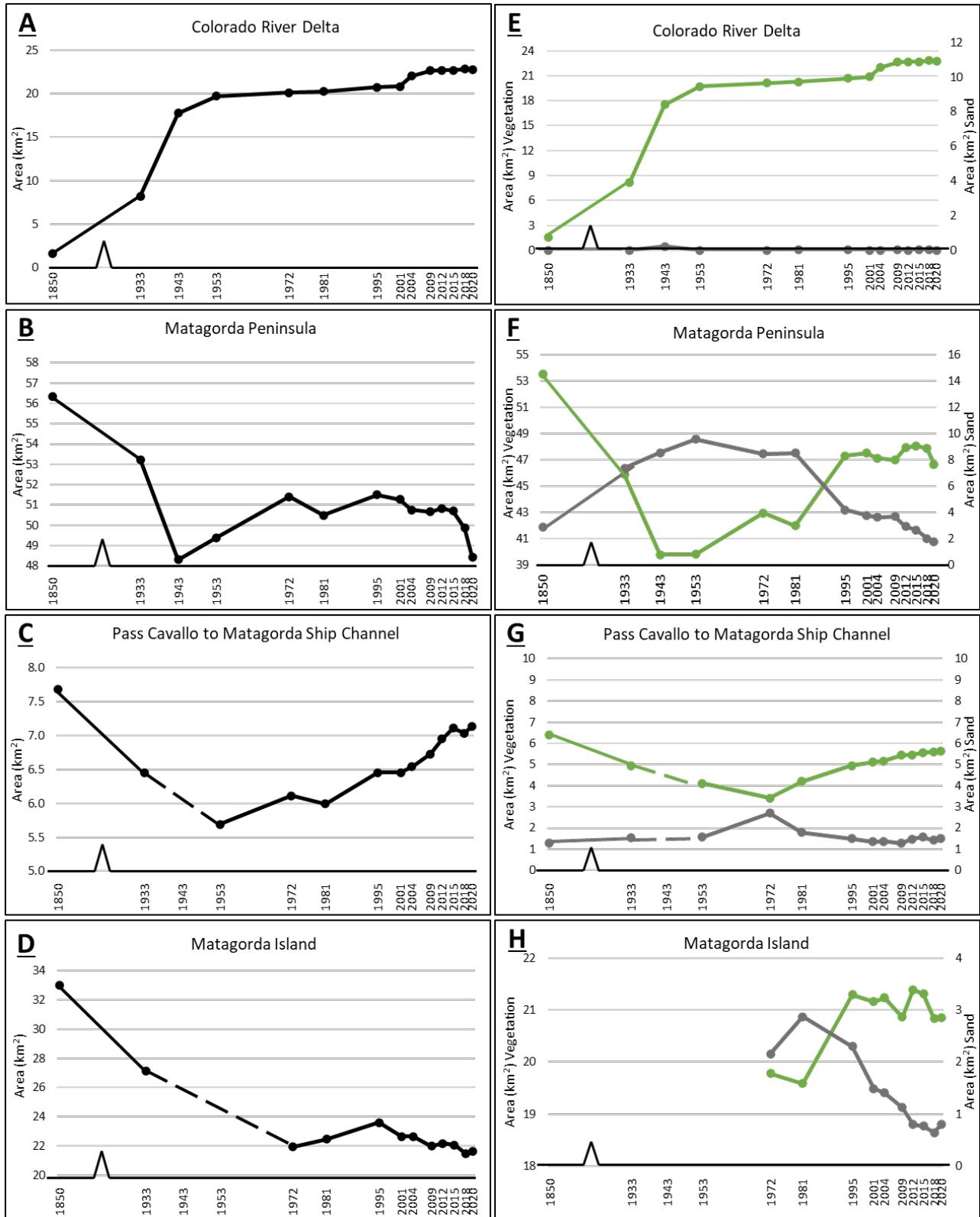


Figure 19. A – D) Area (km²) land cover through time through time by section; and E – H) area (km²) vegetation and sand through time through time by section. The dashed line represents inferred transitions due to data gaps.

Rate of Area Change Through Time

The rate of land, vegetation, and sand change from 1850–2022 varied over time and is depicted in Figure 20. The Colorado River Delta experienced the greatest rate of vegetation increase from 1933–1943 (0.93 km²/yr), which can be attributed to the log raft removal that occurred in 1929. From 1943–2020, and with the exception of 2001–2004, the rate of vegetation growth remained low, under 0.25 km²/yr. Matagorda Peninsula experienced a high rate of vegetation loss from 1933–1943 (0.61 km²/yr), followed by periods of small rate increases and decreases. However, from 2018–2020, the rate of vegetation loss increased again (0.6 km²/yr). Pass Cavallo to Matagorda Ship Channel had a high rate of vegetation gain and sand loss from 1972–1981. However, since 1981 and with the exception of 2004–2009, the rate of vegetation growth has slowed over time. Sand has experienced variable rates of growth and loss over time. Matagorda Island experienced its greatest rate of vegetation growth from 2009–2012 and its greatest rate of loss from 2015–2018. Sand had variable rates of loss from 1981–2018, however experienced a 0.08 km²/yr increase from 2018–2020.

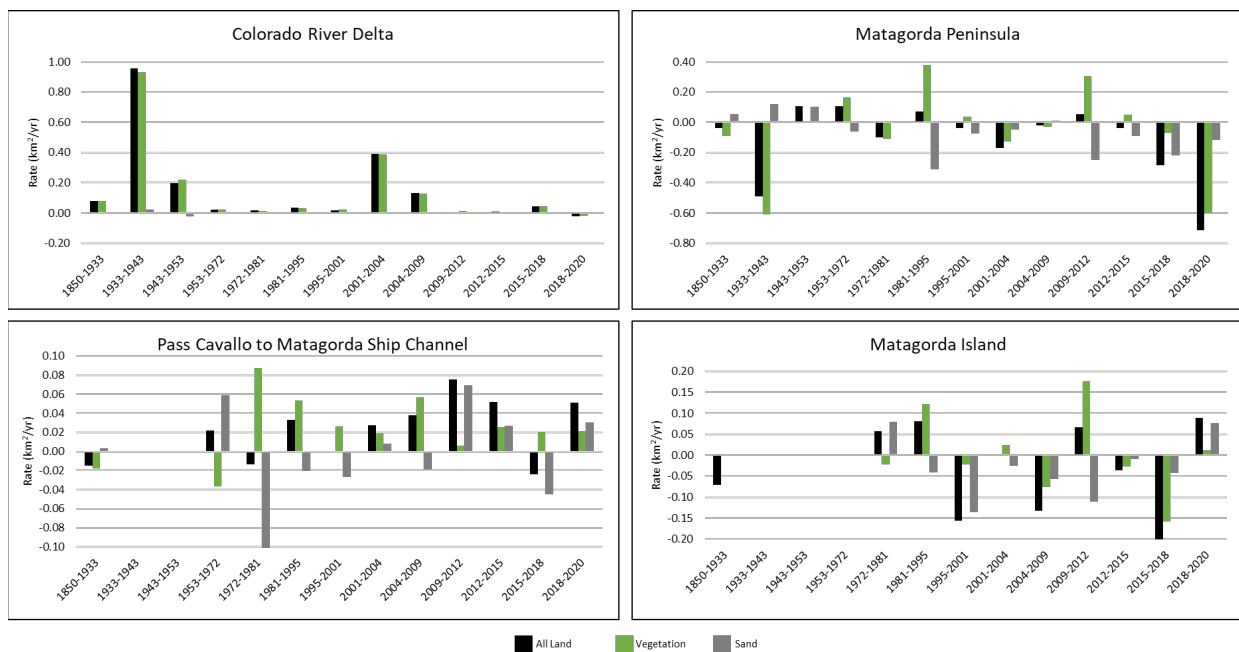


Figure 20. Rate (km²/yr) of land cover change through time by section for total area, vegetation, and sand.

Change Analysis

After unioning sequential years of land cover together, the following nine land cover transitions were analyzed: 1) vegetation to water, 2) vegetation to vegetation, 3) vegetation to sand, 4) water to water, 5) water to vegetation, 6) water to sand, 7) sand to water, 8) sand to

vegetation, and 9) sand to sand. Overall, from 1850–2020, the following transitions were evident which are visually depicted in Figure 21:

1. A net gain in sand from water for Pass Cavallo to Matagorda Ship Channel (1.34 km²), Matagorda Island (0.61 km²), and Matagorda Peninsula (0.28 km²),
2. A net loss of vegetation to water for Matagorda Peninsula (8.17 km²), Matagorda Island (6.95 km²), and Pass Cavallo to Matagorda Ship Channel (1.12 km²),
3. A net gain in vegetation from water for the Colorado River Delta (21.27 km²), and
4. A net gain in vegetation from sand for Matagorda Peninsula (1.25 km²), Pass Cavallo to Matagorda Ship Channel (1.17 km¹), and Matagorda Island (1.97 km¹).

Not considering the Colorado River Delta, the other three study areas experienced a net loss of vegetation (11.82 km²) and sand (2.2 km²). However, when looking at the individual transitions by timeframe, it becomes clear that a lot of swap occurred (ex: vegetation being converted to sand and sand being converted to vegetation throughout the same timeframe; Figure 22).

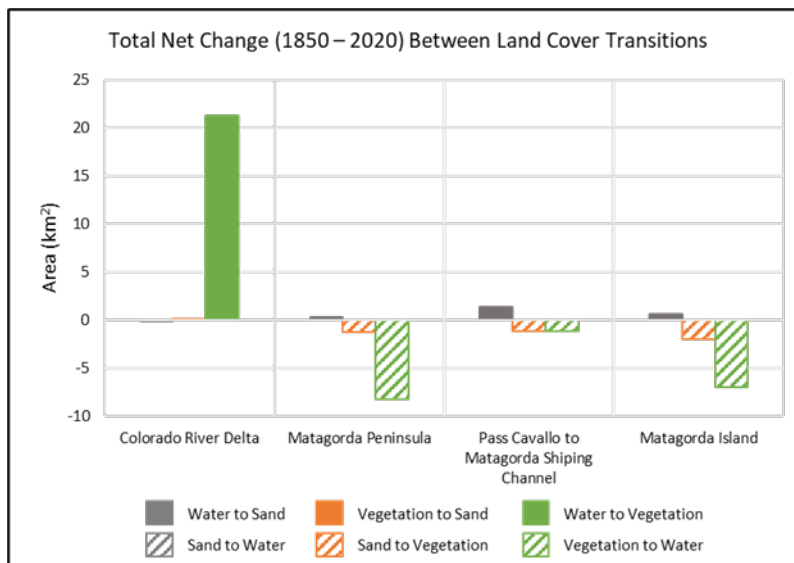


Figure 21. Area (km²) net land cover change occurring from 1850–2020 between landcover transitions (sand and water, vegetation at sand, vegetation and water) for each study area section. Positive Values: 1) gain in sand from water, 2) gain in sand from vegetation, 3) gain in vegetation from water; Negative Values: 1) gain in water from sand, 2) gain in vegetation from sand, 3) gain in water from vegetation

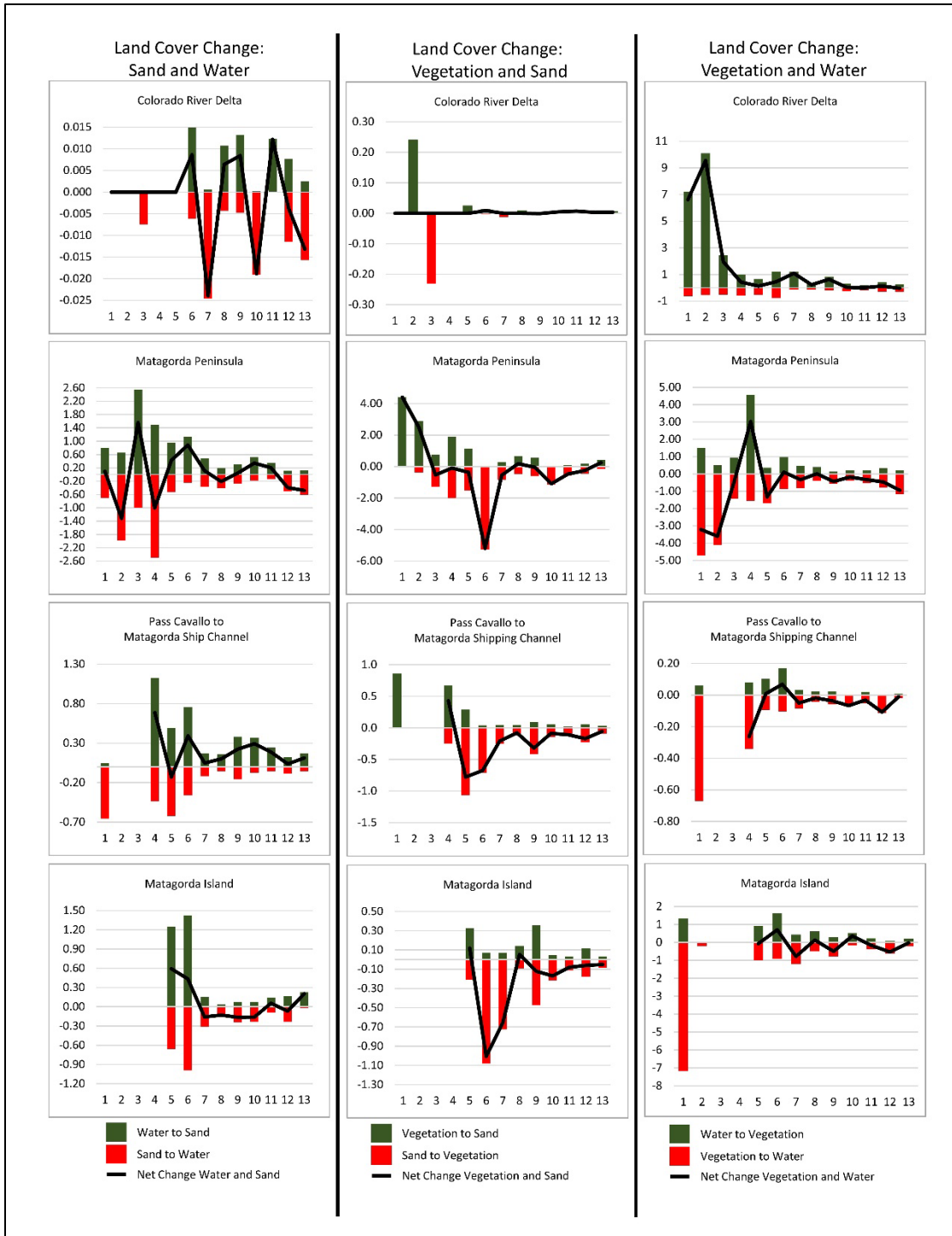


Figure 22. Area (km²) land cover change between sand and water, vegetation and sand, vegetation and water, as well as the net change between covers for Colorado River Delta, Matagorda Peninsula, Pass Cavallo to Matagorda Ship Channel, and Matagorda Island. Numbers 1-13 on the X-axis represent a specific timeframe: 1 = 1850's–1930's; 2 = 1930's–1943; 3 = 1943–1953; 4 = 1953–1972; 5 = 1972–1981; 6 = 1981–1995; 7 = 1995–2001; 8 = 2001–2004; 9 = 2004–2009; 10 = 2009–2012; 11 = 2012–2015; 12 = 2015–2018; 13 = 2018–2020.

Width Through Time

Figure 23 shows the average land, beach, and vegetation width for all transects combined through time for each study area. Figure 24 illustrates the 1850 and 2020 shorelines to demonstrate the significant width changes over time. The average width is useful for showing the general trends through the study area, however due to the long Gulf facing shoreline, the width could vary drastically throughout the study area. Figure 25-Figure 27 show how the width of each land, vegetation, and Gulf beach transect changed through time.

The average land width through time (vegetation and sand combined) decreased for Matagorda Peninsula and Pass Cavallo to Matagorda Ship Channel (Figure 23). Matagorda Peninsula decreased from 1850–1943 (193 m) and remained stable (only decreasing 13 m) from 1943–2020. Pass Cavallo to Matagorda Ship Channel decreased from 1850–1981 (511 m) and then increased from 1981–2020 (165 m). Overall, from 1850–2020, the average land width decreased 206 m for Matagorda Peninsula and 355 m for Pass Cavallo to Matagorda Ship Channel.

Mean Gulf beach width experienced periods of increased and decreased width for Matagorda Peninsula and Pass Cavallo to Matagorda Ship Channel and consistently decreased along Matagorda Island, with the 2020 width being less than in 1850 (1972 for Matagorda Island) for all three areas (Figure 23). During the 1850–1981 timeframes, the closure of numerous storm washover channels throughout Matagorda Peninsula (evident in Figure 27) increased beach widths. Resultingly, the average beach width increased from 1850–1981 (139 m), then decreased from 1981–2020 (173 m). Throughout the entire timeframe, 1953 had the greatest maximum mean beach width of 213 m while 2020 had the minimum each width of 38 m (Figure 23). Pass Cavallo to Matagorda Ship Channel decreased from 1850–2009 (57 m), then experienced periods for rapid increases and decreases from 2009–2020. Matagorda Island consistently decreased from 1972–2020 (323 m). Overall, from 1850–2020, beach width decreased 34 m for Matagorda Peninsula and 23 m for Pass Cavallo to Matagorda Ship Channel, and from 1972–2020, beach width decreased 323 m for Matagorda Island.

Mean vegetation width also experienced periods of increased and decreased width for Matagorda Peninsula and Pass Cavallo to Matagorda Ship Channel, with the 2020 width being less than in 1850 were both areas (Figure 23). For Matagorda Peninsula and Pass Cavallo to Matagorda Ship Channel, vegetation width decreased from 1850–1981, then increased from 1981–2020. Overall, from 1850–2020, vegetation width decreased 172 m for Matagorda Peninsula and 331 m for Pass Cavallo to Matagorda Ship Channel.

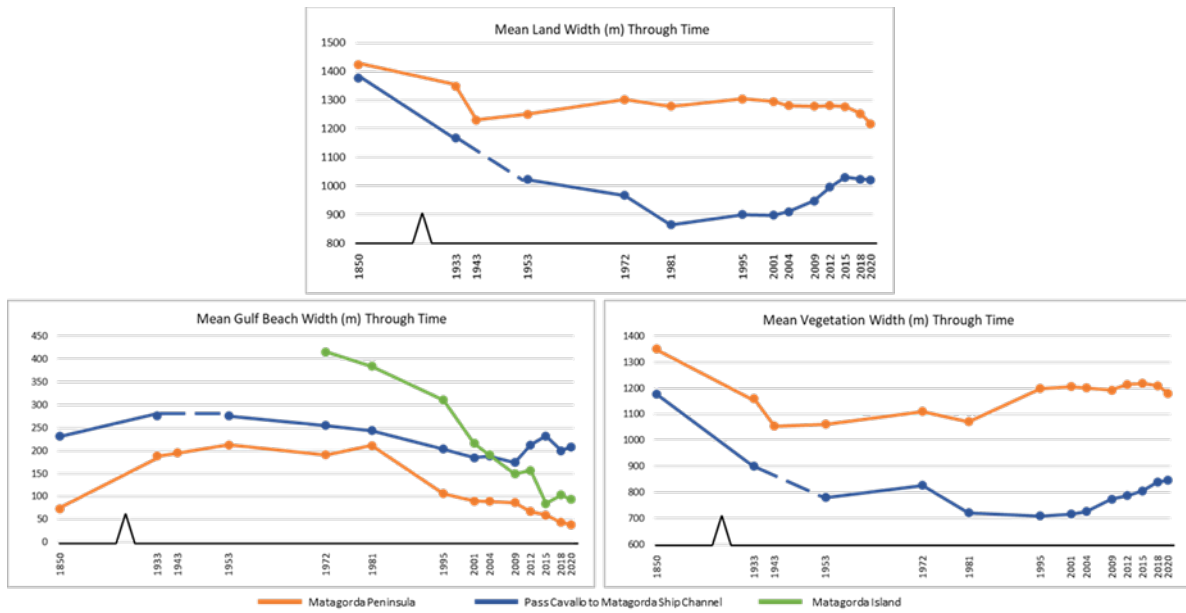


Figure 23. Average land (vegetation and beach combined), beach, and vegetation width through time for each study area.

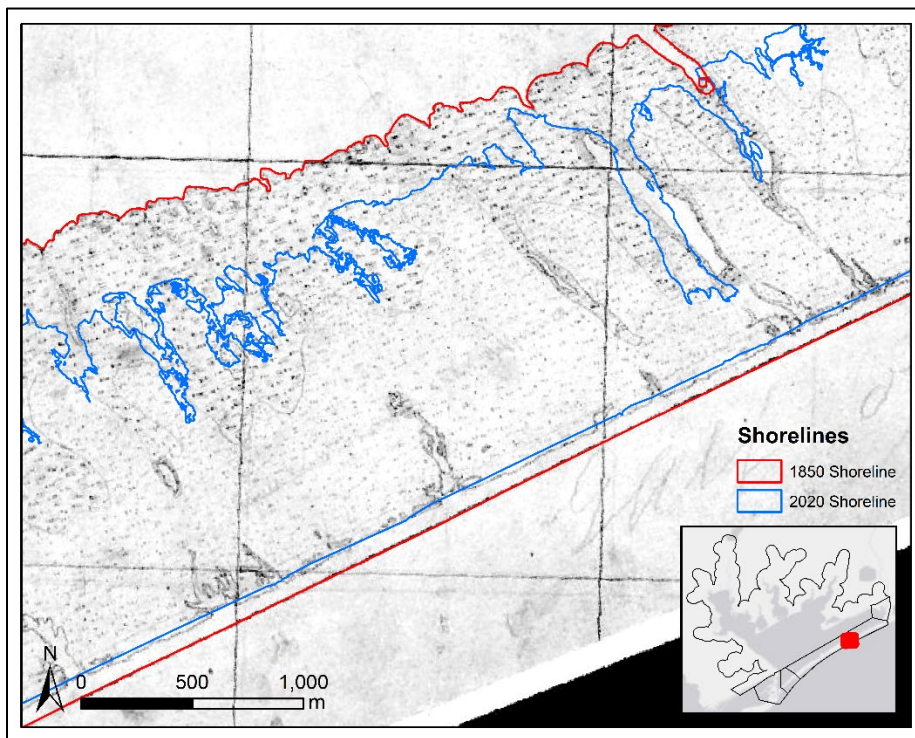


Figure 24. 1850 and 2020 shorelines illustrating the significant width changes.

All Land Width Through Time

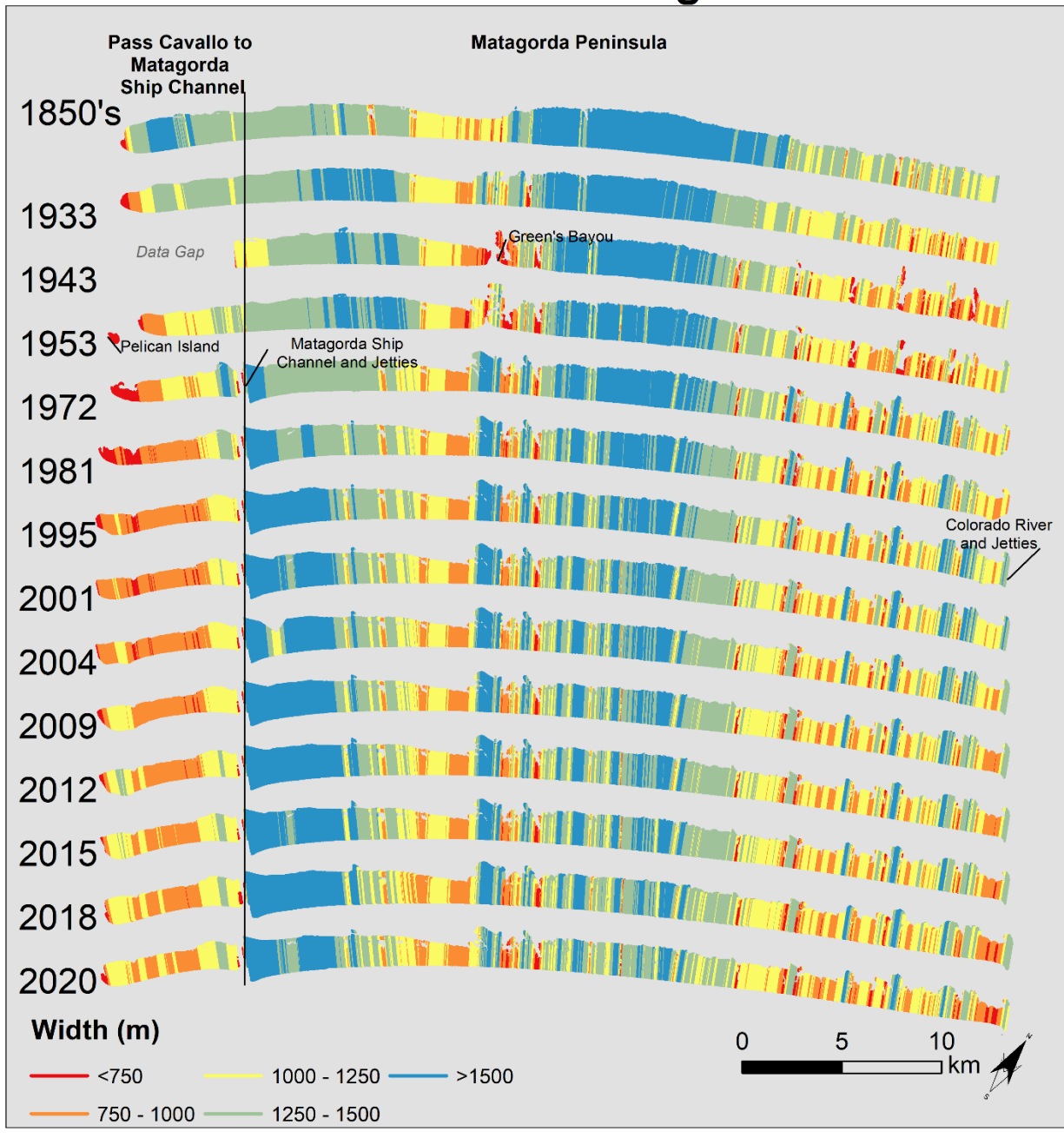


Figure 25. Transects representing the width for the entire island (vegetation and sand combined) through time at 20 m increments.

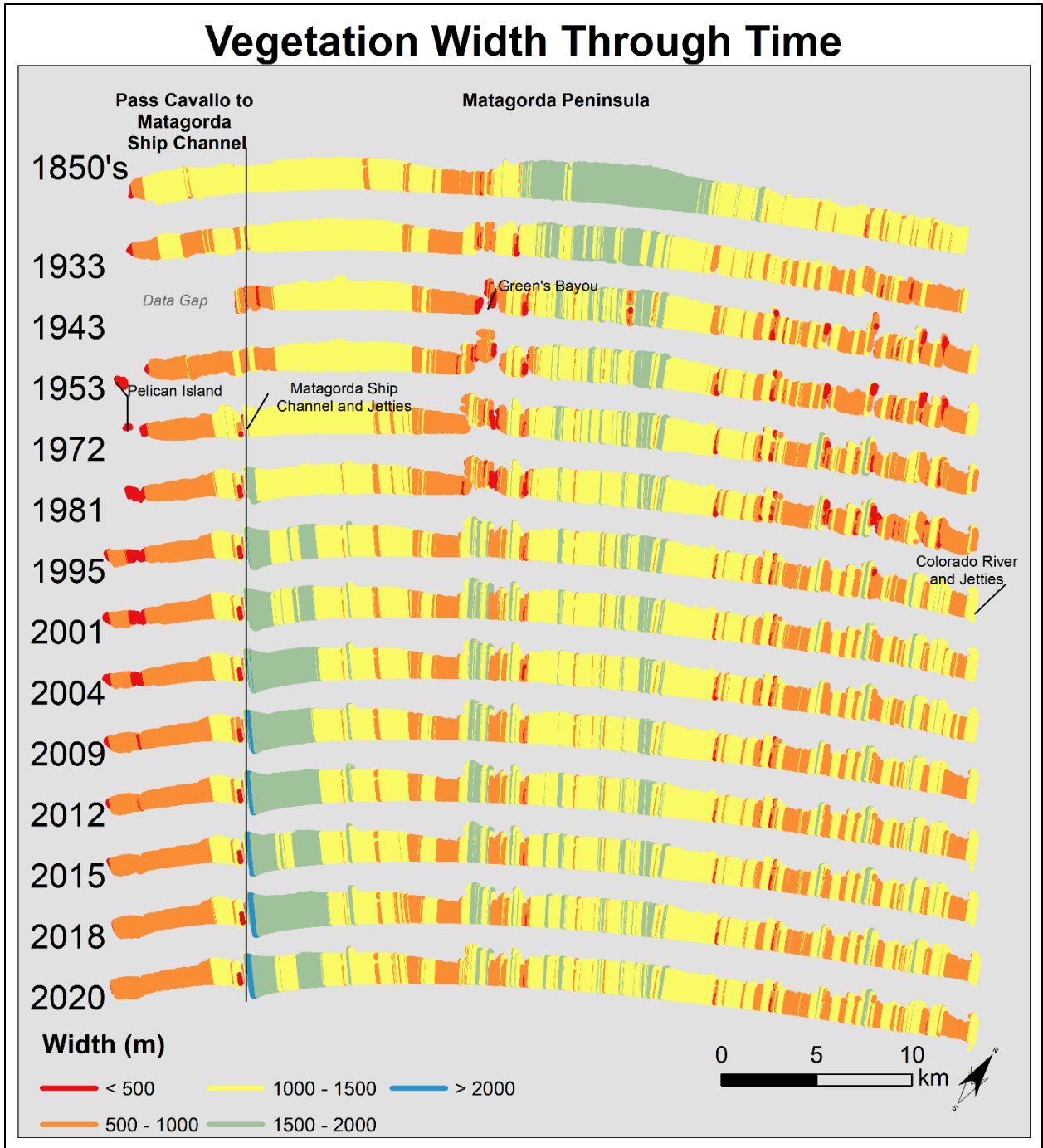


Figure 26. Transects representing the vegetation width through time at 20 m increments.

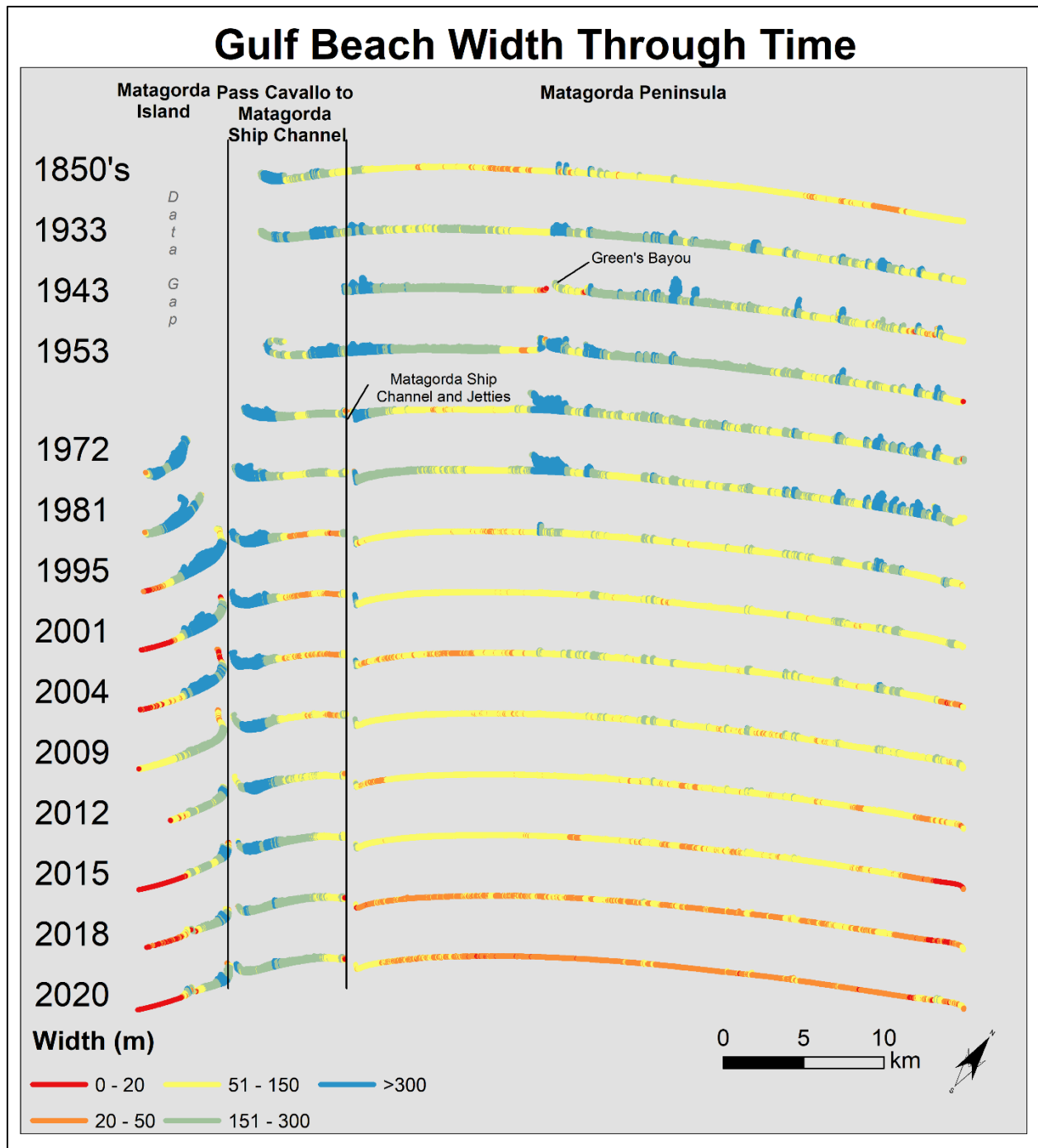


Figure 27. Transects representing the beach width through time at 20 m increments.

Positional Changes of Gulf Shoreline, Gulf Vegetation Line, and Bay Shoreline

Gulf Shoreline

Throughout the entire study area, there were instances of beach erosion and accretion occurring from 1850–2020 (Figure 28 through Figure 30). Extending ~24 km from the Colorado River along Matagorda Peninsula, the shoreline eroded an average of 107 m. Cotton Bayou to

Green's Bayou (located 24–28 km from the Colorado River) are a historic storm washover channels that were opened between 1933 and 1943 (Figure 48, Figure 54, and Figure 60 show this area), and experienced high amounts of accretion (298 m). Similarly, from 30–40 km, there was a continual accretion attributed to the Matagorda Ship Channel north jetty (154 m). Directly west of the Matagorda Ship Channel west jetty (located 40–43 km from the Colorado River), erosion occurred, followed by a high amount of accretion from 43–46 km. Overall Pass Cavallo to Matagorda Ship Channel experienced an average seaward movement of 186 m. Lastly, Matagorda Island experienced seaward movement from 46–50 km and landward movement from 50–53 km, averaging a 13 m landward migration.

Gulf Vegetation Line

A similar trend exists for the sand/vegetation line (Figure 28 through Figure 30) Extending ~24 km from the Colorado River along Matagorda Peninsula, there was a landward migration of the vegetation line (72 m). Cotton Bayou to Green's Bayou and the remainder of Matagorda Peninsula to the Matagorda Ship Channel north jetty experienced a seaward migration of the vegetation line (373 m and 168 m respectively). Directly west of the Matagorda Ship Channel west jetty (located 40–43 km from the Colorado River), the vegetation moved landward, followed by a seaward movement from 43–46 km. Overall Pass Cavallo to Matagorda Ship Channel experienced an average seaward movement of 117 m. Lastly, Matagorda Island experienced seaward movement from 46–50 km and landward movement from 50–53 km, averaging a 119 m seaward migration.

Bay Shoreline

The bay shoreline movement was not calculated for Matagorda Island. With a few exceptions, the bay shoreline migrated seaward for both Matagorda Peninsula and Pass Cavallo to Matagorda Ship Channel (Figure 28 and Figure 29). Extending ~24 km from the Colorado River along Matagorda Peninsula, there was a 237 m seaward migration. Pass Cavallo to Matagorda Ship Channel experienced a seaward migration of 178 m.

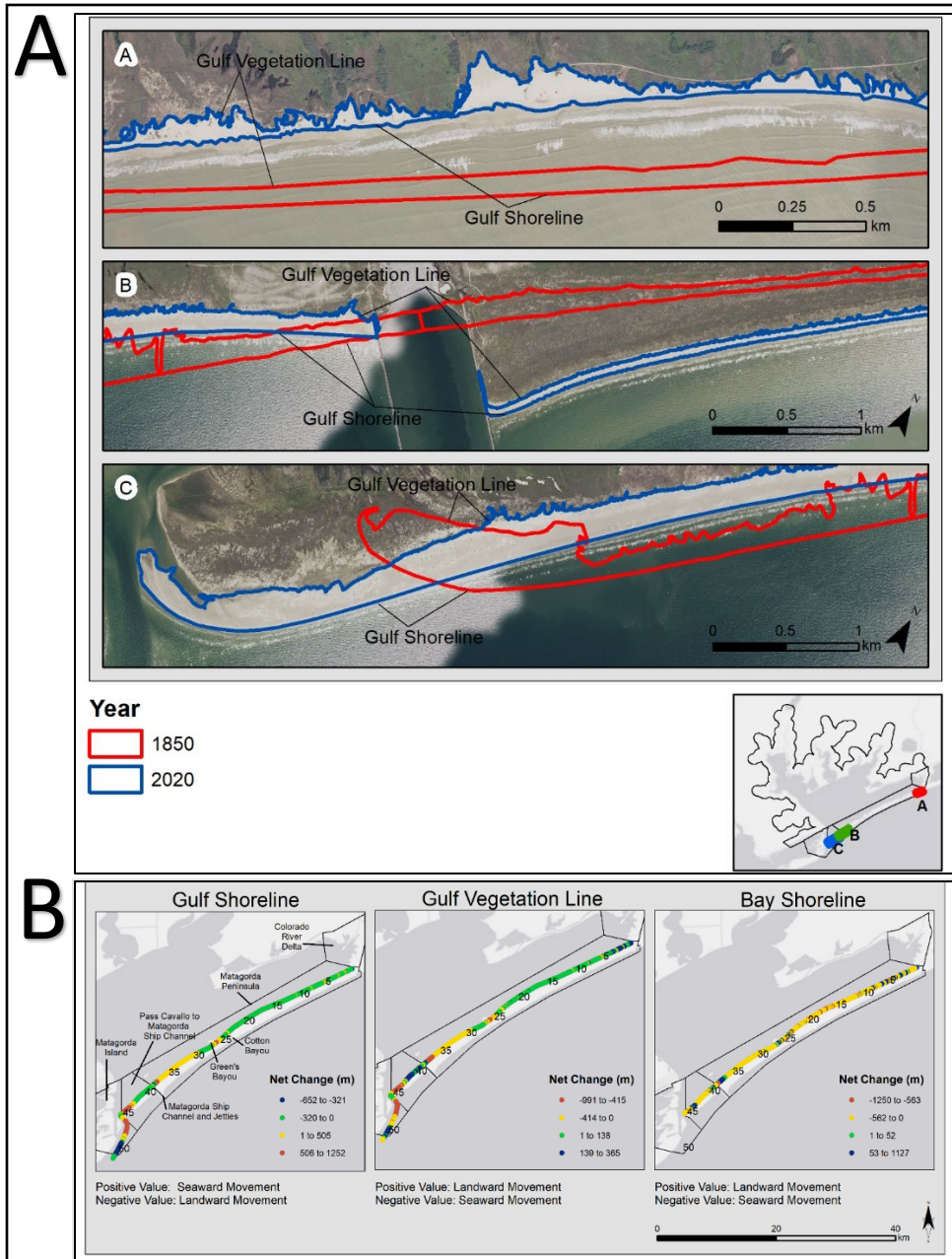


Figure 28. A.) Gulf Shoreline and Gulf Vegetation Line obtained from 1850s NOAA T-Sheets and 2020 NAIP imagery illustrating how these boundaries have shifted seaward or landward due to erosion and accretion along Matagorda Peninsula. B.) Net Movement of the 1) Gulf Beach and Water, 2) Gulf Beach and Vegetation, and 3) Vegetation and Water boundaries over time. Bay shoreline movement was not calculated for Matagorda Island.

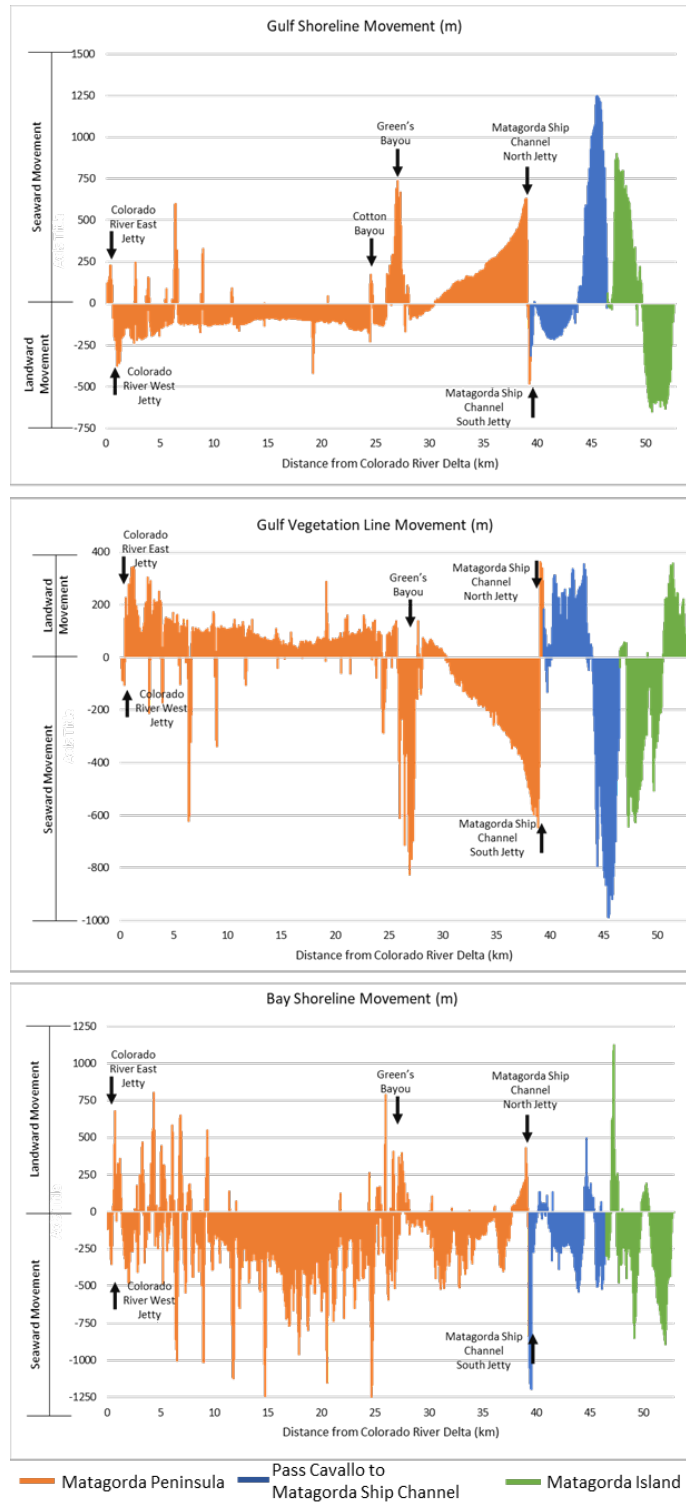


Figure 29. Net Movement of the 1) Gulf Shoreline, 2) Gulf Vegetation Line, and 3) Bay Shoreline over time. Bay shoreline movement was not calculated for Matagorda Island.

Historic Wetlands Trends

Background

Historic wetland data were download from the Bureau of Economic Geology (BEG) for the entire study area (inland and coastal zone) over three time periods (1950's, 1979, and 2000's) (Bureau of Economic Geology, 2021) to illustrate how critical wetland habitats have changed over time. These datasets were mapped in accordance with The Classification of Wetlands and Deepwater Habitats of the United States (Cowardin et al, 1979) and therefore contain more habitats than mapped in the "Mapping Land Cover Through Time" section of this report.

Historic wetland data is available from the Bureau of Economic Geology (BEG) for portions of the Texas coast over three time periods (1950's, 1979, and 2000's) (Bureau of Economic Geology, 2021). The wetland distributions were based on 1950's black-and-white photographs, 1979 CIR photographs, and 2000's CIR photographs. While BEG researchers manually digitized the 2000's wetland habitats, the 1950's and 1979 wetland data were obtained from the USFWS who mapped the wetlands using methods established by the NWI. However, BEG partly revised the older datasets (1950's and 1979) to ensure closer agreement between the older (1950's and 1979) and 2000's wetland codes. Further, due to imagery differences, there were differences among wetland attributes between the three datasets. For example, 1950's wetlands were classified by system (marine, estuarine, riverine, palustrine, lacustrine), subsystem (reflective of hydrologic conditions), and class (description of vegetation and substrate) while the 1979 and 2001 wetlands were further classified by subclasses (subdivisions of vegetation classes), water regime, and special modifiers.

Methods

Historic wetland data were download from the Bureau of Economic Geology (BEG) for the entire study area (inland and coastal zone) over three time periods (1950's, 1979, and 2000's) (Bureau of Economic Geology, 2021). This encompassed two out of the ten BEG regions ("Matagorda Bay" and "Matagorda Peninsula & Island"). First, the historic wetland data were merged for the two regions and a series of steps were taken to convert the wetland attributes to eleven habitats of interest (open water, inland open water, Gulf beach, estuarine beach and flat, inland shore, estuarine emergent wetland, estuarine scrub/shrub wetland, freshwater emergent wetland, swamp, rocky intertidal, and upland) (Table 6).

This involved converting the wetland attributes to SLAMM land covers and then summarizing into the eleven desired habitats. SLAMM already has a well documented process of converting wetland attribute to 23 land cover designations by by taking into account the wetland system, subsystem, class, and when present, subclass and special modifiers (Clough et al., 2010). Thus, this provided an easy avenue for classifying the multitude of NWI values. After assigning SLAMM values, classifications were merged, where necessary, to highlight the eleven desired habitats (Table 6). Then, the land cover was separated into five study area sections (Colorado River Delta, Matagorda Peninsula, Pass Cavallo to Matagorda Ship Channel, Matagorda Island, and Inland Matagorda) which allowed for more localized analysis of trends. However, there were

some data gaps between the BEG historic wetland data and our study areas (Figure 30). Lastly, emphasis was placed on five of the eleven critical habitats and their areal extent through time was calculated: 1) Gulf Beach, 2) Estuarine Emergent Wetland, 3) Estuarine Beaches & Flats, 4) Freshwater Emergent Wetland, and 5) Freshwater Swamps. Only their areal extent was calculated rather than investigating specific transitions due to poor registration of the imagery and overlaying two sequential datasets could identify wetland changes that were actually cartographic errors (Tremblay et al., 2002; Tremblay and Calnan, 2010).

Table 6. Classification system showing our habitat breakdowns and accompanying SLAMM class descriptions.

Habitat	SLAMM Description (SLAMM Code)
Open Water	Estuarine Open Water (17) Open Ocean (19) Riverine Tidal (16)
Inland Open Water	Inland Open Water (15)
Gulf Beach	Ocean Beach (12) Ocean Flat (13)
Estuarine Beach/Flat	Estuarine Beach (10) Tidal Flat (11)
Inland Shore	Inland Shore (22)
Estuarine Emergent Wetland	Irregularly Flooded Marsh (20) Regularly Flooded Marsh (8)
Estuarine Scrub/Shrub Wetland	Mangrove (9) Trans. Salt Marsh (7)
Freshwater Emergent Wetland	Inland Fresh Marsh (5) Tidal Fresh Marsh (6)
Swamp	Swamp (3) Tidal Swamp (23)
Rocky Intertidal	Rocky Intertidal (14)
Upland	Upland

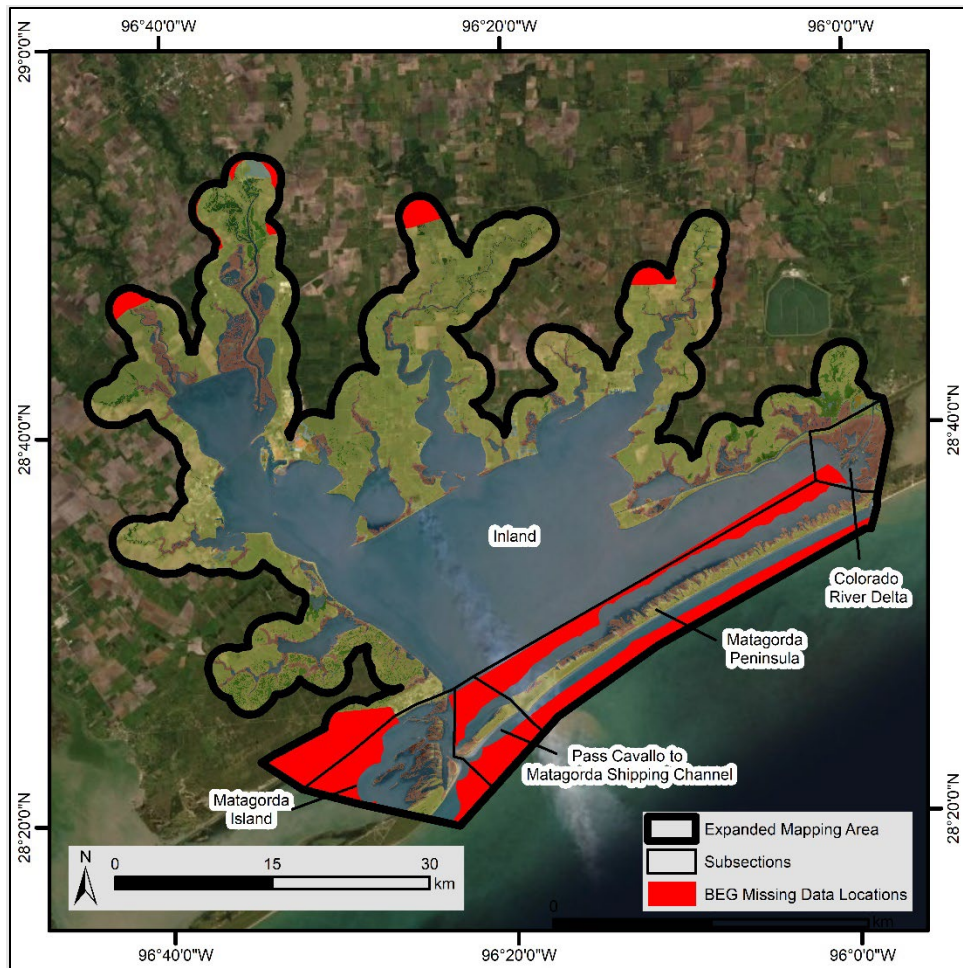


Figure 30. Expanded mapping area, locations of data gaps, and how we divided the study area for analysis.

Results

Figure 31 illustrates the habitat classifications through time for the entire study area while Appendix E: Historic Wetland Trends Through Time contains maps zoomed into each section specifically, allowing for more details to be observed. Throughout the entire study area, there was a large decrease in Swamps (62.5 km²) and Estuarine Flats/Beaches (34.8 km²) and a slight decrease in Gulf Beaches (2.4 km²), Estuarine Emergent Wetlands (2.9 km²), and Freshwater Emergent Wetlands (3.4 km²) (Table 7). Conversely, there was an increase in Open Water (25.6 km²) and Inland Open Water (12.3 km²) (Table 7). However, calculating the areal change through time for the five sections separately resulted in different trends (Figure 32 and Figure 33). The following trends were observed:

1. Matagorda Peninsula, Colorado River Delta, and Pass Cavallo to Matagorda Ship Channel experienced a growth in Estuarine Emergent Wetlands.
2. Matagorda Peninsula, Matagorda Island, and Pass Cavallo to Matagorda Ship Channel had a decrease in Estuarine Beaches & Flats.
3. Matagorda Peninsula experienced a decrease in Gulf Beaches.

4. Within Inland Matagorda County, all four critical habitats (Estuarine Emergent Wetlands, Estuarine Beaches & Flats, Freshwater Emergent Wetlands, and Swamps) experienced a net decrease over time with Freshwater Swamps experiencing the greatest loss.

Some of the transitions observed represent true land cover transitions, however some the observed changes could be due to precipitation/drought occurrences impacting habitat appearance on the imagery. For example, it was noted that there was abnormally high precipitation in 1979 raising water levels and leading to high water extent in classifications whereas the 1956 imagery was obtained prior to a severe drought (Tremblay et al., 2002; Tremblay and Calnan, 2010).

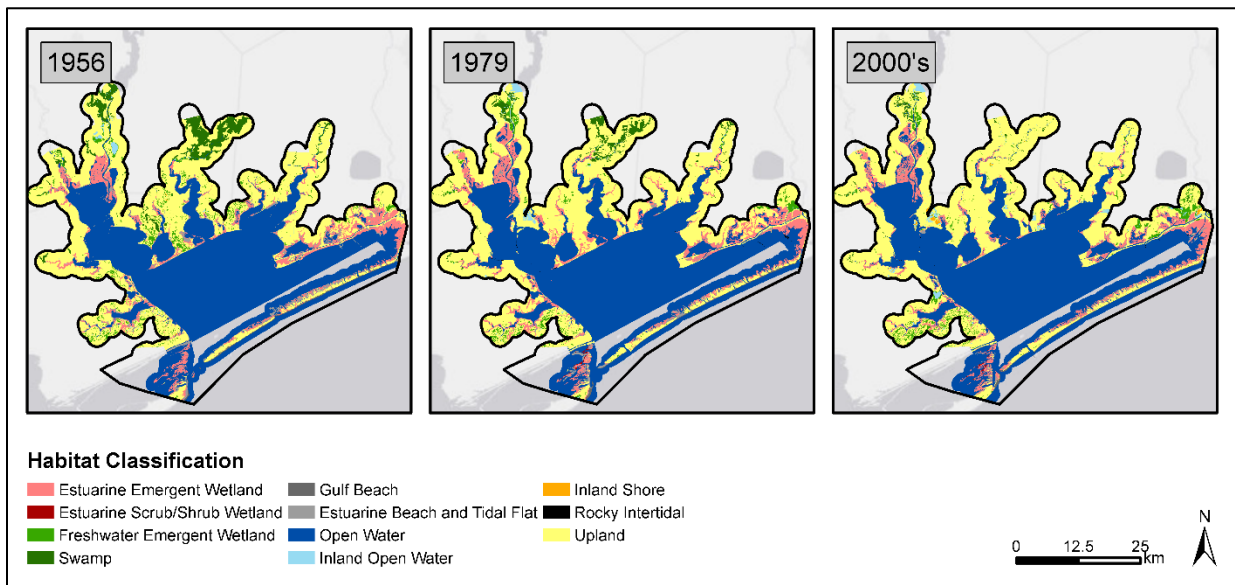


Figure 31. Historic Wetland Classifications Through Time.

Table 7. Habitat classifications and their area (km²) through time (1956 – 1979 – 2000s) for the entire study area.

Classification	1956	1979	2000's
Open Water	1026.0	1044.0	1051.7
Inland Open Water	5.9	10.9	18.2
Gulf Beach	7.7	6.4	5.3
Estuarine Beach/Flat	59.1	24.7	24.3
Inland Shore	0.5	0.1	4.0
Estuarine Emergent Wetland	153.1	182.7	150.2
Estuarine Scrub/Shrub Wetland	0.0	1.5	1.1
Freshwater Emergent Wetland	47.0	32.2	43.6
Swamp	73.3	36.0	10.8

Rocky Intertidal	NA	1.0	0.4
Upland	826.6	859.8	889.7
Not Classified	0.0	0.0	NA

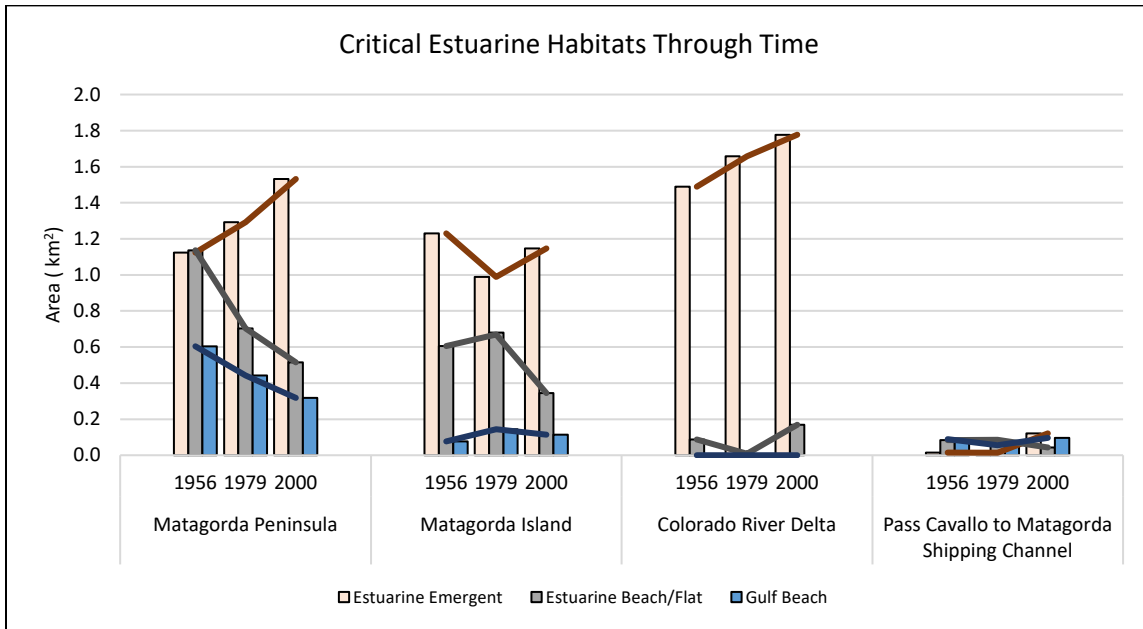


Figure 32. Critical estuarine habitats through time (1956, 1979, 2000's) for Colorado River Delta, Matagorda Peninsula, Pass Cavallo to Matagorda Ship Channel, and Matagorda Island.

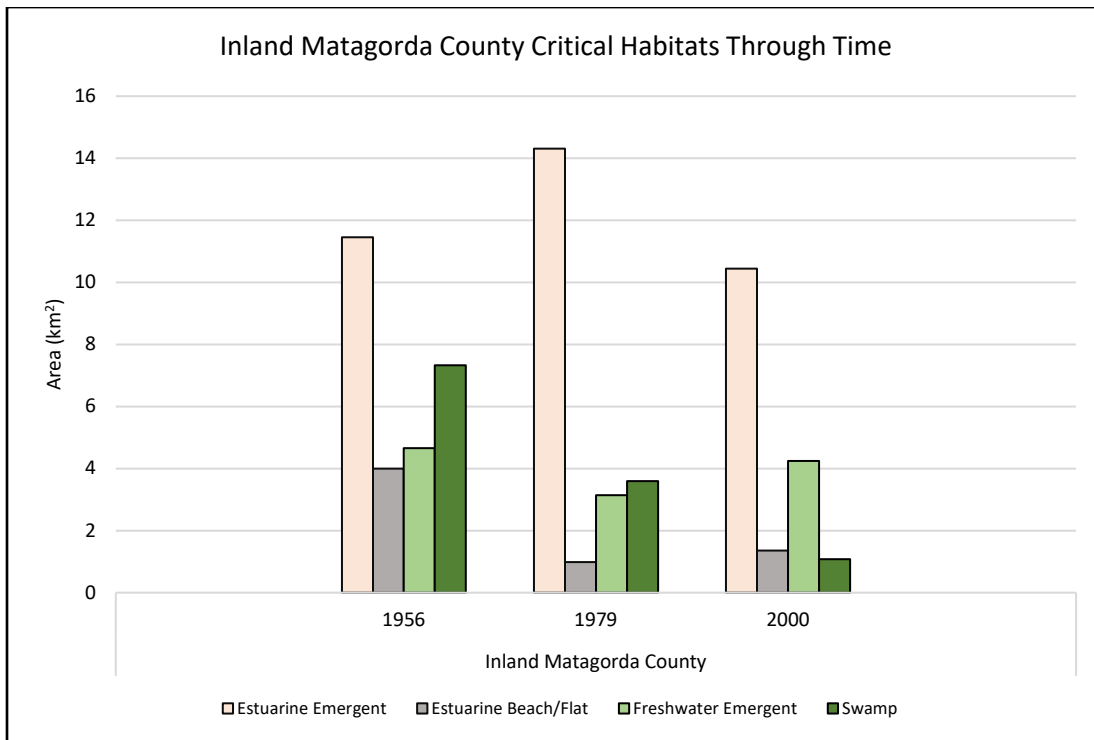


Figure 33. Critical estuarine habitats through time (1956, 1979, 2000's) for Inland Matagorda.

Modeling Landscape Change Under Varying SLR Scenarios

General Overview

This study modeled potential landscape changes under two projected GMSLR scenarios (Intermediate-Low of 0.5 m and Intermediate-High of 1.5 m) by 2100 using the Sea Level Affecting Marshes Model (SLAMM) for the four coastal study areas (Colorado River Delta, Matagorda Peninsula, Pass Cavallo to Matagorda Ship Channel, and Matagorda Island).

Methods

SLAMM (Sea Level Affecting Marshes Model) was used to project future changes for coastal land covers. SLAMM is a rule-based spatial model incorporating: 1) digital elevation data and bathymetry, 2) slope, 3) wetland classifications, 4) development footprints, 5) dikes and shoreline armoring, 6) tidal range, 7) horizontal erosion rates, and 8) vertical accretion rates to simulate how one land cover type converts to another. SLAMM ultimately provides maps of updated elevations and land cover classes in the year 2100 along with numerical outputs. SLAMM has 23 SLAMM land cover designations (Clough et al., 2010) that we aggregated into six for analysis (Table 8). This study followed the strategy and methodology that was used for the Coastal Modeling and Vulnerability Assessment portion of the Texas Coastal Resiliency Master Plan (TCRMP), and details for that effort are extensively documented there (Texas General Land Office 2023). However, the key components and data layers used in SLAMM are presented in Table 9.

NOAA Technical Report NOS CO-OPS 083 Sweet et al., 2007) provides six GMSLR scenarios by 2100: 1) Low (0.3 m), 2) Intermediate-Low (0.5 m), 3) Intermediate (1 m), 4) Intermediate-High (1.5 m), 5) High (2 m), and 6) Extreme (2.5 m). This study used the intermediate-low (0.5 m) and intermediate-high (1.5 m) GMSLR scenarios but took into account local factors such as vertical land surface movement.

Table 8. Classification system showing the aggregation of 21 SLAMM output classes (Clough et al. 2010) to 6 classes for change analysis.

New Description	SLAMM Description (SLAMM Code)
Developed Dry Land	Developed Dry Land (1)
Undeveloped Dry Land	Undeveloped Dry Land (2)
Freshwater Wetlands	Non-Tidal Swamp (3) Cypress Swamp (4) Inland-Fresh Marsh (5)
Salt & Brackish Emergent Wetlands	Tidal-Fresh Marsh (6) Trans. Salt Marsh (7) Regularly Flooded Marsh (8) Mangrove (9) Irregularly Flooded Marsh (20) Tidal Swamp (23)
Beaches & Flats	Ocean Beach (12) Inland Shore (22) Estuarine Beach (10) Tidal Flat (11) Rocky Intertidal (13) Ocean Flat (14)
Open Water	Inland Open Water (15) Riverine Tidal (16) Estuarine Open Water (17) Tidal Creek (18) Open Ocean (19)

Table 9. SLAMM model inputs and data descriptions.

Model Input		Description
1	Digital Elevation Data	A 3 m DEM was created from fusing 35 airborne topographic lidar surveys acquired by various surveyors from 2005 – 2016
2	Slope	A 3 m raster developed from the final 3 m DEM
3	Wetland Classifications	Generated from the latest U.S. Fish and Wildlife Service National Wetlands Inventory (NWI) habitat delineations (U.S. Fish and Wildlife Service, 2017). NWI land cover attributes were then crosswalked to SLAMM land cover codes
4	Development Footprints	Determined from the 2011 National Land Cover Database (NLCD) (USGS 2016) percent impervious raster
5	Dikes and Shoreline Armoring	Cells protected by dikes, levees, or hardened shorelines were identified using a combination of the NWI input file and shoreline information from the Environmental Sensitivity Index (ESI) mapped by the Harte Research Institute (Gibeaut et al. 2013)
6	Tidal Range	NOAA VDATUM tidal datums were used to define the input tide ranges for the study area and the values were verified using nearby NOAA CO-OPS tidal datums. VDATUM's Mean Lower Low Water was subtracted from Mean Higher High Water to get the Great Diurnal Tide Range (GT)
7	Horizontal Erosion Rate	Derived from the Bureau of Economic Geology (BEG) 2016 dataset which has change rates from either 1930's-2010 or 1950's-2012 (Paine et al., 2016) and were based on habitat type (marsh, swamp, and tidal flats)
8	Vertical Accretion Rates	Accretion rates were based on habitat type (low marsh, high marsh, tidal-fresh marsh, inland-fresh marsh, mangrove, beach) and were based on values determined from peer-reviewed studies

Results

Significant effects of SLR are predicted to impact the Matagorda Bay study area, vastly changing the landscape by 2100.

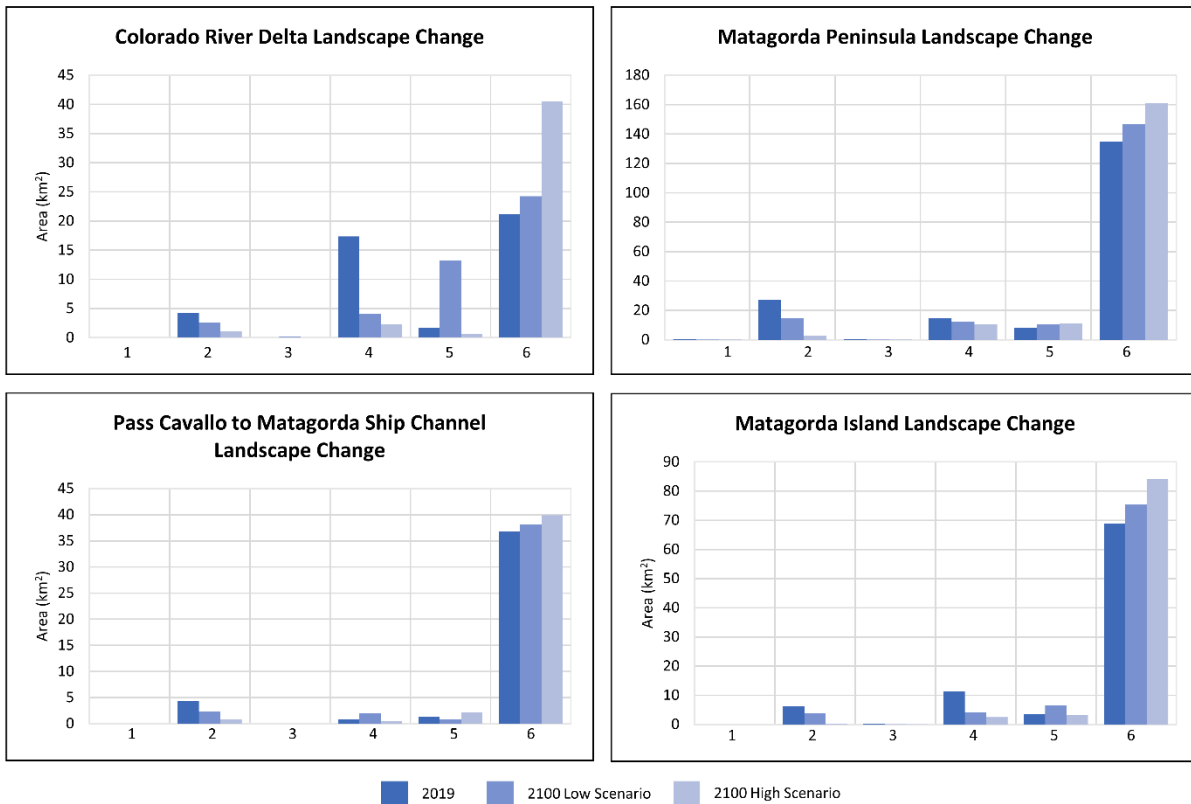
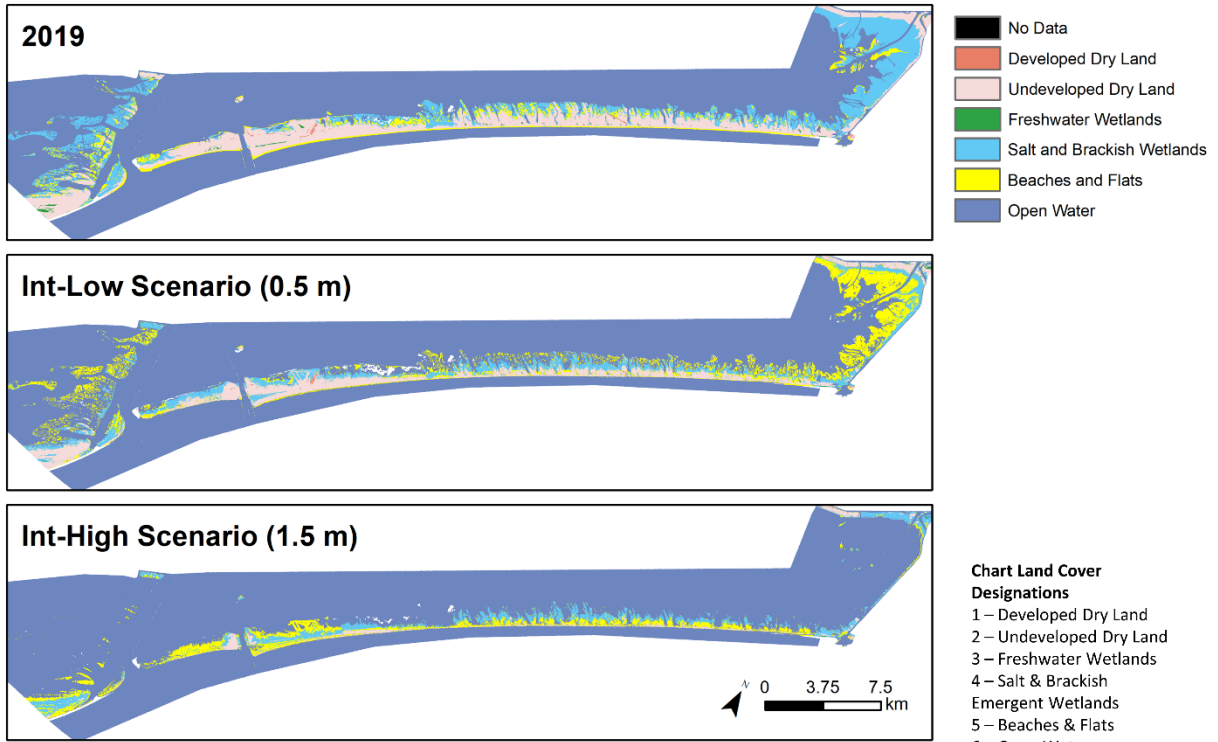
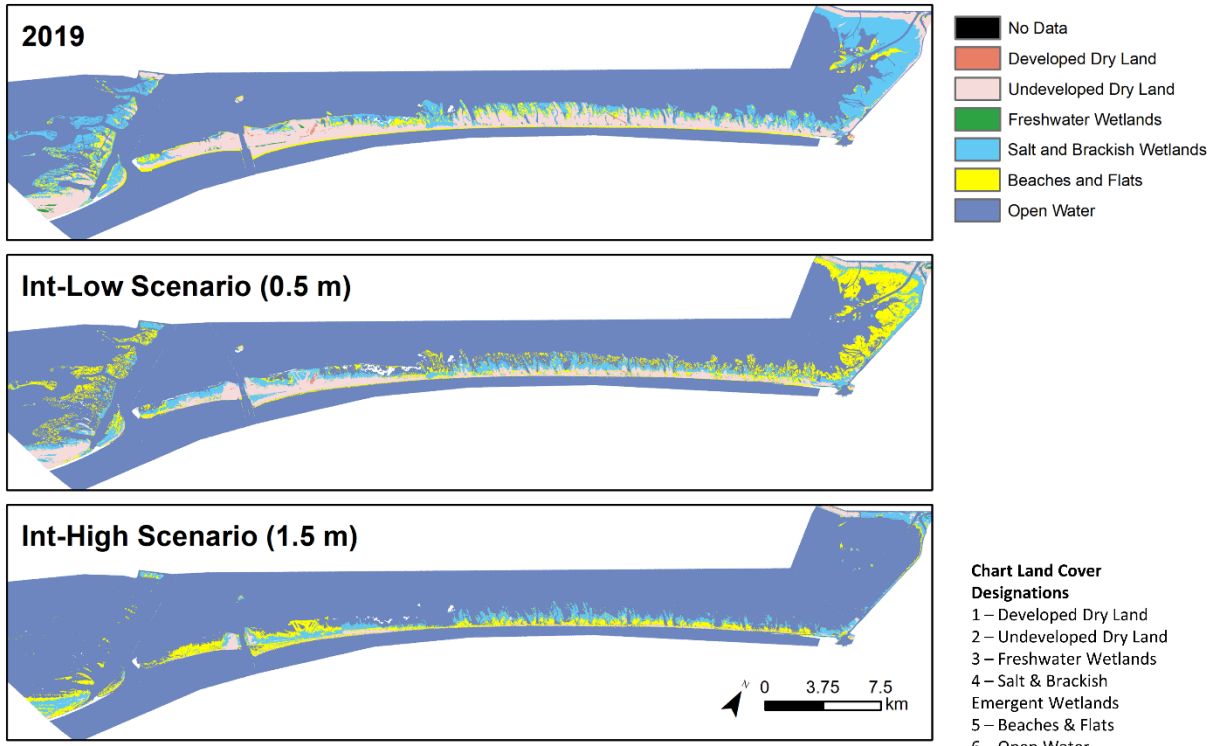


Figure 34 and Table 10 describe the change in each land cover class between the present and modeled future landscape in 2100 under the int-low (0.5 m) and int-high (1.5 m) GMSLR

scenarios. Further, Appendix F: Extent of habitats lost under low and high RSLR scenarios by 2100 contains maps illustrating the present landscape and the modeled future landscape in 2100 under these scenarios. All study areas are predicted to experience an increase in open water in both scenarios. Most notably is the Colorado River Delta which experiences a 14% increase under the 0.5 m scenario but a 91% increase under the 1.5 m scenario (Figure 72). Salt and brackish wetlands are predicted to increase 143% under the 0.5 m scenario for Pass Cavallo to Matagorda Ship Channel, however all study areas are predicted to lose wetlands under the 1.5 m scenario. Beaches and flats are predicted to increase under the 0.5 m scenario for Colorado River Delta, Matagorda Peninsula, and Matagorda Island, however under the 1.5 m scenario are predicted to decrease for Colorado River Delta and Matagorda Island and increase for Matagorda Peninsula and Pass Cavallo to Matagorda Ship Channel. Specifically, for the Colorado River Delta, beaches and flats are predicted to increase 706% under the 0.5 m scenario but decrease 63% under the 1.5 m scenario (Figure 74).



- Chart Land Cover Designations**
- 1 – Developed Dry Land
 - 2 – Undeveloped Dry Land
 - 3 – Freshwater Wetlands
 - 4 – Salt & Brackish Emergent Wetlands
 - 5 – Beaches & Flats
 - 6 – Open Water

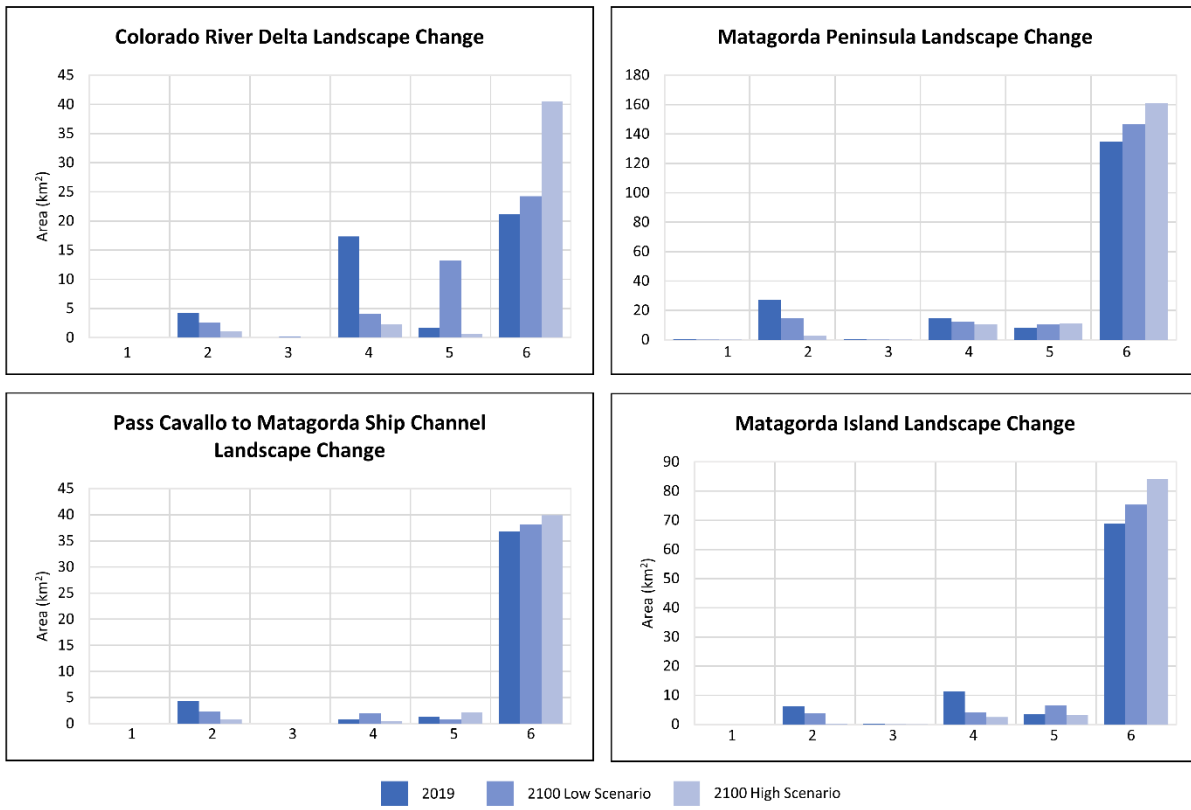


Figure 34. Change in area (km²) of individual land cover types between present condition and the predicted future condition under int-low (0.5 m) and int-high (1.5 m) GMSLR scenarios by the year 2100.

Table 10. Area (km²) and percent difference among individual land cover types between present condition and the predicted future condition under int-low (0.5 m) and int-high (1.5 m) GMSLR scenarios by the year 2100.

Colorado River Delta

Land Cover Class	2019 (km ²)	2100 Low Scenario (km ²)	% Diff	2100 High Scenario (km ²)	% Diff
Developed Dry Land	0	0	-80	0	-100
Undeveloped Dry Land	4	3	-39	1	-74
Freshwater Wetlands	0	0	1393	0	92
Salt & Brackish Emergent Wetlands	17	4	-77	2	-87
Beaches & Flats	2	13	706	1	-63
Open Water	21	24	14	40	91

Matagorda Peninsula

Land cover class	2019 (km ²)	2100 Low Scenario (km ²)	% Diff	2100 High Scenario (km ²)	% Diff
Developed Dry Land	0	0	-61	0	-92
Undeveloped Dry Land	27	15	-45	3	-89
Freshwater Wetlands	0	0	-79	0	-92
Salt & Brackish Emergent Wetlands	15	12	-17	10	-30
Beaches & Flats	8	10	27	11	38
Open Water	135	147	9	161	19

Pass Cavallo to Matagorda Ship Channel

Land cover class	2019 (km ²)	2100 Low Scenario (km ²)	% Diff	2100 High Scenario (km ²)	% Diff
Developed Dry Land	0	0	-13	0	-95
Undeveloped Dry Land	4	2	-47	1	-81
Freshwater Wetlands	0	0	-100	0	-100
Salt & Brackish Emergent Wetlands	1	2	143	0	-44
Beaches & Flats	1	1	-40	2	70
Open Water	37	38	3	40	8

Matagorda Island

Land cover class	2019 (km ²)	2100 Low Scenario (km ²)	% Diff	2100 High Scenario (km ²)	% Diff
Developed Dry Land	0	0	0	0	0
Undeveloped Dry Land	6	4	-39	0	-96
Freshwater Wetlands	0	0	-83	0	-100
Salt & Brackish Emergent Wetlands	11	4	-63	2	-78
Beaches & Flats	3	7	92	3	-7
Open Water	69	75	9	84	22

Habitat Vulnerability

General Overview

Habitat vulnerability maps describe the effect of ongoing geological processes including relative sea-level rise (RSLR), erosion, historic washover locations, storm surge inundation, and future evolution of critical environments in response to RSLR and storm surge by 2100. The habitat vulnerability maps can help inform planners, decision-makers, and the public about the challenges and limitations of living in the coastal plain. These maps also provide a picture of how the Texas coastal plain may look in 2100 in response to the effects of coastal hazards. They not only show areas that are presently exposed to hazardous conditions that might be generally protected by regulations but also shows areas that are not protected and should receive special management consideration. Further, these maps illustrate the vulnerable infrastructure that will be exposed to hazardous conditions in the future and require special attention if progress is to be made in how we live with RSLR.

Methods

Habitat vulnerability maps were created by combining various inputs including:

- Topographic DEMs developed using the latest lidar surveys,
- Various publicly available datasets,
- Future land cover data modeled from SLAMM, and
- Storm surge vulnerability maps (described below).

Ultimately, habitat vulnerability maps were developed for the entire study area for two sea-level rise scenarios: Intermediate Low (0.5 m of GMSLR by 2100) and Intermediate High (1.5 m of GMSLR by 2100).

The storm surge vulnerability map was developed by considering simulated storm surge inundation due to 19 synthetic storms. The 19 storms consisted of varying characteristics and pass throughout the entire Texas coast. The Coastal Modeling and Vulnerability Assessment Section within TCRMP summarizes the 19 storm characteristics and illustrates their storm tracks (Texas General Land Office, 2023). A total of 57 ADCIRC+SWAN model simulations were then forced using meteorological wind and pressure fields for each of the 19 hurricane events. The 19 hurricane events were simulated on the present landscape, and again on the two future 2100 landscapes: Intermediate Low (0.5 m of GMSLR by 2100) and Intermediate High (1.5 m of GMSLR by 2100). The maximum water surface elevation (MAXELE) was then derived for each of the 57 storm simulations and analyzed along the whole Texas coast.

To calculate the storm surge vulnerability score along the Texas coast using these 57 scenarios, each node in the computational mesh was examined to find out how many times it was inundated in the 57 scenarios. It was then divided by the 57 scenarios, resulting in a storm surge vulnerability normalized index ranging from 0 – 1, where a value of 1 means an area is inundated in all 57 scenarios, and 0 means it is not inundated in any scenarios. Once the index value in the range of 0 – 1 was assigned to each node in the computational mesh, a storm surge normalized

vulnerability index raster was generated using Kernel Smoothing interpolation. The Coastal Modeling and Vulnerability Assessment section within TCRMP illustrates the storm surge vulnerability index map (Texas General Land Office, 2023).

Ultimately, a locations habitat vulnerability potential related to RSLR, storm surge, and erosion were grouped into six habitat vulnerability potentials based on the DEM, various publicly available datasets, future land cover, and storm surge vulnerability maps. Table 11 describes the six habitat vulnerability designations.

Table 11. Habitat vulnerability designation and description.

Habitat Vulnerability Designation		Description	How Determined
1	Conversion to Open Water	Historic storm washover channels and future open water	Based on SLAMM output
2	Persisting Critical Habitat	Presently existing critical environments (wetlands, beach/dune system, flats)	Based on latest NWI
3	Conversion to Critical Habitat	Future critical environments	Based on SLAMM output
4	Habitat Prone to Surge Flooding	Uplands prone to storm surge flooding	Storm surge normalized vulnerability index value > 0.5 (inundated by >= 28.5 storms)
5	Stable Upland Habitat	Uplands of high elevation not expected to become critical environments in the future	Storm surge normalized vulnerability index value < 0.5 (inundated by <=28.5 storms)
6	Future Flooding of Existing Infrastructure	Presently developed areas and roads expected to flood	Developed Areas – Based on 2019 NLCD dataset (classes 21–24) Roads – Based on the latest road layer by TxDOT

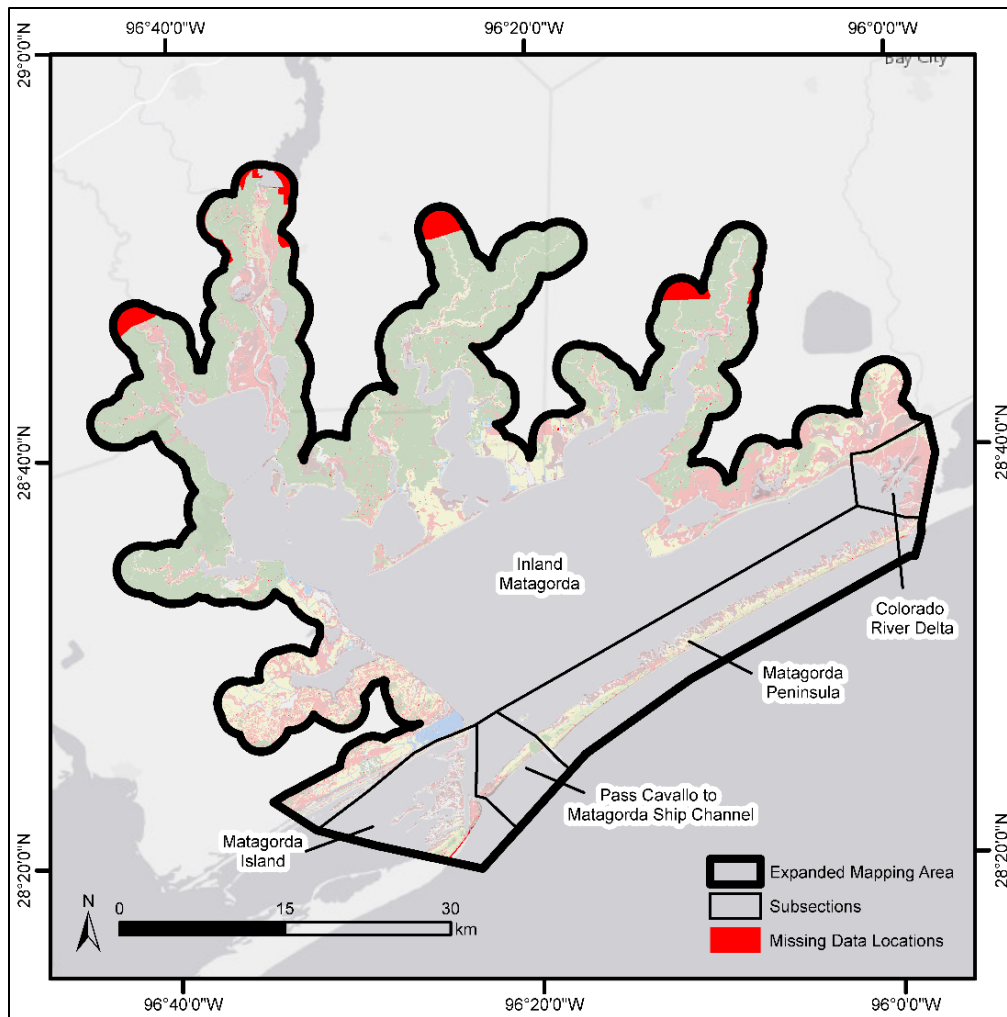


Figure 35. Habitat vulnerability missing data locations.

Results

For the entire study area, under the 0.5 m GMSLR scenario, 239 km² of current marsh, beaches, dunes, and tidal flats are expected to remain as critical habitat, 166 km² are expected to become critical habitat, and 72 km² are expected to become open water. However, under the 1.5 m GMSLR scenario, only 112 km² of current marsh, beaches, dunes, flats are expected to remain as critical habitat, 226 km² are expected to become critical habitat, and 212 km² are expected to become open water. Table 12 describes this area.

Within the Colorado River Delta, only 3.29 km² of current marsh and tidal flats are expected to become open water under the 0.5 m scenario, however, under the 1.5 m scenario, virtually the entire delta (20.19 km²) is expected to become open water.

Table 13 and

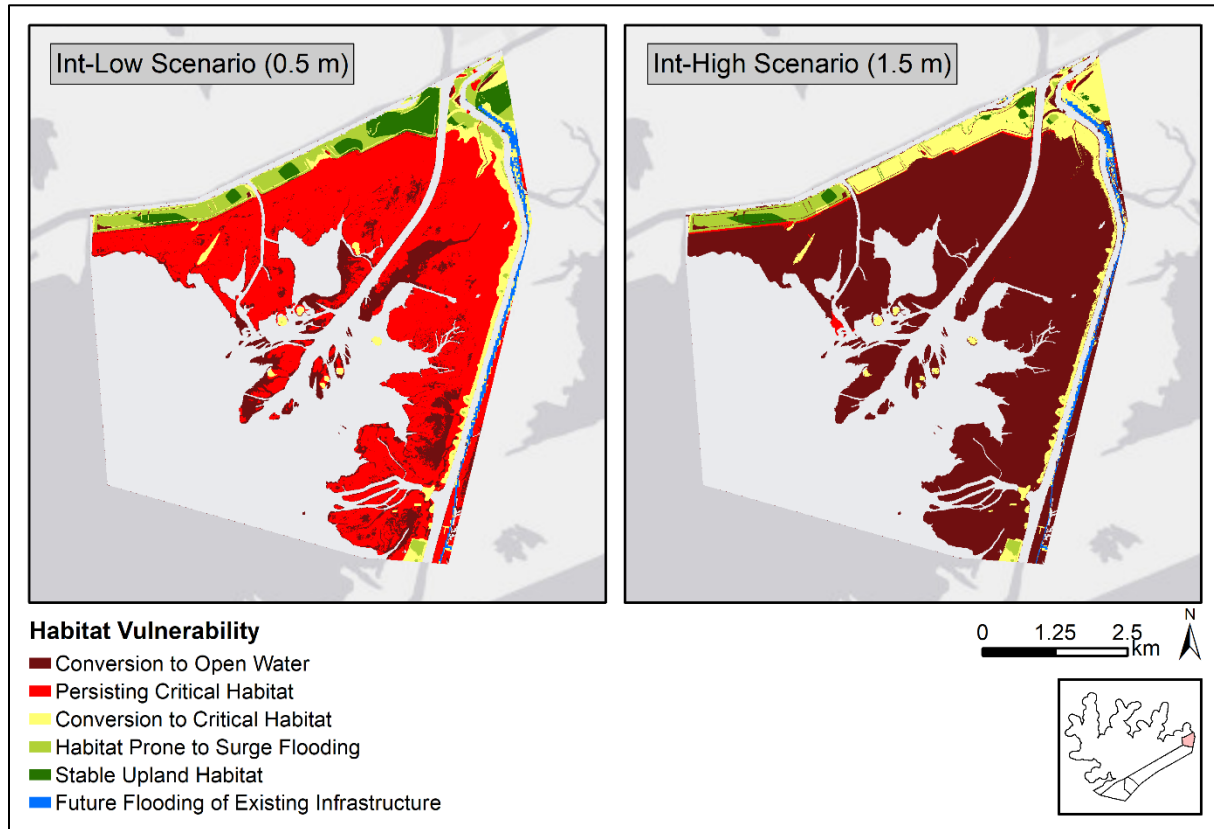


Figure 36 describe this area.

Along Matagorda Peninsula, 12.29 km² of current marsh and tidal flats are expected to become open water under the 0.5 m scenario while 12.21 km² are expected to remain as critical habitat. However, under the 1.5 m scenario, only 1.64 km² of critical habitat remain while the remaining 10.57 km² of critical habitat are expected to convert to open water. Additionally, under the 0.5 m scenario, 13.83 km² of upland habitat are prone to surge flooding, however, under the 1.5 m scenario, only 2.46 km² remain as upland habitat prone to surge flooding while the remaining 11.37 km² are expected to become critical habitat and open water. Under the 1.5 m scenario, this conversion would eliminate almost all current upland habitat.

Table 13 and Figure 37 describe this area.

From Pass Cavallo to the Matagorda Ship Channel, 1.17 km² are expected to remain as critical habitat under the 0.5 m scenario while only 0.38 km² are expected to remain as critical habitat under the 1.5 m scenario. This conversion to open water would ultimately increase the opening of Pass Cavallo and decrease overall marsh and upland habitat. Additionally, under the 0.5 m scenario, 1.40 km² of upland habitat are prone to surge flooding while under the 1.5 m scenario, only 0.18 km² remain as upland habitat prone to surge flooding and the rest is converted to critical habitat.

Table 13 and Figure 38 describe this area.

Along Matagorda Island, 6.87 km² of current marsh and tidal flats are expected to become open water under the 0.5 m scenario while 8.97 km² are expected to remain as critical

habitat. However, under the 1.5 m scenario, only 0.95 km² of critical habitat remain while 16.03 km² are converted to open water. Ultimately, under the 0.5 m scenario, marsh, beach, and tidal flat extent would be reduced, however under the 1.5 m scenario, the entire current marsh extent would be under water. Additionally, in the 1.5 m scenario, upland habitat prone to surge flooding and stable upland habitat are drastically reduced with only 0.19 km² and 0.06 km² remaining.

Table 13 and Figure 39 describe this area.

For Inland Matagorda, under the 0.5 m scenario, 200 km² of current critical habitat are expected to remain, 148.38 km² are expected to become critical habitat, and 48 km² are expected to become open water. However, under the 1.5 m scenario, only 109 km² of current critical habitat are expected to remain, 194.49 km² are expected to become critical habitat, and 149.67 km² are expected to become open water. This results in the disappearance of the current marshland extent of Lavaca River Delta and most marshland surrounding Garcitas Creek, Oyster Lake, Crab Lake, and Mad Island Lake (Figure 40). Additionally, some of the upland habitat prone to surge flooding and stable upland habitat surrounding Crab Lake and Mad Island Lake are expected to remain in the 0.5 m scenario, however are expected to become critical habitat under the 1.5 m scenario (Figure 40).

Table 13 and Figure 40 describe this area.

Table 12. Area (km²) of habitat vulnerabilities under int-low (0.5 m) and int-high (1.5 m) GMSLR scenarios by the year 2100 for the entire study area.

Habitat Vulnerability	Low Scenario (0.5 m)	High Scenario (1.5 m)
Conversion to Open Water	72	212
Persisting Critical Habitat	239	112
Conversion to Critical Habitat	166	226
Habitat Prone to Surge Flooding	55	18
Stable Upland Habitat	614	577
Future Flooding of Existing Infrastructure	15	17

Table 13. Area (km²) of habitat vulnerabilities under int-low (0.5 m) and int-high (1.5 m) GMSLR scenarios by the year 2100 for each study area section.

Colorado River Delta		
Habitat Vulnerability	Int-Low (0.5 m)	Int-High (1.5 m)
Conversion to Open Water	3.29	20.19
Persisting Critical Habitat	16.51	0.26
Conversion to Critical Habitat	1.78	2.82
Habitat Prone to Surge Flooding	1.50	0.71
Stable Upland Habitat	1.17	0.36
Future Flooding of Existing Infrastructure	0.39	0.34

Matagorda Peninsula		
Habitat Vulnerability	Int-Low (0.5 m)	Int-High (1.5 m)
Conversion to Open Water	12.29	26.38
Persisting Critical Habitat	12.21	1.64
Conversion to Critical Habitat	11.64	19.84
Habitat Prone to Surge Flooding	13.83	2.46
Stable Upland Habitat	0.98	0.42
Future Flooding of Existing Infrastructure	0.37	0.75

Pass Cavallo to Matagorda Ship Channel		
Habitat Vulnerability	Int-Low (0.5 m)	Int-High (1.5 m)
Conversion to Open Water	1.27	3.04
Persisting Critical Habitat	1.17	0.38
Conversion to Critical Habitat	1.89	2.45
Habitat Prone to Surge Flooding	1.40	0.18
Stable Upland Habitat	0.88	0.62
Future Flooding of Existing Infrastructure	0.03	0.01

Matagorda Island		
Habitat Vulnerability	Int-Low (0.5 m)	Int-High (1.5 m)
Conversion to Open Water	6.87	16.03
Persisting Critical Habitat	8.97	0.95
Conversion to Critical Habitat	3.25	5.95
Habitat Prone to Surge Flooding	3.30	0.19
Stable Upland Habitat	0.72	0.06
Future Flooding of Existing Infrastructure	0.00	0.00

Inland Matagorda		
Habitat Vulnerability	Int-Low (0.5 m)	Int-High (1.5 m)
Conversion to Open Water	48.00	146.67
Persisting Critical Habitat	200.11	109.16
Conversion to Critical Habitat	147.38	194.49
Habitat Prone to Surge Flooding	35.04	14.78
Stable Upland Habitat	609.86	575.80
Future Flooding of Existing Infrastructure	14.44	16.06

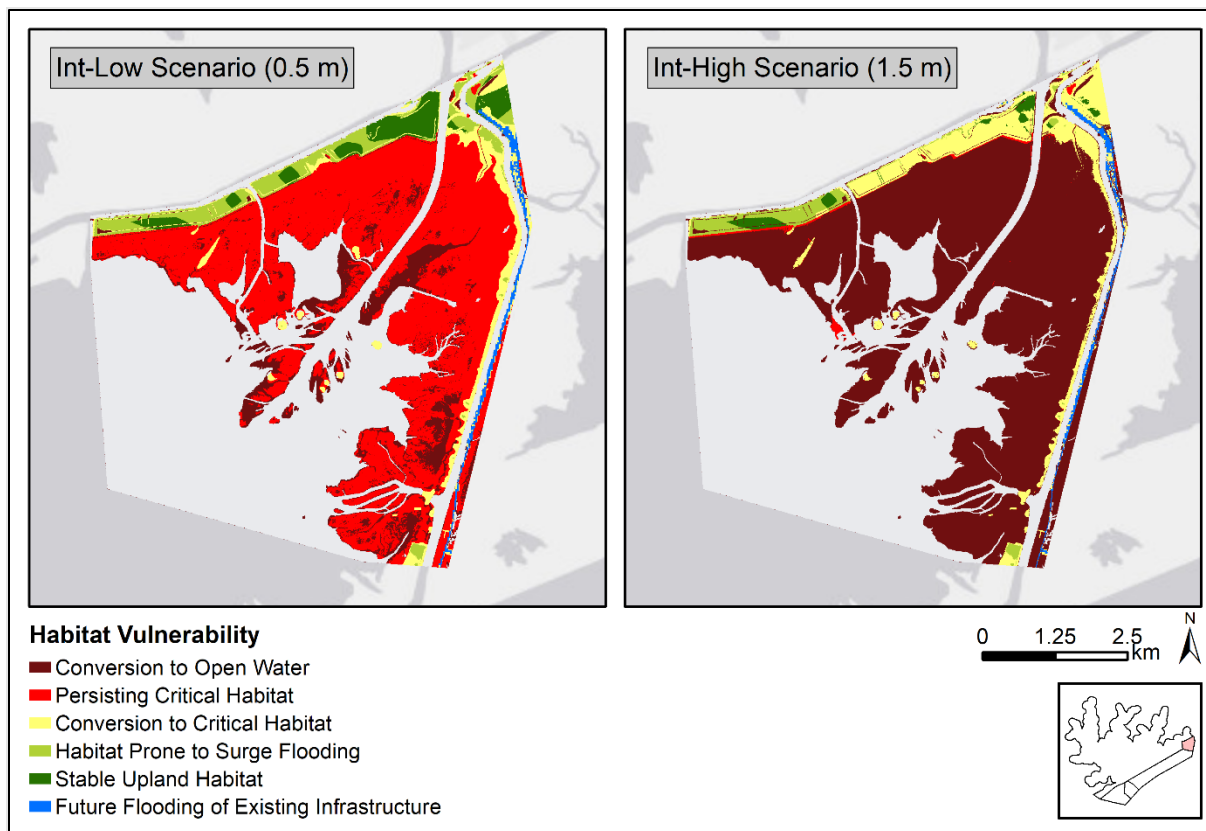


Figure 36. Map showing habitat vulnerability under int-low (0.5 m) and int-high (1.5 m) GMSLR scenarios by the year 2100 within the Colorado River Delta.

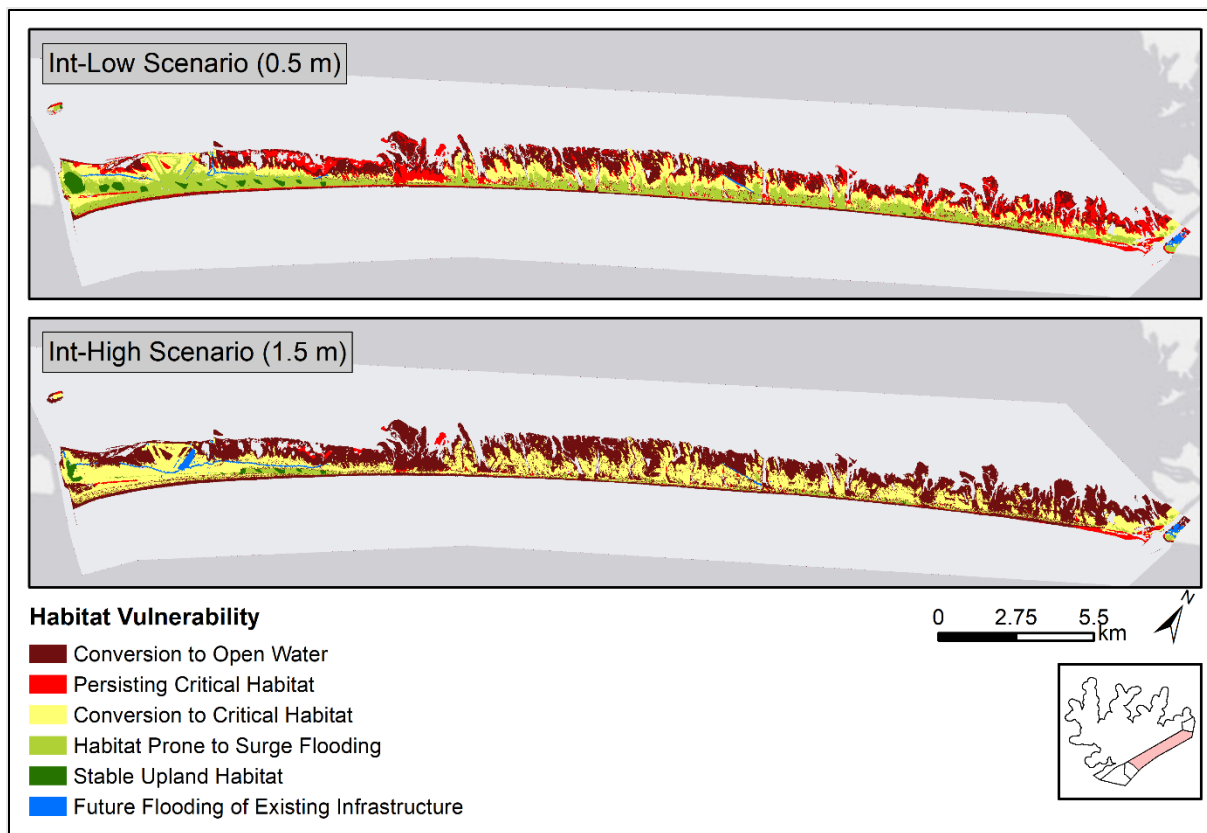


Figure 37. Map showing habitat vulnerability under int-low (0.5 m) and int-high (1.5 m) GMSLR scenarios by the year 2100 within Matagorda Peninsula.

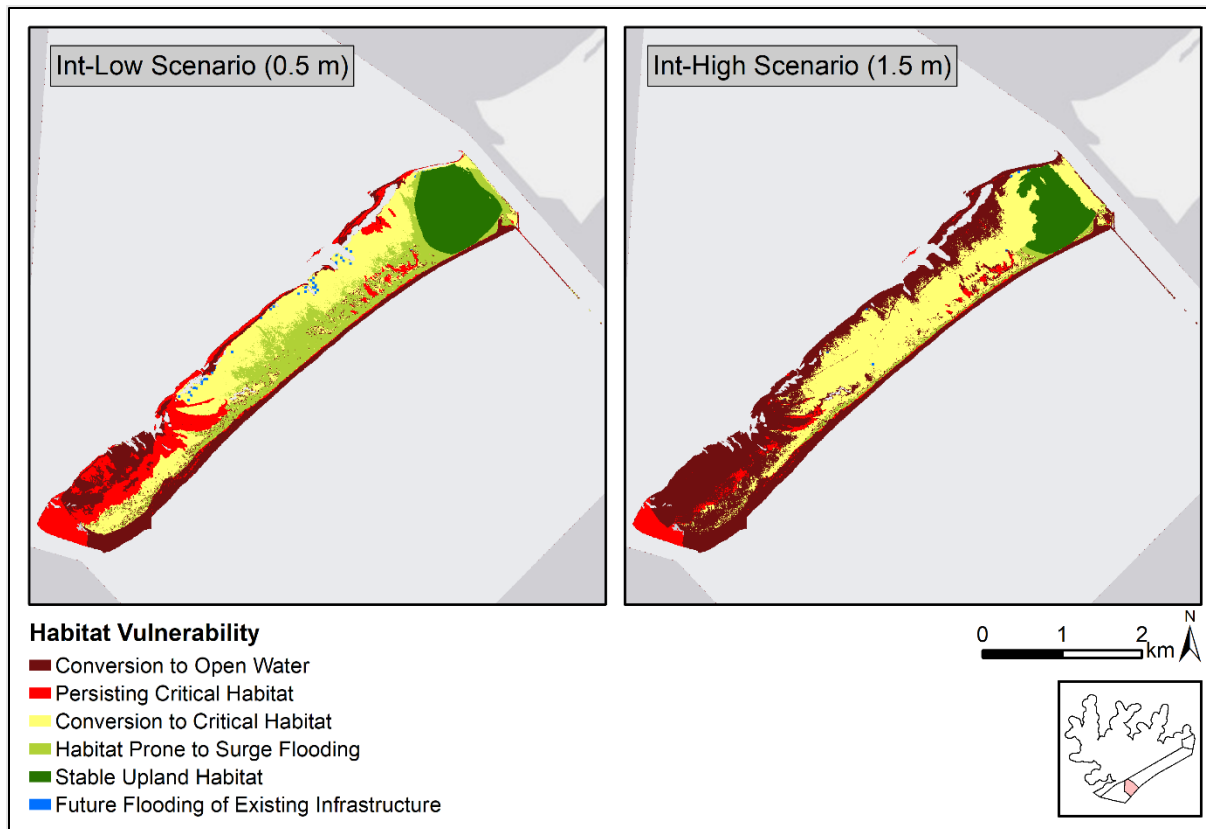


Figure 38. Map showing habitat vulnerability under int-low (0.5 m) and int-high (1.5 m) GMSLR scenarios by the year 2100 from Pass Cavallo to Matagorda Ship Channel.

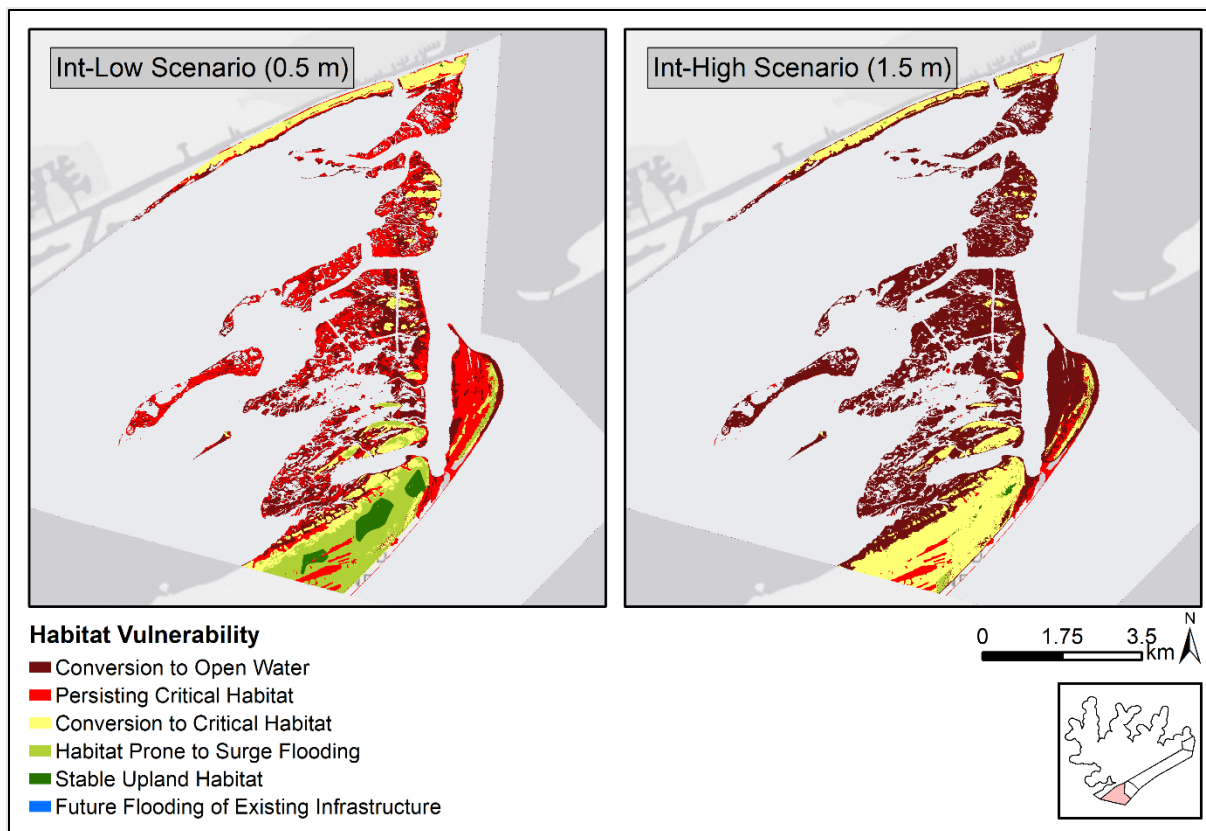


Figure 39. Map showing habitat vulnerability under int-low (0.5 m) and int-high (1.5 m) GMSLR scenarios by the year 2100 within Matagorda Island.

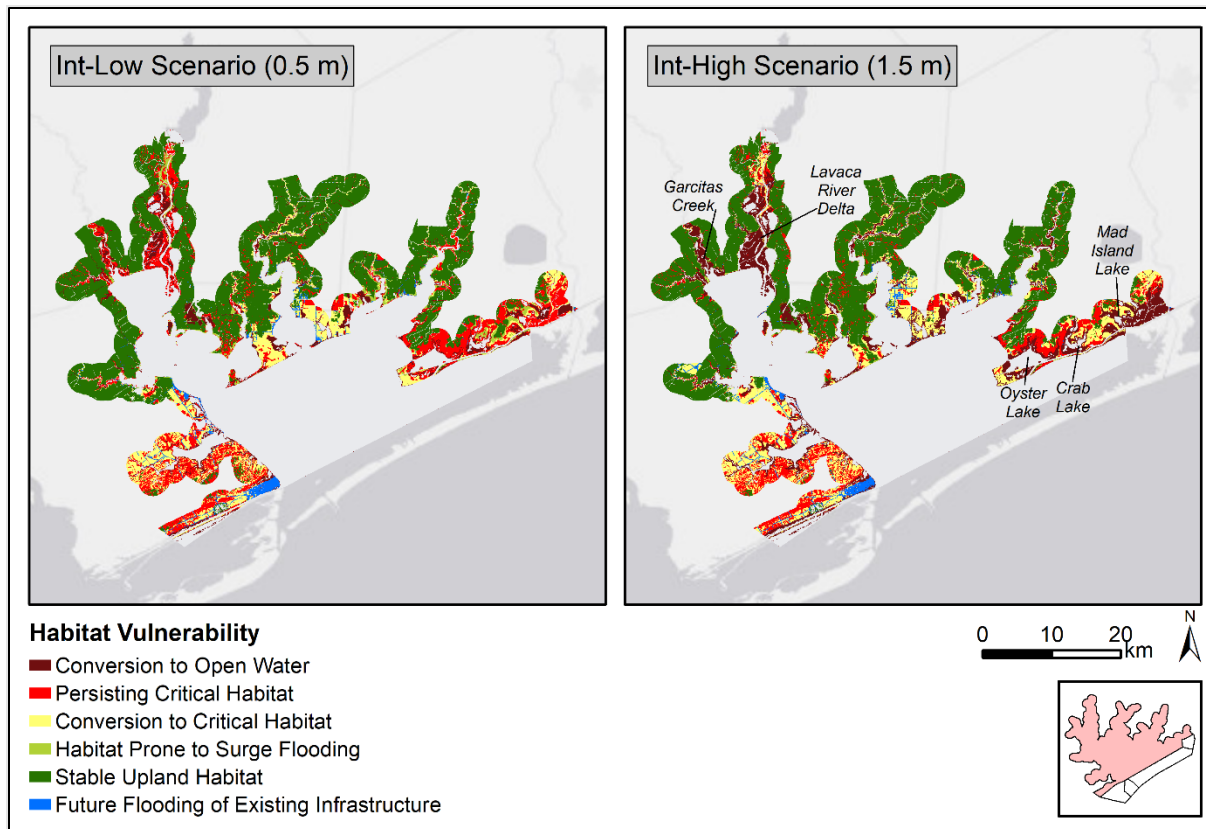


Figure 40. Map showing habitat vulnerability under int-low (0.5 m) and int-high (1.5 m) GMSLR scenarios by the year 2100 within Inland Matagorda.

Discussion

From 1850 to 2020, there were significant fluctuations in vegetation and sand coverage along the stretch from Matagorda Peninsula to Matagorda Island. In total, vegetation declined by 11.8 km², and sand coverage decreased by 2.2 km². Interestingly, the Colorado River Delta experienced a gain of 21 km² in vegetation during the same time period. On average, the width of vegetation along Matagorda Peninsula decreased by 172 m, and from Pass Cavallo to Matagorda Ship Channel, it decreased by 331 m. Similarly, the Gulf beach width decreased by 34 m along Matagorda Peninsula and 23 m from Pass Cavallo to Matagorda Ship Channel from 1850 to 2020. Furthermore, the Gulf beach width on Matagorda Island decreased by 323 m from 1972 to 2020. This decline in vegetation and sand coverage over time is detrimental to the survival and health of various species. Sea turtles depend on Gulf beaches for nesting, colonial waterbirds and shorebirds rely on Gulf beaches and estuarine marshes for nesting and foraging, and rails rely on estuarine marshes for nesting and foraging. The loss of habitat due to the decline in vegetation and sand coverage, coupled with the predicted decline of estuarine marshes under 0.5 m and 1.5 m of Global Mean Sea Level Rise by 2100, will further limit the habitat of these species.

Literature Cited

- Bureau of Economic Geology. (2021). Status and Trends of Texas Wetlands, 1950's to 2000's. Retrieved from <https://www.beg.utexas.edu/research/programs/coastal/wetlands/trends>
- Clough, J. S., Park, R. A., & Fuller, R. (2010). SLAMM 6 Beta Technical Documentation. Retrieved from http://warrenpinnacle.com/prof/SLAMM6/SLAMM6_Technical_Documentation.pdf
- Cowardin, L.M., Carter, V., Golet, F.C., & LaRoe, E.T. (1979). Classification of wetlands and deepwater habitats of the United States. U.S. Department of Interior, Fish and Wildlife Service.
- EagleView. (2022). Pictometry. Retrieved from <https://www.eagleview.com/>
- Gibeaut, J. C., Wood, L. A., & Nichols, W. (2013). Shoreline Type Mapping of the Central and Lower Texas Coast. Final report for the Texas General Land Office Oil Spill Prevention and Response Program. GLO contract 10-094-000-3924.
- NOAA. (2016). C-CAP Regional Land Cover. Retrieved from <https://coast.noaa.gov/digitalcoast/data/ccapregional.html>
- Paine, J. G., Caudle, T., & Andrews, J. R. (2016). Shoreline movement in the Copano, San Antonio, and Matagorda Bay systems, central Texas coast, 1930s to 2010s. The University of Texas at Austin, Bureau of Economic Geology. Final Report prepared for General Land Office under contract no. 13-258-000-7485.
- Research and Distribution Center. (1943). Matagorda 1943 USDA Historic Imagery. Retrieved from <https://data.tnris.org/collection?c=d264b87f-d6ec-4580-9e69-0c244ed7345b#8.68/28.8134/-95.875>
- Strategic Mapping Program. (1996). Texas 1996 TOP Imagery. Retrieved from <https://data.tnris.org/collection?c=85d8fb09-cc72-442f-9b44-287ed8079dbc#4.45/31.34/-100.09>
- Strategic Mapping Program. (2009). Texas 2009 TOP Imagery. Retrieved from <https://data.tnris.org/collection?c=e8a9bba2-b219-47a7-be04-ff6493363c27#5.93/29.732/-96.062>
- Sweet, W. V., Kopp, R. E., Weaver, C. P., Obeysekera, J., Horton, R. M., Thieler, E. R., & Zervas, C. (2017). Global and Regional Sea Level Rise Scenarios for the United States. NOAA Technical Report NOS CO-OPS 083. NOAA/NOS Center for Operational Oceanographic Products and Services.
- Texas General Land Office. (2001). 2001 Aerial Imagery. Retrieved from <https://www.glo.texas.gov/land/land-management/gis/aerials/matagorda11-30-01/index.html>
- Texas General Land Office. (2023). Texas Coastal Resiliency Master Plan - Technical Report. Retrieved from <https://glo.texas.gov/crmp>

- TNRIS. (2015). Texas 2015 TOP Imagery. Retrieved from <https://data.tnris.org/collection?c=b7e5b638-99f0-4676-9411-c88d06d49943#4.45/31.31/-100.12>
- Tremblay, T. A., & Calnan, T. R. (2010). Status and trends of inland wetland and aquatic habitats, Matagorda Bay Area. The University of Texas at Austin, Bureau of Economic Geology. Final report prepared for the Texas General Land Office and National Oceanic and Atmospheric Administration under GLO contract no. 09-046.
- Tremblay, T. A., Vincent, J. S., & Calnan, T. R. (2002). Status and trends of wetland aquatic habitats on Texas barrier islands, Matagorda Bay to San Antonio Bay. The University of Texas at Austin, Bureau of Economic Geology, final report prepared for the Texas General Land Office and National Oceanic and Atmospheric Administration, under GLO contract no. 01-241-R.
- U.S. DOC, NOAA, NESDIS, and NOS. (2016). NOAA Historical Surveys (T-Sheets). Retrieved from <https://shoreline.noaa.gov/data/datasheets/t-sheets.html>
- U.S. Fish and Wildlife Service. (2017). National Wetlands Inventory. Retrieved from <http://www.fws.gov/wetlands/>
- USDA. (1953). Matagorda 1953 USDA Historic Imagery. Retrieved from <https://data.tnris.org/?pg=2&inc=24&s=matagorda&category=Imagery>
- USDA. (2004). Texas 2004 NAIP Imagery. Retrieved from <https://data.tnris.org/collection?c=a8756dac-62a7-4b51-8d07-ab0cecb6e600#4.96/31.31/-100.09>
- USDA. (2012). Texas 2012 NAIP Imagery. Retrieved from <https://data.tnris.org/collection?c=924d3c6f-9f74-4147-8044-d4025f12eac3#4.45/31.46/-100.09>
- USDA. (2018). Texas 2018 NAIP Imagery. Retrieved from <https://data.tnris.org/collection?c=f1d66250-4021-47df-9fe9-9fca286b0f50#4.45/31.41/-100.12>
- USDA. (2020). Texas 2020 NAIP Imagery. Retrieved from <https://data.tnris.org/collection?c=aa5183ca-a1bd-4b5f-9b63-4ba48d01b83d#5.5/31.33/-99.341>
- USGS. (1972). Aerial Photo Single Frame. Retrieved from <https://earthexplorer.usgs.gov/>
- USGS. (1981). National High Altitude Photography. Retrieved from <https://earthexplorer.usgs.gov/>
- USGS. (2016). National Land Cover Database 2016 Land Cover (CONUS). Retrieved from <https://www.mrlc.gov/data/nlcd-2016-land-cover-conus>

USGS. (2018). South Texas Lidar. Retrieved from <https://data.tnris.org/collection?c=6131ecdd-aa26-433e-9a24-97ac1afda7de#6.68/27.576/-98.187>

USGS. (2019). Matagorda Bay Lidar. Retrieved from <https://data.tnris.org/collection?c=8774ed51-b633-4f03-85ca-94c311ee0a88#8.66/28.7509/-96.1562>

Wadsworth, A. H. (1996). Historical Deltation of the Colorado River, Texas. In *Deltas in their geologic framework* (pp. 99-105). Houston, Texas: Houston Geological society

Appendix A: WV-2 Land Cover Classifications Through Time

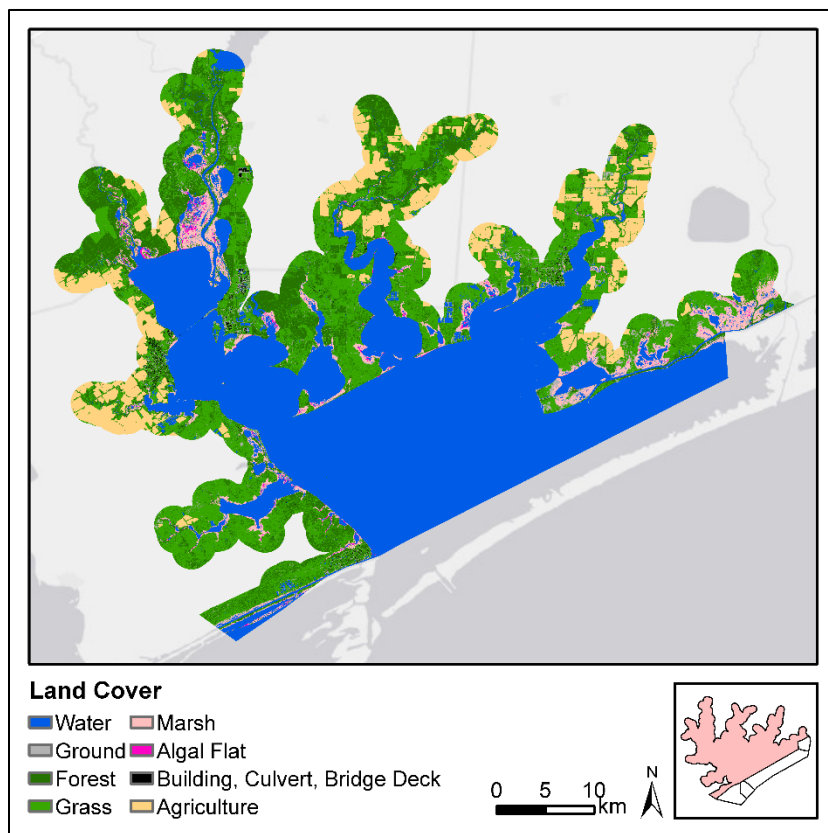


Figure 41. WV-2 Habitat Classification for Inland Matagorda.

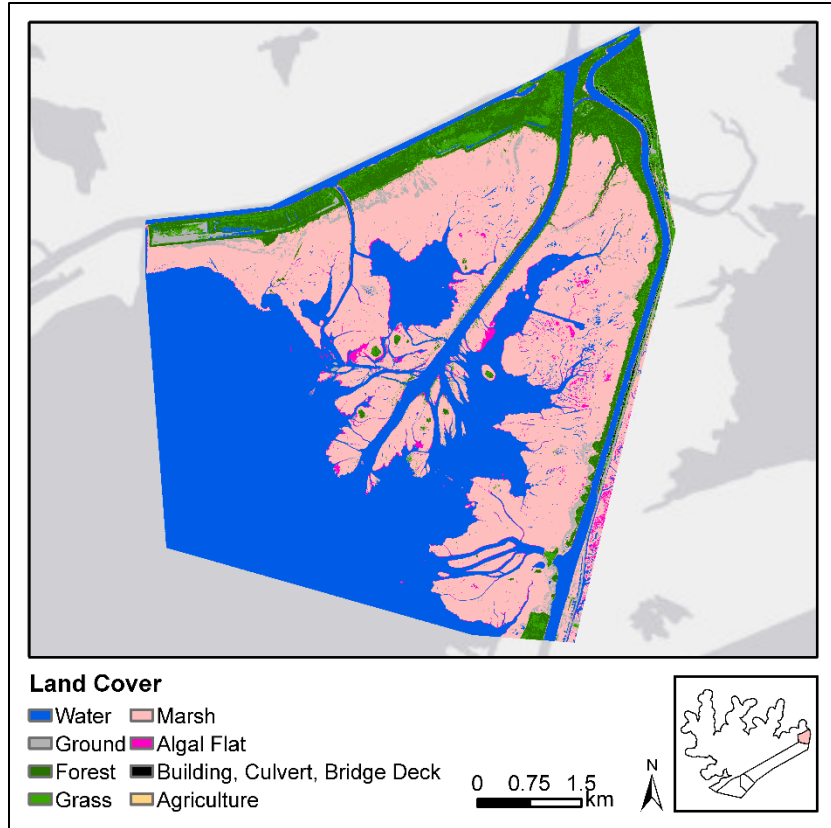


Figure 42. WV-2 Habitat Classification for Colorado River Delta.

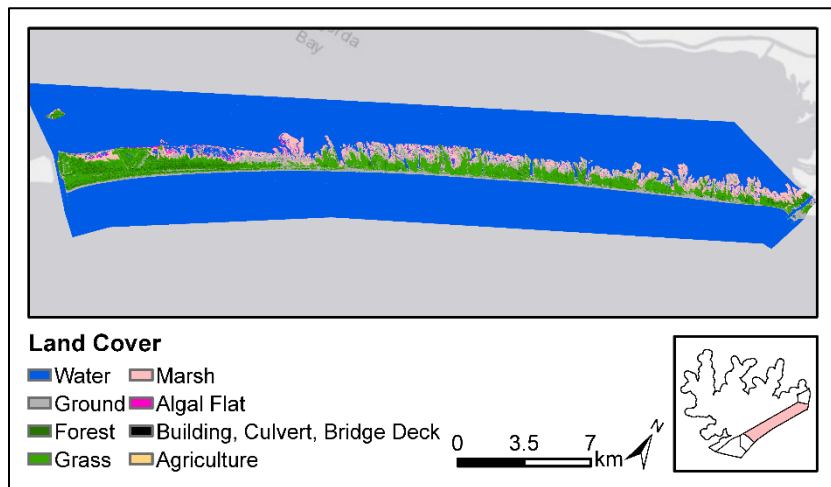


Figure 43. WV-2 Habitat Classification for Matagorda Peninsula.

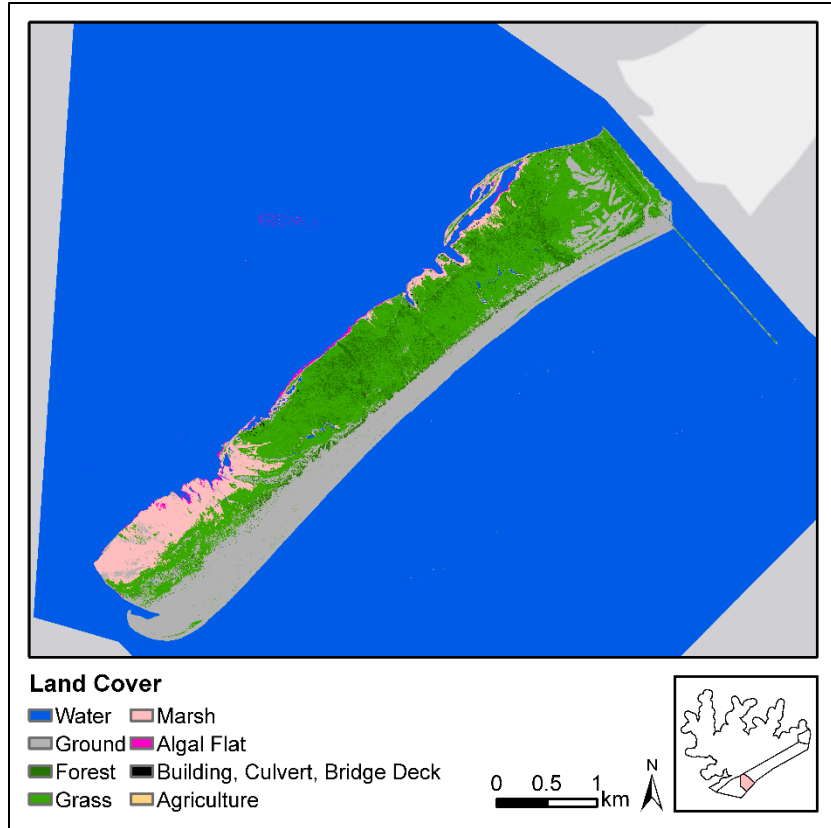


Figure 44. WV-2 Habitat Classification for Pass Cavallo to Matagorda Ship Channel.

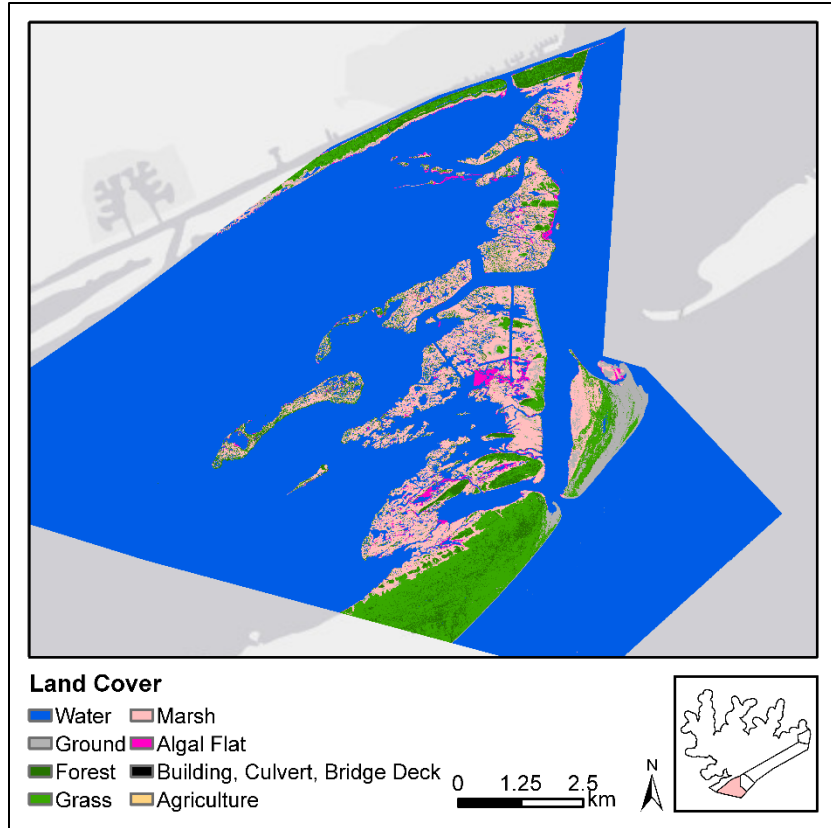


Figure 45. WV-2 Habitat Classification for Matagorda Island.

Appendix B: Imagery Comparisons Along with Classified Land Covers

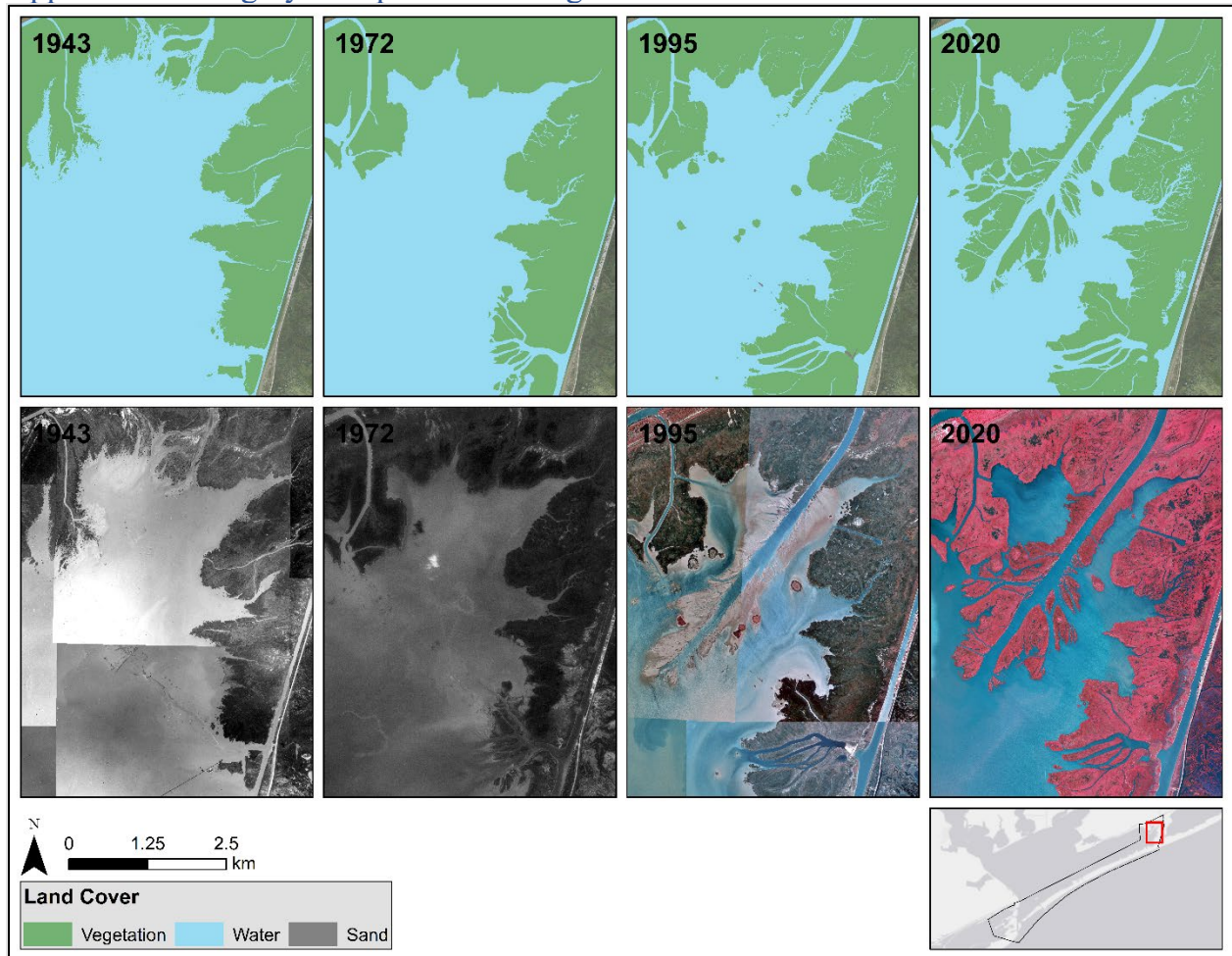


Figure 46. Imagery comparisons along with digitized and classified landcover. Differences between imagery used along with comparisons to their digitized and classified landcovers. This image is focused on the Colorado River Delta and Tiger Island Subdelta.

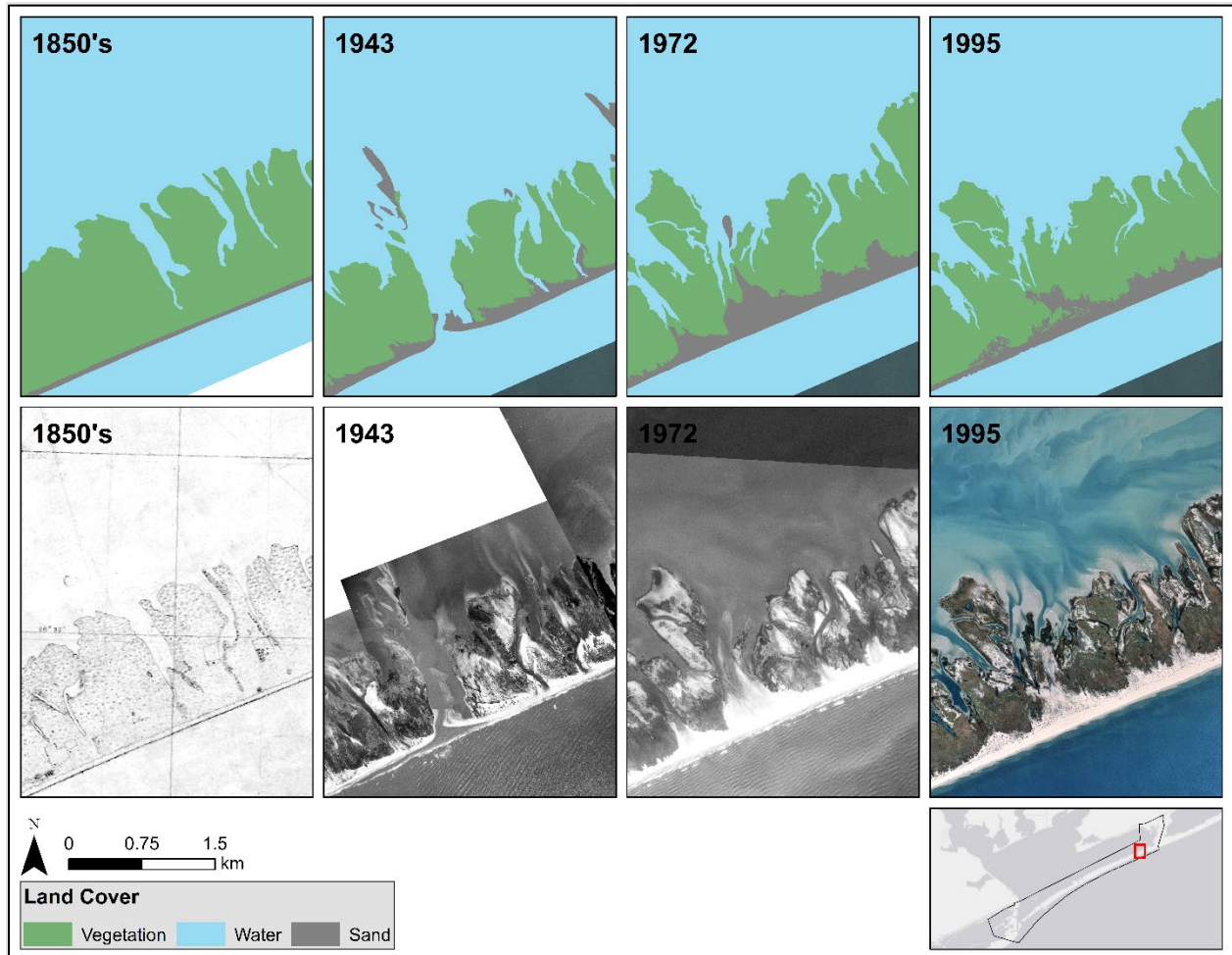


Figure 47. Imagery comparisons along with digitized and classified landcover. Differences between imagery used along with comparisons to their digitized and classified landcovers. This image is focused on Forked Bayou.

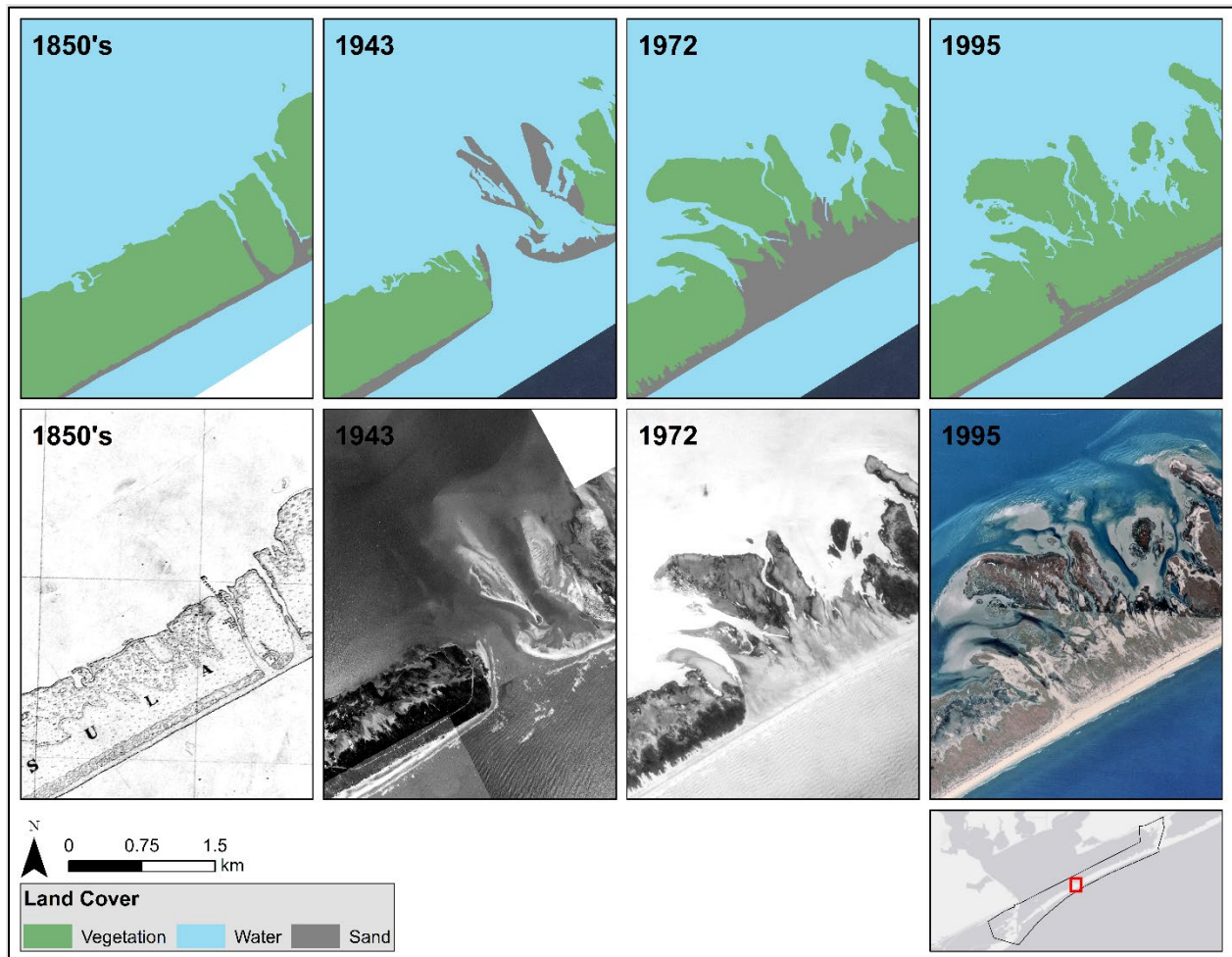


Figure 48. Imagery comparisons along with digitized and classified landcover. Differences between imagery used along with comparisons to their digitized and classified landcovers. This image is focused on Green's Bayou.

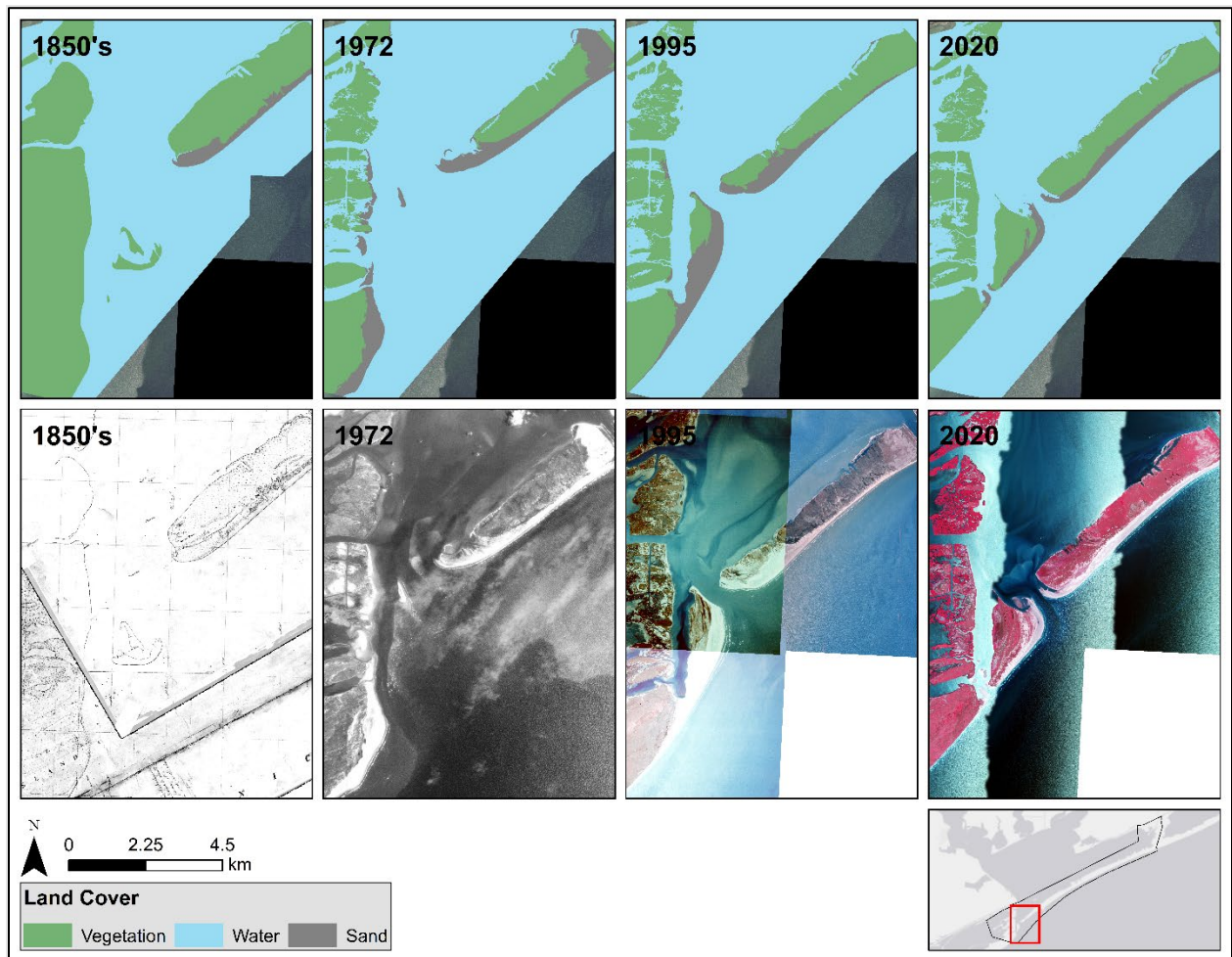


Figure 49. Imagery comparisons along with digitized and classified landcover. Differences between imagery used along with comparisons to their digitized and classified landcovers. This image is focused on Pass Cavallo.

Appendix C: Digitized Land Cover Classifications Through Time

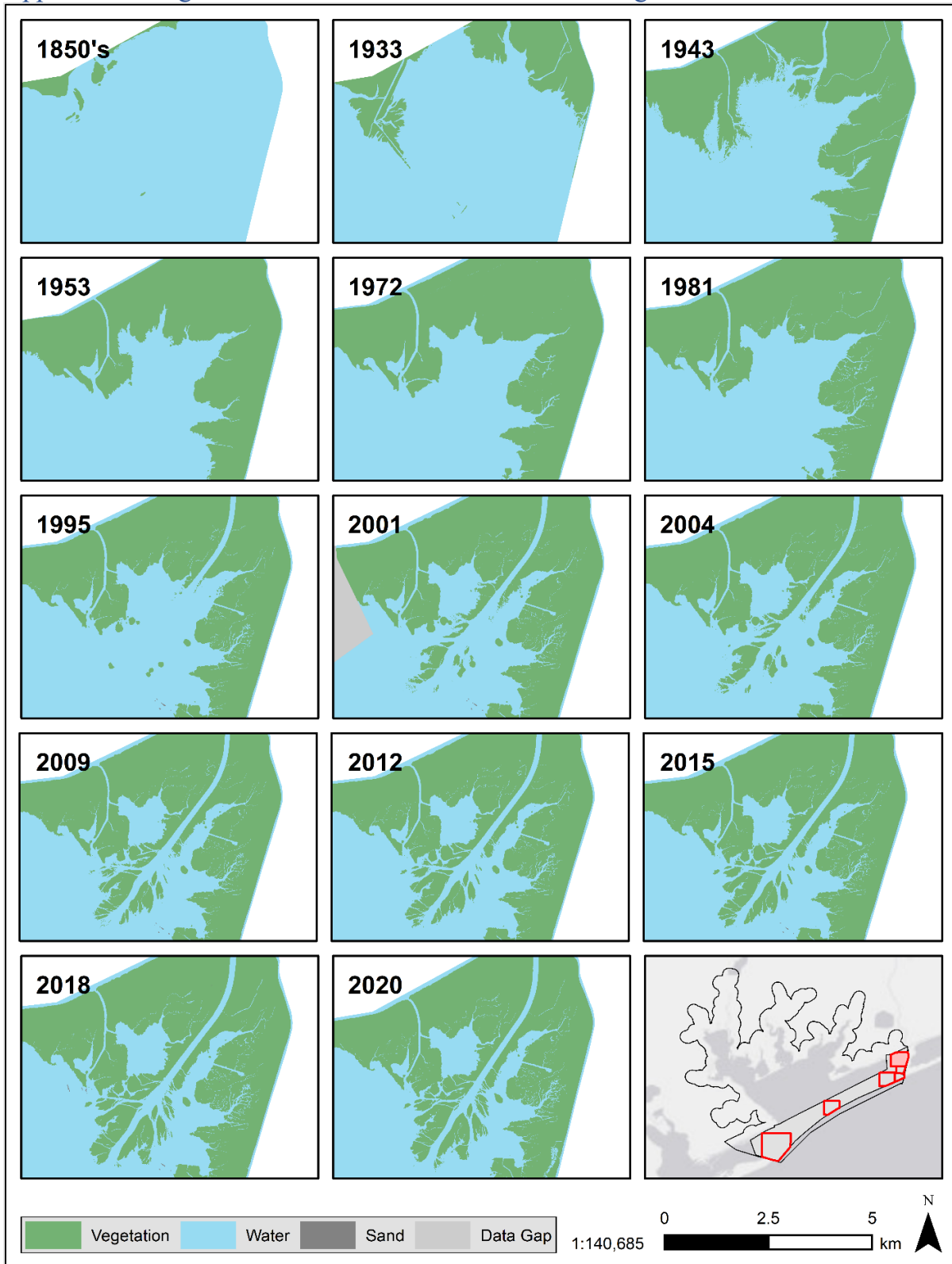


Figure 50. Digitized land cover classifications through time focused on the Colorado River Delta.

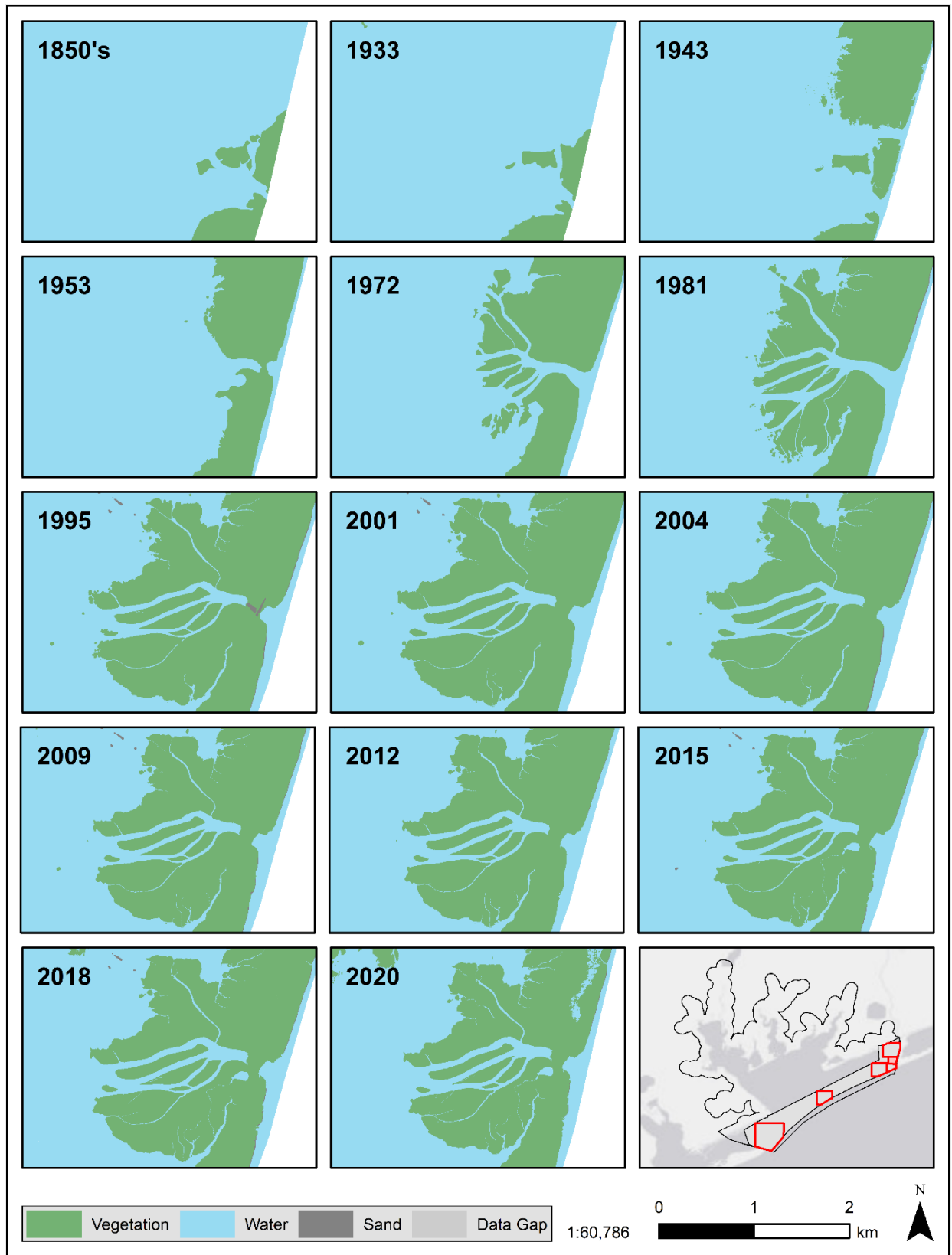


Figure 51. Digitized land cover classifications through time focused on Tiger Island Subdelta.

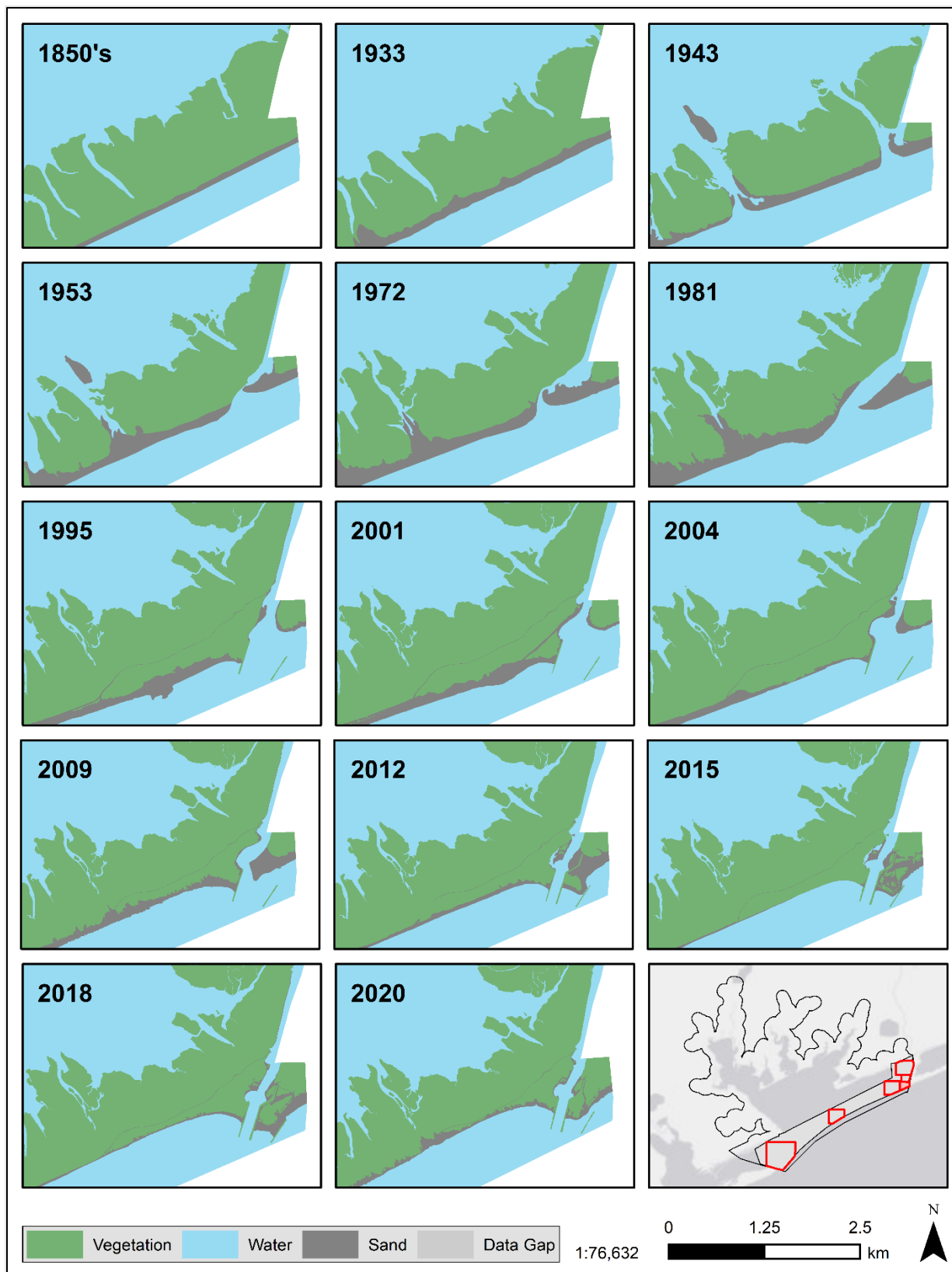


Figure 52. Digitized land cover classifications through time focused on the mouth of the Colorado River.



Figure 53. Digitized land cover classifications through time focused on Forked Bayou.

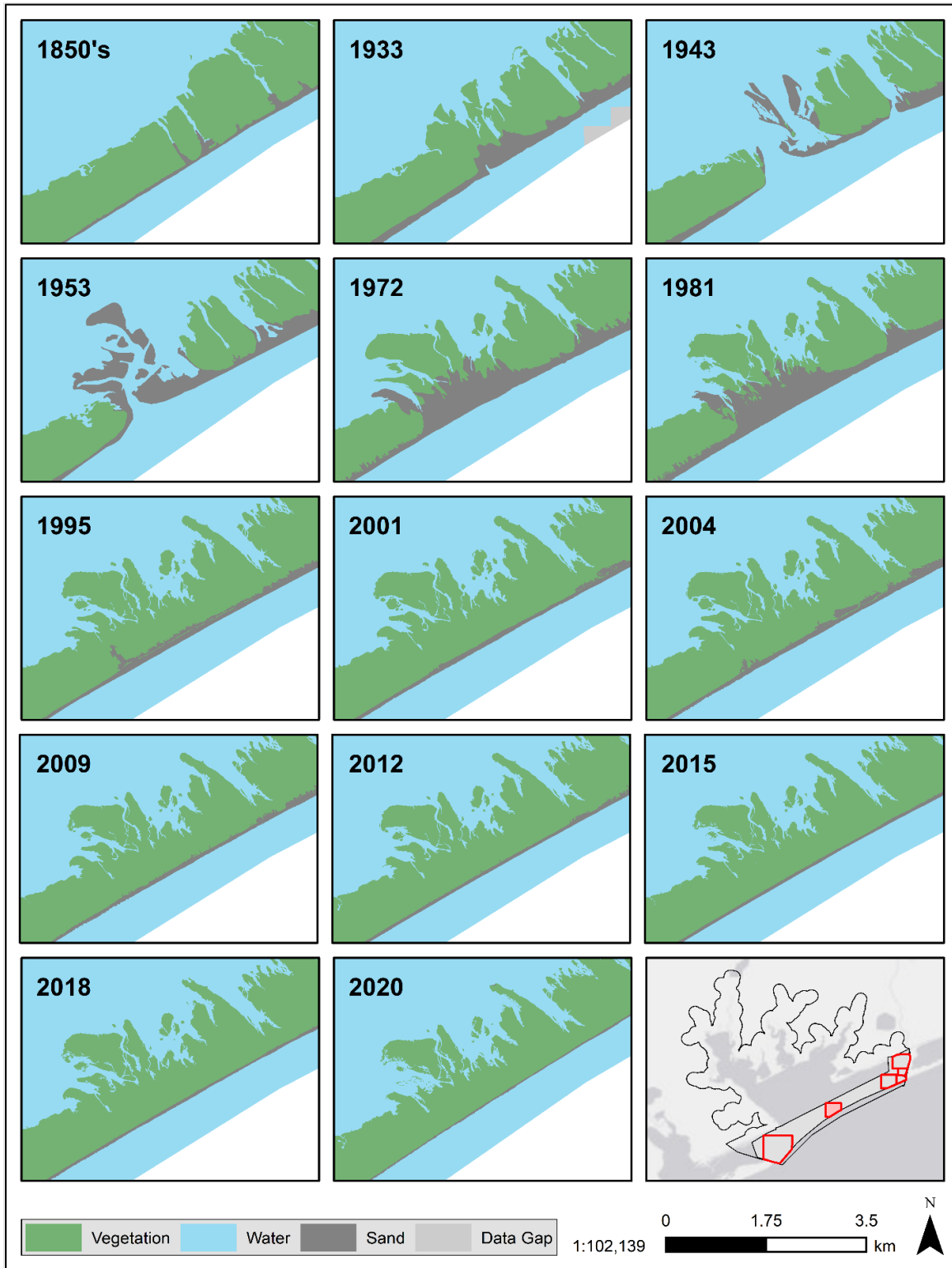


Figure 54. Digitized land cover classifications through time focused on Green's Bayou.

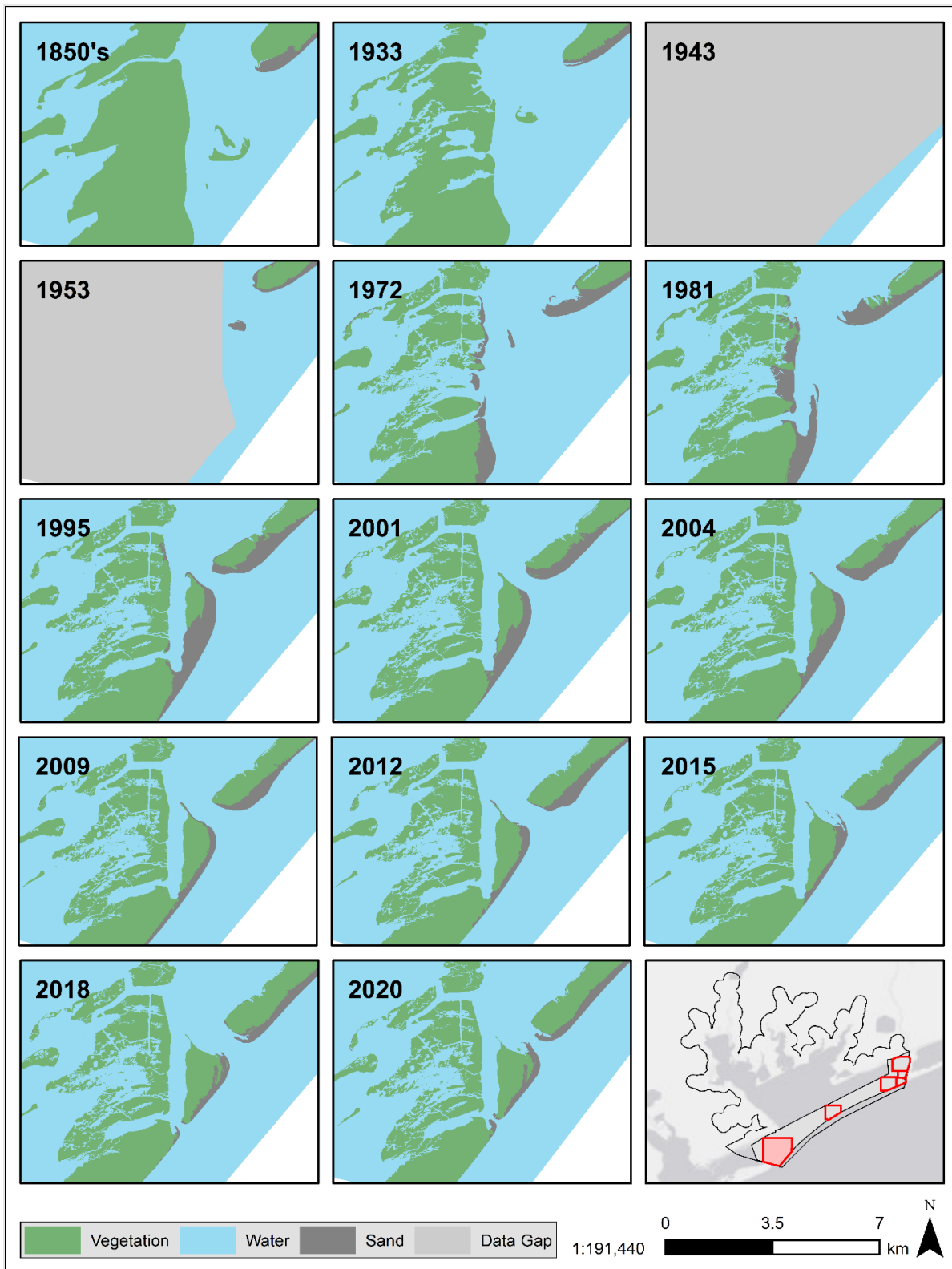


Figure 55. Digitized land cover classifications through time focused on Pass Cavallo and Matagorda Island.

Appendix D: Land cover transitions

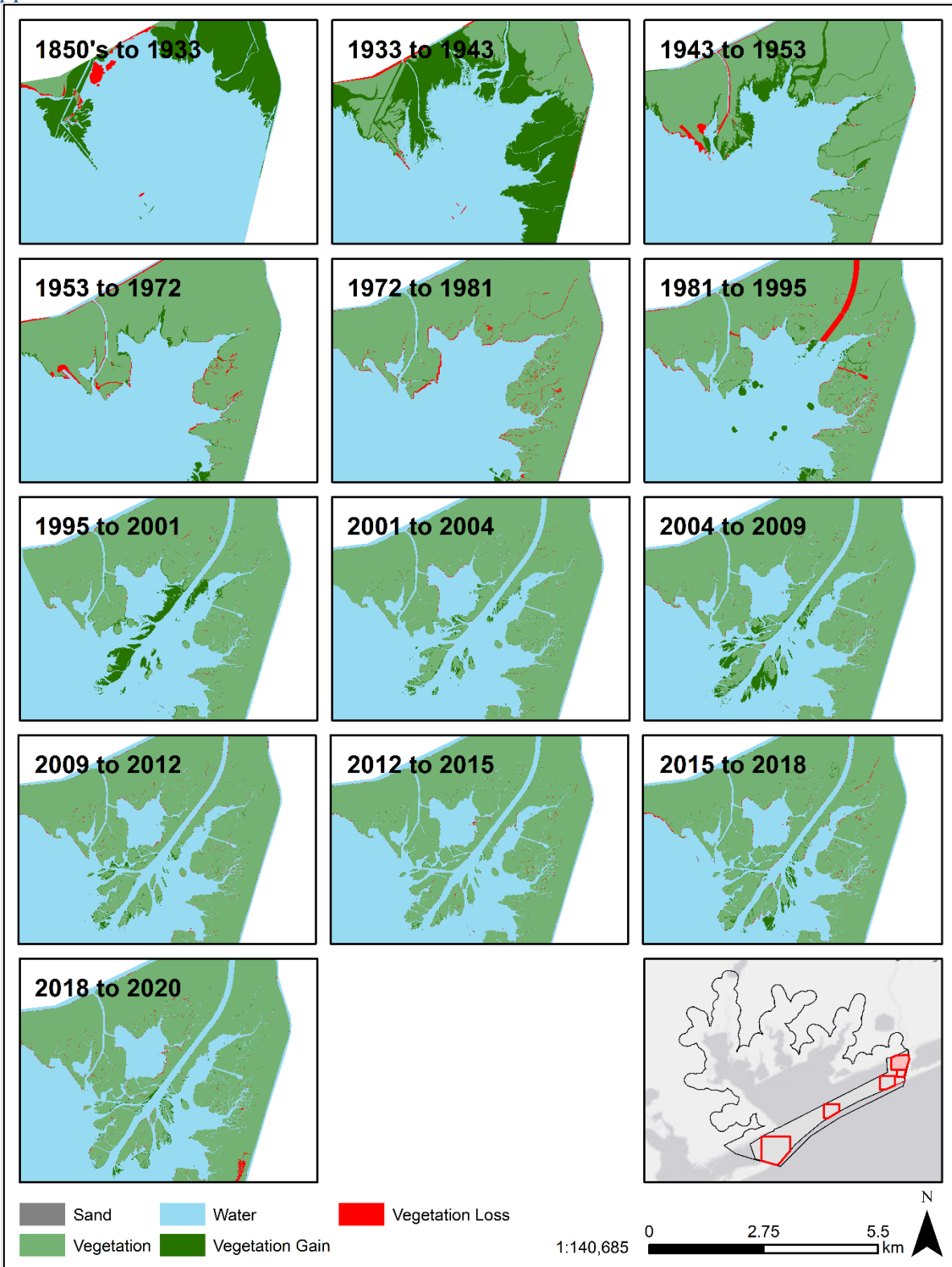


Figure 56. Land cover transitions emphasizing vegetation loss and vegetation gain through time focused on the Colorado River Delta.

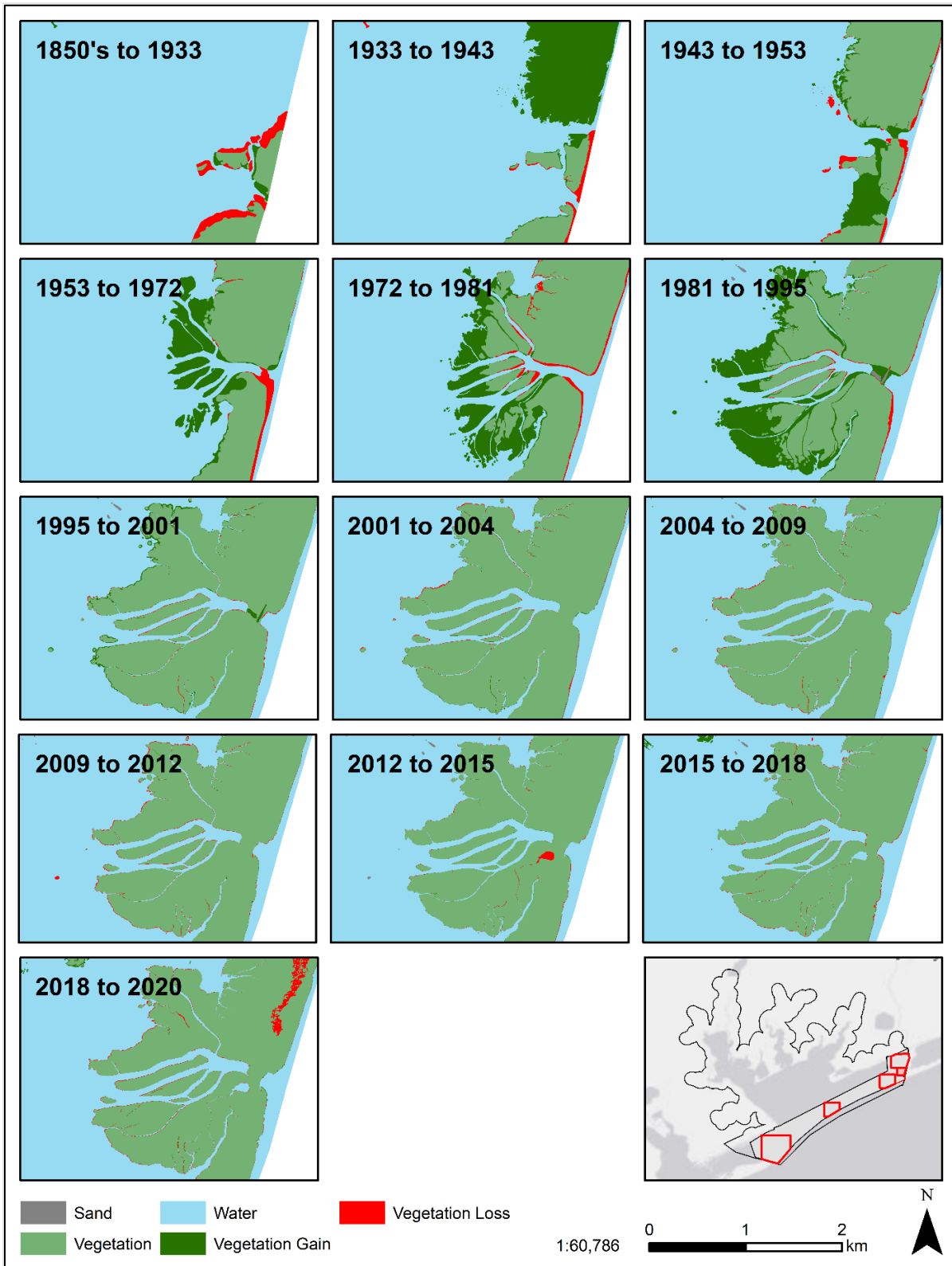


Figure 57. Land cover transitions emphasizing vegetation loss and vegetation gain through time focused on Tiger Island Subdelta.

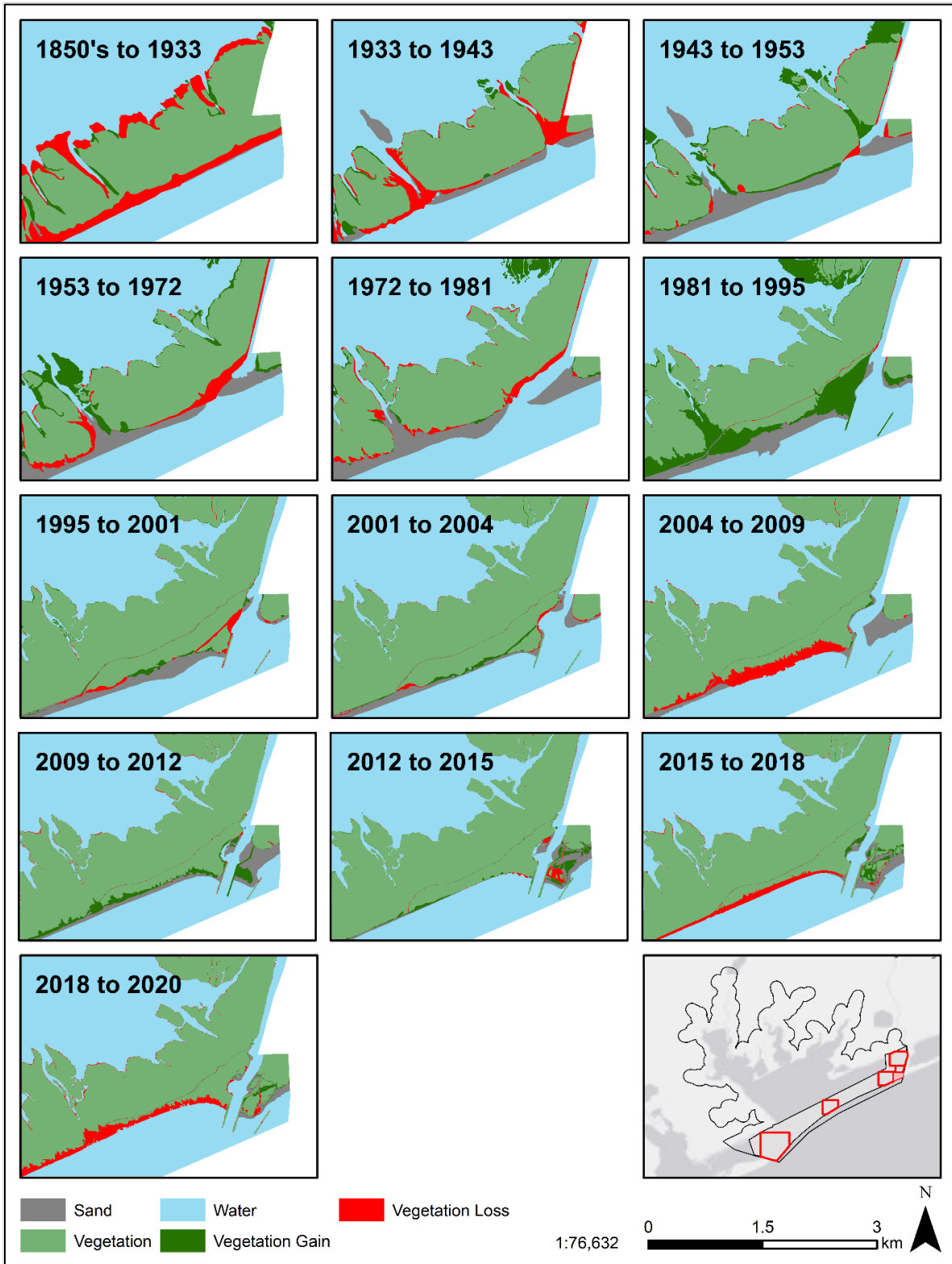


Figure 58. Land cover transitions emphasizing vegetation loss and vegetation gain through time focused on the mouth of the Colorado River.

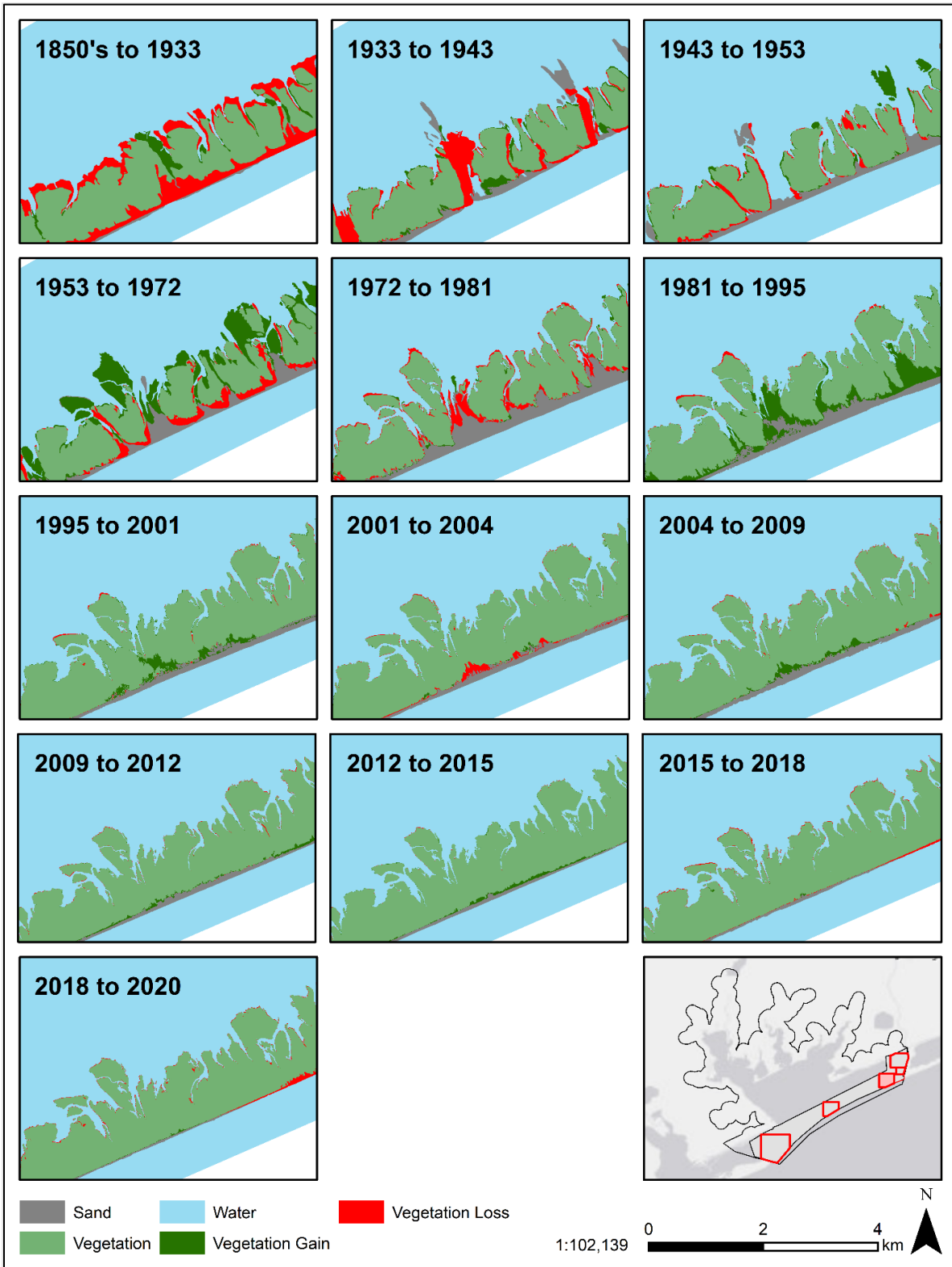


Figure 59. Land cover transitions emphasizing vegetation loss and vegetation gain through time focused on Forked Bayou.

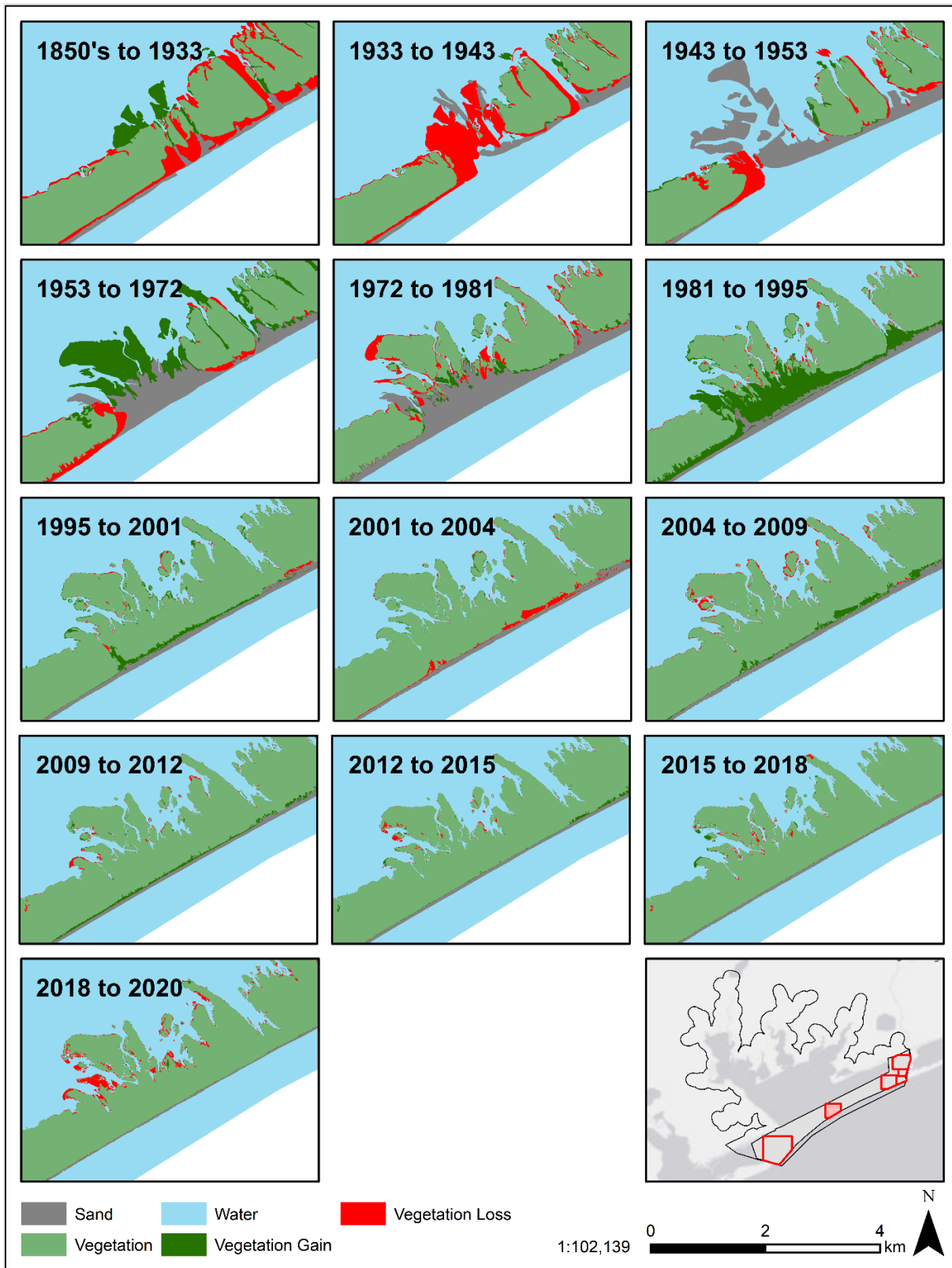


Figure 60. Land cover transitions emphasizing vegetation loss and vegetation gain through time focused on Green's Bayou.

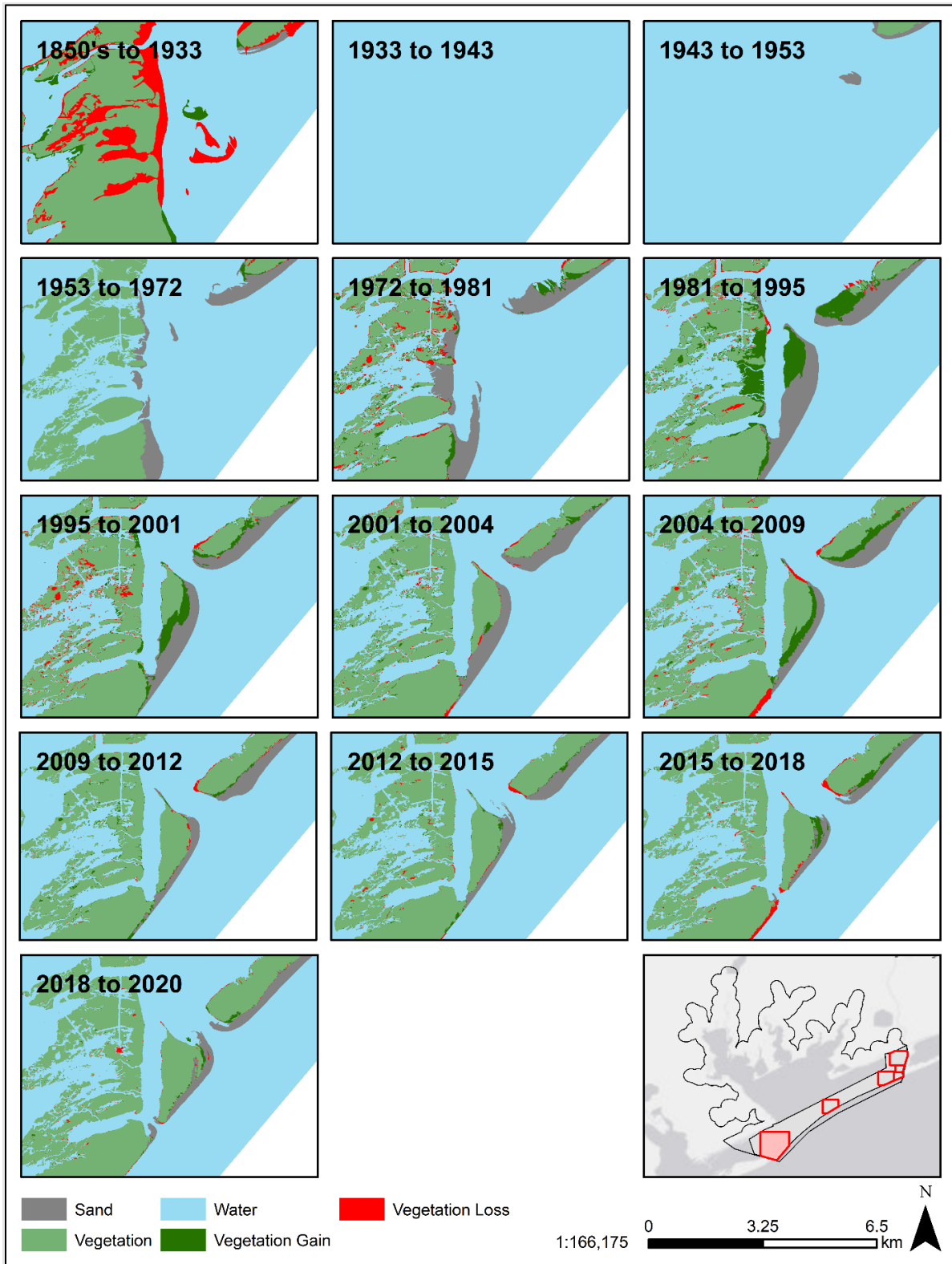


Figure 61. Land cover transitions emphasizing vegetation loss and vegetation gain through time focused on Pass Cavallo and Matagorda Island.

Appendix E: Historic Wetland Trends Through Time

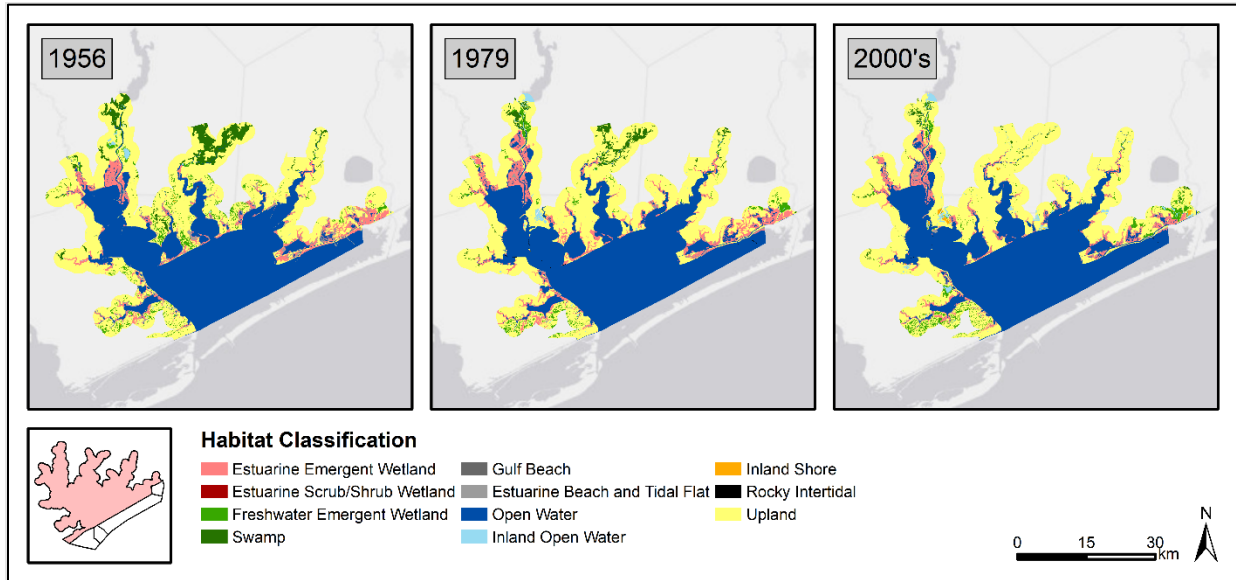


Figure 62. Historic Wetland Classifications for Inland Matagorda County.

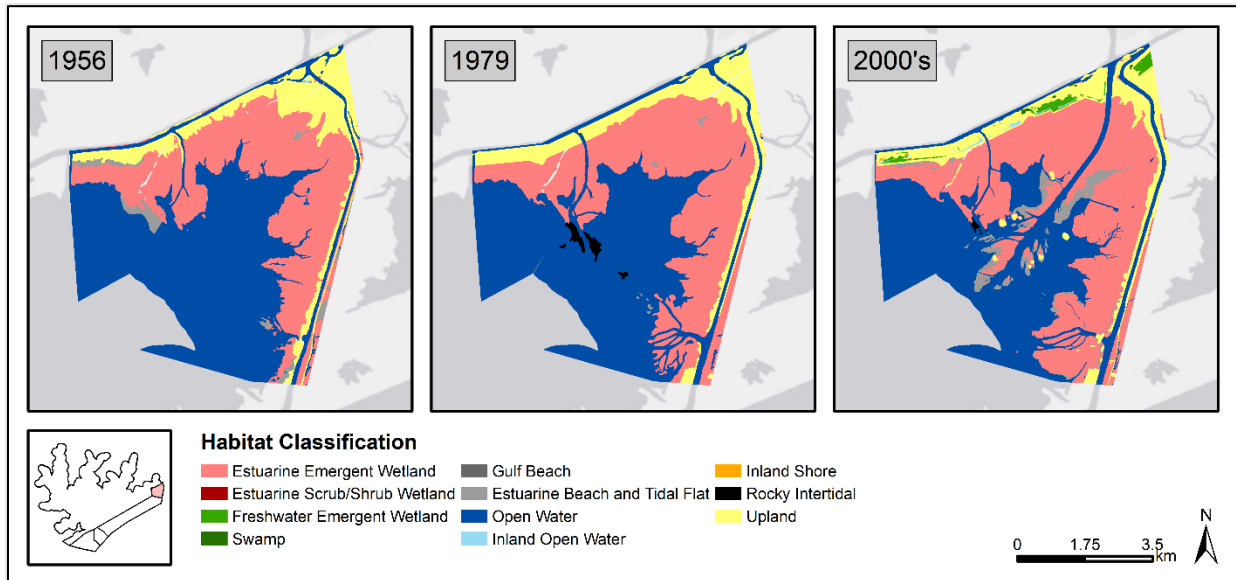
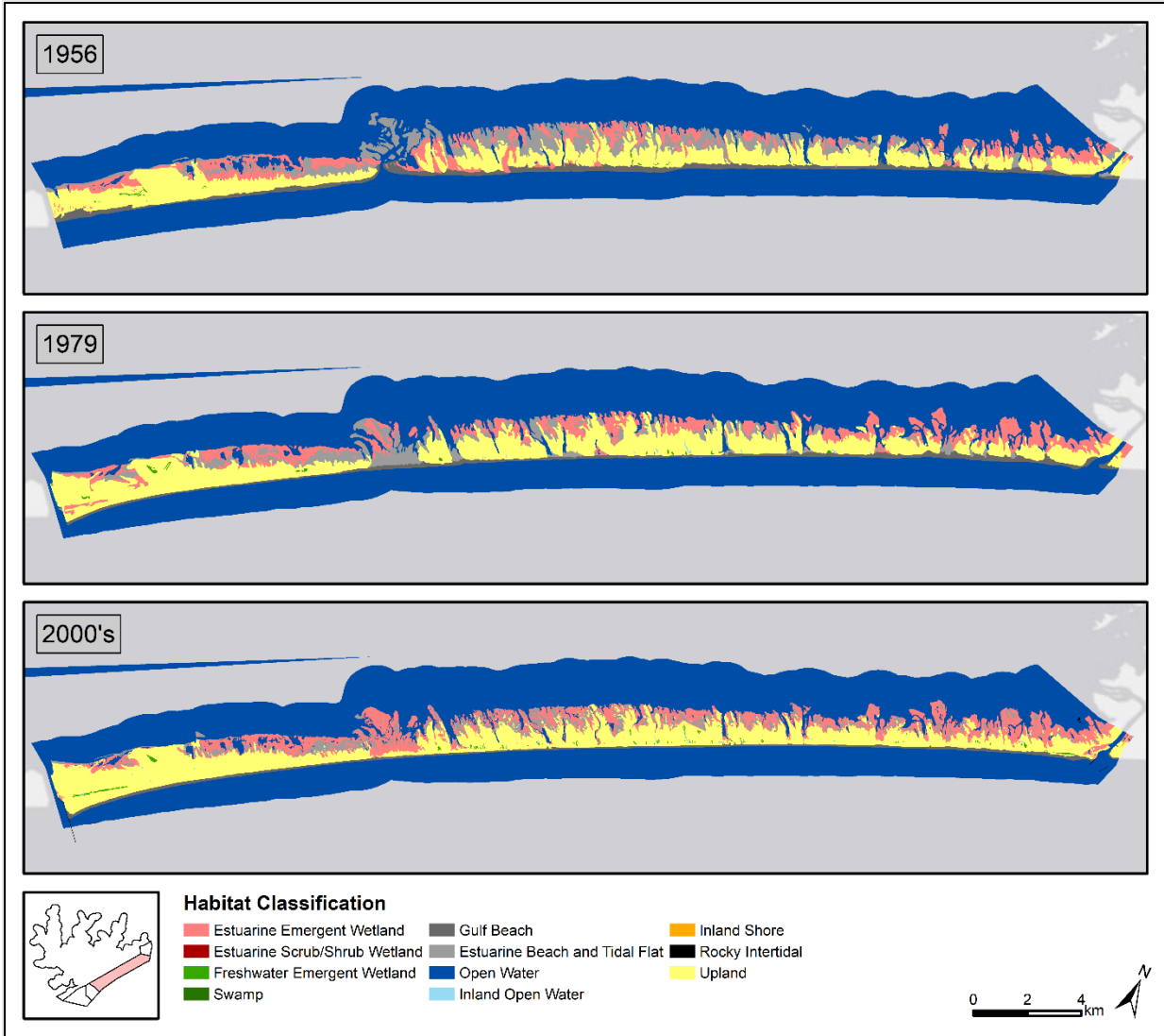


Figure 63. Historic Wetland Classifications for Colorado River Delta.



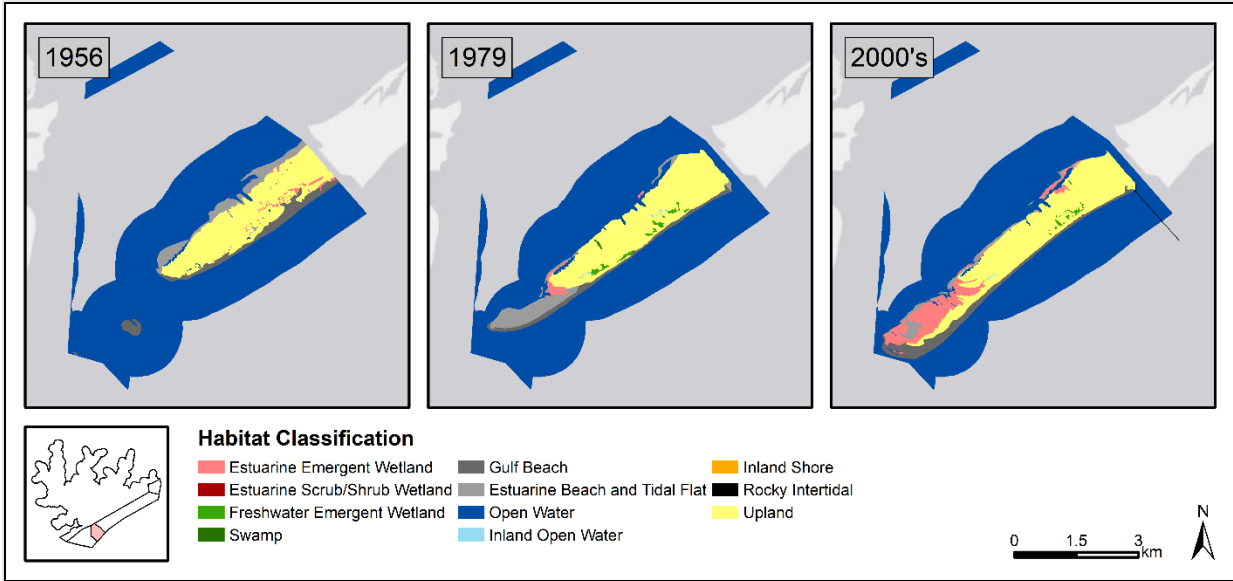


Figure 65. Historic Wetland Classifications for Pass Cavallo to Matagorda Ship Channel.

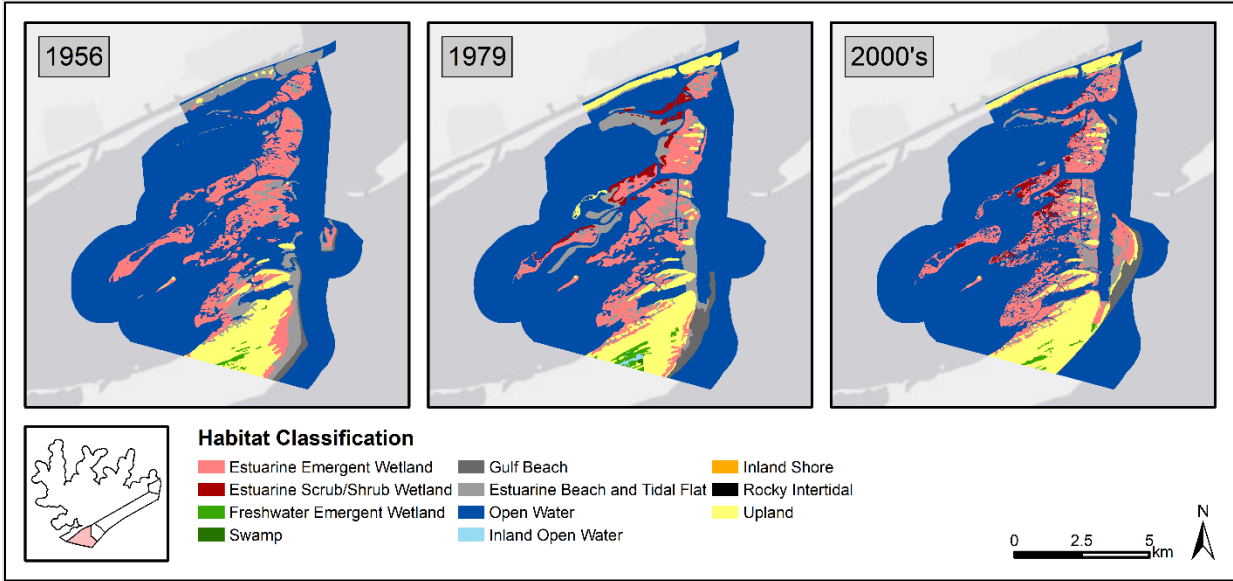


Figure 66. Historic Wetland Classifications for Matagorda Island.

Appendix F: Extent of habitats lost under low and high RSLR scenarios by 2100

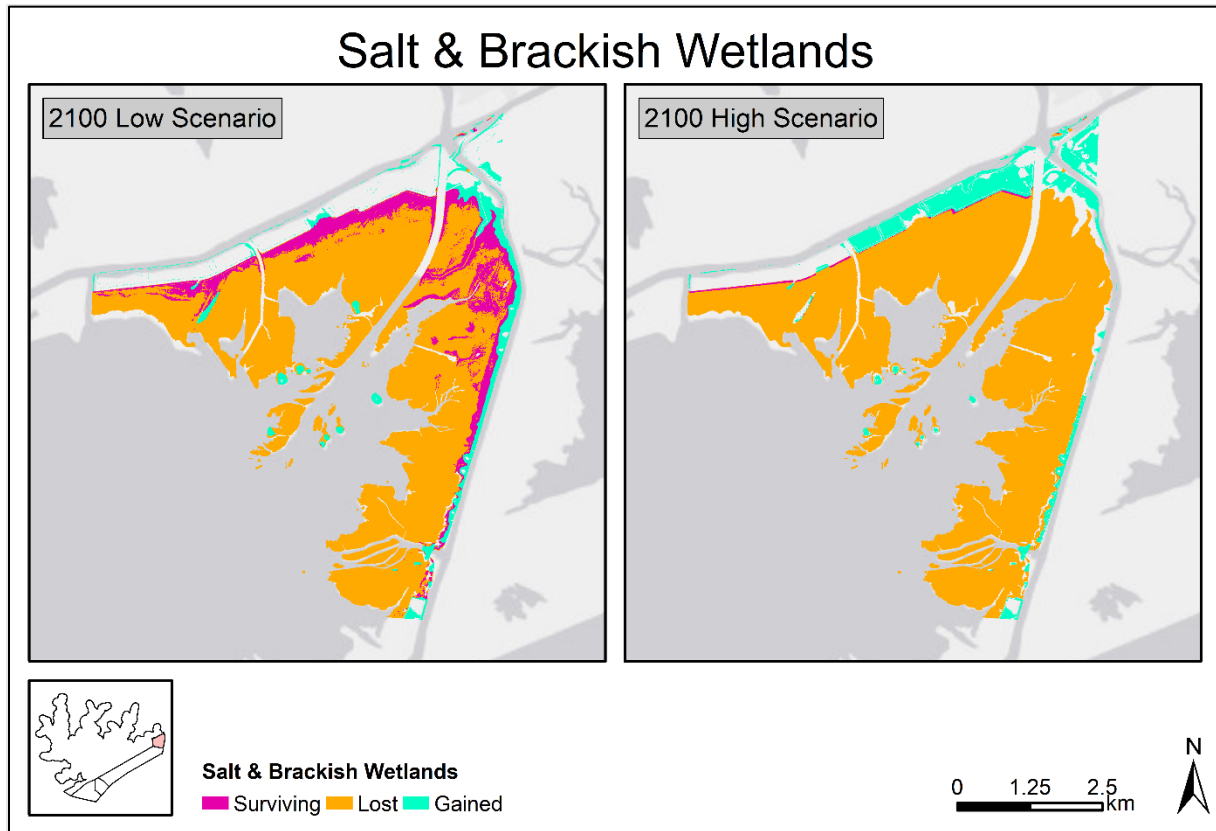


Figure 67. Map showing the extent of salt & brackish emergent wetlands predicted to be lost under low and high RSLR scenarios by the year 2100 within the Colorado River Delta.

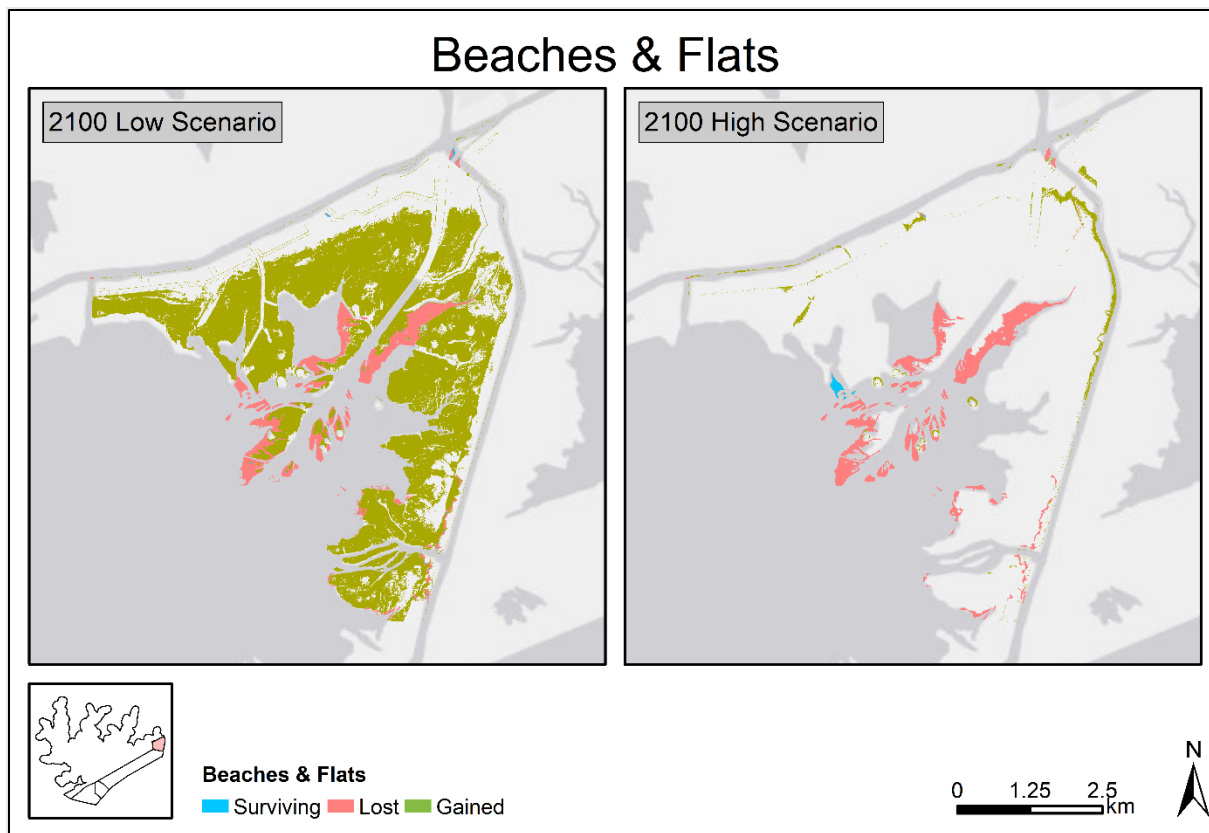


Figure 68. Map showing the extent of beaches & flats predicted to be lost under low and high RSLR scenarios by the year 2100 within the Colorado River Delta.

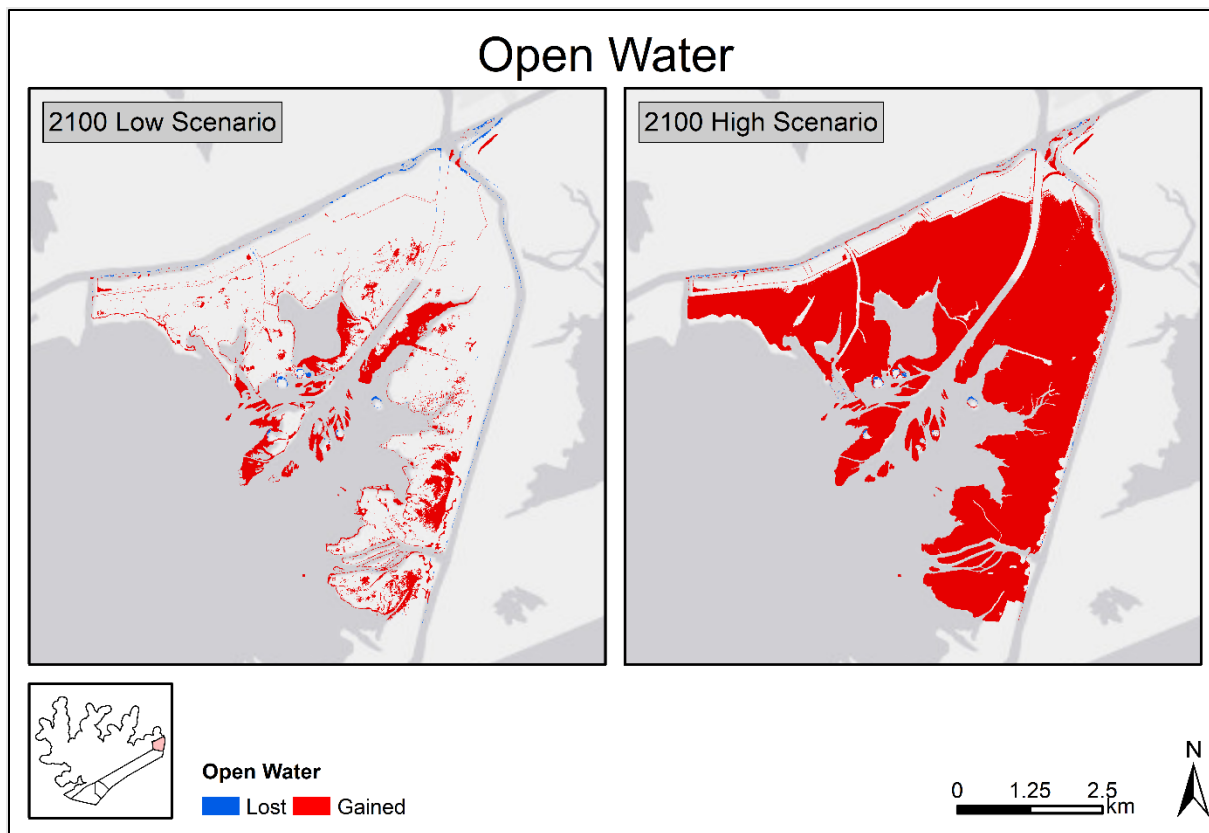


Figure 69. Map showing the extent of open water predicted to be lost under low and high RSLR scenarios by the year 2100 within the Colorado River Delta.

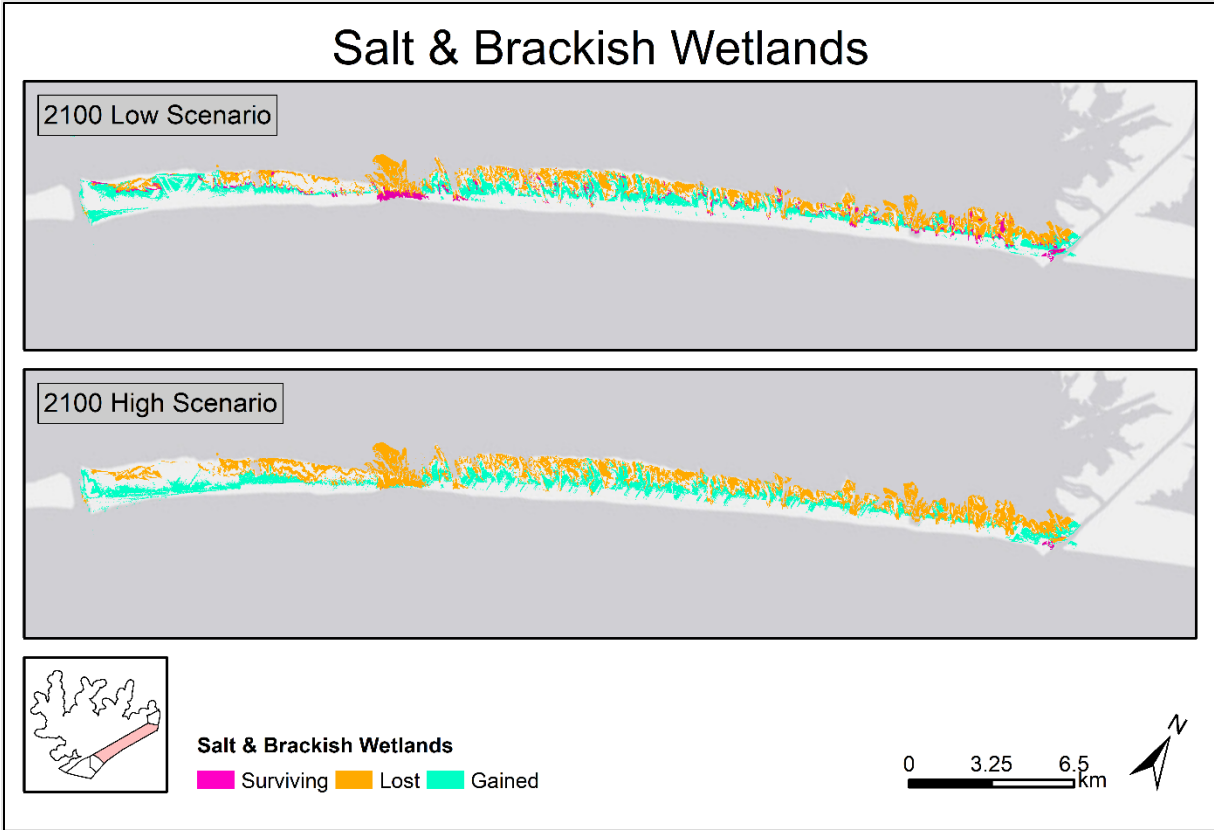


Figure 70. Map showing the extent of salt & brackish emergent wetlands predicted to be lost under low and high RSLR scenarios by the year 2100 within Matagorda Peninsula.

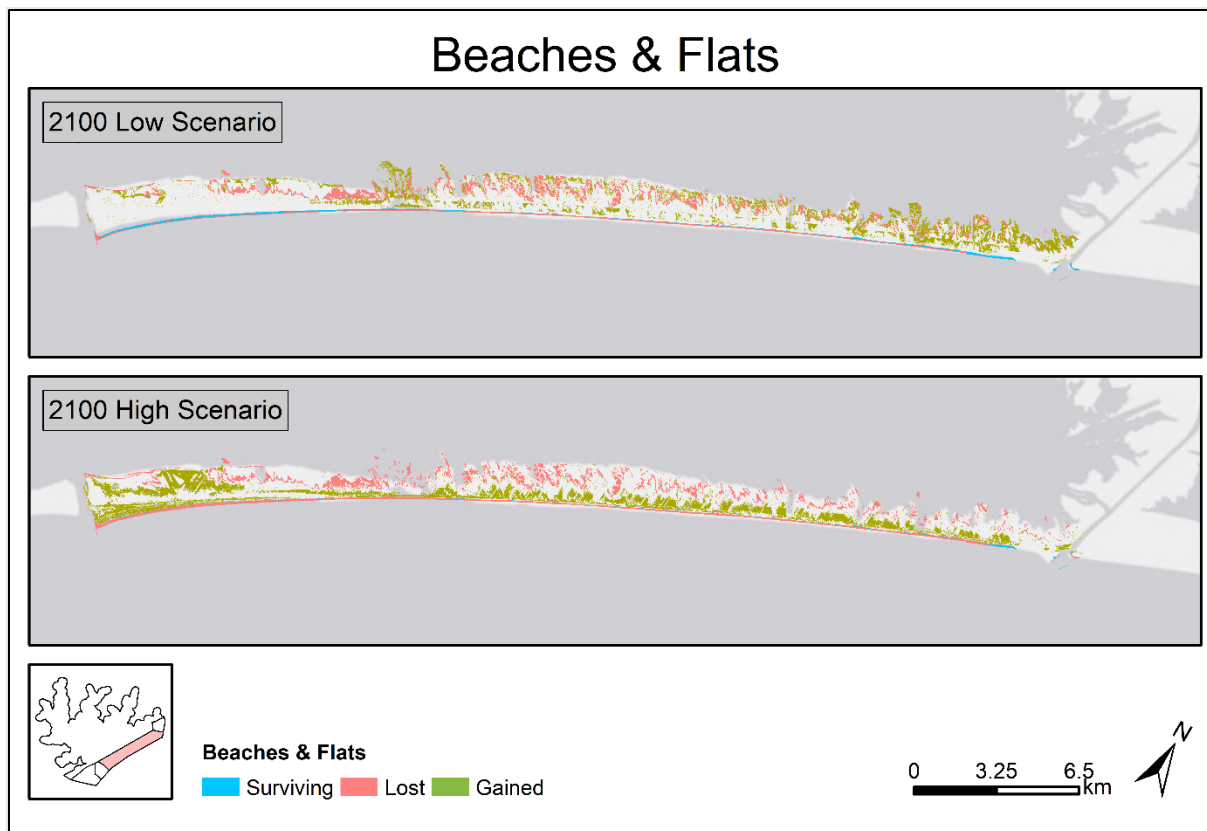


Figure 71. Map showing the extent of beaches & flats predicted to be lost under low and high RSLR scenarios by the year 2100 within Matagorda Peninsula.

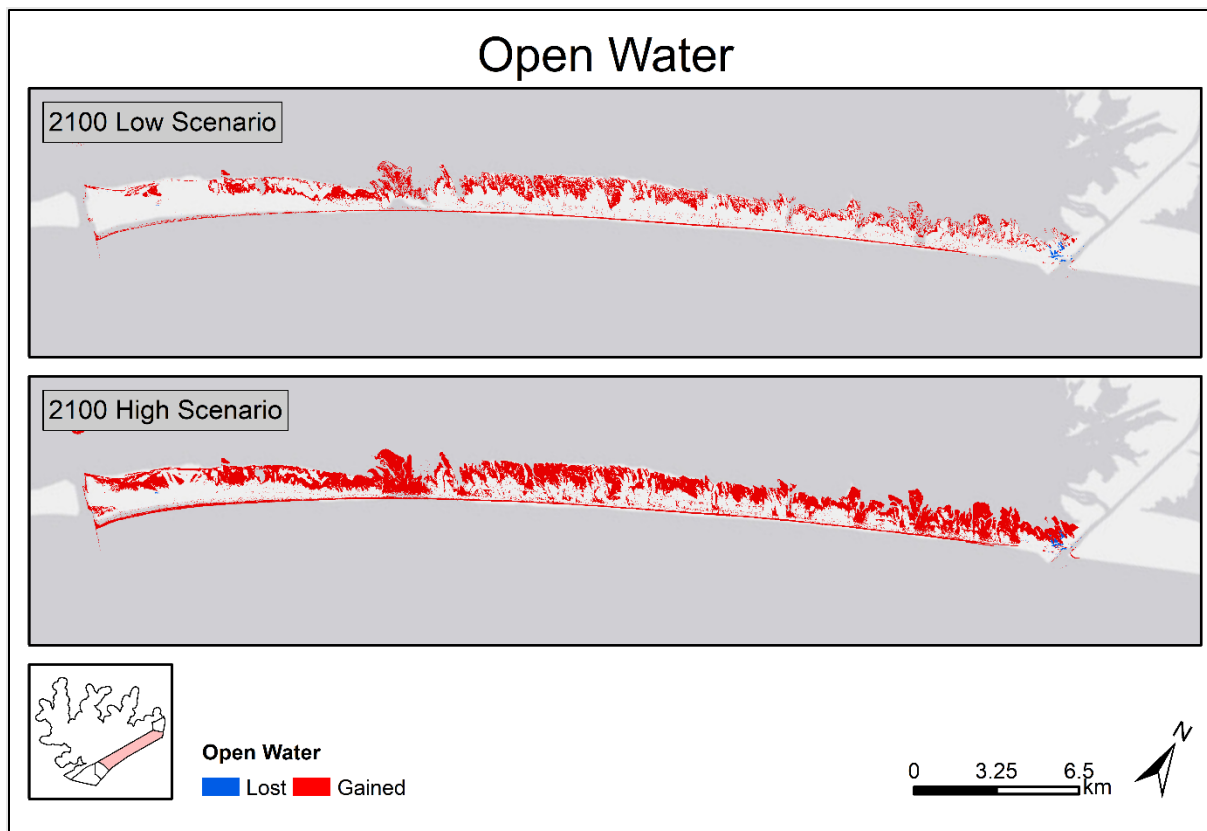


Figure 72. Map showing the extent of open water predicted to be lost under low and high RSLR scenarios by the year 2100 within Matagorda Peninsula.

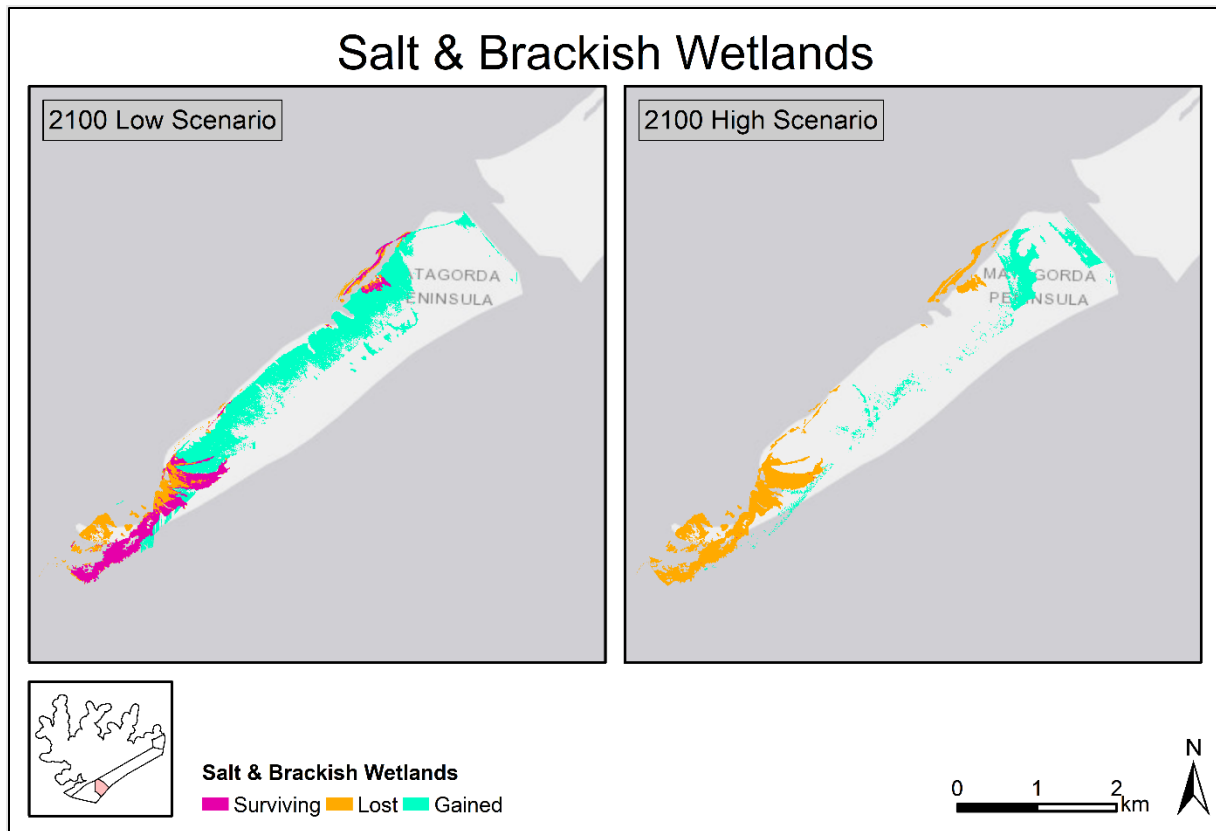


Figure 73. Map showing the extent of salt & brackish emergent wetlands predicted to be lost under low and high RSLR scenarios by the year 2100 within Pass Cavallo to Matagorda Ship Channel.

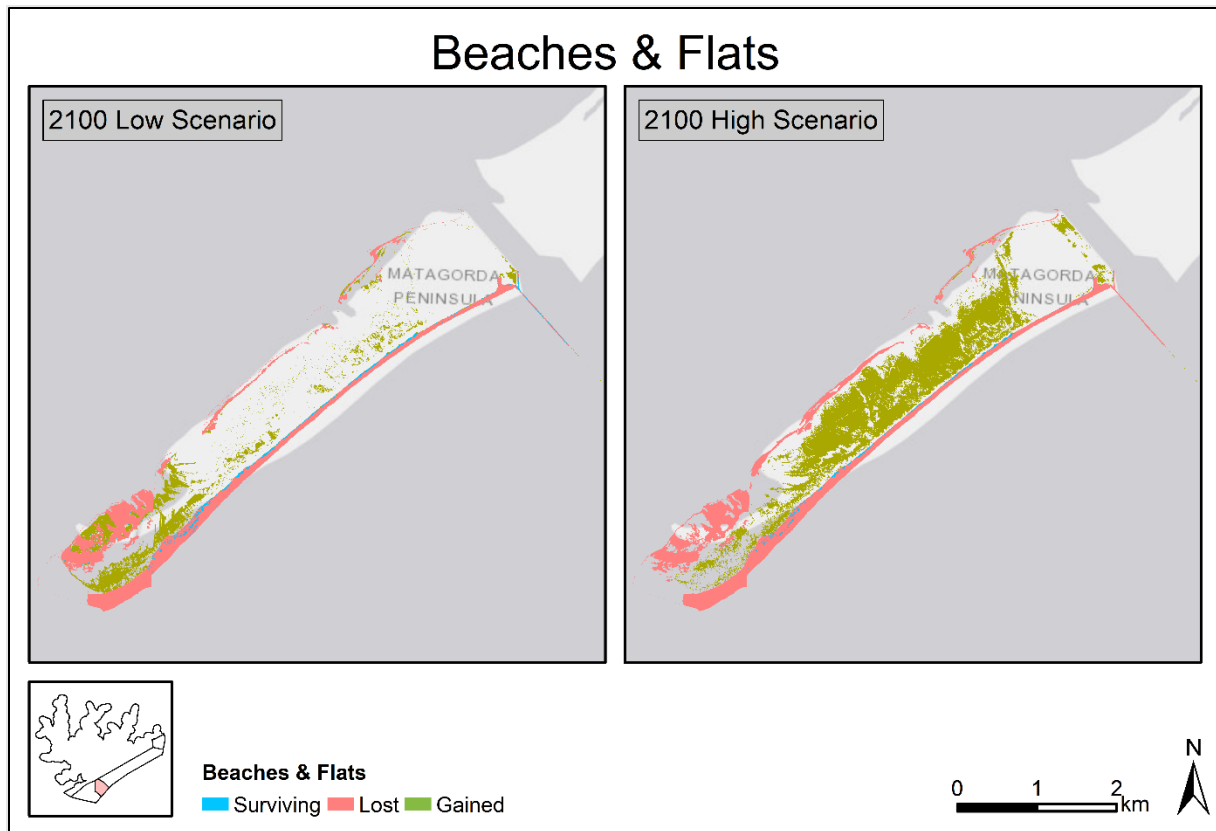


Figure 74. Map showing the extent of beaches & flats predicted to be lost under low and high RSLR scenarios by the year 2100 within Pass Cavallo to Matagorda Ship Channel.

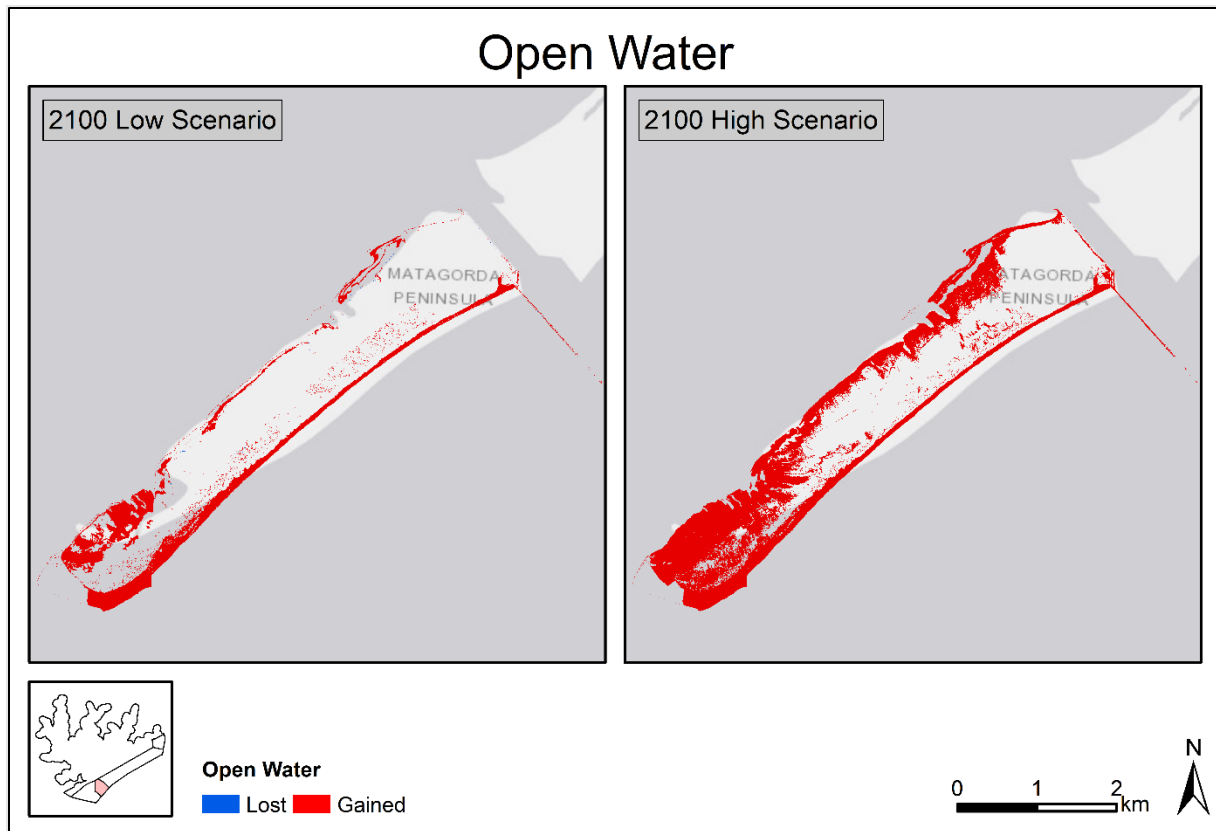


Figure 75. Map showing the extent of open water predicted to be lost under low and high RSLR scenarios by the year 2100 within Pass Cavallo to Matagorda Ship Channel.

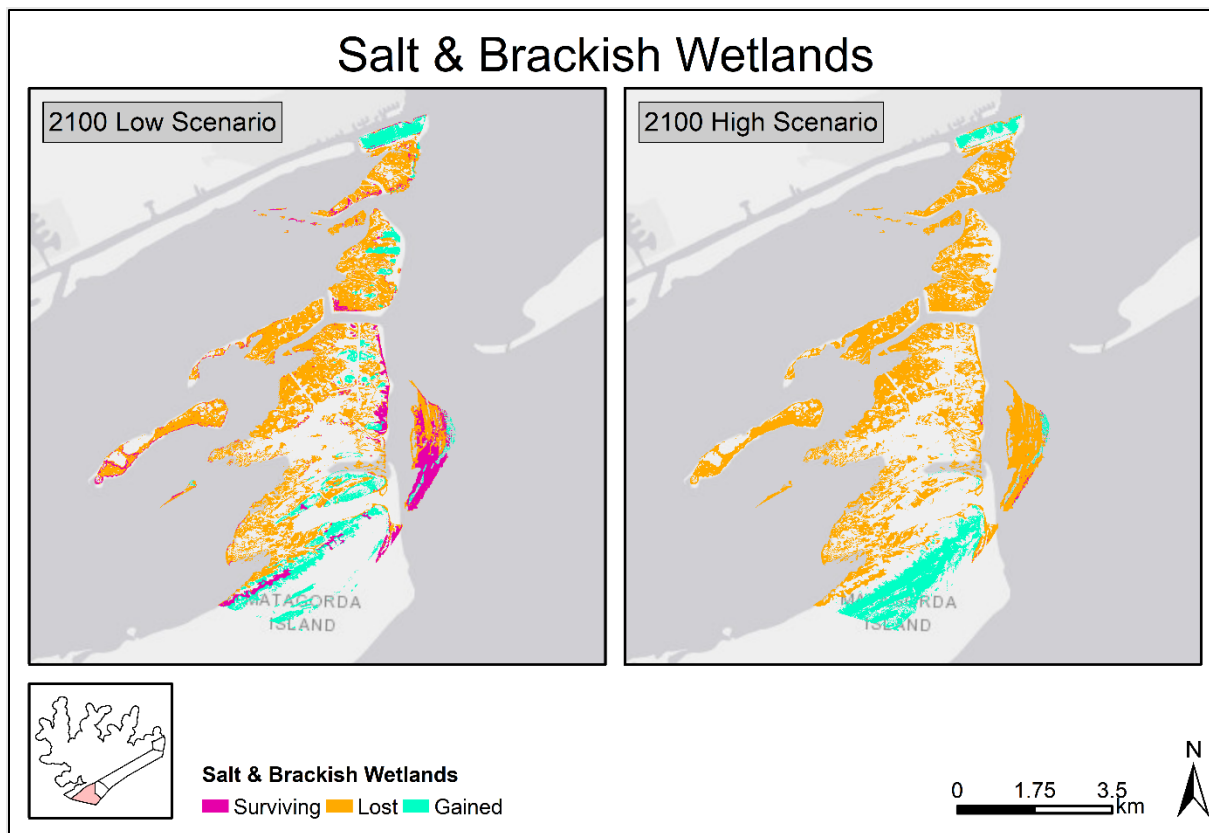


Figure 76. Map showing the extent of salt & brackish emergent wetlands predicted to be lost under low and high RSLR scenarios by the year 2100 within Matagorda Island.

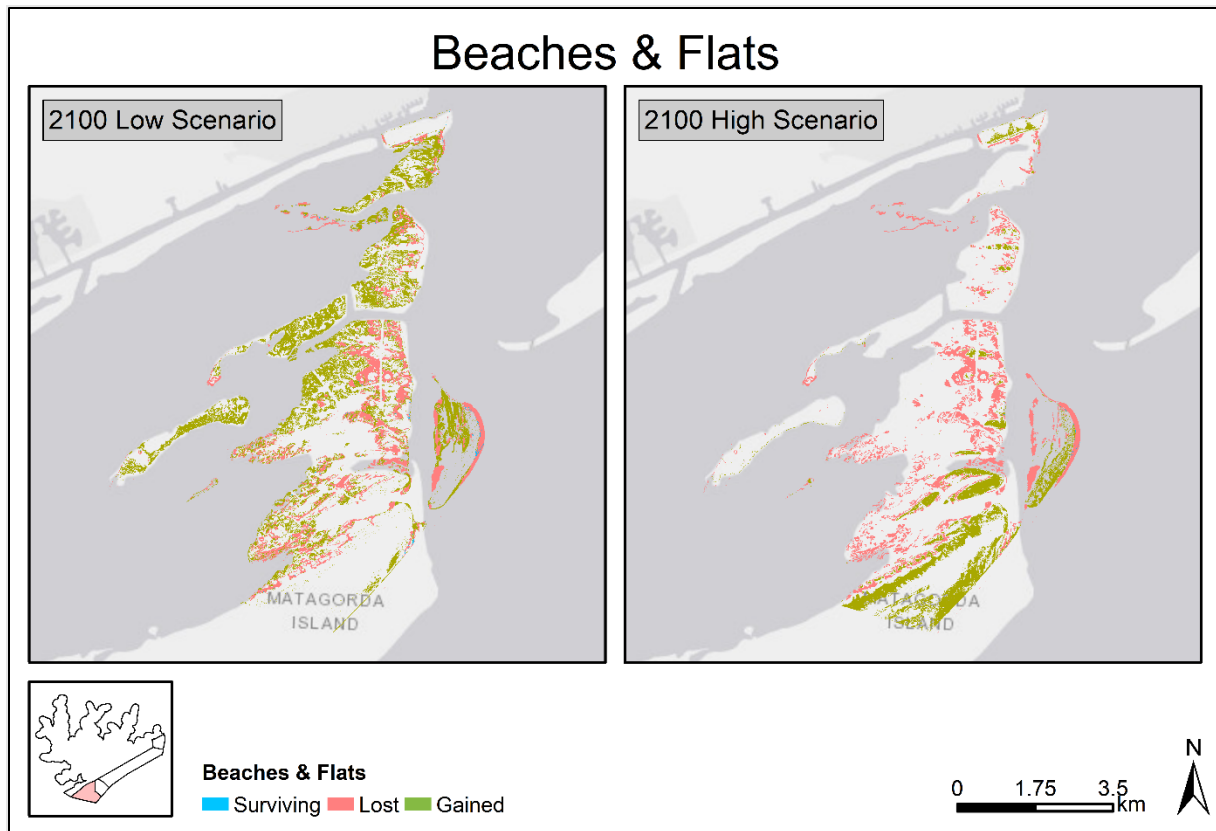


Figure 77. Map showing the extent of beaches & flats predicted to be lost under low and high RSLR scenarios by the year 2100 within Matagorda Island.

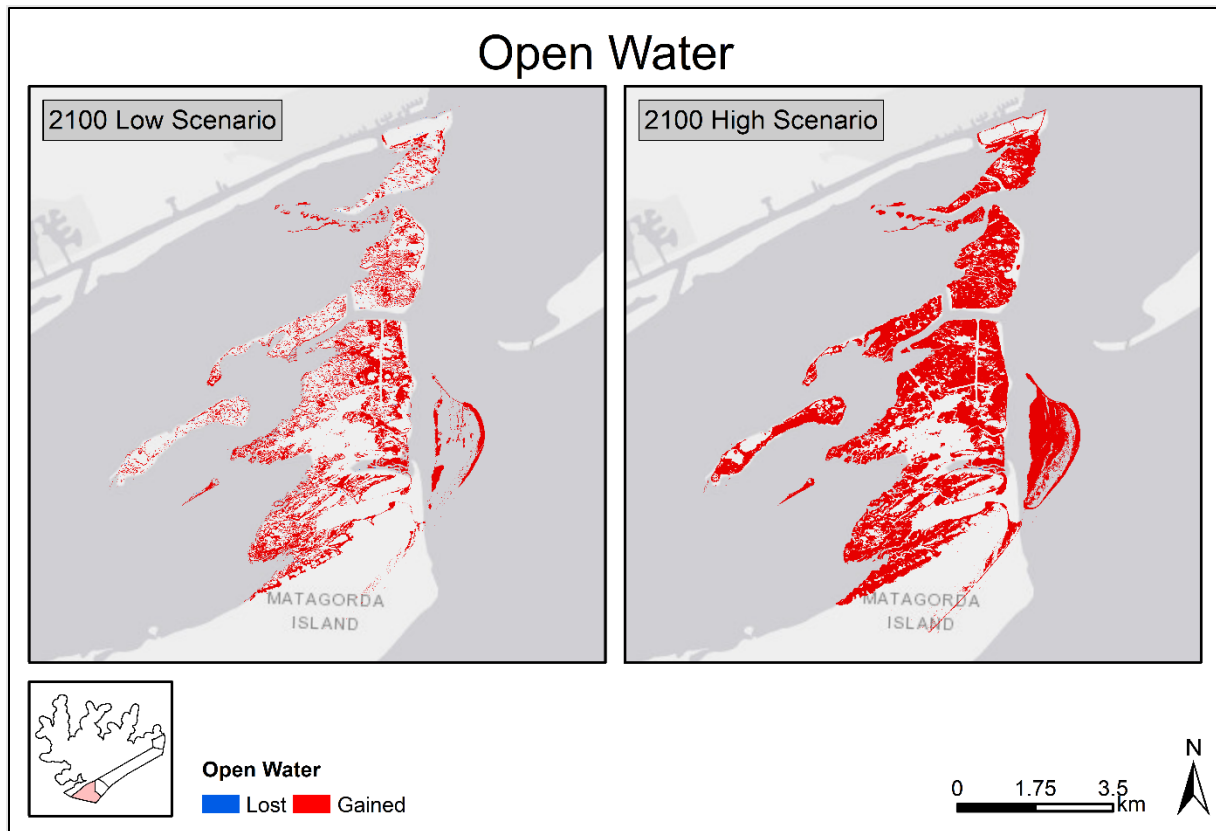


Figure 78. Map showing the extent of open water predicted to be lost under low and high RSLR scenarios by the year 2100 within Matagorda Island.

Seagrass Habitat

Potential seagrass beds in the project area were delineated from benthic habitat imagery coupled with the most recent accessible high-resolution imagery with sufficient water clarity and minimal cloud cover (Google Earth Pro 7.3.3.7786, 12/1/2018, Matagorda Bay, Eye alt 16,920 feet, accessed 7/6/2020). A draft map of potential seagrass beds was generated through geospatial imagery classification of the true color imagery using training samples of visible seagrass beds in Matagorda Bay and was then cleaned to remove terrestrial vegetation with similar pixel values, yielding approximately 2,130 acres classified as seagrass.

Methods

The potential seagrass area is almost entirely within the southwest corner of Matagorda Bay and along the back side of the barrier island and is similar to the area delineated as seagrass by TPWD in 2003. However, seagrass extent likely varies seasonally and annually depending on local salinity levels, freshwater inundation from major storms and other factors, so verification sampling was conducted across the delineated region. Sampling sites were generated by two processes. The potential seagrass area was divided into uniform 5-acre hexagonal polygons and 26 polygons containing delineated seagrass were randomly selected, with several additional “open” polygons in this near-shore area but containing no delineated seagrass also selected for sampling. Then transects were drawn running perpendicular to shore every thousand meters of the outer boundary of potential seagrass bed, creating 35 transect sampling sites (Figure 79). Biologists planned to sample supplemental sites along the delineated outer boundary of seagrass to establish presence/absence but were impeded by water depth and lack of visibility and reverted to the primary verification method after sampling 13 boundary trace sites.

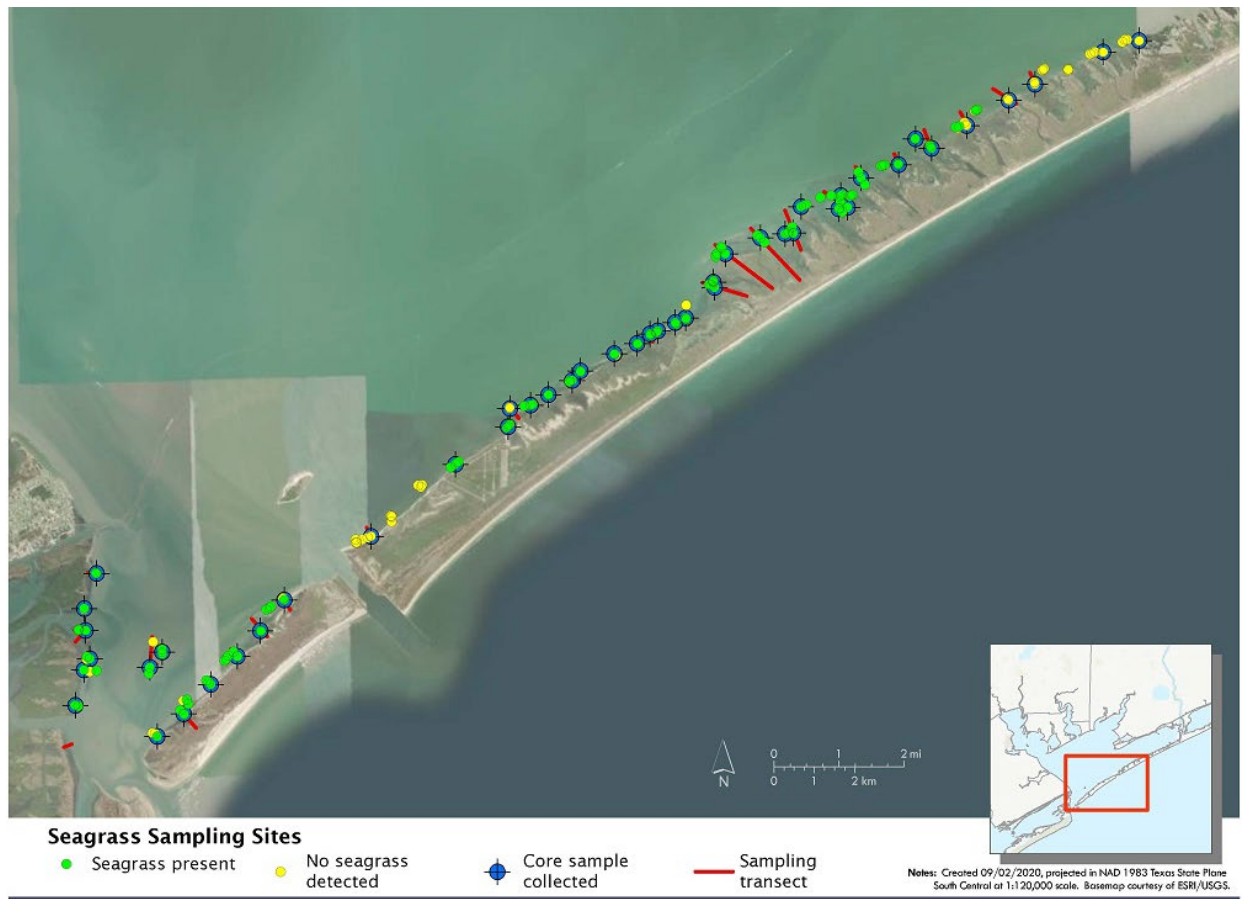


Figure 79. Seagrass Field Verification Sampling Locations and Transects.

During the week of August 10 through 14, biologists conducted seagrass sampling across the southwestern Matagorda Bay region. Sample sites were loaded onto a GPS-enabled tablet and Trimble GPS unit to navigate to sites and record precise sampling locations. At each transect, three samples were collected at intervals along the transect using a 1-meter square sampling plot and recording species presence, coverage across the plot, vegetation height, depth, and visibility (Figure 80). A core sample of the substrate was collected at each transect for use in stable isotope analysis (Figure 80). Sampling randomly selected 5-acre hexagons followed the same protocol with three samples collected at intervals across the site.



Figure 80. Identifying seagrass species coverage in the 1-m plot (left) and depositing substrate core sample into tray (right).

Results

In total, 204 seagrass samples were collected across 77 sites (35 transects, 29 five-acre sites, 13 boundary trace sites), with seagrass found within 136 samples across 51 sites. Shoal grass (*Halodule beaudettei*) was the dominant species across the entire area, followed by sea star grass (*Halophilla engelmannii*) and widgeon grass (*Ruppia maritima*). A few sites also contained large amounts of macroalgae and floating Sargassum was collected at a single site near the channels at the southwestern most extent of Matagorda Bay. 47 substrate core samples for use in stable isotope analysis at TAMU-CC.

Field sampling results were merged back into the potential seagrass beds derived from remote sensing and regions with no seagrass per sampling efforts were removed. Sites with seagrass were amended to reflect actual GPS locations of samples. The extent of seagrass beds was then divided into sections based on sampling sites, and species presence and density were generalized across that section based on species found at samples within the section and the mean density per square meter of these samples. As of mid-August 2020, seagrass beds across the Matagorda Bay study area were estimated to cover approximately 1,908 acres (Figure 81). A species breakdown and approximate intermixing per coverage area is provided in Figure 82.



Figure 81. Seagrass Coverage within Project Area in 2020.



Figure 82. Seagrass Species Breakout in Coverage Area.

Literature Cited

Louisiana Department of Wildlife and Fisheries (LDWF). 2012. Sampling Protocol for Projects in Public Oyster Areas. Pp. 6. Rev. January 1, 2012

Texas Parks and Wildlife Department (TPWD), 2020a. Recommended Survey Protocols for Oyster Habitat for Permitting Review of Pipeline Installation Project in Deep Waters (>2.5 feet). pp. 4

Texas Parks and Wildlife Department (TPWD), 2020b. Recommended Survey Protocols for Oyster Habitat for Permitting Review of Non-Pipeline Dredging Projects in Deep Waters (>2.5 feet). pp. 4

Sea Turtle Movement and Ecosystem Connectivity

Overview

Matagorda Bay was once the epicenter of a commercial sea turtle fishery that began in the mid-1800s and removed millions of pounds of sea turtles from Texas bays and estuaries, the Gulf of Mexico, and the wider Caribbean within a few decades. It has been more than 120 years since this commercial fishery crashed and eventually ceased to exist in Texas. Since then, multiple management and conservation measures have been implemented to save sea turtles from extinction. Most notable among these measures was the U.S. Endangered Species Act of 1973, which provided sea turtles with protection on land and at sea, and the 1990 federal requirement for U.S. fishing vessels to use turtle excluder devices (TEDs) in their nets to reduce the incidental capture and mortality of sea turtles.

Long-term research conducted by the Texas Parks and Wildlife Department (TPWD), as part of their in-water systematic gill net survey since 1980, has demonstrated increasing numbers of sea turtles in the west Matagorda Bay complex beginning in 1993 (the complex includes Lavaca Bay, Cox Bay, Keller Bay, Carancahua Bay, and Tres Palacios Bay). Prior sea turtle studies conducted in west Matagorda Bay in the 1990s and 2000s also demonstrated increasing numbers of sea turtles in the region. These studies identified the different sea turtle species living in the bay, some of the areas occupied by sea turtles, and their movements within and outside the bay. These foundational studies were small in scope, focused on sea turtles only, and provided critical biological information about the sea turtles in Matagorda Bay. Beginning in 2009, sea turtles were captured annually by the TPWD survey, the number of captures increased significantly, and the species captured were primarily green turtles (*Chelonia mydas*) and Kemp's ridleys (*Lepidochelys kempii*). Loggerhead sea turtles (*Caretta caretta*) and hawksbill sea turtles (*Eretmochelys imbricata*) were also captured in TPWD surveys, though in lower numbers. Collectively, these studies have demonstrated the importance of Matagorda Bay to threatened and endangered sea turtles.

The aim of the current study was to use an ecosystem-based approach to study the west Matagorda Bay ecosystem. While single-species studies provide key inputs on population demographic parameters and other valuable biological information, management without an in-depth understanding of the fundamental underlying ecological processes and stressors that interact to structure a resilient ecosystem may be ineffective. This first-of-its-kind study was designed to provide an in-depth understanding of the ecosystem that supports threatened and endangered sea turtles. Robust science on the estuarine ecosystem that supports sea turtles can enhance recovery and long-term sustainability of their populations. Data generated from an ecosystem-based approach are crucial to developing effective management and conservation strategies and can be used to identify and prioritize areas to protect for sea turtles within the estuarine complex.

Our overarching goal was to determine the spatiotemporal distribution of sea turtles in west Matagorda Bay to identify critical habitat within the bay, to determine if these habitats are used year-round or seasonally, to document sea turtle migration to other bay systems and the Gulf of Mexico, and to understand the environmental drivers of these migrations. We also sought to understand the ecological roles of the sea turtles in this estuarine complex, the health of the sea turtles, and the ecosystem processes that impact them and their survival outlook.

Introduction

Goals

Our overarching goal was to determine the spatiotemporal distribution of threatened and endangered sea turtles in west Matagorda Bay. Specifically, we were interested in examining the spatiotemporal distribution of threatened and endangered sea turtles in west Matagorda Bay. Seasonal changes in movement patterns and habitat use were analyzed to determine if sea turtles have seasonally and spatially divergent patterns of habitat use within west Matagorda Bay. We were also interested to determine if sea turtles spend more time near deeper waters (e.g., near the Gulf Intracoastal Waterway, Matagorda Ship Channel) during the winter months and show more dispersal to shallower waters during the summer. The influence of ecosystem processes on sea turtle habitat trends in west Matagorda Bay were believed to be influenced strongly by water quality variability and trends, a hypothesis we tested herein. Finally, we examined the functional roles that sea turtles have within the ecosystem and the linkages among these supporting habitats in Matagorda Bay.

Objectives

Several key questions were answered from sampling and data collection as a result of this study. Specifically, we determined if threatened and endangered sea turtles reside in Matagorda Bay year-round, or if they migrate to other bay systems and into the Gulf of Mexico and what the environmental drivers are of such movements. We also wanted to classify specific areas of west Matagorda Bay as important habitat for sea turtles and examine if the home range and habitat use of threatened and endangered species in Matagorda Bay is related to the particular types or quality of the habitats occupied. The ecological roles of sea turtles in these habitats was analyzed by determining where they feed and at what trophic level. The impact of seasonal and annual habitat variability (biological and physical characteristics) and its influence on the distribution, abundance, demography and movements of sea turtles was further examined. While handling the sea turtles, we were able to determine their overall health and nutritional state (e.g., epibiont load, body-condition-index, general obvious emaciation) and examine if seasonal and temporal changes affected their nutritional state. Finally, the distribution, abundance, demography and movements of sea turtles in west Matagorda Bay was compared to historically available data.

Prior Research

Estuaries represent one of the most productive aquatic ecosystems on the planet, and much of their function is derived from the plentiful habitat types that characterize these systems. Estuarine habitats such as seagrass meadows, tidal marsh, tidal flats, oyster reefs, and associated upland habitats support abundant and diverse communities and provide nursery habitat for many

economically and ecologically important species (Beck et al. 2001, Chambers 1992). These foundational habitats are essential components for estuarine systems that support marine life. Quantifying the availability of nursery and juvenile habitat is essential when determining the dynamics and structure of marine populations as these nurseries serve as hotspots of secondary production that support higher trophic levels (Connell and Jones 1991). Given that secondary production in these nursery habitats supports higher order consumers (sportfish, coastal birds, sea turtles, etc.), an improved understanding of the functional roles and linkages between habitats and the species that inhabit them is critical to the development of effective ecosystem-based restoration and conservation strategies. Unfortunately, for many species, including threatened or endangered, previous research has often focused on individual species, while often ignoring ecosystem processes that may be important drivers of population recovery, maintenance, or decline. Consequently, recovery plans for these species remain hindered by a lack of research supporting ecosystem-based management and conservation strategies. Thus, the principal goal of this project is to provide key scientific insight supporting these needs for these species of interest.

Species of Interest

Approaches to study sea turtles in the U.S. since the 1950s have relied heavily on data collected from long-term monitoring projects that studied adult females nesting at beaches (National Research Council 2010). In the 1990s, the need to study sea turtles in the water became widely recognized as a priority by the federal agencies with regulatory authority for these threatened and endangered species, who needed to delineate sea turtle critical habitat (Magnuson et al. 1990, National Marine Fisheries Service and U.S. Fish and Wildlife Service 1991a, 1991b, 1992, Turtle Expert Working Group 1998, 2000, U.S. Fish and Wildlife Service and National Marine Fisheries Service 1992). Great progress was made during the 1990s and 2000s to initiate in-water studies for sea turtles in U.S. waters. These studies established that inshore waters such as bays and estuaries provide important developmental habitat for sea turtles across the eastern seaboard and the Gulf of Mexico. Studies conducted in Texas inshore waters in the 1990s documented the distribution and abundance of threatened and endangered sea turtles and concluded that these waters are critical developmental habitat for juvenile sea turtles (Shaver 1994, Shaver 2000, Landry et al. 1997, Landry and Costa 1999, Landry et al. 2005, Renaud and Williams 2005, Metz and Landry 2013, Metz and Landry 2016). While these studies have provided important information about the occurrence and abundance of juvenile sea turtles in Texas inshore waters, their functional role in and use of these inshore ecosystems remain poorly known, and data are insufficient to define priority conservation areas for sea turtles. Unfortunately, these important first studies were discontinued a decade ago and only intermittent sampling has occurred at some of the study sites.

Since the 1990s, sea turtles in Texas waters have increased significantly. The best available data to document this is the increase in the number of Kemp's ridleys nesting in Texas annually (Shaver et al. 2016), and the nearly annual mass sea turtle stranding that occurs in the winter months when air and water temperatures decline rapidly and hundreds of green turtles become

immobilized by the cold temperatures (i.e. cold-stunning) (Shaver et al. 2017). Despite this increase in sea turtles in Texas, research, monitoring, and conservation of sea turtles in Texas and the greater Gulf of Mexico has not advanced as far as it has in other regions, nor as quickly as needed (Bjorndal et al. 2011, Plotkin et al. 2016).

Texas beaches, bays and estuaries, and Gulf of Mexico waters are essential habitat for five sea turtle species: loggerhead (*Caretta caretta*), Kemp's ridley (*Lepidochelys kempii*), green (*Chelonia mydas*), hawksbill (*Eretmochelys imbricata*) and leatherback (*Dermochelys coriacea*). Sea turtles nest on Texas beaches, they live inshore, nearshore, and in the open ocean, and all life stages migrate through these waters.

Loggerhead sea turtle (Caretta caretta):

The loggerhead sea turtle occurs in all the world's oceans ranging from temperate to subtropical regions (Plotkin 2003). Loggerheads are broadly distributed in U.S. waters. They occur hundreds of miles out to sea, as well as in bays, lagoons, salt marshes, creeks, ship channels, and the mouths of large rivers. The Gulf of Mexico provides critical habitat for post-hatchling, juvenile and adult loggerheads (Amos and Plotkin 1990, Plotkin et al. 1993, Plotkin 1996, NMFS and USFWS 2008, Hart et al. 2012, 2013). Like most sea turtle species, post-hatchling and small juvenile loggerheads occur in oceanic waters, where they feed near or at the surface of the water column. As they mature, small juvenile loggerheads migrate to nearshore waters, become benthic feeders (e.g., crabs), and as adults typically migrate seasonally north to south along the coastline (Plotkin 2003, Plotkin and Spotila 2002).

The status and abundance of loggerheads in Texas waters is poorly known. Loggerheads were once the most abundant sea turtle in Texas waters (Rabalais and Rabalais 1980, Hildebrand 1982), but for many years, little was known about them because they rarely nest on Texas beaches. Research was therefore limited to studies on loggerheads that washed ashore (Rabalais and Rabalais 1980, Hildebrand 1982, Plotkin and Amos 1988, Plotkin et al. 1993, Plotkin 1996), that were visible from oil-production platforms (Rosman et al. 1987), jetties (Metz and Landry 2013), or aerial surveys (Fritts et al. 1983), and from one in-water study conducted in the 1990s and early 2000s (Landry and Costa 1999).

Small juvenile loggerheads regularly occupy inshore waters along the eastern seaboard (Hopkins-Murphy et al. 2003), but they do not appear to be abundant in Texas bays and estuaries. Only a few captures of loggerheads have been reported in Texas inshore waters (Landry et al. 1997), and their use of these inshore habitats remains very much in question.

Kemp's ridley sea turtle (Lepidochelys kempii):

The Kemp's ridley sea turtle has a restricted distribution compared to most other sea turtle species (Plotkin 2003, Morreale et al. 2007). Adults occur primarily in the nearshore waters of the Gulf of Mexico (Manzella and Williams 1992, Plotkin 2003, Shaver and Rubio 2008, Seney and Landry 2011, Shaver et al. 2013, Hughes and Landry 2016). Nesting occurs predominantly on the beaches of the western Gulf of Mexico, primarily in Tamaulipas, Mexico with some nesting also occurring in Veracruz, Mexico and south Texas (Shaver et al. 2016). Post-hatchling and juvenile Kemp's ridleys are broadly distributed throughout the Gulf of Mexico and

southeastern U.S. waters, where small juveniles regularly occupy inshore waters from New England to Texas (Manzella and Williams 1992, Morreale et al. 2007).

The Kemp's ridley is still considered critically endangered (NMFS et al. 2011), but its abundance in Texas waters has increased significantly since the population decline in the mid-1980s when it reached a low point. The number of adult females nesting in Mexico and Texas has increased significantly since then (Gallaway et al. 2016, Shaver et al. 2016). We do not know if there has been a corresponding increase in juvenile Kemp's ridleys in Texas inshore waters because there has not been a consistent effort to study sea turtles there since the early 2000s (Metz and Landry 2016). The Lavaca-Matagorda Bay system was identified as an important developmental habitat for juvenile Kemp's ridleys (Landry et al. 1997, Landry and Costa 1999, Landry et al. 2005), and more recent studies indicate Matagorda Bay still provides important habitat for the species including prey resources (Seney and Landry 2011, Metz and Landry 2016).

Green turtle (Chelonia mydas):

Green turtles occur throughout the tropical and subtropical oceans of the world (Plotkin 2003). As adults, green turtles are primarily herbivorous and most often reside in association with seagrass beds. Green turtles nest on tropical beaches worldwide, but relatively little nesting occurs in the U.S. Gulf of Mexico. Sporadic nesting occurs on south Texas beaches. There are several major nesting beaches located along the Mexico coast from Tamaulipas, Mexico (Jaime Peña, personal communication) through the Yucatán Peninsula (SWOT 2010, Zavaleta-Lizárraga and Morales-Mávil 2013, Uribe-Martínez et al. 2021). Historically, adult green turtles were very abundant in Texas' bays and estuaries. These turtles were fished extensively in the 1890s, and by the early 1900s this commercial fishery based in Aransas Bay, Matagorda Bay, and the lower Laguna Madre collapsed (Doughty 1984).

Juvenile green turtles are now the most abundant sea turtle in Texas waters. Hatchling green turtles from beaches in Florida, Mexico, and the wider Caribbean spend their first few years in oceanic waters and as they mature, they return to nearshore areas, associate with jetties for some time, and then enter the bays and estuaries where they feed on algae and seagrasses. Several studies have documented the distribution and abundance of green turtles from Sabine Pass in north Texas down to the Port Mansfield Channel in south Texas and in the Laguna Madre (Shaver 1994, Landry and Costa 1999, Metz and Landry 2013). Studies conducted in Lavaca-Matagorda Bays indicated juvenile green turtles are using the bays, but their abundance there is lower than in other bay systems in Texas and the Laguna Madre (Metz and Landry 2013). Recent cold-stunning events in Texas suggest that there are a very large number of juvenile green turtles inhabiting the inshore waters of Texas and despite their growing numbers, relatively little is known about their role in these inshore ecosystems.

Hawksbill (Eretmochelys imbricata):

Hawksbills are widespread, occurring in the tropical and subtropical seas of the Atlantic, Pacific, and Indian Oceans (Plotkin 2003). Like most sea turtle species, post-hatchling and small juvenile hawksbills occur in oceanic waters where they feed near or at the surface of the water column. As they mature, they return to nearshore areas and become resident near coral reefs,

rocky areas, other hard bottom habitats, seagrass and algae beds, shallow coastal areas, lagoons and oceanic islands, narrow creeks, and mangrove bays where they feed on sponges, corals, algae, soft coral and other prey. In the Gulf of Mexico, adult hawksbills nest mostly on Yucatán Peninsula beaches in the southern Gulf (Cuevas et al. 2010). Hatchlings from this nesting beach are carried by the current through the Yucatán Channel north into the Gulf of Mexico and post-hatchlings and juveniles are frequently found stranded on Texas beaches (Amos 1989, Amos and Plotkin 1990), or swimming in passes near jetties (Amos 1989, Shaver 1994, Plotkin, personal observation). Hawksbills have not been documented in Texas inshore waters and their use of these inshore habitats remains an open question.

Leatherback (Dermochelys coriacea):

Leatherbacks are cosmopolitan and range globally (Plotkin 2003). This species has the widest distribution, reaching into subarctic waters as far north as Alaska and Norway and as far south as Cape Agulhas in Africa and the southernmost tip of New Zealand. It is also found in all tropical and subtropical oceans, and nests on beaches in these regions. There is very little leatherback nesting in the Gulf of Mexico. Leatherback distribution and abundance is poorly known in the Gulf of Mexico. The species feeds primarily on jellyfish and other gelatinous invertebrates; it has been documented in association with dense concentrations of jellyfish (Leary 1957), occurs primarily in deep waters far from land, and is not known to occur regularly within inshore waters in any part of its range. As such, we know very little about the post-hatchling and juvenile leatherback life stages and we know virtually nothing about adult males and the locations of their breeding areas.

Methods

Permits

We applied for and obtained all of the required federal and state permits to conduct scientific research on threatened and endangered species before we began the field research component of this project. We also obtained approval from the Texas A&M University Institutional Animal Care and Use Committee (IACUC) which governs the use of vertebrate animals in research studies at the university. We received these permissions in 2019 (Table 14) and were restricted to very specific methods including where we sampled, when we sampled, how we sampled and with whom we sampled. All research activities reported herein were conducted pursuant to approved Animal Use Protocol (AUP) No. 2019-0001, Texas Park and Wildlife Department (TPWD) Permit No. SPR-0219-021, and National Marine Fisheries Services (NMFS) Permit No. 18029 and 22822/22822-01/22822-02.

Table 14. List of permits issued to conduct research activities on sea turtles in Matagorda Bay. AUP: Animal Use Protocol; IACUC: Institutional Animal Care and Use Committee; TPWD: Texas Park and Wildlife Department; NMFS: National Marine Fisheries Services

Issuing agency	Permit Number	Permit holder	Timeframe	Purpose
TAMU AUP IACUC	2019-0001	Dr. Pamela Plotkin	Mar 13, 2019 – Mar 23, 2022	To establish the protocols to be used when capturing and handling sea turtles
TPWD	SPR-0219-021	Dr. Pamela Plotkin	Feb 8, 2019 – Oct 16, 2019	Permit issued to Dr. Pamela Plotkin to live-capture (entanglement netting, bottom trawl) sea turtles in West Matagorda Bay, sample tissue (skin/scute), attach tags (Iridium satellite transmitters, coded acoustic transmitters), and release unharmed at capture site for scientific purposes.
	SPR-0219-021	Dr. Pamela Plotkin	Oct 17, 2019 – Sep 24, 2020	Modification to add Dr. Christine Figgenger as Subpermittee
	SPR-0219-021	Dr. Pamela Plotkin	Sep 25, 2020 – Sep 24, 2020	Modification to add Dr. Natalie Wildermann as Subpermittee
	SPR-0219-021	Dr. Pamela Plotkin	Apr 9, 2021 – Feb 8, 2022	Modification to add Quentin Hall, Jeffrey Kaiser, Jason Williams as Subpermittees
NMFS	18029	Dr. Tasha Metz	June 4, 2019 – Sep 26, 2019	Dr. Pamela Plotkin added as permit Co-PI
	22822	Dr. Pamela Plotkin	Sep 26, 2019 – Jan 1, 2020	Permit issued to Dr. Pamela Plotkin (PI) to determine the spatiotemporal distribution of sea turtles in Matagorda Bay, Texas
	22822-01	Dr. Pamela Plotkin	Jan 2, 2020 – July 7, 2021	Modification to add Dr. Natalie Wildermann as permit Co-PI
	22822-02	Dr. Pamela Plotkin	July 8, 2021 – Dec 31, 2021	Modification to increase annual catch quota of green turtles, which had been reached by May 31, 2021

Study area

We focused our efforts on the south-western region of Matagorda Bay, between Magnolia Beach (28.562178°N, -96.541145°E) and Green Fields (28.499641°N, -96.239034°E). Several species of sea turtles (i.e. green turtles, Kemp’s ridley turtles and loggerhead turtles) were previously recorded in the area by researchers (Landry et al. 1997, Renaud and Williams 1997, Metz, 2004, Metz and Landry 2013, Metz et al. 2020) and during the current study by citizen scientists using the iSeaTurtle app (see Outreach section for further details). Matagorda Bay is the third largest estuarine system in Texas with an approximate surface area of 1,093 km². It is a shallow bay system with average depths of 2-2.5 m, and mostly mud/sand bottom with some patchy areas of seagrass (mainly shoal grass, *Halodule beaudettei*; star grass, *Halophila engelmannii*; and widgeon grass, *Ruppia maritima*) and some oyster reef patches (Ward and

Armstrong 1980, Pulich and Calnan 1999, TPWD 2022, BIO-WEST this study). The bay connects to the Gulf of Mexico through two channels located in the western end of the bay, namely Pass Cavallo and the Matagorda Ship Channel (MSC) that serve the ports of Port O'Connor and Port Lavaca. Pass Cavallo is a shallow natural inlet west of the MSC, while the MSC is a 11.5 m deep and 91 m wide entrance channel that extends through an inlet fringed by jetties (Lambert et al 2013). Sea turtles are commonly sighted feeding between the rocks in these jetties. Matagorda Bay represents an important resource for the local and regional economy, with commercial fisheries (e.g., shrimp, oysters, blue crabs, finfish), recreational and sport fisheries as primary activities (Harte Research Institute for Gulf of Mexico Studies 2016). There is a relative lack of urban and industrial development around Matagorda Bay compared to other estuarine systems in Texas, which has likely favored the maintenance of healthy ecosystems in the bay (Ward and Armstrong 1980).

Historical sea turtle captures

Historical sea turtle catch data from Matagorda Bay were obtained from the TPWD coastwide fisheries-independent surveys conducted as part of their Coastal Fisheries Resource Monitoring Program. Data generated by this program are collected using a stratified cluster sampling design; each bay system and Gulf area serves as non-overlapping strata with a fixed number of samples per month or season. Sample locations are drawn independently and without replacement for each combination of gear, stratum, and month (season) (Martinez-Andrade 2015).

We analyzed the gill net survey data for west Matagorda Bay from 1980 – 2021 to determine the historical catch per unit effort of sea turtles, the locations of these captures, the species captured, and the size of the captures. This area included all saltwater bayous, between the surf line from the eastern edge of the lower Colorado River (below the Gulf Intracoastal Waterway) to the eastern edge of the Chain of Islands in Pass Cavallo and the lower portion of the Tres Palacios and Lavaca Rivers. Gill nets were set each spring and fall in west Matagorda Bay perpendicular to the shoreline. Gill nets covered the water column from the bottom to as much as 1.2 m above the bottom, measured 182.9 m in total length, were constructed of four continuous 45.7 m long panels with stretched mesh monofilament webbing sizes of 152 mm, 127 mm, 102 mm, and 76 mm, with the smallest mesh deployed nearest the shoreline. Gill nets were set 1 h before sunset, fished overnight, and retrieved within 4 h of sunrise the following day. There were 90 samples collected per year. Sea turtles captured were identified to species and the maximum curved carapace length was measured.

Sea turtle sampling plan

The initial sampling plan included two types of methods to capture sea turtles in Matagorda Bay: entanglement netting, and if permitted by the National Oceanic and Atmospheric Administration (NOAA), bottom trawling without a turtle excluder device (TED) in the net and brief tow time (<30 minutes). The latter was not permitted, thus we relied only on entanglement netting. We planned on capturing juvenile sea turtles in locations where previous studies had successfully captured sea turtles in Matagorda Bay (Landry et al. 1997, Metz and Landry 2016).

In order to address our hypotheses, it was crucial to attach 20 satellite and 12 acoustic transmitters to sea turtles in years 1 and 2 of the study. Thus, our goal was to sample as often as possible to catch the necessary number of turtles. In addition, the type of transmitter used and the number of transmitters attached to each turtle depended on the size of the turtle (as specified by our NOAA ESA permit). Ideally, we would have attached a satellite and an acoustic transmitter to each turtle. However, we were limited to the combined weight of the transmitters and attachment not exceeding 5% of the turtle's body weight. Therefore, our plan needed to be flexible to stay within this guideline. Larger turtles captured could receive both transmitters, and smaller turtles could receive only one type of transmitter.

Sea turtle capture and handling

Net setting

We set two entanglement nets in nearshore waters between Magnolia Beach (28.562819°N, -96.541863°E) and Green Fields (28.499641°N, -96.239034°E) for 2 to 8 hours and monitored them continuously for sea turtle capture from a Carolina Skiff flat-bottom boat with 3 to 5 observers. To minimize incidental capture of other protected species (i.e. bottlenose dolphins, *Tursiops truncatus*), nets were only set if no dolphins were observed in the vicinity of the area and monitored constantly for the presence of this species.

The entanglement nets were set in line next to each other and were 91.4 m long each, 2.7–4.9 m deep with 12.7–25.4 cm bar mesh of No. 9 twisted nylon. We attached highly visible buoys to the float line of each net spaced at intervals of every 20 m or less, and visually monitored the float line continuously for movement. The net was checked immediately upon movement of the float line; otherwise, it was checked at intervals of no more than 30 minutes or no more than 20 minutes if the water temperature was $\leq 10^{\circ}\text{C}$ or $\geq 30^{\circ}\text{C}$. To check the net, we pulled up on the top line of the net until the full depth of the net was viewed along its entire length as an indicator that an animal had hit the net.

Turtle handling

As soon as a turtle was captured in the net, it was immediately removed from the net by hand, brought on board the boat, and restrained in a small plastic pool for data collection and to assess its overall health. The purpose of restraint was to prevent injury to turtles during data collection, sample collection and transmitter attachment and to minimize stress. If the turtle was in good condition, we arranged a shaded workstation either on the boat or on the nearest beach, depending on weather conditions and staff availability. We handled sea turtles always using non-sterile disposable gloves and covered the head and flippers with wet towels to keep the turtles moist. After releasing a sea turtle, we cleaned and disinfected all surfaces that came in contact with the animal and changed the wet towels.

Handling of turtles with fibropapillomatosis

Fibropapillomatosis is a viral disease that affects sea turtles, especially green turtles, causing tumors called fibropapillomas (FPs) to grow on the external tissues and skin of the animals (Herbst 1994, Page-Karjian 2019). To minimize exposure and cross-contamination between turtles with and without FPs, we exercised all possible safety measures including the use of

disposable gloves and thoroughly disinfecting all items that contacted turtles with FP with a 10% bleach solution between the processing of the animals. When working with turtles with FPs, we assessed the location and degree of FPs (as per Shaver 2019) to decide whether we could attach a transmitter or not. We only attached a transmitter if the turtle with FP was in very good apparent health condition, with a maximum of Grade 1 FPs located in non-critical areas (i.e. not on eyes).

Data collected from captured sea turtles

We recorded standard morphometric measurements for sea turtles as required by the Cooperative Marine Turtle Tagging Program (CMTTP) managed by the Archie Carr Center for Sea Turtle Research (ACCSTR). We used calipers to record standard straight carapace length notch-to-tip (SCL \pm 0.1 cm), straight carapace width (SCW \pm 0.1 cm) and straight carapace depth (SCD \pm 0.1 cm), a flexible measuring tape to record standard curved carapace length notch-to-tip (CCL \pm 0.1 cm) and curved carapace width (CCW \pm 0.1 cm), and a digital postal scale to record body weight (\pm 0.1 kg) of each sea turtle. We marked each sea turtle with two Inconel tag Style 681 (National Band and Tag Company), by thoroughly cleaning and disinfecting the second large scale on the posterior edge of each front flipper with betadine scrub followed by 70% isopropyl alcohol and then cinching the tag on the flippers. Every sea turtle was photo-documented throughout the data collection, transmitter attachment and release process.

Skin samples were collected for stable isotope analysis, by cleaning the surface of the skin in the “shoulder” area using betadine followed by alcohol prep pads prior to sampling. We used a sterile 6-mm biopsy punch to collect one skin sample to the depth of the ~epidermis/dermis on just one side of each turtle. Each skin sample was placed in a single vial in 70% ethanol and properly labeled. Following skin biopsy, we applied betadine solution followed by 70% alcohol and an antibacterial ointment to the shoulder area of the turtle. In addition, fecal material was collected from turtles if they naturally expressed material while in the workstation.

Data collected from stranded turtles

Between February 13-17, 2021, Winter storm Uri brought extreme cold temperatures to Texas. As a result, thousands of sea turtles stranded along the Texas coast. On February 20-21 and 27-28, 2021, we worked with TPWD staff to survey the coast between Port O'Connor (28.450950°N, -96.400671°E) and Green Fields (28.499641°N, -96.239034°E) in Matagorda Bay by boat searching for stranded sea turtles. We photo documented each sighting and when possible, recorded presence/absence of flipper tags, passive integrated transponder (PIT) tags, fibropapillomas, and measured SCL, SCW, SCD, CCL and CCW. After assessing the state of the turtle, if it was determined that it was deceased, we obtained skin samples from the neck and/or flippers for genetic and stable isotope analyses. In addition, we performed a necropsy on 18 turtles to identify the sex of the individual and collect, when possible, samples from the skin, muscle, blood and the gastrointestinal tract for stable isotope and/or per- and polyfluoroalkyl substance (PFAS) analyses. We provided the stranding data to the Texas State Coordinator of the NOAA's Sea Turtle Stranding and Salvage Network (STSSN).

Satellite and Acoustic Transmitters

Selection of satellite transmitters

Based on successful previous experience with transmitters using the Iridium satellite constellations (Figgner et al. 2018), four transmitters from the manufacturer Telonics, Inc. were tested. The Iridium system has been operating since 1998, is used by the military and commercial GPS phone providers, consists of 66 cross-linked satellites in low earth orbit, and provides continuous (24/7) coverage world-wide. The Telonics GPS-Iridium transmitters use the Short Burst Data (SBD) Service on the Iridium Satellite Network to transmit the data and are designed for marine animals that spend very little time at the surface and can obtain the data necessary to calculate a GPS position with an accuracy of 9-12 m in as little as 3 seconds. Two units were the experimental SeaTrkr-4170-4 Iridium transmitter, which is a smaller model measuring 5.6 x 3.5 x 3.1 cm and that weighs only 85 g. The two other units were the larger SeaTrkr-4370-4 model, measuring 10.3 x 4.5 x 3.6 cm and weighing 190 g. These transmitters are designed with internal antennas, so there is no need for an external whip antenna, which is subject to breakage and a point of weakness in many transmitters.

Unfortunately, the Telonics transmitters did not perform well on sea turtles in Matagorda Bay, likely due to the behavior of the turtles in the study area (i.e., juvenile sea turtles tend to spend longer periods submerged, surfacing very briefly – less than the 3 seconds needed for the transmitter to connect to the satellite constellation). Thus, we compared other available transmitters in the market in April 2020. We compared different models from three manufacturers (i.e., Wildlife Computers, Lotek NZ Ltd, and Telonics, Inc.) based on dimensions, weight, type of data transmitted (e.g., ARGOS, GPS, Iridium), operational life and costs (e.g., unit price, transmission costs) (Appendix B). After multiple communications with the manufacturers and careful consideration, we selected Lotek transmitters, model F6G 276F. These transmitters are FastGPS Argos-linked transmitters, that provide both ARGOS (lower resolution) and GPS (high resolution) locations needed to assess sea turtle positions and movements at a very fine scale. The transmitters were also smaller (dimensions were 10.1 x 4.4 x 3.2 cm and weight 144 g) than the Telonics SeaTrkr-4370-4 model, allowing us to attach the instrument on smaller turtles (minimum 30 cm SCL). While the Lotek transmitters do have a whip antenna, they also have sacrificial bumps on top of the tag that protect the antenna from breaking. Locations collected by the Lotek F6G 276F model are transmitted through the ARGOS satellite system, with coverage provided in North America by the Woods Hole Group, Inc. (formerly CLS America). This system is made up of a constellation of 8 polar orbiting satellites at an altitude of 850 km, completing an orbit around Earth approximately every 100 minutes. FastGPS transmitters have the advantage to be accurate, they can collect GPS locations in a fraction of a second, store these locations and transmit them during subsequent surfacing events. The transmitters were programmed to sample six locations per day every four hours at: 01:00:00, 05:00:00, 09:00:00, 13:00:00, 17:00:00, and 21:00:00 UTC, a re-try transmission schedule with transmission interval of 15 seconds and daily transmission limit of 207 ARGOS locations, and history (the rotating log of transmittable data) of the last 6 samples (which covers last ~36

hours). After successfully testing five transmitters and receiving above satisfactory data, we ordered 10 additional transmitters with the same configuration.

We partnered with the U.S. Animal Telemetry Network (ATN) to make the data from the satellite transmitters publicly available on the ATN Portal (<https://portal.atn.ioos.us>), in exchange for the ATN covering all fees associated with ARGOS transmission (i.e., \$63.00 per month per transmitter).

Selection of acoustic transmitters

Our intent was to use the acoustic transmitters as 1) a secondary method of location data collection in the event a satellite transmitter became detached or failed, 2) to collect sea turtle location data outside of the 6 transmission periods programmed in the satellite transmitters, and 3) to monitor movements of sea turtles too small to equip with a satellite transmitter. We deployed two different acoustic transmitter models (Innovasea Systems, NS, Canada): V13-1x-069k-1 (2 units; 3.6 x 1.3 cm; 11 g in air, 6.3 g in water) and V16-4x-069k-2 (10 units; 6.8 x 1.6 cm, 24 g in air, 10.3 g in water). Each transmitter emits a uniquely-coded 'pulse train' on a pseudo-random repeat rate of 40-80 seconds at a frequency of 69 kHz. The expected battery life of the V13 model was 817 and 331 days on low and high-power mode, respectively, and of the V16 model was 1613 days on high-power mode.

An extensive spatial array of 23 acoustic monitoring receivers were strategically-placed in Matagorda Bay to passively track sea turtles equipped with acoustic transmitters (Figure 83). Receivers (VR2W-69 kHz and VR2Tx; 30.8 x 7.3 cm, 1190 g in air, 50 g in water; Innovasea Systems, NS, Canada) were deployed primarily in seagrass habitats where sea turtles are likely to forage and channel and pass areas to monitor for ingress and egress from Matagorda Bay. Receivers were mounted subsurface on channel markers (with U.S. Coast Guard approval) and PVC pipes driven into the substrate. One receiver was deployed at Chester Island (28.455°N, -96.343°E) and a VR2AR Acoustic Release receiver (40.1 x 8.1 cm, 2350 g in air, 500 g in water; Innovasea Systems, NS, Canada) was deployed near the entrance of the MSC in the Gulf of Mexico (28.413°N, -96.318°E); however, we were unable to recover these receivers and therefore these receivers were excluded from further analysis. Of the remaining 21 acoustic receivers, one located at Halfmoon Reef (MB5) and another positioned at the entrance to Saluria Bayou (MB23) had temporal overlap with only the first two acoustically-tagged turtles (Cm5 and Cm6). Receivers record the unique identification number and date and time of detection from successfully decoded pulse trains as a tagged sea turtle travels within the receiver detection range. Previous range tests by Dr. Wells' Lab at Half Moon Reef in Matagorda Bay indicated a 50% detection rate at a distance of 183 m (range at which 50% of transmitter signals are detected by a receiver; TinHan et al. 2018). Acoustic receivers were retrieved, downloaded, and cleaned of biofouling approximately every 6 months. Additional acoustic receivers positioned along the Texas coast are maintained by Dr. Stunz as part of the Texas Acoustic Array Network (TEXAAN), a permanent observation system for documenting the movement patterns and habitat for a host of acoustically tagged species associated with Texas' coastal waters. Furthermore, Drs. Rooker and Wells maintain acoustic receiver arrays inside and outside the

Galveston Bay complex. Collectively, these additional acoustic receiver networks provided the capacity for opportunistically tracking the movements of tagged sea turtles outside of Matagorda Bay.

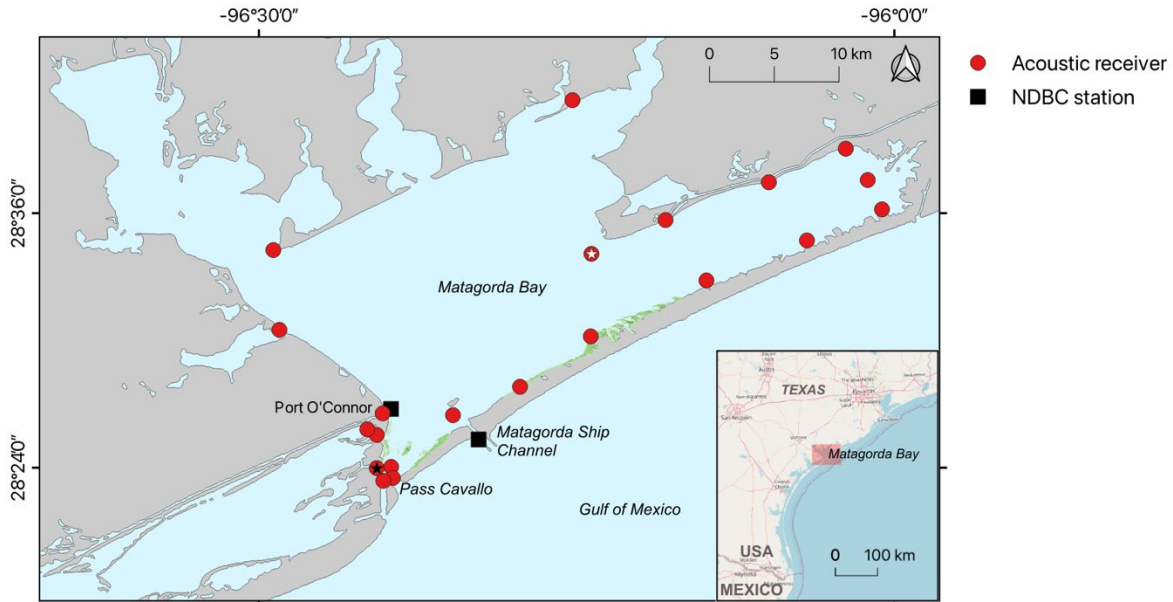


Figure 83. Spatial array of acoustic monitoring receivers (red circles) within Matagorda Bay. Only receivers included within the analyses performed in this study are shown. White and black stars denote the MB5 and MB23 receivers, respectively, which had temporal overlap only with the two green turtles equipped with acoustic transmitters in 2019. National Data Buoy Center (NDBC) stations, which record meteorological and hydrological environmental parameters, are represented by black squares.

Transmitter Attachment

If a sea turtle was large enough to receive a transmitter (Table 15), we attached the satellite transmitter slightly posteriorly to the peak of the turtle’s carapace to reduce drag, and the acoustic transmitters to the posterior carapace adhered to the marginal scutes. We first prepped the attachment surfaces (base of transmitters and carapace) by thoroughly cleaning them with distilled water to remove all debris and epibionts. The cleaned carapace was then sanded with 60-grit sandpaper, being especially careful on the growth areas around the edges of the scutes to avoid tissue bleeding. After sanding the carapace, we cleaned it with 70% isopropyl followed by acetone to accelerate drying time. The first 3 transmitters were attached using only a fast-drying and low exothermic epoxy adhesive (3M™ 08217 clear two-part epoxy adhesive). However, to increase the retention time of the transmitters on the sea turtles we switched to a two-step epoxy method. First, we used the same epoxy adhesive as before to attach strips of fiberglass cloth connecting the transmitter to the carapace. Once this layer of epoxy was dry, we used a fast-drying low-exothermic putty epoxy (West Marine Epoxy Putty Stick) to strengthen the attachment and streamline the shape of the attachment to make it more hydrodynamic. We finished the process with two coats of anti-fouling paint (Interlux Micron 66 with Biolux) applied to the transmitter and epoxy.

Table 15. List of different transmitter models and specifications used to track sea turtles in Matagorda Bay. As a general rule, the total combined weight of the transmitters should not exceed 5% of the turtle's body weight.

Type	Manufacturer	Model	Dimensions	Weight	Minimum SCL of turtle	Number of units attached
Satellite	Telonics, Inc.	SeaTrkr-4170-4	5.6 x 3.5 x 3.1 cm	85 g	24 cm	2
Satellite	Telonics, Inc.	SeaTrkr-4370-4	10.3 x 4.5 x 3.6 cm	190 g	32 cm	2
Satellite	Lotek NZ Ltd	F6G 276F	10.1 x 4.4 x 3.2 cm	144 g	30 cm	16
Acoustic	Vemco	V13	3.6 cm length – 1.3 cm diameter	11 g in air – 6.3 g in water	-	2
Acoustic	Vemco	V16	6.8 cm length – 1.6 cm diameter	24 g in air – 10.3 g in water	-	10

Data analysis

Sea turtle demographics and Body Condition Index (BCI)

Demographic parameters of captured and stranded sea turtles included relative abundance (as Catch Per Unit Effort, CPUE), size composition (straight carapace length and weight) and sex ratio (as percentage of females). We calculated the means (\pm SD) for each of these parameters.

The sea turtle CPUE was calculated following the equation employed by Metz and Landry (2016):

$$\frac{N_T}{T(L)}$$

where N_T is the total number of sea turtles captured in entanglement nets, T is the total soak time (in hours) of all nets deployed, and L is the length of one net (0.0914 km). CPUE was calculated for each sample day and then averaged to calculate the monthly and yearly means. We also mapped the spatial distribution of the CPUE by averaging the daily CPUE values that fell within each 500 m cell of a hexagonal grid.

The Body Condition Index (BCI) of captured sea turtles was calculated using Fulton's K index (Bjorndal 2000, Avens et al 2012):

$$BCI = \frac{mass}{SCL^3 \times 10^4}$$

where *mass* is the weight (kg) of the turtle, and *SCL* the Straight Carapace Length (cm). We calculated the BCI for each turtle and then calculated the average BCI by month.

Satellite tracking data processing and analysis

GPS locations and other data (i.e. diving data) acquired by Telonics GPS-Iridium transmitters were downloaded and decoded using the Telonics Data Converter software (TDC). The data output is provided as CSV and KML files. Data were downloaded once a month, until no new data were acquired. Of the four Telonics GPS-Iridium transmitters deployed, the two SeaTrkr-4370-4 tags transmitted limited data and the two SeaTrkr-4170-4 tags never reported.

Argos and GPS locations acquired by the Lotek FastGPS Argos-linked transmitters are frequently and automatically downloaded on the Lotek Argos Web Service (<https://nz.lotekdata.com/>). This website provides processed location data that can be visualized in near real-time on a map and a data table and can be downloaded as CSV and KML files. Data from deployed transmitters were checked at least once a week on the web portal, and downloaded at the end of each deployment (i.e., when no new locations had been received in >4 weeks). All sixteen Lotek FastGPS Argos-linked transmitters deployed successfully transmitted useable data.

We applied a data-driven filter to the downloaded Argos and GPS (derived from ≥ 4 satellites) locations to remove temporal and spatial duplicates, and locations with unlikely traveling speeds and turning angles using the 'SDLfilter' package (Shimada et al. 2012, 2016) in R (R Core Team 2022), and further filtered the data by removing visually obvious erroneous fixes (e.g., locations on land or those with implausible pathways over land). We computed utilization distributions (UDs) using the filtered GPS locations of each turtle by applying a movement-based kernel density estimation (MKDE) analysis based on a biased random bridge

model (BRB) (Benhamou 2011) with the ‘adehabitatHR’ package (Calenge 2006) in R. The MKDE considers the timestep between successive locations, thus accounting for temporal autocorrelation between locations (Benhamou 2011). Due to the reduced accuracy of Argos locations, only high-resolution GPS locations were used in these calculations. With the resulting UDs we then estimated home ranges (95% UD) and core use areas (50% UD) for each satellite tracked individual and calculated the size (km²) of each area. High Use Areas (HUA) were calculated by averaging the probability densities of all individual UDs in 100 m grid cells using the ‘mean’ function in the ‘Cell Statistics’ tool in QGIS 3.22.1.

Of the 18 satellite tags that successfully transmitted data, 6 tags revealed emigration from Matagorda Bay with 4 tags transmitting more than 5 locations outside of the bay. One Telonics GPS-Iridium transmitter (Cm8) provided limited data and was thus excluded, yielding a total of three individual satellite tracks (Cm9, Cm10, Cm11) from Lotek FastGPS Argos-linked transmitters to investigate environmental drivers of green turtle movement patterns. We fit a continuous-time move persistence model in state-space form to the temporally irregular, filtered GPS and Argos location data from these three satellite-tracked green turtles to estimate changes in movement behavior using the ‘aniMotum’ package (Jonsen et al. 2020, 2023) in R. This approach accounted for location uncertainty and provided modeled location estimates at regular time steps along each track using the maximum observed swim speed of 5.3 km/h. The maximum linear swim speed was calculated using the data-driven filter fit to these three individual tracks using high-resolution GPS locations derived from ≥ 6 satellites and corresponds well with previous studies on green turtles (Luschi et al. 1998; Hart and Fujisaki 2010; Metz et al. 2020). Given that 90% of temporal gaps between locations in our tracks were ≤ 12 h, we used a time step of 12 h in the model to produce two positions per day for each green turtle. To reduce spurious modeled location estimates associated with long gaps in satellite transmissions, tracks were segmented when gaps between filtered satellite locations were > 5 days (corresponding to $< 0.1\%$ of gaps) and reassembled after modeling (see Bailey et al. 2008). Tracks (or track segments) with less than 10 transmissions and 5 transmit days in duration were excluded. Erroneous modeled location estimates interpolated onto land were corrected using the ‘pathroutr’ package (London 2021) in R.

The move persistence model calculates a time-varying move persistence index (γ_t) between successive location estimates along the track, which provides an index of how an animal’s movement behavior varies in space and time based on the autocorrelation in speed and directionality. The move persistence index objectively identifies changes in behavior along a continuum ranging from 0 (low speed and directionality indicative of area-restricted behavior) to 1 (high speed and directionality indicative of transiting behavior), rather than as switches between discrete behavioral states (e.g., Bailey et al. 2008; Michelot et al. 2017). Move persistence index estimates were normalized jointly across the tracks, which preserves the relative magnitudes of move persistence across individuals and can often better resolve subtle changes in movement behavior. One-step-ahead (prediction) residuals were calculated to evaluate model performance.

To investigate which factors are associated with changes in move persistence, we modeled the response of γ_t to a suite of environmental factors encountered by sea turtles along their track using generalized additive mixed models (GAMMs). Bathymetry (m) was extracted from the NOAA National Geophysical Data Center (1/3 arc-second resolution; NGDC 2001) and meteorological data, including wind speed (m/s), wind gust (m/s), atmospheric pressure (mb), air temperature (°C), and water temperature (°C), was extracted from NOAA National Data Buoy Center (NDBC; <http://www.ndbc.noaa.gov/>) stations overlapping in time (averaged across each 12-h time step) and space ($\leq 0.01^\circ$ or 11.1 km) with each modeled location estimate. Location estimates during the first 24 h post-release were excluded to eliminate potential bias in movement resulting from the capture and handling event. Prior to model fitting, data exploration was carried out per Zuur et al. (2010). Collinearity between candidate predictor variables was assessed with Pearson correlation coefficients and variance inflation factors (VIF) using the ‘corvif’ function (Zuur et al. 2009) in R. High absolute Pearson correlation coefficients (>0.93) and VIF (>3) indicated high collinearity between wind speed and gust and air and water temperatures. Therefore, wind speed and air temperature were retained as candidate predictor variables due to more complete NDBC data records.

Move persistence was logit transformed and modeled using a Gaussian distribution with an identity link function using the ‘mgcv’ package (Wood 2017) in R. Thin plate regression splines were estimated for each candidate predictor variable and automatically penalized from a specified maximum degrees of freedom ($df = 5$; Keele 2008). We included a correlation structure with an autoregressive process of order 1 (AR1) to account for serial correlation in time series data. As observations were repeated measures collected from the same individuals, we modeled individual green turtles as a random effect to account for variation among individual responses to environmental variables. Model selection was based upon an information-theoretic approach through minimization of the second-order Akaike Information Criterion (AICc; Burnham and Anderson 2002) using the ‘MuMIn’ package (Bartoń 2020). Models with substantial support were selected based on a $\Delta AICc < 2$ from the model with the lowest AICc. The final model was used for graphical representation of terms, calculation of deviance explained, and adherence to statistical assumptions of residuals.

Acoustic tracking data processing and analysis

Acoustic detection data were filtered to remove potential false detections due to echoes and signal collisions, including detections that occurred within the minimum delay rate (40 s) of each other for a given individual, single detections recorded within a 24-h period, and subsequent detections between two receivers resulting in unrealistic rates of movement based on the 50% detection radius (183 m) and maximum linear swim speed from satellite locations described above (Pincock 2012; Simpfendorfer et al. 2015). A single acoustic detection was recorded simultaneously on the two closest receivers (MB18 and MB19 spatially separated by 778 m) and was treated as a single detection, whereby the first detection in the database (MB19) was retained and the second was discarded. Previous range tests by Dr. Stunz’s Lab in Mesquite Bay indicated a similar 50% detection rate at a distance of 170 m and a 7% detection rate at a distance of 398 m

(i.e., half the distance between MB18 and MB19; Hall et al. 2019). Based on these data, receiver detection range overlap is unlikely throughout the Matagorda Bay array.

Detections during the first 24 h post-release were excluded to eliminate potential bias in movement resulting from the capture and handling event. Juvenile green turtles are fast-growing and may shed their scutes and the externally attached acoustic transmitters much more quickly than adults, thus causing detections to cease prematurely (Hart and Fujisaki 2010; Seney et al. 2010; Smith et al. 2019). Since the nominal battery life of each tag likely exceeded their attachment duration, we examined abacus detection plots for each individual to ensure shed tags were not resulting in background positive detections (e.g., continuous detections by a single receiver for >24 h).

To visualize green turtle movements and connectivity within and outside the Matagorda Bay array, acoustic detections were used to create networks representing movements among all receivers using the ‘igraph’ package (Csardi and Nepusz 2006) in R. Within the network, each receiver represents a node with their size indicating the relative detection frequency. Movements between nodes (subsequent detections) are represented by edges (connections) weighted by the frequency of movements between two receivers divided by the total number of movement edges in the network (Jacoby et al. 2012).

We calculated the number and duration of green turtle visits to each receiver. Visit duration was calculated as the time elapsed from the first transmitter detection to when either the transmitter was not detected for 30 min (96.6% of all detections occurred within 30 mins of each other), or the transmitter was detected on a different receiver. The low spatiotemporal overlap of tagged green turtles detected within the Matagorda Bay array (maximum of three for a given monitoring period) made signal collisions and false detections less likely to occur. Therefore, visits consisting of single transmitter detections were considered valid and estimated to last 2.7 min (equivalent to the transmitter pulse train duration of 3.6 s, preceded and followed by listening periods equivalent to the maximum nominal delay of 80 s). Diel differences in detection frequencies were explored by calculating the average proportion of detections per green turtle within the Matagorda Bay array during each hour based on local sunrise and sunset times.

To examine patterns of residency in Matagorda Bay, a weighted residency index ranging from 0 (no residency) to 1 (full residency) was calculated for each green turtle using two fractions. The first fraction corresponds to the total number of calendar days the green turtle was detected at least twice on any receiver within the Matagorda Bay array divided by the monitoring period, which is weighted by a second fraction, the period between the first and last detections divided by the monitoring period (Kraft et al. 2023). Due to reduced tag retention (as described above), we standardized the monitoring period for all green turtles to the longest number of days at liberty (the number of days between the tagging date and the last day it was detected on a receiver) observed in this study (Cm14: 163 days). This monitoring period marginally exceeds the longest number of days at liberty observed for a satellite-tracked green turtle (Cm11: 155 days) in this study and corresponds well with retention rates from previous studies on juvenile green turtles (Smith et al. 2019; Griffin et al. 2020; Metz et al. 2020). A roaming index was

calculated from the number of receivers at which an individual was detected, divided by the total number of receivers available in the Matagorda Bay array to assess the extent of movement by individual green turtles within the array (Heupel and Simpfendorfer 2015). A total of 21 receivers were available to the first two green turtles tagged in 2019 (Cm5 and Cm6) and 19 receivers were available to the remaining green turtles tagged in 2021. The roaming index ranged from 0 to 1, where values close to 1 indicated an individual was detected on all available receivers within the Matagorda Bay array.

To examine patterns of space use, the mean geographic location of each green turtle was estimated every hour based on short-term centers of activity (Simpfendorfer et al. 2002) using the ‘Animal Tracking Toolbox’ extension (Udyawer et al. 2018) to the ‘VTrack’ package (Campbell et al. 2012) in R. The center-of-activity locations provide a more accurate representation of movement than the fixed receiver locations, and were used in the subsequent calculation of UD_s to quantify the spatial area used by acoustically-tagged green turtles detected on at least three receivers (Cm5, Cm6, Cm18). Similar to analyses of satellite-derived locations, UD_s were estimated using the Brownian bridge kernel method in the ‘Animal Tracking Toolbox’ in conjunction with the ‘adehabitatHR’ package in R, which accounts for autocorrelated locations and applies a conditional random walk to model both the green turtle positions and the expected path traveled between receivers. A smoothing parameter (δ_2) of 183 m was included to account for the acoustic receiver detection range within Matagorda Bay (TinHan et al. 2018).

To investigate which environmental factors are associated with residency within Matagorda Bay, we modeled the response of the daily presence of a green turtle detected on any receiver within the Matagorda Bay array using a GAMM framework. Daily meteorological data, including wind speed, atmospheric pressure, and air temperature, was extracted from the NDBC station (Station PCNT2, Port O’Connor, Matagorda Bay, TX, 28.446°N, -96.396°E) in the closest proximity to the receivers within the Matagorda Bay array that recorded detections. Gaps in daily meteorological records were supplemented from the second closest NDBC station (Station MBET2, Matagorda Bay Entrance Channel, TX, 28.422°N, -96.327°E). The number of days at liberty (the number of days between the tagging date and the last day it was detected on a receiver) were converted to daily presence-absence for each individual sea turtle and modeled using a binomial distribution with a logit link function in R as described above. To reduce biases associated with few and sporadic detections, only individual sea turtles detected on more than 10 calendar days on any receiver within the Matagorda Bay array were included in models and as a random effect.

Outreach

We used multiple approaches to engage the Matagorda Bay communities in Calhoun County and Matagorda County throughout this project. COVID-19 quarantine hindered some of our original plans, but also inspired new ideas and opportunities to extend our reach including virtual events and a citizen science project and tool to provide us with scientific information necessary to locate sea turtles once COVID-19 restrictions were lifted.

iSeaTurtle app development

During the early stages of field work in 2019, we identified an interest from the fishing community in sharing their knowledge about where they sighted sea turtles. In 2020, the COVID-19 pandemic resulted in an increase of recreational fishers in the US (Midway et al. 2021), which we saw as an opportunity to provide a tool to encourage citizens to share this knowledge and be involved in science by providing useful data on the distribution of sea turtles sighted in Matagorda Bay. In May 2020 we contracted Dr. Dustin Baumbach, who has extensive experience in the design and development of citizen science apps for sea turtle research, to create a smartphone app with an easy user-friendly interface through which to report sea turtles sighted in the water. The app was built using AppStudio for ArcGIS Mapping API provided by ESRI and released in the Apple Store and Google Play Store in June 2020. Texas Sea Grant developed a web-based platform to host the real-time data submitted through the iSeaTurtle app and made it publicly available for visualization (tx.ag/iSeaTurtle).

Results

Historical distribution of sea turtle captures

Gill net surveys were conducted in Matagorda Bay during the fall and spring from 1980 – 2019. A total of 50 sea turtles were captured from 1993 – 2019. Multiple sea turtles were captured from 1993 through 2009, but not annually (Figure 84-Figure 86). Beginning in 2009, sea turtles were captured annually, the number of captures increased significantly, and the species captured were primarily green turtles and Kemp’s ridleys. The species captured across all years included green turtles (n= 36), Kemp’s ridleys (n= 11), loggerheads (n=2), and hawksbills (n=1) (Figure 85). Fishing effort was consistent across all years during the nearly 40-year span, indicating that the increase in number of sea turtles was independent of the effort.

Sea turtles were captured in 31 different locations in the area including Matagorda Bay, Lavaca Bay, Cox Bay, Keller Bay, and near the entrances to Carancahua Bay and Tres Palacios Bay (Figure 84). Multiple sea turtle captures occurred at 11 of the 31 locations. Green turtles were captured as far north as Chocolate Bay and as far east as the backside of Matagorda Peninsula, across from Oyster Lake, between Phillips Bayou and Maverick Bayou (Figure 84). Most of the green turtles were captured in the area from south of Powderhorn Lake, down to Pass Cavallo and east to the area between Phillips Bayou and Maverick Bayou. Most of the Kemp’s ridleys were captured in Lavaca Bay, Cox Bay, and Keller Bay. Kemp’s ridleys were also captured near Pass Cavallo, and along the backside of the Matagorda Peninsula east of Maverick Bayou. The two loggerheads were captured in Keller Bay and near the mouth of Carancahua Bay. The hawksbill was captured in Keller Bay.

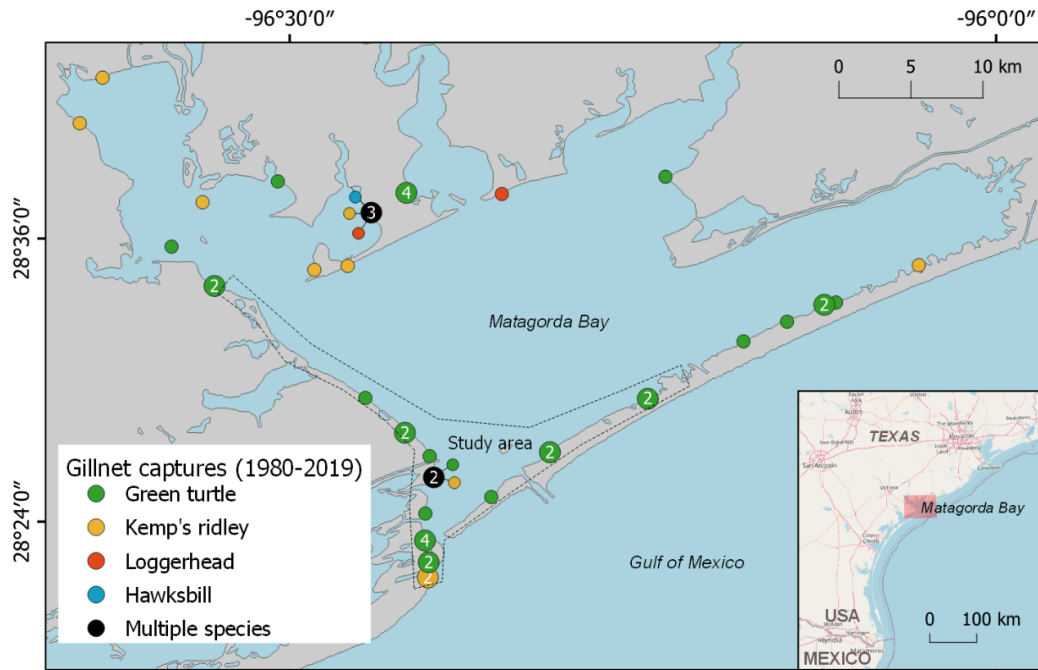


Figure 84. Map of study area (dotted line) in Matagorda Bay overlapped with historical data on sea turtles captured with gillnets by the Texas Parks and Wildlife Department (TPWD) between 1980 and 2019. Value in circles represent number of individuals, and the color indicates the species.

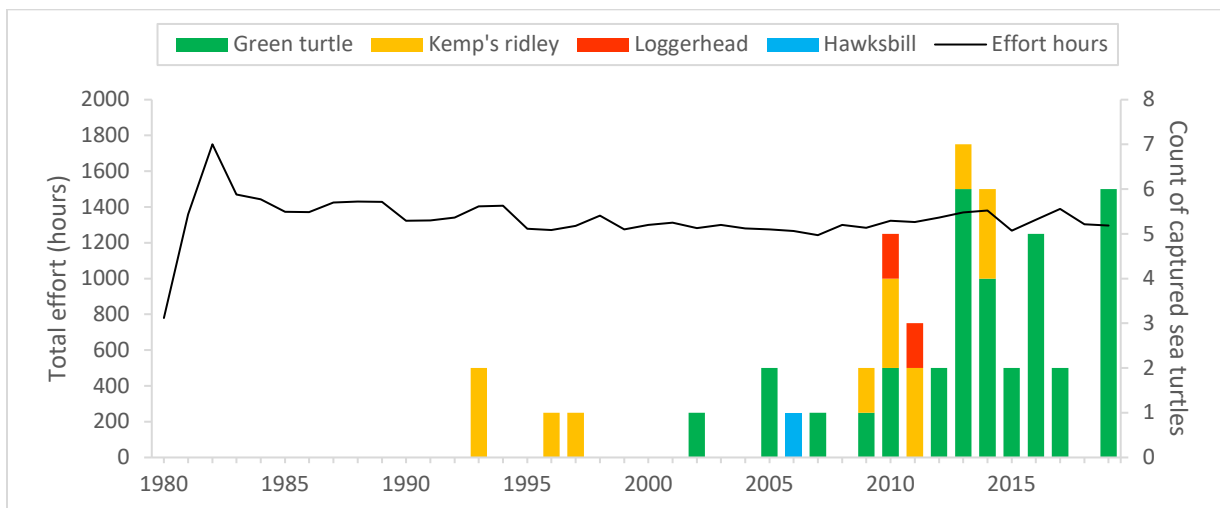


Figure 85. Total number of effort hours spent in gillnet fishing by TPWD (black line) and total number of sea turtles captured during these fishing trips (columns colored by species), between 1980 and 2019 in Matagorda Bay

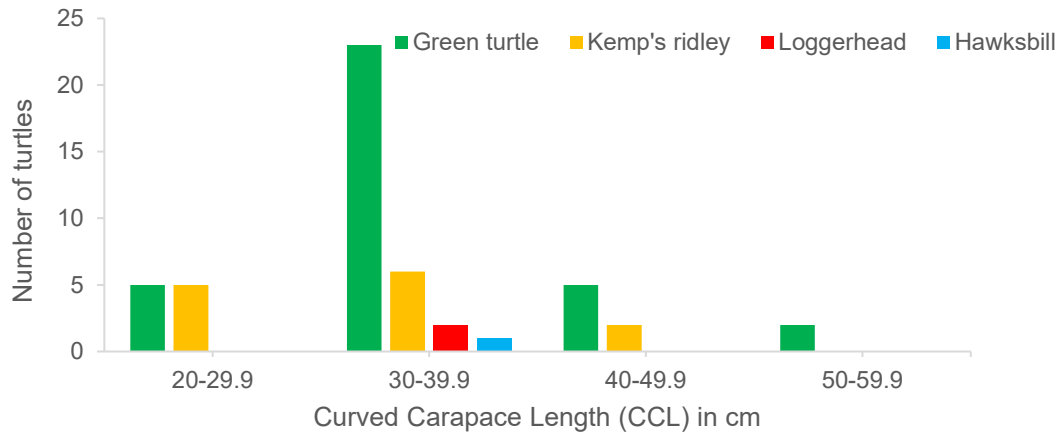


Figure 86. Size distribution of sea turtles captured in gillnets by TPWD between 1980 and 2019 in Matagorda Bay.

Sampling distribution and effort

During the first field season (August-November 2019) we had limited success capturing sea turtles and the satellite transmitters we purchased provided limited data. The chance of encountering a sea turtle was much lower than we had anticipated, and it was difficult to locate the specific areas where the chance of capturing a sea turtle was higher. After November 2019 there was a hiatus of field work due to changes in staff; Dr. Figgner left for another position and Dr. Wildermann was contracted in February 2020. Unfortunately, the COVID-19 pandemic began, and field work had to be put on hold until October 2020 when university travel restrictions were relaxed, and the team felt safe enough to resume activities. During this time, we researched and purchased new satellite tags, and had a strong outreach component spearheaded by the development and launching of the iSeaTurtle citizen app, which would later greatly help identify sites to search for sea turtles. The 2021 field season was very successful, being able to capture and track turtles in the middle of winter before the freeze event in February 2021. The freeze caused the death of many if not all the sea turtles that remained in the bay, but we saw it as an unfortunate opportunity to collect additional data for the project, that otherwise would have been very difficult to gather. We returned to the field after the freeze two times before we started to catch turtles again in early April 2021. After this, our catch success increased significantly, and we reached our permitted annual catch quota for green turtles on May 31, 2021. Thus, we had to stop research activities until the extension of our annual catch quota was approved on July 8, 2021. In the meantime, we developed in-house training on how to capture and handle sea turtles for the staff at Dr. Stunz's Lab, whose team provided great field support upon resuming field activities. We returned to the field on July 10, 2021 and captured all the remaining turtles needed by the end of July.

We carried out a total of 31 field trips between August 2019 and July 2021, captured sea turtles on 17 of these trips (45% success rate), and captured on average 1.1 ± 1.3 sea turtles/trip (Table 16). We invested a total of 330.6 hours of netting effort, but effort was not equal across months and years due to logistical challenges (i.e., COVID-19 pandemic, weather conditions) (Figure 87). We captured at least one turtle each month and recorded the highest CPUE values in September 2019 (1.8 turtles/km-hr) and July 2021 (2 turtles/km-hr). CPUE in January 2020 was higher than other winter months (1.1 turtles/km-hr), but we consider this circumstantial due to a very short net setting in which we captured one turtle and removed the nets right after the capture due to weather conditions.

After the pilot surveys in 2019 we selected netting sites based on our previous netting success or lack thereof, as well as the input of sea turtle sightings recorded through the iSeaTurtle app (see iSeaTurtle app development and outreach and engagement sections). Based on these data, we identified three hotspots to set nets for sea turtles (Figure 87), from west to east: the J-hook area between the entrance of Mule Slough and Saluria Bayou, the area from Decros Point through the eastern side of Matagorda Island, and the area near Greens Bayou. Figure 87 also shows a location with very high CPUE near Port O'Connor, which we could only sample once when the tide was extremely low; otherwise, the area was too deep to set our nets.

Table 16. Netting details and effort to capture sea turtles in Matagorda Bay between 2019 and 2021. We set two contiguous 91.4 m long entanglement nets of either 2.7 (shallow water) or 3.7 m (deep water) depth.

Date	Latitude	Longitude	Type of entanglement net	Daily Soak Time (hours)	# Turtles Captured	CPUE (#turtles/km-h)
2019-08-03	28.55915	-96.52755	Deep water	12.2	1	0.45
2019-08-04	28.5479	-96.51726	Deep water	13.1	0	0.00
2019-08-10	28.55998	-96.52655	Deep water	14.3	0	0.00
2019-09-28	28.47913	-96.43338	Deep water	9.1	0	0.00
2019-09-28	28.55923	-96.5288	Deep water	5.8	0	0.00
2019-09-29	28.40905	-96.37288	Deep water	6.2	3	2.65
2019-11-09	28.40805	-96.37213	Shallow water	7.0	0	0.00
2019-11-10	28.40660	-96.37456	Shallow water	3.3	0	0.00
2019-11-23	28.37661	-96.40331	Shallow water	10.6	4	2.06
2020-10-03	28.48033	-96.26187	Shallow water	6.6	0	0.00
2020-10-04	28.40443	-96.37525	Shallow water	12.0	1	0.46
2020-10-24	28.37797	-96.40396	Shallow water	12.0	0	0.00
2020-10-25	28.49735	-96.23913	Shallow water	10.1	0	0.00
2021-01-16	28.42431	-96.38976	Shallow water	5.1	1	1.07
2021-01-17	28.41443	-96.37128	Shallow water	10.0	0	0.00
2021-02-06	28.37698	-96.40373	Shallow water	12.7	0	0.00
2021-02-07	28.41443	-96.37128	Shallow water	10.1	1	0.54
2021-03-30	28.40695	-96.37759	Shallow water	16.1	0	0.00
2021-04-03	28.37533	-96.40294	Shallow water	16.2	2	0.68
2021-04-04	28.37801	-96.40209	Shallow water	13.3	0	0.00
2021-04-05	28.40699	-96.37322	Shallow water	11.7	2	0.93
2021-05-29	28.40795	-96.37173	Shallow water	10.9	2	1.01
2021-05-30	28.38348	-96.40351	Shallow water	10.5	1	0.52
2021-05-31	28.42703	-96.3524	Shallow water	12.0	1	0.46
2021-07-10	28.40310	-96.37627	Shallow water	12.8	4	1.72
2021-07-11	28.40841	-96.37041	Shallow water	13.1	0	0.00
2021-07-13	28.40956	-96.37022	Shallow water	14.8	2	0.74
2021-07-14	28.40635	-96.37391	Shallow water	14.3	2	0.77
2021-07-28	28.40670	-96.37437	Deep water	9.2	1	0.60
2021-07-29	28.40735	-96.37556	1x deep water, 1x shallow water	5.2	1	1.06
2021-07-31	28.49215	-96.24545	Shallow water	10.7	4	2.04

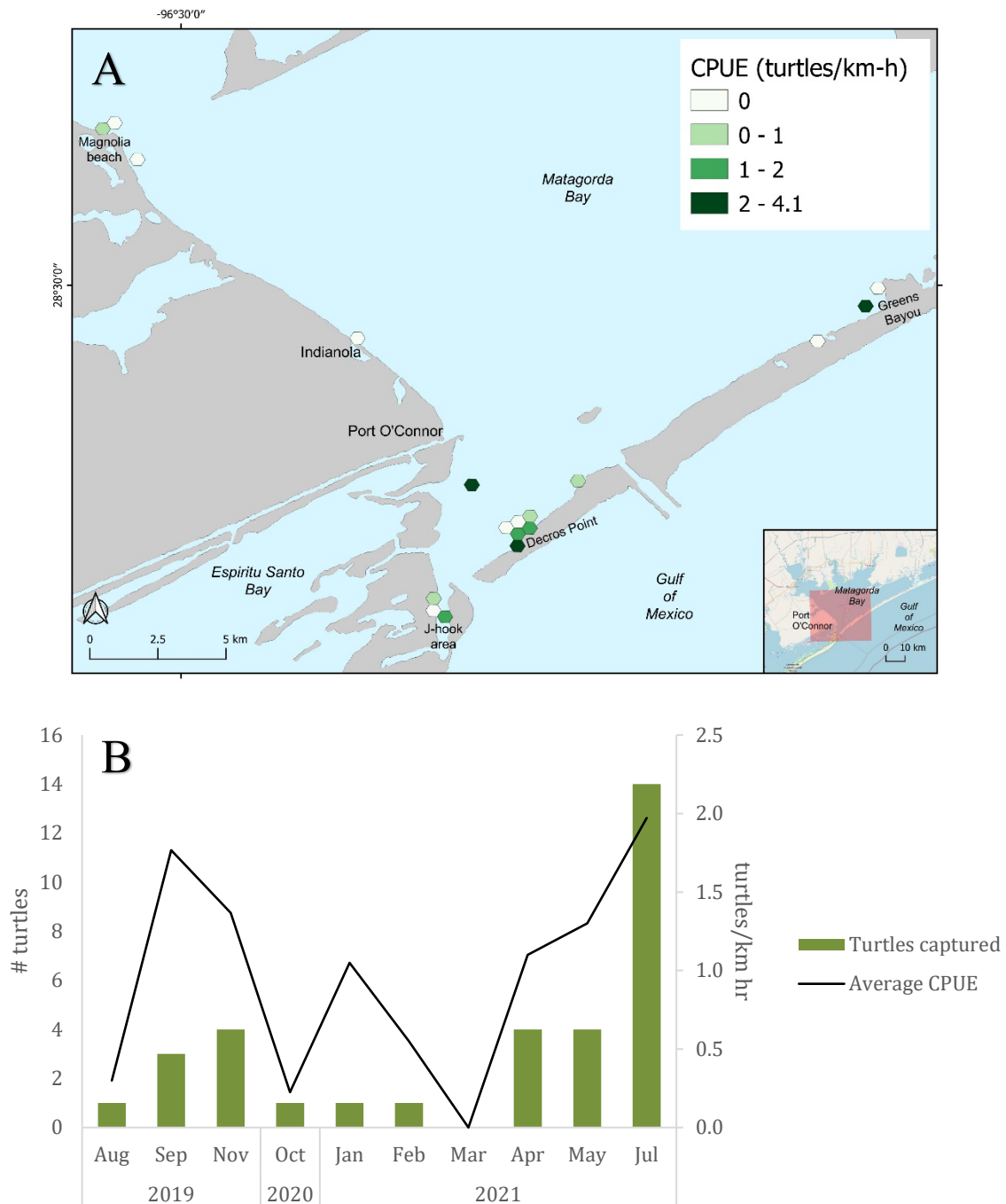


Figure 87. Spatial (a) and temporal (b) distribution of catch per unit effort (CPUE) of green turtles in Matagorda Bay between 2019 and 2021.

Sea turtle demographics and body condition index

Average CPUE in Matagorda Bay between 2019 and 2021 was 1.1 ± 1.3 (mean \pm SD) turtles/km-hr, with daily CPUE ranging between 0 – 2.65 turtles/km-hr (Table 16). We captured a total of 32 green turtles (*Chelonia mydas*) and one Kemp’s ridley turtle (*Lepidochelys kempii*)

using nets and recorded 62 green turtles during stranding surveys. All individuals were juveniles and subadults, ranging between 29.8 and 47.2 cm CCL (mean = 39.2 ± 5.5 cm) for captured green turtles (Figure 88, Table 17) and 26.5 – 71.0 cm CCL (mean = 45.1 ± 8.6 cm) for stranded green turtles. Captured green turtles weighed on average 6.6 ± 3.1 kg (Table 17). The Kemp's ridley turtle was also a juvenile measuring 27.5 cm CCL and weighed 4.9 kg and displayed chromatic leucism (Table 17). Sex ratio of green turtles was determined from necropsies of a random subset of stranded green turtles, yielding a slightly female-dominated sex ratio of 58%, or a female:male ratio of 1.4:1.

Green turtles exhibited better body condition during warmer months (Figure 89), with the highest value (BCI = 1.7 ± 0.3) recorded in September and the lowest in January (0.7). The average BCI was 1.3 ± 0.3 . Overall, captured green turtles appeared to be in good health. Only about 20% (N = 7) of turtles had epibionts on the carapace and/or plastron, most of which were few leeches and/or small barnacles. The carapaces of five turtles captured in November 2019 and January 2021 were covered by a thick biofilm of microalgae and mud. Two turtles had small scars on the flippers, and one turtle had large, healed propeller scars on the central/anterior side of the carapace, as well as multiple notches on the marginal scutes. Fibropapillomas were present in approximately a third of the green turtles we sampled, with a 31% prevalence in captured turtles and 29% prevalence in stranded turtles. All the green turtles with presence of tumors were juveniles.

Table 17. Capture, tagging and morphometric data of sea turtles captured with entanglement nets in Matagorda Bay between 2019 and 2021. SCL: Straight Carapace Length, SCW: Straight Carapace Width, SCD: Straight Carapace Depth, CCL: Curved Carapace Length, CCW: Curved Carapace Width, PTT: Platform Transmitting Terminal.

Species	Turtle ID	Date (mm/dd/yy)	Latitude	Longitude	Right Flipper Tag	Left Flipper Tag	CCL (cm)	CCW (cm)	SCL (cm)	SCW (cm)	SCD (cm)	Mass (Kg)	Acoustic Tag ID	PTT ID	Name
Green turtle	Cm1	08/03/19	28.55915	-96.5276	KKP0378	KKP0377	34.1	28.8	31.5	24.5	12.4	4.4	-	710243	"Gina"
Green turtle	Cm2	09/29/19	28.40905	-96.3729	KKP0380	KKP0379	35.1	31.6	33.5	27.7	13.2	5	-	-	"Sting"
Green turtle	Cm3	09/29/19	28.40905	-96.3729	-	-	31.4	29.8	26.4	23.8	11.3	3.6	-	-	"Squirt"
Green turtle	Cm4	09/29/19	28.40905	-96.3729	KKP0382	KKP0381	47.2	44.7	38.6	33.5	16.2	10.6	-	710244	"Greta"
Green turtle	Cm5	11/23/19	28.37662	-96.4033	-	-	31.2	21.3	29.6	23.8	11.0	3.2	19075	-	"Leechy"
Green turtle	Cm6	11/23/19	28.37662	-96.4033	KKP0384	KKP0383	35.8	30.0	34.1	37.2	11.9	4.6	14594	-	"Claudia"
Green turtle	Cm7	11/23/19	28.37662	-96.4033	-	-	32.2	27.2	30.5	24.1	12.0	3.4	-	-	"Slashy"
Green turtle	Cm8	11/23/19	28.37662	-96.4033	KKP0386	KKP0385	37.6	30.7	35.8	27.5	12.2	5.2	-	712549	"Grace"
Green turtle	Cm9	10/04/20	28.40443	-96.3753	KKP0303	KKP0302	34.1	29.4	32.4	26.2	11.9	4.2	-	202704	"Uri"
Green turtle	Cm10	01/16/21	28.4233	-96.3883	KKP0304	KKP0305	45.9	38.1	43.8	33.8	14.6	~6	58010	202700	"Tom"
Green turtle	Cm11	02/07/21	28.41443	-96.3713	KKP0308	KKP0307	36.4	30.1	34.1	25.2	11.9	4.5	58011	202703	"Pickle"
Green turtle	Cm12	04/03/21	28.37533	-96.4029	KKP0309	KKP0310	35.7	30.7	33.2	27.0	12.4	4.5	58012	202701	"Coddiwomple"
Green turtle	Cm13	04/03/21	28.37544	-96.4031	KKP0311	KKP0312	36.0	30.8	33.6	27.2	18.1	4.7	58013	202702	"Windy"
Green turtle	Cm14	04/05/21	28.40699	-96.3732	KKP0313	KKP0314	29.8	25.4	27.7	22.9	9.8	2.9	58014	-	"Pi"
Green turtle	Cm15	04/05/21	28.40699	-96.3732	KKP0315	KKP0317	33.5	28.4	32.1	25.4	13.2	4.2	-	712548	"Cinco"
Green turtle	Cm16	05/29/21	28.40795	-96.3717	KKP0318	KKP0316	39.6	34.1	36.3	28.7	15.1	6.1	58015	215057	"Mindy"
Green turtle	Cm17	05/29/21	28.40795	-96.3717	KKP0319	KKP0320	46.9	40.2	43.6	33.2	18.1	15.5	58016	215058	"Mork"
Green turtle	Cm18	05/30/21	28.38348	-96.4035	KKP0322	KKP0321	45.7	38.9	41.8	33.5	16.9	9.8	58017	215060	"Smalls"
Green turtle	Cm19	05/31/21	28.42703	-96.3524	KKP0324	KKP0323	43.0	36.9	39.8	32.7	14.5	6.6	58018	215062	"Cinderella"
Green turtle	Cm20	07/10/21	28.40310	-96.37627	KKP0326	KKP0327	33.9	29.1	30.8	24.7	11.6	3.8	-	215063	"Stergil"
Green turtle	Cm21	07/10/21	28.40310	-96.37627	KKP0330	KKP0328	33.9	30.7	30.6	25.0	11.8	-	-	-	"Scar"
Green turtle	Cm22	07/10/21	28.40310	-96.37627	KKP0329	KKP0331	41.7	37.1	38.4	31.2	16.2	7.0	58019	215061	"Flakey"
Green turtle	Cm23	07/10/21	28.40310	-96.37627	KKP0332	-	42.7	35.9	40.6	31.6	15.1	9.0	-	-	"Gulf Ball"
Green turtle	Cm24	07/13/21	28.40956	-96.37022	KKP0334	KKP0333	45.9	39.6	42.4	34.8	15.7	-	-	215066	"Michael"
Green turtle	Cm25	07/13/21	28.40956	-96.37022	KKP0335	-	46.6	38.2	43.7	33.4	16.9	-	-	-	"No Name"
Green turtle	Cm26	07/14/21	28.40635	-96.37391	KKP0336	KKP0337	39.5	31.3	36.4	27.0	13.6	6.4	-	215065	"Julio"

Green turtle	Cm27	07/14/21	28.40635	-96.37391	KKP0338	KKP0339	45.4	39.2	41.7	32.6	17.3	9.9	-	215059	"Slow Poke"
Green turtle	Cm28	07/28/21	28.40670	-96.37437	KKP0341	KKP0340	46.2	38.6	43.1	31.7	16.3	9.9	-	202704	"Squirtle"
Green turtle	Cm29	07/29/21	28.40735	-96.37556	KKP0343	KKP0342	40.0	35.4	37.2	30.7	13.8	6.9	-	215064	"Susan"
Green turtle	Cm30	07/31/21	28.49215	-96.24545	KKP0345	KKP0344	44.7	36.2	41.6	31.8	15.4	9.4	-	-	"Ginger"
Green turtle	Cm31	07/31/21	28.49215	-96.24545	KKP0347	KKP0346	38.4	32.6	41.4	38.5	13.0	7.4	-	-	"Mary Anne"
Kemp's ridley	Lk1	07/31/21	28.49215	-96.24545	KKP0349	KKP0348	27.5	25.7	25.5	22.1	8.9- 10.3	4.9	-	-	"Phoenix"
Green turtle	Cm32	07/31/21	28.49215	-96.24545	KKP0351	KKP0350	42.9	36.4	40.2	30.5	15.7	12.5	-	-	

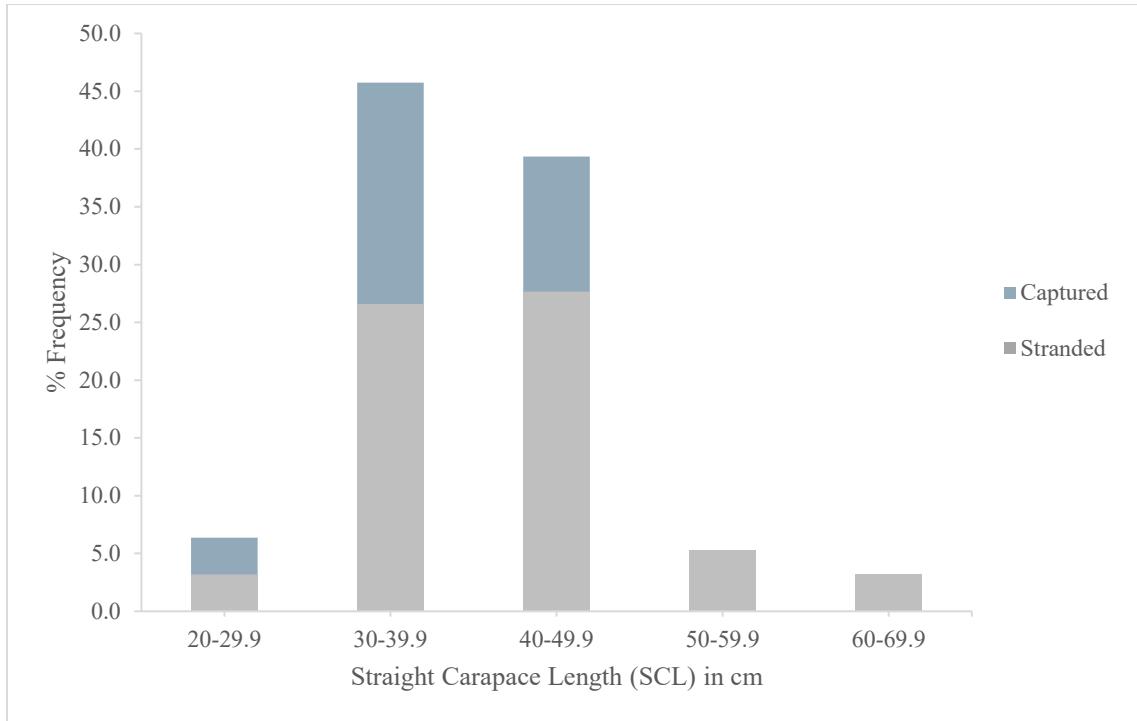


Figure 88. Size distribution of green turtles captured in Matagorda Bay between 2019 and 2021.

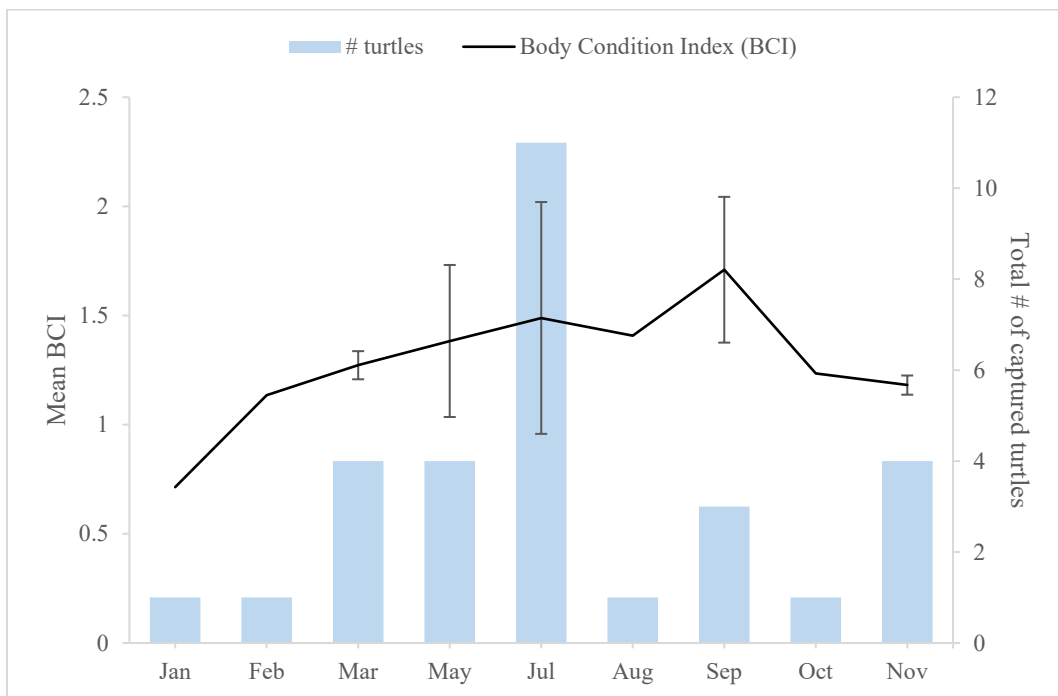


Figure 89. Mean body condition index (BCI) of green turtles captured in Matagorda Bay between 2019 and 2021.

Sea turtle home ranges and high use areas derived from satellite tracking data

The number of days a turtle was tracked (or track days) ranged from 18 days (Telonics transmitter) to 155 days (Lotek transmitter), with an average of 84.2 ± 43.3 days (Table 18). The majority of tracked turtles (N =13) remained resident in Matagorda Bay for the duration of their transmissions (Figure 96-Figure 108), however there was also evidence of connectivity between Matagorda Bay and other Texas Bays (i.e. Espiritu Santo Bay, Aransas Bay, Laguna Madre) (Figure 92- Figure 95), as well as the use of Mexican waters (Figure 95). The total distance travelled by green turtles varied, with resident turtles moving 88.4 ± 47.9 km on average and migratory turtles moving 613.6 ± 295.8 km on average.

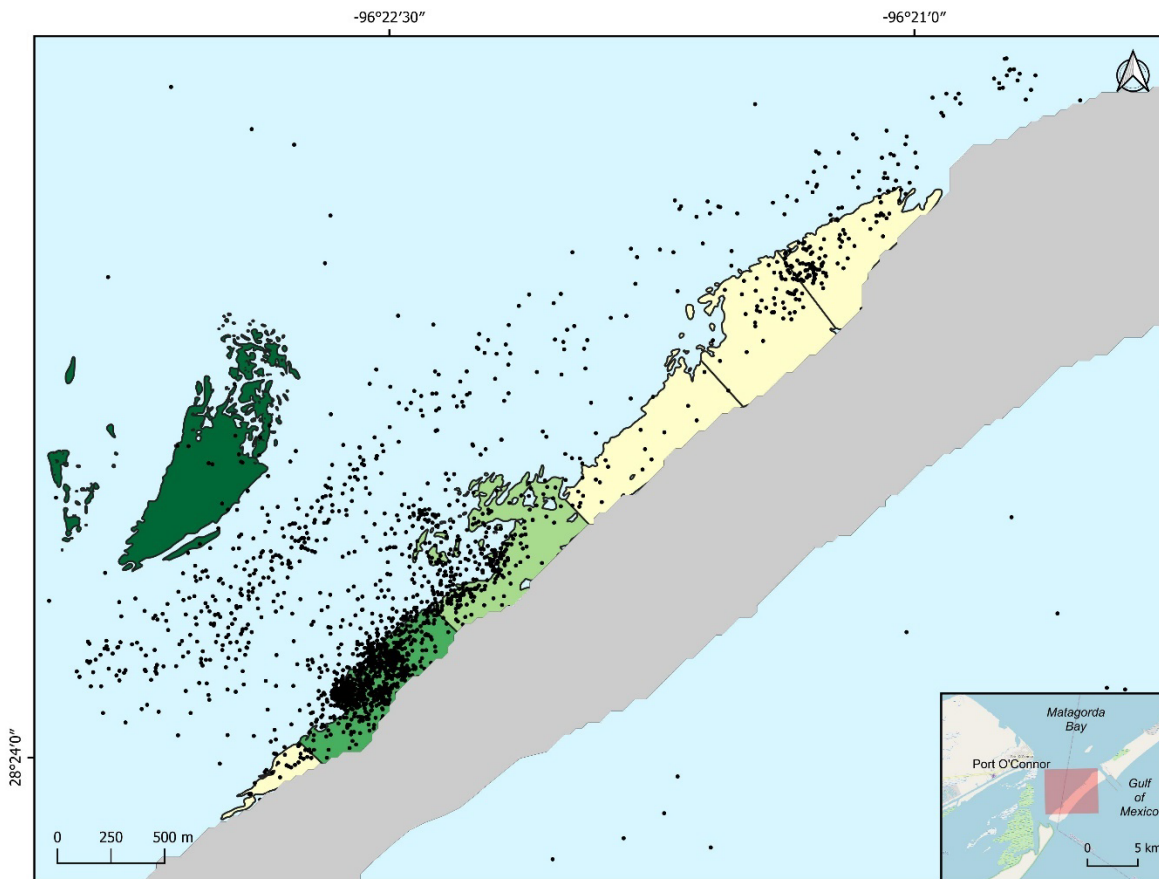
The area of green turtle home ranges (95% UD) in Matagorda Bay measured on average 3.0 ± 1.7 km² (range 0.4 – 6.1 km²), with core areas (50% UD) measuring on average 0.5 ± 0.4 km² (range 0.1 – 1.4 km²) (Table 19). We identified two main sea turtle high use areas based on satellite tracking data: (a) the seagrass beds on the backside of Matagorda Island, namely around Decros Point and on the eastern side of the island, and (b) the J-hook area between the entrance of Mule Slough and Saluria Bayou (**Error! Reference source not found.**, Figure 91). Most sea turtle locations overlapped with areas covered by seagrass beds, in particular in areas where the seagrass species diversity was high (i.e. composed by *Halodule beaudettei*, *Halophilla engelmannii*, *Ruppia maritima*). Moreover, we also detected the use of deeper areas further into the bay, where the seabed is primarily composed by mud (Appendix D).

Table 18. Satellite tracking details of green turtles captured in Matagorda Bay between 2019 and 2021. PTT: Platform Transmitting Terminal.

Tag Manufacturer	Tag Model	Turtle ID	PTT ID	Deployment ID	Deployment Status	Transmission Start Date (yyyy-mm-dd)	Transmission Stop Date (yyyy-mm-dd)	# Track Days	Deployment Latitude	Deployment Longitude	# Locations transmitted (ARGOS/GPS)	# GPS Locations retained for Analysis
Telonics, Inc.	SeaTrkr-4170-4	Cm1	710243	710243_KKP0378	Did not transmit	2019-08-03	-	-	28.55915	-96.52755	0	0
Telonics, Inc.	SeaTrkr-4170-4	Cm4	710244	710244_KKP0382	Did not transmit	2019-09-29	-	-	28.40905	-96.372883	0	0
Telonics, Inc.	SeaTrkr-4370-4	Cm8	712549	712549_KKP0386	Complete - Transmitted limited data	2019-11-23	2020-04-21	150	28.376617	-96.403317	24 Iridium	24
Lotek NZ Ltd	F6G 276F	Cm9	202704	202704_KKP0303	Complete	2020-10-04	2020-12-25	82	28.401552	-96.37514	1611 (1316/295)	244
Lotek NZ Ltd	F6G 276F	Cm10	202700	202700_KKP0304	Complete	2021-01-16	2021-03-13	56	28.4233	-96.388317	421 (293/128)	71
Lotek NZ Ltd	F6G 276F	Cm11	202703	202703_KKP0308	Complete	2021-02-07	2021-07-12	155	28.414433	-96.371283	2282 (1949/333)	261
Lotek NZ Ltd	F6G 276F	Cm12	202701	202701_KKP0309	Complete	2021-04-03	2021-07-15	103	28.375334	-96.402943	2216 (1825/391)	364
Lotek NZ Ltd	F6G 276F	Cm13	202702	202702_KKP0311	Complete	2021-04-03	2021-08-20	139	28.375436	-96.403142	1904 (1555/349)	333
Telonics, Inc.	SeaTrkr-4370-4	Cm15	712548	712548_KKP0315	Complete - Transmitted limited data	2021-04-05	2021-04-23	18	28.40699	-96.37322	12 Iridium	12
Lotek NZ Ltd	F6G 276F	Cm16	215057	215057_KKP0318	Complete	2021-05-29	2021-07-27	59	28.40795	-96.371733	764 (585/179)	166
Lotek NZ Ltd	F6G 276F	Cm17	215058	215058_KKP0319	Complete	2021-05-29	2021-09-04	98	28.40795	-96.371733	1451 (1186/265)	223
Lotek NZ Ltd	F6G 276F	Cm18	215060	215060_KKP0322	Complete	2021-05-30	2021-08-10	72	28.383483	-96.403517	1326 (1033/293)	258
Lotek NZ Ltd	F6G 276F	Cm19	215062	215062_KKP0324	Complete	2021-05-31	2021-08-08	69	28.427033	-96.3524	1047 (839/208)	186
Lotek NZ Ltd	F6G 276F	Cm20	215063	215063_KKP0326	Complete	2021-07-10	2021-10-31	113	28.4031	-96.37627	1927 (1566/361)	319
Lotek NZ Ltd	F6G 276F	Cm22	215061	215061_KKP0329	Complete	2021-07-10	2021-08-13	34	28.4031	-96.37627	667 (505/162)	127
Lotek NZ Ltd	F6G 276F	Cm24	215066	215066_KKP0334	Complete	2021-07-13	2021-09-18	67	28.40956	-96.37022	1220 (982/238)	198
Lotek NZ Ltd	F6G 276F	Cm26	215065	215065_KKP0336	Complete	2021-07-14	2021-12-09	148	28.40635	-96.37391	991 (783/208)	188
Lotek NZ Ltd	F6G 276F	Cm27	215059	215059_KKP0338	Complete	2021-07-14	2021-09-26	74	28.40635	-96.37391	1309 (1003/306)	272
Lotek NZ Ltd	F6G 276F	Cm28	202704	202704_KKP0341	Complete	2021-07-28	2021-09-27	61	28.4067	-96.37437	599 (490/109)	72
Lotek NZ Ltd	F6G 276F	Cm29	215064	215064_KKP0343	Complete	2021-07-29	2021-08-16	18	28.40735	-96.37556	392 (322/70)	46

Table 19. Size of home ranges (95% UD) and core areas (50% UD) of satellite and acoustically tracked green turtles inside Matagorda Bay between 2019 and 2021. The table does not include areas of movements, migrations and foraging areas outside of Matagorda Bay.

Deployment ID	Satellite Telemetry		Acoustic Telemetry	
	Home range (km ²)	Core area (km ²)	Home range (km ²)	Core area (km ²)
Cm5			2.9	0.9
Cm6			1.6	0.3
Cm9	6.1	0.3		
Cm10	2.3	0.1		
Cm11	4.0	0.2		
Cm12	1.0	0.3		
Cm13	1.0	0.4		
Cm16	2.9	0.6		
Cm17	2.3	0.5		
Cm18	2.7	0.7	0.4	0.1
Cm19	3.6	0.8		
Cm20	2.0	0.2		
Cm22	0.4	0.1		
Cm24	3.6	0.8		
Cm26	4.2	0.3		
Cm27	5.3	1.4		
Cm28	1.2	0.3		
Cm29	4.8	1.1		
Mean ± SD (Range)	3.0 ± 1.7 (0.4-6.1)	0.5 ± 0.4 (0.1-1.4)	1.6 ± 1.3 (0.4-2.9)	0.4 ± 0.4 (0.1-0.9)



- Sea turtle locations received from satellite transmitters

Seagrass species diversity*

Halodule beaudettei

Halodule beaudettei, Halophilla engelmannii

Halodule beaudettei, Halophilla engelmannii, Ruppia maritima

Halodule beaudettei, Halophilla engelmannii, yellow macroalgae, floating Sargassum

*Seagrass data provided by BIO-WEST

Figure 90. Overlap between sea turtle locations received from satellite transmitters and seagrass distribution in Matagorda Bay. Color scheme of seagrass areas represents the diversity in seagrass and macroalgae species (darker colors = higher diversity)

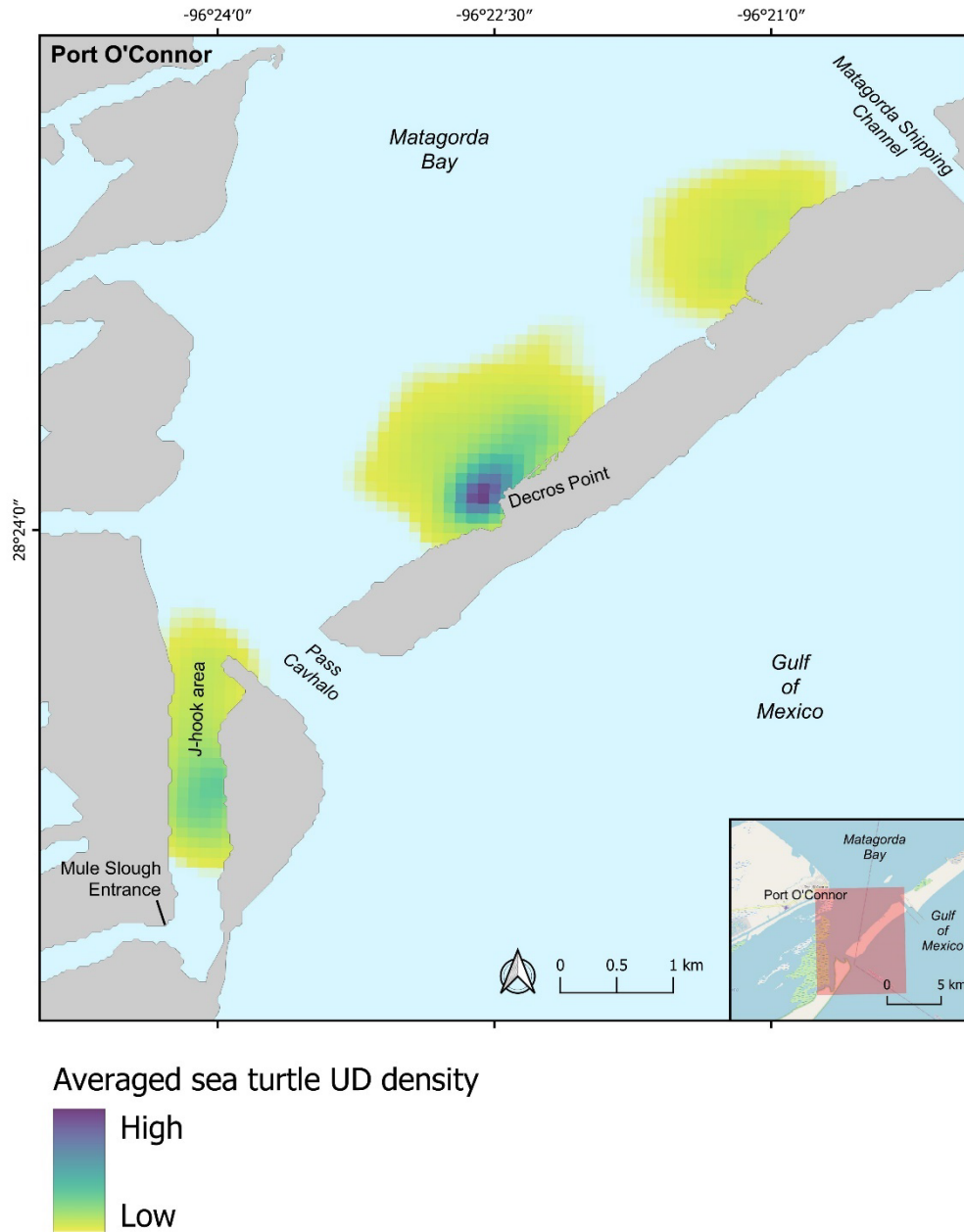


Figure 91. Areas highly used by satellite-tracked green turtles in Matagorda Bay between 2020 and 2021. Color scale represents the averaged density of all green turtle Utilization Distributions (UDs), from yellow (low density = fewer green turtle UD) to dark blue (high density = greater green turtle UD).

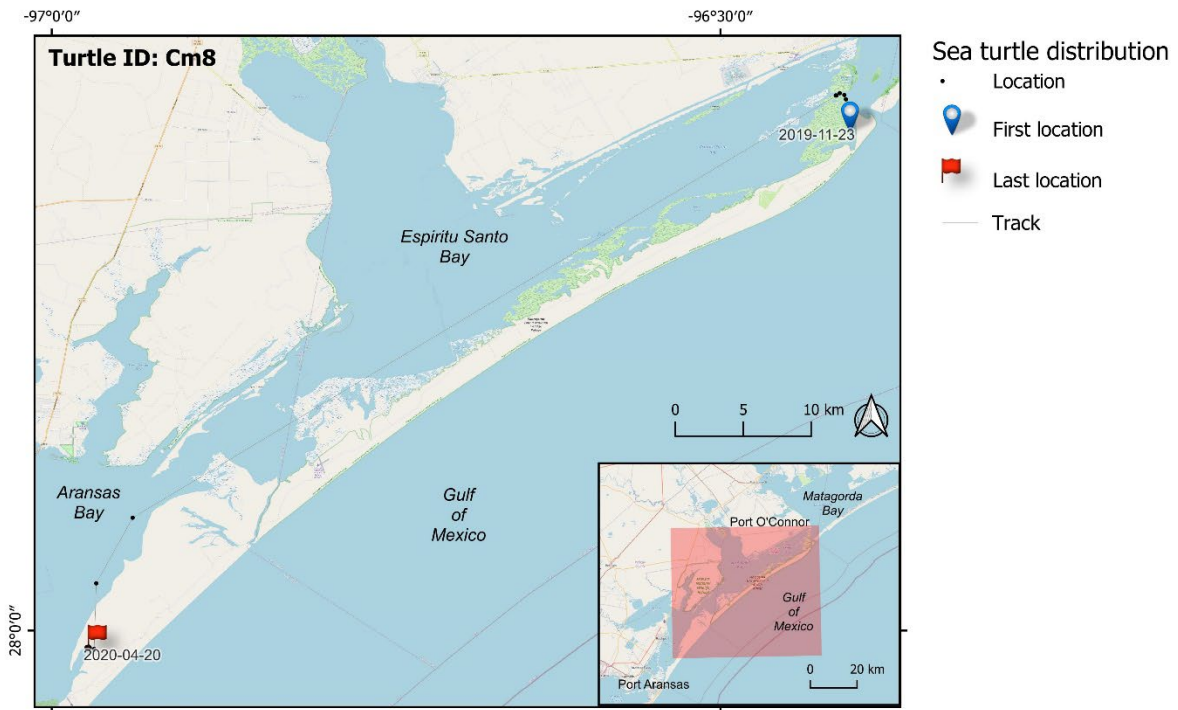


Figure 92. Movement of a juvenile green turtle (ID Cm8) from Matagorda Bay, tracked with a Telonics GPS-Iridium transmitter in 2019. There was no available data on seagrass distribution for this area.

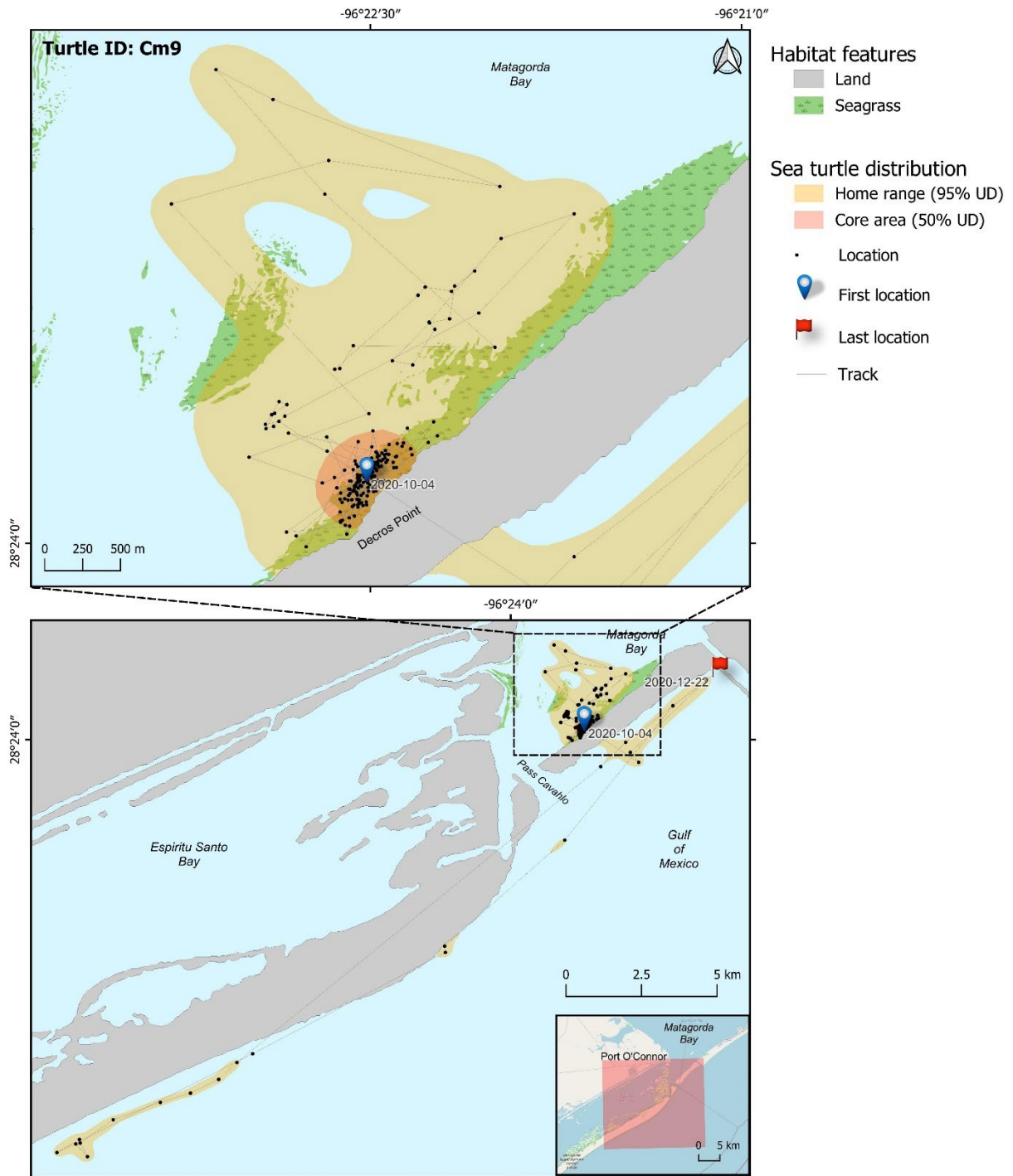


Figure 93. Movement of a juvenile green turtle (ID Cm9) from Matagorda Bay, tracked with a Lotek Fast-GPS Argos-linked transmitter in 2020. Seagrass distribution data provided by BIO-WEST.

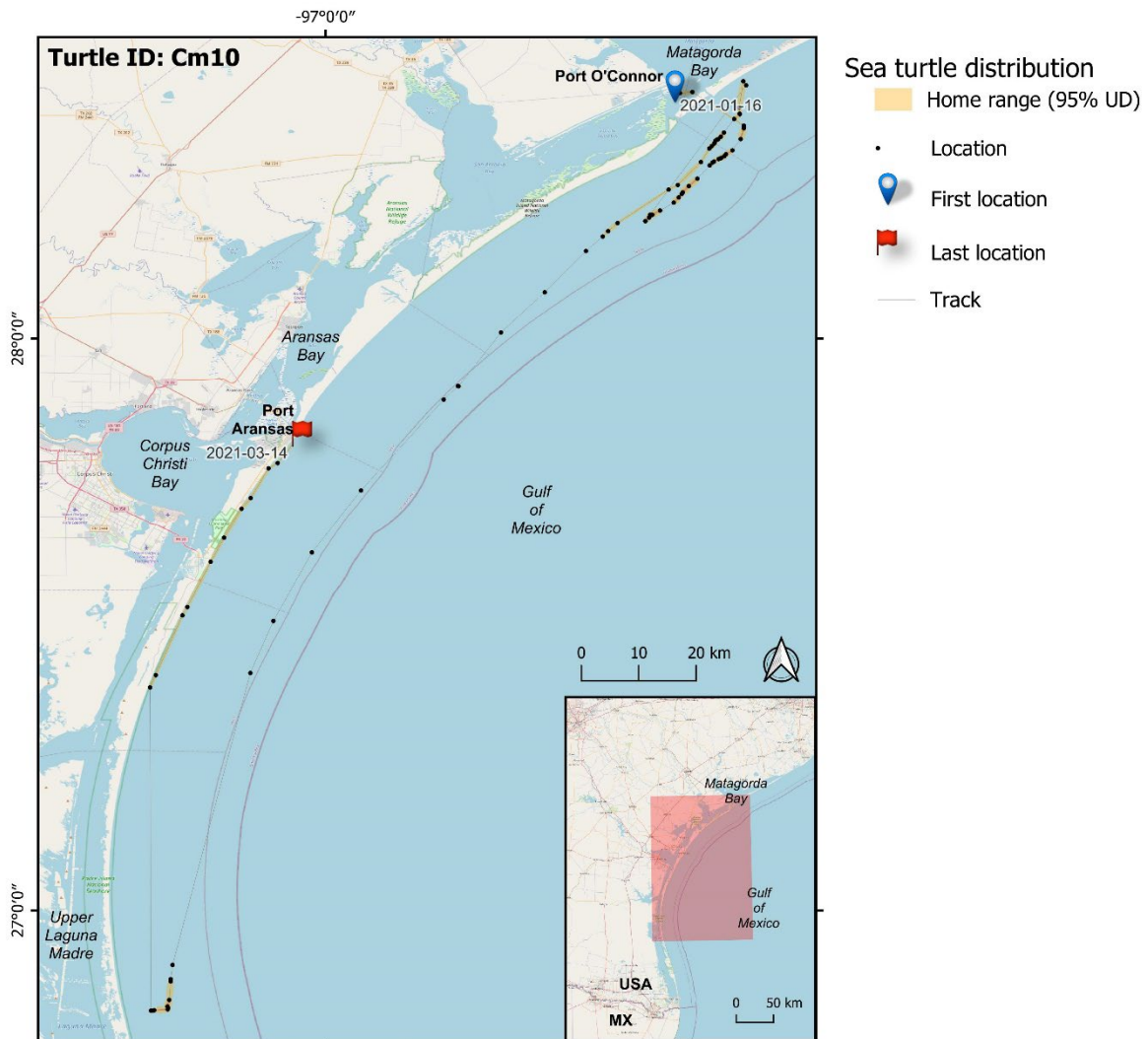


Figure 94. Movement of a juvenile green turtle (ID Cm10) from Matagorda Bay, tracked with a Lotek Fast-GPS Argos-linked transmitter in 2021.

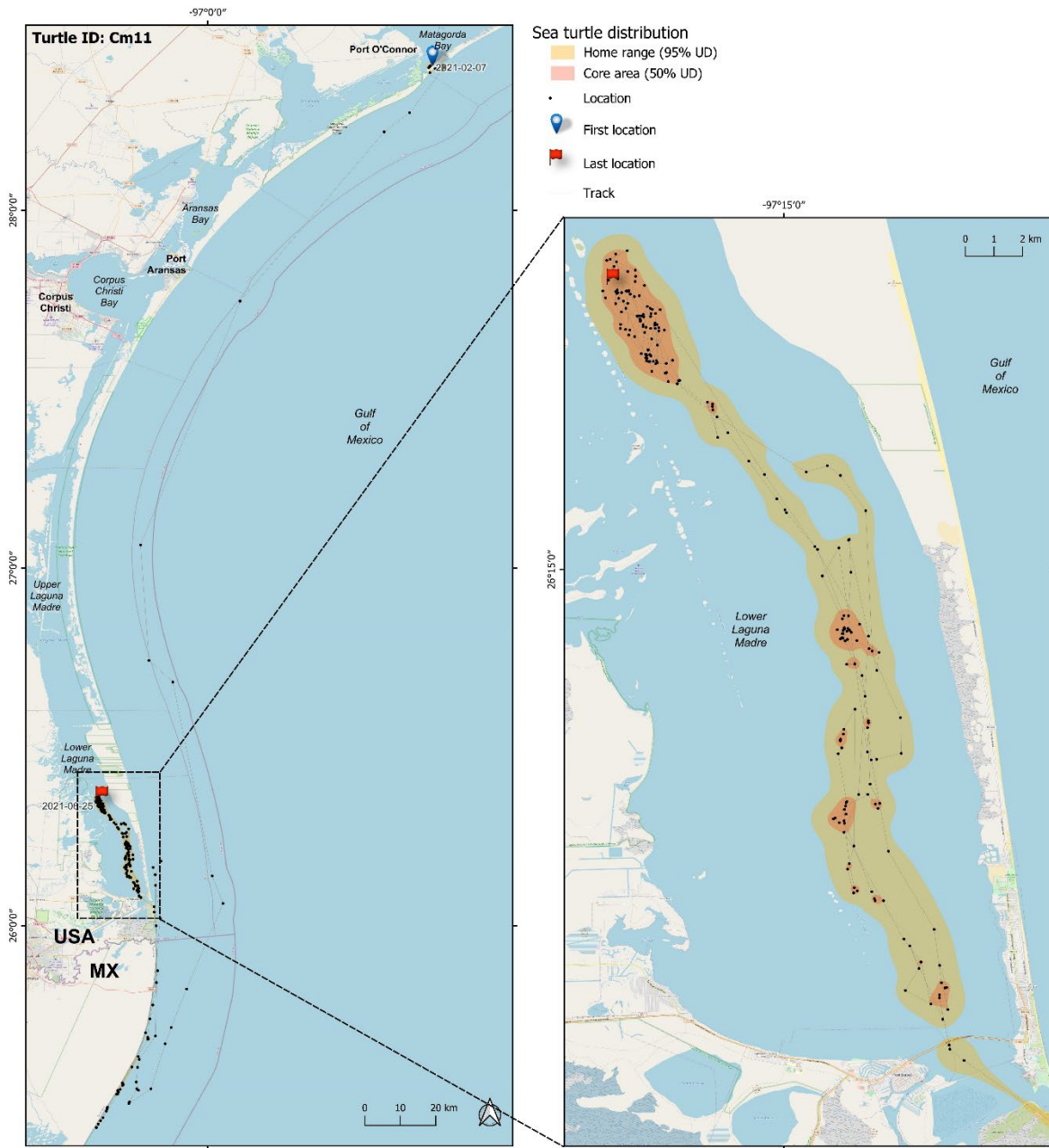


Figure 95. Movement of a juvenile green turtle (ID Cm11) from Matagorda Bay, tracked with a Lotek Fast-GPS Argos-linked transmitter in 2021. There was no available data on seagrass distribution for this area.

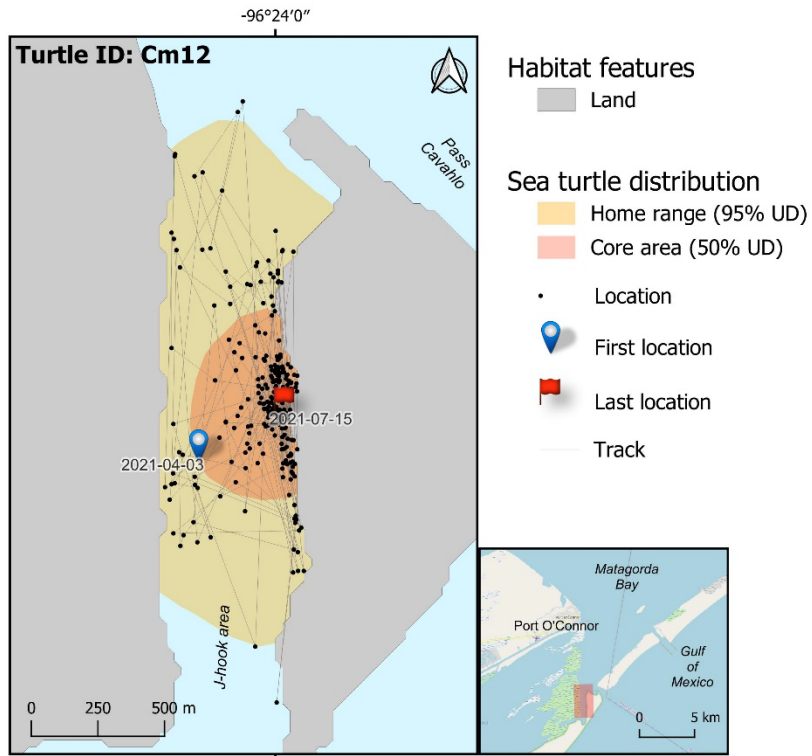


Figure 96. Movement of a juvenile green turtle (ID Cm12) from Matagorda Bay, tracked with a Lotek Fast-GPS Argos-linked transmitter in 2021. No benthic surveys were carried out in this area, therefore it was not possible to overlay seagrass distribution and sea turtle tracks.

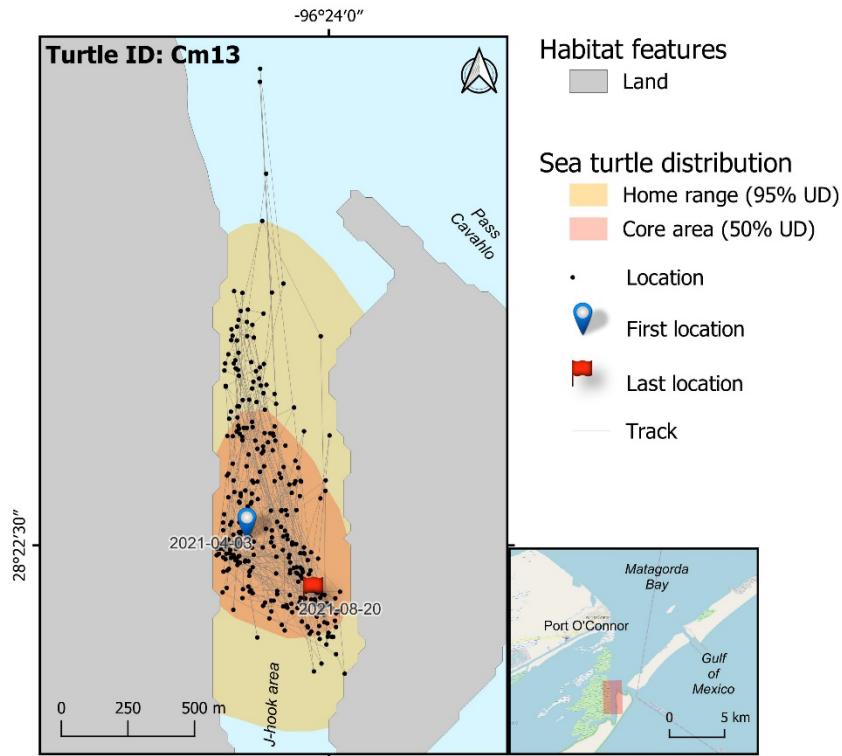


Figure 97. Movement of a juvenile green turtle (ID Cm13) from Matagorda Bay, tracked with a Lotek Fast-GPS Argos-linked transmitter in 2021. No benthic surveys were carried out in this area, therefore it was not possible to overlay seagrass distribution and sea turtle tracks

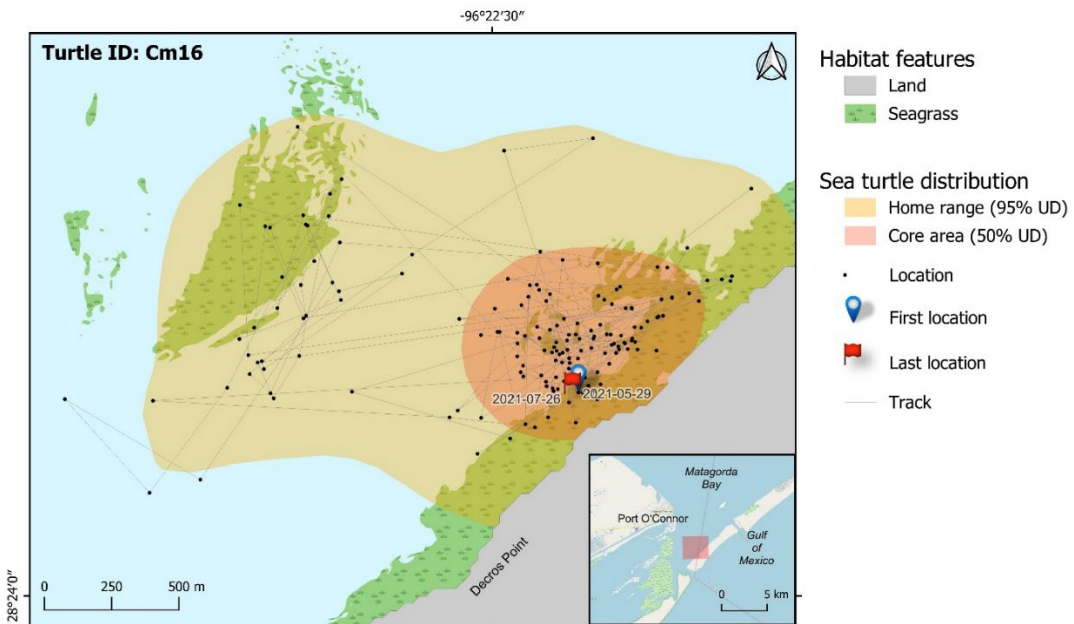


Figure 98. Movement of a juvenile green turtle (ID Cm16) from Matagorda Bay, tracked with a Lotek Fast-GPS Argos-linked transmitter in 2021. Seagrass distribution data provided by BIO-WEST.

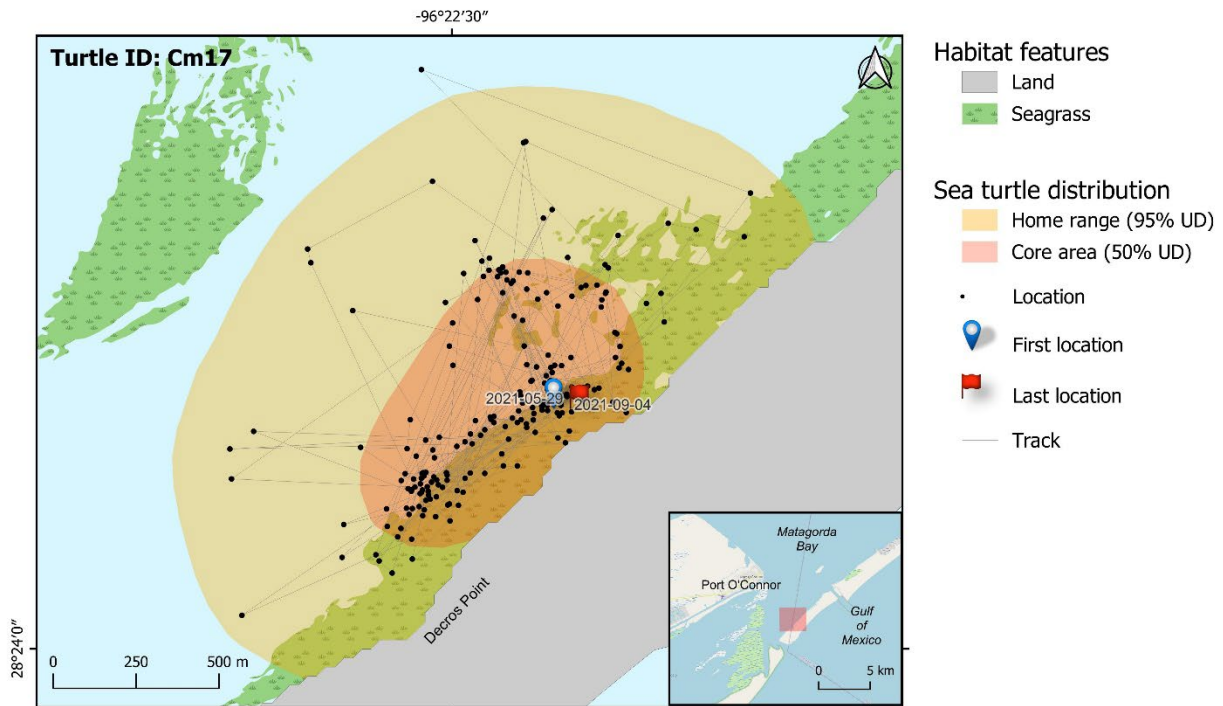


Figure 99. Movement of a juvenile green turtle (ID Cm17) from Matagorda Bay, tracked with a Lotek Fast-GPS Argos-linked transmitter in 2021. Seagrass distribution data provided by BIO-WEST.

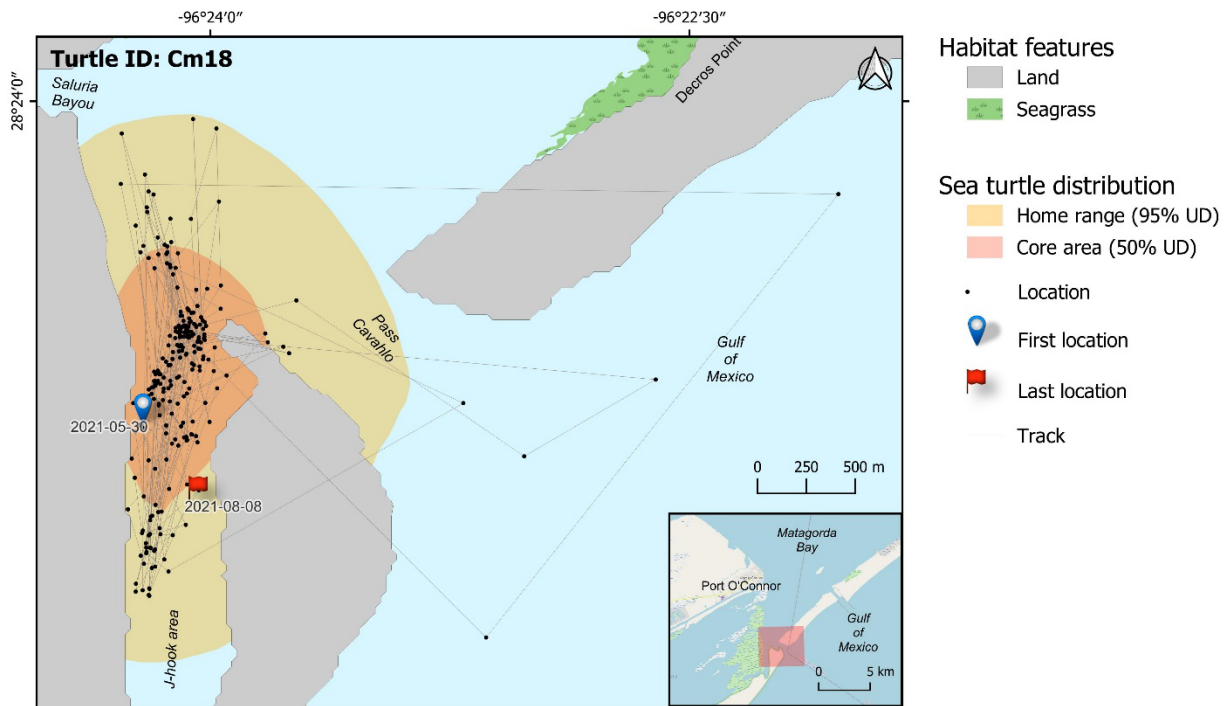


Figure 100. Movement of a juvenile green turtle (ID Cm18) from Matagorda Bay, tracked with a Lotek Fast-GPS Argos-linked transmitter in 2021. No benthic surveys were carried out in this area, therefore it was not possible to overlay seagrass distribution and sea turtle tracks.

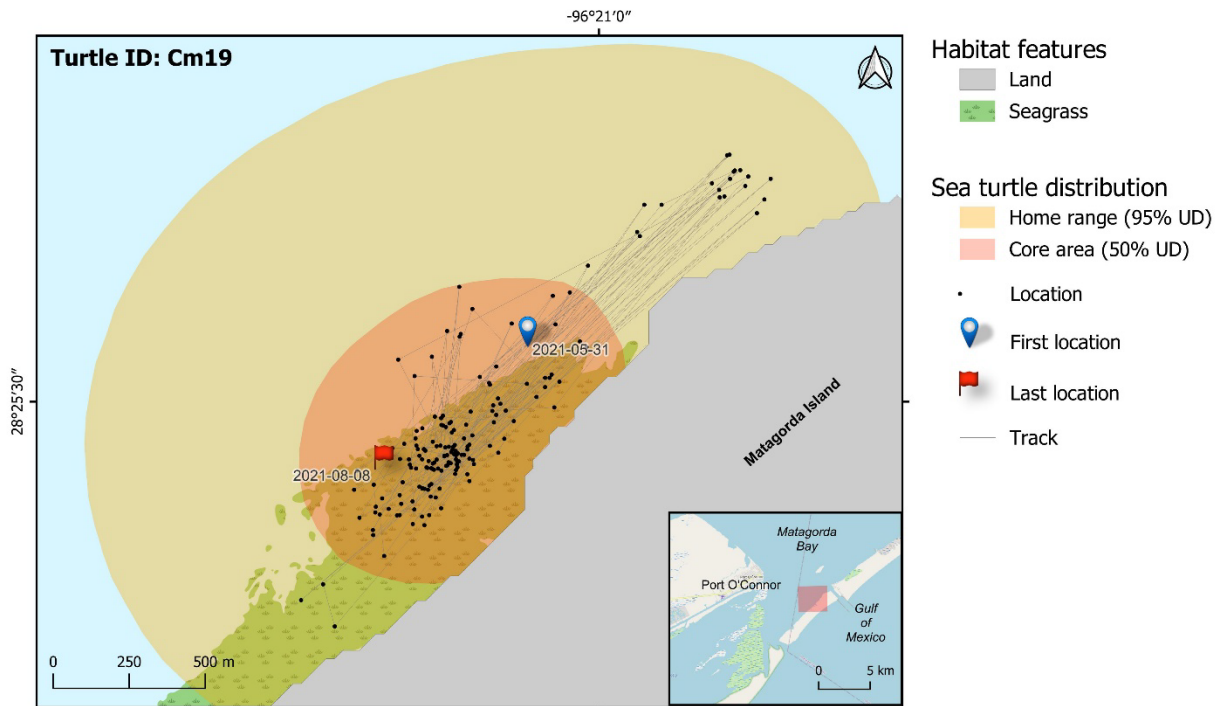


Figure 101. Movement of a juvenile green turtle (ID Cm19) from Matagorda Bay, tracked with a Lotek Fast-GPS Argos-linked transmitter in 2021. Seagrass distribution data provided by BIO-WEST.

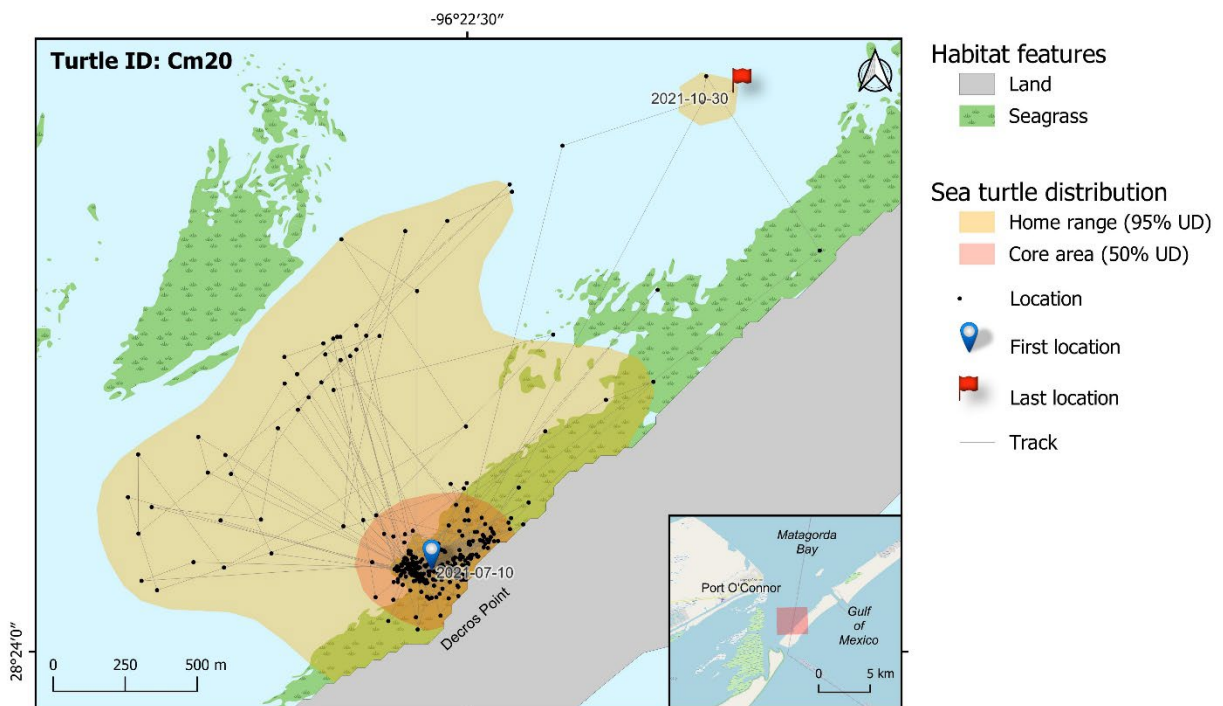


Figure 102. Movement of a juvenile green turtle (ID Cm20) from Matagorda Bay, tracked with a Lotek Fast-GPS Argos-linked transmitter in 2021. Seagrass distribution data provided by BIO-WEST.

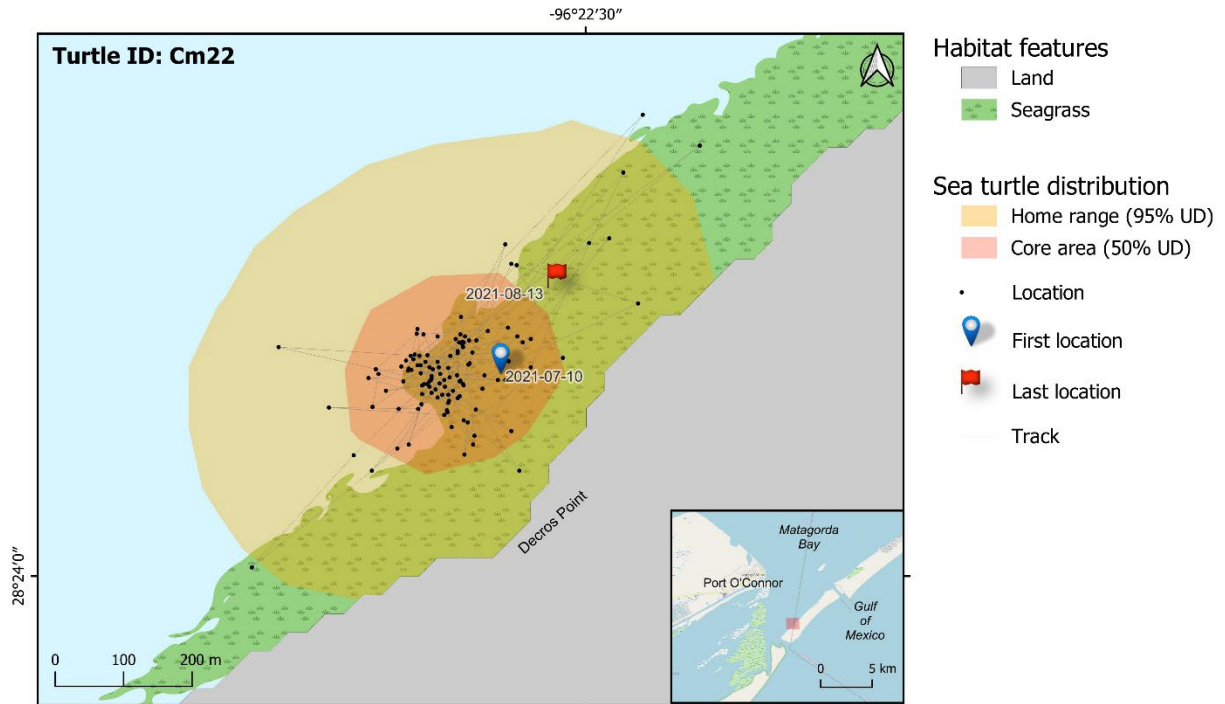


Figure 103. Movement of a juvenile green turtle (ID Cm22) from Matagorda Bay, tracked with a Lotek Fast-GPS Argos-linked transmitter in 2021. Seagrass distribution data provided by BIO-WEST.

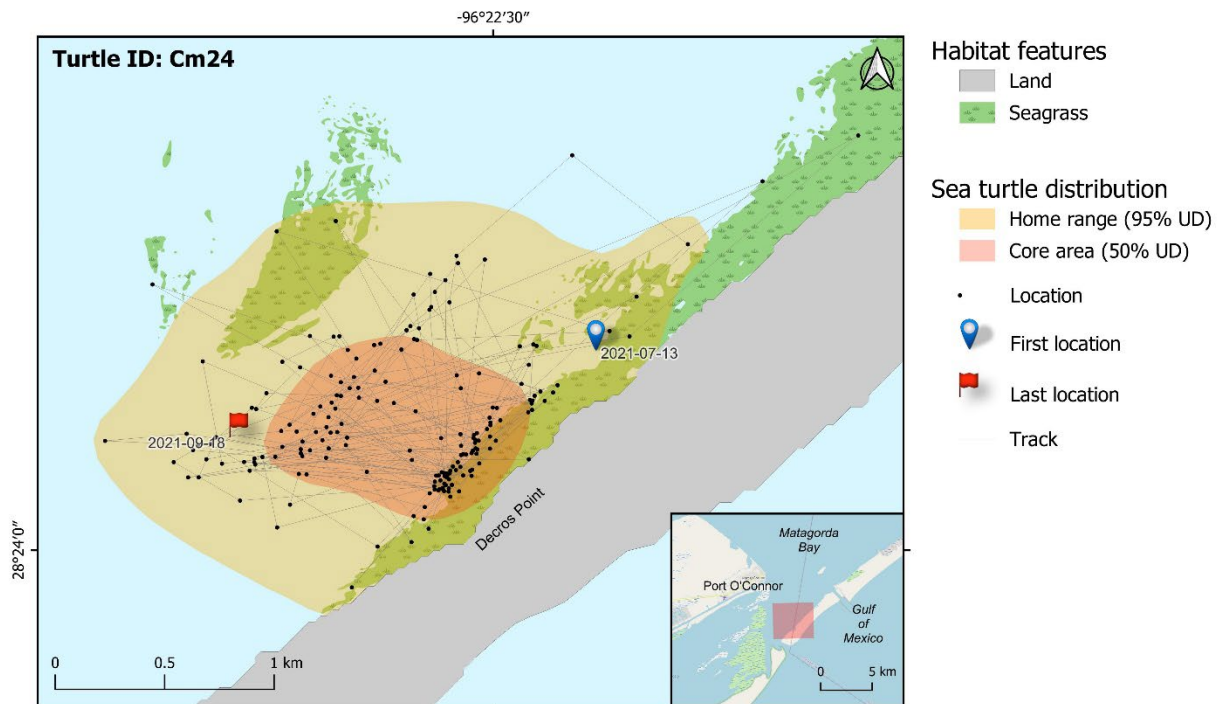


Figure 104. Movement of a juvenile green turtle (ID Cm24) from Matagorda Bay, tracked with a Lotek Fast-GPS Argos-linked transmitter in 2021. Seagrass distribution data provided by BIO-WEST.

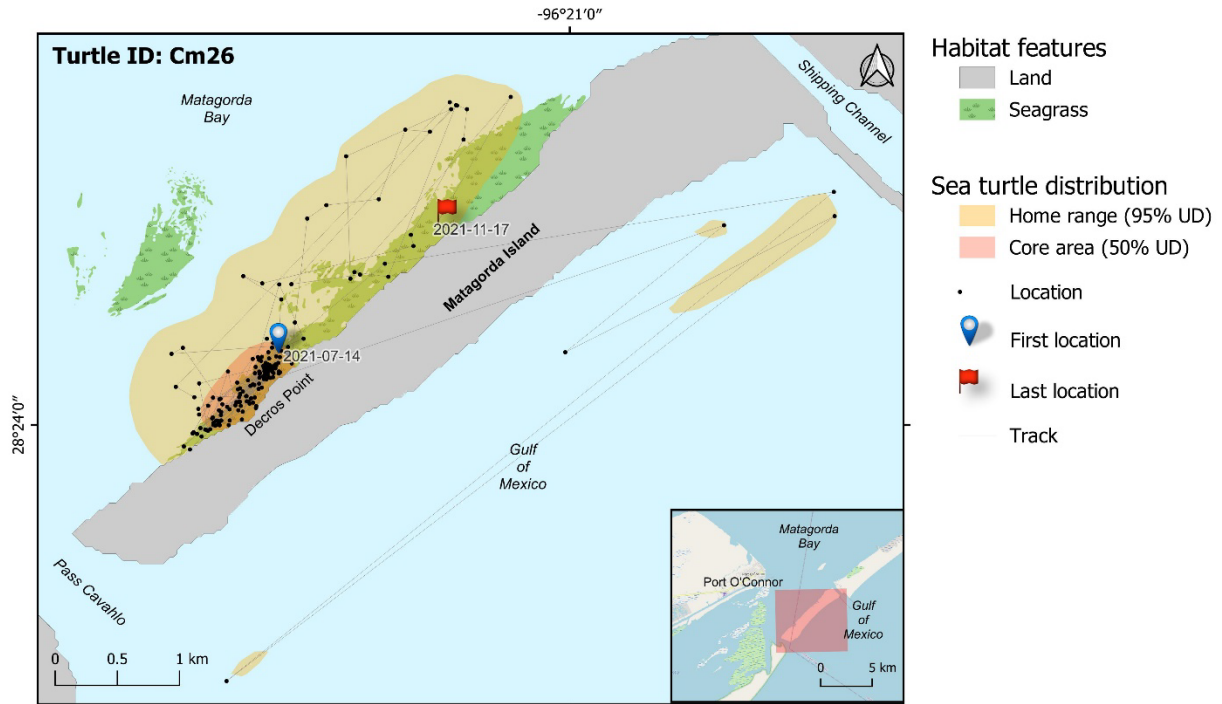


Figure 105. Movement of a juvenile green turtle (ID Cm26) from Matagorda Bay, tracked with a Lotek Fast-GPS Argos-linked transmitter in 2021. Seagrass distribution data provided by BIO-WEST.

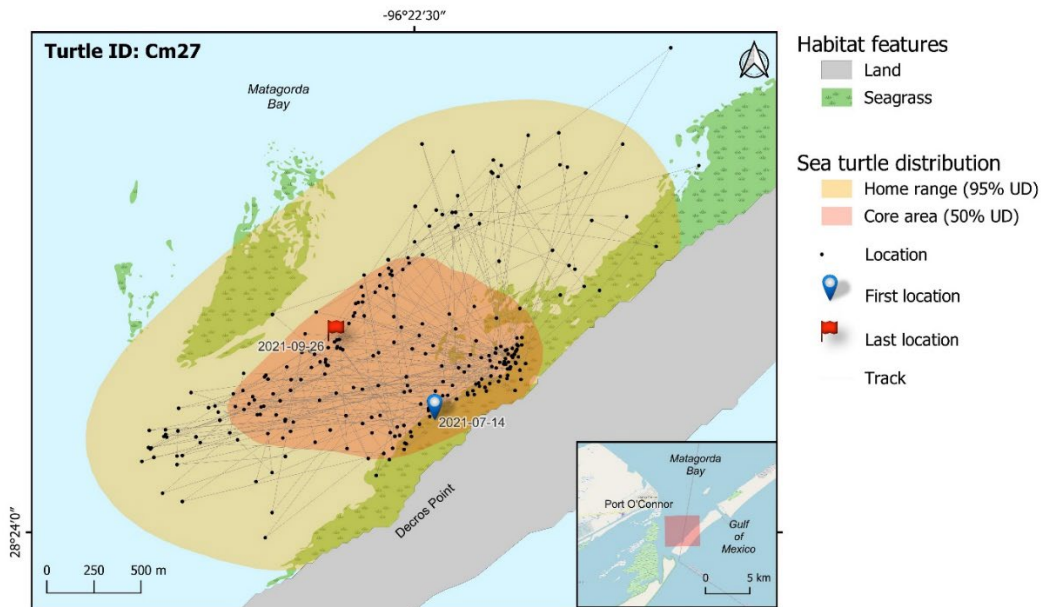


Figure 106. Movement of a juvenile green turtle (ID Cm27) from Matagorda Bay, tracked with a Lotek Fast-GPS Argos-linked transmitter in 2021. Seagrass distribution data provided by BIO-WEST.

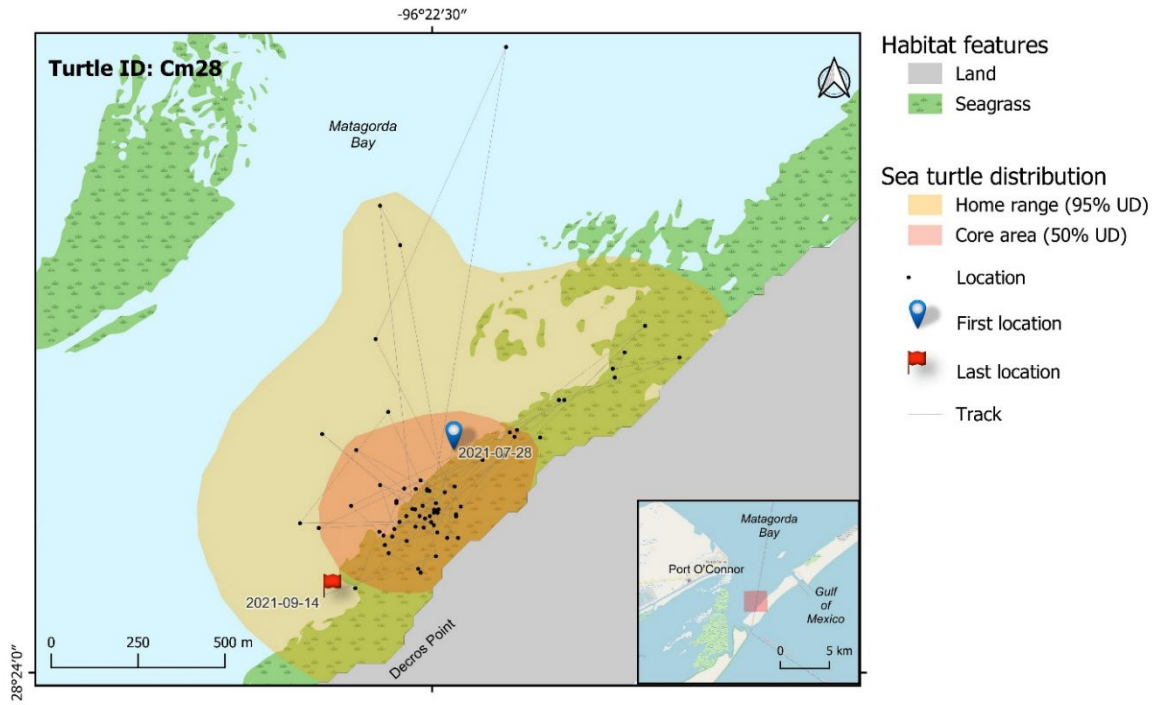


Figure 107. Movement of a juvenile green turtle (ID Cm28) from Matagorda Bay, tracked with a Lotek Fast-GPS Argos-linked transmitter in 2021. Seagrass distribution data provided by BIO-WEST.

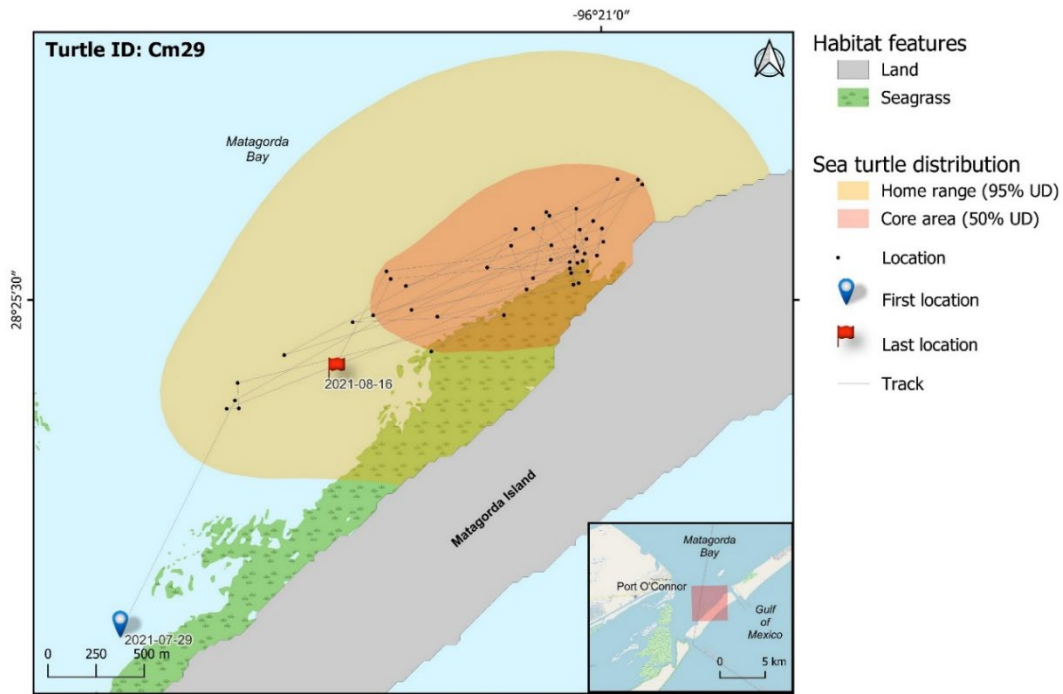


Figure 108. Movement of a juvenile green turtle (ID Cm29) from Matagorda Bay, tracked with a Lotek Fast-GPS Argos-linked transmitter in 2021. Seagrass distribution data provided by BIO-WEST.

Sea turtle home ranges derived from acoustic tracking data

Eleven (91.7%) of 12 acoustically-tagged green turtles were detected (total filtered detections = 9,611) between November 2019 to September 2021 (Table 20; Figure 109, Figure 110). Cm19 was never detected on any receiver. However, this green turtle was also equipped with a Lotek Fast-GPS Argos-linked transmitter, which revealed residency within Matagorda Bay outside the detection range of the acoustic array. Individuals were at liberty (period between the tagging date and last detection) for 10-163 days (mean \pm SD: 62 ± 48 days) with detection spans (period between the first and last detections) of 2.5 hours to 158 days (55 ± 50 days). Green turtles were detected on 4 (19.0%; MB17, MB18, MB19, and MB23) of the 21 receivers in the Matagorda Bay array, positioned within 0.78-1.22 km of one another near the entrance to Pass Cavallo and the J-hook area between the entrance of Mule Slough and Saluria Bayou. These four receivers were positioned closest (0.68-2.87 km) to the tagging locations for sea turtles detected within the Matagorda Bay array resulting in a spatial bias of detections given the relatively small home ranges of juvenile green turtles observed in this study calculated from satellite-derived GPS locations (see above). Cm10 was never detected within the Matagorda Bay array and was only detected on two acoustic receivers positioned 91.3 km (entrance to Aransas Pass) and 105.5 km (a 47.2-m steel cargo ship, *M/V Kinta S*, submerged as an artificial reef structure within the Corpus Christi Nearshore Reef), respectively, south from its tagging location (Figure 109, Figure 110). This green turtle was also equipped with a Lotek Fast-GPS Argos-linked transmitter, which revealed it emigrated from Matagorda Bay within 24 h post-release into the Gulf of Mexico. Cm11 had a single 35.7 min visit to MB17 42 h post-release and was subsequently detected 35 days later on a receiver inside the entrance to the Brazos Santiago Pass (269.2 km to the south and maintained by Dr. Kline at The University of Texas Rio Grande Valley). This sea turtle was also equipped with a Lotek Fast-GPS Argos-linked transmitter, which corroborated its emigration from Matagorda Bay 4 days post-release into the Gulf of Mexico and immigrated into the lower Laguna Madre on the same day on which it was acoustically detected at the Brazos Santiago Pass.

The receiver deployed closest to the J-hook area between the entrance of Mule Slough and Saluria Bayou (MB19) recorded the most detections (85.6% of all detections) with the receiver deployed closest to Pass Cavallo (MB18) recording the fewest detections (1.1%) within the Matagorda Bay array (Figure 111). Interestingly, movements between these two receivers (separated by a distance of 0.78 km) had the highest frequency (58.8%) of all movements in the acoustic network with an equivalent number of combined directed movements (MB18 to MB19: 53 connections; MB19 to MB18: 54 connections) by the same four green turtles (Cm5, Cm6, Cm13, Cm18). Network analyses demonstrated that while visits to MB18 were relatively brief (3.9 ± 3.1 min; range: 2.7-21.6 min), green turtles would pass through this area near the entrance to Pass Cavallo when visiting the J-hook area (MB19: 49.1 ± 105.5 min; range: 2.7 min to 12.5 h) more frequently than directed movements from any other receiver, thus highlighting the centrality (level of connectedness) of this receiver despite a low detection frequency (Figure 111).

Although, the monitoring period for the receiver deployed closest to the entrance of Saluria Bayou (MB23) temporally overlapped with only two acoustically-tagged sea turtles (Cm5 and Cm6; Figure 90), it accounted for the second highest frequency of detections (7.1%) and movements (21.4% between MB23 and MB17) in the acoustic network and the second longest mean and maximum visit duration (39.0 ± 102.6 min; range: 2.7 min to 9.2 h). Detections at receivers outside Matagorda Bay ($n = 3$) consisted of single visits (10.4-38.0 min) and directed movements (Figure 111). Detection frequencies were relatively consistent across the time of day with no clear diel differences observed (Figure 112).

Residency indices were variable among individual green turtles and ranged from 0 (Cm10) to 0.13 (Cm18) with a mean of 0.03 ± 0.05 (Table 19); however, these estimates are likely conservative given the relatively small detection range and spatial distribution of the receivers in Matagorda Bay. Roaming indices ranged from 0 (Cm10) to 0.19 (Cm5 and Cm6) with a mean of 0.09 ± 0.06 (Table 19), indicating that all green turtles were detected on less than 20% of the available receivers. There was a significant positive quadratic relationship between roaming and residency ($n = 11$, $R^2 = 0.936$, $F_{1,8} = 3.6 \times 10^{-6}$, $P = 0.0002$) that reached a maximum roaming index of 0.19 at a residency index of 0.08 (Figure 113). The decrease in roaming at the highest observed residency index of 0.13 is due to the loss of two receivers within the Matagorda Bay array while this green turtle (Cm18) was at liberty, including MB23 located near its home range (see below).

The area of acoustically-tagged green turtle home ranges (95% UD) in Matagorda Bay measured on average 1.6 ± 1.3 km² (range 0.4 – 2.9 km²), with core areas (50% UD) measuring on average 0.4 ± 0.4 km² (range 0.1-0.9 km²) (Table 19; Figure 114-Figure 116). Despite limited same sizes for estimating UD for green turtles from acoustic tracking data, home ranges were approximately half the size of GPS-based home ranges while core areas were very strikingly similar in size. Similarly, the J-hook area between the entrance of Mule Slough and Saluria Bayou was identified as a high use area based on acoustic tracking data.

Table 20. Acoustic tracking details of green turtles captured in Matagorda Bay between 2019 and 2021. PTT: Platform Transmitting Terminal, DAL: Days at Liberty.

Tag Model	Turtle ID	Acoustic Tag ID	PTT ID	Release Date (yyyy-mm-dd)	Detection Start Date (yyyy-mm-dd)	Detection Stop Date (yyyy-mm-dd)	DAL (d)	Detection Span (d)	Detection Days	Residency Index	Roaming Index
V13-1x-069k-1	Cm5	19075		2019-11-24	2019-11-25	2020-03-23	121	120	22	0.08	0.19
V13-1x-069k-1	Cm6	14594		2019-11-24	2019-11-24	2019-02-24	93	93	22	0.10	0.19
V16-4x-069k-2	Cm10	58010	202700	2021-01-17	2021-02-17	2021-03-14	57	25	2	0	0
V16-4x-069k-2	Cm11	58011	202703	2021-02-08	2021-02-09	2021-03-15	37	35	2	<0.01	0.05
V16-4x-069k-2	Cm12	58012	202701	2021-04-04	2021-04-13	2021-04-30	27	18	2	<0.01	0.06
V16-4x-069k-2	Cm13	58013	202702	2021-04-04	2021-04-07	2021-06-17	76	72	10	0.03	0.11
V16-4x-069k-2	Cm14	58014		2021-04-06	2021-04-10	2021-09-15	163	159	2	0.01	0.06
V16-4x-069k-2	Cm16	58015	215057	2021-05-30	2021-06-02	2021-06-16	18	15	5	<0.01	0.06
V16-4x-069k-2	Cm17	58016	215058	2021-05-30	2021-06-04	2021-06-17	19	14	4	<0.01	0.06
V16-4x-069k-2	Cm18	58017	215060	2021-05-31	2021-06-01	2021-08-04	66	65	54	0.13	0.17
V16-4x-069k-2	Cm19	58018	215062	2021-05-31	-	-	-	-	-	-	-
V16-4x-069k-2	Cm22	58019	215061	2021-07-11	2021-07-20	2021-07-20	11	1	1	<0.01	0.06

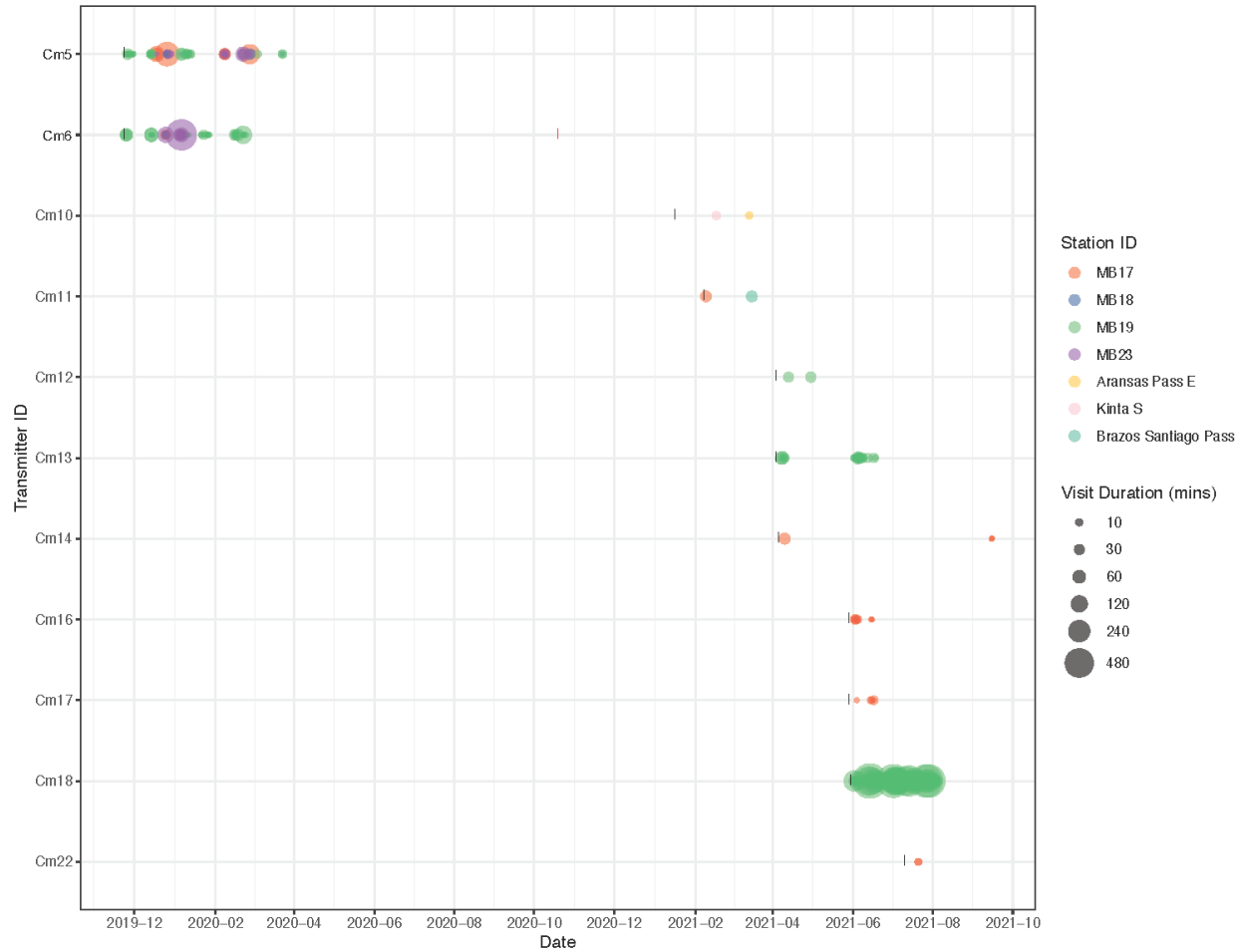


Figure 109. Acoustic detections recorded over the monitoring period for each tagged green turtle. The size of each point indicates the visit duration recorded by each receiver (color) for each individual. Black vertical lines represent deployment dates of each transmitter, while red vertical lines indicate the estimated transmitter battery life end date.

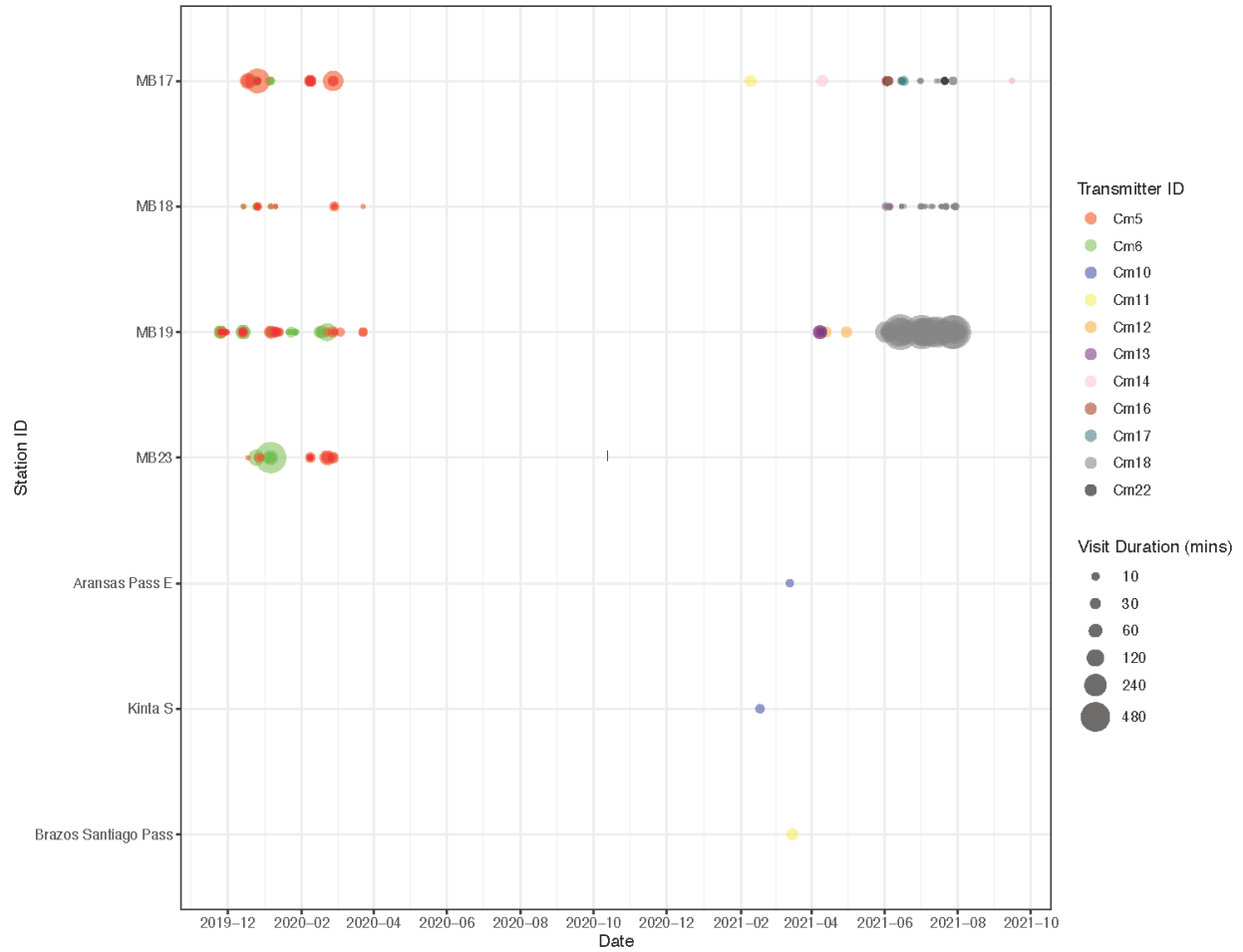


Figure 110. Green turtle acoustic detections recorded over the monitoring period for each receiver. The size of each point indicates the visit duration recorded for each individual (color) at each receiver. Black vertical lines represent the last receiver download date.

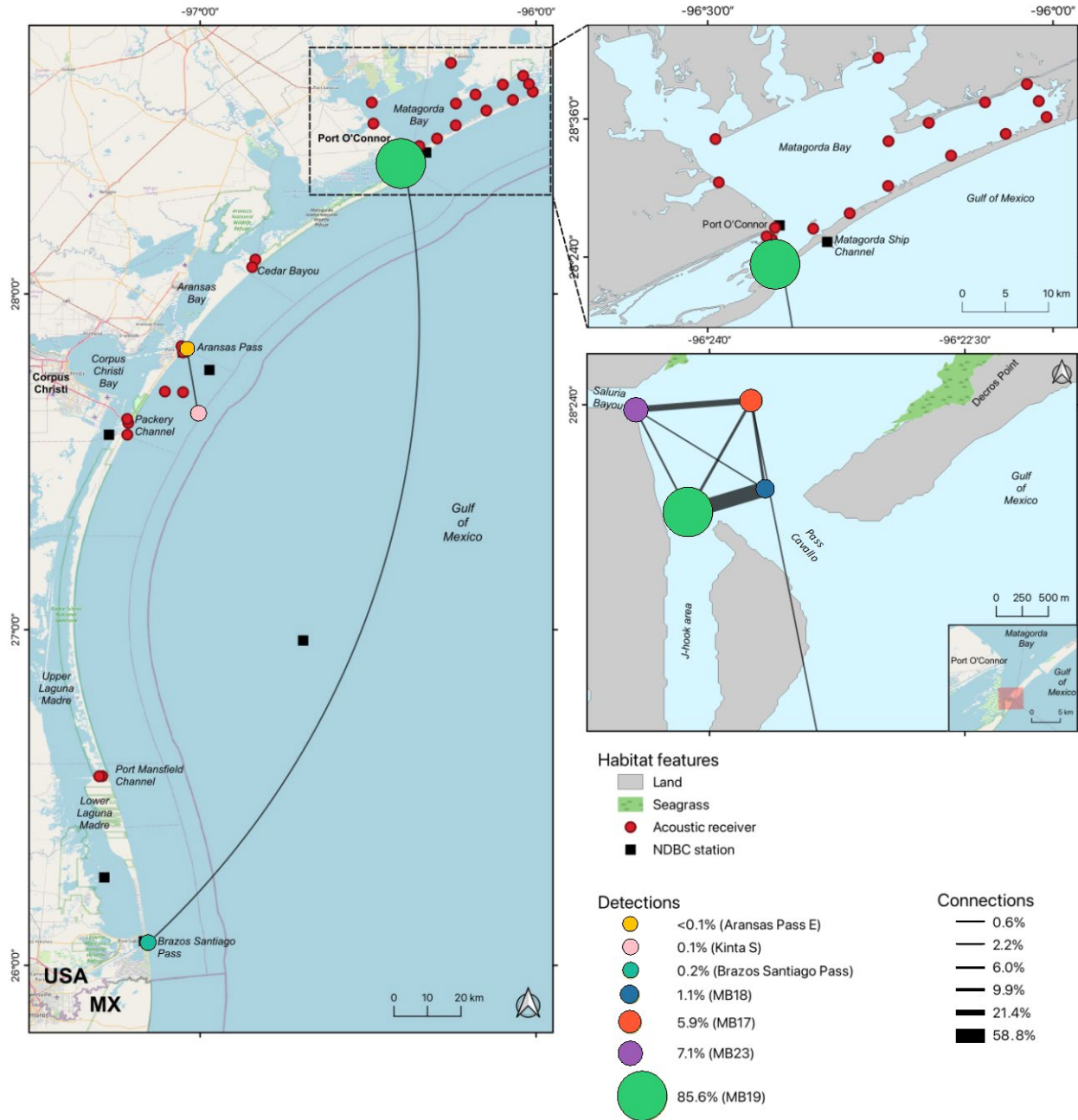


Figure 111. Green turtle acoustic detections and acoustic receiver network map. The color and size of each node corresponds to the percentage of detections recorded at each receiver. The network map represents the frequency of movements (connections) between each pair. The relative thickness of the edge (black line) connecting the nodes corresponds to the frequency of movements (connections) between each pair of acoustic receivers. Acoustic receivers which did not record detections are represented by red circles. National Data Buoy Center (NDBC) stations, which record meteorological and hydrological environmental parameters, are represented by black squares.

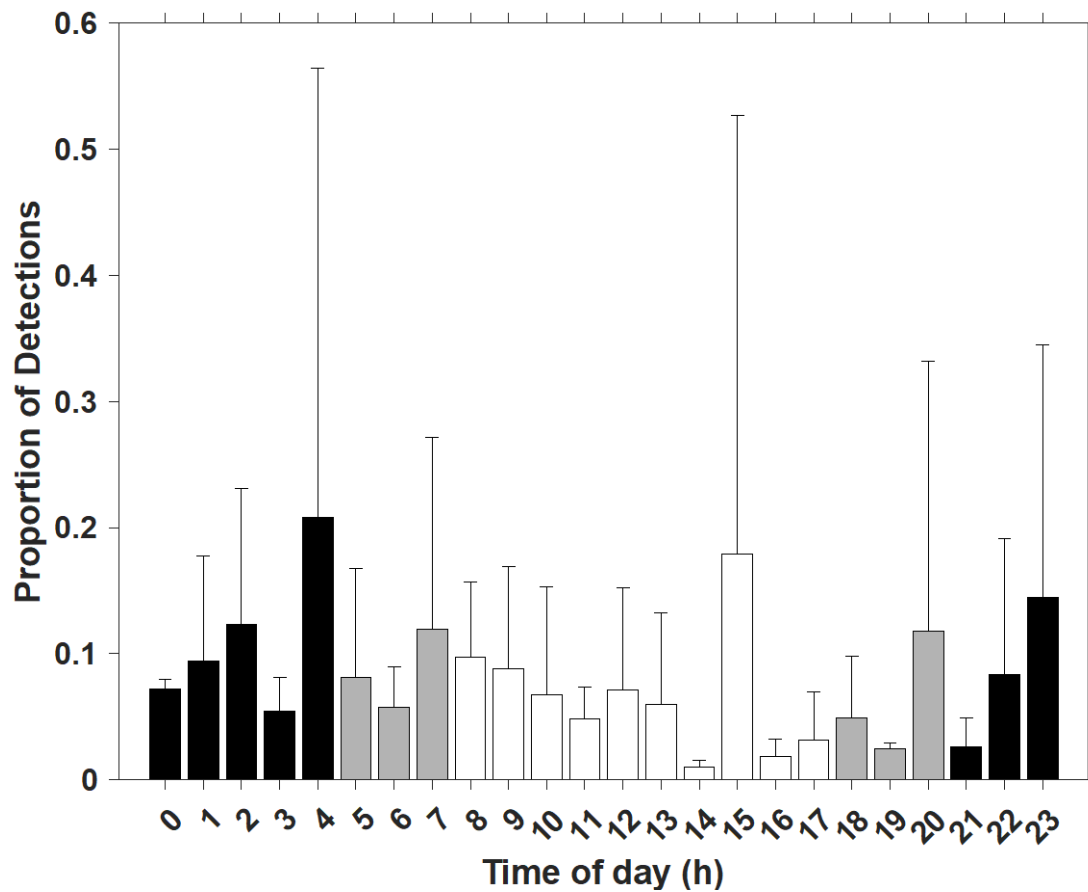


Figure 112. Diel variation in green turtle acoustic transmitter detections within the Matagorda Bay array calculated as the mean proportion of detections per individual by time of day based on local times. Colors correspond to night (black), day (white), and dawn/dusk (grey). Error bars represent the standard deviation among individual green turtles.

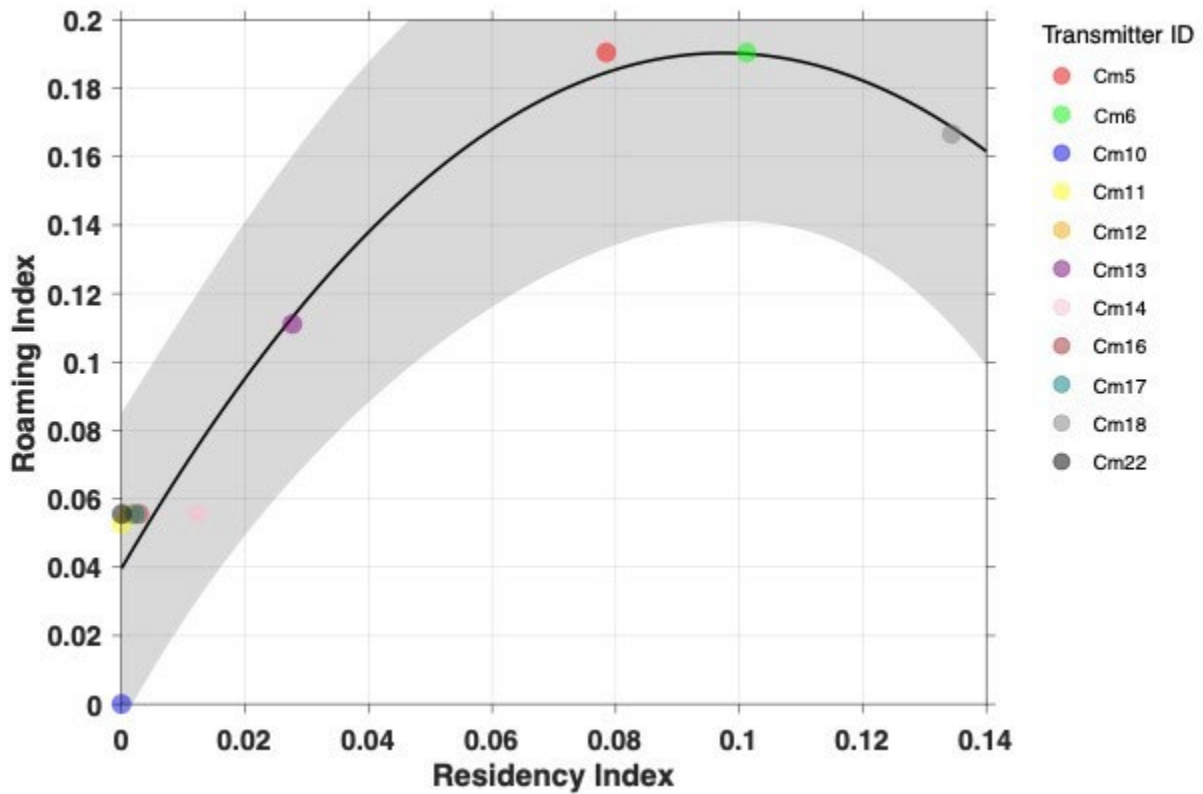


Figure 113. Roaming-residency indices plot for green turtles (color) detected within the Matagorda Bay acoustic array. The quadratic relationship ($\text{Roaming Index} = -15.867 \times \text{Residency Index}^2 + 3.0923 \times \text{Residency Index} + 0.0397$) between roaming and residency is represented by the black solid line. Shaded areas represent 95% confidence limits.

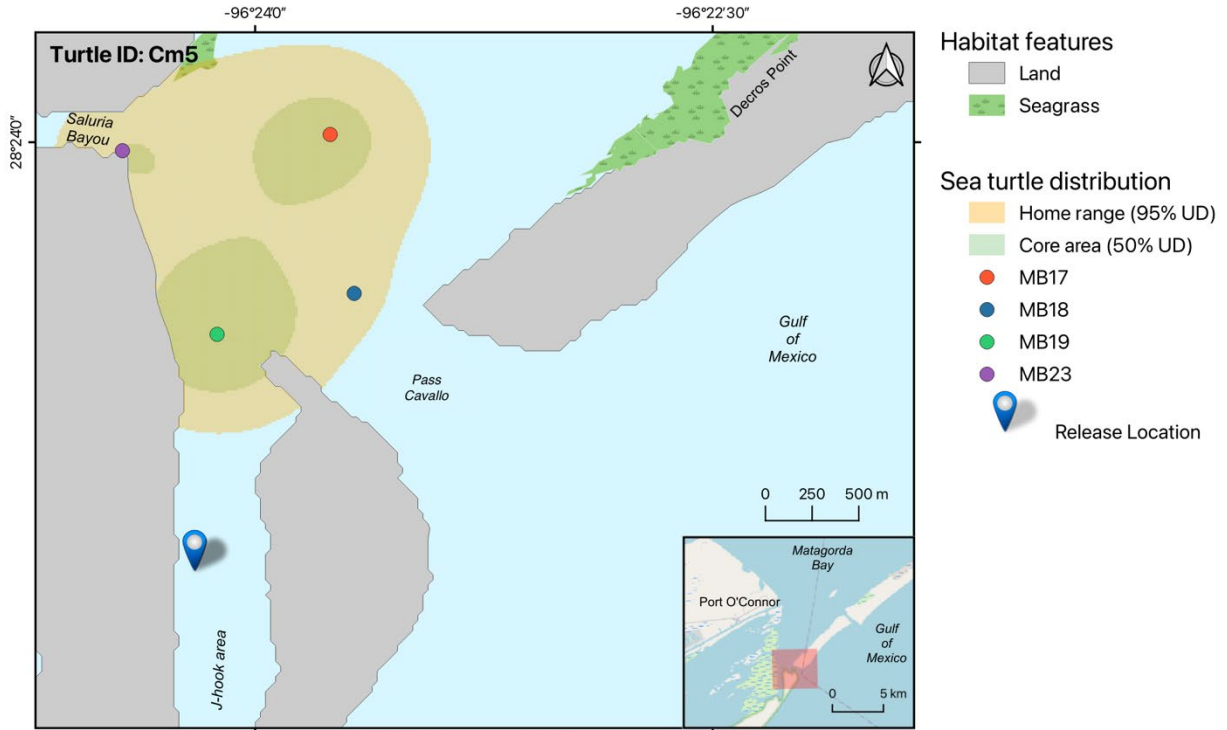


Figure 114. Home range (95% utilization distribution) and core area (50% utilization distribution) of a juvenile green turtle (ID Cm5), tracked with an acoustic transmitter from 2019-2020. Colored points represent the receiver locations where the individual was detected. No benthic surveys were carried out in this area, therefore it was not possible to overlay seagrass and green turtle utilization distributions.

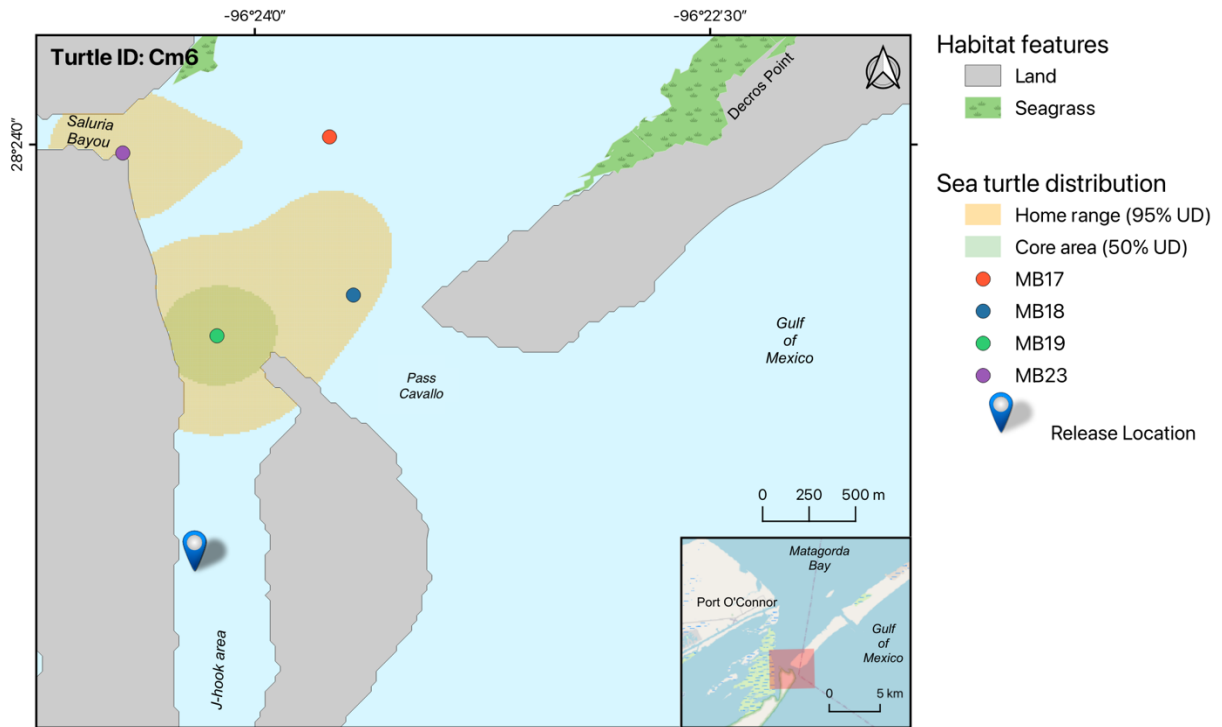


Figure 115. Home range (95% utilization distribution) and core area (50% utilization distribution) of a juvenile green turtle (ID Cm6), tracked with an acoustic transmitter from 2019-2020. Colored points represent the receiver locations where the individual was detected. No benthic surveys were carried out in this area, therefore it was not possible to overlay seagrass and green turtle utilization distributions.

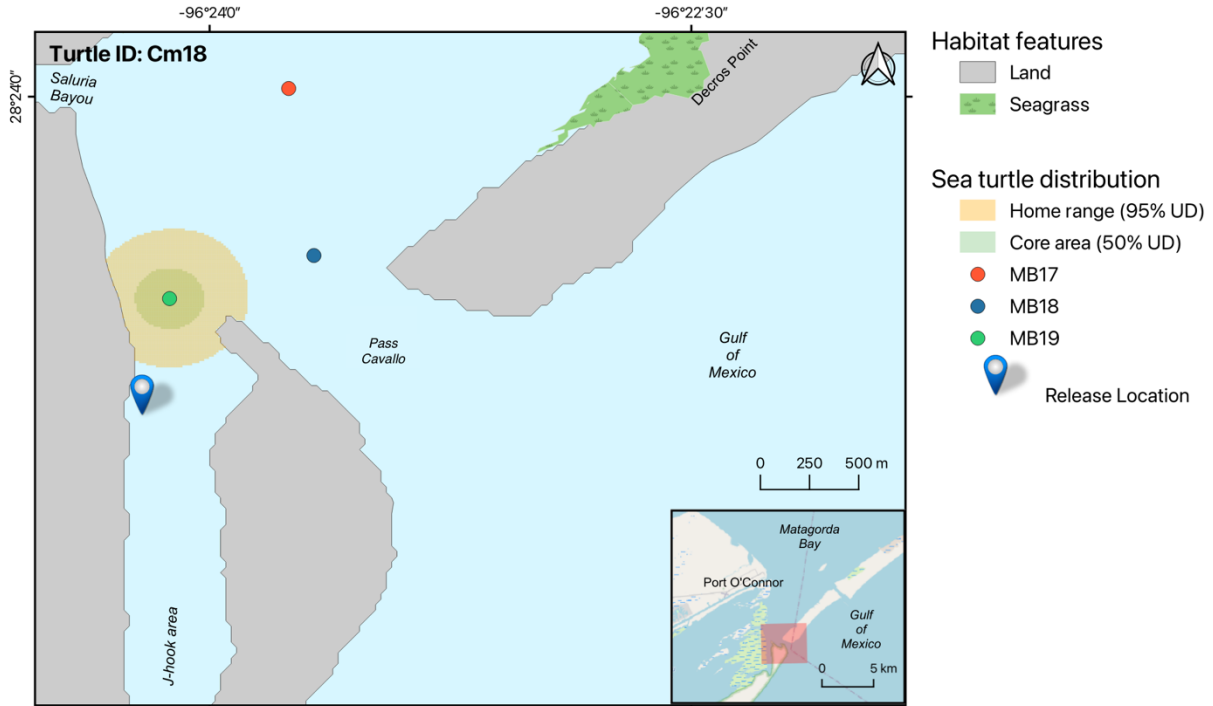


Figure 116. Home range (95% utilization distribution) and core area (50% utilization distribution) of a juvenile green turtle (ID Cm18), tracked with an acoustic transmitter in 2021. Colored points represent the receiver locations where the individual was detected. Note the absence of the MB23 receiver in 2021 near the entrance to Saluria Bayou. No benthic surveys were carried out in this area, therefore it was not possible to overlay seagrass distribution and sea turtle tracks.

Seasonal changes in sea turtle habitat use

Environmental factors were examined for their influence on green turtle move persistence (Figure 117-Figure 119) and residency within Matagorda Bay using satellite and acoustic tracking data, respectively. Air temperature was the only candidate predictor variable retained in the GAMM that best fit the move persistence index (Table 21). The model explained 6.5% of deviance in move persistence by green turtles, indicating there are additional factors beyond our model explaining the majority of variation in their movement behavior. Nevertheless, green turtles dramatically increase speed and directionality indicative of transiting behavior when air temperatures decline below 10°C with the shift towards increased move persistence occurring below 15°C (Figure 120).

Air temperature was also retained in the GAMM that best predicted the presence of green turtles within the Matagorda Bay array (Table 22). The probability of green turtles being detected within the array increased linearly with air temperature with a significantly higher presence at temperatures above 18°C (Figure 121). Atmospheric pressure was retained in the final GAMM, but was marginally non-significant and only able to predict sea turtle presence at relatively high pressures above 1029 mb, indicative of calm weather. The model explained 20.1% of deviance in sea turtle presence indicating air temperature, and to a lesser degree atmospheric pressure, are key drivers of green turtle presence within the Matagorda Bay array.

Table 21. Summary statistics from the final generalized additive mixed model on green turtle move persistence. $n = 350$, $df = 6$, maximum log-likelihood = -434.57, adjusted $R^2 = 0.068$, $AICc = 881.39$, Akaike weight = 0.544, deviance explained = 6.49%.

Term	edf	F-ratio	P
f(Air Temperature, °C)	3.52	13.77	< 0.00001

edf, estimated degrees of freedom

Table 22. Summary statistics from the final generalized additive mixed model on green turtle residency within Matagorda Bay. $n = 292$, $df = 7$, maximum log-likelihood = -638.38, adjusted $R^2 = 0.241$, $AICc = 1291.15$, Akaike weight = 0.999, deviance explained = 20.06%.

Term	edf	F-ratio	P
f(Air Temperature, °C)	1.00	16.16	< 0.00001
f(Atmospheric Pressure, mb)	2.94	2.91	0.0511

edf, estimated degrees of freedom

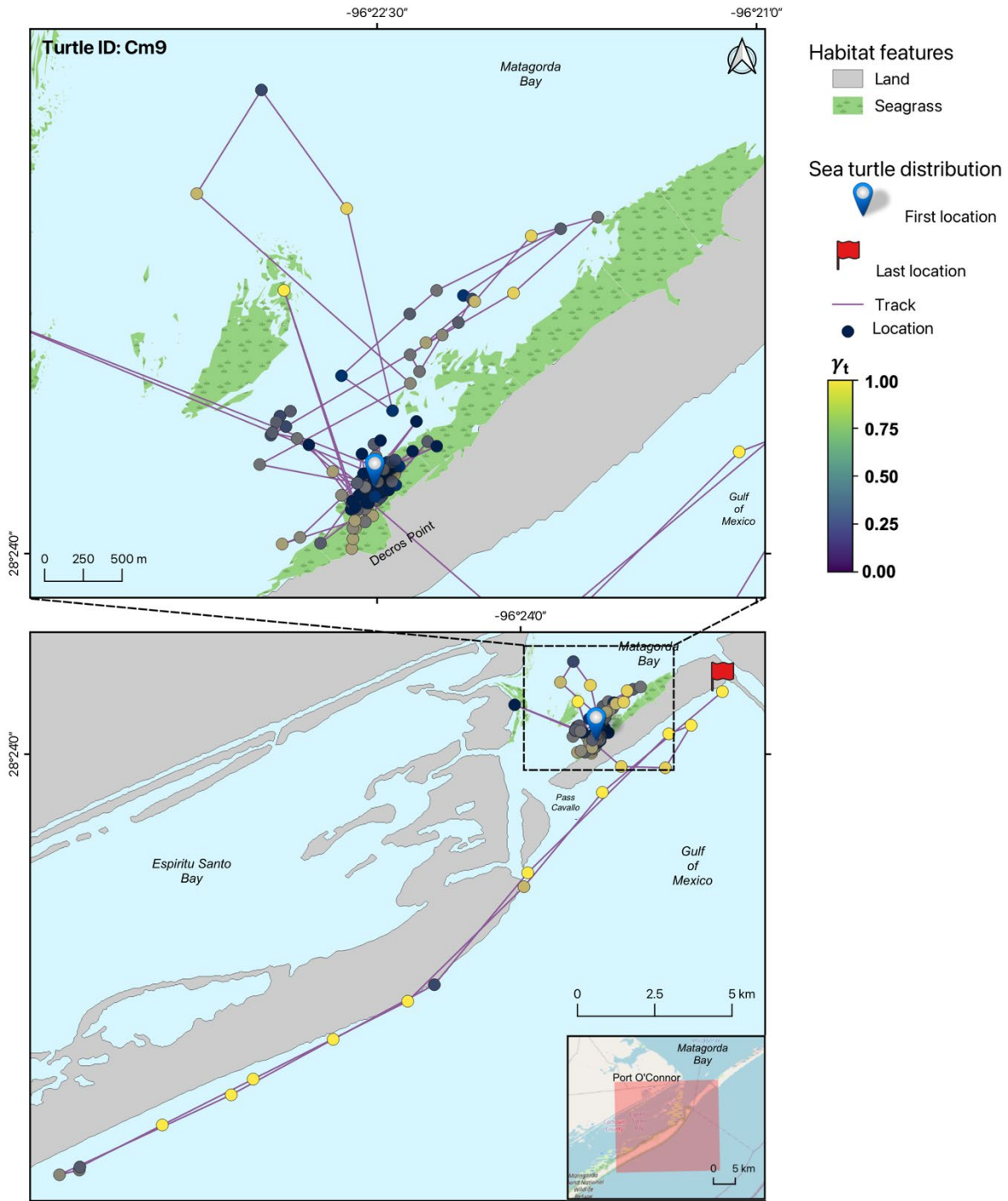


Figure 117. Movement of a juvenile green turtle (ID Cm9) from Matagorda Bay, tracked with a Lotek Fast-GPS Argos-linked transmitter in 2020. Points represent twelve-hour location estimates from the continuous-time move persistence model and are colored according to its move persistence index (γ_t). The move persistence index identifies changes in behavior along a continuum ranging from 0 (low speed and directionality indicative of area-restricted behavior) to 1 (high speed and directionality indicative of transiting behavior). Seagrass distribution data provided by BIO-WEST.

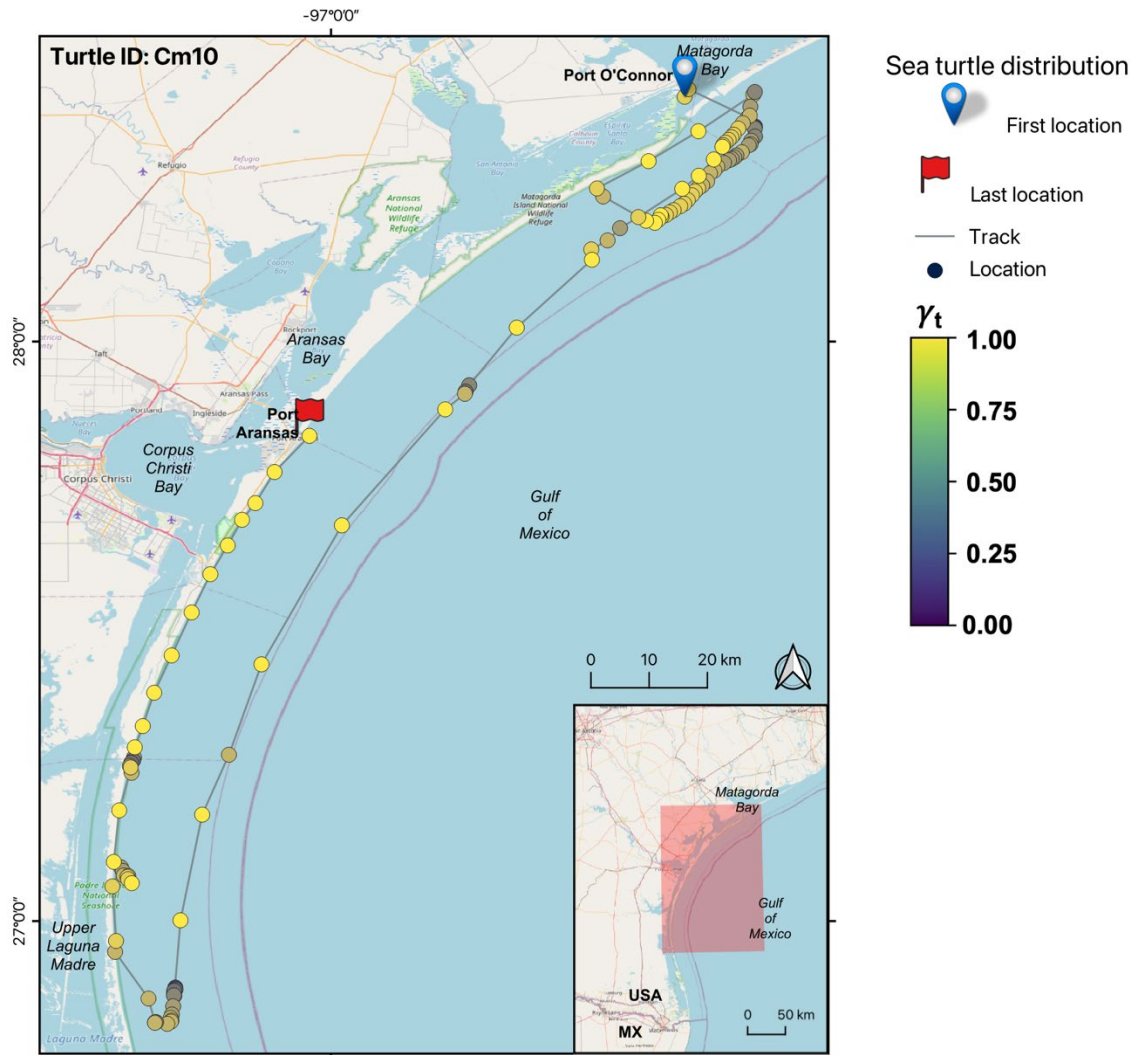


Figure 118. Movement of a juvenile green turtle (ID Cm10) from Matagorda Bay, tracked with a Lotek Fast-GPS Argos-linked transmitter in 2021. Points represent twelve-hour location estimates from the continuous-time move persistence model and are colored according to its move persistence index (γ_t). The move persistence index identifies changes in behavior along a continuum ranging from 0 (low speed and directionality indicative of area-restricted behavior) to 1 (high speed and directionality indicative of transiting behavior).

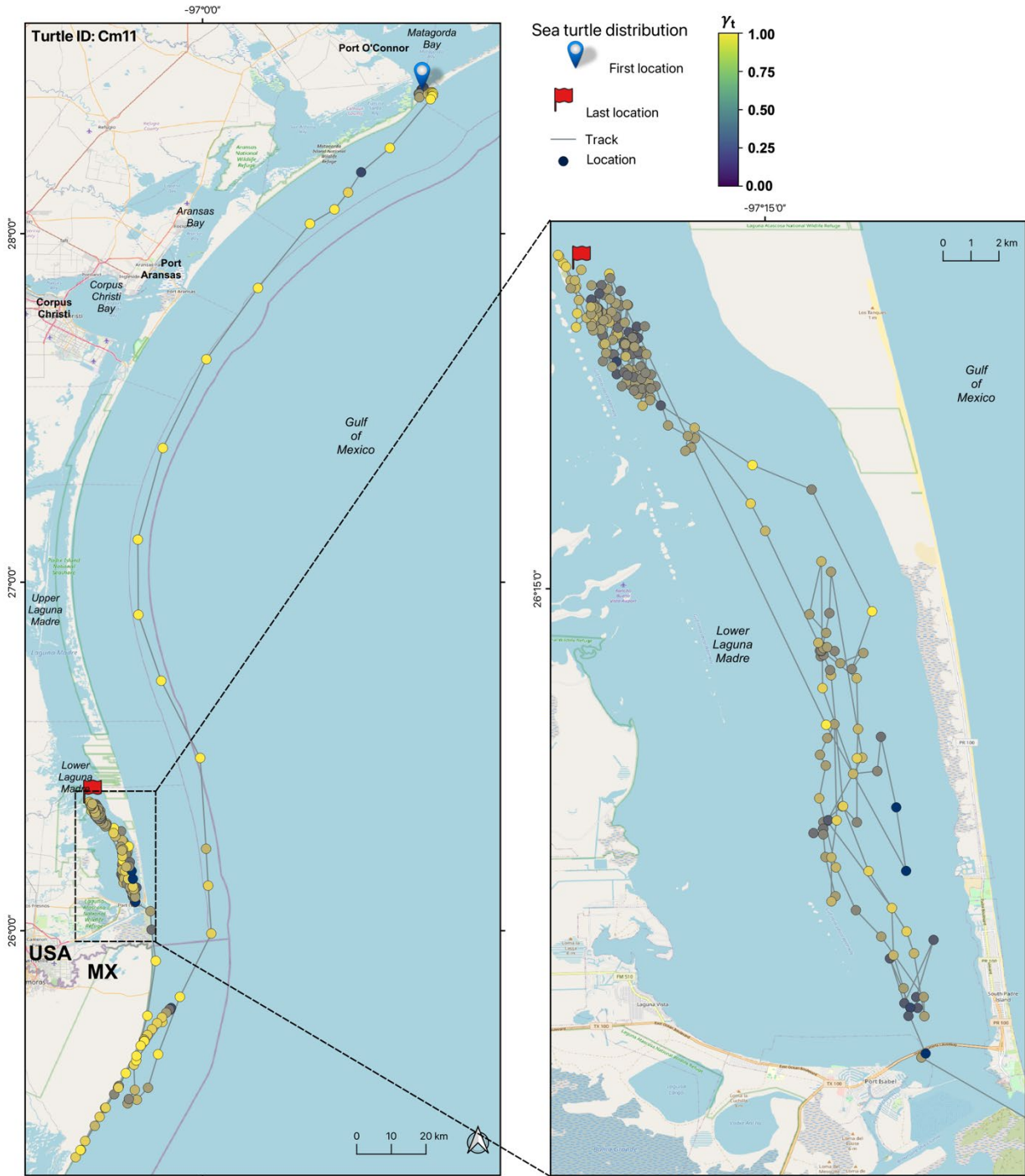


Figure 119. Movement of a juvenile green turtle (ID Cm11) from Matagorda Bay, tracked with a Lotek Fast-GPS Argos-linked transmitter in 2021. Points represent twelve-hour location estimates from the continuous-time move persistence model and are colored according to its move persistence index (γ_t). The move persistence index identifies changes in behavior along a continuum ranging from 0 (low speed and directionality indicative of area-restricted behavior) to 1 (high speed and directionality indicative of transiting behavior). There was no available data on seagrass distribution for this area.

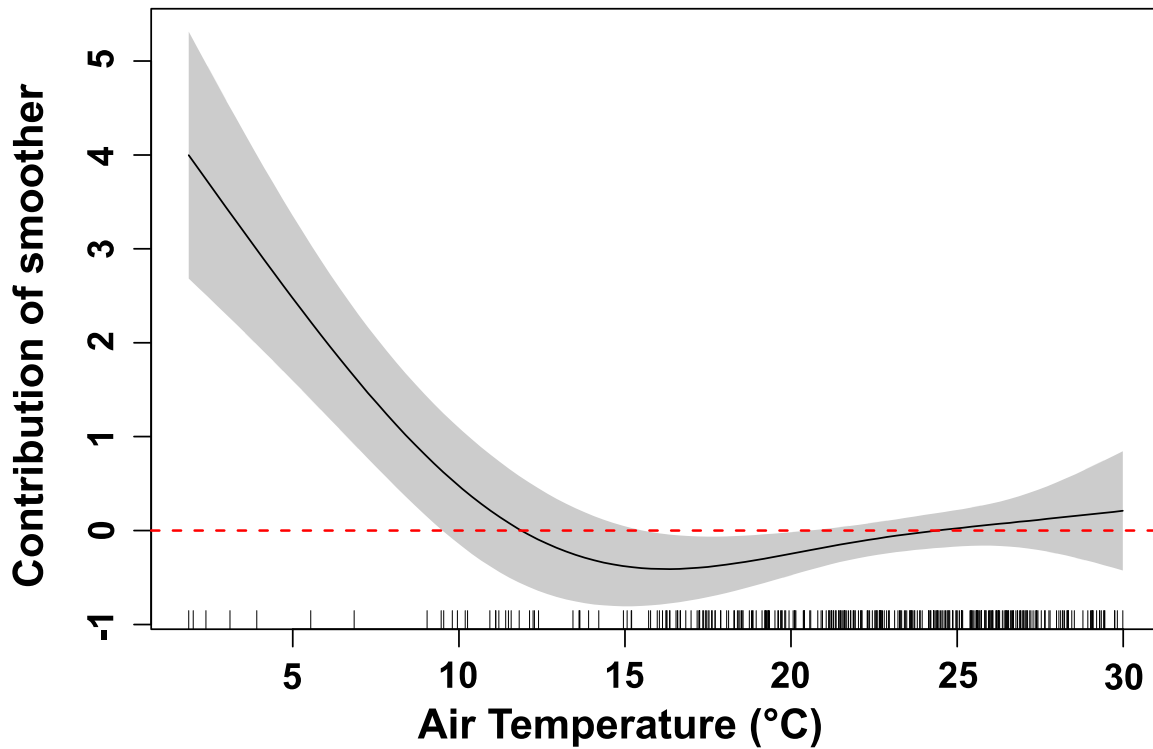


Figure 120. Estimated response curve (black solid line) of component smooth functions for air temperature on move persistence of satellite-tracked green turtles from the best-fit generalized additive mixed model. Shaded areas represent 95% confidence limits of uncertainty in the centered smooth. Vertical axes are partial responses (estimated, centered smooth functions) on the scale of the linear predictor. Ticks on x-axis denote values for which there are data. Positive values on y-axis (above red dashed line) indicate increased move persistence (high speed and directionality indicative of transiting behavior) by green turtles.

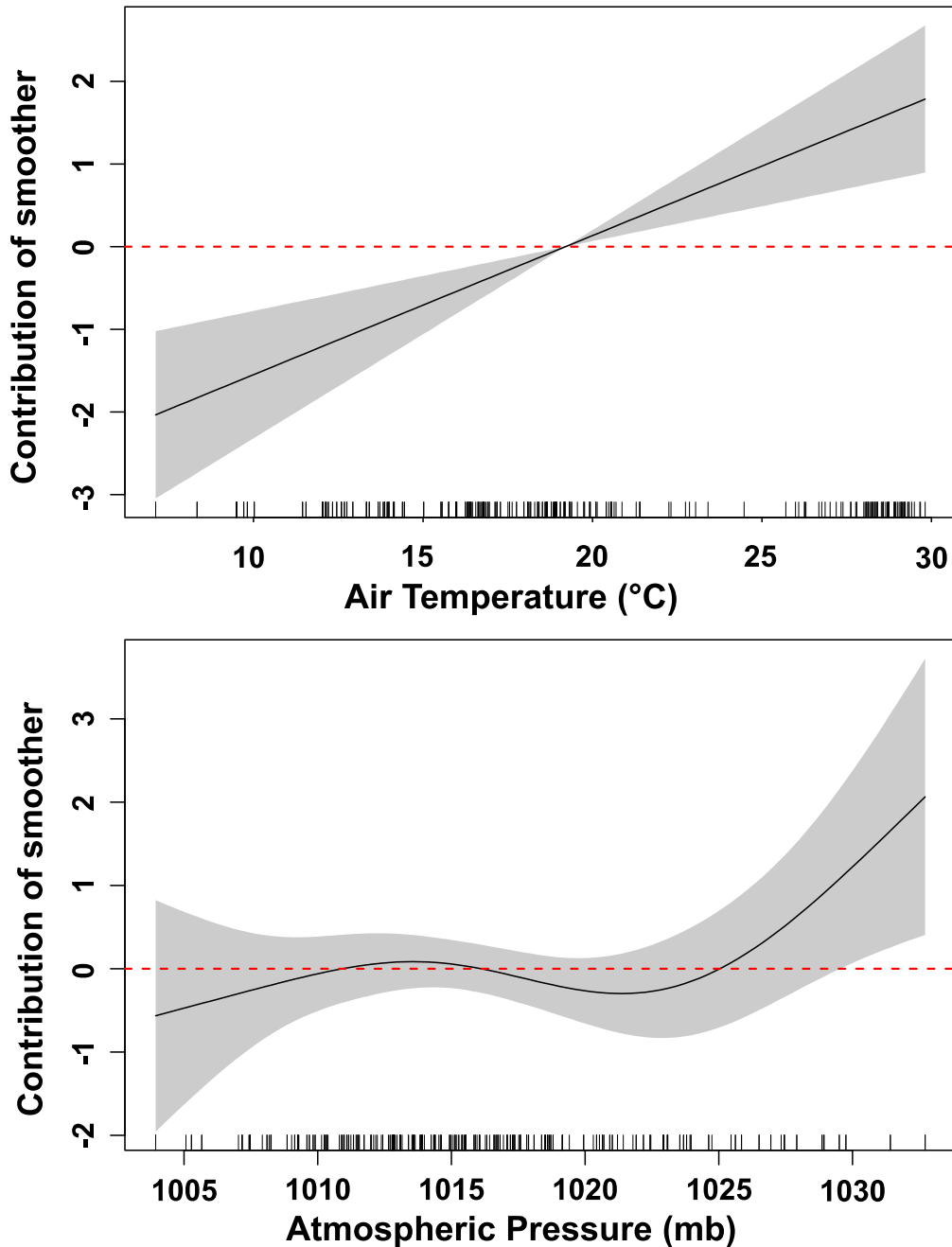


Figure 121. Estimated response curves (black solid line) of component smooth functions for air temperature and atmospheric pressure on the daily presence (residency) of acoustically-tracked green turtles in Matagorda Bay from the best-fit generalized additive mixed model. Shaded areas represent 95% confidence limits in the centered smooth. Vertical axes are partial responses (estimated, centered smooth functions) on the scale of the linear predictor. Ticks on x-axis denote values for which there are data. Positive values on y-axis (above red dashed line) indicate an increased probability of presence (residency) within Matagorda Bay by green turtles.

Outreach and engagement

From 2019 through 2022, we used multiple approaches to provide outreach, education, and engagement in the Matagorda Bay communities and beyond to reach a broad audience. We began by doing an inventory of existing sea turtle outreach materials developed by Texas Sea Grant and others in Texas and the Gulf of Mexico, and this led us to develop a Texas Sea Turtles poster (24" x 36"). The aim was to provide a visually attractive and informative poster to educate Texans about sea turtles in Texas including the different species present, where they come from, and their diverse habitats. Previous posters developed by Texas Sea Grant in the 1980s and later in the 2010s were all very well received and have been the most frequently requested educational materials. The Texas sea turtle poster was developed during December 2019 – January 2020 by Dawn Witherington (artist), and Drs. Blair Witherington and Pamela Plotkin. Texas Sea Grant supported the poster development and printing. These posters have been distributed across Texas, and specifically in Matagorda Bay communities during outreach events held since 2019.

We next developed a citizen science app, iSeaTurtle. The aim of iSeaTurtle was to involve the Matagorda Bay communities in our research by enabling them to easily upload sea turtle sightings via their cell phones and contribute to our research as citizen scientists. The app was developed from March 2020 – July 2020 by Drs. Dustin Baumbach and Natalie Wildermann. Before its release, the app was field tested by R. J. Shelly, Calhoun County Agent, and charter fishing guides from the Matagorda Bay area, and improvements to the app were made based on their recommendations. The Android version of the app was published on July 15, 2020 and the IOS version was published on July 16, 2020. An updated version of iSeaTurtle was published in May 2021 to expand its reach across the Texas coast in partnership with the Turtle Island Restoration Network. The major improvement to the app included adding a link on the home page to report sea turtles that are injured, stranded or nesting on beaches in Texas. From July 2020 through July 2022, the app has been downloaded 507 times on IOS devices and 417 times on Androids. We have received 202 sea turtle sightings during this time period.

In tandem with the development of iSeaTurtle, we developed a web page (tx.ag/iseaturtle) on the Texas Sea Grant site to host iSeaTurtle general information and a map that publicly displays all of the sea turtle sightings uploaded into the app by citizen scientists. The web page was developed March 2020 – July 2020 by Sara Carney, Texas Sea Grant Communications Manager. Since the launch of this website, September 14, 2020: There have been 569 people who have visited the iSeaTurtle page since launch, 431 visitors are unique users (not the same person visiting multiple times), and for August and September 2020, it was the second most viewed page on Texas Sea Grant's website, following the homepage.

We also developed iSeaTurtle stickers to give to the charter boat fishermen who partnered with us as citizen scientists, and to K-12 classes and summer camps. We printed 2,000 stickers and have distributed most of these in Matagorda and Calhoun County, as well as other areas across the TX coast.

Social Media:

We used 3 different social media platforms to communicate news about the sea turtle project and iSeaTurtle. This included Twitter: @iSeaTurtleTX (launched June 17, 2020) and @TXSeaGrant, and the Texas Sea Grant Facebook page. Our most effective engagements were on the Texas Sea Grant Facebook platform which is a well-established and well-visited resource.

Webinars:

We held one webinar during the quarantine entitled, “Turtle-y Texas”, in partnership with the Inland Ocean Coalition, North Texas Chapter’s April Tovar. This webinar was held on August 25, 2020, Presenters included Dr. Natalie Wildermann who spoke about the Matagorda Bay sea turtle research, Laura Picariello who discussed her work to save sea turtles by training fishermen how to use turtle excluder devices to reduce the incidental capture of sea turtles in Texas, and Jace Tunnell, Director of the Mission-Aransas National Estuarine Research Reserve, who presented results of his research and outreach project to document plastic nurdles in Texas. There were 234 attendees for the webinar, which was recorded and can be viewed on-line: <https://www.youtube.com/watch?v=c5YaqII-SPI>

Summer Camp Programs:

R.J. Shelly, Calhoun County Extension Agent, used our outreach materials developed for the Matagorda Bay Ecosystem Assessment during the youth summer camp programs held in 2020 and 2021. The aim was to teach the children of these communities about sea turtles in Matagorda Bay and the research we were doing there to understand the sea turtles’ use of the bay. Between June-August 2020, there were 102 youth participants and from June-August 2021 there were 139 youth participants. Participants received posters, stickers, coloring books, and sea turtle cards.

Media Coverage:

We had multiple news and magazine articles published by various outlets during the project, including the Port O’Connor Dolphin Talk, the Victoria Advocate, Texas A&M Today, the Corpus Christi Caller Times, KIIITV, and Texas Shores Magazine (Appendix B). In addition, the Texas Farm Bureau produced 3 radio programs about our research and aired these in July 2022:

https://soundcloud.com/texasfarmbureau/070622-texas-sea-turtle-research/s-2StWrShoIJa?in=texasfarmbureau/sets/tfb-archives-6/s-yfjsWxcvjOb&utm_source=clipboard&utm_medium=text&utm_campaign=social_sharing,

https://soundcloud.com/texasfarmbureau/070722-threatened-endangered-sea-turtles-call-texas-bay-home/s-wPPiJ0hFasD?in=texasfarmbureau/sets/tfb-archives-6/s-yfjsWxcvjOb&utm_source=clipboard&utm_medium=text&utm_campaign=social_sharing,

https://soundcloud.com/texasfarmbureau/070822-ecosystem-assessment-reveals-valuable-information-about-sea-turtles/s-k6kPetUjJ5O?in=texasfarmbureau/sets/tfb-archives-6/s-yfjsWxcvjOb&utm_source=clipboard&utm_medium=text&utm_campaign=social_sharing

Scientific Presentations:

Dr. Wildermann presented preliminary results from iSeaTurtle at a first-ever “Sea Turtle Twitter Talks” event organized by the International Sea Turtle Society (ISTS) during the COVID quarantine in September 2021 and intended for sea turtle scientists to share their research via Twitter. The title of this presentation, “iSeaTurtle: Discovering Sea Turtles in Texas Waters” summarized the iSeaTurtle app and data that had been collected in Matagorda Bay. Sea turtle high use areas were mapped and identified during this presentation using the data collected by the iSeaTurtle app, and its success as a tool to engage citizen scientists was also noted.

Our presentation was one of 24 Twitter presentations highlighting the full breadth of sea turtle research, management, and conservation efforts from over a dozen countries. This included participants from non-profit organizations, government agencies, and academia. Within the first 48 hours of this event, @SeaTurtleTalks tweets were viewed >18,000 times and presentations were shared >400 times and liked >1,700 times (mean 18 shares and 71 likes per talk).

The presentation can be accessed here: N. Wildermann, D. Baumbach, R.J. Shelly, J. Steinhaus, and P.T. Plotkin. 2021. iSeaTurtle, discovering sea turtles in Texas waters. Sea Turtle Talks <https://twitter.com/seaturtletalks>.

Dr. Wildermann also presented a poster at the 40th International Sea turtle Symposium, held on a virtual platform March 2022. The presentation entitled “Should I Stay or Should I Go? Movements of Sea turtles During Extreme Weather Events” described the movements and behavior of Matagorda Bay sea turtles during and after winter storm Uri which impacted the entire state of Texas, and Hurricane Nicholas which made landfall 80 km east of Matagorda Bay.

Preliminary Conclusions

(i) Do threatened and endangered sea turtles reside in Matagorda Bay year-round, or do they migrate to other bay systems and into the Gulf of Mexico? What are the environmental drivers of such movements?

From 2019-2021 we captured 33 sea turtles (32 green turtles and 1 Kemp’s ridley) in west Matagorda Bay between Magnolia Beach and Green Fields using entanglement nets set in shallow water and deep-water areas in multiple locations. The majority of the green turtles we tracked with satellite and acoustic transmitters remained resident in Matagorda Bay for the duration of their transmissions, however, we also found connectivity with other Texas bays as well as the Gulf of Mexico and Mexican waters. All of these migrations occurred in advance of or during approaching cold fronts and are consistent with previous studies that found migration initiated in response to cold fronts that reduce ambient and water temperatures (Renaud and Williams 1997, Metz and Landry 2013, Metz et al. 2020).

Collectively, this study demonstrated some green turtles switch from area-restricted, resident behavior to more directed transiting behavior when air temperatures decline below 15°C and especially below 10°C. These results correspond well with the previously reported movements of juvenile green turtles satellite-tracked over winter in nearshore waters along the Texas coast, which remained within waters >15°C, suggesting a threshold temperature at which migration behavior may be initiated (Metz et al. 2020). Residency in shallow, inshore waters

over winter make juvenile green turtles more susceptible to cold stunning. Cold stunning is associated with an abrupt drop in air and water temperatures, strong northerly winds, and a mean water temperature of 8.0°C (Shaver et al. 2017). Therefore, some green turtles are capable of making seasonal southward migrations in response to declining water temperatures, which minimizes the risk of cold stunning as temperatures at higher latitudes become physiologically stressful or lethal (Metz et al. 2020).

Combined with the data on stranded turtles, our results provide evidence of a year-round presence of green turtles in Matagorda Bay, with expected seasonal fluctuations in the abundance of turtles. Virtually all turtles that remained inside Matagorda Bay during the deep freeze died due to extended continued exposure to very cold temperatures. After this event, we started to consistently capture sea turtles starting in late April, with numbers increasing into the summer months. This influx of sea turtles is likely driven by incoming sea turtles migrating from southern regions in the Caribbean, with natal origins primarily in Mexican beaches (i.e. mostly from Tamaulipas, and in a lower proportion from Quintana Roo) (Shamblin et al. 2017). Green turtle nesting trends in most of the Greater Caribbean have been steadily increasing (e.g., Troëng and Rankin 2005, NMFS and USFWS 2014), and nesting populations, particularly in Mexico, have shown a positive trend over the last two decades (Marquez-M et al. 2004, Cuevas et al. 2021). This increase consecutively supports the recruitment of more juvenile turtles to foraging grounds along the different Texas bays.

While in-water captures provided a snapshot of a very specific size-class of sea turtles (mostly 30 – 45 cm SCL), the stranding data provided evidence that also recruits (< 30 cm SCL) and larger immature and subadult sea turtles (> 50 cm SCL) reside in Matagorda Bay. The netting method used in this study was very effective at capturing transitioning and inshore sea turtles foraging in very shallow waters (74% of our net settings were in waters up to 1 m depth). It is likely that there is some degree of habitat partitioning by sea turtles based on size classes. For example, local fishermen made observations that larger sea turtles are more often sighted in the Greens Bayou area, a more secluded coastal area further inside the bay. Even though we did not sample the jetties, it is also a hotspot of sea turtle sightings (based on citizen science data obtained through the iSeaTurtle app). The jetties provide foraging habitat, mostly composed of macroalgae, to immature turtles and in particular smaller turtles recruiting from their oceanic life stage, as has been well reported for different locations in Texas (Coyne 1994, Renaud et al. 1995, Metz and Landry 2013, Howell and Shaver 2021).

(ii) Which portions of west Matagorda Bay can be classified as important habitat for sea turtles? Is the home range and habitat use of threatened and endangered species in Matagorda Bay related to particular types/quality of the habitats occupied?

Eleven of the sixteen satellite-tracked green turtles moved into areas also surveyed by the BioWest team. The other five green turtles and all acoustically-tagged turtles were in areas outside the range of their survey (i.e., the J-hook area), and thus are not included in the assessment of the types of habitat occupied by tracked green turtles.

High-Use Area (HUA) of tracked sea turtles covered both seagrass beds and soft bottom habitats, with the highest sea turtle use density overlapping mostly with seagrass areas in which the seagrass species diversity was higher, but not necessarily dense. A particular difference between the seagrass area with higher sea turtle use and contiguous areas, was the presence of widgeon grass (*Ruppia maritima*) in addition to shoal grass (*Halodule beaudettei*) and star grass (*Halophila engelmannii*). These seagrass species have been identified as common diet items of green turtles in Texas (Coyne 1994; Howell and Shaver 2021), with shoal grass being the second most important diet item after turtle grass (*Thalassia testudinum*) (Howell and Shaver 2021). Both widgeon grass and star grass are easily digestible (Prof. Anitra Thorhaug pers. comm.) and have also been identified as common diet items for green turtles in Texas, particularly in inshore turtles (≥ 40.1 cm) that have established residency in seagrass habitats (Howell and Shaver, 2021). Feeding selectivity is well reported in green turtles in general (Balazs 1980, Bjorndal 1985, López-Mendilaharsu et al. 2008) and in Texas (Coyne 1994) and could likewise be one of the main drivers of the foraging distribution of green turtles in Matagorda Bay.

Additionally, by exploring the dataset we identified diel patterns in the movement of satellite-tracked green turtles. Some turtles (N=6) regularly shifted areas during daytime (6:00 – 18:00) and nighttime (18:00 – 6:00). These turtles mostly spent nighttime in deeper waters (1-3 m depth), especially within a channel characterized by soft bottom that runs parallel to the coast (aprox. 1 km into the bay) (Appendix D). This is consistent with observations made by Hildebrand (1982) in reference to the locations where fishermen deployed nets during the commercial fishing of green turtles in Texas, stating that most turtles were caught while they were moving to shallower foraging grounds from their nightly resting places in deeper waters of the bay. While some of the turtles consistently moved into deeper waters to rest, two of the turtles that used the channel at night also appeared to have resting areas over the seagrass bed, which were distinct to the areas they used during the day. Furthermore, other tracked sea turtles used areas over the seagrass indistinctively during day and night. This highlights the prevalence of intraspecific differences in the movement patterns of sea turtles, for which we recommend a further in-depth analysis of this dataset to answer in more detail the differences and similarities of the nightly resting areas at the individual-level.

(iii) How do seasonal and annual habitat variability (biological and physical characteristics) in west Matagorda Bay influence the distribution, abundance, demography and movements of sea turtles?

The relatively few satellite-tracked green turtles that emigrated from Matagorda Bay increased speed and directionality indicative of transiting behavior when air temperatures declined below 10°C with the shift towards increased move persistence occurring below 15°C. Similarly, the probability of acoustically-tagged green turtles being detected within Matagorda Bay increased linearly with air temperature with a significantly lower presence at temperatures below 18°C. These patterns suggest a threshold temperature around 15°C at which migration behavior may be initiated for some green sea turtles to leave shallow bays to find refuge at

southern latitudes and/or the deeper waters of the Gulf of Mexico during cold climatic conditions.

Green turtles that remained in Matagorda Bay during cold fronts in 2019 and 2020 increased their home range and spent more time in deeper water. Our late fall/early winter sampling in 2019 showed that green turtles had been buried in the soft-bottom substrate as evidenced by the mud and algae covering their carapaces. The winter freeze of 2021 however was prolonged and too severe for green turtles in Matagorda Bay to survive. Water temperatures along the Texas Gulf coast declined to a low of 1.1°C (34°F) and an ambient low temperature of -6.7°C (~20°F). Sea turtles that remained in the bay were cold-stunned and died because there were no efforts directed to this area to rescue sea turtles. The cold freeze provided an opportunity to ascertain the number of sea turtles residing in west Matagorda Bay at that moment. We can assume with confidence that the sea turtle population residing in the bay during warmer months should be considerably larger, and that Matagorda Bay provides habitat for at least several hundreds of sea turtles annually.

Sea turtle movements in response to a hurricane were also observed in the current study. When Hurricane Nicholas, a category 1 storm, made landfall 80 km east of Matagorda Bay, we observed an increase in the home range of turtles that had the smallest home ranges.

(iv) What is the overall health and nutritional state of sea turtles in west Matagorda Bay (e.g., epibiont load, body-condition-index, general obvious emaciation)? Are there seasonal and temporal changes to the nutritional state?

Prior studies in Matagorda Bay and other bay systems in Texas have not investigated the overall health, nutritional status, or body condition of sea turtles. A few studies have reported an increase in size of recaptured sea turtles, indicating the turtles were surviving and growing (Shaver 1994, Landry et al. 1997, Metz and Landry 2013). Our study is the first to apply a body condition index (BCI) to assess sea turtle health status as a function of the turtle's weight and carapace size. All of the turtles we captured in water were visually healthy animals that exhibited their best body condition during the warmer months of the year. During the colder months, turtles often had mud and microalgae films on their shells, indicating that they had spent time on or in the mud substrate of the bay – a possible sign of torpid behavior, which is known to occur when water temperatures are below 15°C (59°F) (Felger et al. 1976, Davenport 1997). Lower BCI values are expected during winter months, as has been documented in sea turtle foraging aggregations in Australia (Heithaus et al. 2005).

Potential health impacts to sea turtles in the upper reaches of Matagorda Bay and Lavaca Bay have been mentioned in association with the Formosa plastic plant though no turtles were observed near the plant's effluent areas (Renaud and Williams 1997). Toxicological impacts of the wastewater effluent from the plant were investigated by measuring various heavy metals present in sea turtle blood (Landry et al. 1997). This single study captured sea turtles in Lavaca Bay and Matagorda Bay and compared these turtles to similar size Kemp's ridley sea turtles captured near Sabine Pass, TX. The results indicated that mercury levels of Kemp's ridley sea turtles in Matagorda Bay were significantly higher than the sea turtles captured at Sabine Pass.

The study included only one sample from a green turtle and this individual also had a significantly higher concentration of mercury compared to sea turtles captured at Sabine Pass. Copper, lead, silver, and zinc were also measured but no significant differences were detected.

Early studies in the 1990s did not report fibropapillomatosis in the sea turtles they captured. The first documented reports of this disease in Texas occurred in 2010 (Tristan et al. 2010). A Texas-wide assessment in 2019 (Shaver et al. 2019) based on stranded sea turtles found that the prevalence of fibropapillomatosis in Texas has been increasing from <4% in 2010 to 35.2% in 2019. Few additional studies have reported this disease and it is unclear if they did not find evidence of tumors or they did not provide these data in their publications because it was tangential to their study goals. Our findings suggest that fibropapillomatosis is present in a significant portion of the green turtle population based on the sea turtles we captured in-water and the sea turtles we found stranded (roughly 1/3 of the turtles). The prevalence of fibropapillomatosis in Matagorda Bay in our study was however higher than reported by Shaver et al. (2019), in which only 10.7% of the sea turtles in the northern region (encompassing Matagorda Bay) had presence of tumors. Compared to sea turtle populations in the northeastern Gulf of Mexico (67.5% prevalence of tumors; Chabot et al. 2021), sea turtles in Texas seem to exhibit a considerably lower prevalence of fibropapilloma. Most of the tumors were small in size, were not restricting turtle vision, movement, or feeding ability and thus appeared to be early-stages of the disease. In addition, all sea turtles that presented tumors were in the juvenile life stage.

Acute extreme events such as winter storms in Texas present significant threats to the health and survival of sea turtles that become cold-stunned if they are residing in the bays and estuaries when ambient and water temperatures decline (Shaver 1990, Metz and Landry 2013, Shaver et al. 2017). Sea turtle stranding and mortality along the entire Texas coast in 2021 in association with winter storm Uri demonstrated this very clearly during our study. Although we were unable to measure body condition in the sea turtles that stranded and died in Matagorda Bay during the storm, we were able to document other aspects of their overall health. The turtles we found stranded during the first cold-stunning trip were in generally good condition with no evidence of external injuries, and coverage of epibionts, primarily algae coverage and barnacles, as expected during colder months. The carapaces of a small proportion of turtles were very clean with no epibionts. The turtles during the subsequent weekend were already too decomposed to assess. About a third of the stranded turtles had fibropapillomatosis.

Efforts to retrieve cold-stunned sea turtles in Texas during and immediately following winter storms have focused on areas from Corpus Christi Bay south to the Texas-Mexico border. Little effort has been provided further north from Aransas Bay through to east Matagorda Bay. Many local fishermen relayed stories to us about hundreds of sea turtles stranding in these bays during winter storms in recent years (personal communication), and the hundreds of sea turtles recovered during winter storm Uri confirmed that the high density of sea turtles in this area also requires targeted search and rescue efforts (Brigid Berger, personal communication). These

stranded turtles can and should be used to investigate the long-term health status of sea turtles in Texas with blood and tissues collected and preserved for toxicological and other studies.

(v) How do distribution, abundance, demography and movements of sea turtles in west Matagorda Bay compare to historical available data?

The results from the current study complement previous investigations, provide more robust data about the distribution and movements of green turtles in west Matagorda Bay, and provide additional support for a previously noted increase in the abundance of juvenile green turtles observed along the Texas coast (Metz and Landry 2016, Shaver et al. 2017, 2020). The increase is believed to be a result of rising numbers of adult green turtles nesting in the southern Gulf of Mexico and the wider Caribbean (Metz and Landry 2013, Shaver et al. 2020).

The distribution of green turtles captured during the current study parallels the historical data available that documents green turtle distribution in west Matagorda Bay. Small-scale short-term studies in the 1990s captured green turtles from bay waters near Magnolia and Indianola Beaches in the north, south to Pass Cavallo (Renaud and Williams 1997, Landry et al. 1997). High frequency areas of sea turtle distribution noted in these studies were centered in the lower reaches, near Pass Cavallo and the Matagorda Ship Channel. TPWD survey data from 1980 to the present are also consistent with previous studies that documented the greatest abundance of sea turtles occupying the lower reaches of west Matagorda Bay (unpublished). The green turtles tracked by satellite and acoustic transmitters in the current study confirm the location of these high use areas in west Matagorda Bay and provides additional information about specific locations utilized as home range and core areas, and the diel use and movement between these areas.

Within this documented range, green turtles have been recorded in close proximity to the shoreline (Renaud and Williams 1997), feeding in the seagrass beds located near their site of capture (Renaud and Williams 1997). The current study provides further support that green turtles reside near their point-of-capture, feed in shallow waters where seagrass is abundant and diverse, and rest in nearby deeper-waters with soft-bottoms comprised of mud. Hendrickson (1982) noted that commercial sea turtle fishermen were aware of this diel behavior, and regularly set their gill nets to capture green turtles leaving their deep-water habitat every morning, *en route* to shallow water feeding areas in the seagrass beds.

Like other rock-jettied passes on the Texas coast, the Matagorda Ship Channel is a high use area for sea turtles, as indicated by citizen scientists who observed sea turtles there and recorded their observations using the iSeaTurtle app developed for the current study. The rock jetties provide important developmental habitat for juvenile sea turtles that are transitioning from an oceanic-stage to a neritic-stage (Shaver 1994, Renaud et al. 1997). Juvenile green turtles feed on the abundant macroalgae that grow on these rocks (Coyne 1994, Arms 1996).

We captured only one Kemp's ridley sea turtle during the current study, we did not attach a transmitter to this turtle, and we are therefore unable to assess the current distribution of this species from the present study. Previous studies documented Kemp's ridley distribution as the

western perimeter of west Matagorda Bay and Lavaca Bay, with movements of tracked turtles into Carancahua Bay and Tres Palacios Bay (Renaud and Williams 1997). TPWD long-term surveys have captured Kemp's ridleys in Lavaca Bay in the north, south to Pass Cavallo and the backside of Matagorda Peninsula in Matagorda Bay (Unpublished data). We sampled many of the same locations where previous studies captured Kemp's ridleys and we did not capture any until 2021 at the end of our field work in the shallow waters on the backside of Matagorda Peninsula. We do not know the cause for the low number of Kemp's ridley captures in the current study. Recent trends in Kemp's ridley abundance and distribution indicate they are still present in west Matagorda Bay though they have not increased in parallel with the significant increase in the number of adult females nesting in the western Gulf of Mexico (Metz and Landry 2016) and the increased protection provided to the nests, eggs, and hatchlings since the Deepwater Horizon Oil Spill, as part of the Sea Turtle Early Restoration Project.

One loggerhead turtle was opportunistically observed from the boat during one field trip in July 2021 in the Greens Bayou area, and another loggerhead turtle was reported by users of iSeaTurtle who not only submitted the location of the sighting near the south jetty but also directly contacted the research team to send photos for identification (Appendix E). In contrast, historical records of loggerhead turtles captured by TPWD are closer to the inshore bays adjacent to Matagorda Bay (i.e. Keller Bay and Carancahua Bay).

Increasing sea turtle abundance in Texas' bays and estuaries has been evident in the systematic surveys conducted by the TPWD (unpublished data), the number of sea turtle strandings during extreme cold weather events (Shaver et al. 2017), parallels the historical data available that documents green turtle distribution in west Matagorda Bay), and in directed studies using in-water capture methods (Metz and Landry 2013). In our study area, juvenile green turtles were previously determined to be less abundant than other bay systems in Texas (Metz and Landry 2013). Nevertheless, our CPUE results (1.1 ± 1.3 turtles/km h) are much higher than those reported for Matagorda Bay between 1991-2010 (0.07 turtles/km h), and comparable to those found in the Lower Laguna Madre (1.5 turtles/km h) in the same study (Metz and Landry, 2013).

The movements of green turtles in the current study also parallels the limited historical data available that documents green turtle movements in west Matagorda Bay, and the influence of changing ambient and water temperatures as drivers of these movements. Renaud and Williams (1997) and Metz and Landry (2013) reported seasonal migrations out of the bay, with winter departures followed by spring arrivals and returns to the bay. These studies also documented connectivity with other bay systems located south of Matagorda Bay including Espiritu Santo Bay, Aransas Bay, Corpus Christi Bay, and the lower Laguna Madre. Movements out of Matagorda Bay occurred via Espiritu Santo Bay, the Matagorda Ship Channel, and Pass Cavallo. Green turtles that left Matagorda Bay and swam into Gulf of Mexico waters, also migrated south, crossed into Mexican waters, and returned to Texas bays and estuaries when temperatures increased. The current study provided further support to our understanding of the seasonal movements within and outside Matagorda Bay.

In terms of demographical parameters, the *size distribution* of green turtles recorded in this study (stranded + captured) aligns with the historical sizes recorded by TPWD as well as a previous study in Matagorda Bay (Landry et al. 1997) with a clear prevalence of green turtles in the 30 to 39.9 cm range. Nevertheless, during the stranding event the majority were larger turtles (>40 and up to 76 cm SCL) which could suggest two possible scenarios: (a) that larger turtles are more likely to overwinter inside the Bay and thus the higher proportion of larger animals, or (b) that size composition could be a reflection of the areas surveyed and the captured method that is employed and thus additional capture methods are needed to sample more accurately the entirety of the population. The *sex ratio* of green turtles in Matagorda Bay from this study is consistent with a female-biased ratio reported in Matagorda Bay (N=6 turtles, 66.7% females) (Stabenau et al. 1996) and other locations in Texas (Shaver 2009) and the northeastern Gulf of Mexico (Florida) (Foley et al. 2007, Avens et al. 2012, Sanchez 2013).

Future Management Recommendations

Texas bays and estuaries provide one of the most important developmental habitats for green turtles in the western Gulf of Mexico. Our study confirms that Matagorda Bay provides important developmental feeding and resting areas for green turtles and extends the range of critical habitat for the species further north than previously appreciated. The high use areas we identified in this study, including the seagrass beds and the jetties in west Matagorda Bay, require special management consideration or protections for immature and juvenile green turtles that use these areas daily to feed, rest, develop and grow. We recommend prioritizing areas of high seagrass diversity for protection of green turtle foraging habitat. We also recommend managing the seagrass beds present to maintain their abundance and diversity of seagrass species critical to the green turtles in Matagorda Bay. Interventions to reduce or manage commercial and recreational boat activity as well as other human activities in these high use areas is also important. Examples include reducing boat speed in these areas, increasing education and outreach to recreational boaters about the presence of sea turtles and what to do if they capture/injure a turtle, and preventing removal or destruction of seagrass.

We also recommend special consideration of the jetties in the Matagorda Ship Channel due to the high number of sea turtles sighted and the multiple species observed there. Recent dredging of Aransas Pass had immediate impacts on the jetty habitat, sea turtles were disturbed by these activities, and they left the area (Personal Observation). Fewer sea turtles were sighted there for as long as a year following the dredging (Personal Observation). Activities that alter these habitats, even temporarily, can adversely impact immature sea turtles that depend on these areas as they transition from oceanic waters to bay and estuarine developmental habitats. In addition to providing areas for sea turtles to feed and rest, the channel is used by green turtles for transit from Matagorda Bay to the Gulf of Mexico during extreme weather events. Restricting this access could threaten a greater number of sea turtles during future winter freezes.

Winter storm Uri confirmed that the high density of sea turtles in Matagorda Bay and surroundings bays from Aransas Bay to east Matagorda Bay require targeted search and rescue efforts during extreme cold weather events. These efforts should begin when the water

temperature declines to 10°C. Current efforts for sea turtle search and rescue are concentrated near South Padre Island, North Padre Island, Mustang Island, Corpus Christi, and in the Galveston Bay region. If recovered quickly, cold-stunned turtles can be released offshore into warmer water and held temporarily in rehabilitation facilities if necessary. Deceased turtles can and should be used for future investigations, including the long-term health status of sea turtles in Texas.

Lastly, fibropapillomatosis was detected in a third of the green turtles we studied. Further investigation of the prevalence of this disease in Texas turtles and factors contributing to its spread are needed.

Literature Cited

- Amos, A.F. 1989. The occurrence of hawksbills (*Eretmochelys imbricata*) along the Texas Coast. Proceedings, 9th Annual Workshop on Sea Turtle Conservation and Biology, Jekyll Island, GA, USA, pp 9–12.
- Amos, A.F. and P.T. Plotkin. 1990. Anthropogenic and natural debris on a south Texas barrier island beach. Pp. 367-368. Proceedings of the Second International Conference on Marine Debris. NOAA TM-NMFS-SWFSC-154.
- Arms, S.A. 1996. Overwintering behavior and movement of immature green sea turtles in south Texas waters. Doctoral dissertation, Texas A&M University.
- Avens, L., Goshe, L.R., Harms, C.A., Anderson, E.T., Hall, A.G., Cluse, W.M., Godfrey, M.H., Braun-McNeill, J., Stacy, B., Bailey, R. and M.M. Lamont. 2012. Population characteristics, age structure, and growth dynamics of neritic juvenile green turtles in the northeastern Gulf of Mexico. Marine Ecology Progress Series 458:213-229.
- Bailey H., Shillinger, G., Palacios, D., Bograd, S., Spotila, J., Paladino, F. and B. Block. 2008. Identifying and comparing phases of movement by leatherback turtles using state-space models. Journal of Experimental Marine Biology and Ecology 356(1-2):128-35.
- Balazs, G.H. 1980. Field method for sampling the dietary components of green turtles, *Chelonia mydas*. Herpetology Review 11:5-6
- Bartoń, K. 2022. MuMIn: Multi-Model Inference. R package version 1.47.1.
- Beck, M.W., Heck, K.L., Able, K.W., Childers, D.L., Eggleston, D.B., Gillanders, B.M., Halpern, B., Hays, C.G., Hoshino, K., Minello, T.J. and R.J. Orth. 2001. The identification, conservation, and management of estuarine and marine nurseries for fish and invertebrates: a better understanding of the habitats that serve as nurseries for marine species and the factors that create site-specific variability in nursery quality will improve conservation and management of these areas. Bioscience 51(8):633-641.
- Benhamou, S. 2011. Dynamic approach to space and habitat use based on biased random bridges. PLoS One 6(1):e14592.
- Bjorndal, K.A. 1985. Nutritional ecology of sea turtles. Copeia 736–751.
- Bjorndal, K.A., Bolten, A.B. and M.Y. Chaloupka. 2000. Green turtle somatic growth model: evidence for density dependence. Ecological Applications 10(1):269-282.

- Bjorndal, K.A., B.W. Bowen, M. Chaloupka, L.B. Crowder, S.S. Heppell, C.M. Jones, M.E. Lutcavage, D. Policansky, A.R. Solow and B.E. Witherington. 2011. Better science needed for restoration of the Gulf of Mexico. *Science*. 331:537-538.
- Blumenthal, J. M., T.J. Austin, J.B. Bothwell, A.C. Broderick, G. Ebanks-Petrie, J.R. Olynik, M.F. Orr, J.L. Solomon, M.J. Witt and B.J. Godley. 2009. Diving behavior and movements of juvenile hawksbill turtles *Eretmochelys imbricata* on a Caribbean coral reef. *Coral Reefs* (2009) 28:55–65.
- Burnham, K.P. and D.R. Anderson. 2002. Model selection and multimodel inference: A practical information-theoretic approach, 2nd edn New York Springer.
- Calenge, C. 2006. The package adehabitat for the R software: a tool for the analysis of space and habitat use by animals. *Ecological Modelling* 197:516-51.
- Campbell, H.A., Watts, M.E., Dwyer, R.G. and C.E. Franklin.. 2012. V-Track: software for analysing and visualizing animal movement from acoustic telemetry detections. *Marine and Freshwater Research* 63:815-820.
- Chabot, R.M., Welsh, R.C., Mott, C.R., Guertin, J.R., Shamblin, B.M. and B.E. Witherington. 2021. A sea turtle population assessment for Florida's Big Bend, Northeastern Gulf of Mexico. *Gulf and Caribbean Research* 32(1):19-33.
- Chambers, J.R. 1992. Coastal degradation and fish population losses. In: Stroud, R.H. (ed.), Stemming the tide of coastal fish habitat loss. Proceedings of a symposium on conservation of coastal fish habitat. Baltimore, MD: Marine Recreational Fisheries Symposium 14. p. 45-51.
- Connell, S.D. and G.P. Jones. 1991. The influence of habitat complexity on post recruitment processes in a temperate reef fish population. *Journal of experimental marine biology and ecology* 151(2):271-294.
- Coyne, M.S. 1994. Feeding ecology of subadult green sea turtles in south Texas waters. Master's thesis, Texas A&M University.
- Csardi, G and T. Nepusz. 2006. The igraph software package for complex network research. *InterJournal, Complex Systems* 1695:1-9.
- Cuevas E, de los Ángeles Liceaga-Correa A. and I. Mariño-Tapia. 2010. Influence of beach slope and width on hawksbill (*Eretmochelys imbricata*) and green turtle (*Chelonia mydas*) nesting activity in El Cuyo, Yucatán, Mexico. *Chelonian Conservation and Biology* 9:262–267.

- Cuevas, E., Guzmán-Hernández, V., Sarti Martínez, A.L., López-Castro, M., Tzeek-Tuz, M., Liria Reyes, D., Gómez Nieto, L., Castañeda-Ramírez, D.G., Uribe-Martínez, A., Cáceres-G-Cantón, C., Ortíz-Hernández, A. and Quintana-Pali, G. 2021. Mexico. In: Nalovic, M.A., Ceriani, S.A., Fuentes, M.M.P.B., Pfaller, J.B., Wildermann, N.E., Uribe-Martínez, A., Cuevas, E. (eds.). 2021. Sea turtles in the North Atlantic & Wider Caribbean Region. MTSG Annual Regional Report 2021. Draft Report to the IUCN SSC Marine Turtle Specialist Group.
- Davenport, J. 1997. Temperature and the life-history strategies of sea turtles. *Journal of thermal biology* 22(6):479-488.
- Doughty, R.W. 1984. Sea turtles in Texas: A forgotten commerce. *The Southwestern Historical Quarterly*, 88(1):43-70.
- Felger, R.S., Clifton, K. and P.J. Regal. 1976. Winter dormancy in sea turtles: independent discovery and exploitation in the Gulf of California by two local cultures. *Science* 191(4224):283-285.
- Figgenger, C., Bernardo, J. and P.T. Plotkin. 2018. Successful use of the Iridium satellite system to study the fine-scale movements of interesting marine turtles, International Sea Turtle Society, Kobe, Japan.
- Foley, A.M., Singel, K.E., Dutton, P.H., Summers, T.M., Redlow, A.E. and J. Lessman. 2007. Characteristics of a green turtle (*Chelonia mydas*) assemblage in northwestern Florida determined during a hypothermic stunning event. *Gulf of Mexico Science* 25(2):4.
- Fritts, T.H., Hoffman, W. and M.A. McGehee. 1983. The Distribution and Abundance of Marine Turtles in the Gulf of Mexico and Nearby Atlantic Waters. *Journal of Herpetology*, 17(4):327-344.
- Gallaway, B.J., Gazey, W.J., Caillouet, Jr., C.W., Plotkin, P.T. and 34 others. 2016. Development of a Kemp's Ridley Sea Turtle Stock Assessment Model. *Gulf of Mexico Science* 33(2):138-157.
- Griffin, L.P., Smith, B.J., Cherkiss, M.S., Crowder, A.G., Pollock, C.G., Hillis-Starr, Z., Danylchuk, A.J. and K.M. Hart. 2020. Space use and relative habitat selection for immature green turtles within a Caribbean marine protected area. *Animal Biotelemetry*. 8:22.
- Hall, Q.A., Curtis, J.M., Williams, J. and G.W. Stunz. 2019. The importance of newly-opened tidal inlets as spawning corridors for adult Red Drum (*Sciaenops ocellatus*). *Fisheries Research*. 212:48-55.

- Hart, K.M. and I. Fujisaki. 2010. Satellite tracking reveals habitat use by juvenile green sea turtles *Chelonia mydas* in the Everglades, Florida, USA. *Endangered Species Research* 11:221-232.
- Hart, K.M., M.M. Lamont, I. Fujisaki, A.D. Tucker and R.R. Carthy. 2012. Common coastal foraging areas for loggerheads in the Gulf of Mexico: opportunities for marine conservation. *Biological Conservation* 145:185–194.
- Hart K.M., M.M. Lamont, A.R. Sartain, I. Fujisaki, and B.S. Stephens. 2013. Movements and Habitat-Use of Loggerhead Sea Turtles in the Northern Gulf of Mexico during the Reproductive Period. *PloS ONE* 8(7): e66921.
- Harte Research Institute for Gulf of Mexico Studies. 2016. GulfBase: Resource Database for Gulf of Mexico Research, Education, and Management. Texas A&M University-Corpus Christi. World Wide Web electronic publication. <http://www.gulfbase.org>, November 2016.
- Heithaus, M.R., Frid, A., Wirsing, A.J., Bejder, L. and L.M. Dill. 2005. Biology of sea turtles under risk from tiger sharks at a foraging ground. *Marine Ecology Progress Series* 288:285-294.
- Herbst, L.H. 1994. Fibropapillomatosis of marine turtles. *Annual Review of Fish Diseases* 4:389-425.
- Heupel, M.R. and C.A. Simpfendorfer. 2015. Long-term movement patterns of a coral reef predator. *Coral Reefs* 34:679-691.
- Hildebrand, H. 1982. A historical review of the status of sea turtle populations in the western Gulf of Mexico. In: Bjorndal, K. (ed.). *Biology and Conservation of Sea Turtles*. Smithsonian Institution Press, Washington D.C. p.447-453.
- Hildebrand, H.H. 1983. Random notes on sea turtles in the western Gulf of Mexico. In: Owens, D.W. et al. (eds.). *Western Gulf of Mexico Sea Turtle Workshop Proceedings*. Sea Grant, Texas A&M University, College Station, Texas, p. 34-41. TAMU-SG-86-402.
- Hopkins-Murphy, S.R., Owens, D.W. and T.M. Murphy. 2003. Ecology of immature loggerhead on foraging grounds and adults in interesting habitat in the Eastern United States. In: Bolten AB, Witherington BE (eds.) *Loggerhead sea turtles*. Smithsonian Books, Washington, DC, USA, pp 79–92.
- Howell, L.N. and D.J. Shaver. 2021. Foraging habits of green sea turtles (*Chelonia mydas*) in the Northwestern Gulf of Mexico. *Frontiers in Marine Science* 8:658368.

- Hughes, C.L. and A.M. Landry, Jr. 2016. Long-term movements of an adult male Kemp's ridley sea turtle (*Lepidochelys kempii*) in the northwestern Gulf of Mexico. *Gulf of Mexico Science* 33(2):205-212.
- Jacoby, D.M., Brooks, E.J., Croft, D.P. and D.W. Sims. 2012. Developing a deeper understanding of animal movements and spatial dynamics through novel application of network analyses. *Methods in Ecology and Evolution* 3(3):574-583.
- Jonsen, I.D., Grecian, W.J., Phillips, L., Carroll, G., McMahon, C., Hartcourt, R.G., Hindell, M.A. and T.A. Patterson. 2023. aniMotum, an R package for animal movement data: Rapid quality control, behavioural estimation and simulation. *Methods in Ecology and Evolution* 14(3):806-816.
- Jonsen, I.D., Patterson, T.A., Costa, D.P., Doherty, P.D., Godley, B.J., Grecian, W.J., Guinet, C., Hoenner, X., Kienle, S.S., Robinson, P.W. and S.C. Votier. 2020. A continuous-time state-space model for rapid quality control of Argos locations from animal-borne tags. *Movement Ecology* 8:31.
- Kraft, S., Gandra, M., Lennox, R.J., Mourier, J., Winkler, A.C., and D. Abecasis. 2023. Residency and space use estimation methods based on passive acoustic telemetry data. *Movement Ecology* 11:12.
- Keele, L.J. 2008. Semiparametric regression for the social sciences. John Wiley & Sons, Ltd.
- Lambert, S.S., Willey, S.S., Campbell, T., Thomas, R.C., Li, H., Lin, L. and T.L. Welp. 2013. Regional sediment management studies of Matagorda Ship Channel and Matagorda Bay System, Texas. US Army Engineer Research and Development Center (ERDC). ERDC/CHL TR-13-10.
- Landry, Jr., A.M. and D. Costa. 1999. Status of sea turtle stocks in the Gulf of Mexico with emphasis on the Kemp's ridley. In: Kumpf, H., Steidinger, K., Sherman, K. (eds.) *The Gulf of Mexico large marine ecosystem: assessment, sustainability, and management*. Blackwell Science, Malden, MA, pp. 248–268.
- Landry, Jr., A.M., Costa, D.T., Kenyon, F.L., St. John, K.E., Coyne, M.S. and M.C. Hadler. 1997. Distribution of sea turtles in Lavaca and Matagorda Bays, Texas – A preliminary survey of ecology and toxicology of sea turtles as related to Formosa Plastics Corporation's wastewater discharge. Final Report submitted to the Environmental Protection Agency, August 1997.
- Landry, Jr., A.M., Costa, D.T., Kenyon, F.L. and M.S. Coyne. 2005. Population characteristics of Kemp's ridley sea turtles in nearshore waters of the upper Texas and Louisiana coasts. *Chelonian Conservation and Biology* 4: 801–807.

- Leary, T.R. 1957. A schooling of leatherback turtles, *Dermochelys coriacea*, on the Texas coast. *Copeia* 1957:232.
- London, J.M. 2021. Pathroutr: An R package for (re-)routing paths around barriers (version 0.2.1). <http://zenodo.org/record/5522909#.ZCDPFuzMKrN>
- López-Mendilaharsu, M., Gardner, S. C., Riosmena-Rodrigues, R., and J.A. Seminoff. 2008. Diet selection by immature green turtles (*Chelonia mydas*) at bahía Magdalena foraging ground in the pacific coast of the baja California Peninsula, México. *Journal of the Marine Biological Association of the United Kingdom* 88(3):641-647.
- Luschi, P., Hays, G.C., Del Seppia, C., Marsh, R and F. Papi. 1998. The navigational feats of green sea turtles migrating from Ascension Island investigated by satellite telemetry. *Proceedings of the Royal Society of London. Series B: Biological Sciences* 265:2279-2284.
- Magnuson, J.J., K.A. Bjorndal, W.D. DuPaul, G.L. Graham, D.W. Owens, C.H. Peterson, P.C.H. Pritchard, J.I. Richardson, G.E. Saul and C.W. West. 1990. *Decline of the sea turtles: causes and prevention*. National Research Council, National Academy Press, Washington, DC.
- Manzella, S.A. and J.S. Williams. 1992. The distribution of Kemp's ridley sea turtles (*Lepidochelys kempii*) along the Texas coast: An atlas. NOAA Technical Report NMFS 110.
- Marquez-M, R., Diaz, J., Guzman, V., Bravo, R. and M. Jimenez. 2004. Marine turtles of the Gulf of Mexico. Abundance, distribution and protection. *Special Publication Series* 1:89-107.
- Metz, T. L. 2004. Factors influencing Kemp's ridley sea turtle (*Lepidochelys kempii*) distribution in nearshore waters and implications for management. Doctoral dissertation, Texas A&M University.
- Metz, T.L. and A.M. Landry, Jr. 2013. An Assessment of green turtle (*Chelonia mydas*) stocks along the Texas coast, with emphasis on the lower Laguna Madre. *Chelonian Conservation Biology* 12(2):293-302.
- Metz, T.L. and A.M. Landry, Jr. 2016. Trends in Kemp's Ridley Sea Turtle (*Lepidochelys kempii*) Relative Abundance, Distribution, and Size Composition in Nearshore Waters of the Northwestern Gulf of Mexico. *Gulf of Mexico Science* 33(2):179-191.

- Metz, T.L., Gordon, M., Mokrech, M. and G. Guillen. 2020. Movements of juvenile green turtles (*Chelonia mydas*) in the nearshore waters of the northwestern Gulf of Mexico. *Frontiers in Marine Science* 7:647.
- Michelot, T., Langrock, R., Bestley, S., Jonsen, I. D., Photopoulou, T. and T. A. Patterson. 2017. Estimation and simulation of foraging trips in land-based marine predators. *Ecology* 98(7):1932-1944.
- Midway, S.R., Lynch, A.J., Peoples, B.K., Dance, M. and R. Caffey. 2021. COVID-19 influences on US recreational angler behavior. *PloS one* 16(8):e0254652.
- Morreale, S.J., Plotkin, P.T., Shaver, D.J. and H.J. Kalb. 2007. Adult Migration and Habitat Utilization: Ridley Turtles in their Element. In: P.T. Plotkin (ed.). *Biology and Conservation of Ridley Sea Turtles*. Johns Hopkins University Press, Baltimore, MD.
- National Geophysical Data Center (NGDC). 2001. U.S. Coastal Relief Model Vol. 5 – Western Gulf of Mexico. National Oceanic and Atmospheric Administration National Centers for Environmental Information.
- National Marine Fisheries Service and U.S. Fish and Wildlife Service. 1991a. Recovery Plan for U.S. Population of Loggerhead Turtle, *Caretta caretta*. National Marine Fisheries Service: Washington, D.C., 64 pp.
- National Marine Fisheries Service and U.S. Fish and Wildlife Service. 1991b. Recovery Plan for U.S. Population Atlantic Green Turtle, *Chelonia mydas*. National Marine Fisheries Service: Washington, D.C., 52 pp.
- National Marine Fisheries Service and U.S. Fish and Wildlife Service. 1992. Recovery Plan for Hawksbill Turtles, *Eretmochelys imbricata*, in the U.S. Caribbean Sea, Atlantic Ocean, and Gulf of Mexico. National Marine Fisheries Service: St. Petersburg, FL, 52 pp.
- National Marine Fisheries Service and U.S. Fish and Wildlife Service. 2008. Recovery Plan for the Northwest Atlantic Population of the Loggerhead Sea Turtle (*Caretta caretta*), Second Revision Silver Spring, MD, National Marine Fisheries Service. 325 pages.
- National Marine Fisheries Service and U.S. Fish and Wildlife Service. 2014. Green turtle (*Chelonia mydas*) Status Review under the U.S. Endangered Species Act. Report of the Green Turtle Status Review Team. May 2014. 567 pp.
- National Marine Fisheries Service, U.S. Fish and Wildlife Service, and SEMARNAT. 2011. Bi-National Recovery Plan for the Kemp's Ridley Sea Turtle (*Lepidochelys kempii*), Second Revision. National Marine Fisheries Service. Silver Spring, Maryland 156 pp. + appendices.

- National Research Council. 2010. Assessment of Sea-Turtle Status and Trends: Integrating Demography and Abundance. Washington, DC: The National Academies Press.
- Page-Karjian, A. 2019. Fibropapillomatosis in Marine Turtles. *Fowler's Zoo and Wild Animal Medicine Current Therapy* 9:398-403.
- Pincock DG. 2012. False detections: what they are and how to remove them from detection data. Vemco Application Note DOC-004691 Version 03, Amirix Systems Inc., Halifax, NS, Canada, 1-11.
- Plotkin, P.T. and A.F. Amos. 1988. Entanglement in and ingestion of marine debris by sea turtles stranded along the south Texas coast. Pp. 79-82. *Proceedings of the Eighth Annual Workshop on Sea Turtle Conservation and Biology*. NOAA TM-NMFS-SEFC-214.
- Plotkin, P.T., M.K. Wicksten and A.F. Amos. 1993. Feeding ecology of the loggerhead sea turtle *Caretta caretta* in the northwestern Gulf of Mexico. *Marine Biology* 115:1-5.
- Plotkin, P.T. 1996. Occurrence and diet of juvenile loggerhead sea turtles, *Caretta caretta*, in the northwestern Gulf of Mexico. *Chelonian Conservation and Biology* 2:78-80.
- Plotkin, P.T. and J.R. Spotila. 2002. Post-nesting migrations of loggerhead turtles *Caretta caretta* from Georgia, U.S.A.: Conservation implications for a genetically distinct sub-population. *Oryx* 36(4).
- Plotkin, P.T. 2003. Adult migrations and habitat use. Pp. 225-241. In: P. Lutz, J. Musick, and J. Wyneken (eds.). *The Biology of Sea Turtles: II*. CRC Press, Boca Raton, FL.
- Plotkin, P.T., C. Ragland, C. Figgner, C. Campbell, V. Cornish, E. Fetherston, B. Wallace and T. Shearer. 2016. Research, Monitoring and Conservation Needs for Gulf of Mexico Sea Turtles. Gulf of Mexico Oil Spill and Ecosystem Science Conference, Tampa, FL.
- Pulich Jr, W. and T. Calnan. 1999. Seagrass conservation plan for Texas. Texas Parks and Wildlife Department, Austin, Texas. 79pp.
- Rabalais, S.C. and N.N. Rabalais. 1980. The occurrence of sea turtles on the south Texas coast. *Contributions in Marine Science* 23:123-129.
- R Core Team. 2022. R: A language and environment for statistical computing. R Foundation for Statistical Computing, Vienna, Austria. <http://www.R-project.org/>.
- Renaud, M.L. and J.A. Williams. 1997. Movements of Kemp's ridley (*Lepidochelys kempii*) and green (*Chelonia mydas*) sea turtles using Lavaca Bay and Matagorda Bay, 1996-1997.

- Environmental Protection Agency Office of Planning and Coordination, Dallas, TX. p. 53.
- Renaud, M.L., Carpenter, J.A., Williams, J.A., and S.A. Manzella-Tirpak. 1995. Activities of juvenile green turtles, *Chelonia mydas*, at a jettied pass in south Texas. *Oceanographic Literature Review* 5(43):488.
- Renaud, M.L. and J.A. Williams. 2005. Kemp's ridley sea turtle movements and migrations. *Chelonian Conservation and Biology* 4:808–816.
- Rosman, I., Boland, G.S., Martin, L.R. and C.R. Chandler. 1987. Underwater sightings of sea turtles in the Northern Gulf of Mexico. OCS Study MMS 87/0107. Minerals Management Service, Washington, DC, USA. 37 pp.
- Sanchez, C. 2013. Sex ratios of juvenile green turtles (*Chelonia mydas*) in three developmental habitats along the coast of Florida. Master's thesis, University of Central Florida.
- Seney, E.E., Higgins, B.M. and A.M. Landry Jr. 2010. Satellite transmitter attachment techniques for small juvenile sea turtles. *Journal of Experimental Marine Biology and Ecology* 384(1-2):61-67.
- Seney, E.E. and A.M Landry, Jr. 2011. Movement patterns of immature and adult female Kemp's ridley sea turtles in the northwestern Gulf of Mexico. *Marine Ecology Progress Series* 440:241-254.
- Shamblin, B.M., Dutton, P.H., Shaver, D.J., Bagley, D.A., Putman, N.F., Mansfield, K.L., Ehrhart, L.M., Peña, L.J. and C.J. Nairn. 2017. Mexican origins for the Texas green turtle foraging aggregation: a cautionary tale of incomplete baselines and poor marker resolution. *Journal of Experimental Marine Biology and Ecology* 488:111-120.
- Shaver, D.J. 1990. Hypothermic stunning of sea turtles in Texas. *Marine Turtle Newsletter* 48:25-27.
- Shaver, D.J. 1994. Relative Abundance, Temporal Patterns, and Growth of Sea Turtles at the Mansfield Channel, Texas. *Journal of Herpetology*, 28(4):491-497.
- Shaver, D.J. 2019. Texas Sea Turtle Nesting and Stranding Manual (revised in 2019). National Park Service, Department of the Interior. 68 pp.
- Shaver, D.J. 2000. Distribution, residency, and seasonal movements of the green sea turtle, *Chelonia mydas* (Linnaeus, 1758), in Texas. Doctoral dissertation, Texas A&M University.

- Shaver, D. J., and C. Rubio. 2008. Post-nesting movement of wild and head-started Kemp's ridley sea turtles (*Lepidochelys kempii*) in the Gulf of Mexico. *Endangered Species Research* 4:43–55.
- Shaver, D.J., Frandsen, H.R., George, J.A. and C. Gredzens. 2020. Green turtle (*Chelonia mydas*) nesting underscores the importance of protected areas in the northwestern Gulf of Mexico. *Frontiers in Marine Science* 7:673.
- Shaver, D.J., Hart, K.M., Fujisaki, I., Rubio, C. , Sartain, S.R., Peña, J., Burchfield, P.M., Gomez Gamez, D., and J. Ortiz. 2013. Foraging area fidelity for Kemp's ridleys in the Gulf of Mexico. *Ecology and Evolution* 3(7):2002-2012.
- Shaver, D.J., Rubio, C., Walker, J.S., George, J., Amos, A.F., Reich, K., Jones, C. and T. Shearer. 2016. Nesting on the Texas coast: Geographic, temporal, and demographic trends through 2014. *Gulf of Mexico Science* 33(2):158-178.
- Shaver, D.J., Tissot, P.E., Streich, M.M., Walker, J.S., Rubio, C., Amos, A.F., George, J.A. and M.R. Pasawicz. 2017. Hypothermic stunning of green turtles in a western Gulf of Mexico foraging habitat. *PLoS ONE* 12(3): e0173920.
- Shaver, D.J., Walker, J.S. and T.F. Backof. 2019. Fibropapillomatosis prevalence and distribution in green turtles *Chelonia mydas* in Texas (USA). *Diseases of Aquatic Organisms* 136(2):175-182.
- Shimada, T., Jones, R., Limpus, C. and M. Hamann. 2012. Improving data retention and home range estimates by data-driven screening. *Marine Ecology Progress Series*,457:171–180.
- Shimada, T., Jones, R., Limpus, C., Groom, R. and M. Hamann. 2016. Long-term and seasonal patterns of sea turtle home ranges in warm coastal foraging habitats: Implications for conservation. *Marine Ecology Progress Series* 562:163–179.
- Simpfendorfer, C.A., Heupel, M.R., Hueter, R.E. 2002. Estimation of short-term centers of activity from an array of omnidirectional hydrophones and its use in studying animal movements. *Canadian Journal of Fisheries and Aquatic Sciences*. 59:23-32.
- Simpfendorfer, C.A., Huveneers, C., Steckenreuter, A., Tattersall, K., Hoenner, X., Harcourt, R. and M.R. Heupel. 2015. Ghosts in the data: false detections in VEMCO pulse position modulation acoustic telemetry monitoring equipment. *Animal Biotelemetry* 3:55.
- Smith, B.J., Selby, T.H., Cherkiss, M.S., Crowder, A.G., Hillis-Starr, Z., Pollock, C.G. and K.M. Hart. 2019. Acoustic tag retention rate varies between juvenile green and hawksbill sea turtles. *Animal Biotelemetry* 7:15.

- Stabenau, E.K., Stanley, K.S. and A.M. Landry. 1996. Sex ratios from stranded sea turtles on the upper Texas coast. *Journal of Herpetology* 30(3):427-430.
- SWOT. 2010. The green turtle: The most valuable reptile in the world. Report Volume VI. Arlington, VA, USA. 62 pp.
- Texas Park and Wildlife Department (TPWD). 2022. Marine Vegetation in Texas. (01-05-2022). <https://txmarspecies.tamug.edu/veglislist.cfm>
- TinHan, T.C., Mohan, J.A., Drumensnil, M., DeAngelis, B.M. and R.J.D. Wells. 2018. Linking habitat use and trophic ecology of spotted seatrout (*Cynoscion nebulosus*) on a restored oyster reef in a subtropical estuary. *Estuaries and Coasts* 41:1793-1805.
- Tristan, T., Shaver, D.J., Kimbro, J., deMaar, T., Metz, T., George, J. and A. Amos. 2010. Identification of fibropapillomatosis in green sea turtles (*Chelonia mydas*) on the Texas coast. *Journal of Herpetological Medicine and Surgery* 20(4):109-112.
- Troëng, S. and E. Rankin. 2005. Long-term conservation efforts contribute to positive green turtle *Chelonia mydas* nesting trend at Tortuguero, Costa Rica. *Biological Conservation* 121(1):111-116.
- Turtle Expert Working Group. 1998. An assessment of the Kemp's ridley (*Lepidochelys kempii*) and loggerhead (*Caretta caretta*) sea turtle populations in the western North Atlantic. NOAA Technical Memorandum NMFS-SEFSC-409, 96 pp.
- Turtle Expert Working Group. 2000. Assessment update for the Kemp's ridley and loggerhead sea turtle populations in the western North Atlantic. NOAA Technical Memorandum NMFS-SEFSC-444, 115 pp.
- U.S. Fish and Wildlife Service and National Marine Fisheries Service. 1992. Recovery Plan for the Kemp's ridley Sea Turtle (*Lepidochelys kempii*). National Marine Fisheries Service: St. Petersburg, FL, 40 pp.
- Uribe-Martínez, A., Liceaga-Correa, M.D.L.A. and E. Cuevas. 2021. Critical in-water habitats for post-nesting sea turtles from the southern Gulf of Mexico. *Journal of Marine Science and Engineering*, 9(8):793.
- Udyawer, V., Dwyer, R.G., Hoenner, X., Babcock, R.C., Brodie, S., Campbell, H.A., Harcourt, R.G., Huveneers, C., Jaine, F.R., Simpfendorfer, C.A. and M.D. Taylor. 2018. A standardised framework for analysing animal detections from automated tracking arrays. *Animal Biotelemetry* 6:17.

Ward, G.H. and N.E. Armstrong. 1980. Matagorda Bay, Texas: its hydrography, ecology and fishery resources. U.S. Fish and Wildlife Service, Biological Services Program, Washington, D.C. FWS/OBS-81/52.

Wood SN. 2017. Generalized Additive Models: An Introduction with R. Second ed. Boca Raton, FL: CRC Press.

Zavaleta-Lizárraga, L. and J.E. Morales-Mávil. 2013. Nest site selection by the green turtle (*Chelonia mydas*) in a beach of the north of Veracruz, Mexico. *Revista Mexicana de biodiversidad* 84(3):927-937.

Zuur, A. F., Ieno, E.N. and C.S. Elphick. 2010. A protocol for data exploration to avoid common statistical problems. *Methods in Ecology and Evolution* 1:3-14.

Zuur, A.F., Ieno, E.N., Walker, N.J., Saveliev, A.A. and G.M. Smith. *Mixed Effects Models and Extensions in Ecology with R*. Gail M, Krickeberg K, Samet JM, Tsiatis A, Wong W, editors. New York, NY: Springer; 574 p.

Appendix A: List of project collaborators and supporters

1. Matagorda Bay Ecosystem Assessment Sea Turtle Project Participants

A. Fieldwork Volunteers - Students

Cora Garcia

Kelsey Gibbons

Alexis High

Brandon Mason

Charlotte Miller

Kimberly Nguyen

Cassandra Rivas

Sara Rodrigues

Alyssa Walker

Arisa Furata

Meredith Faix

Mona Birgisson

Rachel Calame

Sangeetha Puthigai

Drew Anderson

Nicole Long

B. Fieldwork Associated Scientists

Christine Figgner, Post-doctoral Research Associate

Tasha Metz, permit holder; contractor;

Jennifer Wetz, TAMUCC-HRI, Logistical support

Jeffrey Kaiser, TAMUCC-HRI, Field Assistant

Daniel Coffey, TAMUCC-HRI, Field Assistant

Jason Williams, TAMUCC-HRI, Field Assistant

Quentin Hall, TAMUCC-HRI, Field Assistant

Chloe Dannenfelser, Texas Sea Grant Research Assistant

Kimber DeSalvo-Anderson, TIRN Gulf Coordinator

Alicia Walker, ARK Program Coordinator, The University of Texas at Austin, on-call veterinarian support

C. Boat Operations

James Helms, Captain

Jason Williams, TAMUCC-HRI, Boat operator

Quentin Hall, TAMUCC-HRI, Boat operator

2. Outreach

Sara Carney, Texas Sea Grant Communications Manager, iSeaTurtle Website and App

Callie Rainosek, Texas Sea Grant Communications Intern

Kimber DeSalvo-Anderson, Texas Sea Grant Communications Program Assistant, iSeaTurtle Website and App

R.J. Shelley, Calhoun County Extension Agent – Coastal & Marine Resources, Texas Sea Grant College Program & Texas A&M Agrilife Extension

Nicole Pilson, Matagorda County Extension Agent – Coastal & Marine Resources, Texas Sea Grant College Program & Texas A&M Agrilife Extension

3. *Other*

Brigid Berger, Texas Master Naturalist, support during freeze

Kelley Kowal, San Antonio Bay Ecosystem Leader, Texas Parks & Wildlife Department, Coastal Fisheries, support during freeze

Dustin Baumbach, ProTECTOR Inc., contractor for development of iSeaTurtle app

Joanie Steinhaus, Turtle Island Restoration Network, partnership to expand iSeaTurtle Texas-wide.

Brent Thuet, Contractor for Net repairs.

Appendix B: Comparison of potential satellite transmitter models to deploy on sea turtles in Matagorda Bay.

Manufacturer	Transmitter Model	Dimensions (cm)	Weight (gr)	GPS Operational Life (days)	QFP Operational Life (days)	Unit cost in US\$ (in 2020)	Comments
Telonics, Inc.	SeaTrkr-4370-4	10.3 x 4.5 x 3.6	190	657 (GPS every 4 hours and Iridium transmitting GPS every 2 days)	401 (hourly QFP positions and hourly Iridium transmission)		
Wildlife Computers	SPLASH10-F-351D	8.6 x 5.5 x 2.5	149	240 (hourly Fastloc attempts and 250 Argos transmissions/day)	N/A	5000	Four protection bumpers
	SPLASH10-BF-351E				N/A	3400	Same as SPLASH10-F-351D BUT no depth sensor
	SPOT-395A	7.5 x 4.0 x 1.9	86	345 (hourly Fastloc attempts and 250 Argos transmissions/day).	N/A	1450	For turtles 40-55 cm CCL, only ARGOS. "Rhino" tag with raised wet/dry sensors
Lotek NZ Ltd	F6G 276E	10.0 x 4.4 x 3.1	140	281 (hourly Fastloc attempts and 200 Argos transmissions/day)	N/A	2225	Better suited for green turtles
	F6G 276F	10.1 x 4.4 x 3.2	144	281 (hourly Fastloc attempts and 200 Argos transmissions/day)	N/A	2750	Same as 276E but with sacrificial bumps and dive sensors (optional)
	F6G 376A	11.5 x 6.4 x 4.35	220	-	N/A	2225	Better suited for Kemp's ridley turtles. Dimensions comparable to tag K2G 376A, used extensively on Kemp's ridley turtle research.

Appendix C: Outreach material

1. Sea Turtles in Texas poster. Art by: Dawn Witherington. Produced by: Dr. Blair Witherington and Dr. Pamela Plotkin.

Sea Turtles in Texas

The Texas coast provides important nesting beaches, bays, estuaries, and offshore habitats for five sea turtle species. All are threatened with extinction, but thanks to long-term conservation programs, our state's sea turtles are on the rise!

Where Do They Come From?

A sea turtle's origin is its nesting beach. The map to the left highlights major nesting beaches for sea turtles of the Gulf of Mexico. Many turtles swimming in the gulf emigrated as hatchlings from nests on gulf beaches, but most green turtles and leatherbacks probably came from beaches farther south in the Caribbean Sea. Significant gulf loggerhead nesting occurs in southwestern Florida and the Panhandle. Important hawksbill nesting takes place along the gulf's southern beaches. Nearly all of the world's Kemp's ridleys nest on beaches of the western Gulf of Mexico.

The Species

Of seven sea turtle species worldwide, five species occur in Texas.

Kemp's Ridley — The official Texas state sea turtle. This rarest of all sea turtles resides mostly in the Gulf of Mexico and nests on beaches in Texas and Mexico. Texas bays and nearshore waters provide crucial feeding habitat and migratory corridors for Kemp's ridleys. Adults feed primarily on crabs.

Hatchling: 0.6 oz Juvenile Adult: 12 to 30+ years, average 85 lb.

Loggerhead Sea Turtle
Adult and subadult loggerheads found in Texas' nearshore waters feed on crabs, mollusks, and sea pens (a soft coral). They also live and feed offshore in association with hard substrates such as oil platforms and both natural and artificial reefs.

Hatchling: 0.7 oz Juvenile Adult: 30 to 60+ years, average 265 lb.

Green Turtle
A commercial sea turtle harvest in Texas almost eliminated green turtles from the state's waters by the early 1900s. But the tide has turned — thanks to over 30 years of successful conservation programs, juvenile green turtles are now the most abundant sea turtle in Texas. These turtles live in shallow waters and feed on algae near rock jetties and on seagrasses within bays and estuaries. Adult females nest on beaches in Texas and Mexico, as well as throughout the southeastern U.S. and western Caribbean.

Hatchling: 1 oz Juvenile Adult: 30 to 70+ years, average 310 lb.

Hawksbill
Hawksbills are most commonly found on reefs, but also associate with mangroves, feeding primarily on sponges and colonial anemones. Most of the hawksbills found in Texas' nearshore waters are juveniles.

Hatchling: 0.5 oz Juvenile Adult: 25 to 42+ years, average 130 lb.

Leatherback
The world's largest turtle lives mostly in the high seas and occurs in the Atlantic from Canada to tropical Caribbean waters. Leatherbacks forage on jelly animals and are occasionally seen feeding on jellyfish within Texas bays.

Hatchling: 1.6 oz Juvenile Adult: 15 to 30+ years, average 800 lb.

Where in Texas Do Sea Turtles Live?

Sea turtles depend on a variety of coastal and open-sea habitats in the gulf.

- Beaches** — Female sea turtles lay eggs in nests on sandy beaches. After incubating for about 2 months, nests produce hatchlings that disperse away from land.
- Open sea** — Juveniles grow up in rafts of Sargassum seaweed. Leatherbacks spend the majority of their lives in open, blue water.
- Coastal waters** — Loggerheads, Kemp's ridleys, and green turtles feed in estuaries and other shallow coastal waters.
- Seagrass pastures** — All species other than the leatherback depend on seagrasses. Green turtles eat seagrass, and the other species feed on invertebrates living in seagrass.
- Reefs** — Deep offshore reefs support foraging loggerheads, and shallow coral reefs are the principal habitat for hawksbills.
- Migration corridors** — Sea turtles need unimpeded corridors for their migration routes between foraging areas and nesting beaches.

AT TEXAS A&M UNIVERSITY
 7805 DC 35 • P.O. Box 1980 • College Station, TX 77843-1980
 U.S. Coastal Program • Sea Grant Texas • Texas Sea Grant College
 National Oceanic and Atmospheric Administration
 U.S. Department of Commerce

A non-profit organization
 www.inwater.org

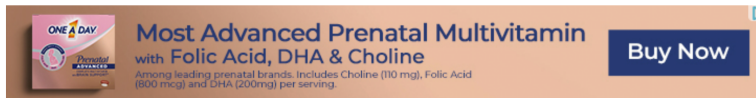
Copyright © 2014 Dawn Witherington

2. Sea turtle card distributed in Calhoun County and Matagorda County. Art by: Dawn Witherington. Produced by: Texas Sea Grant.



3. Press releases

A. November 21, 2019 (updated December 26, 2020) – Victoria Advocate - “Researchers persevere through challenges at start of endangered sea turtle study”. By: Kali Venable. URL: https://www.victoriaadvocate.com/news/environment/researchers-persevere-through-challenges-at-start-of-endangered-sea-turtle/article_4c040ecc-071e-11ea-bd07-f3d9b1bf21ef.html



Conservation

Researchers persevere through challenges at start of endangered sea turtle study



By Kali Venable | kvenable@vicad.com Nov 21, 2019 Updated Dec 26, 2020  0



Island Life... By Clint Bennetsen

Riding Out The Island Storm

Clint & Corky
 Greetings from the island everyone. I hope that all of you are doing well and coping with this real south Texas August heat we have been having. As has been the case since last month, I continue to do my outside chores and projects during the early morning and late evening hours. It's just too dang hot I'm miserable trying to work in this scorching heat and high humidity. Thank goodness for the shaded front porch and Gulf of Mexico sea breeze.

Well, a few Saturdays ago, July 25th to be exact, Hurricane Isiah made landfall about 100 miles south of me, and I am very thankful that it made that south turn. Coming in as a strengthening high (Cat 1, sustained winds of 90 mph, I wasn't overly concerned about and stayed in place on the island.

I spent the day Friday picking up and securing all the loose items, and took down the flags, hammock and wind chimes, as the winds would be in the 30-40 mph range. I also moved my boat over I secured it with extra lines to neighbors Britton and Susan's dock, swinging their dock was higher and much stronger... I'm very glad that it did this.

As far as riding out a storm, this one was not terrible, except the tidal surge was higher than I expected. After becoming a strengthening hurricane, the predicted tide rise for our area of the coastline was 3-5', and with my house being at a 4' sea level, I knew there was a chance I would get water into my downstairs kitchen/bathroom. And sure enough, during the 12 noon High Tide time of the day, while sitting at my kitchen table, I saw water start coming inside for the front door and along the baseboards of the octagon house. NG!! That's not a sight that you ever really want to see. Not much more to that point except start picking stuff up off the floor, and hope it doesn't get higher than several inches and damage the propane fridge. Luckily, just under 2" of Matagorda Bay water came inside, so I was able to sweep it out the front door as it receded. My cat, Jetty, mainly did not enjoy walking in the water on the floor, so she jumped on the table and spent the afternoon there.

These storms, even minimal hurricanes, have so much power and opportunities of destruction behind them, you really have to prepare a plan for them. I had very minimal damage, mostly consisting of baseboards on my pier coming loose from the surge and washing away. This was the fourth time in my 20+ years on the island to have water intrusions, so in that respect I am very fortunate.

As of this writing, the wooden floor in my 12'x26' tractor garage is almost finished, needing only seven more boards to complete the job. Yay!! All projects out here are a slow methodical process, going out a few materials at a time on my mainland supply runs. I always say that the latest building project will be my last one... but as yet to turn out that way, after the two-story house w/decks and porch, and now seven outbuildings. Geez!!

Well, that's it from the island for now. Everyone please take care, stay cool and have a great day.

The Treasure Chest
Accents for You and Your Home!
361.983.2696
 1304 Adams
 Port O'Connor, TX
Specializing in Texas Artists

tisd.net

TOP RESIDENTIAL PLANS

25 MBPS \$84.99 PER MONTH	15 MBPS \$64.99 PER MONTH	10 MBPS \$54.99 PER MONTH
-------------------------------------	-------------------------------------	-------------------------------------

PRICES BASED ON 24-MONTH COMMITMENT

CALL TODAY FOR MORE INFORMATION

510 NORTH VIRGINIA ST. 1502 EAST RED RIVER
PORT LAYACA, TX VICTORIA, TX
361-552-2000 361-573-1102

“State of the County”

Republican Club will meet Monday, September 7, at the Red Barn, 3187 Hwy 35 South between the 4-way at SH2433 and Bucces's. Dinner (\$11 by reservation only) from 5-5:45 p.m., meeting to begin 6:00 p.m. County Judge Richard Meyer will speak on the 'State of the County'.

Public is invited. Complimentary coffee and tea. For dinner reservations, call Connie (552-0917) or Lisa (552-6313).

Help Study Sea Turtles

Download the iSeaTurtle app on Google Play or Apple App Store and help Texas A&M University Scientists study Sea Turtles in the Matagorda Bay Ecosystem. The Matagorda Bay Ecosystem Assessment is a cooperative project between Texas Sea Grant, The Harte Research Institute for Gulf of Mexico Studies, the Texas Comptrollers Office and the Plotkin Lab.

Part of the Ecosystem Assessment will study Sea Turtles in Matagorda Bay. There are 3 different species of Sea Turtles that live in this area. Scientists at Texas A&M University have developed the iSeaTurtle app which will allow the public to report Sea Turtles that they see when they are in the bay. Several of the local fishing guides have assisted Texas Sea Grant by field testing the app so modifications could be made before it was released to the general public.







The iSeaTurtle app is available for both iPhone and Android devices. The app is free to download and easy to use. Once the user has downloaded the app to their phone all they have to do is open the app and click the "Send Location" button when they observe a sea turtle. Once this is done the app will open a map showing the user's location and allow the user to hit the "Submit" button. The location will be sent anonymously to a website that will show the reported location. If you want to see the map showing the locations of the sea turtle sightings go to tx.ag/iSeaTurtle.

When you mark your first sea turtle sighting get someone on your boat to take a picture of you doing it or take a selfie and email it to me at rj.shelly@tamu.edu. We will post it on Texas Sea Grant social media. Thanks for helping us out. RJ Shelly, Calhoun County Extension Agent – Coastal and Marine Resources



“A Beautiful Day begins with a Beautiful Mindset.”

C. May 4, 2021 – Texas A&M Today – “iSeaTurtle App Expands To Track Turtles Over Entire Texas Coast”. By: Sara Carney. URL: <https://today.tamu.edu/2021/05/04/iseaturtle-app-expands-to-track-turtles-over-entire-texas-coast/>

TEXAS A&M TODAY SCIENCE & TECH BUSINESS & GOVERNMENT ARTS & HUMANITIES CAMPUS LIFE HEALTH & ENVIRONMENT COVID-19      

Subscribe Press Room Search 

HEALTH & ENVIRONMENT

iSeaTurtle App Expands To Track Turtles Over Entire Texas Coast

Following a successful period of tracking sea turtles in Matagorda Bay, the turtle sighting app is expanding to cover the Texas coast thanks to a partnership between Texas Sea Grant and Turtle Island Restoration Network.

By Sara Carney, Texas Sea Grant at Texas A&M University • MAY 4, 2021

D. May 5, 2021 – Caller Times – “Track sea turtles in Texas waters with this app created by Texas A&M scientists”. By: Ashlee Burns. URL: <https://www.caller.com/story/news/local/2021/05/05/track-sea-turtles-texas-waters-app-created-texas-a-m-university-scientists/4945410001/>

CYBER SALE IS ON \$1 for 6 Months. Save 98%.

Caller Times

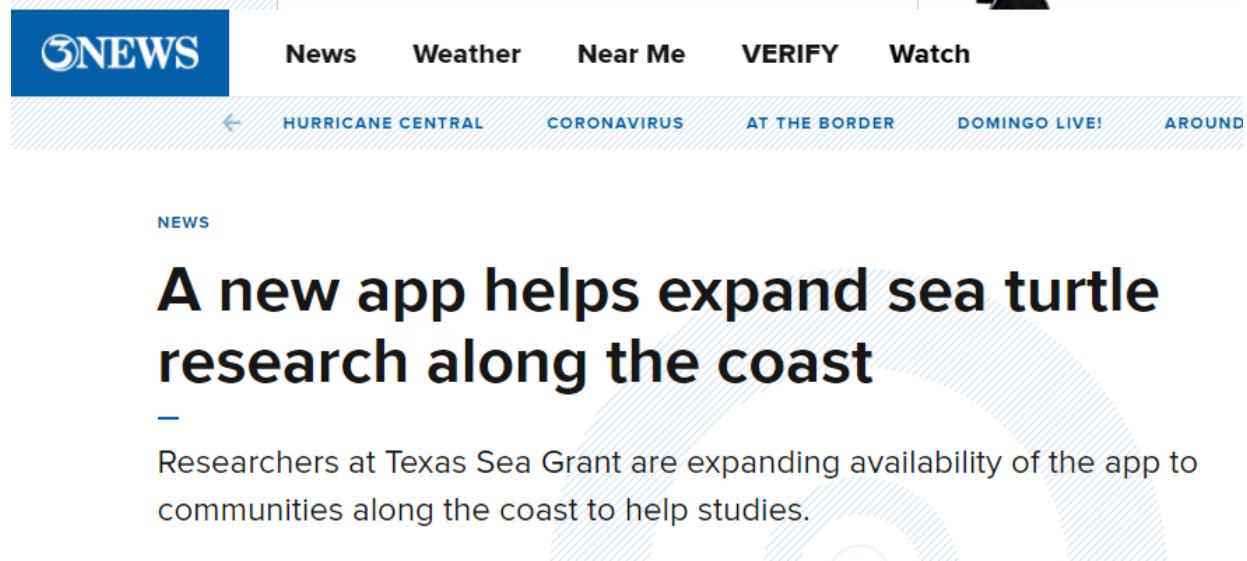
[News] Sports Business Opinion Lifestyle Obituaries E-Edition Legals 

Track sea turtles in Texas waters with this app created by Texas A&M scientists

Ashlee Burns Corpus Christi Caller Times
Published 7:15 a.m. CT May 5, 2021

[View Comments](#)    

E. May 13, 2021 – KIIITV – “A new app helps expand sea turtle research along the coast”.
By: Mariah Gallegos. URL: <https://www.kiiitv.com/article/news/a-new-app-helps-expand-sea-turtle-research-along-the-coast/503-fd761002-2f8d-42cb-9bab-3e3b41371eab>



F. May 23, 2021 – Port O’Connor Dolphin Talk Newspaper – “iSeaTurtle App Expands”.
Posted by: Joyce Rhyne. URL: <https://thedolphintalk.com/?p=27472>



G. 2021 – Texas Sea Grant – “The Mysteries of Matagorda Bay's Sea Turtles”. By: Callie Rainosek. URL: <https://stories.texaseagrant.org/the-mysteries-of-matagorda-bay-s-sea-turtles/index.html>

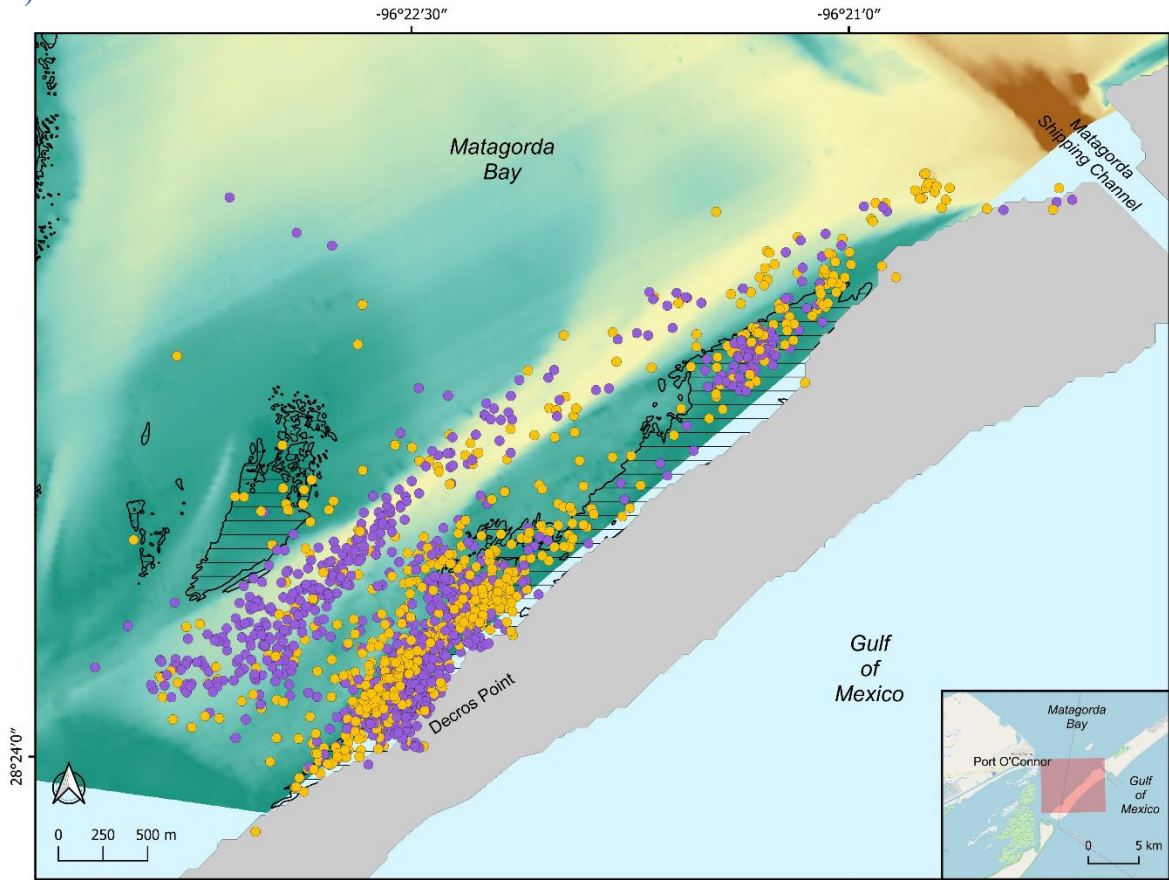
A wide-angle photograph of a beach at sunset. The sky is a mix of orange, yellow, and grey, with the sun just below the horizon. The ocean is calm with small waves lapping at the shore. The foreground shows a sandy beach with some dark rocks and pebbles.

The Mysteries of Matagorda Bay's Sea Turtles

Tracking Sea Turtles' Movements, Developing a Deeper Understanding of Matagorda Bay's Ecosystem

The author of this story, Callie Rainosek, M.S., is a science writer who has worked for Texas Sea Grant for two consecutive summers as a communications intern. She is also a doctoral student at the Texas A&M University School of Public Health.

Appendix D: Satellite locations of sea turtles received during day (orange) and night (purple) hours.



- Sea turtle satellite locations
 - day
 - night
- Seagrass
- Bathymetry (feet)
 - >50
 - 0

*Seagrass and bathymetry data provided by BIO-WEST

Appendix E: Photo of a loggerhead turtle sighted and reported by an iSeaTurtle user.
Photo credits: Captain Kenneth Gregory.



Appendix F: Data management

1. Main outputs for satellite tracking analysis:

Zip file “Matagorda_turtle_datasets.zip”, which includes four types of datasets:

A. SRTM_Region2

High-resolution and very detailed polygon layer of Texas, provided by Marissa Dotson from Dr. Gibeaut’s lab).

B. Filtered tracks and locations:

Folder: filtered

All shapefiles are already projected in EPSG:32614 - WGS 84 / UTM zone 14N

Matagorda_filtered_proj – Locations filtered using the SDLfilter package

Matagorda_filtered_all_proj_manualfilter – Additional filter to remove locations on land, using layer SRTM_R2 as overlay

Matagorda_filtered_tXXXXXX_KKPxxxx_proj – filtered locations by individual.

tXXXXXX_KKPxxxx refers to Deployment_ID (PPT number + flipper tag number)

lines_Matagorda_filtered_tXXXXXX_KKPxxxx_proj –tracks for filtered locations by individual. tXXXXXX_KKPxxxx refers to Deployment_ID (PPT number + flipper tag number)

C. Home ranges and Core areas:

noland_sing_tXXXXXX_KKPxxxx_udvol50 – 50% UD by ID, estimated using the BRB function in adehabitatHR package. tXXXXXX_KKPxxxx refers to Deployment_ID (PPT number + flipper tag number)

noland_sing_tXXXXXX_KKPxxxx_udvol95 – 95% UD by ID, estimated using the BRB function in adehabitatHR package. tXXXXXX_KKPxxxx refers to Deployment_ID (PPT number + flipper tag number)

D. SSM Simulated locations

Folder: SSM

Subfolders:

t202700_KKP-0304 and t202703_KKP0308: These are two turtles that were tagged with Lotek tags in Jan-Feb 2021, and migrated shortly after to the south. The folder includes one *.csv file with the simulated points and associated behavioral index (“g”, for gamma) for both turtles, and for each turtle there are *.pdf files of (a) Residual plots to check model performance, (b) Time series plot of the simulated locations colored by the value of the behavioral index, and (c) Map of simulated locations colored by the value of the behavioral index.

t202704_KKP0303: This is one turtle that was tagged with a Lotek tag in Oct-2020 and remained for the most part inside MB, but moved considerably during cold fronts. The folder includes one *.csv file with the simulated points and associated behavioral index (“g”, for gamma), and *.pdf files of (a) Residual plots to check model performance, (b) Time series plot of the simulated locations colored by the value of the behavioral index, and (c) Map of simulated locations colored by the value of the behavioral index.

t712549: This is one turtle tagged with an Iridium Telonics tag, which provided very limited and sparse -but highly accurate-raw data. Due to the large temporal gaps, there is huge uncertainty in the simulated track, and I would not use this turtle for further analysis. he folder includes one *.csv file with the simulated points and associated behavioral index (“g”, for gamma), and *.pdf files of (a) Residual plots to check model performance, (b) Time series plot of the simulated locations colored by the value of the behavioral index, and (c) Map of simulated locations colored by the value of the behavioral index.

Appendix G: Sample Sea Turtle Data Collection Sheet



TURTLE DATA SHEET

ENTRY ID:
 Mata20- _____
 Recorded by: _____

CAPTURE

DATE (mm/dd/yyyy): _____ / _____ / _____ TIME (hh:mm): _____

COORDINATES: _____ , _____ GPS WAYPOINT: _____

DEPTH (m): _____ NET TYPE (shallow, deep, other-specify): _____

TURTLE DATA

SPECIES: Cm Lk Cc Ei Dc TAG SCARS: Yes No

RIGHT FLIPPER TAG: _____ Present, OR Applied

LEFT FLIPPER TAG: _____ Present, OR Applied

CCL - Curved Carapace Length (cm): _____

CCW – Curved Carapace Width (cm): _____

SCL – Straight Carapace Length (cm): _____

SCW – Straight Carapace Width (cm): _____

SCD – Straight Carapace Depth (cm): _____

MASS (kg): _____

FIBROPAPILLOMA No Yes Grade (1-3): _____ Location: _____

Observations (e.g. injuries, epibionts, name):

SAMPLES

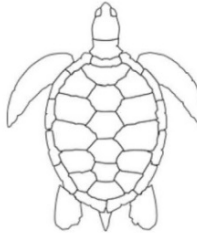
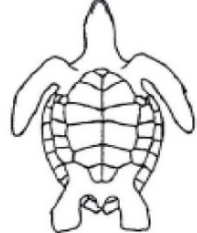
Skin No Yes, ID _____

Scute No Yes, ID _____

Blood No Yes, ID _____

Other: _____ ID _____

Other: _____ ID _____

TRANSMITTER DATA

Acoustic tag: Yes No Acoustic Tag ID: _____

Satellite tag: Yes No Satellite Tag ID: _____

PHOTOS

Turtle: Yes

Acoustic tag: Yes

Satellite tag: Yes

RELEASE SAME AS CAPTURE

DATE (mm/dd/yyyy): _____ / _____ / _____ TIME (hh:mm): _____

COORDINATES: _____ , _____ GPS WAYPOINT: _____

Appendix H: Transmitter Attachment Protocol

See adjacent PDF file: Satellite Transmitter_Attachment protocol.pdf

Appendix I: Research permits

See adjacent PDF files:

NMFS permits: 22822-01_permit_iss_fully executed.pdf

22822 auth letter sat tags.pdf

22822-02_permit and cover letter.pdf

TPWD permit: Plotkin, Pamela.20200925.TPWD.SPR.pdf

Biological Sampling Across Habitats

Introduction and Project Goals

Estuaries are productive and diverse ecosystems that support a wide range of aquatic flora and fauna (Seitz et al. 2014). The complex mix of habitats that comprise estuarine seascapes (e.g., seagrass, saltmarsh, oyster reefs) influences ecosystem services provided as well as the resilience of associated communities to environmental change (Stachowicz et al. 2007, Barbier et al. 2011). For example, seagrass, saltmarsh, and oyster reefs along the Gulf of Mexico serve as nursery habitats, and the presence of these habitats have been shown to enhance production of many species of commercial and recreational value (zu Ermgassen et al. 2021). Along the Gulf Coast, the primary types of aquatic vegetation found in estuaries are seagrass meadows and inundated saltmarsh. These foundational habitats are essential components of estuarine seascapes in this region and both habitats support a diverse range of marine life and serve as critical nurseries for invertebrates and fishes (McDevitt-Irwin et al. 2016, Baker et al. 2020, Hollweg et al. 2020).

Nursery habitats are areas within a system used by juvenile fishes that contribute disproportionately more recruits to adult populations (Beck et al. 2001, Dahlgren et al. 2006). The functional role of nurseries is linked to their ability to enhance foraging success (Nunn et al. 2012) and minimize predation mortality (Walters and Juanes 1993). Habitat complexity afforded by both seagrass and saltmarsh habitats is of considerable value to juvenile fishes because the complexity of the vegetation represents shelter or refuge (physical or visual barriers) that reduces the encounter rates or capture success of predators, enhancing early life survival (Scharf et al. 2006, Flaherty-Walia et al. 2015). In addition, prey availability for juvenile fishes is typically higher in aquatic vegetation such as seagrass and saltmarsh relative to adjacent non-vegetated areas of the estuary, enhancing the growth, condition, and survival of fishes during the vulnerable early life interval (Houde 1987). Apart from antipredator and foraging benefits afforded by aquatic vegetation, the physical complexity of this vegetation also alters the delivery and settlement of recruits in these habitats, thus indirectly influencing the spatial distribution of fishes as well as the structure of estuarine communities (Jenkins and Sutherland 1997, Jenkins et al. 1998).

Previous research evaluating the community structure of fishes using seagrass and saltmarsh habitats indicated that the density and diversity of the juvenile fishes can differ significantly between these two habitats and across seasons (Rozas and Minello 1998, Bloomfield 2005, Baillie et al. 2015). Moreover, studies have documented that the nutritional condition and growth of juvenile fishes associated with these and other estuarine nursery habitats (e.g., oyster reefs) may be significantly different, suggesting that ‘habitat quality’ both within and among these habitats is variable (‘not all habitats are equal in terms of quality’) (Westerman and Holt 1994, Rooker and Holt 1996, Stunz et al. 2002, Glass et al. 2008). Several approaches are commonly used to assess habitat quality, with the most common being measures of abundance (Rooker et al. 1998, Minello et al. 2003, Baillie et al. 2015) and diversity (Rozas and Minello 1998, Morris et al. 2014). Using these approaches, habitats or sites with higher relative

abundance or higher assemblage diversity are deemed to be of greater quality relative to habitats or sites with lower measures. For example, Rooker et al. (1998) showed patches of turtle grass (*Thalassia testudinum*) supported significantly lower densities of juvenile red drum (*Sciaenops ocellatus*) and spotted seatrout (*Cynoscion nebulosus*) in a south Texas estuary relative to shoal grass (*Halodule wrightii*) and hypothesized that shoal grass represented higher quality habitat for these species. Apart from abundance, elevated biological diversity is often associated with enhanced ecosystem stability and resiliency (Duffy 2006, Worm et al. 2006), and is commonly used as an indicator of habitat quality (Naeem 1998). A comprehensive review on the subject indicated that areas with higher species richness resisted environmental disturbances better and were faster to recover from disturbances when they did occur (Worm et al. 2006). Similarly, this review determined that coastal ecosystems with higher taxonomic richness had lower rates of collapse and extinction of commercially important species than less diverse systems. Therefore, diverse communities of fishes associated with seagrass and saltmarsh habitats may reinforce the stability of estuarine ecosystems, and also serve as a useful indicator of high-quality habitat.

Fishes in the family Sciaenidae (drums and croakers) are highly abundant in estuarine habitats along the Gulf coast (Rooker et al. 1998, Geary et al. 2001). Species from this diverse family use a breadth of habitats and vary in their habitat use throughout ontogeny (Neahr et al. 2010, Akin and Winemiller 2015). The wide range of morphological characteristics exhibited by sciaenids allow them to occupy not only multiple habitats but several different ecological niches (Chao and Musick 1977, Deary et al. 2017). During early life history stages, this divergence in habitat use and feeding strategy exhibited by adults is diminished. Many different species will use the same estuarine habitats including seagrass (Rooker et al. 1998) and saltmarsh edges (Geary et al. 2001) but differ in the timing of settlement into these habitats. For example, Rooker et al. (1998) reported that settlement of red drum *Sciaenops ocellatus* and Atlantic croaker *Micropogonias undulatus* both occurred during the fall but entry into estuarine nursery habitats was temporally partitioned (early October vs. late October/early November), with limited overlap in peak settlement times between the two species. These two species were both characterized as generalist feeders during early life based on feeding apparatus morphology and stomach contents (Deary et al. 2017) and appear to share a preference for the same prey items in Texas estuaries (Soto et al. 1998). This suggests that staggered entry into these nurseries may be critical for the recruitment success of both species given the high degree of overlap in prey resources. Several species of sciaenids including red drum, Atlantic croaker, spotted seatrout *Cynoscion nebulosus*, silver perch *Bairdiella chrysoura*, and spot *Leiostomus xanthurus* are commonly harvested recreationally or commercially for food, sport, and bait (Green and Campbell 2010). Their economic significance and ecological importance make sciaenids an ideal focal group for studying species-specific patterns of nursery habitat use. Understanding patterns of estuarine nursery habitat use by these important fishes is essential for prioritizing the management of estuarine habitats.

Spanning roughly 1070 square kilometers along the central coast of Texas, Matagorda Bay is a bar-built estuary at the confluence of the Colorado River that serves as critical habitat for a

wide range of taxa including fishes (Gelwick et al. 2001, TinHan et al. 2018), shore birds (Withers 2002), and sea turtles (Renaud and Williams 1997). The relatively undeveloped shorelines and diverse seascapes found throughout Matagorda Bay are important ecologically and provide important ecosystem services that support this idyllic estuary as well as the local economy (Green and Campbell 2010, Comptroller 2019). Despite its ecological and economic importance, our current understanding of the functional role of Matagorda Bay as nursery habitat is limited and more research is needed to develop effective conservation strategies to ensure the long-term sustainability of this unique ecosystem. The lack of basic ecological data for Matagorda Bay prompted the Texas Comptroller of Public Accounts to initiate a baseline assessment of this estuary with the goal of determining the best way to balance economic activity and sustainable use of its ecological resources (Comptroller 2019).

The primary aim of this study was to identify habitats, regions, and environmental conditions in Matagorda Bay that support post-settlement fishes. Two general metrics were used to assess the function of putative nurseries used by fishes in Matagorda Bay: 1) relative abundance of post-settlement fishes and 2) taxonomic diversity (family level) of the entire post-settlement fish assemblage. Abundance and diversity metrics were linked to environmental conditions in the estuary to determine which conditions were most favorable for post-settlers during the early life period. In addition, abundance of species within a single family (Sciaenidae) was quantified to further evaluate the role putative nurseries in Matagorda Bay serve for a suite of sport fishes heavily targeted by anglers and to highlight the impact of temporal shifts in nursery habitat use by species from a single family on overall assemblage diversity. One ancillary benefit of the study was to establish baseline estimates of abundance and diversity of post-settlement fishes for assessing future impacts to these nurseries and the Matagorda Bay ecosystem. Findings from this study will prove instrumental for developing priority areas regarding management and the conservation of natural resources in this and other estuarine ecosystems.

Methods

Study Area

The study was conducted in Matagorda Bay located centrally along the Texas Gulf Coast (Figure 122). Matagorda Bay is a tidally influenced bar-built estuary with two inlets (Matagorda Ship Channel and Pass Cavallo) that connect the bay to the Gulf of Mexico. Matagorda Bay experiences diurnal tides with a fairly limited range averaging approximately 0.2 m (NOAA NDBS station 8773701). Freshwater enters the bay directly via the Colorado River to the far east and the Tres Palacios River to the northeast and indirectly through Lavaca Bay, a small-sub bay in the northwest corner. Compared to other major bays in Texas, freshwater inflow from the Colorado River (the major contributor of freshwater) is relatively low (Wilber and Bass 1998). This leads to fairly high average salinity across the bay of 23.7 ppt (Palmer et al. 2011), with higher salinities occurring in the southwestern portion of the bay (closest to the tidal passes) and lower salinities occurring close to the Colorado River. The sampling locations for this study were concentrated along Matagorda Peninsula to take advantage of the abundant seagrass and intact

saltmarsh found in these areas. Similarly, selection of this area allowed for sampling across a salinity gradient observed west (higher) to east (lower). Seagrass meadows dominated by shoal grass *Halodule wrightii* and widgeon grass *Ruppia maritima* are restricted to higher salinity, lower turbidity waters closest to the pass (Figure 122), while *Spartina alterniflora* marsh is found throughout the bay.

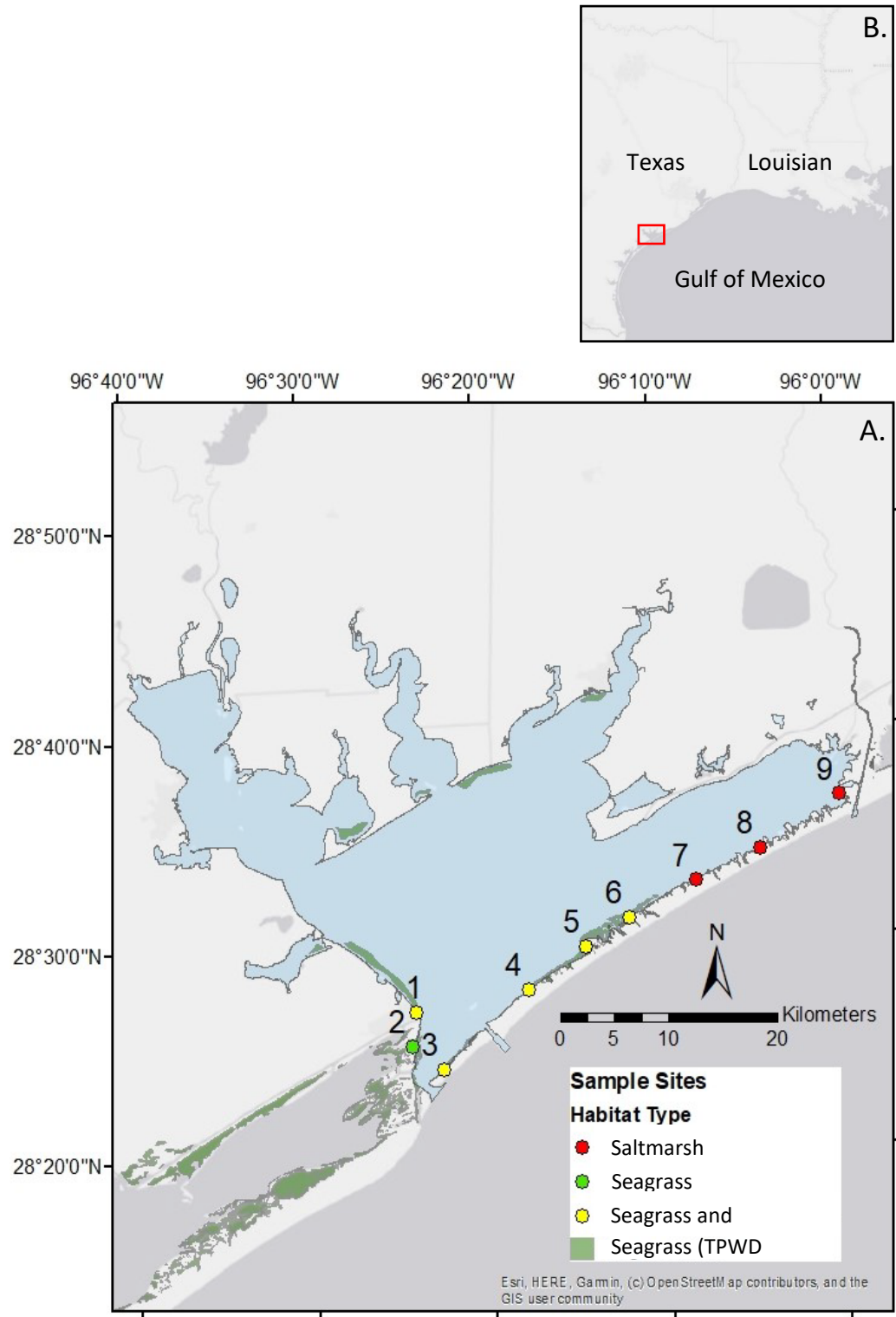


Figure 122. A) Map of Matagorda Bay and historic extent of seagrass (green) (TPWD 2001). Sample sites 1-9 shown as points containing seagrass only (●), saltmarsh only (●), or both habitats (●). B) Shows the location of Matagorda Bay (red box) in the northwestern Gulf of Mexico.

Sample Collection

Collections of post-settlement fishes and invertebrates were conducted at nine sites with seagrass and/or saltmarsh edge (hereafter “saltmarsh”) habitat(s) in Matagorda Bay (Figure 122). Every site was visited quarterly with sampling occurring in March, June, September, and December of 2020 and 2021. A subset of these sites (sites 1, 3 and 5) contained both seagrass and saltmarsh habitats was sampled monthly from May through October to coincide with periods of peak recruitment for several species of interest in Texas bays (Rooker et al. 1998). Low water levels related to northerly cold fronts reduced the ability to sample saltmarsh in December of 2020. Additionally, no seagrass was present at site 6 in September or December following direct landfall of hurricane Nicholas in this area on September 12, 2021. Of the nine sites, not all include both seagrass and saltmarsh habitats. The three sites closest to the Colorado River (7, 8, and 9) contained only saltmarsh habitat adjacent to bare substrate. At site 2, seagrass was present but no inundated saltmarsh and therefore no edge habitat. Sites 1, 3, 4, 5, and 6 contained seagrass and saltmarsh; habitats were separated by a band (1- 2 m wide) of bare substrate directly adjacent to the saltmarsh edge.

All fishes and invertebrates were collected using an epibenthic sled 60-cm wide and 75-cm tall attached to a 1.5-m conical net with 1-mm mesh. The rope attached to the epibenthic sled was pulled by hand at a constant speed (~1.5 m/second) for 16.7 m to cover a total area of 10 m². The epibenthic sled has been proven effective for sampling post-settlement sized fishes and invertebrates from both seagrass beds and marsh edges (Rooker et al. 1998, Hall et al. 2016, Williams et al. 2016). A total of 443 sled pulls were conducted between March 2020 and December 2021. GPS coordinates were taken at the beginning and end of each pull using a handheld Garmin GPS unit. After each sample, the net was rinsed down towards the cod end and contents were emptied into a bucket. Pulls were made in triplicate through each habitat type present at each site and replicate samples were preserved and sorted separately. Individual fishes larger than the target “post-settlement size” were identified, measured, and released alive. For taxa with elongate body shapes (e.g., Syngnathidae, Ophichthidae), all individuals were collected regardless of length. Post-settlement fishes were placed into a clean collection jar and humanely euthanized by rapid cooling in an ice slurry (TAMU IACUC 2020-0019) before immersion in 95% ethanol for fixation and preservation. Ethanol in each sample was changed 24 hours (95%) and again one week after collection (70%) to ensure proper preservation and to reduce acidification of preservative.

Environmental parameters were recorded at each site during every collection period. In situ water temperature (°C), dissolved oxygen (mg/L), salinity (ppt), and turbidity (NTU) were recorded at each site using a YSi ProDSS model handheld multiparameter water quality meter. Measurements were taken immediately prior to collections to minimize disturbance of sediment in the site. The sonde was lowered into the water until sensors were ten centimeters from the bottom to accurately approximate water conditions. Tide cycle and time of sunrise were recorded from the nearest NOAA data buoy (NOAA NDBS station 8773701) located near Port O’Connor.

The “distance to pass” variable was calculated in ArcGIS using the start coordinates collected at the beginning of every pull and coordinates for Pass Cavallo (28.387657, -96.386605) and the Matagorda ship channel (28.434182, -96.33577). The distance in meters between the nearest tidal pass and each pull was calculated in ESRI ArcMap Pro using the Near tool in the Analysis tool pack.

Sample Preparation

Preserved benthic sled samples were first rough sorted with the naked eye before remaining material was sorted under a Leica M80 dissecting scope (0.75 – 2.5 x magnification) to separate smaller fishes and invertebrates from detritus. All fishes removed from the bulk sample were separated into two categories: 1) sciaenids and 2) non-sciaenids before being placed in jars of 70% ethanol. Non-sciaenid fishes were identified to family level. Individuals above the minimum length of sexual maturity or likely greater than age 0 as determined from literature values were excluded from analysis (Supplemental 1). Some uncommon resident species for whom the necessary life history information was lacking were not separated into juveniles and adults. These species were included in the analysis as they are important constituents of the communities in these habitats, but their low abundances did not significantly affect estimates of post-settlement fish density. Similarly, fishes from the families Engraulidae (anchovies) and Clupeidae (herrings, shads, sardines, menhadens) were excluded from analysis because these taxa inhabit the water column and are not necessarily reflective of communities in the benthic habitats targeted in this study. Sciaenids were identified to species using morphological characteristics outlined by Ditty and Shaw (1994) and length (standard length [SL], total length [TL]) was measured for each individual.

Data Analysis

Data analysis was conducted in R using several packages: *vegan*, *mgcv*, *tidyverse*, *dplyr*, *ggplot2*, and *multcomp* (Hothorn et al. 2008, Oksanen et al. 2022, Wickham et.al. 2016, Wickham et.al. 2019, Wickham et.al. 2022, Wood et al, 2016). Density of post-settlement fishes (all families including sciaenids) was calculated for each pull as number of recruits per square meter. To quantify biodiversity of recruits in each site, Shannon diversity (H') was calculated at the family level for all pulls (Morris et al. 2014). Taxonomic richness to the family level (T_F) was calculated for each pull and used in lieu of the commonly used species richness (S).

Analysis of density, T_F , and H' data was conducted using only quarterly samples (March, June, September, and December collections) when all sites and habitat types were sampled. Limiting the analysis to quarterly samples eliminated the likelihood of inflated diversity measures related to higher sampling effort during these collections compared to monthly collections. Further mention to seasonal variation refers only to quarterly collections: March = spring, June = summer, September = fall, and December = winter. To ensure comparisons between habitat types were not influenced by differences in geographic location within Matagorda Bay, parametric analysis was limited to sites containing both seagrass and saltmarsh (1, 3, 4, 5, and 6) (hereafter referred to as “paired sites”). Density, T_F , and H' of all post-

settlement fishes collected at paired sites was evaluated using a three-way analysis of variance (ANOVA) with year, season, and habitat type as the main factors. When the three-way ANOVA revealed significant interactions among the main factors, Tukey's honestly significant difference (Tukey's HSD) post-hoc test was used to determine which levels of each factor differed from one another. Density of the five most abundant species of sciaenids (spot, silver perch, spotted seatrout, red drum, and Atlantic croaker) was compared using two-way ANOVAs with year and habitat type as the main factors for each model. These species-specific models were limited to monthly collection data when a given species was present. Alpha of 0.05 was used to determine significance for all statistical analyses in this study.

Community structure of post-settlement fishes in seagrass and saltmarsh habitats across all four seasons was analyzed with a Bray-Curtis dissimilarity matrix based on the abundance (density) of families present in each habitat. Bray-Curtis indices require at least one taxon per sample and thus pulls without any fish were removed prior to this step. Next, a permutational multivariate analysis of variance (PERMANOVA) with 999 permutations was used to compare community structure of families by habitat type and season from quarterly collections. The two-way PERMANOVA revealed a significant interaction between habitat type and season, and thus community structure of post-settlement fishes in seagrass and saltmarsh habitats were compared separately for each season. P-values from these comparisons were then adjusted using Holm's adjustment for multiple comparisons to account for potential inflation of type I error. PERMANOVAs were paired with Similarity Percentage (SIMPER) analysis (again with 999 permutations) to determine families that were driving the differences between habitat types. A SIMPER analysis calculates the average percent differences in community structure attributed to a given family across all permutations. The five highest-ranked families by percent contribution were reported.

Relationships between response variables (density, T_F , and H') and environmental variables were analyzed using generalized additive models (GAMs), which are commonly used to elucidate fish-habitat relationships between a response variable and biotic or physicochemical explanatory variables (Furey and Rooker 2013). GAMs employ the sum of smoothed predictor functions that can be used to model both linear and high order non-linear responses (Tibshirani 1986). This allows GAMs to better predict response variables given inputs that may show a non-linear relationship to said response. Similarly, GAMs allow for the inclusion of categorical variables, the relationship of which is not smoothed. Each of the models used a gaussian distribution, and splines were estimated using restricted maximum likelihood (REML). The number of basis functions (k) was limited to four for each variable to avoid over fitting while allowing the model to follow natural variation common in ecological relationships. Prior to GAM selection, a linear model was constructed using all potential variables and the collinearity of these variables was tested using variable inflation factors (VIF). Collinear variables ($VIF > 10$) were used to build separate GAMs and the variable that resulted in a model with higher deviance explained (DE) and lower corrected Akaike Information Criterion (AICc) was used to start model selection while the other collinear variable was omitted. For example, the variables "start

time” and “minutes after sunrise” are collinear and essentially provide the same information to the model. Minutes after sunrise resulted in a higher percent deviance explained (DE) and lower AICc, and thus this variable was chosen over start time. Optimal GAMs were selected using backwards stepwise selection procedure based on minimizing AICc. First a full model containing all of the environmental variables (habitat type, year, water temperature, dissolved oxygen, salinity, turbidity, minutes after sunrise, distance from tidal pass, tide height, and Julian day) was constructed, and the AICc and DE was recorded. Next, the least significant variable was removed from the model and again the AICc and DE were recorded. This procedure was repeated until the AICc of a given model increased by greater than 2 following the removal of an explanatory variable (Symonds and Mousalli 2011, Richards 2005). The AICc, DE, and adjusted coefficient of determination (r^2) of models were recorded and used to determine its fit and explanatory power. When multiple environmental variables showed a significant relationship ($p < 0.05$) with the response variable in the final model, each was removed one at a time and the change in percent deviance explained (Δ DE) and change in AICc (Δ AICc) of the new model was recorded. This procedure was used to determine the relative explanatory power of each variable in the final model.

Results

Collection Summary

A total of 30,963 fishes from 27 families were collected during the course of this study, of those 20,631 were post-settlement fishes from 25 families. The majority of adult fishes that were excluded from data analysis were from the families Gobiidae (gobies), Fundulidae (killifishes), Cyprinodontidae (pupfishes), and Atherinopsidae (silversides). For both 2020 and 2021, the five most abundant families of post-settlement fishes were Gobiidae, Sparidae (porgies), Gerriidae (mojarras), Sciaenidae (drums and croakers) and Fundulidae, which combined represented 91.0% of the catch in 2020 and 91.2% of the catch in 2021 (Table 23). Gobiids alone accounted for 48.3% of the total catch and were present in 89.0% and 52.3% of the individual net pulls in seagrass and saltmarsh, respectively.

For invertebrates, a total of 196,241 decapod invertebrates were collected. These represented 10 taxonomic groups wherein most were identified to family, with some identified to genus. In 2020, the most abundant families were Palaemonidae, Hippolytidae, Penaeidae, and the most abundant genera were *Tozeuma* and *Callinectes*. These groups combined represented 99.07% (only included the taxa $> 1\%$) of all the invertebrates collected. In 2021, most abundant families were Palaemonidae, Penaeidae, Hippolytidae, and the most abundant genus was *Callinectes*. These groups combined represented 99.62% (only included the taxa $> 1\%$) of all invertebrate species collected. Palaemonidae alone represented 78.82% of the total catch and occurred in 94.44% of Seagrass pulls and 96.08% of saltmarsh pulls (Table 24).

Table 23: Count and percent composition post-settlement fishes (by family) captured in seagrass and saltmarsh habitats of Matagorda Bay in 2020 and 2021.

	2020			2021		
	Seagrass	Saltmarsh	Percent	Seagrass	Saltmarsh	Percent
Archiridae	0	1	0.01	0	0	0
Atherinopsidae	1	37	0.50	74	211	2.20
Batrachoididae	4	1	0.07	2	0	0.02
Blenniidae	0	0	0.00	3	0	0.02
Carangidae	0	1	0.01	1	3	0.03
Cynoglossidae	36	18	0.70	32	3	0.27
Cyprinodontidae	4	80	1.09	318	131	3.47
Elopidae	0	0	0	1	0	0.01
Eleotridae	0	0	0	19	8	0.21
Fundulidae	13	622	8.27	74	511	4.51
Gerreidae	466	250	9.33	1359	146	11.62
Gobiidae	2988	841	49.90	5650	487	47.36
Gobiesocidae	1	2	0.04	0	0	0
Haemulidae	4	0	0.05	0	0	0
Lutjanidae	7	3	0.13	4	0	0.03
Mugilidae	0	62	0.81	73	40	0.87
Ophichthidae	1	1	0.03	2	2	0.03
Ophidiidae	1	0	0.01	3	0	0.02
Paralichthyidae	29	4	0.43	80	19	0.76
Poeciliidae	2	259	3.40	2	3	0.04
Sciaenidae	379	310	8.98	525	307	6.42
Scorpaenidae	0	1	0.01	2	0	0.02
Sparidae	860	221	14.09	2150	606	21.27
Syngnathidae	119	10	1.68	78	10	0.68
Tetraodontidae	2	0	0.03	1	1	0.02
Unknown	18	15	0.43	8	8	0.12
Total	4935	2739	100	10461	2496	100

Table 24: Count and percent composition of invertebrates (to lowest taxonomic level) captured in seagrass and saltmarsh habitats of Matagorda Bay in 2020 and 2021.

	2020			2021		
	Seagrass	Saltmarsh	Percent	Seagrass	Saltmarsh	Percent
<i>Alpheidae</i>	16	1	0.02	0	0	0.00
<i>Callinectes</i>	2074	899	3.36	3693	621	4.00
<i>Hippolytidae</i>	10002	467	11.83	1765	393	2.00
<i>Menippidae</i>	2	0	<0.01	2	0	<0.01
<i>Ocypodidae</i>	0	0	0.00	0	1	<0.01
<i>Palaemonidae</i>	35619	27739	71.61	40786	50542	84.74
<i>Penaeidae</i>	4455	1708	6.97	5973	3602	8.88
<i>Porcellanidae</i>	13	3	0.02	6	0	0.01
<i>Tozeuma</i>	4493	195	5.30	28	0	0.03
<i>Xanthidae</i>	274	511	0.89	227	130	0.33
<i>Unknown</i>	1	0	<0.01	0	0	0.00
Total	56949	31523	100	52480	55289	100

Density

The main effects of habitat and year were identified as significant factors in the three-way density model for post-settlement fishes at sites with paired habitats (Table 25). Overall density from all collections was higher in seagrass (Mean + SE: $5.92 + 0.54$ ind. m^{-2}) relative to saltmarsh ($2.37 + 0.43$ ind. m^{-2}), and density varied as a function of season and year (Figure 123). Both season x year and habitat x season interactions were significant, indicating that habitat-specific trends in density were not consistent over seasons or years. In 2020, fish density in seagrass was highest during the fall ($8.66 + 1.66$ ind. m^{-2}) relative to the spring ($4.50 + 1.13$ ind. m^{-2}), summer ($2.77 + 0.36$ ind. m^{-2}), and winter ($0.94 + 0.29$ ind. m^{-2}) surveys (Tukey's HSD $p < 0.05$). In 2021, fish density in seagrass was statistically similar among the four seasons with modest differences in mean density between the highest observed value in the winter ($10.50 + 2.43$ ind. m^{-2}) and the other three seasons (range: 5.81 to 7.70 ind. m^{-2} ; Figure 123). Fish density in saltmarsh was highest in the spring 2020 ($2.99 + 0.98$ ind. m^{-2}) and summer 2021 ($4.65 + 2.00$ ind. m^{-2}) surveys; however, densities were statistically similar among seasons and between years in this habitat (Figure 123). Although density within each habitat varied as a function of season and year, mean fish density in seagrass compared to saltmarsh was higher during every season in both 2020 and 2021.

Season was identified as a significant factor in the three-way density model for invertebrates at sites with paired habitats (Table 26). The overall density was higher in seagrass (Mean + SE: $76.0 + 8.74$ ind. m^{-2}) relative to saltmarsh ($63.6 + 8.27$ ind. m^{-2}), and density varied as a function of season (Figure 124). The habitat x season interaction was significant, indicating

that habitat-specific trends in density were not consistent over the various seasons. In 2020, the mean density was highest in the seagrass during the summer, followed by the fall, winter, then spring (Figure 124). However, for the salt marsh habitat invertebrate density was nearly equal during the spring and summer, decreasing in the fall and winter. Interestingly, in 2021 those trends changed and the peak density for invertebrates found in seagrass habitat was highest in the fall, followed by winter, summer, then spring. The salt marsh also had a change in peak mean density, with summer and winter, and then spring and fall densities almost equal to each other.

Table 25. Results of three-way ANOVAs, comparing the density, taxonomic richness (TF), and family level Shannon diversity (H') of post settlement fishes collected from paired sites containing seagrass and saltmarsh habitats during four seasonal collections in Matagorda Bay in 2020 and 2021. Resulting degrees of freedom (df), F, and p-values for each comparison are given, significant p-values shown in bold and indicated with an asterisk

MODEL	COMPARISON	DF	F VALUE	P VALUE
DENSITY	Year	1	9.48	0.002*
	Season	3	0.56	0.644
	Habitat Type	1	30.01	<0.001*
	Year x Season	3	5.95	0.001*
	Year x Habitat type	1	2.07	0.152
	Season x Habitat Type	3	4.33	0.006*
	Year x Season x Habitat Type	3	1.07	0.362
RICHNESS	Year	1	0.00	0.988
	Season	3	3.44	0.018*
	Habitat Type	1	53.55	<0.001*
	Year x Season	3	6.78	<0.001*
	Year x Habitat type	1	3.75	0.054
	Season x Habitat Type	3	1.39	0.248
	Year x Season x Habitat Type	3	1.71	0.165
DIVERSITY	Year	1	9.76	0.002*
	Season	3	6.55	<0.001*
	Habitat Type	1	13.08	<0.001*
	Year x Season	3	0.97	0.410
	Year x Habitat type	1	0.45	0.505
	Season x Habitat Type	3	1.57	0.198
	Year x Season x Habitat Type	3	3.22	0.024*

Table 26: Results of three-way ANOVAs, comparing the density, taxonomic richness (TF), and Shannon diversity (H') of invertebrates collected from paired sites containing seagrass and saltmarsh habitats during four seasonal collections in Matagorda Bay in 2020 and 2021. Resulting degrees of freedom (df), F, and p-values for each comparison are given, significant p-values shown in bold and indicated with an asterisk.

MODEL	COMPARISON	DF	F VALUE	P VALUE
DENSITY	Year	1	0.182	0.670
	Season	3	5.61	0.001*
	Habitat Type	1	1.50	0.222
	Year x Season	3	1.79	0.151
	Year x Habitat Type	1	0.81	0.371
	Season x Habitat Type	3	3.64	0.014*
	Year x Season x Habitat Type	3	1.10	0.350
RICHNESS	Year	1	64.37	<0.001*
	Season	3	9.07	<0.001*
	Habitat Type	1	31.19	<0.001*
	Year x Season	3	3.66	0.013*
	Year x Habitat Type	1	3.95	0.048*
	Season x Habitat Type	3	1.47	0.225
	Year x Season x Habitat Type	3	1.01	0.390
DIVERSITY	Year	1	19.44	<0.001*
	Season	3	4.12	0.008
	Habitat Type	1	30.44	<0.001*
	Year x Season	3	0.66	0.580
	Year x Habitat Type	1	0.03	0.866
	Season x Habitat Type	3	12.31	<0.001*
	Year x Season x Habitat Type	3	1.15	0.331

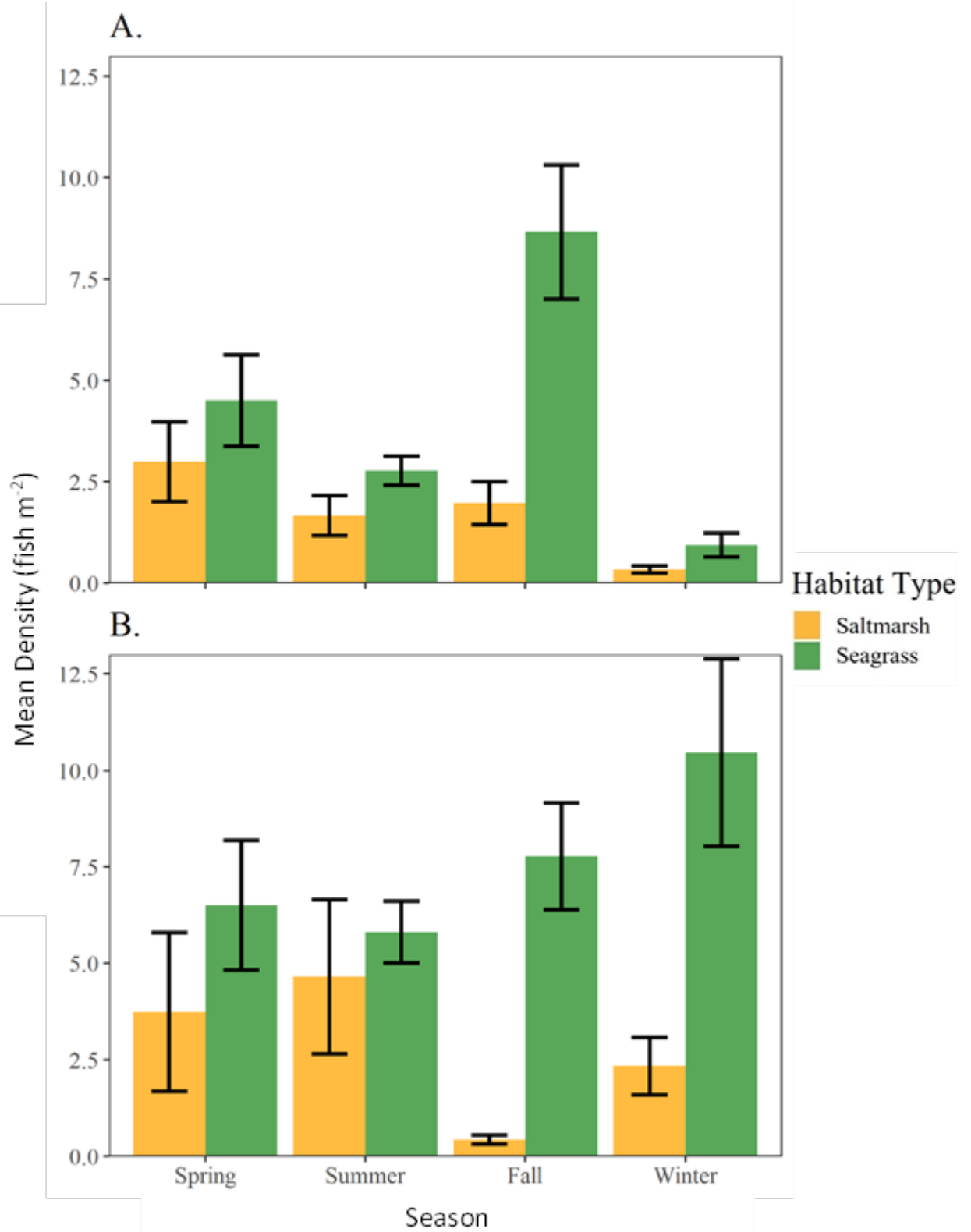


Figure 123. Mean density (fish m⁻²) of post-settlement fishes collected from paired sites containing seagrass (green) and saltmarsh (yellow) habitats during quarterly sampling of Matagorda Bay in 2020 (A) and 2021 (B). Error bars represent ± 1 standard error.

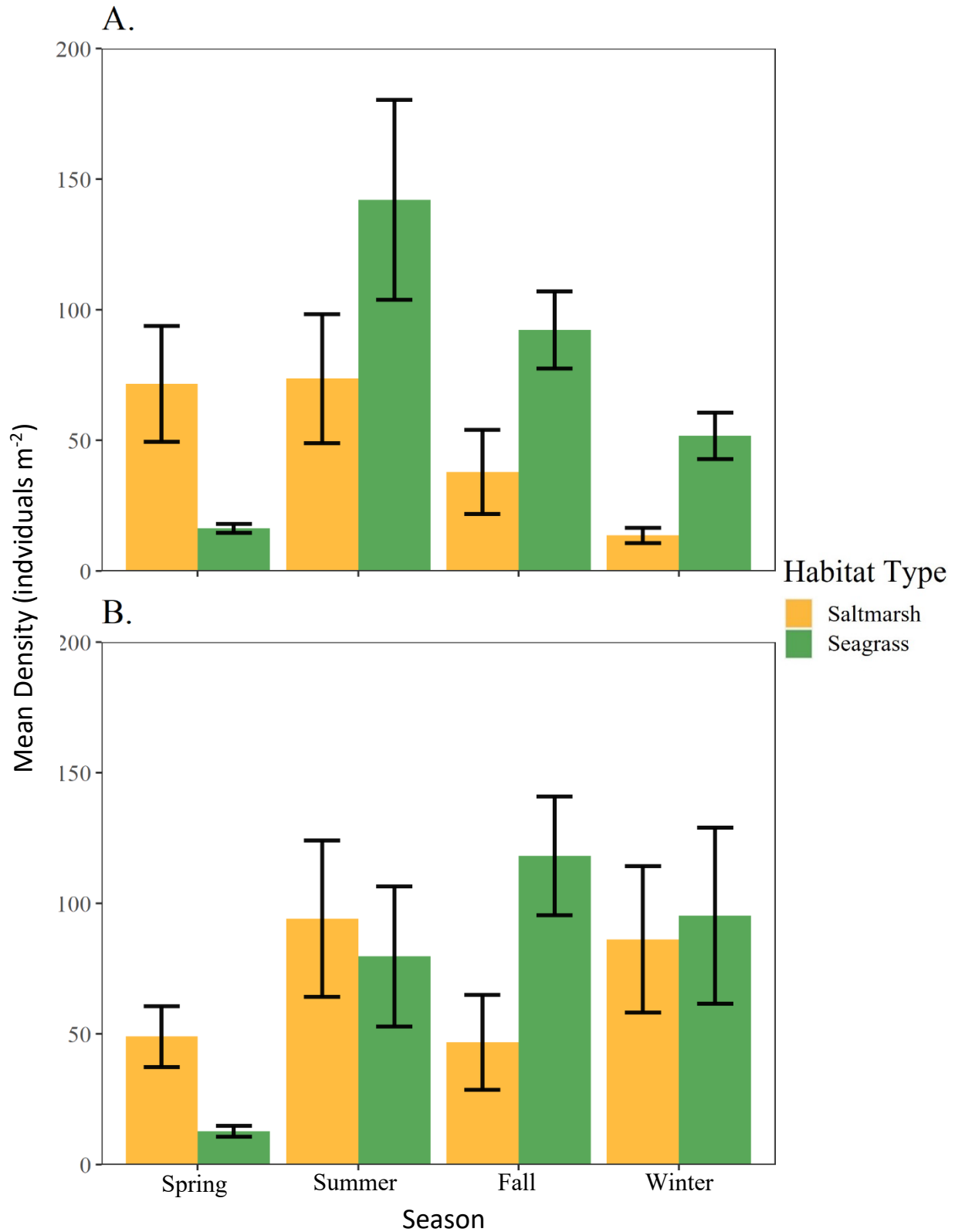


Figure 124: Mean density (individuals m⁻²) of invertebrates collected from paired sites containing seagrass (green) and saltmarsh (yellow) habitats during quarterly sampling of Matagorda Bay in 2020 (A) and 2021 (B). Error bars represent ± 1 standard error.

Taxonomic Richness (T_F)

Taxonomic richness at the family level (T_F) of post-settlement fishes was influenced by the main effects month and habitat type (Table 25). Taxonomic richness at paired sites was higher in seagrass (3.76 ± 0.12) than saltmarsh (2.49 ± 0.14) and highest in summer surveys in both years (Figure 125). A significant season by year interaction was observed indicating that seasonal trends in T_F were not consistent among years. Seasonal variation in T_F was observed in seagrass and mean values generally peaked in the summer in both 2020 (4.33 ± 0.23) and 2021 (4.33 ± 0.43). Taxonomic richness in seagrass for the spring (3.13 ± 0.29) and winter (2.47 ± 0.26) surveys was significantly lower than the summer and fall (4.13 ± 0.22) surveys in 2020 (Tukey's HSD, $p < 0.01$) but statistically similar between all seasons in 2021 (Figure 125). In contrast, T_F in saltmarsh was not significantly different between season or years (Tukey's HSD $p > 0.05$).

For invertebrates, T_F was influenced by all of the variables tested (year, season, habitat type; Table 26). Taxonomic richness at paired sites was higher in seagrass (4.22 ± 0.115) than saltmarsh (3.39 ± 0.114 ; Figure 126). Significant season by year and year by habitat type interactions were observed indicating that yearly trends in T_F were not consistent among season or habitat type. Seasonal variation in T_F was similar for the summer, fall, and winter, but significantly different in the spring for both habitat types in 2020. In contrast, for 2021 there was no significant seasonal difference in the seagrass beds, however the salt marsh summer months had the lowest T_F as compared to the fall and winter months.

Shannon Diversity (H')

Shannon diversity (H') at the family level of post-settlement fishes was influenced by all three main effects (Table 25). In paired sites across both years, H' was higher in seagrass (0.773 ± 0.030) than saltmarsh (0.588 ± 0.044) (Figure 127). A significant year x season x habitat interaction was observed and indicates that habitat specific difference in diversity were not the same between seasons or years. Shannon diversity in seagrass in 2020 was significantly higher in the summer (1.080 ± 0.054) relative to both fall (0.657 ± 0.053) and winter (0.744 ± 0.099) surveys (Tukey's HSD, $p \leq 0.05$). In 2021, H' in seagrass peaked in the spring (0.912 ± 0.053) and was significantly higher in the spring and summer (0.806 ± 0.099) surveys than fall survey (0.469 ± 0.068) (Tukey's HSD, $p < 0.01$ and $p < 0.05$). For saltmarsh, H' was statistically similar among the four seasons in 2020 (range: 0.437 – 0.844; Tukey's HSD, $p > 0.05$) and 2021 (range: 0.387 – 0.678; Tukey's HSD, $p > 0.05$).

For invertebrates, H' was influenced by all of the variables tested (Table 26). Similarly to post-settlement fishes, H' at paired sites was higher in seagrass (0.709 ± 0.0256) than saltmarsh (0.464 ± 0.0428) and significantly higher in the spring and summer than the fall and winter (Figure 128). Shannon diversity in the fall and winter months is similar between habitats, with the exception of the winter where the saltmarsh has higher H' than the seagrass.

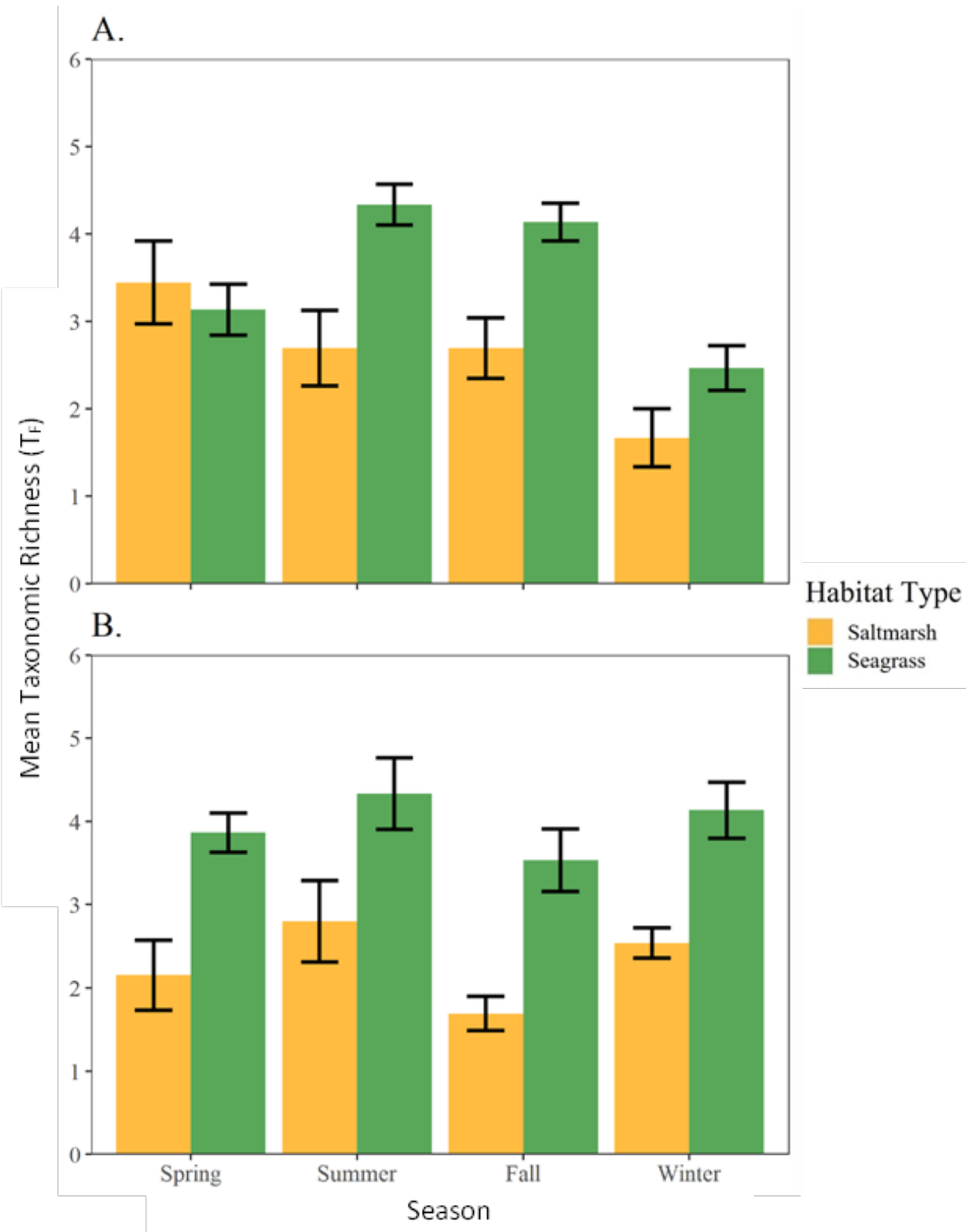


Figure 125. Mean taxonomic richness (T_F) at family level for post-settlement fishes collected from paired sites containing seagrass (green) and saltmarsh (yellow) habitats during quarterly sampling of Matagorda Bay in 2020 (A) and 2021 (B). Error bars represent ± 1 standard error.

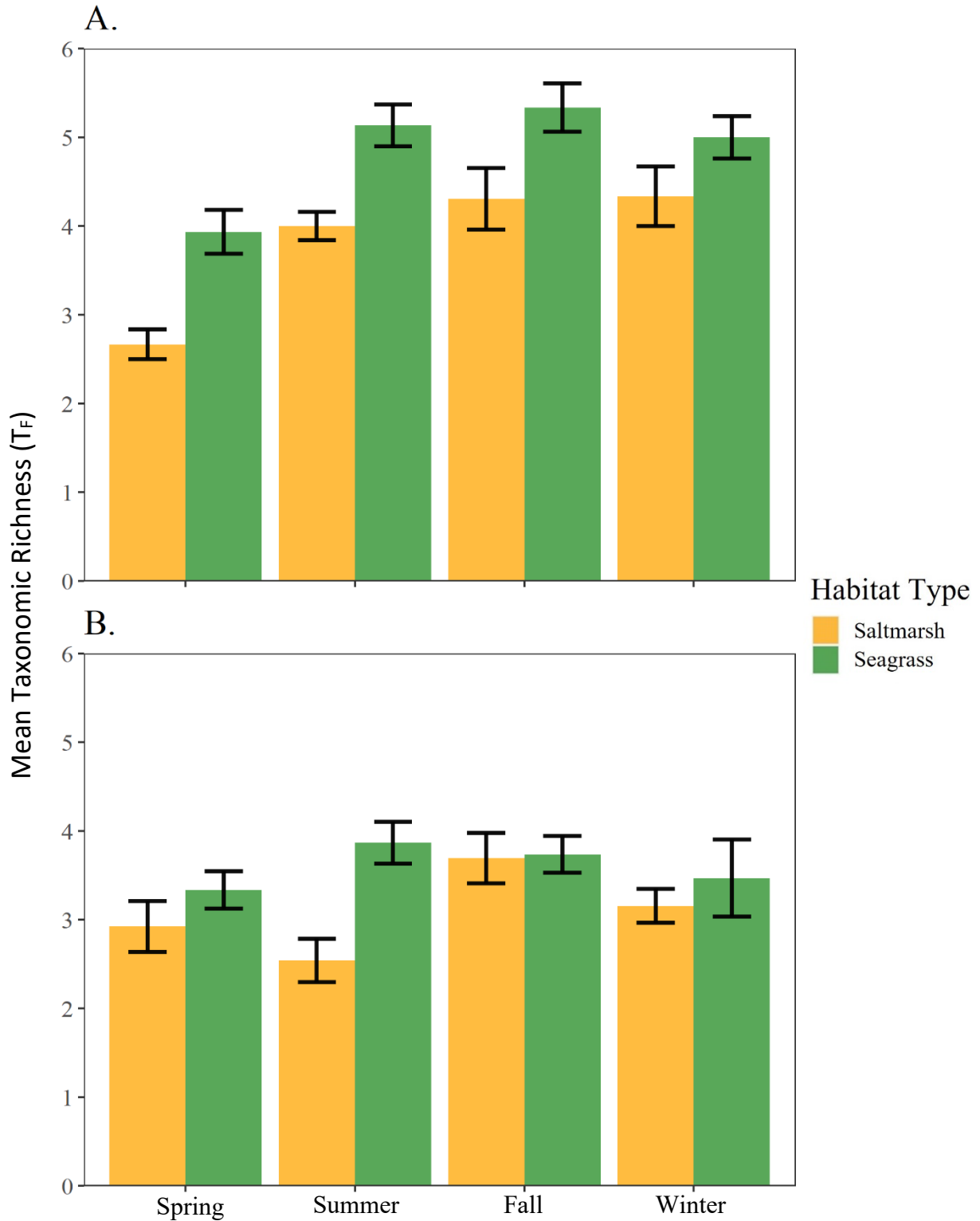


Figure 126. Mean taxonomic richness (T_F) at family level for invertebrates collected from paired sites containing seagrass (green) and saltmarsh (yellow) habitats during quarterly sampling of Matagorda Bay in 2020 (A) and 2021 (B). Error bars represent ± 1 standard error.

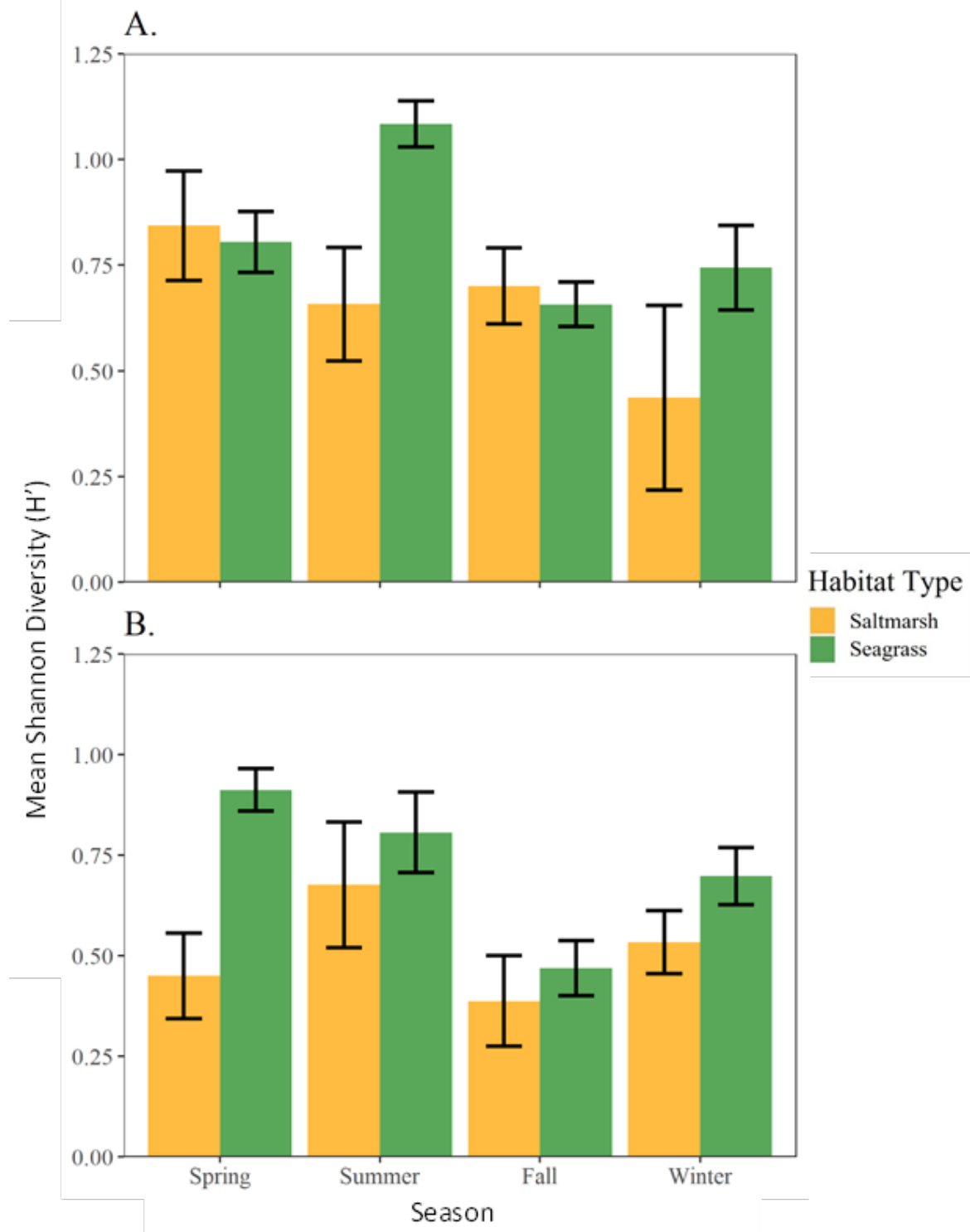


Figure 127. Mean Shannon diversity (H') at family level for post-settlement fishes collected from paired sites containing seagrass (green) and saltmarsh (yellow) habitats during quarterly sampling of Matagorda Bay in 2020 (A) and 2021 (B). Error bars represent ± 1 standard error.

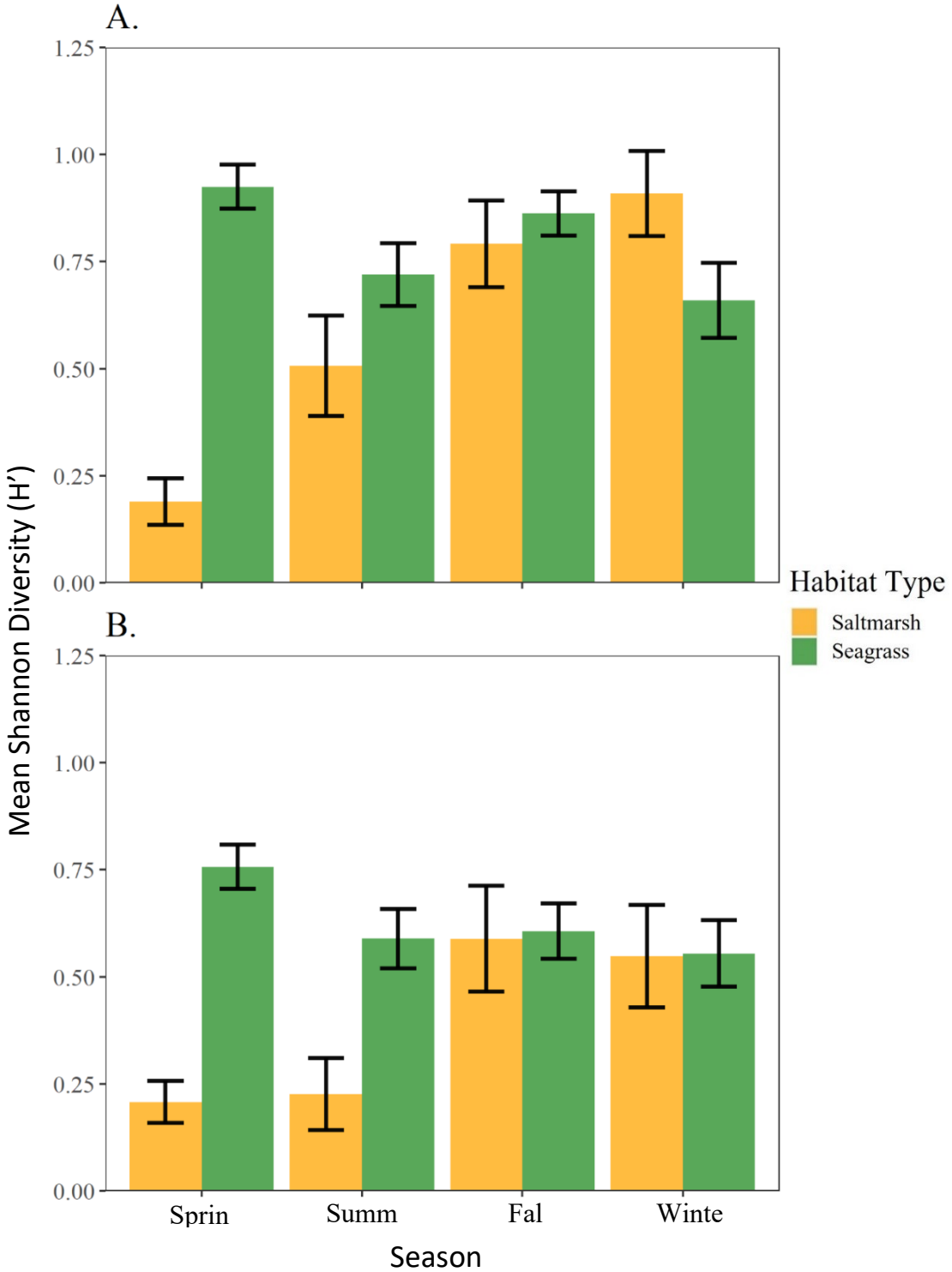


Figure 128. Mean Shannon diversity (H') at family level for invertebrates collected from paired sites containing seagrass (green) and saltmarsh (yellow) habitats during quarterly sampling of Matagorda Bay in 2020 (A) and 2021 (B). Error bars represent ± 1 standard error.

Community Structure

A significant habitat x season interaction was detected for the community structure of post-settlement fishes in Matagorda Bay (PERMANOVA, $R^2 = 0.04$, $p < 0.001$). In response, the community structure between habitat types was compared within each season separately. In spring, the community structure of post-settlement fishes varied significantly between seagrass and saltmarsh habitat (PERMANOVA, $R^2 = 0.055$, $p_{adj} < 0.01$). This difference was driven primarily by five families: Sparidae (28.0%), Gobiidae (20.7%), Sciaenidae (12.9%), Paralichthyidae (sand flounders) (5.5%), and Fundulidae (3.1%), which combined accounted for 70.2% of the dissimilarity in community structure between the two habitats. Sparids, gobiids, sciaenids, and paralichthyids were all more abundant in seagrass, while fundulids were more abundant in saltmarsh (Figure 129).

In the summer, community structure differed significantly between seagrass and saltmarsh habitat (PERMANOVA, $R^2 = 0.10$, $p_{adj} < 0.01$). Habitat-specific variation was driven primarily by families Gobiidae (26.9%), Sparidae (16.4%), Cyprinodontidae (10.5%), Fundulidae (9.9%), and Gerreidae (6.8%), which combined accounted for 70.5% of the dissimilarity in community structure between the two habitats. Gobiids, sparids, cyprinodontids and gerreids were more abundant in seagrass (Figure 129). Gobiids and sparids were again the most abundant taxa, but unlike in spring, gobiids contributed more to the differences in community structure than sparids. Cyprinodontids contributed the third most to differences in community structure and along with gerreids, and this family replaced sciaenids and paralichthyids as the top-five most abundant taxa. Fundulids were again more abundant in saltmarsh and contributed slightly more to the differences in community structure (4.2% increase) than in spring.

In the fall, community structure differed significantly between seagrass and saltmarsh habitat (PERMANOVA, $R^2 = 0.198$, $p_{adj} < 0.01$). Habitat-specific variation was driven primarily by families Gobiidae (61.6%), Gerreidae (10.3%), Sciaenidae (5.0%), Sparidae (1.8%), and Fundulidae (0.9%), which accounted for 79.6% of the dissimilarity in community structure between the two habitats. Gobiids, gerreids, sciaenids, and fundulids were more abundant in seagrass while sparids were more abundant in saltmarsh (Figure 129). This is a shift from spring and summer, when sparids were more abundant in seagrass and fundulids were more abundant in saltmarsh.

Similar to the three other seasons, a significant difference in community structure between seagrass and saltmarsh was also detected for the winter survey (PERMANOVA, $R^2 = 0.103$, $F = 6.761$, $p_{adj} < 0.01$). Habitat-specific variation was driven primarily by families Gobiidae (35.7%), Sparidae (22.3%), Sciaenidae (14.8%), Syngnathidae (pipefishes and seahorses) (3.7%), and Paralichthyidae (2.8%), which combined accounted for 79.3% of dissimilarity in community structure between the two habitats. Gobiids, sparids, syngnathids, and paralichthyids were more abundant in seagrass than in saltmarsh, while sciaenids were more abundant in saltmarsh (Figure 129).

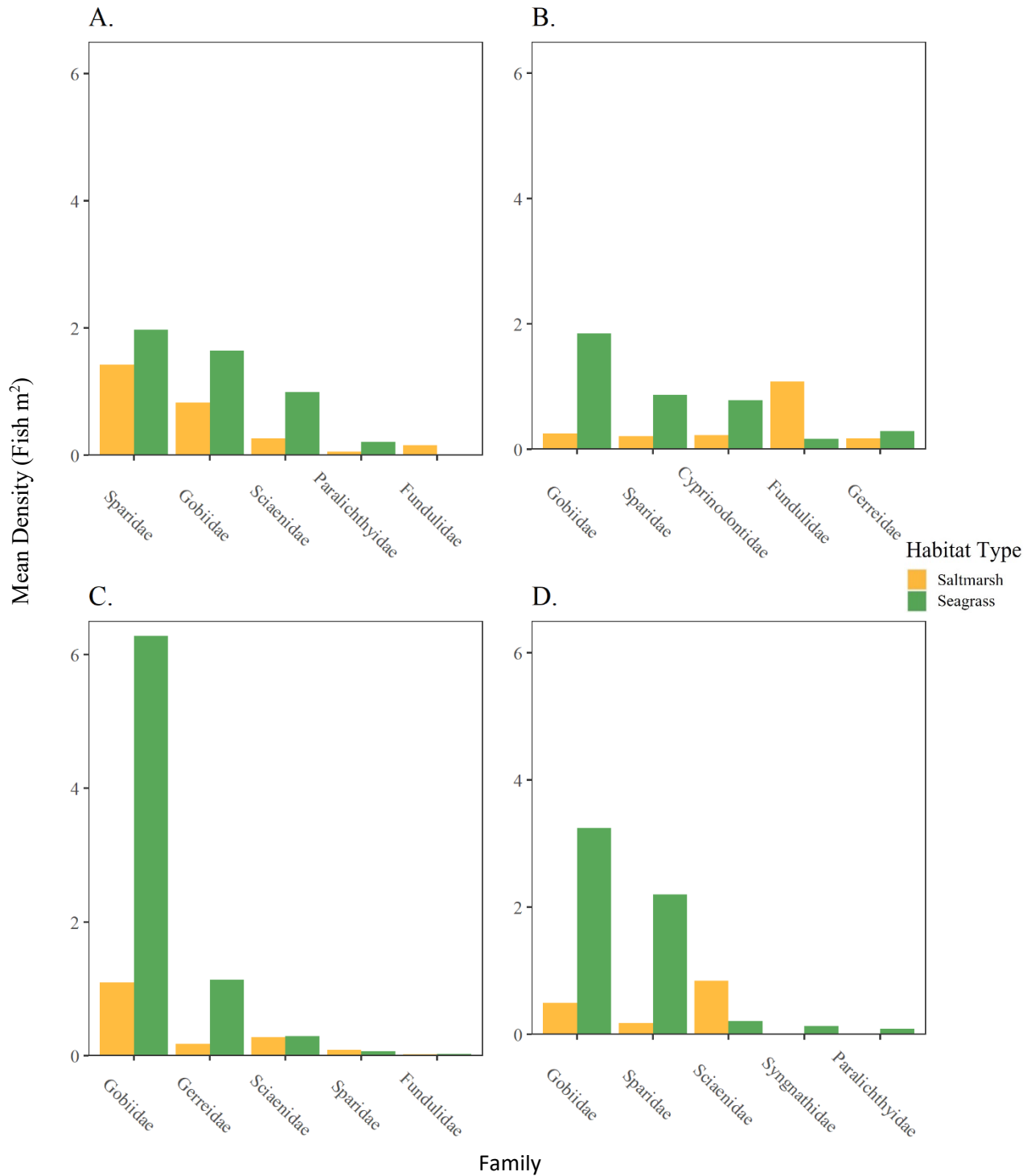


Figure 129: Density of top five families of post- settlement fishes (left to right in rank order) that drive community structure differences between seagrass (green) and saltmarsh (yellow) habitats in Matagorda Bay shown for four seasons sampled: A) spring (March), B) summer (June), C) fall (September), and D) winter (December).

Environmental Modelling

A generalized additive model (GAM) based on collections from all sites (1-9) in Matagorda Bay indicated that the density of post-settlement fishes was influenced by several environmental factors. Fish density was influenced by habitat type ($\Delta DE = 9.6\%$), minutes after sunrise (6.8%), water temperature (3.1%), dissolved oxygen (2.4%), salinity (2.3%), distance to tidal pass (2.3%), year (1.2%), and turbidity (0.9%) (Table 27). All variables retained in the final model (AICc 1718.2; DE 30.2%) were significant ($p \leq 0.05$) (Table 27). The model showed that fish density was higher in seagrass than saltmarsh and higher in 2021 relative to 2020. Response curves showed that fish density was higher at sunrise and sunset, and lower between 300 and 400 minutes after sunrise (Figure 130). Fish density increased with increasing dissolved oxygen and generally increased with water temperature until around 23°C before decreasing at higher temperatures. Salinity also showed a positive relationship with fish density for most of the observed range. Both distance to tidal pass and turbidity displayed positive relationships with fish density (Figure 130).

The GAM evaluating family level taxonomic richness (T_F) of post-settlement fishes indicated this diversity measure was influenced by habitat type ($\Delta DE = 12.2\%$), distance to tidal pass (6.3%), water temperature (3.7%), turbidity (1.7%), tide height (1.5%), and dissolved oxygen (1.2%). All variables retained in the final model (AICc 969.4; DE 37.9%) were significant ($p < 0.05$) (Table 27). Habitat type significantly affected T_F and was higher in seagrass than in saltmarsh (Figure 131). Taxonomic richness generally decreased with increasing distance from tidal pass up to approximately 30 km and then increased at the farthest location from the pass. The response curve for water temperature showed a positive relationship with T_F throughout most of the observed range, particularly at lower (12-18°C) and higher (28-36°C) water temperatures. A positive relationship was present for turbidity and T_F , while reductions in both tide height and dissolved oxygen negatively affected T_F (Figure 131).

The GAM evaluating family level Shannon diversity (H') of post-settlement fishes indicated this diversity measure was influenced by distance to tidal pass ($\Delta DE = 9.2\%$), salinity (7.1%), minutes after sunrise (3.6%), dissolved oxygen (2.9%), tide height (2.8%), habitat type (2.3%), and year (2.3%). All variables in the final model (AICc 200.2; DE 33.4%) were significant ($p \leq 0.05$) (Table 27). The response curve displaying the relationship between H' and distance to tidal pass was similar to T_F with the highest values observed at both closest (< 10 km) and farthest (> 30 km) sites from the tidal pass (Figure 132). Salinity and H' were inversely related with peak values observed in mixing zones with lower salinity (~5-15 ppt). Time of day also influenced H' and this diversity measure increased throughout the day. Increases in dissolved oxygen and tide height were associated with lower H' values. Similar to T_F , habitat type influenced H' and this diversity measure was higher in seagrass than in saltmarsh (Figure 132). The effect of year on H' was higher in 2020 than in 2021.

Table 27: Environmental variables retained in final generalized additive models (in order of ΔDE) for density, taxonomic richness (T_F) at the family level, and Shannon diversity (H') at the family level of post-settlement fishes in Matagorda Bay including estimated degrees of freedom (edf), p-value, change in deviance explained (ΔDE), and change in AICc ($\Delta AICc$) for each variable.

MODEL	VARIABLE	EDF	P	ΔDE	$\Delta AICc$
DENSITY FINAL AIC _c : 1718.24 FINAL DE: 30.2%	Habitat Type	n/a	0.011	9.6%	35.04
	Minutes After Sunrise	2.77	<0.001	6.8%	25.57
	Water Temperature (°C)	2.42	0.015	3.1%	7.24
	Dissolved Oxygen (mg/L)	1.0	0.001	2.4%	8.67
	Salinity (ppt)	1.94	0.015	2.3%	6.73
	Distance to Tidal Pass (m)	1.0	0.007	2.3%	4.71
	Year	n/a	0.035	1.2%	1.38
	Turbidity (NTU)	1.0	0.021	0.9%	3.62
RICHNESS (T_F) FINAL AIC _c : 969.42 FINAL DE: 37.9%	Habitat Type	n/a	<0.001	12.2%	53.39
	Distance to Tidal Pass (m)	2.77	<0.001	6.3%	21.84
	Water Temperature (°C)	2.70	0.002	3.7%	10.73
	Turbidity (NTU)	1.0	0.004	1.7%	7.28
	Tide Height (m)	1.0	0.009	1.5%	4.77
	Dissolved Oxygen (mg/L)	1.0	0.040	1.2%	3.17
DIVERSITY (H') FINAL AIC _c : 200.24 FINAL DE: 33.4%	Distance to Tidal Pass (m)	2.97	<0.001	9.2%	33.47
	Salinity (ppt)	2.84	<0.001	7.1%	26.87
	Minutes After Sunrise	1.95	<0.001	3.6%	12.58
	DO	1.0	<0.001	2.9%	10.88
	Tide Height (m)	1.0	<0.001	2.8%	9.12
	Habitat Type	n/a	0.002	2.3%	7.57
	Year	n/a	0.005	2.3%	6.22

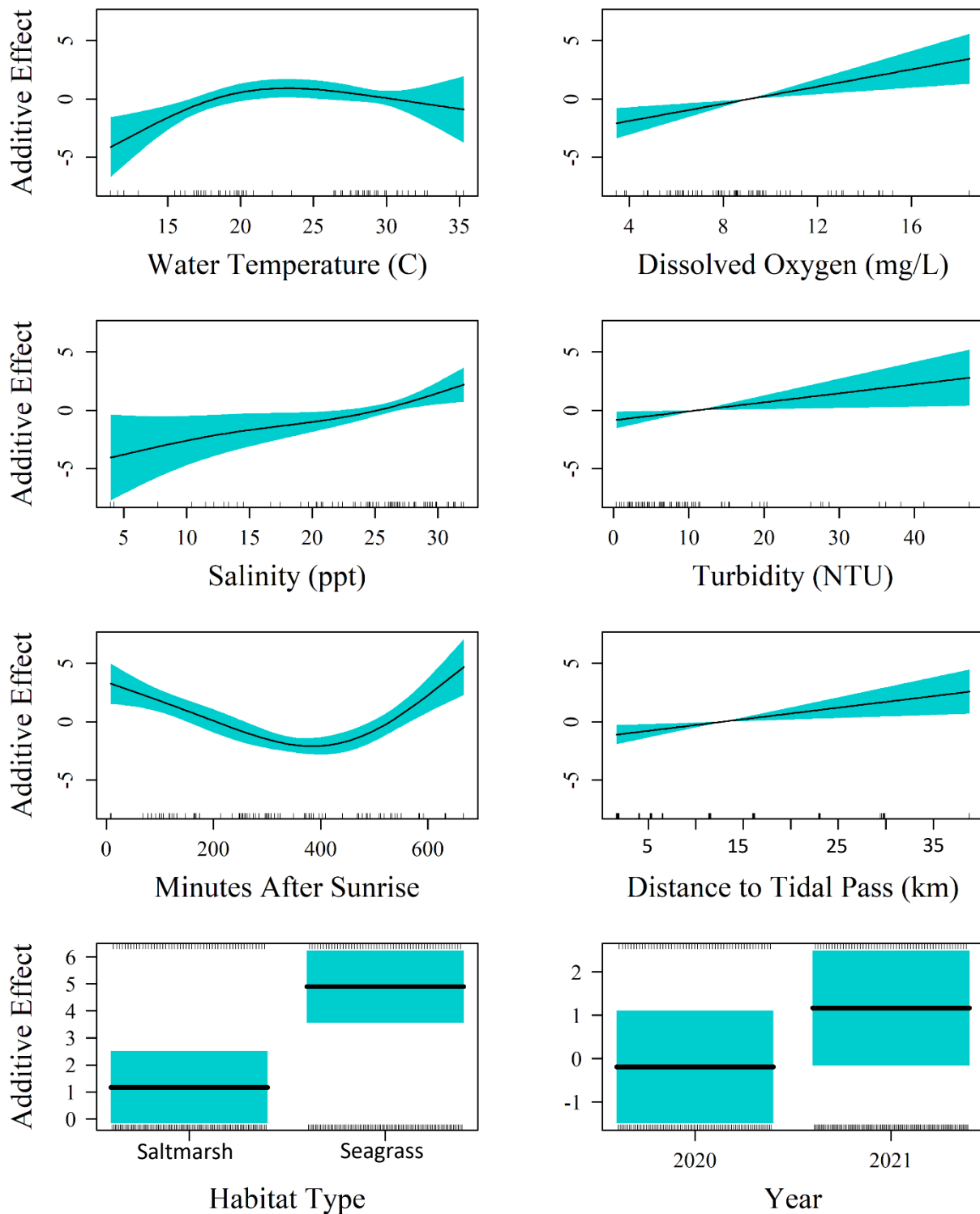


Figure 130: Response plots of environmental variables with significant influence on the density of post-settlement fishes in Matagorda Bay in 2020 and 2021 based on the generalized additive model (GAM). Black lines represent model estimate, surrounding shading represents 95% C.I.

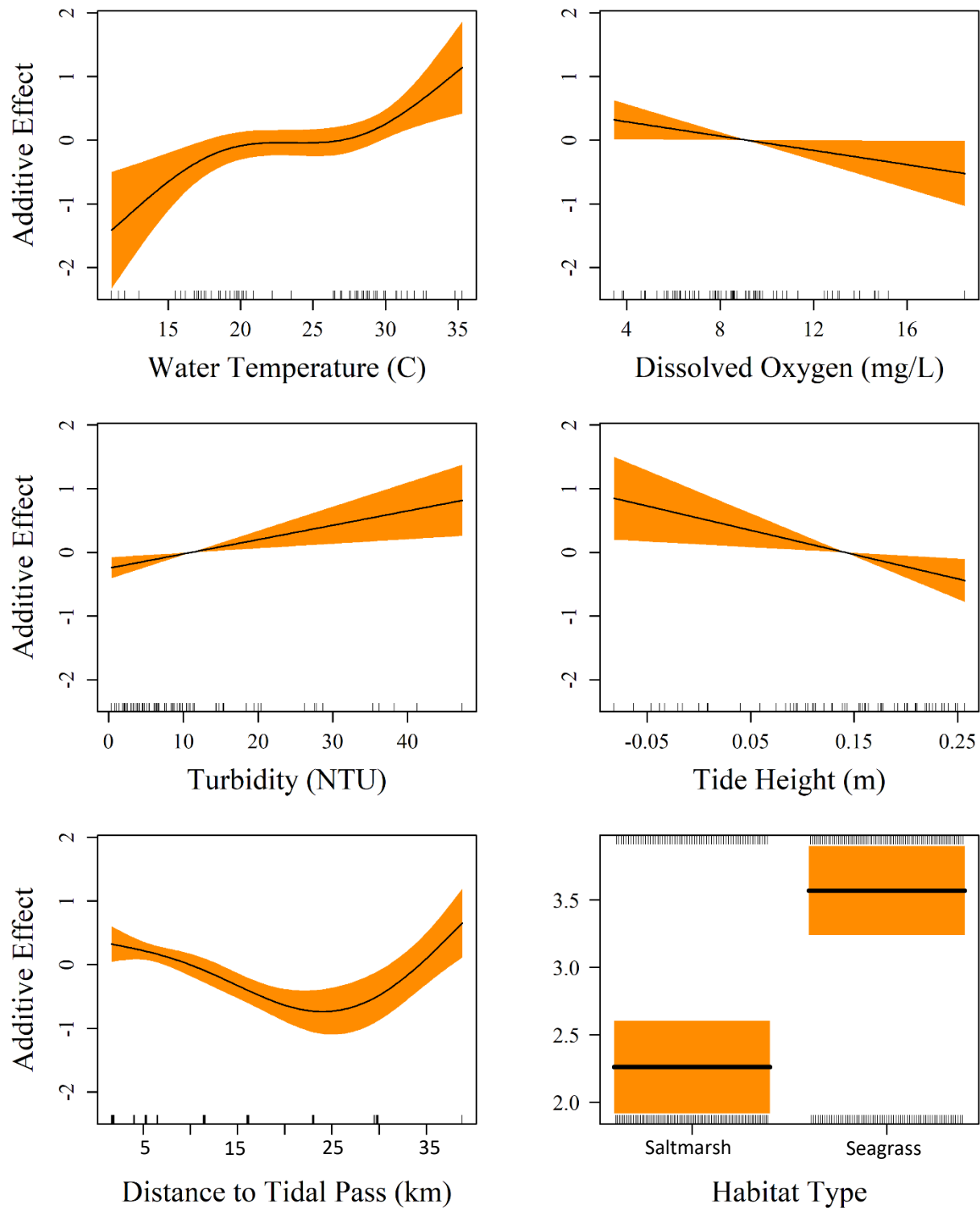


Figure 131: Response plots of environmental variables with significant influence on the taxonomic richness (T_F) of post-settlement fishes in Matagorda Bay in 2020 and 2021 based on the generalized additive model (GAM). Black lines represent model estimate, surrounding shading represents 95% C.I.

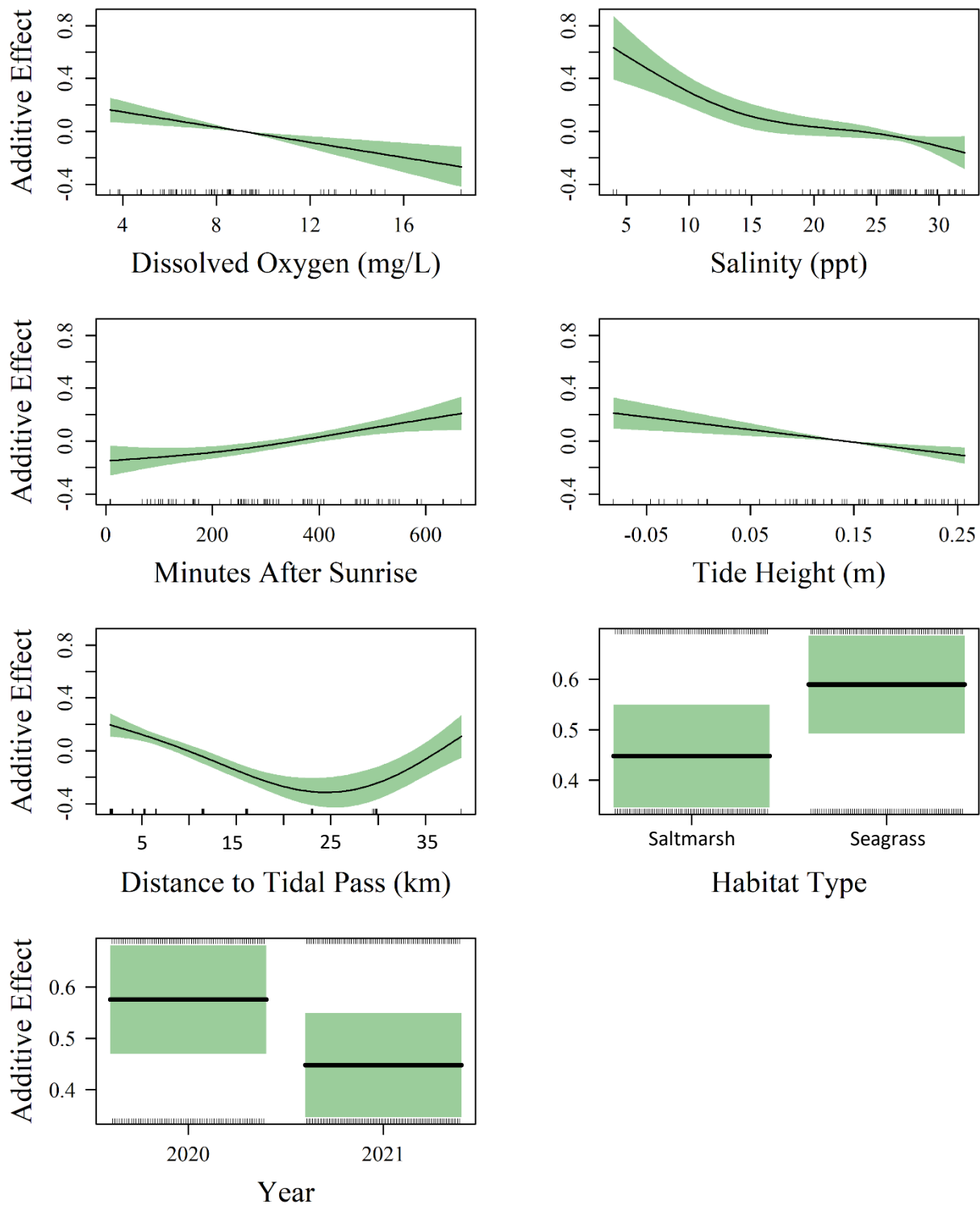


Figure 132: Response plots of environmental variables with significant influence on the Shannon diversity (H') of post-settlement fishes in Matagorda Bay in 2020 and 2021 based on the generalized additive model (GAM). Black lines represent model estimate, surrounding shading represents 95% C.I.

Species-Specific Patterns: Family Sciaenidae (drums and croakers)

A total of 1,490 post-settlement (SL < 40 mm) sciaenids from six species were collected during quarterly surveys (March, June, September, and December) and supplemental monthly surveys (May, July, August, and October) in both years. The sciaenid assemblage was comprised almost entirely (99.7%) of five species: spot *Leiostomus xanthurus*, silver perch *Bairdiella chrysoura*, spotted seatrout *Cynoscion nebulosus*, red drum *Sciaenops ocellatus*, and Atlantic croaker *Micropogonias undulatus* (Table 28). Five southern kingfish *Menticirrhus americanus* were collected from a single saltmarsh site in September but not included in the analysis because of the small sample size. Although size distributions varied among the five primary species (Tukey's HSD, $p \leq 0.05$), the majority of sciaenids collected were between 4-20 mm SL. Despite modest overlap in occurrence, peak density of each species (pooled between both habitats) occurred during a different month of the year, and the primary settlement period with the highest observed density was consistent among the five species in both 2020 and 2021: spot (March), silver perch (June), spotted seatrout (September), red drum (October), and Atlantic croaker (December) (Figure 133).

Density data used to assess habitat specific and interannual differences in post-settlement abundances for each species were limited to months when individuals were present. Spot was the most numerically abundant sciaenid and accounted for 30.9% of the total catch (Table 28). A significant year x habitat interaction was observed for spot density (ANOVA, $p \leq 0.05$). Density of spot in seagrass (0.24 ± 0.11 ind. m^{-2}) and in saltmarsh (0.16 ± 0.10 ind. m^{-2}) was statistically similar during the observed settlement period (March-May) in 2020 (ANOVA, $p \geq 0.05$), but significantly higher in seagrass (1.10 ± 0.39 ind. m^{-2}) than in saltmarsh (0.18 ± 0.08 ind. m^{-2}) in 2021 (ANOVA, $p \leq 0.05$) (Table 29). Red drum density was also significantly higher in seagrass (0.34 ± 0.09 ind. m^{-2}) than in saltmarsh (0.06 ± 0.01 ind. m^{-2}) during the observed settlement period (September-December) (ANOVA, $p \leq 0.01$) and did not differ significantly between years. Silver perch and spotted seatrout were observed from May to July and June to October, respectively. Density for both species was similar statistically between the two habitats; however, a year effect was observed with density significantly higher in 2020 compared to 2021 for silver perch (0.29 ± 0.12 ind. m^{-2} and 0.02 ± 0.01 ind. m^{-2}) and spotted seatrout (0.102 ± 0.03 ind. m^{-2} and 0.02 ± 0.01 ind. m^{-2}) (ANOVA, $p < 0.05$). Atlantic croaker was observed from October to December, and the highest density was present in collections from saltmarsh in 2021 (0.39 ± 0.19 ind. m^{-2}); however, density was not significantly different between habitats or years (ANOVA, $p \geq 0.05$).

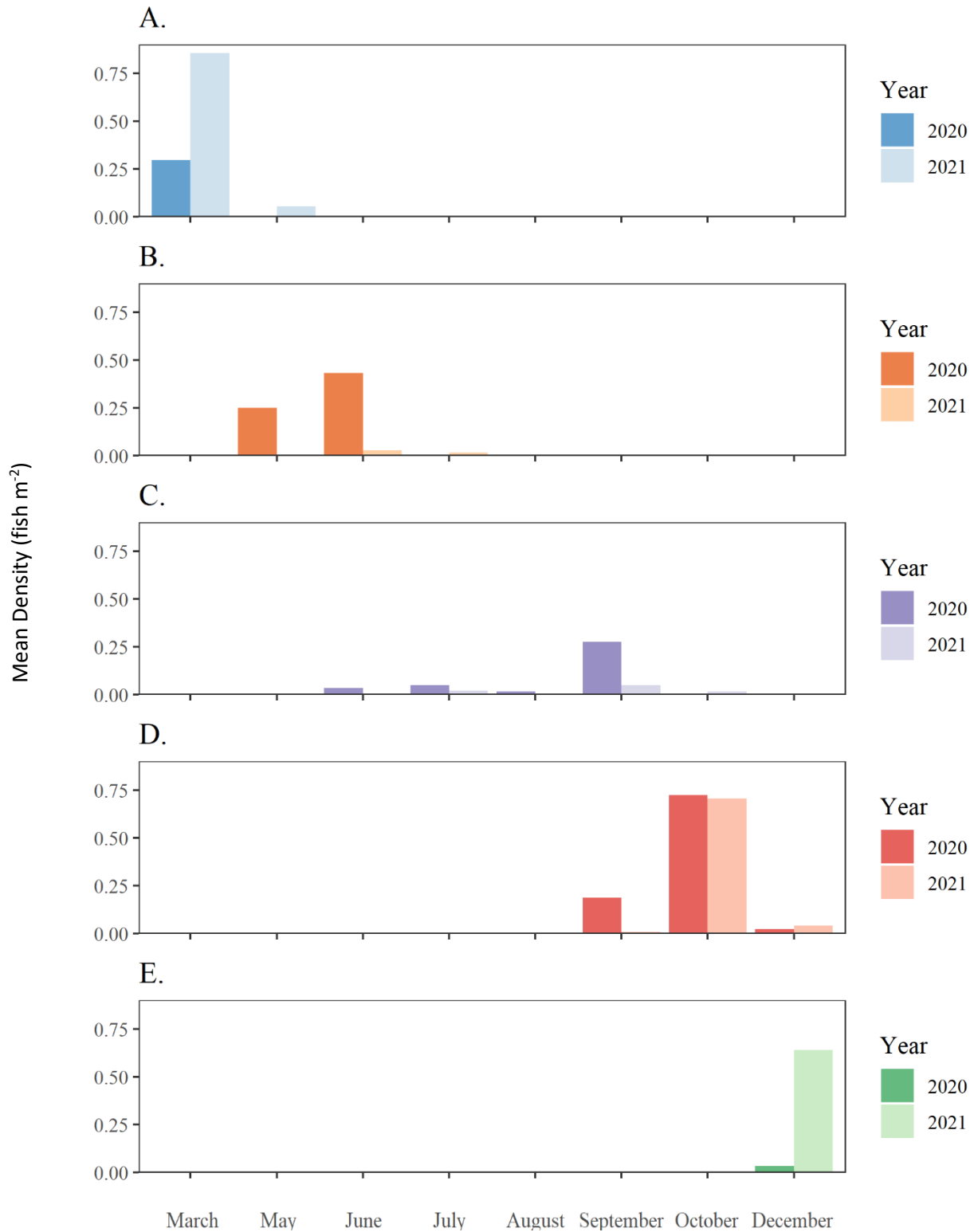


Figure 133: Density of post-settlement (< 40mm SL) spot (A), silver perch (B), spotted seatrout (C), red drum (D), and Atlantic croaker (E) collected monthly in seagrass and saltmarsh habitats of Matagorda Bay in 2020 and 2021.

Table 28: Count and percent composition of post-settlement (<40mm) sciaenids collected during monthly sampling in seagrass and saltmarsh habitats of Matagorda Bay in order of occurrence.

Species	Common Name	Count 2020	Count 2021	Total	Percent
<i>Leiostomus xanthurus</i>	spot	107	353	460	30.87
<i>Bairdiella chrysoura</i>	silver perch	220	16	236	15.84
<i>Cynoscion nebulosus</i>	spotted seatrout	137	28	165	11.07
<i>Sciaenops ocellatus</i>	red drum	210	147	357	23.96
<i>Micropogonias undulatus</i>	Atlantic croaker	7	260	267	17.92
<i>Menticirrhus americanus</i>	southern kingfish	0	5	5	0.34
Total		681	809	1490	100.00

Table 29: Count, mean density, standard error, and max density of post settlement sciaenids collected in seagrass and saltmarsh habitats of Matagorda Bay monthly in 2020 and 2021. Resulting p-values given for each comparison from two-way ANOVA comparing density by habitat type and year. Significant results shown in bold and indicated with asterisk.

Species	Year	Habitat Type	Count	Mean Density	Standard Error	Max	Habitat P	Year P	Interaction P
<i>Leiostomus xanthurus</i> (spot)	2020	Saltmarsh	42	0.156	0.104	2.8	0.017*	0.040*	0.046*
		Seagrass	65	0.241	0.112	2.8			
	2021	Saltmarsh	57	0.181	0.083	2.0			
		Seagrass	296	1.100	0.386	9.0			
<i>Bairdiella chrysoura</i> (silver perch)	2020	Saltmarsh	156	0.390	0.212	5.6	0.369	0.027*	0.317
		Seagrass	64	0.175	0.079	2.8			
	2021	Saltmarsh	4	0.008	0.008	0.3			
		Seagrass	12	0.031	0.009	0.3			
<i>Cynoscion nebulosus</i> (spotted seatrout)	2020	Saltmarsh	74	0.104	0.049	3.3	0.847	0.004*	0.681
		Seagrass	63	0.100	0.018	0.5			
	2021	Saltmarsh	8	0.012	0.005	0.2			
		Seagrass	20	0.030	0.009	0.4			
<i>Sciaenops ocellatus</i> (red drum)	2020	Saltmarsh	37	0.109	0.033	0.7	0.004*	0.390	0.976
		Seagrass	173	0.384	0.123	4.7			
	2021	Saltmarsh	11	0.021	0.007	0.3			
		Seagrass	136	0.302	0.145	6.0			
<i>Micropogonias undulatus</i> (A. croaker)	2020	Saltmarsh	0	0.000	0.000	0	0.140	0.059	0.255
		Seagrass	7	0.016	0.014	0.6			
	2021	Saltmarsh	206	0.387	0.194	7.9			
		Seagrass	54	0.120	0.039	1.5			

Discussion

Density and Diversity of Post-Settlement Fishes

The post-settlement fish assemblage in Matagorda Bay was composed of both resident taxa that spend their entire life cycles in estuaries and estuarine-dependent taxa that may only occupy these systems during early life. On average, the density and diversity of post-settlement fishes in seagrass and saltmarsh was relatively similar to that observed in other studies conducted with comparable gear types in the northern Gulf of Mexico (Hollweg et al. 2020, Minello 1999) and more specifically Texas (Froeschke et al. 2016, Geary et al. 2001, Glass et al. 2009, Rozas and Minello 1998). The taxonomic richness observed in Matagorda Bay (25 families) was higher than that observed in similar estuaries along the Texas coast. For example, Hall et al. (2016) observed 14 families in the Aransas Bay system while Geary et al. (2001) observed 22 families in Christmas Bay (part of the Galveston Bay Complex). However, sampling effort was higher in this study and taxonomic richness is known to increase with increasing sampling effort (Foggo et al. 2003). Dominant families collected were very similar among surveys conducted in Texas estuaries and several families of fishes common in previous studies (e.g., gobiids, sparids, fundulids, syngnathids) were collected during this study. The numerical dominance of gobiids and sparids in seagrass and saltmarsh habitats of Matagorda Bay was not unexpected because a meta-analysis of nekton communities from estuaries along the northern Gulf coast found that across 106 studies, gobies and sparids were among the most numerically abundant taxa (Hollweg et al. 2020). Families of commercial and recreational fishes collected in this study (e.g., Sciaenidae, Carangidae (jacks), Lutjanidae (snappers), and Paralichthyidae) were also similar to those collected in studies conducted in the Aransas Bay, Texas (Froeschke et al. 2016, Hall et al. 2016, Rooker et al. 1998) and Christmas Bay, Texas (Geary et al. 2001).

Pronounced patterns in the density and diversity (T_F , H') of post-settlement fishes were observed between seagrass and saltmarsh habitats in Matagorda Bay, with all three measures higher on average in seagrass. The role of both seagrass and saltmarsh as nursery habitat for fishes has been well documented (e.g., Heck et al. 2003, Minello et al. 2003, Stunz et al. 2002). Both habitat types are structurally complex and potentially benefit juvenile fishes by enhancing foraging success and decreasing predation (Rooker et al. 1998, Stunz et al. 2002). A review by Heck et al. (2003) evaluated the nursery role of seagrass and found enhanced abundance of juvenile fishes in this habitat when compared to bare substrates but did not detect consistent differences between seagrass and other structurally complex submerged habitats. This implies that the presence of complex structure may be more important than the habitat type in determining the abundance and potentially the success (i.e., survival) of juvenile fishes. However, a more recent meta-analysis revealed that seagrass increased the foraging success of juvenile fishes and in so doing, this habitat may increase growth, survival, and recruitment success compared to other habitats including saltmarsh (McDevitt-Irwin et al. 2016). Moreover, this meta-analysis showed that increased growth rate associated with prey availability was more pronounced in subtropical regions relative to temperate and tropical regions. The increased

abundance and diversity of juvenile fishes in seagrass relative to saltmarsh in subtropical waters of Matagorda Bay are in accord with the previously mentioned studies. This suggests that seagrass meadows within this bay system likely enhanced the foraging success and post-settlement survival of fishes, and therefore declines or fragmentation of this foundational habitat that have been reported in other estuaries along the Gulf of Mexico (Hensgen et al. 2014, Ray et al. 2014) may negatively impact the survival and recruitment of several taxa that occupy seagrass during early life.

Lower density and diversity of post-settlement fishes in saltmarsh compared to seagrass does not negate the importance of this presumed nursery habitat in Matagorda Bay. Saltmarsh habitat, particularly the interface or edge that is regularly inundated with water, has been shown to host diverse assemblages of juvenile fishes in estuaries across the globe (Whitfield 2017). Given the large spatial coverage of saltmarsh edge habitat relative to seagrass in Matagorda Bay, this nursery habitat remains critically important and influential in determining recruitment success and year-class strength of many marine fishes. The significance of saltmarsh edge as nursery habitat was highlighted in a meta-analysis conducted by Minello et. al. (2003), which concluded that while this habitat had a lower density of fish than seagrass, the density of fishes along the saltmarsh edge was higher than that found in oyster reef, unvegetated bottom, and the saltmarsh interior. Most of the families captured in the present study were collected in both seagrass and saltmarsh habitats, suggesting that both habitats serve as effective nurseries and that connectivity between these two habitats may be beneficial to the growth and survival of post-settlement fishes in Matagorda Bay.

Density of post-settlement fishes in Matagorda Bay differed seasonally across the two-year survey. Variation in timing of spawning and subsequent settlement or recruitment of juveniles into nursery habitats is common among marine fishes (Edworthy and Strydom 2016, Lowerre-Barbieri et al. 2011, Munsch et al. 2016), and the timing of reproductive events appears largely responsible for observed seasonal variation in both total fish density and assemblage diversity. For example, in 2020 total fish density was significantly greater in fall compared to all other seasons, and this appears due in part to increased spawning activity in the late summer and fall by many of the numerically dominant taxa including sciaenids, gerreids, and especially gobiids (Darcy 1980, Heremma et al. 1985, Rooker et al. 1998). These taxa are common constituents of both seagrass and saltmarsh habitats during the first year of life in the western Gulf (Rooker et al. 1998, Stunz et al. 2002), eastern Gulf (Carassou et al. 2011) and more northern regions along the eastern seaboard (Bailee et al. 2016). Several species within these numerically dominant families are known to spawn during late summer and/or fall such as spotfin mojarra *Eucinostomus argenteus* and darter goby *Ctenogobius boleosoma*. Therefore, the timing of spawning and then entry into nurseries likely played a role in the elevated density of post-settlers observed in the fall (Richards 2005).

Differences in density and diversity between years sampled are due to complex biological (spawning stock biomass, timing of spawning, prey availability for recruits) and physical (hydrography) interactions that influence the transport of eggs/larvae, early life survival,

and ultimately settlement into estuarine nurseries (Brown et al. 2005, Holt et al. 1989, Jenkins et al. 1998). These processes fluctuate widely in time and space, and significant year-to-year variability in the abundance of settlers in estuarine nurseries is common (Able 1999, Bolle et al. 2009, Rooker et al. 1998). Environmental conditions in the estuary including water temperature, turbidity, dissolved oxygen, and salinity vary spatially and temporally as a result of water inflow and normal climatic variation, and corresponding shifts in abundance of nekton have been associated with changing physicochemical conditions in the estuary (Belgrad et al. 2021). Characterizing the relationships between environmental conditions and both density and diversity (T_F , H') of post-settlement fishes allows for a better understanding of environmental drivers of seasonal and annual differences in recruitment.

Environmental Conditions: GAMs

GAMs were used to further evaluate the influence of environmental conditions on the density and diversity (T_F , H') of post-settlement fishes in Matagorda Bay. All of the retained explanatory variables were influential in multiple models (salinity, water temperature, turbidity, minutes after sunrise, year) and several were influential in all three models (dissolved oxygen, distance from tidal pass, habitat type). As expected, habitat type was included in all final models and again shown to be an important determinant of density and diversity for post-settlement fishes in Matagorda Bay. In fact, habitat type was deemed to be the most influential variable explaining fish density and taxonomic richness (T_F) in this system. Several other studies applying multivariate models to assess the importance of environmental conditions on juvenile fish abundance and diversity, particularly for models including similar estuarine habitats, have also reported habitat type to be a significant factor (Froeschke et al. 2016, Schaffler et al. 2013), with elevated density and diversity associated with structured habitats for both estuarine (Adams et al. 2004, Stunz et al. 2002, Ofanidis et al. 2021) and coastal (Dance et al. 2021, Rooker et al. 2004) species.

Final models revealed that distance to tidal pass was a significant predictor of density, T_F , and H' of post-settlement fishes. The general pattern observed for both diversity measures was higher fish diversity near and far from the passes and lower values for collection sites at intermediate distances from the pass. Larval settlement in estuaries is the product of both biological and physical factors, and a variety of potential causes exist for the observed relationship, including hydrodynamic processes that regulate the transport of larvae into nursery areas (Brown et al. 2005, Jenkins et al. 1997). This is especially true for species that spawn proximal to tidal inlets and rely on physical factors (i.e., tidal stream transport) to deliver larvae into estuarine nursery habitats (Norcross and Shaw 1984, Islam et al. 2007, Secor 2015). Brown et al. (2005) demonstrated that proximity of settlement habitat to the tidal pass played an important role in determining the spatial distribution of settlers, with increased particle inputs (virtual larvae) and eventual settlement numbers found closer to the tidal pass. Similarly, other studies in Gulf estuaries have reported that nekton density and diversity are inversely related to distance from the primary tidal pass (Bushon 2006, Reese et al. 2008). Since both the density and diversity of fish larvae are presumed to be highest proximal to the entrance point into the bay, the

isolation-by-distance phenomenon may also explain the decrease in diversity as distance from the tidal pass increases. These observations are in agreement with elevated T_F and H' measures closest to the pass but fail to explain the modest increase in T_F and H' at the farthest sampling site from the tidal pass. Interestingly, the complexity of saltmarsh at the site farthest from the tidal pass in Matagorda Bay is notably increased and contains large, continual patches of *Spartina* with added seascape complexity provided by the presence of tidal creeks. Because both the patch size and complexity of saltmarsh habitat positively correlate with increased abundance and diversity of organisms (Green et al. 2012, Meyer and Posey 2009), the added complexity of the saltmarsh habitat farthest from the pass may explain the increased density and subtle increase in diversity metrics at this site.

Dissolved oxygen (DO) was included in all three final models, and this environmental factor is known to affect the distribution, abundance, and diversity of fishes in estuarine and coastal environments (Brennan et al. 2016, Craig and Crowder 2005, Roman et al. 2019). Hypoxic conditions ($DO < 2\text{mg L}^{-1}$) (Pinckney et al. 2001) have been shown to negatively affect the growth and survivorship of many marine fishes (Breitburg 2002, Miller et al. 2002), and even subtle changes in survival associated with low DO can produce marked declines in recruitment and fish production (Houde 2016). Measured DO in Matagorda Bay was above hypoxic levels during all collections; however, sub-hypoxic effects due to low DO have been reported for several species of fish (Breitburg 2002). Campbell and Rice (2014) documented active avoidance of low DO areas of the Neuse River Estuary in NC, including some of the same species collected in Matagorda Bay (e.g., spot and Atlantic croaker). The ability of these and other taxa to detect and move to areas of more favorable DO levels may explain the positive relationship observed between density and DO in Matagorda Bay. While the aforementioned explanation appears plausible and is well supported by the literature, there was also a decrease in both T_F and H' at the highest DO levels. A possible explanation for this finding is that exposed sites in Matagorda Bay often experience strong wind-induced mixing, which increases DO but also leads to more challenging conditions for juvenile fishes. As a result, some taxa capable of moving away from the area may do so, leading to reductions in T_F and H' without a corresponding decrease in density.

Turbidity was retained in both the density and T_F models and showed a positive relationship with both. Changes in precipitation, surface water mixing, and primary productivity all influence turbidity, and previous studies have linked higher turbidity to increased juvenile fish growth and survival due to both increased prey availability and decreased predation rates by visual predators (Blaber and Blaber 1980, Fisker et al. 2002, Lunt and Smee 2020). While not directly measured, higher turbidity may correspond to periods of higher productivity and therefore better foraging opportunities for post-settlement fishes in nursery habitats. Apart from biological factors linked to foraging and predation, another plausible explanation for the observed relationship is gear avoidance. As turbidity increases, visual detection of the benthic sled likely decreases, potentially leading to higher catch numbers. Williams and Fabrizio (2011) concluded that increased catches of spottail shiner *Notropis hudsonius* (a small fish similar in

size to post-settlement fishes in this study) in turbid waters may be due in part to reduced detectability of net gears. Similarly, elevated turbidity at certain times or in specific areas of Matagorda Bay may have reduced the ability of post-settlers to detect the benthic sled, resulting in higher catches (density) and increased diversity of fishes in these collections.

Minutes after sunrise was retained in the final GAMs for both density and diversity. The relationship between fish abundance and time of day has been well studied, and many juvenile fishes are thought to be most active during times of low light (Carpentierie et al. 2005, Guest et al. 2003, Morrison et al. 2002, Stoner et al. 1991). In Matagorda Bay, density of post-settlers was highest in the early morning (10-100 mins after sunrise), and evening before sunset (600+ mins after sunrise). Similar to density, H' was highest for collections performed late in the day near sunset. While post-settlement fishes are generally more active during times of low light, increased density and H' observed in this study may also be due in part to gear avoidance (i.e., sampling bias) because reduced light has been associated with higher catches of ichthyoplankton and juvenile fishes (Bruno et al. 2008, Carpentieri et al. 2005). Interestingly, Guest et al. (2003) found that higher diversity was observed when seagrass beds were surveyed at night and hypothesized that nighttime collections may be more reflective of actual assemblage composition in this habitat. It stands to reason that some sampling bias may have been introduced by collecting strictly during daylight hours; however, sites were visited at different times of day throughout the study, and thus any bias is likely distributed across sampling sites and habitats.

Water temperature was retained in both density and T_F models, and this is not unexpected because this factor is an important determinant of the distribution of many teleosts (Aida 1991, De Vlaming 1972, Freitas et al. 2021). Post-settlement fish density in Matagorda Bay showed a parabolic relationship to water temperature and peaked at intermediate temperatures, suggesting that moderate water temperatures may be more suitable for several families that use these nursery habitats. Similarly, Akin et. al (2003) found that peak densities of fishes in Mad Island Marsh, TX (adjacent to Matagorda Bay) occurred when water temperatures were moderate in April and June. In contrast, T_F generally increased with rising water temperatures, plateauing briefly in the intermediate temperature range. The increase in T_F without a corresponding increase in density or H' indicates that more taxa are settling into these nursery habitats as temperatures increase but these taxa occur at relatively low densities. Diversity incorporates both the number of taxa (T_F) and each taxa's relative abundance, and therefore an increase in T_F without an increase in H' indicates the increased presence of less common families. Findings from this study suggest that a wider breadth of taxa use nursery habitats when higher temperatures occur, but the most abundant taxa settle at intermediate water temperatures. Rare taxa like scorpaenids (scorpionfishes) carangids, ophidids (cusk eels), and lutjanids were present in these warm water periods but in low numbers.

Community Structure

Community structure of fishes differed between habitat types and seasons in Matagorda Bay, and results from PERMANOVAs revealed that for every season, community structure differed significantly between seagrass and saltmarsh habitats. Further SIMPER revealed that a

difference between the two habitats may be consistent but the primary families of fishes driving these differences varied among seasons. Influential families that primarily contributed to dissimilarity in community structure included resident fishes (e.g., gobiids, sparids, fundulids, syngnathids) and estuarine-dependent fishes (e.g., paralichthyids, sciaenids, gerreids), with the latter being major drivers of community structure only during their principal spawning/settlement period.

It is common for the most abundant taxa to be primary drivers of community structure (Plumlee et al. 2020, Reese et al. 2008, Froeschke et al. 2016). For example, fishes in the family Gobiidae were by far the most abundant taxon in this study and were responsible for a substantial percent of the dissimilarity between seagrass and saltmarsh habitats during every season. The high density of gobiids in seagrass and lower abundance in saltmarsh by contrast was primarily responsible for the differences in community structure between the two habitats across every season. Additionally, the protracted spawning exhibited by species in this family ensured that some post-settlement individuals were always present (Darcy 1980). Sparids were also significant drivers of community structure differences between seagrass and saltmarsh habitats in every season; however, the abundance and rank importance of this family decreased from the beginning of their settlement period (winter) to the end of their nursery habitat use (fall). Peak abundance of sparids occurred in the winter and spring which coincides with the documented spawning of the numerically dominant species pinfish *Lagodon rhomboides* (Nelson 2002, Chacin et al. 2016). This would explain why post-settlement pinfish start appearing in high number in the winter and continue to decrease in abundance and therefore influence on community structure, as these fish grow and possibly become less vulnerable to the sampling gear.

Some families (Gobiidae, Gerreidae, Fundulidae, Paralichthyidae) were consistently more abundant in either seagrass or saltmarsh, and species within each of these families are known to prefer specific habitat types (Froeschke 2013, McDonald et al. 2015, Nelson et al. 2014). Others such as Sciaenidae were more abundant in seagrass in one season and saltmarsh in another, indicating difference in habitat preference can occur among species from the same family. For example, sciaenids contributed to community structure differences in spring, fall and winter surveys. Sciaenids were more abundant in seagrass in the spring and fall and more abundant in saltmarsh in the winter. Identifying settlement patterns and nursery habitat preference for sciaenid species can help explain some of the observed patterns in community structure driven by this family and others with multiple species.

Species-Specific Patterns: Family Sciaenidae

Peak abundances of the five sciaenid species within seagrass and saltmarsh habitats in Matagorda Bay were observed at different times (months) of the year: spot (March), silver perch (June), spotted seatrout (September), red drum (October), Atlantic croaker (December). The degree of overlap of co-occurring species in these nursery areas was limited, and the observed pattern of temporal partitioning observed in Matagorda Bay was in accord with findings from previous studies of habitat use by newly settled sciaenids (Rooker et al. 1998, Geary et al. 2001).

Decades earlier, Chao and Musick (1977) speculated that the coexistence of juvenile sciaenids in estuarine tributaries of the Chesapeake Bay was made possible by their temporal partitioning of entry into these nursery areas. During times when post-settlers of two species did overlap in Matagorda Bay, the month with the highest abundance for each species remained different. For example, silver perch and spotted seatrout were both present in seagrass and saltmarsh habitats throughout the summer, but silver perch abundance peaked in May while spotted seatrout peaked in September. Similarly, red drum and Atlantic croaker were both present through the fall and winter, but red drum abundance peaked in October while Atlantic croaker abundance peaked in December. Due to the rapid growth of post-settlement sciaenids (Rooker et al. 1996, Searcy et al. 2007, Hendon and Rakocinski 2016) and ontogenetic shifts in feeding that occur for this species complex during the juvenile stage (Deary et al. 2016, Llanso et al. 1998, Soto et al. 1998), it is likely that most of the individuals of the species arriving a month or two earlier would be significantly larger and consuming different sizes or types of prey than newly settled individuals from another species, thus limiting any potential overlap in food and/or space requirements between the co-occurring species (Akin and Winemiller 2015).

While peak settlement periods (i.e., month) was consistent for all five species across the two years, the density of settlers often differed between the two years. Spotted seatrout and silver perch were significantly more abundant (4.8x and 13.7x, respectively) in 2020 than in 2021. While interannual variation in recruitment is natural, both of these species are particularly sensitive to cold weather (McEacheron 1994) and a freeze that occurred in February of 2021 potentially reduced the spawning stock biomass of both species, which remain in the bay as adults and thus are subject to freeze events. Texas Parks and Wildlife estimated that spotted seatrout and silver perch were the most severely affected species of game and non-game fish, respectively, to be affected by the freeze event that killed an estimated 3.8 million fish in Texas Bays (TPWD 2021). Spot and Atlantic croaker also displayed interannual variability but unlike spotted seatrout and silver perch, these species were markedly more abundant in 2021. Spot and Atlantic croaker along with red drum form aggregations in near shore waters and rely heavily on the physical transport of larvae into estuarine nursery habitats (Anderson et al. 2018, Powell and Gordy 1980, Wilson and Neiland 1994). This reliance on tidal transport and dynamic hydrographic conditions often leads to pronounced interannual fluctuations in the delivery of pre-settlement fishes into estuarine nursery areas (Norcross and Shaw 1984). As a result, I would expect interannual variability to be more pronounced for these tidal pass or coastal spawners over bay spawners such as spotted seatrout and silver perch.

In addition to temporal differences, habitat preference was observed for several sciaenid species. Red drum and spot were both more abundant in seagrass than saltmarsh habitat. The higher abundance of red drum in seagrass relative to other available nursery habitat alternatives in Matagorda Bay is consistent with previous studies (Stunz et al. 2002). Spot were similarly more abundant in seagrass in 2021, with three times more spot collected as compared to 2020. While some studies have shown spotted seatrout and silver perch to exhibit an association with seagrass habitats as juveniles (Brown Peterson 2002, Rooker et al. 1998), others have collected

these species in similar abundance from saltmarsh (Geary et al. 2001, Nahear and Stunz 2010) indicating a reliance on vegetated habitat in general rather than preference for one type over the other. Atlantic croaker were substantially more abundant (~4x) in saltmarsh than seagrass when both habitats were sampled equally (2021), and this finding is in agreement with other studies that have observed high abundance and occurrence of this species in saltmarsh habitat (Froeschke et al. 2016, Geary et al. 2001, Hall, et al. 2016). Differences in habitat use of post-settlement fishes observed across this single family highlight the value of both seagrass and saltmarsh as critical nursery habitats of post-settlement fishes in Matagorda Bay.

Conclusions

This study has highlighted the importance of seagrass and saltmarsh habitat for supporting diverse assemblages of post-settlement fishes in Matagorda Bay. Density, diversity, and composition of post-settlement fishes varied spatially, temporally and between the two habitats. The density and diversity of fishes were both consistently higher in seagrass than saltmarsh, indicating the importance of this habitat for sustaining fish populations in Matagorda Bay. Although the post-settlement fish assemblage in saltmarsh was less dense and diverse, the quantity of fishes supported by this habitat type as a function of its extensive cover throughout the bay speaks to the critical role saltmarsh plays as nursery habitat. The community structure of post-settlement fishes also differed significantly between the two habitats and these differences were driven by a combination of highly abundant resident species and estuarine-dependent species. While resident species such as gobiids were consistent drivers of community structure differences, estuarine-dependent taxa including paralichthyids and sciaenids only influenced community structure differences during peak recruitment periods for numerically dominant species within each family.

Generalized additive modeling revealed that the density and diversity of post-settlement fishes were both influenced by a mix of both environmental conditions (e.g., dissolved oxygen, water temperature, salinity, turbidity, and tide height) and spatial variables (e.g., distance from tidal pass). All three metrics (density, T_F and H') estimated for post-settlement fishes were significantly affected by distance from tidal pass, with both diversity measures elevated at sites closest to the primary tidal pass. This finding appears to suggest tidal transport plays an important role in the delivery and settlement of fish into nurseries in Matagorda Bay. Additionally, heightened density and diversity of post-settlement fishes farthest from the tidal pass where marsh habitat is most complex, suggests that these regions may be critical for sustaining fish populations in Matagorda Bay. Dissolved oxygen was the only physicochemical variable retained in all three models, likely indicating the strength of this variable for shaping post-settlement fish assemblages. Other environmental variables including water temperature, turbidity, salinity, tide height and minutes after sunrise all had a significant effect on more than one of the metrics. Post-settlement fish density, T_F and H' are all a product of complex relationships between temporal, spatial and environmental factors and this study highlights the importance of several of these conditions in shaping fish assemblages in Matagorda Bay.

Species-specific patterns of nursery habitat use for fishes in the family Sciaenidae were examined to identify habitats and seasons that support these commercially and recreationally important species. Temporal partitioning of nursery habitat use by sciaenids was pronounced and species-specific trends were consistent between both years of the study. Red drum and spot were more abundant in seagrass while Atlantic croaker were more abundant in saltmarsh. Silver perch and spotted seatrout were equally abundant in both habitats but occurred in much lower densities in 2021 than in 2020, indicating a decrease in recruitment to both nursery habitats for these species in 2021. The identification of these habitat-specific associations can be used to direct management of a given species by highlighting the importance of minimizing impacts on preferred habitat(s), especially during peak recruitment periods. Similarly, the observed decrease in spotted seatrout and silver perch in 2021, may be indicative of a reduction in spawning stock biomass and should be further investigated to ensure the long-term sustainability of both species in Matagorda Bay.

Seagrass and saltmarsh habitat in Matagorda Bay support diverse assemblages of post-settlement fishes which are further influenced by the complex interactions of environmental conditions within the estuary. The results of this study add to the rich body of knowledge surrounding nursery habitat use for post-settlement fishes in subtropical estuaries. Additionally, these findings can be used to inform management of nursery habitats that sustain Matagorda Bay fishes and should act as a baseline against which the effects of any future disturbances are measured.

Literature Cited

- Able, K. W. (1999). Measures of juvenile fish habitat quality: examples from a National Estuarine Research Reserve. In *American Fisheries Society Symposium* (Vol. 22, pp. 134-147).
- Adams, A. J., Locascio, J. V., & Robbins, B. D. (2004). Microhabitat use by a post-settlement stage estuarine fish: evidence from relative abundance and predation among habitats. *Journal of Experimental Marine Biology and Ecology*, 299(1), 17-33.
- Aida, K. (1991). Environmental regulation of reproductive rhythms in teleosts. *Bulletin of Institution of Zoology Academia Sinica Monographs*, 16, 173-187.
- Akin, S., Winemiller, K. O., & Gelwick, F. P. (2003). Seasonal and spatial variations in fish and macrocrustacean assemblage structure in Mad Island Marsh estuary, Texas. *Estuarine, Coastal and Shelf Science*, 57(1-2), 269-282.
- Akin, S., & Winemiller, K. O. (2015). Habitat use and diets of juvenile spot (*Leiostomus xanthurus*) and Atlantic croaker (*Micropogonias undulatus*) in a small estuary at Mad Island Marsh, Texas. *Texas Journal of Science*, 64(1), 1-29.
- Anderson, J., McDonald, D., Bumguardner, B., Olsen, Z., & Ferguson, J. W. (2018). Patterns of maturity, seasonal migration, and spawning of Atlantic croaker in the western Gulf of Mexico. *Gulf of Mexico Science*, 34(1), 3.
- Baillie, C. J., Fear, J. M., & Fodrie, J. F. (2015). Ecotone effects on seagrass and saltmarsh habitat use by juvenile nekton in a temperate estuary. *Estuaries and Coasts*, 38(5), 1414-1430.
- Baker, R., Taylor, M. D., Able, K. W., Beck, M. W., Cebrian, J., Colombano, D. D., Conolly, R. M., Currin, C., Deegan, L. A., Feller, I. C., Gilby, B. L., Kimball, M. E., Minello, T. J., Rozas, L. P., Simenstad, C., Turner, R. E., Waltham, N. J., Weinstein, M. P., Ziegler, S. L., zu Ermgassen, P. S. E., Alcott, C., Alford, S. B., Barbeau, M. A., Crosby, S. C., Dodds, K., Frank, A., Goeke, J., Goodridge Gaines, L. A., Hardcastle, F. E., Henderson, C. J., James, W. R., Kenworthy, M. D., Lesser, J., Mallick, D., Martin, C. W., McDonnald, A. E., McLuckie, C., Morrison, B. H., Nelson, J. A., Norris, G. S., Ollerhead, J., Pahl, J. W., Ramsden, S., Rehage, J. S., Reinhardt, J. F., Rezek, R. J., Risse, L. M., Smith, J. A. M., Sparks, E. L., Staver, L. W. (2020). Fisheries rely on threatened salt marshes. *Science*, 370(6517), 670-671.
- Barbier, E. B., Hacker, S. D., Kennedy, C., Koch, E. W., Stier, A. C., & Silliman, B. R. (2011). The value of estuarine and coastal ecosystem services. *Ecological Monographs*, 81(2), 169-193.
- Beck, M. W., Heck, K. L., Able, K. W., Childers, D. L., Eggleston, D. B., Gillanders, B. M., Halpern, B., Hays, C. G., Hoshino, K., Minello, T. J., Orth, R. J., Sheridan, P. F., & Weinstein, M. P. (2001). The identification, conservation, and management of estuarine and marine nurseries for fish and invertebrates: a better understanding of the habitats that serve as nurseries for marine species and the factors that create site-specific variability in nursery quality will improve conservation and management of these areas. *BioScience*, 51(8), 633-641.

- Belgrad, B. A., Correia, K. M., Darnell, K. M., Darnell, M. Z., Hayes, C. T., Hall, M. O., Furman, B. T., Martin, C. W., & Smee, D. L. (2021). Environmental drivers of seagrass-associated nekton abundance across the northern Gulf of Mexico. *Estuaries and Coasts*, 44(8), 2279-2290.
- Blaber, S. J. M., & Blaber, T. G. (1980). Factors affecting the distribution of juvenile estuarine and inshore fish. *Journal of Fish Biology*, 17(2), 143-162.
- Bloomfield, G. (2005). Fish and invertebrate assemblages in seagrass, mangrove, saltmarsh, and nonvegetated habitats. *Estuaries and Coasts*, 28(1), 63-77.
- Bolle, L. J., Dickey-Collas, M., van Beek, J. K., Erftemeijer, P. L., Witte, J. I., van der Veer, H. W., & Rijnsdorp, A. D. (2009). Variability in transport of fish eggs and larvae. III. Effects of hydrodynamics and larval behaviour on recruitment in plaice. *Marine Ecology Progress Series*, 390, 195-211.
- Breitburg, D. (2002). Effects of hypoxia, and the balance between hypoxia and enrichment, on coastal fishes and fisheries. *Estuaries*, 25(4), 767-781.
- Brennan, C. E., Blanchard, H., & Fennel, K. (2016). Putting temperature and oxygen thresholds of marine animals in context of environmental change: a regional perspective for the Scotian Shelf and Gulf of St. Lawrence. *PloS one*, 11(12), e0167411.
- Brown, C. A., Jackson, G. A., Holt, S. A., & Holt, G. J. (2005). Spatial and temporal patterns in modeled particle transport to estuarine habitat with comparisons to larval fish settlement patterns. *Estuarine, Coastal and Shelf Science*, 64(1), 33-46.
- Brown-Peterson, N. J. (2002). The reproductive biology of spotted seatrout. In *Biology of the spotted seatrout* (pp. 113-148). CRC Press.
- Bruno, D. O., Delpiani, S. M., & Acha, E. M. (2018). Diel variation of ichthyoplankton recruitment in a wind-dominated temperate coastal lagoon (Argentina). *Estuarine, Coastal and Shelf Science*, 205, 91-99.
- Bushon, A. (2006). Recruitment, spatial distribution, and fine-scale movement patterns of estuarine dependent species through tidal inlets in Texas. *Texas A&M University Corpus-Christi, Department of Life Sciences*.
- Campbell, L. A., & Rice, J. A. (2014). Effects of hypoxia-induced habitat compression on growth of juvenile fish in the Neuse River Estuary, North Carolina, USA. *Marine Ecology Progress Series*, 497, 199-213.
- Carassou, L., Dzwonkowski, B., Hernandez, F. J., Powers, S. P., Park, K., Graham, W. M., & Mareska, J. (2011). Environmental influences on juvenile fish abundances in a river-dominated coastal system. *Marine and Coastal Fisheries*, 3(1), 411-427.
- Carpentieri, P., Colloca, F., & Ardizzone, G. D. (2005). Day–night variations in the demersal nekton assemblage on the Mediterranean shelf-break. *Estuarine, Coastal and Shelf Science*, 63(4), 577-588.

- Chacin, D. H., Switzer, T. S., Ainsworth, C. H., & Stallings, C. D. (2016). Long-term analysis of spatio-temporal patterns in population dynamics and demography of juvenile Pinfish (*Lagodon rhomboides*). *Estuarine, Coastal and Shelf Science*, 183, 52-61.
- Chao, L. N., & Musick, J. A. (1977). Life-history, feeding-habits, and functional-morphology of juvenile Sciaenid fishes in York River Estuary, Virginia. *Fishery Bulletin*, 75(4), 657.
- Comptroller, T. P. A. (Producer). (2019). Matagorda bay economic and ecological resources report. Texas Comptroller of Public Accounts memorandum.
- Craig, J. K., & Crowder, L. B. (2005). Hypoxia-induced habitat shifts and energetic consequences in Atlantic croaker and brown shrimp on the Gulf of Mexico shelf. *Marine Ecology Progress Series*, 294, 79-94.
- Dahlgren, C. P., Kellison, G. T., Adams, A. J., Gillanders, B. M., Kendall, M. S., Layman, C. A., Ley, J. A., Nagelkerken, I., & Serafy, J. E. (2006). Marine nurseries and effective juvenile habitats: concepts and applications. *Marine Ecology Progress Series*, 312, 291-295.
- Dance, M. A., Rooker, J. R., Kline, R. J., Quigg, A., Stunz, G. R., Wells, R. J. D., Lara, K., Lee, J., & Suarez, B. (2021). Importance of low-relief nursery habitat for reef fishes. *Ecosphere*, 12(6), e03542.
- Darcy, G. H. (1980). Comparison of ecological and life history information on gobiid fishes, with emphasis on the southeastern United States. NOAA Technical Report.
- Deary, A. L., Latour, R. J., & Hilton, E. J. (2017). Niche partitioning in early life history stage, estuarine-dependent fishes (Sciaenidae). *Estuaries and Coasts*, 40(6), 1757-1770.
- Deary, A. L., & Hilton, E. J. (2016). Comparative ontogeny of the feeding apparatus of sympatric drums (Perciformes: Sciaenidae) in the Chesapeake Bay. *Journal of Morphology*, 277(2), 183-195.
- De Vlaming, V. L. (1972). Environmental control of teleost reproductive cycles: a brief review. *Journal of Fish Biology*, 4(1), 131-140.
- Ditty, J. G., & Shaw, R. F. (1994). *Preliminary guide to the identification of the early life history stages of sciaenid fishes from the Western Central Atlantic*. NOAA Technical Memorandum
- Duffy, J. E. (2006). Biodiversity and the functioning of seagrass ecosystems. *Marine Ecology Progress Series*, 311, 233-250.
- Edworthy, C., & Strydom, N. (2016). Habitat partitioning by juvenile fishes in a temperate estuarine nursery, South Africa. *Scientia Marina*, 80(2), 151-161.
- Fiksen, Ø., Aksnes, D. L., Flyum, M. H., & Giske, J. (2002). The influence of turbidity on growth and survival of fish larvae: a numerical analysis. In *Sustainable Increase of Marine Harvesting: Fundamental Mechanisms and New Concepts* (pp. 49-59).
- Flaherty-Walia, K. E., Matheson, R. E., & Paperno, R. (2015). Juvenile spotted seatrout (*Cynoscion nebulosus*) habitat use in an eastern Gulf of Mexico estuary: the effects of

- seagrass bed architecture, seagrass species composition, and varying degrees of freshwater influence. *Estuaries and Coasts* 38(1), 353-366.
- Foggo, A., Rundle, S. D., & Bilton, D. T. (2003). The net result: evaluating species richness extrapolation techniques for littoral pond invertebrates. *Freshwater Biology*, 48(10), 1756-1764.
- Freitas, C., Villegas-Ríos, D., Moland, E., & Olsen, E. M. (2021). Sea temperature effects on depth use and habitat selection in a marine fish community. *Journal of Animal Ecology*, 90(7), 1787-1800.
- Froeschke, B. F., Stunz, G. W., Robillard, M. M. R., Williams, J., & Froeschke, J. T. (2013). A modeling and field approach to identify essential fish habitat for juvenile Bay Whiff (*Citharichthys spilopterus*) and Southern Flounder (*Paralichthys lethostigma*) within the Aransas Bay complex, TX. *Estuaries and Coasts*, 36(5), 881-892.
- Froeschke, B. F., Reese Robillard, M. M., & Stunz, G. W. (2016). Spatial biodiversity patterns of fish within the Aransas Bay complex, Texas. *Gulf and Caribbean Research*, 27(1), 21-32.
- Furey, N. B., & Rooker, J. R. (2013). Spatial and temporal shifts in suitable habitat of juvenile southern flounder (*Paralichthys lethostigma*). *Journal of Sea Research*, 76, 161-169.
- Geary, B. W., Rooker, J. R., & Webb, J. W. (2001). Utilization of saltmarsh shorelines by newly settled sciaenids in a Texas estuary. *Gulf and Caribbean Research* 13(1), 29-41.
- Gelwick, F., Akin S., Arrington D.A., Winemiller K. O. (2001). Fish Assemblage Structure in Relation to Environmental Variation in a Texas Gulf Coastal Wetland. *Estuaries*, 24(2), 285-296.
- Glass, L. A., Rooker, J. R., Kraus, R. T., & Holt, G. J. (2008). Distribution, condition, and growth of newly settled southern flounder (*Paralichthys lethostigma*) in the Galveston Bay Estuary, TX. *Journal of Sea Research*, 59(4), 259-268.
- Green, L. M., & Campbell, R. P. (2010). *Trends in finfish landings of sport-boat anglers in Texas marine waters, May 1974-May 2008*: Texas Parks and Wildlife Department, Coastal Fisheries Division Technical Report.
- Green, B. C., Smith, D. J., & Underwood, G. J. (2012). Habitat connectivity and spatial complexity differentially affect mangrove and salt marsh fish assemblages. *Marine Ecology Progress Series*, 466, 177-192.
- Guest, M. A., Connolly, R. M., & Loneragan, N. R. (2003). Seine nets and beam trawls compared by day and night for sampling fish and crustaceans in shallow seagrass habitat. *Fisheries Research*, 64(2-3), 185-196.
- Hall, Q. A., Robillard, M. M. R., Williams, J. A., Ajemian, M. J., & Stunz, G. W. (2016). Reopening of a remote tidal inlet increases recruitment of estuarine-dependent nekton. *Estuaries and Coasts*, 39(6), 1769-1784.
- Heck Jr, K. L., Hays, G., & Orth, R. J. (2003). Critical evaluation of the nursery role hypothesis for seagrass meadows. *Marine Ecology Progress Series*, 253, 123-136.

- Hensgen, G. M., Holt, G. J., Holt, S. A., Williams, J. A., & Stunz, G. W. (2014). Landscape pattern influences nekton diversity and abundance in seagrass meadows. *Marine Ecology Progress Series*, 507, 139-152.
- Hendon, J. R., & Rakocinski, C. F. (2016). Habitat-specific growth, survival and diet of late juvenile hatchery-reared spotted seatrout (*Cynoscion nebulosus*). *Journal of Experimental Marine Biology and Ecology*, 484, 1-10.
- Herrema, D. J., Peery, B. D., Williams-Walls, N., & Wilcox, J. R. (1985). Spawning periods of common inshore fishes on the Florida East Coast. *Gulf of Mexico Science*, 7(2).
- Hollweg, T. A., Christman, M. C., Cebrian, J., Wallace, B. P., Friedman, S. L., Ballesterro, H. R., Huisenga, M. T., & Benson, K. G. (2020). Meta-analysis of nekton utilization of coastal habitats in the northern Gulf of Mexico. *Estuaries and Coasts*, 43(7), 1722-1745.
- Holt, S. A., Holt, G. J., & Arnold, C. R. (1989). Tidal stream transport of larval fishes into non-stratified estuaries. *Rappoert et Process-Verbauex Reun Cons Int Explor Mer*, 191, 100-104.
- Hothorn T., Bretz F., and Westfall P. (2008). Simultaneous Inference in General Parametric Models. *Biometrical Journal*, 50(3), 346-363.
- Houde, E. (1987). Fish early life dynamics and recruitment variability. *Transactions of the American Fisheries Society*(2), 17-29.
- Houde, E. D. (2016). Recruitment variability. *Fish reproductive biology: implications for assessment and management*, 98-187.
- Islam, M., Hibino, M., & Tanaka, M. (2007). Tidal and diurnal variations in larval fish abundance in an estuarine inlet in Ariake Bay, Japan: implication for selective tidal stream transport. *Ecological Research*, 22(1), 165-171.
- Jenkins, G., Keough, M., & Hamer, P. (1998). The contributions of habitat structure and larval supply to broad-scale recruitment variability in a temperate zone, seagrass-associated fish. *Journal of Experimental Marine Biology Ecology* 226(2), 259-278.
- Jenkins, G. P., Black, K. P., Wheatley, M. J., & Hatton, D. N. (1997). Temporal and spatial variability in recruitment of a temperate, seagrass-associated fish is largely determined by physical processes in the pre-and post-settlement phases. *Marine Ecology Progress Series* 148, 23-35.
- Llanso, R. J., Bell, S. S., & Vose, F. E. (1998). Food habits of red drum and spotted seatrout in a restored mangrove impoundment. *Estuaries*, 21(2), 294-306.
- Lowerre-Barbieri, S. K., Ganas, K., Saborido-Rey, F., Murua, H., & Hunter, J. R. (2011). Reproductive timing in marine fishes: variability, temporal scales, and methods. *Marine and Coastal Fisheries*, 3(1), 71-91.
- Lunt, J., & Smee, D. L. (2020). Turbidity alters estuarine biodiversity and species composition. *ICES Journal of Marine Science*, 77(1), 379-387.

- McDevitt-Irwin, J. M., Iacarella, J. C., & Baum, J. K. (2016). Reassessing the nursery role of seagrass habitats from temperate to tropical regions: a meta-analysis. *Marine Ecology Progress Series*, 557, 133-143.
- McDonald, R. B., Moody, R. M., Heck, K. L., & Cebrian, J. (2016). Fish, macroinvertebrate and epifaunal communities in shallow coastal lagoons with varying seagrass cover of the northern Gulf of Mexico. *Estuaries and coasts*, 39(3), 718-730.
- McEachron, L. W., Matlock, G. C., Bryan, C. E., Unger, P., Cody, T. J., & Martin, J. H. (1994). Winter mass mortality of animals in Texas bays. *Gulf of Mexico Science*, 13(2), 6.
- Meyer, D. L., & Posey, M. H. (2009). Effects of life history strategy on fish distribution and use of estuarine salt marsh and shallow-water flat habitats. *Estuaries and Coasts*, 32(4), 797-812.
- Miller, D., Poucher, S., & Coiro, L. (2002). Determination of lethal dissolved oxygen levels for selected marine and estuarine fishes, crustaceans, and a bivalve. *Marine Biology*, 140(2), 287-296.
- Minello, T. J. (1999). Nekton densities in shallow estuarine habitats of Texas and Louisiana and the identification of essential fish habitat. In *American Fisheries Society Symposium* (Vol. 22, pp. 43-75).
- Minello, T. J., Able, K. W., Weinstein, M. P., & Hays, C. G. (2003). Salt marshes as nurseries for nekton: testing hypotheses on density, growth and survival through meta-analysis. *Marine Ecology Progress Series*, 246, 39-59.
- Morris, E. K., Caruso, T., Buscot, F., Fischer, M., Hancock, C., Maier, T. S., Meiners, T., Muller, C., Obermaier, E., Prati, D., Socher, S. A., Sonnemann, I., Waschke, N., Wubet, T., Wurst, S., & Rillig, M. C. (2014). Choosing and using diversity indices: insights for ecological applications from the German Biodiversity Exploratories. *Ecology and Evolution*, 4(18), 3514-3524.
- Morrison, M. A., Francis, M. P., Hartill, B. W., & Parkinson, D. M. (2002). Diurnal and tidal variation in the abundance of the fish fauna of a temperate tidal mudflat. *Estuarine, Coastal and Shelf Science*, 54(5), 793-807.
- Munsch, S. H., Cordell, J. R., & Toft, J. D. (2016). Fine-scale habitat use and behavior of a nearshore fish community: nursery functions, predation avoidance, and spatiotemporal habitat partitioning. *Marine Ecology Progress Series*, 557, 1-15.
- Naeem, S. (1998). Species redundancy and ecosystem reliability. *Conservation Biology*, 12(1), 39-45.
- Neahr, T., Stunz, G., & Minello, T. (2010). Habitat use patterns of newly settled spotted seatrout in estuaries of the north-western Gulf of Mexico. *Fisheries Management Ecology*, 17(5), 404-413.
- Nelson, G. A. (2002). Age, growth, mortality, and distribution of pinfish (*Lagodon rhomboides*) in Tampa Bay and adjacent Gulf of Mexico waters.

- Nelson, T. R., Sutton, D., & DeVries, D. R. (2014). Summer movements of the Gulf Killifish (*Fundulus grandis*) in a northern Gulf of Mexico salt marsh. *Estuaries and coasts*, 37(5), 1295-1300.
- Norcross, B. L., & Shaw, R. F. (1984). Oceanic and estuarine transport of fish eggs and larvae: a review. *Transactions of the American Fisheries Society*, 113(2), 153-165.
- Nunn, A. D., Tewson, L. H., & Cowx, I. G. (2012). The foraging ecology of larval and juvenile fishes. *Reviews in Fish Biology Fisheries*, 22(2), 377-408.
- Orfanidis, G. A., Touloumis, K., Stenberg, C., Mariani, P., Støttrup, J. G., & Svendsen, J. C. (2021). Fish assemblages in seagrass (*Zostera marina* L.) meadows and mussel reefs (*Mytilus edulis*): Implications for coastal fisheries, restoration and marine spatial planning. *Water*, 13(22), 3268.
- Oksanen, J., Simpson G., Blanchet F., Kindt R., Legendre P., Minchin P., O'Hara R., Solymos P., Weedon J. (2022). Vegan: Community Ecology Package. R package version 2.6-2, <https://CRAN.R-project.org/package=vegan>.
- Palmer, T. A., Montagna, P. A., Pollack, J. B., Kalke, R. D., & DeYoe, H. R. (2011). The role of freshwater inflow in lagoons, rivers, and bays. *Hydrobiologia*, 667(1), 49-67.
- Pinckney, J. L., Paerl, H. W., Tester, P., & Richardson, T. L. (2001). The role of nutrient loading and eutrophication in estuarine ecology. *Environmental health perspectives*, 109(suppl 5), 699-706.
- Plumlee, J. D., Dance, K. M., Dance, M. A., Rooker, J. R., TinHan, T. C., Shipley, J. B., & Wells, R. J. (2020). Fish assemblages associated with artificial reefs assessed using multiple gear types in the northwest Gulf of Mexico. *Bulletin of Marine Science*, 96(4), 655-678.
- Powell, A. B., & Gordy, H. R. (1980). *Leiostomus xanthurus* (Sciaenidae). *Fishery Bulletin*, 78(3), 701.
- Ray, B. R., Johnson, M. W., Cammarata, K., & Smee, D. L. (2014). Changes in seagrass species composition in northwestern Gulf of Mexico estuaries: effects on associated seagrass fauna. *PloS one*, 9(9), e107751.
- Reese, M. M., Stunz, G. W., & Bushon, A. M. (2008). Recruitment of estuarine-dependent nekton through a new tidal inlet: the opening of Packery Channel in Corpus Christi, TX, USA. *Estuaries and Coasts*, 31(6), 1143-1157.
- Renaud, M. L., & Williams, J. A. (1997). Movements of Kemp's ridley (*Lepidochelys kempii*) and green (*Chelonia mydas*) sea turtles using Lavaca Bay and Matagorda Bay, 1996-1997. *Environmental Protection Agency*.
- Richards, W. J. (2005). *Early Stages of Atlantic Fishes: an Identification Guide for the Western Central North Atlantic, Two Volume Set*. CRC Press.
- Richards, S. A. (2005). Testing ecological theory using the information-theoretic approach: examples and cautionary results. *Ecology*, 86(10), 2805-2814.

- Roman, M. R., Brandt, S. B., Houde, E. D., & Pierson, J. J. (2019). Interactive effects of hypoxia and temperature on coastal pelagic zooplankton and fish. *Frontiers in Marine Science*, 6, 139.
- Rooker, J. R., & Holt, G. J. (1996). Application of RNA: DNA ratios to evaluate the condition and growth of larval and juvenile red drum (*Sciaenops ocellatus*). *Marine Freshwater Research*, 47(2), 283-290.
- Rooker, J. R., Holt, S. A., Soto, M. A., & Holt, G. J. (1998). Postsettlement patterns of habitat use by sciaenid fishes in subtropical seagrass meadows. *Estuaries*, 21(2), 318-327.
- Rooker, J. R., Landry Jr, A. M., Geary, B. W., & Harper, J. A. (2004). Assessment of a shell bank and associated substrates as nursery habitat of postsettlement red snapper. *Estuarine, Coastal and Shelf Science*, 59(4), 653-661.
- Rozas, L. P., & Minello, T. J. (1998). Nekton use of salt marsh, seagrass, and nonvegetated habitats in a south Texas (USA) estuary. *Bulletin of Marine Science*, 63(3), 481-501.
- Scharf, F. S., Manderson, J. P., & Fabrizio, M. C. (2006). The effects of seafloor habitat complexity on survival of juvenile fishes: species-specific interactions with structural refuge. *Journal of Experimental Marine Biology and Ecology* 335(2), 167-176.
- Schaffler, J. J., Montfrans, J. V., Jones, C. M., & Orth, R. J. (2013). Fish species distribution in seagrass habitats of Chesapeake Bay are structured by abiotic and biotic factors. *Marine and Coastal Fisheries*, 5(1), 114-124.
- Searcy, S. P., Eggleston, D. B., & Hare, J. A. (2007). Environmental influences on the relationship between juvenile and larval growth of Atlantic croaker *Micropogonias undulatus*. *Marine Ecology Progress Series*, 349, 81-88.
- Secor, D. H. (2015). *Migration ecology of marine fishes*. JHU Press.
- Seitz, R. D., Wennhage, H., Bergström, U., Lipcius, R. N., & Ysebaert, T. J. (2014). Ecological value of coastal habitats for commercially and ecologically important species. *ICES Journal of Marine Science*, 71(3), 648-665.
- Soto, M. A., Holt, G. J., Holt, S. A., & Rooker, J. R. (1998). Food habits and dietary overlap of newly settled red drum (*Sciaenops ocellatus*) and Atlantic croaker (*Micropogonias undulatus*) from Texas seagrass meadows. *Gulf and Caribbean Research* 10(1), 41-55.
- Stachowicz, J. J., Bruno, J. F., & Duffy, J. E. (2007). Understanding the effects of marine biodiversity on communities and ecosystems. *Annual Review of Ecology, Evolution, and Systematics*, 38, 739-766.
- Stoner, A. W. (1991). Diel variation in the catch of fishes and penaeid shrimps in a tropical estuary. *Estuarine, Coastal and Shelf Science*, 33(1), 57-69.
- Stunz, G. W., Minello, T. J., & Levin, P. S. (2002). A comparison of early juvenile red drum densities among various habitat types in Galveston Bay, Texas. *Estuaries*, 25(1), 76-85.

- Symonds, M. R., & Moussalli, A. (2011). A brief guide to model selection, multimodel inference and model averaging in behavioural ecology using Akaike's information criterion. *Behavioral Ecology and Sociobiology*, 65(1), 13-21.
- Tibshirani, T. H. R. (1986). Generalized additive models *Statistical Science*, 1(3), 297-318.
- TinHan, T. C., Mohan J. A., Dumesnil M., DeAngelis B. M., & Wells R. J. D. (2018). Linking habitat use and trophic ecology of spotted seatrout (*cynoscion nebulosus*) on a restored oyster reef in a subtropical estuary. *Estuaries and Coasts*, 41, 1793-1805.
- Texas Parks and Wildlife Department (2021). 2021 Winter Storm Coastal Fisheries Impacts Texas Parks and Wildlife Department March 2021.
- Walters, C. J., & Juanes, F. (1993). Recruitment limitation as a consequence of natural selection for use of restricted feeding habitats and predation risk taking by juvenile fishes. *Canadian Journal of Fisheries Aquatic Sciences* 50(10), 2058-2070.
- Westerman, M., & Holt, G. (1994). RNA: DNA ratio during the critical period and early larval growth of the red drum *Sciaenops ocellatus*. *Marine Biology*, 121(1), 1-9.
- Whitfield, A. K. (2017). The role of seagrass meadows, mangrove forests, salt marshes and reed beds as nursery areas and food sources for fishes in estuaries. *Reviews in Fish Biology and Fisheries*, 27(1), 75-110.
- Wickham H. (2016). ggplot2: Elegant Graphics for Data Analysis. *Springer-Verlag New York*
- Wickham et al. (2019). Welcome to the tidyverse. *Journal of Open Source Software*, 4(43), 1686 <https://doi.org/10.21105/joss.01686>
- Wickham H., François R. S., Henry L., Müller. K. (2022). dplyr: A Grammar of Data Manipulation. R package version 1.0.9, <<https://CRAN.R-project.org/package=dplyr>>.
- Wilber, D., & Bass, R. (1998). Effect of the Colorado River diversion on Matagorda Bay epifauna. *Estuarine, Coastal Shelf Science* 47(3), 309-318.
- Williams, B. D., & Fabrizio, M. C. (2011). Detectability of estuarine fishes in a beach seine survey of tidal tributaries of lower Chesapeake Bay. *Transactions of the American Fisheries Society*, 140(5), 1340-1350.
- Williams, J. A., Holt, G. J., Robillard, M. M. R., Holt, S. A., Hensgen, G., & Stunz, G. W. (2016). Seagrass fragmentation impacts recruitment dynamics of estuarine-dependent fish. *Journal of Experimental Marine Biology Ecology* 479, 97-105.
- Withers, K. (2002). Shorebird use of coastal wetland and barrier island habitat in the Gulf of Mexico. *The Scientific World*, 2.
- Wilson, C. A., & Nieland, D. L. (1994). Reproductive biology of red drum, *Sciaenops ocellatus*, from the neritic waters of the northern Gulf of Mexico. *Fishery Bulletin*, 92(4), 841-850.
- Wood, S.N., N. Pya, and B. Saefken. 2016. Smoothing parameter and model selection for general smooth models (with discussion). *Journal of the American Statistical Association* 111,1548-1575.

- Worm, B., Barbier, E. B., Beaumont, N., Duffy, J. E., Folke, C., Halpern, B. S., . . . al, e. (2006). Impacts of biodiversity loss on ocean ecosystem services. *Science*, *314*(5800), 787-790.
- zu Ermgassen, P. S., DeAngelis, B., Gair, J. R., Ermgassen, S. Z., Baker, R., Daniels, A., MacDonald, T. C., Meckley, K., Powers, S., Ribera, M., Rozas, L. P., & Grabowski, J. H. (2021). Estimating and applying fish and invertebrate density and production enhancement from seagrass, salt marsh edge, and oyster reef nursery habitats in the Gulf of Mexico. *Estuaries and Coasts*, *44*(6), 1588-1603.

Marsh Ecosystem Sampling for Flooding/Sea Level Rise Assessment

Introduction

The Colorado-Lavaca Estuary, or Matagorda Bay system, is located along the upper-mid Texas coast and is bordered by Matagorda, Jackson, Victoria, and Calhoun Counties. The Matagorda Bay system is the second largest estuary in Texas with an area of 244,490 acres and consists of a series of interconnected bays and riverine systems. This estuary includes Matagorda Bay, Lavaca Bay, and several smaller bays including Carancahua, Tres Palacios Bay, Keller Bay, Cox Bay, and Turtle Bay. As the terminus of the Colorado, Lavaca, and Tres Palacios rivers, this system typically receives about 3.5 million acre-feet of freshwater inflow annually (Texas Water Development Board 2022). This study was conducted in West Matagorda Bay, along the bay margins of the barrier island, the Colorado River Delta, and two areas associated with the Gulf Intracoastal Waterway (GIWW), including Mad Island Marsh Preserve and Oyster Lake (Figure 134). Utilizing these relatively ecologically and geographically disparate regions provided a more appropriate context for assessing the variation in floral and faunal spatiotemporal trends within the Bay.

The Bay hosts approximately 28 miles of barrier island chain stretching from Pass Cavallo to the Colorado River. From Gulf to Bay side, the habitat types of the barrier island shift from open sandy beach to dune ridge, to coastal prairie dotted with freshwater to brackish ponds and marshes, and finally to saltmarsh (Hice & Schmidly 2002). Along the bay margins of the barrier island, the saltmarsh is comprised of saline to brackish bayous surrounded predominately by cordgrass marsh (Teal and Teal 1969). Other major components of the tidally influenced bay margins include tidal flats, oyster reefs, shell hash, and open water areas (White et al 2005). Generally, the broad range of distinct habitat types and associated plant communities present within barrier island ecosystems is considered to be of paramount importance for most taxa (Scherber et al 2018). Moreover, barrier islands provide habitat for both year-round residents and migratory coastal birds, representing critical habitat for many species (Rosenfeld 2004; Foster et al. 2009).

The Colorado River Delta (Delta) is one of the few deltas along the entire Gulf of Mexico Coast that is presently expanding and has a unique history of development (White and Calnan 1990). Its progradation across the eastern arm of the Bay occurred within six years following the removal of a log raft along the channel (Wadsworth 1966). As the Delta continues to expand it creates sites of new marsh development as salt-water and brackish-water marsh plants colonize the new land (Van Beek et al. 1980). The Delta provides a wide array of habitat-types, including highly channelized lower and upper estuarine marsh, open water, oyster reefs, and some coastal prairie at higher elevations. Located along the GIWW, Mad Island Marsh Preserve is a 7,063-acre area consisting of fresh, intermediate, brackish, and saline marshes with surrounding upland prairie and shrub land habitats. The marshes on the preserve provide important habitat for many aquatic organisms, shore birds and wading birds, and are an important wintering ground for millions of neotropical migrants (Mangham & Williams 2007). Located further west along the

GIWW, Oyster Lake is a 2,400-acre saltwater lake hosting similar habitats to that of the Mad Island Marsh Preserve. This tidally influenced lake represents tidal flat and saltmarsh habitat directly adjoining land utilized primarily for agricultural and recreational purposes.

Marsh Vegetation Assessment

Forming along lagoons protected by barrier islands, at the mouths of river deltas and along the edges of protected estuaries, salt marshes occur in protected areas which are supplied with a source of sediment. As grasses and shrubs colonize these areas the substrate is stabilized, and accretion of marsh is further facilitated. Salt marshes are generally dominated by one to a few species of salt-tolerant grasses and shrubs, and often exhibit distinct zonation created by regular patterns of tidal inundation and salinity (Chapman 1976; Greenberg et al. 2014). Specifically, the temporal and spatial distribution of halophytic vegetation within salt marshes is not random, but organized into patches based on physical, chemical, and biotic factors (Marani et al. 2003). This organization means that salt marshes are unique, exhibiting differences in dominant plant taxa and source of colonizing fauna (Greenberg et al 2014). In addition to providing habitat for a wide variety of flora and fauna, salt marshes reduce coastal erosion, attenuate nutrient inputs to the marine environment, and protect shorelines by dissipating energy from storm surges (Bertness 1999). An important natural resource within the Bay, salt and brackish coastal marshes are highly productive systems which provide habitat in which birds can breed, feed, and roost (Adam 1990; Greenberg et al. 2014). A multi-season marsh vegetation sampling plan was established to determine a baseline for marsh vegetation within study sites and explore the relationships between avian distribution and habitat.

Site Selection

Six sites were selected in 2020 to evaluate longitudinal trends in coastal bird assemblages and marsh vegetation conditions across the Bay. Three sites were selected along the bay margins of the barrier island, including Site 1 (BI-1) located approximately 6 miles east of the Matagorda Ship Channel, Site 2 (BI-2) located approximately mid-way between Pass Cavallo and the Delta, and Site 3 (BI-3) located in the eastern arm of the Bay. Site 4 (CRD-4) was located within the Colorado River Delta along the diversion channel approximately 2 miles from the tip of the Delta. Site 5 (MIM-5) was located in the Mad Island Marsh Preserve along the margins of the GIWW. Site 6 (OL-6) occurred within Oyster Lake which drains directly into the upper open-water portions of the Bay (**Figure 135. Matagorda Bay study sites utilized for avian community and marsh vegetation assessments.**).



Figure 134. Overview of Matagorda Bay including general study areas (white).

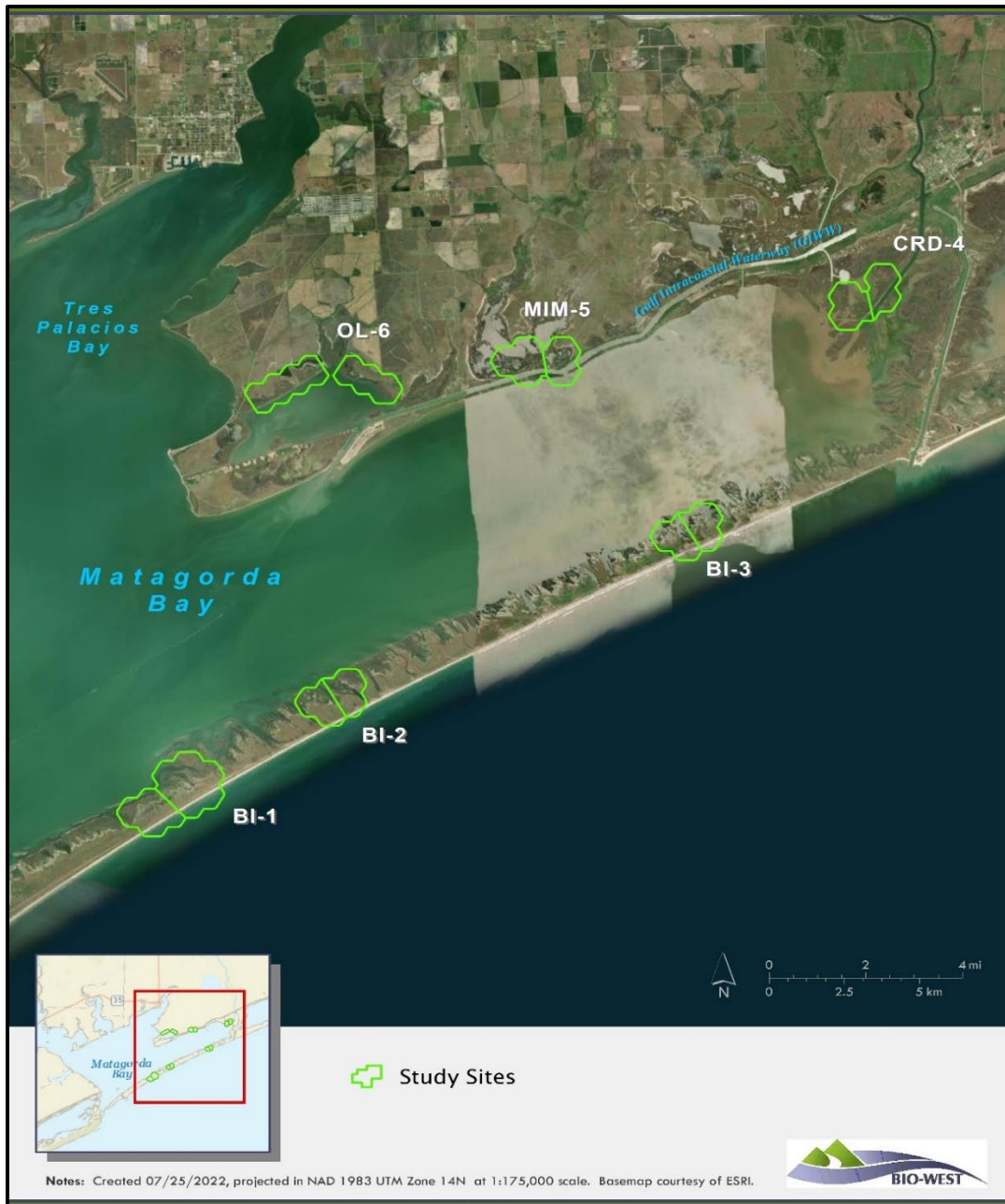


Figure 135. Matagorda Bay study sites utilized for avian community and marsh vegetation assessments.

Methods

Quadrat Sampling

Vegetation survey sites were selected by digitizing the shoreline from aerial imagery using supervised landcover classification, then randomly selecting start points along the shoreline in each study area using GIS software (ArcMap 10.6). A 200 m transect was digitized perpendicular to the shoreline from each start point, with six transects generated per study site for each seasonal sampling event (Figure 136). Four transects were surveyed in the field per

study area for each sampling event, and two excess (alternate) transects discarded based on tidal stream depths, impenetrable thorn scrub, shoreline debris or other barriers to access. Each transect contained 20 temporal monitoring plots along the length of the transect starting directly on the shoreline and proceeding at ten meters intervals along the length of the transect. For each temporal monitoring plot, a 1m² quadrat was laid on the substrate, and within this quadrat the dominant vegetation taxa, relative abundance of dominant taxa, stem counts per species, vegetation height, and species life stage (vegetative, flowering, fruiting, seeding, dormant) were recorded. Common and scientific names for wetland plants follow Stutzenbaker (1999). Plant species richness in the areas surrounding each transect was also recorded to help note the presence of species which may not have been captured in the transect plots. Standard water quality and environmental parameters (temperature [°C], inundation [cm], and salinity [ppt]) were measured at each site at the time of surveys. Presence of algal mats within and adjacent to the quadrat was also noted.

Data Analysis

To summarize general community trends, taxa richness, counts, and relative abundance (%) were calculated for each study site per season and year. Trends in community metrics, taxa-site associations, and marsh vegetation assemblage structure were examined based on the transect level and as independent observations. Transect-level observations were calculated by summing counts per taxa across all quadrat samples within a transect per site for each seasonal sampling event. Taxa richness, diversity, and evenness were calculated for each transect-level observation. Taxa diversity was calculated based on the Shannon Diversity Index, which was then used to calculate taxa evenness. Boxplots were then used to quantify and visualize spatiotemporal patterns (e.g., central tendency, variation) for each community metric among study sites per season.

To assess assemblage structure, abundances were $\log(x+1)$ transformed and taxa that occurred at <5% of transect-level observations were omitted ($n = 95$ taxa examined). Permutational multivariate analysis of variance (Adonis; $\alpha = 0.05$, 1,000 permutations; method = Bray-Curtis) was used to test for meaningful differences in avian assemblage structure between sites, seasons, and their interactive effects. Adonis results supported meaningful differences ($P < 0.05$) in the interactive effect between sites and seasons, meaning that independent evaluations of mean distances for each main effect was not warranted. Therefore, mean within- and between-group dissimilarities (method = Bray-Curtis) were calculated to further assess differences in assemblages for each site-season combination and visualized using a mean-dissimilarity dendrogram to potentially identify insightful hierarchical clustering.

To generalize from vegetation surveys to landscape level, data from temporal surveys was split into two fields of vegetated versus non-vegetated (open sand or algal flats), and then interpolated across the sampling areas GIS software. This interpolated vegetation coverage was then merged with the classified landcover from aerial imagery, and landcover type was updated to reflect presence of vegetation or open sand or algal flats from the temporal monitoring quadrat data. Finally, the updated landcover per sampling area was intersected with Lidar data provided by TAMU-CC and vegetation and open areas were reclassified based on their altitude into

categories of low, medium, high and very high altitude relative to the range of altitude values across the study areas (from inundated and open water areas below sea level or a value of 0 to 8.18 feet at the highest point), and the vegetated or open areas were reclassified according to altitude into low marsh or tidal flats (low), high marsh or open flats (medium), low marsh dune or open dune (high), and high marsh dune/bluff or open dune/bluff (very high) and total coverage values per vegetation-altitude landcover classification were calculated per sampling area.

Environmental characteristics were assessed among sites using landscape cover and vegetation community parameters. Landscape variables were quantified per site using the proportion of areal coverage for the 12 unique Landcover type (i.e., Marsh, Open) and DEM class (e.g., Dune/Bluff, High Marsh) combinations. Patterns in vegetation communities across sites were quantified based on taxa richness, Shannon diversity, and taxa evenness values calculated using the transect-level dataset previously processed to assess trends in assemblage structure. Vegetation community composition was summarized per site by calculating the median (i.e., central tendency) and interquartile range (i.e., variation/stability) for each metric. Principal components analysis (PCA) was used to examine environmental variation across sites and identify latent gradients in landscape ($n = 12$ variables) and vegetation community ($n = 6$ variables) characteristics within the bay. For analysis, landscape and vegetation variables were $\arcsin(\sqrt{x})$ and $\log(x)$ transformed, respectively. PCA results were visualized by plotting scores of the first two PC axes per site. Percent variation explained for each PC axis and variables highly correlated ($r > |0.70|$) with either axis is also presented. All statistical analyses were performed using the R (4.2) packages ‘ggplot2’ (Lin Pedersen 2022) and ‘vegan’ (Oksanen 2020).



Figure 136. Study site sampling area with example of vegetation transects and quadrat points.

Results

A complete list of plant species observed, including site occurrence, relative abundance, proportion of plots containing algal mats, and total number of species observed by site can be found in the Appendix for this section. Vegetation community sampling was conducted at each of the six study sites, with each area visited in spring (April/May) and fall (October/November) of 2020 and 2021. Spring sampling of study site BI-3 produced the highest median taxa richness (11.5) across all study sites and seasons. In general, study sites located in proximity to the GIWW (CRD-4, MIM-5, and OL-6) exhibited relatively similar median taxa richness with the highest values for fall MIM-5 (7.5). Median diversity was generally greatest in the spring, with the highest values observed at BI-3 (1.492) followed by MIM-5 (1.226). In contrast to BI-3, the other barrier island sites generally showed lower scores for median taxa richness, Shannon diversity, and taxa evenness (Figure 137).

Assessments of assemblage structure were based on 17 taxa and 72 transects from the entire study duration. Results from Adonis supported meaningful differences in assemblage structure between sites ($F = 8.48$, $P = 0.001$), but not seasons ($F = 2.02$, $P = 0.094$). Meaningful differences were also well supported for site-season interactive effects ($F = 3.22$, $P = 0.001$). Based on this, independent evaluations of mean distances among sites were not conducted. Mean distance calculations showed that mean dissimilarities within-groups (0.30) were less than between-groups (0.43) for each site-season combination, providing additional evidence that assemblages differed on average (Figure 138).

Principal component axis 1 explained 46.51 % of variation and PC axis 2 explained 24.99%, totaling 71.50 %. Variables positively correlated to PC 1 were Marsh - Low Marsh (0.97) and Shannon Diversity - Median (0.80). Variables negatively correlated with PC 1 were Taxa Evenness – IQR (-0.90), Marsh - Dune/Bluff, and four Open DEM classes: Dune/Bluff (-0.94), High Marsh/Low Dune (-0.91), Low Marsh (-0.90), and High Marsh (-0.83). Lastly, variables positively correlated with PC 2 were Marsh - Water (0.91), Open - Water (0.88), Taxa Richness - IQR (0.82), Taxa Richness – Median (0.81). No variables displayed a strong negative correlation with PC 2. Landscape and vegetation community characteristics showed clear separation in multivariate space for most sites. All BI sites had a greater proportion of higher elevation DEM classes compared to other sites. BI-3 separated from other BI sites based on the presence of Marsh – Water, as well as higher and more variable patterns in taxa richness. BI-1 was distinguished from all sites due to lower values for all vegetation community metrics. In contrast, CRD-4, MIM-5, and OL-6 had a greater proportion of Marsh - Low Marsh and had higher median Shannon diversity values (Figure 139).

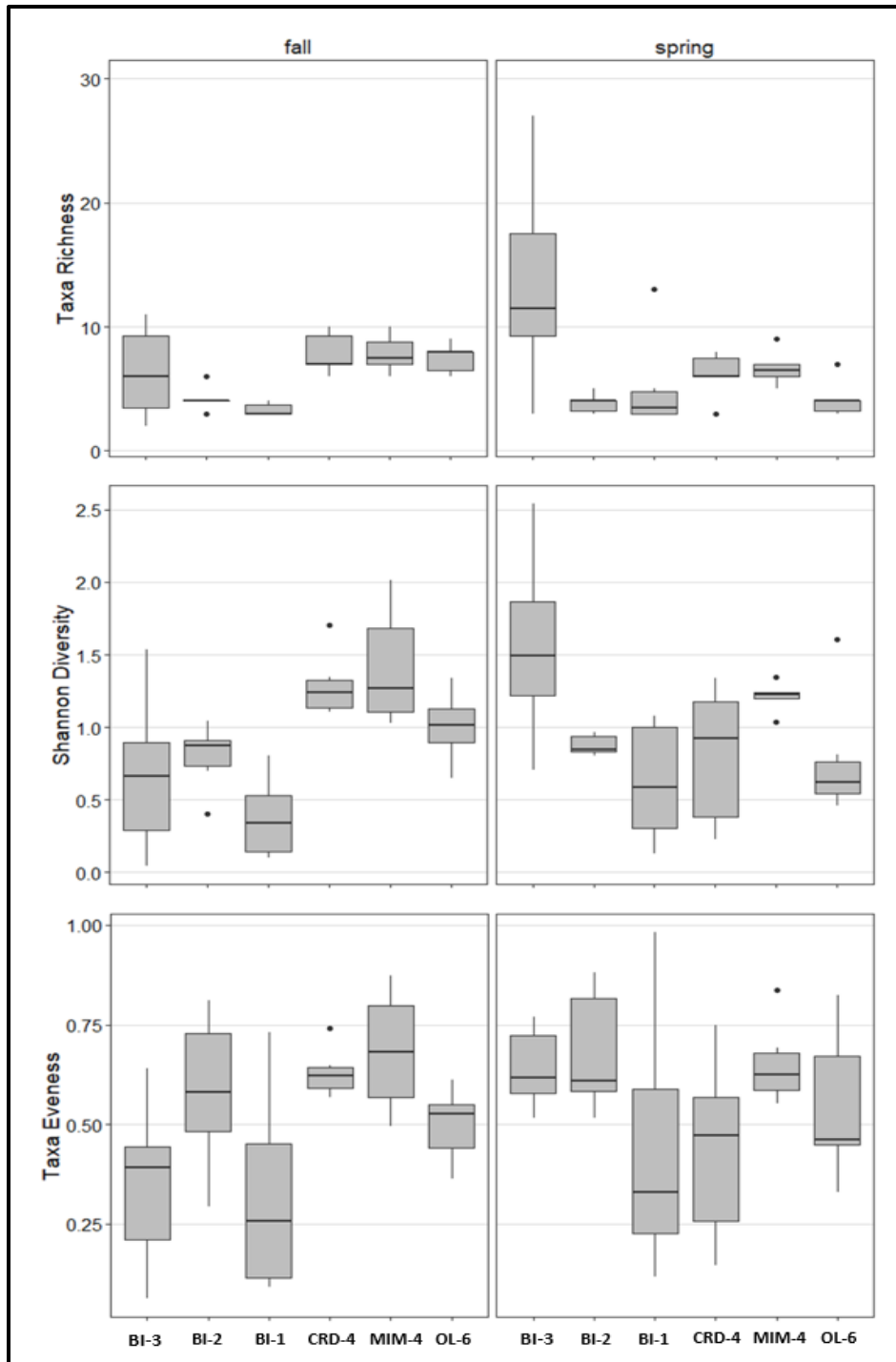


Figure 137. Boxplots displaying seasonal trends in taxa richness (top), Shannon Diversity (middle), and taxa evenness (bottom) of vegetation assemblages across sites. The thick horizontal line in each box is the median and the upper/lower bounds of each box represents the interquartile range. Whiskers represent minimum/maximum values up to 1.5 times the interquartile range, and outliers beyond this are designated with solid black circles.

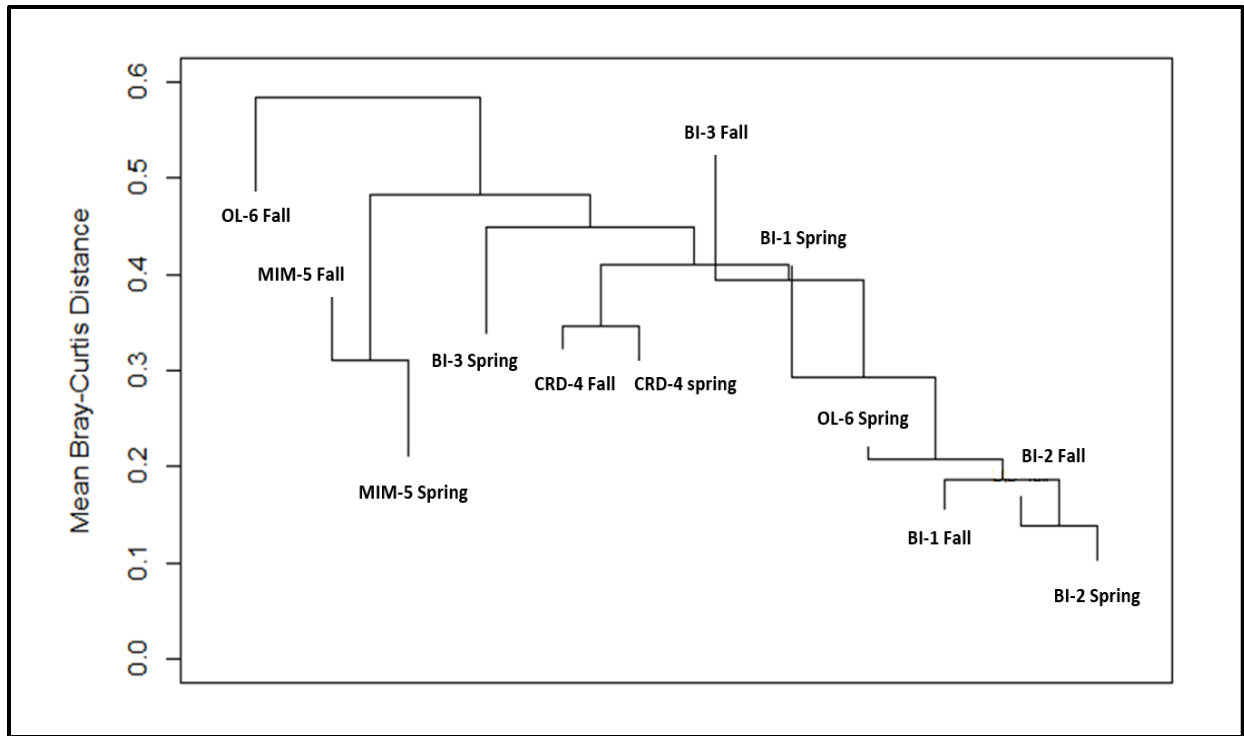


Figure 138. *Dendrogram displaying dissimilarities in vegetation assemblage structure grouped by each site-season combination via mean Bray Curtis distance. Reversed leaf segments demonstrate heterogeneous assemblage structure within a particular group.*

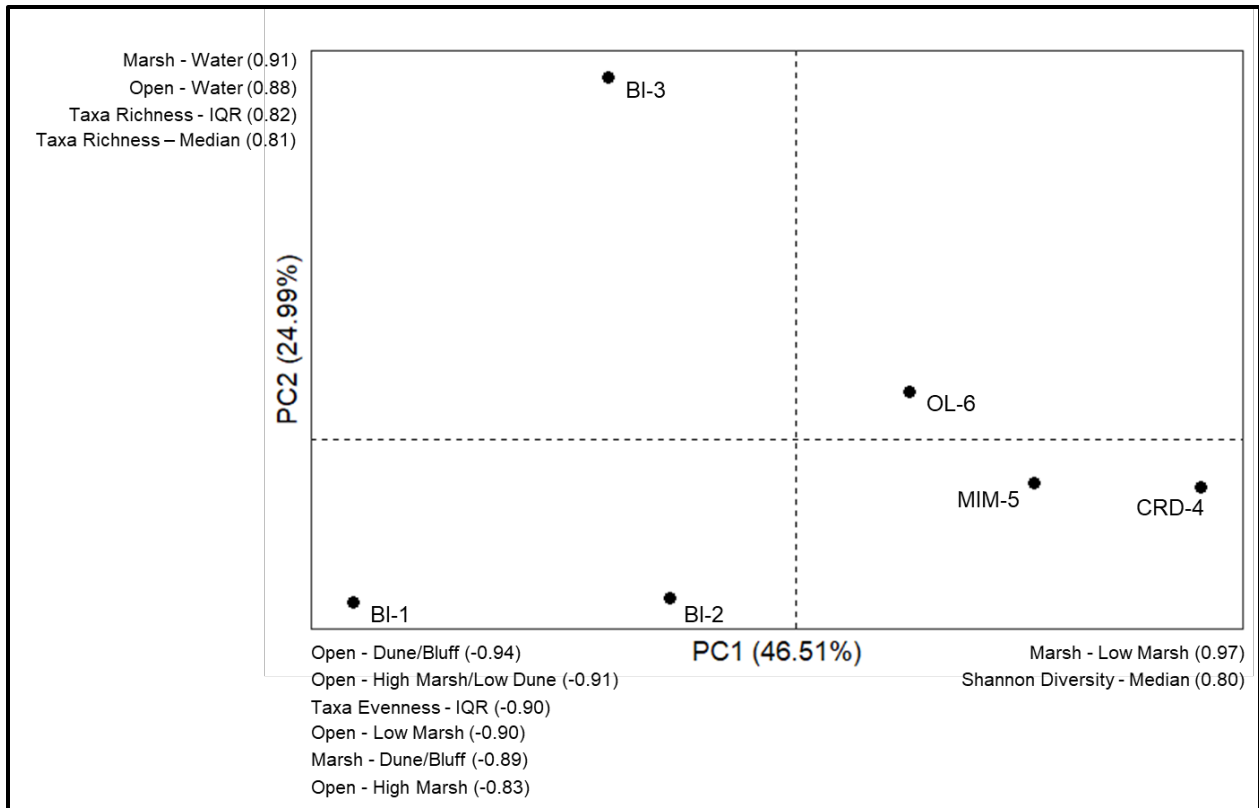


Figure 139. Principal components (PC) analysis displaying environmental variation among sites in multivariate space based on PC scores the first two axes. Landscape cover and vegetation community metric variables strongly correlated ($r > |0.70|$) with PC 1 and PC 2 are also presented. Dashed lines denote zero on the x- and y-intercept.

Appendix

Site occurrence (as denoted by the presence of a relative abundance value) and relative abundance (%) calculated by site for each plant species observed during marsh vegetation sampling. Number of plots, proportion of plots containing algal mats, and total number of species observed by site are presented at the bottom of the table.

Taxa		Relative Abundance (%) by Site					
Common Name	Scientific Name	BI-3	BI-2	BI-1	CRD-4	MIM-5	OL-6
Altamisa	<i>Ambrosia cumanensis</i>	0.3	0	0.1	0	0	0
Amaranth Family	<i>Suaeda sp.</i>	<0.1	0.2	<0.1	0	0.1	0
American Glasswort	<i>Salicornia virginica</i>	7.0	0	0.3	0	2.3	1.1
Black Mangrove	<i>Avicennia germinans</i>	0	0	<0.1	0	0	0
Blanket Flower	<i>Gaillardia pulchella</i>	0	0	<0.1	0	0	0
Blue Eyed Grass	<i>Sisyrinchium bellum</i>	<0.1	0	0	0	0	0
Blue Mistflower	<i>Conoclinium coelestinum</i>	<0.1	0	0	0	0	0
Broadleaf Arrowhead	<i>Sagittaria latifolia</i>	0	0	0	0	0	<0.1
Broadleaf Signalgrass	<i>Brachiara platyphylla</i>	<0.1	0	0	0	0	0
Bushy Bluestem	<i>Andropogon glomeratus</i>	2.1	0	0.2	0	0	0
Bushy Seaside Tansy	<i>Borrichia frutescens</i>	0.7	<0.1	0.2	5.6	2.6	1.4
Carolina Sealavender	<i>Limonium carolinianum</i>	0	0	0	0	0	<0.1
Carolina Wolfberry	<i>Lycium carolinianum</i>	0.1	0	0	0.3	0.8	0.3
Common Ragweed	<i>Ambrosia artemesiifolia</i>	<0.1	0	0	0	0	0
Common Reed	<i>Phragmites australis</i>	0	0	0	<0.1	0	0
Common Threesquare	<i>Scirpus pungens</i>	<0.1	0	0	0	0	0
Composite Family	<i>Rudbeckia sp.</i>	<0.1	0	<0.1	0	0	0
Daisy Family	<i>Thistle sp.</i>	<0.1	0	0	0	0	0
Dayflower	<i>Commalina erecta</i>	<0.1	0	0	0	0	0
Dayflower Family	<i>Commalina sp.</i>	<0.1	0	0	0	0	0
Dwarf Saltwort	<i>Salicornia bigelovii</i>	4.0	14.7	11.2	15.8	12.2	10.2
Eastern Annual Saltmarsh Aster	<i>Symphotrichum subulatum</i>	<0.1	0	0	0	0	0
Gentian Family	<i>Eustoma sp.</i>	0	0	0	0	0	<0.1
Grass Family	<i>Distichlis sp.</i>	0	0.1	0	0	0	0

Taxa		Relative Abundance (%) by Site					
Common Name	Scientific Name	BI-3	BI-2	BI-1	CRD-4	MIM-5	OL-6
Grass Family	<i>Leersia sp.</i>	<0.1	0	0	0	0	0
Grass Family	<i>Sporobolus sp.</i>	0	0	0	0	0.1	<0.1
Gulf Coast Swallow-wort	<i>Cynanchum angustifolium</i>	<0.1	0	0	<0.1	<0.1	0
Gulf Cordgrass	<i>Spartina spartinae</i>	1.9	0	0	0	0.7	18.8
Horseweed	<i>Conyza canadensis</i>	0.7	0	0	0	0	0
Knotgrass	<i>Paspalum distichum</i>	<0.1	0	0	0	0	0
Lanceleaf Nightshade	<i>Solanum cinerescens</i>	<0.1	0	0	0	0	0
Largeleaf Pennywort	<i>Hydrocotyle bonariensis</i>	<0.1	0	0	0	0	0
Little Bluestem	<i>Schizachyrium scoparium</i>	<0.1	0	0	0	0	0
Morning Glory Family	<i>Cuscuta sp.</i>	0	0	0	<0.1	0	0
Morning Glory Family	<i>Ipomaea sp.</i>	<0.1	0	0	0	0	0
Orchid Family	<i>Spiranthes sp.</i>	<0.1	0	0	0	0	0
Partridge Pea	<i>Chamaecrista fasciculata</i>	<0.1	0	0	0	0	0
Redseed Plantain	<i>Plantago rhodosperma</i>	<0.1	0	0	0	0	0
Saline Aster	<i>Aster tenuifolia</i>	0	0	0	10.6	0.1	0
Saltmarsh Bulrush	<i>Scirpus_maritimus</i>	0	0	0	0.1	0	0
Saltmeadow Cordgrass	<i>Spartina patens</i>	10.8	0	0.1	0.3	<0.1	8.0
Saltwort	<i>Batis maritima</i>	8.5	22.2	11.2	10.1	20.4	3.6
Sea Myrtle	<i>Baccharis halimifolia</i>	0.1	0	0	0.6	0	0
Seashore Dropseed	<i>Sporobolus virginicus</i>	0.9	0	0.5	0.3	39.6	1.0
Sedge Family	<i>Scirpus sp.</i>	0	0	0	0	<0.1	0
Shoregrass	<i>Monanthochloe littoralis</i>	0.14	<0.1	9.9	0	12.1	13.6
Smallflower Groundcherry	<i>Physalis cinerescens</i>	0.4	0	0	0	0	0
Smooth Cordgrass	<i>Spartina alterniflora</i>	38.8	62.6	66.1	54.3	8.9	41.5
Southern Dewberry	<i>Rubus trivialis</i>	<0.1	0	0	0	0	0
Sturdy Bulrush	<i>Bulboschoenus robustus</i>	0	0	0	<0.1	0	0
Sunflower Family	<i>Aster sp.</i>	0.2	0	0	2.1	<0.1	0
Tamarisk Family	<i>Tamarisk sp.</i>	0	0	0	<0.1	0	0
Texas Sunflower	<i>Helianthus praecox</i>	<0.1	0	0	0	0	0

Taxa		Relative Abundance (%) by Site					
Common Name	Scientific Name	BI-3	BI-2	BI-1	CRD-4	MIM-5	OL-6
Turkey Tangle Frogfruit	<i>Phyla incisa</i>	0.2	0	0	0	0	0
Water-plantain Family	<i>Echinodorus sp.</i>	0	0	0	0	0	0.3
Whitetop Sedge	<i>Rhynchospora colorata</i>	<0.1	0	0	0	0	0
Willowherb Family	<i>Ludwigia sp.</i>	0	0	0	0	0	<0.1
Number of Plots		248	249	251	233	238	249
Proportion of Plots with Algal Mats		0.16	0.19	0.12	0	0	0.1
Total Number of Species		41	7	14	16	16	16

Summary/Discussion

Over the three-year study period the observed bird community was typical of a Texas Gulf Coast estuarine ecosystem, with multiple species of rail inhabiting the lower marsh habitats, an abundance of tern, heron, and wading bird species utilizing the marsh fringe, and large flocks of shorebirds foraging and roosting on the tidal flats. Across all study sites taxa richness showed little variation between winter and spring sampling, with a notable decrease in overall richness in the fall. Across sampling years, taxa richness was consistently more variable in the winter than in other seasons. This is most likely attributable to differences in the rate and timing of large flocks arriving to over-winter in the Bay in addition to the larger fluctuations in within-season bird activity due to the more severe weather patterns typical of the Texas Gulf Coast winter. Median diversity and taxa evenness was mostly consistent among seasons and sites. The barrier island study sites generally displayed higher diversity than the GIWW-associated study sites. Most notably BI-1, which exhibited considerably higher avian diversity than all other study sites. Taxa evenness was much lower during the winter for the Oyster Lake study site, as large numbers of migratory single-species flocks of Sandhill Crane (*Antigone canadensis*) and waterfowl were commonly observed utilizing the smaller more wind-protected lake for roosting. Analysis of assemblage structure supported that there is a meaningful difference in the observed avian communities in the Bay, differing by both study site and season. In general spring assemblage structures were most dissimilar from those of other seasons. Additionally, there were higher levels of between-group variation in spring assemblages, with BI-1 displaying the most heterogeneity. This distinctive clustering suggests that the seasonal variation in avian assemblage structure may be largely driven by the diversity of birds present in the Bay during spring months.

Relative to species of interest, the barrier island study sites hosted the most species, including American Oystercatcher (winter), Black Skimmer (spring and winter), Eastern Black Rail (fall), and Piping Plover (winter). However, Whooping Cranes were only observed at the GIWW-associated study sites (MIM-5 and OL-6) during fall and winter sampling. Red Knots were not observed during this study. This is most likely a function of study site location wherein sampling efforts were restricted to interior bay areas and did not include the beach habitat commonly used by this species. In general, the seasonality and habitat associations observed for species of interest in the Bay were consistent with the available literature for these species. During winter sampling, several small groups of American Oystercatcher were observed roosting on shell hash and open water areas of the barrier islands as well as the more inland lake areas of the GIWW. Large numbers of American Oystercatcher were observed as flyovers during spring sampling, suggesting these groups were returning to established breeding areas in the Bay. At the barrier island study sites, Black Skimmers congregated in small numbers during the winter to forage along open water fringing saltmarsh and algal flats. Perhaps consistent with reports of its cryptic habits, only one Eastern Black Rail was observed during this study. This individual was observed at study site BI-1 in the fall when flushed by a researcher traveling through dense emergent marsh. Over-wintering Piping Plover were only recorded once during this study. Five individuals were observed along the partially inundated intertidal zone of BI-2, foraging along

the shoreline. Whooping Crane were observed once at OL-6 and occurred seasonally in the same area of the MIM-5 study site, arriving in early November and inhabiting the area until late January during both 2020 and 2021 sampling. Passive sampling using acoustic recording devices did not produce any observations of the target species, demonstrating the difficulty of studying species with narrow and seasonal distribution (Whooping Crane) or highly cryptic behavior (Eastern Black Rail).

Two years of seasonal marsh vegetation sampling within the Bay demonstrated the high degree of temporal and spatial variation in estuarine saltmarsh communities, differing both across and within study sites. At a broader scale, study sites were generally dominated by one to a few species. However, quadrat sampling indicated that regions of the Bay vary considerably relative to community indices. Of the barrier island study sites, BI-1 exhibited the lowest plant diversity. On a landscape scale, principal components analysis supported that this study site was associated more closely with a lower number of landcover types (count = 2), including more tidally inundated open water areas. Conversely, this study site produced the most species of interest and highest levels of avian diversity observed across the study. This provides evidence to suggest that coastal bird diversity in the Bay may be driven largely by the amount tidally inundated open water habitat interspersed throughout the saltmarsh rather than the availability of higher numbers of landcover types or levels of plant diversity. The BI-1 study site was more closely associated with a larger number of landcover types (count = 5) and higher-elevation landcover types (dune/bluff, high marsh). When compared to the other barrier island study sites, BI-1 had relatively lower values for both avian species richness and diversity. This demonstrates that the barrier island is heterogenous at landscape scale with respect to habitat availability and coastal bird response. More specifically, the barrier island varies regionally with respect to saltmarsh extent and relative proportion of lower marsh and high marsh which in turn may have an influence on coastal bird distribution and abundance in the Bay. Relative to vegetation, analyses indicated that the GIWW-associated study sites were generally more closely associated with lower marsh habitats and higher levels of species diversity. The expansive lower marshes prevalent throughout MIM-5 and OL-6 represented habitat commonly utilized by migratory waterfowl and cranes. These areas also maintained higher levels of Carolina Wolfberry, an important forage species for Whooping Crane. While the barrier island study sites presented higher levels of bird diversity and hosted more avian species of interest, the GIWW-associated study sites, particularly MIM-5 and OL-6, represent demonstrably suitable habitat for Whooping Crane.

The analysis presented herein and compiled data resources are intended to support overall ecological recommendations for mitigation and restoration activities targeting flooding, sea rise, and extended drought in the project area (*Matagorda Bay Ecosystem Assessment: Integrated Synopsis and Future Management Report, September 2022*). Restoration efforts along the barrier islands are recommended to focus on shoreline protection, rookery island development, and seagrass protection in support of birds, habitat including algal flats, and sea turtles. Restoration efforts on the inland side of the GIWW and in the expanding Colorado River Delta are

recommended to focus on freshwater inflow enhancement to support long-term habitat as well as short-term refuges. These marsh habitats support key components of the food web and nursery areas that will be vital to sustain the productivity of the Bay into the future.

Appendix

Seasonal occurrence, site occurrence, count (#), relative abundance (%) and dominant habitat type of the avian communities observed during spring, summer, fall and winter sampling. Habitat types included emergent marsh (EM), open water (OW), shoreline (SL), woody debris (WD), algal flat (AF), grassland (GL), exposed oyster (EO), and scrubland (SR). Observations of species-of-interest shown in bold.

Taxa	Season			Site						Count	Relative Abundance (%)	Dominant Habitat Type						
	Winter	Spring	Fall	BI-3	BI-2	BI-1	CRD-4	MIM-5	OL-6			EM	OW	SL	WD	AF	GL	EO
American Avocet	X	X	X	X	X	X	X	X	X	301	1.4	X	X	X		X		
American Bittern	X		X	X	X	X	X		X	21	<0.1	X					X	
American Kestrel	X		X			X	X	X	X	4	<0.1	X						
American Oystercatcher	X			X		X			X	8	<0.1		X					
American White Ibis	X	X	X	X	X	X	X	X	X	813	3.8	X	X	X	X	X	X	
American White Pelican	X	X	X	X	X	X	X	X	X	843	4.0	X	X	X	X	X	X	
American Wigeon								X		34	0.2		X					
Bald Eagle ^a	X			X						1	<0.1							
Barn Swallow		X	X	X	X	X	X	X	X	241	1.1	X			X	X	X	
Barred Owl	X			X						1	<0.1	X						
Belted Kingfisher	X		X				X	X		26	0.1	X	X	X	X			X
Black-bellied Whistling Duck			X				X		X	4	<0.1	X						
Black Rail			X			X				1	<0.1	X						
Black Skimmer	X	X			X	X	X			98	0.5		X			X		
Black Tern		X				X	X	X	X	211	1.0	X	X			X		
Black Vulture	X	X			X			X		6	<0.1						X	
Black-bellied Plover	X	X	X	X	X	X	X	X	X	155	0.7	X	X	X		X		X
Black-crowned Night Heron	X	X	X		X	X				45	0.2	X				X		
Black-necked Stilt	X	X	X	X	X	X		X	X	56	0.3	X	X	X		X		
Blue-winged Teal	X	X	X	X		X	X	X	X	228	1.1	X	X					

Taxa	Season			Site						Count	Relative Abundance (%)	Dominant Habitat Type							
	Winter	Spring	Fall	BI-3	BI-2	BI-1	CRD-4	MIM-5	OL-6			EM	OW	SL	WD	AF	GL	EO	SR
Boat-tailed Grackle	X	X	X	X	X	X	X	X	X	757	3.6	X			X	X			
Bonaparte's Gull ^a	X								X	6	<0.1								
Brown Pelican	X	X	X	X	X	X	X	X	X	567	2.7	X	X	X	X	X	X		
Brown-headed Cowbird	X		X							18	<0.1								
Bufflehead	X					X				105	0.5		X						
Canvasback	X					X			X	66	0.3	X	X						
Caspian tern	X	X	X	X	X	X	X	X	X	250	1.2	X	X	X		X		X	
Cattle Egret	X	X	X			X	X			154	0.7	X			X				
Cave Swallow			X	X						10	<0.1	X							
Chimney Swift		X				X				1	<0.1					X			
Chipping Sparrow	X		X	X	X	X	X		X	26	0.1	X			X	X			
Cinnamon Teal		X				X	X			7	<0.1	X							
Clapper Rail	X	X	X	X	X	X	X	X	X	79	0.4	X					X		
Cliff Swallow		X	X	X	X				X	159	0.8	X				X	X		
Common Grackle	X	X	X	X	X	X	X	X	X	843	4.0	X	X	X	X	X	X		X
Common Loon		X	X			X	X			2	<0.1			X					
Common Nighthawk	X	X		X	X	X		X	X	15	<0.1	X			X	X	X		
Common Tern		X				X	X	X	X	11	<0.1	X	X			X			
Crested Caracara	X	X	X	X	X	X		X	X	20	0.1	X		X					
Dickcissel		X							X	33	0.2	X				X	X	X	
Double-crested Cormorant	X	X		X	X	X	X		X	152	0.7	X	X	X	X				
Dunlin	X	X	X		X	X			X	479	2.3	X	X	X		X			
Eared Grebe		X							X	3	<0.1			X					
Eastern Kingbird		X		X						70	0.3						X		
Eastern Meadowlark	X	X	X	X	X	X	X	X	X	295	1.4	X				X	X		
Eastern Phoebe			X					X		4	<0.1	X							

Taxa	Season			Site						Count	Relative Abundance (%)	Dominant Habitat Type							
	Winter	Spring	Fall	BI-3	BI-2	BI-1	CRD-4	MIM-5	OL-6			EM	OW	SL	WD	AF	GL	EO	SR
Forster's Tern	X	X	X	X	X	X	X	X	X	495	2.3	X	X	X	X	X			
Franklin's Gull	X	X	X	X			X	X	X	33	0.2	X	X	X		X			
Gadwall	X							X		11	<0.1		X						
Glossy Ibis		X		X				X		5	<0.1	X							
Grasshopper Sparrow	X				X					2	<0.1	X							
Great Blue Heron	X	X	X	X	X	X	X	X	X	301	1.4	X	X	X	X	X			
Great Egret	X	X	X	X	X	X	X	X	X	521	2.5	X	X	X		X			
Greater Yellowlegs	X	X	X	X	X	X	X	X	X	50	0.2	X		X		X	X		
Great-tailed Grackle	X	X	X	X	X	X	X	X	X	411	1.9	X	X		X	X	X		
Green Heron		X					X	X		6	<0.1	X							
Green-winged Teal	X		X			X			X	153	0.7	X				X			
Gull-billed Tern	X		X					X		6	<0.1			X					
Herring Gull			X		X		X	X		59	0.3			X	X	X			
Hooded Merganser			X				X			4	<0.1			X					
Horned Lark				X	X	X			X	22	0.1	X				X	X		
House Wren	X							X		4	<0.1							X	
Killdeer	X	X	X	X	X		X	X	X	126	0.6	X	X	X		X	X	X	
Laughing Gull	X	X	X	X	X	X	X	X	X	732	3.4	X	X	X	X	X	X		
LeConte's Sparrow	X			X						2	<0.1	X							
Least Bittern		X	X			X	X	X		5	<0.1	X							
Least Sandpiper	X	X	X	X	X	X	X	X	X	235	1.1	X	X	X		X			
Least Tern	X	X			X	X	X		X	237	1.1	X		X		X	X		
Lesser Scaup	X			X	X	X				125	0.6		X						
Lesser Yellowlegs	X	X	X	X	X	X	X	X	X	225	1.1	X	X	X		X	X	X	
Lincoln's Sparrow	X					X				5	<0.1	X							
Little Blue Heron	X	X	X		X	X	X	X	X	60	0.3	X	X	X		X		X	
Long-billed Curlew	X	X	X	X	X	X			X	214	1.0	X	X	X		X	X	X	

Taxa	Season			Site						Count	Relative Abundance (%)	Dominant Habitat Type							
	Winter	Spring	Fall	BI-3	BI-2	BI-1	CRD-4	MIM-5	OL-6			EM	OW	SL	WD	AF	GL	EO	SR
Long-billed Dowitcher	X		X			X					42	0.2	X	X	X				
Magnificent Frigatebird		X	X			X	X	X			8	<0.1	X	X					
Mallard	X								X		8	<0.1	X						
Marbled Godwit	X	X	X	X	X	X	X		X		90	0.4	X	X				X	
Marsh Wren	X	X	X	X	X	X	X	X	X		247	1.2	X		X	X		X	
Mottled Duck		X	X	X	X				X		71	0.3	X		X				
Mourning Dove	X	X		X			X	X	X		18	<0.1	X				X	X	X
Neotropic Cormorant	X	X	X	X	X	X	X	X	X		449	2.1	X	X	X	X	X	X	
Northern Bobwhite		X			X	X			X		11	<0.1	X				X		
Northern Cardinal	X	X	X						X		17	<0.1	X			X			X
Northern Harrier	X	X	X	X	X	X	X	X	X		83	0.4	X			X	X	X	X
Northern Mockingbird	X	X	X						X		43	0.2	X		X				X
Northern Pintail	X					X		X	X		108	0.5	X	X					
Northern Shoveler ^a	X								X		28	0.1							
Osprey	X		X	X			X	X			20	0.1	X	X	X	X			
Painted Bunting		X						X			3	<0.1							X
Pied-billed Grebe	X		X	X				X	X		6	<0.1	X	X					
Piping Plover	X					X					5	<0.1		X					
Reddish Egret	X	X	X	X	X	X	X	X	X		190	0.9	X	X	X	X	X		
Redhead	X					X					100	0.5		X					
Red-tailed Hawk	X							X			3	<0.1	X			X			
Red-winged Blackbird	X	X	X	X	X	X	X	X	X		616	2.9	X			X	X	X	X
Ring-billed Gull	X	X	X	X		X	X	X	X		73	0.3	X	X	X	X	X		
Roseate Spoonbill	X	X	X	X	X	X	X	X	X		435	2.1	X	X	X			X	
Royal Tern	X	X	X	X	X	X	X	X			279	1.3	X	X				X	

Taxa	Season			Site						Count	Relative Abundance (%)	Dominant Habitat Type							
	Winter	Spring	Fall	BI-3	BI-2	BI-1	CRD-4	MIM-5	OL-6			EM	OW	SL	WD	AF	GL	EO	SR
Ruby-throated Hummingbird			X						X		1	<0.1							X
Ruddy Turnstone	X	X	X	X	X	X					42	0.2	X		X		X		X
Sanderling	X	X	X	X	X	X			X	X	173	0.8	X	X	X		X		
Sandhill Crane	X		X					X		X	908	4.3	X	X			X	X	
Sandwich Tern	X	X	X	X	X	X	X	X	X	X	44	0.2	X	X	X		X		X
Savannah Sparrow	X				X			X		X	10	<0.1	X					X	
Scissor-tailed Flycatcher		X			X				X		3	<0.1	X					X	
Seaside Sparrow	X	X	X	X	X	X	X	X	X	X	194	0.9	X				X	X	X
Sedge Wren	X	X			X	X		X	X	X	17	<0.1	X						
Semipalmated Plover	X	X			X	X	X		X		83	0.4	X				X		
Semipalmated Sandpiper	X	X	X		X	X			X	X	32	0.2	X	X			X		
Sharp-shinned Hawk			X						X		1	<0.1	X						
Short-billed Dowitcher	X	X	X	X	X	X				X	167	0.8	X	X	X		X		
Snow Goose			X							X	1928	9.1	X		X				
Snowy Egret	X	X	X	X	X	X	X	X	X	X	352	1.7	X	X	X	X	X	X	X
Snowy Plover	X					X					13	<0.1		X					
Sooty tern		X			X	X	X	X			297	1.4	X		X		X	X	
Spotted Sandpiper	X	X						X	X	X	6	<0.1	X	X	X				
Stilt Sandpiper			X			X					2	<0.1						X	
Swamp Sparrow	X				X	X	X			X	40	0.2	X				X	X	
Tree Swallow	X	X	X	X	X	X	X				98	0.5	X		X		X	X	
Tricolored Heron	X	X	X	X	X	X	X	X	X	X	279	1.3	X	X	X	X	X	X	X
Turkey Vulture	X	X	X	X	X		X	X	X	X	146	0.7	X	X	X	X	X	X	X
Western Meadowlark	X		X			X			X		9	<0.1	X						
Western Sandpiper	X	X	X	X	X	X	X	X	X	X	1,072	5.0	X	X	X		X		X

Taxa	Season			Site						Count	Relative Abundance (%)	Dominant Habitat Type							
	Winter	Spring	Fall	BI-3	BI-2	BI-1	CRD-4	MIM-5	OL-6			EM	OW	SL	WD	AF	GL	EO	SR
Whimbrel	X	X	X	X	X	X			X	29	0.2	X		X		X	X	X	
White-faced Ibis ^a	X						X			1	<0.1				X				
White-tailed Hawk		X				X				1	<0.1								
Whooping Crane	X		X					X		13	<0.1	X							
Willet	X	X	X	X	X	X	X	X	X	965	4.5	X	X	X	X	X	X	X	
Wilson's Phalarope		X				X				5	<0.1	X				X			
Wilson's Plover		X		X	X	X	X		X	93	0.4	X	X			X			
Wood Duck	X						X			6	<0.1	X							
Yellow-billed Cuckoo		X							X	1	<0.1							X	
Yellow-crowned Night Heron			X						X	1	<0.1	X							

a: flyover only, habitat associations not recorded.

Avian Assessment

Introduction

Bird species that depend on coastal habitats (coastal birds) are represented by several taxonomic groups, however, all share a reliance on marine environments as a source of food, nesting habitat, or both (Ogden et al 2014). Some generic representatives are Pelecaniformes (wading birds, pelicans, cormorants, and frigate birds), Charadriiformes (shorebirds, gulls, and terns), Anseriformes (waterfowl), and some Falconiformes (osprey and eagles). Coastal birds are represented by a great diversity of species with a variety of life history strategies (Foster et al. 2009). Their utilization of coastal habitats may vary from year-round to seasonal. They use a variety of different strategies to exploit food resources, including fishes, mollusks, crustaceans, and insects. In contrast to passerines, coastal birds are generally long-lived (20 to 60 years), can defer maturity, and have smaller clutch sizes in many cases (Schrieber and Burger 2002). Many coastal birds are colonial nesters, making them susceptible to mass clutch mortalities in unfavorable conditions (Burger and Gochfeld 1991). The combination of all these life-history traits makes coastal birds distinctly susceptible to population declines related to increasing human population trends (Foster 2009). In fact, coastal birds may be at greatest risk because of the tendency of people to settle along coasts (Myers et al. 1987). Coastal birds are also susceptible to environmental pressures including the effects of global climate change as nesting and foraging sites are lost due to sea rise, increased tropical storm systems, and altered rainfall patterns (Ogden et al. 2014).

Bird species and bird community compositions are often utilized as biological indicators (Caro and O'Doherty 1999). They are well-suited for this purpose as they represent important energetic components of ecosystems, are often high in trophic webs, exhibit notable vagility in response to both adversity and opportunity, and are conspicuous allowing for straightforward quantification in space and time (Ogden et al. 2014). Moreover, because birds are globally distributed and historically well-studied, they are ideal candidates for assessing ecosystem health (Foster et al. 2009). There are many instances wherein links between avian status and environmental variation have been capably demonstrated (Noss 1990). For example, it has been shown that populations of herons, egrets, ibises, and storks react reproductively to specific hydrological patterns in the Everglades predominately as a function of prey availability (Ogden 1994; Frederick and Spalding 1994). These community-level responses represent a continuous link at the landscape scale between water management and functional response of coastal birds (Frederick et al. 2009; Ogden et al 2014).

The Gulf Coast encompasses some of the most important coastal bird habitat in North America. For both migrating and wintering birds utilizing the Interior Flyway, the barrier islands and wetlands present within this area provide the first substantial areas of suitable habitat between northern breeding grounds and wintering grounds in South America (Withers 2002). Along the Texas Gulf Coast there are four general types of coastal habitat consistently utilized by coastal birds including beach, washover pass, tidal flat, and marsh habitat (Elliott and McKnight 2000). The beach habitat includes the marine intertidal zone as well as berm habitats

above mean sea level (MSL) of the barrier islands. The intertidal zone is characterized by sand substrate, strong wave action, and regular tidal fluctuations and is primarily used for foraging by several species, most notably plovers (Chapman 1984). Washover passes along the Texas barrier islands serve as nesting habitat for a few species of shorebirds and are important roost sites for plovers and other species (Zonick 1996). These areas are formed when tides and winds from strong storms cause a temporary pass between the Gulf and Bays, resulting in a non-vegetated, channel-like landform terminating in sand and mud tidal flats (Withers 2002). Tidal flats are characterized as large gradually sloping bayside habitats from about 1-m below MSL to 2-m above MSL, and smaller areas bordering bay margins and tidal creeks. In these areas vegetation is sparse and typically dominated by blue-green algal mats growing on the substrate surface (Withers 2002). The majority of Texas shorebirds utilize tidal flat habitat, and it represents particularly important winter foraging habitat for Piping Plover (*Charadrius melodus*) and Snowy Plover (*Charadrius nivosus*; Zonick and Ryan 1994). Tidal flats can exhibit an extreme abundance of shorebirds along the central and southern Texas coast during winter and migratory periods (Withers and Chapman 1993). Marsh habitat is typically a fringe of vegetation along the margins of bays and estuaries within the intertidal area. These muddy and vegetated areas support a diversity of coastal bird species, including larger species such as Black-necked Stilt (*Himantopus mexicanus*) and some sandpipers. Smaller birds, including sandpipers and plovers, are often confined to areas of non-vegetated habitat within the marsh mosaic (Withers 2002).

Between the expansive saltmarsh and tidal flats along the Delta and interior regions of the GIWW to the fringing marsh, algal flats, and coastal prairie of the barrier Islands, Matagorda Bay represents a diverse mosaic of coastal habitats which provide numerous opportunities for both nesting and foraging of many coastal birds. To explore the relationships between avian communities and the Matagorda Bay ecosystem, BIO-WEST conducted seasonal avian community sampling with an emphasis on species of interest to investigate the distribution, abundance, seasonality and habitat associations of coastal birds.

Literature Review: Species of Interest

To contextualize findings of this report within the framework of species-specific management, a literature review of each species of interest was conducted. The specific life histories and habitat associations of these species should be considered when formulating potential management activities. This review also highlights the importance of each species' ecological role within the Matagorda Bay system. These species are considered to be good indicators of the representative pressures on waterbirds in the Matagorda Bay estuaries and marine habitats, representative of the major coastal habitat types in this region or warranting of conservation efforts due to population declines.

American Oystercatcher

The American oystercatcher (*Haematopus palliatus*) is a large shorebird that has been proposed as a 'sentinel' bio-indicator of ecosystem integrity due to its specialized dependence on oysters and associated marine invertebrates and known reproductive responses to several natural and anthropogenic pressures (Nol and Humphrey 1994; Ogden et al. 2014). Along the Gulf

Coast, Texas hosts a resident breeding population within appropriate habitat as well as a wintering population (Oberholser 1974; Nol and Humphrey 1994). Oystercatchers utilize a laterally compressed bill to feed on bivalves and other marine invertebrates (Nol 1989). Because of this specialized diet they reside only in coastal areas supporting intertidal shellfish beds. American oystercatchers are typically associated with undeveloped barrier beaches, sandbars, sand spits and inlets, shell rakes, salt marsh islands, dredged spoil material islands, and oyster reefs. During the breeding season, nests sites are predominately restricted to the coast or nearshore islands within 5 m of open water, almost exclusively on rock or sand beaches (Schulte et al. 2010). In Texas, this species is locally common along the central coast and rare to locally uncommon on the upper and lower coasts (Lockwood and Freeman 2004). Because of their narrow niche it is believed that the species has declined as widespread coastal development and coastal disturbance increases (Ogden et al. 2014). In addition to direct habitat loss, breeding and non-breeding populations face threats from recreational disturbance, increases in nest predators, potential contamination of food resources, and alteration of habitat through beach stabilization (Clay et al. 2014). This species has historically been utilized as an ecological indicator because of its close affiliation with oysters and because of the tendency for wintering populations to utilize the Gulf Coast as refuge (Koczur et al. 2014; Ogden et al. 2014).

Black Skimmer

The North American subspecies of Black Skimmer (*Rynchops niger niger*) is a large tern-like migratory species with unique adaptations to nocturnal foraging (Vieira et al. 2018). This species has a lower mandible extending beyond the upper mandible as well as a slit pupil shape with five times more rods than cones, allowing for increased ability to see in low light. These adaptations allow individuals to skim the water surface with their bill to catch fish prey and engage in nocturnal foraging habits ((Murphy 1936; Zusi and Bridge 1981). Black Skimmer breeding range in the United States extends from Massachusetts to Florida along the Atlantic Coast, the entirety of the Gulf Coast, and to an isolated area of Southern California (Gochfeld and Burger 1994). Commonly found with a mixed-species assemblage, Black Skimmers are strongly colonial and nest in large colonies (Clapp et al. 1983). This species prefers open shell hash and fine silt nesting substrate, breeding along the Texas coast from mid-March to early September (TBBAP 2022). On the central Texas coast, the Black Skimmer breeding population has declined over 60% in the last 30 years (Texas Colonial Waterbird Database 2005). Threats to this species include environmental pollutants, avian terrestrial predation, human disturbance, and habitat loss (Fern 2013).

Eastern Black Rail

Eastern Black Rail (*Laterallus jamaicensis jamaicensis*) is the smallest member of the family Rallidae found in North America and may be one of the most secretive marsh birds. The shy nature and small body size of this species, paired with its preference for occupying dense marsh vegetation makes this species particularly difficult to detect and study (Haverland 2019). In Texas, this species is generally restricted to moist soil intermediate to brackish cordgrass marshes interspersed with open water (Tolliver et al. 2018), where it feeds on aquatic beetles,

spiders, snails, and small crustaceans (Cornell University 2019). Along the Gulf Coast, Eastern Black Rails can also be found in higher elevation wetland zones with moderate shrubby vegetation (USFWS 2019). Pairing occurs from April to August with calling activity peaking during the courtship and egg-laying period of spring and early summer (Davidson 1992; Conway 2009). This species was recently added to the USFWS threatened species list following identification of several threats to the population including habitat fragmentation, climate change, altered hydrology, and human disturbance (Federal Register 2020). It has been estimated that populations have decreased at least 75% over the past 10 to 20 years (Watts 2016). Data on the distribution and abundance of this species in Texas is sparse. Given the relatively large extent of marsh habitat available along the Gulf Coast, Texas may have an abundance of Eastern Black Rails, representing a knowledge gap for this species (Haverland 2019).

Piping Plover

The habitat requirements of shorebirds in wintering and migratory staging areas such as the Gulf Coast were largely ignored in the U.S. until the Piping Plover (*Charadrius melodus*) was added to the U.S. Fish and Wildlife Service's list of threatened and endangered species in 1985 (Withers 2002). One of the least common members of the plover family (Charadriidae), the Piping Plover is a small, sand colored shorebird which breeds on undisturbed beaches (Haig 1983). From March through April, this migratory shorebird nests in the Great Lakes watershed, on the northern Great Plains of the United States and Canada, and along the Atlantic Coast from Newfoundland to South Carolina (Federal Register 1985). Along the barrier beach systems of the Atlantic Coast, the Piping Plover serves as an umbrella species, where nesting habitat is associated with barrier beaches. Federally threatened (Atlantic Coast and Great Plains population) and endangered (Great Lakes population) in portions of its nesting range, the Piping Plover and associated habitat is afforded extra protection in these areas, extending benefits to other species of flora and fauna (Hecker 2008). The Texas Gulf Coast represents winter foraging range for 35 percent of the known population of Piping Plovers (TPWD 2022). They begin arriving late July or early August, regularly utilizing beach, washover, and tidal flat habitats (Zonick and Ryan 1994). In these areas, Piping Plover commonly move between habitats in response to flooding and exposure of barrier island tidal flats, foraging on marine worms, beetles, spiders, crustaceans, mollusks, and other small marine animals (Zonick and Ryan 1994). For wintering populations, loss of habitat to beach development and shoreline stabilization and human disturbance represent the largest threat to this species (USFWS 2009).

Red Knot

The Western Hemisphere's subspecies of Red Knot (*Calidris canutus rufa*) is a medium-sized migratory shorebird listed as threatened by the USFWS in 2015 (USACE 2018). The *rufa* subspecies migration is one of the longest in the world, with populations commonly flying over 18,000 miles between breeding habitat in the Canadian Arctic and wintering grounds in parts of the United States, the Caribbean, and South America (USACE 2018). Along the Texas coastline, Red Knot exhibit a pattern of peak presence on gulf beaches during the spring and fall months, presumably on passage to more southerly latitudes for wintering (Skagen et al. 1999). Red Knots

commonly utilize sandy, gravel, or cobble beaches, tidal flats on the bay sides of barrier islands, salt marshes, shallow coastal impoundments and lagoons, and peat banks (Ecoservices 1993), foraging on mussels, clams, snails, and other mollusks within intertidal areas (USACE 2018). Populations of Red Knot have declined significantly over the last 30 years (Baker et al. 2004). This species was listed due to loss of breeding and non-breeding habitat most likely due to disruption of natural predator cycles on breeding grounds and reduced prey availability throughout its wintering range. Additionally, climate change may be a factor in population declines as the timing of the bird's annual migratory cycle relative to favorable food and weather conditions become increasingly disrupted by the highly interrelated effects of sea level rise (USFWS 2014).

Whooping Crane

A flagship species for the North American wildlife conservation movement, the Whooping Crane (*Grus americana*) is the tallest North American bird. The status of this species as federally endangered is attributed to habitat loss and degradation, power lines, and illegal hunting (USFWS 2007). The only migratory population of Whooping Crane breeds in Wood Buffalo National Park, Alberta and Northwest Territories, Canada, and winters along the Texas Gulf Coast predominately within the Aransas National Wildlife Refuge (USFWS 2007). Mature Whooping Cranes exhibit site fidelity, returning to established territories within both breeding and wintering grounds (Stehn and Prieto 2010). Along the Texas Gulf Coast wintering grounds, territories are generally restricted to saltmarsh habitat adjacent to or within open areas suitable for foraging (Bonds 2000). Dominant food items within their winter range include blue crabs (*Callinectes sapidus*) when tidal flats are flooded as well as Carolina Wolfberry (*Lycium carolinianum*) during fall and winter seasons (Wozniak et al. 2012). The availability of both these forage items have been linked to fluctuations in freshwater inflows which affect the salinity of saltmarsh areas utilized by wintering Whooping Cranes (Hamlin 2005).

Methods

To assess the avian community and presence of species of interest within the Bay, a multi-year seasonal sampling across an array of habitat types. This effort included both active sampling (timed avian point counts) and passive sampling (automated acoustic recorders).

Study Site Delineation

Each of the six designated study sites were divided into two approximately 100-acre sampling areas (Figure 140). The establishment of discrete sampling areas allowed for sampling to occur relatively equally across multiple habitat types (within saltmarsh and open areas such as algal flats, mud flats, and low dunes) and facilitated landscape-scale comparisons. These sampling areas were also large enough to encompass a gradient ranging from shoreline, lower marsh, upper marsh, and to coastal prairie, with variation depending on the site-specific availability of these habitats. Using supervised classification aerial imagery, the sampling areas were split into three landcover categories including vegetation, bare earth (open), and open water, with open water subsequently removed from the analysis. Eight avian survey points were chosen within each sampling area, with a set of eight points representing one walking 'circuit'.

Each sampling area contained one circuit, for a total of two circuits per site (or 16 survey points per site). The locations of timed avian survey points chosen through random stratified selection with equal numbers of points in each of the vegetation and bare earth landcover categories. Best path between points was determined on-the-ground based on tide and weather conditions and private land access. New avian survey point locations were selected for each sampling period in order to effectively survey the majority of each sampling area across the three-year study.

Timed Point Counts

Timed point counts were conducted for a fixed 10-minute period. During timed point counts, all avian species observed (identified either aurally or visually), number of individuals, habitat associations and behavior at the time of observation, and relevant climate parameters (wind average, wind max, ambient temperature, humidity, and cloud cover) were recorded (Verner 1985; USDA 1997). For large flocks of the same species, individuals were counted if less than 100 were observed. Above 100 individuals of the same species, counts were estimated.

Acoustic Recording Devices

To increase the probability of observing rare and migrant species (Whooping Crane) or cryptic species (Eastern Black Rail) whose often secretive habits and infrequent vocalizations may preclude them from detection during timed point counts, automated acoustic recorders were deployed during each field sampling event. At the onset of each sampling event, one to two Song Meter SM4 Bioacoustic Recorders (Wildlife Acoustics, Inc., Maynard, MA, USA) were deployed at each study site. Within each study site, recorder placement was chosen based on the presence of suitable habitat for Eastern Black Rails (i.e., cordgrass marsh interspersed with small pockets of open water) or Whooping Cranes (saltmarsh or tidal flats) depending on the sampling season. Recorders were affixed to t-posts approximately 0.5 to 1.5-m off the ground. All recorders were programmed to record continuously throughout the duration of the sampling event (three to five days). Following the conclusion of all seasonal sampling efforts, recorders were retrieved, and all auditory data was analyzed.



Figure 140. Study site sampling area with landcover classification and example of seasonal avian survey points.

Data Analysis

Timed Point Counts

To summarize general avian community trends, taxa richness, counts, and relative abundance (%) were calculated for each study site per season and year. For the species of interest, raw counts were summed for each site and habitat type (fly-over observations omitted). Trends in community metrics, taxa-site associations, and avian assemblage structure were examined based on point count circuits as independent observations to help control for imperfect detection of rarer species at the point-count-level and thus, increase the number of taxa available for analysis. Circuit-level observations were calculated by summing counts per taxa across all point-count locations within a circuit per site for each seasonal sampling event. Taxa richness, diversity, and evenness were calculated for each circuit-level observation. Taxa diversity was calculated based on the Shannon Diversity Index, which was then used to calculate taxa evenness. Boxplots were then used to quantify and visualize spatiotemporal patterns (e.g., central tendency, variation) for each community metric among sites per season.

To assess assemblage structure, abundances were $\log(x+1)$ transformed and taxa that occurred at <5% of circuit-level observations were omitted ($n = 95$ taxa examined). Permutational multivariate analysis of variance (Adonis; $\alpha = 0.05$, 1,000 permutations; method = Bray-Curtis) was used to test for meaningful differences in avian assemblage structure between sites, seasons, and their interactive effects. Adonis results supported meaningful differences ($P < 0.05$) in the interactive effect between sites and seasons, meaning that independent evaluations of mean distances for each main effect was not warranted. Therefore, mean within- and between-group dissimilarities (method = Bray-Curtis) were calculated to further assess differences in assemblages for each site-season combination and visualized using a mean-dissimilarity dendrogram to potentially identify insightful hierarchical clustering. All statistical analyses were conducted using the R (4.2) packages ‘ggplot2’ (Lin Pedersen 2022) and ‘vegan’ (Oksanen 2020).

Acoustic Recording Devices

To review all recordings for evidence of calling Eastern Black Rail and Whooping Crane, auditory data was analyzed using the software package Kaleidoscope Pro[®] (version 5.1.9; Wildlife Acoustics, Inc., Maynard, MA, USA). Kaleidoscope’s Cluster Analysis feature uses Hidden Markov Models to build a clustering algorithm to automatically detect and sort similar acoustic events (i.e., detections) into groups, or clusters. Manual identification of detections of interest from target species can be used to create a more discriminating advanced classifier (i.e., recognizer) trained to automatically identify species-specific detections. This feature was implemented to create a species-specific recognizer for both Eastern Black Rails and Whooping Cranes using call recordings obtained from the Macaulay Library at the Cornell Lab of Ornithology (Cornell Lab of Ornithology 2020) and other personal recordings. After initially training the recognizer models to detect calls of the target species, the models were further refined to improve their ability to discriminate between target species and the calls of other similar species, until well-performing models were produced. These algorithms were subsequently used to analyze the entire data set of field recordings by each site, and then

qualified observers manually reviewed every putative detection identified by the recognizer both aurally and visually (i.e., listening to the detection and inspecting the spectrogram, respectively).

Results

Timed Avian Point Counts

To establish a baseline of avian distribution across study sites and available habitats and capture the seasonal variation in community assemblage, timed point counts were conducted from 2020 to 2022 at each site during the spring, fall, and winter seasons (Table 30).

A complete list of avian species observed, including seasonality, site occurrence, count, relative abundance, and observed habitat associations by dominant habitat type can be found in the Appendix following this section. A total of 22,236 individuals represented by 150 taxa (136 unique species) were observed during avian community sampling from 2020 to 2022. Among species of interest, Black Skimmer was the most abundant, with the highest counts at CRD-4 (80 ind.). Greater counts of American Oystercatcher were observed at two barrier sites, BI-1 (4 ind.) and BI-3 (2 ind.). Eastern Black Rail and Piping Plover were exclusively observed at barrier island sites, BI-1 (1 ind.) and BI-2 (5 ind.), respectively. Whooping Crane were observed consistently at MIM-5 (10 ind.) over two winter sampling seasons with one pair observed at OL-6 (2 ind.). No Red Knot were observed. Counts among habitat types were highest in open water for American oystercatcher (6 ind.), Black Skimmer (8 ind.), and Piping Plover (5 ind.). Whooping Crane were found exclusively within emergent marsh habitat (10 ind.). The single Eastern Black Rail was observed in emergent marsh (Table 31).

Ranges in median taxa richness were similar across study sites in winter (17.50-28.00) and spring (22.00-28.50) and were both higher than observations in fall (17.00-23.50). Between sites, median taxa richness was generally higher at barrier island study sites (17.00-28.00), though exceeded 20.00 at least once at all sites. Variation in taxa richness, as represented by the interquartile range (i.e., upper/lower bounds of each box), demonstrated winter was consistently more variable (6.25-18.75) than other seasons, with the exception of CRD-4 in spring (19.75). Median diversity and taxa evenness was mostly consistent among seasons and sites. Notable within-season trends in median diversity and taxa evenness included much lower winter values at OL-6 (1.55 and 0.54, respectively), higher spring values at BI-1 (2.90 and 0.83, respectively) and lower spring values at CRD-4 (2.03 and 0.66, respectively). Variation in diversity across sites was higher in winter (0.22-0.61) and fall (0.03-0.54) compared to spring (0.07-0.33). In contrast, variation in taxa evenness showed no notable trends other than the much higher variation at OL-6 in fall (0.20) (Figure 141).

Assessments of assemblage structure were based on 95 taxa and 81 sampling events from the entire study duration. Results from Adonis supported meaningful differences in assemblage structure for main effects site ($F = 3.71$, $P = 0.001$) and season ($F = 6.68$, $P = 0.001$). Meaningful differences were also well supported for site-season interactive effects ($F = 1.24$, $P = 0.018$). Based on this, independent evaluations of mean distances for each main effect were not conducted. Mean distance calculations showed that mean dissimilarities within-groups (0.62)

were less than between-groups (0.72), providing additional evidence that assemblage structure among each site-season combination is different on average.

Mean dissimilarities between site-season groups visualized by the dendrogram displayed four distinct hierarchical clusters. Spring avian assemblages across all sites formed one distinct cluster with high levels of variation between-groups. Moreover, the reversed leaf segment for BI-1-spring displays that assemblage structure was more heterogenous within this group in comparison. The remaining three clusters differentiate assemblages in the winter and fall across sites. Distinct clusters included OL-6, all barrier island sites, and MIM-5 grouped with CRD-4. Among these winter-fall clusters, assemblage structure was more dissimilar across barrier island sites. Lastly, higher levels of within-group variation occurred for BI-1 winter, BI-1-fall, and MIM-5-fall (Figure 142).

Table 30. Seasonal avian community sampling, including number of sampling events per year, season, and month sampled.

Year	# Sampling Events	Season	Month
2020	4	Winter	January
			November & December
		Spring	May
		Fall	October
2021	4	Winter	February & March
			December
		Spring	May
		Fall	October
2022	1	Winter	January & February

Table 31. Total counts of the six species of interest in Matagorda Bay among sites and habitat types. Habitat types represent habitat associations observed at the time of species observation and include emergent marsh (EM), algal flat (AF), open water (OW), and shell hash (SH). Habitat type counts do not include flyovers.

Species	Study Site Counts						Habitat Type Counts			
	BI-1	BI-2	BI-3	CRD-4	MIM-5	OL-6	EM	AF	OW	SH
American Oystercatcher	4	0	2	0	0	2	0	0	6	2
Black Skimmer	15	3	0	80	0	0	0	1	8	0
Eastern Black Rail	1	0	0	0	0	0	1	0	0	0
Piping Plover	0	5	0	0	0	0	0	0	5	0
Red Knot	0	0	0	0	0	0	0	0	0	0
Whooping Crane	0	0	0	0	10	3	10	0	0	0
Total Count	20	8	2	80	10	2	2	1	13	2
Total Species	3	2	1	1	1	2	2	1	3	1

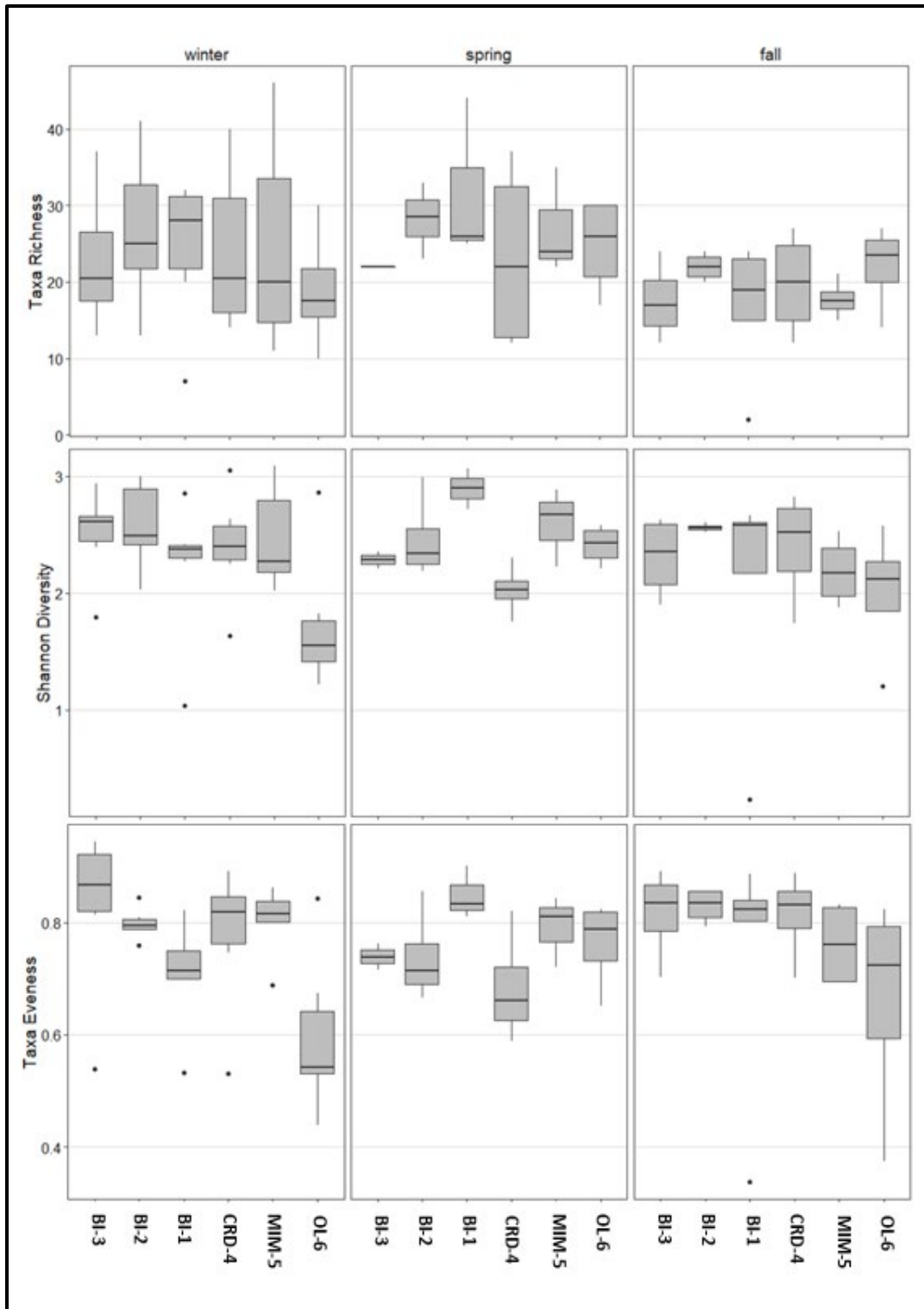


Figure 141. Boxplots displaying seasonal trends in taxa richness (top), Shannon Diversity (middle), and taxa evenness (bottom) of avian assemblages across sites. The thick horizontal line in each box is the median and the upper/lower bounds of each box represents the interquartile range. Whiskers represent minimum/maximum values up to 1.5 times the interquartile range, and outliers beyond this are designated with solid black circles.

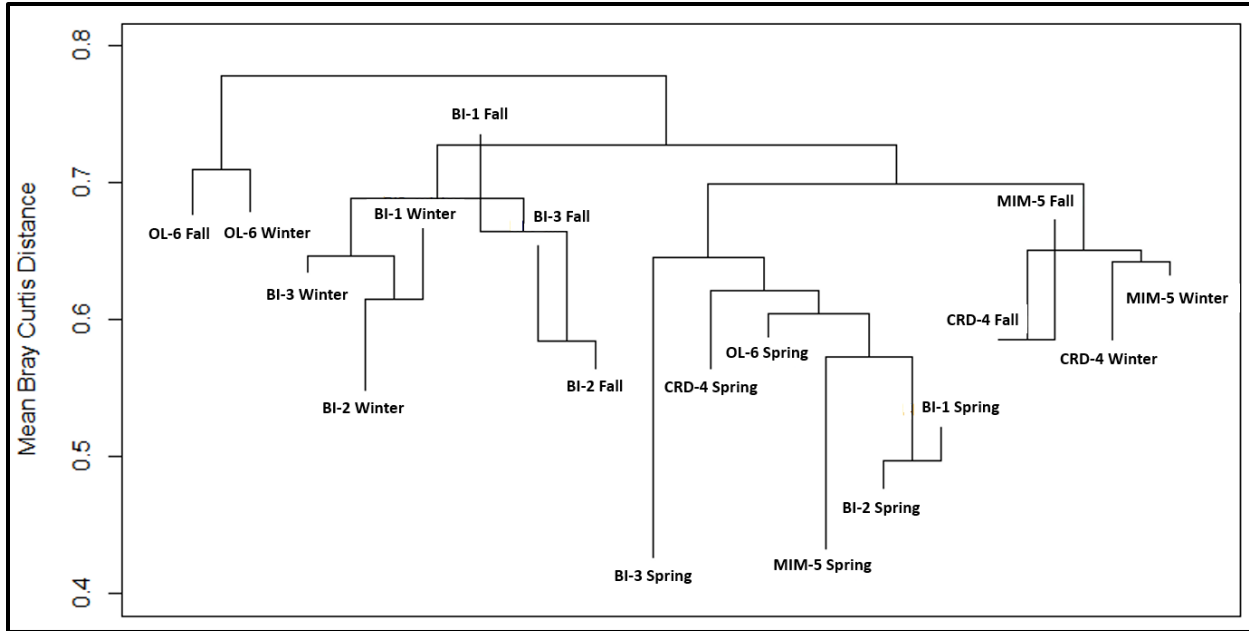


Figure 142. Dendrogram displaying dissimilarities in avian assemblage structure grouped by each site-season combination via mean Bray Curtis distance. Reversed leaf segments demonstrate heterogeneous assemblage structure within a particular group.

Acoustic Recording Devices

The automated acoustic recorders deployed during the 2020 to 2022 sampling events produced approximately 4,333 hours (916 gigabytes [GB]) of recorded auditory data across all six sites. During review of data for calling Eastern Black Rail, analysis produced a total of 125,173 detections (distance from cluster = 0.5), of which the recognizer automatically identified 15,431 putative detections (12.3% of total detections). During review of data for calling Whooping Crane, analysis produced a total of 1,909,289 detections (distance from cluster = 0.5), of which the recognizer automatically identified 21,551 putative detections (1.1% of total detections). Manual review of detections for both species found all putative detections were, in fact, false-positive detections and not true target species calls.

Literature Cited

- Adam, P. 1990. Salt Marsh Ecology. Cambridge University Press, Cambridge, UK, 461 pp.
- Baker, A.J., P.M. Gonzalez, T. Piersma, L.J. Niles, I. de Lima, S. Nascimento, P.W. Atkinson, N.A. Clark, C.D.T. Minton, M.K. Peck and G. Aarts. 2004. Rapid population decline in red knots: fitness consequences of refueling rates and late arrival in Delaware Bay. Proc. Royal Soc. Lond. 271: 875–882.
- Bertness, M.D. 1999. The Ecology of Atlantic Shorelines. Sinauer Associates, Sunderland, Massachusetts.
- BIO-WEST (BIO-WEST, Inc.). 2020. Benthic Habitat Technical Memorandum.
- BIO-WEST (BIO-WEST, Inc.). 2022. Matagorda Bay Ecosystem Assessment: Integrated Synopsis and Future Management Report.
- Burger, J., and M. Gochfeld. 1991. Black skimmer: social dynamics of a colonial species. New York: Columbia University Press. 355.
- Caro, T.M., and O’Doherty, G., 1999. On the use of surrogate species in conservation biology. Conservation Biology. 13: 805–881.
- Chapman, V.J. 1976. Coastal Vegetation. Second ed. Pergamon Press, Oxford. 292.
- Chapman, B.R. 1984. Seasonal abundance and habitat-use patterns of coastal bird populations on Padre and Mustang Island Barrier beaches. U.S. Fish and Wildlife Service FWS/OBS83/31, Washington, D.C.
- Clapp, R.B., D. Morgan-Jacobs and R. C. Banks. 1983. Marine birds of the southeastern United States. U.S. Fish and Wildlife Service, FWS/OBS 83/30, Washington, D.C.
- Conway, C.J. 2009. Standardized North American marsh bird monitoring protocols. Wildlife Research Report #2009-02. U.S. Geological Survey. Arizona Cooperative Fish and Wildlife Research Unit, Tucson, Arizona.
- Cornell Lab of Ornithology. 2020. Macaulay Library at the Cornell Lab of Ornithology. <https://www.macaulaylibrary.org>. (accessed 08.05.21).
- Cornell University. 2019. Black rail. All About Birds.
- Davidson, L. M. 1992. Black Rail, *Laterallus jamaicensis*. In: Migratory nongame birds of management concern in the Northeast. K. J. Schneider and D. M. Pence (Eds.) Newton Corner, Massachusetts: U.S. Fish and Wildlife Service.

- Ecoservices. 1993. Laguna Madre Bird Project from Yarborough Pass to Mansfield Channel during July 1992 through April 1993. Report to Padre Island National Seashore, Contract no. 1443PX7000092582. Corpus Christi, Tex. 82.
- Elliott, L. and K. McKnight 2000. Lower Mississippi/Western Gulf Coast regional shorebird plan. U.S. Shorebird Conservation Plan, Report: U.S. Fish and Wildlife Service.
- Federal Register. 1985. Determination of endangered and threatened status for the piping plover. 50: 50726-50734.
- Federal Register. 2020. Threatened Species Status for Eastern Black Rail with a Section 4(d) Rule. 85: 63764-63803.
- Fern, R. 2013. Reproductive success of nesting terns and black skimmers on the Central Texas coast. Texas A&M University. Master's Thesis.
- Foster, C.R., and A.F. Amos. 2009. Trends in abundance of coastal birds and human activity on a Texas barrier island over three decades. *Estuaries and Coasts*. 32(6): 1079-1089.
- Gratto-Trevor, C.L., and S. Abbott. 2011. Conservation of piping plover (*Charadrius melodus*) in North America: science, successes, and challenges. *Canadian Journal of Zoology*. 89(5): 401-418.
- Gochfeld, M. and J. Burger. 1994. Black Skimmer (*Rynchops niger*). In: *The Birds of North America*, No. 108 (A. Poole and F. Gill, Eds.). The Academy of Natural Sciences; Washington, D.C.: The American Ornithologists' Union.
- Greenberg, R., A. Cardoni, B.J. Ens, X. Gan, J.B. Isacch, K. Koffijberg, and R. Loyn. The distribution and conservation of birds of coastal salt marshes. In: *Coastal Conservation*. Ed. B. Maslo, and J.L. Lockwood. Cambridge University Press.
- Haig, S. 1983. The Piping Plover. *Natural Areas Journal*. 3(3): 35-37.
- Hamlin, L. 2005. The abundance and spatial distribution of blue crabs (*Callinectes sapidus*) in the Guadalupe estuary related to low freshwater inflow conditions. San Marcos, Texas State University: Master's thesis. 103.
- Haverland, A.A. 2019. Determining the status and distribution of eastern black rail (*Laterallus jamaicensis*) in coastal Texas. Texas State University. Master's Thesis.
- Hecker, S. 2008. The piping plover as an umbrella species for the barrier beach ecosystem. In: Askins et al. *Saving Biological Diversity*. 59-74.

- Hice, C. L., and D.J. Schmidly. 2002. The Mammals of Coastal Texas: A Comparison between Mainland and Barrier Island Faunas. *The Southwestern Naturalist*, 47(2): 244.
- Koczur, L.M., A.E. Munters, S.A. Heath, B.M. Ballard, M.C. Green, S.J. Dinsmore and F. Hernández. 2014. Reproductive Success of the American Oystercatcher (*Haematopus palliatus*) in Texas. *Waterbirds*. 37(4): 371-380.
- Lin Pedersen, T. 2017. ggplot2: Create Elegant Data Visualizations Using the Grammar of Graphics. R package version 3.3.6. <https://rdocumentation.org/packages/ggplot2>.
- Lockwood, M. W., and B. Freeman. 2004. The TOS handbook of Texas birds. Texas A&M University Press, College Station.
- Oksanen, J. 2017. vegan: Community Ecology Package. R package version 2.4.2. <https://www.rdocumentation.org/packages/vegan>.
- Mangham, W., and H. Williams. 2007. GPS-based analysis of shoreline change, 1995-2005, Mad Island Marsh Preserve, Matagorda County, Texas. *The Texas Journal of Science*. 59(1): 61.
- Marani, M., E. Belluco, A. D'Alpaos, A. Defina, S. Lanzoni, and A. Rinaldo. 2003. On the drainage density of tidal networks. *Water Resources Research*. 39: 1040.
- Murphy R.C. 1936. Oceanic birds of South America. American Museum of Natural History, New York.
- Myers, J.P., R.I.G. Morrison, P.Z. Antas, B.A. Harrington, T.E. Lovejoy, M. Sallaberry, S.E. Senner, and A. Tarak. 1987. Conservation strategy for migratory species. *American Scientist* 75: 19-26.
- Nol, E. 1989. Food supply and reproductive performance of the American Oystercatcher in Virginia. *Condor*. 91: 429-435.
- Nol, E., and R.C. Humphrey. 1994. American oystercatcher (*Haematopus palliatus*). In: Poole, A. (Ed.), *The Birds of North America*. Cornell Lab of Ornithology, Ithaca, NY, <http://bna.birds.cornell.edu/bna/species/154> (accessed 07.01.13).
- Noss, R.F. 1990. Indicators for monitoring biodiversity: a hierarchical approach. *Conservation Biology*. 4(4): 355-364.
- Oberholser, H. C. 1974. *The bird life of Texas*. University of Texas Press, Austin.

- Ogden, J.C., J.D. Baldwin, O.L. Bass, J.A. Browder, M.I. Cook, P.C. Fredericke, P.E. Frezza, R.A. Galvez, A.B. Hodgson, K.D. Meyer, L.D. Oberhofer, A.F. Paul, P.J. Fletcher, S.M. Davis, and J.J. Lorenz. 2014. Waterbirds as indicators of ecosystem health in the coastal marine habitats of southern Florida: Selection and justification for a suite of indicator species. *Ecological Indicators*. 44: 148-163.
- Roman, C.T., M.J. James-Pirri, and J.F. Heltshe. 2001. Monitoring salt marsh vegetation. Technical Report: Long-term Coastal Ecosystem Monitoring Program at Cape Cod National Seashore, Wellfleet, MA. 47p.
- Rosenfeld, K.M. 2004. Ecology of Bird Island, North Carolina: An Uninhabited, Undeveloped Barrier Island. Masters Thesis, North Carolina State University.
- Scherber, C., H. Andert, R. Niedringhaus, and T. Tschardtke. 2018. A barrier Island perspective on species-area relationships. *Ecology and Evolution*. 8(24): 12879-12889).
- Schulte, S., S. Brown, and D. Reynolds. 2010. American Oystercatcher Working Group: A Conservation Action Plan for the American Oystercatcher (*Haematopus palliatus*) for the Atlantic and Gulf Coasts of the United States. American Oystercatcher Conservation Plan.
- Schreiber, E.A., and J. Burger. 2002. Seabirds in the marine environment. In: *Biology of Marine Birds*, ed. Boca Raton, FL. 1-16.
- Stehn, T.V. and F. Prieto. 2010. Changes in winter whooping crane territories and range 1950-2006. In *Proceedings of the North American Crane Workshop 11*. (ed): 146-151.
- Stolen, E.D., D.R. Breining, and P.C. Frederick. 2005. Using waterbirds as indicators in estuarine systems: successes and perils. In: Bartone, S. (Ed.), *Estuarine Indicators*. CRC Press, Boca Raton, FL. 409-422.
- Teal, J., and M. Teal. 1969. *Life and death of the salt marsh*. Random House, Inc., New York.
- Texas Colonial Waterbird Database. 2005. <https://www.quickbase.com/db/bbqnb2ty4>.
- TBBAP (Texas Breeding Bird Atlas Project). 2022. Texas A&M University.
- Tolliver, J.D., A. Moore, M.C. Green, and F.C. Weckerly. 2018. Coastal black rail population states and survey effort. *The Journal of Wildlife*. 83(2): 312-324.
- TWDB (Texas Water Development Board). Colorado-Lavaca Estuary (Matagorda Bay). https://www.twdb.texas.gov/surfacewater/bays/major_estuaries/colorado_lavaca/index.asp (accessed 07.05.22).

- TWDB (Texas Water Development Board). 2011. Coastal Hydrology for the Lavaca-Colorado Estuary. Bays & Estuaries Program Surface Water Resources Division Texas Water Development Board. Technical Report.
- Texas Wetlands. Barrier Island Interior Wetlands. <https://texaswetlands.org/wetland-types/barrier-island-interior-wetlands>. (accessed 07.05.22).
- USACE (U.S. Army Corps of Engineers). 2018. Biological Assessment for Matagorda Ship Channel Deficiency Project, Matagorda County, Texas. Report and Environmental Assessment.
- USFWS (U.S. Fish and Wildlife Service). 2007. International recovery plan for the whooping crane (*Grus americana*). Revision 3.
- USFWS (U.S. Fish and Wildlife Service). 2009. Piping Plover (*Charadrius melodus*) 5-year review: summary and evaluation. Northeast Region, Hadley, Mass.
- USFWS (U.S. Fish and Wildlife Service). 2014. Rufa Red Knot Background Information and Threats Assessment. Supplement to: Endangered and Threatened Wildlife and Plants; Final Threatened Status for the Rufa Red Knot (*Calidris canutus rufa*). Docket No. FWS-R5-ES-2013-0097; RIN AY17.
- USFWS (U.S. Fish and Wildlife Service). 2019. Species status assessment for the eastern black rail (*Laterallus jamaicensis jamaicensis*), Version 1.3. Atlanta, Georgia. 175.
- Van Beek, J. L., B.T. Gael, M.K. Harris, G.J. Irish, C.D. McLindon, S.S. Dugan, and K.M. Wicker. 1980. Delta building potential of the Colorado River, Central Texas, in U.S. Army Corps of Engineers, 1981, Mouth of Colorado River, Texas phase I: general design memorandum and environmental impact statement (diversion features): Galveston, Texas, U.S. Army Corps of Engineers, 209 p.
- Wadsworth, A H., Jr., 1966. Historical delatation of the Colorado River, Texas, in Shirley, M. L., ed., Deltas in their geologic framework: Houston Geological Society. 99-105.
- Watts B.D. Status and distribution of the eastern black rail along the Atlantic and Gulf Coasts of North America. 2016. College of William and Mary/Virginia Common wealth University, Williamsburg, VA.: The Center for Conservation Biology Technical Report Series. 148.
- White, W.A., and T.R. Calnan. 1990. Sedimentation and historical changes in fluvial-deltaic wetlands along the Texas Gulf Coast with emphasis on the Colorado and Trinity river deltas. Bureau of Economic Geology. Technical Report.

- White, W.A., T.A Tremblay, R.L. Waldinger, T.L. Hepner, and T.R. Calnan. 2005. Status and trends of wetland and aquatic habitats on barrier islands, Freeport to East Matagorda Bay, and South Padre Island. Final Report: Coastal Coordination Division, General Land Office.
- Withers, K. and B.R. Chapman. 1993. Seasonal abundance and habitat use of shorebirds on an Oso Bay mudflat, Corpus Christi, Texas. *Journal of Field Ornithology*. 64, 382-392.
- Withers, K. 1994. The relationship of macrobenthic prey availability to shorebird use of blue-green algal flats in the upper Laguna Madre. Ph.D. dissertation, Texas A&M University, College Station
- Withers, K. 2002. Shorebird use of the coastal wetland and barrier island habitat in the Gulf of Mexico. *The scientific World*. 2: 514-536.
- Wozniak, J.R., T.M. Swannack, R. Butzler, C. Llewellyn, and S.E.III Davis. 2012. River inflow, estuarine salinity, and Carolina wolfberry fruit abundance: linking abiotic drivers to Whooping Crane food. *Journal of Coastal Conservation* 16:345-354.
- Van Beek, J. L., B.T. Gael, M.K. Harris, G.J. Irish, C.D. McLindon, S.S. Dugan, and K.M. Wicker. 1980. Delta building potential of the Colorado River, Central Texas, in U.S. Army Corps of Engineers, 1981, Mouth of Colorado River, Texas phase I: general design memorandum and environmental impact statement (diversion features): Galveston, Texas, U.S. Army Corps of Engineers, 209 p.
- Zonick, C. and M. Ryan, M. 1994. Ecology and conservation of Piping Plovers and Snowy Plovers wintering along the Texas Gulf Coast. Report to Texas Parks and Wildlife Department, Resource Protection and U.S. Fish and Wildlife Service, Ecological Services. Corpus Christi
- Zonick, C. 1996. Key residual questions associated with the ecology of Piping Plovers and Snowy Plovers along the Texas Gulf Coast. Report to Texas Parks and Wildlife Department, Resource Protection and U.S. Fish and Wildlife Service, Ecological Services, Corpus Christi.
- Zusi R.L. and D. Bridge. 1981. On the slit pupil of the Black Skimmer (*Rynchops niger*). *Journal of Field Ornithology*. 51: 338-340.

Trophic Ecology and Food Web Analysis

Introduction

An improved understanding of the functional roles and linkages between habitats and the species that inhabit them is critical to the development of effective ecosystem-based restoration and conservation strategies. Estuaries are often subject to anthropogenic and climatic activity that affect local conditions, habitat quality, and community composition. Thus, investigating the structure and function of an estuarine food web gives valuable insight into these habitats and is an important step in establishing baseline ecological information for susceptible ecosystems. Specifically, investigating trophic interactions of estuarine communities can provide valuable data on sources of production and energy pathways.

Stable isotopes of carbon ($\delta^{13}\text{C}$), nitrogen ($\delta^{15}\text{N}$), and sulfur ($\delta^{34}\text{S}$) provide a long-term measure of diet and are commonly used to determine trophic position and delineate trophic pathways (Peterson and Fry 1987, Fry 2007). $\delta^{13}\text{C}$ and $\delta^{34}\text{S}$ of consumers are useful for discerning contributions from different primary producers. Especially in an estuarine environment, $\delta^{34}\text{S}$ reflects signatures on a benthic – pelagic scale, and on a freshwater-marine scale (Connolly et al. 2004). $\delta^{15}\text{N}$ signatures are useful for estimating trophic position among members within a food web, particularly when primary producer $\delta^{15}\text{N}$ values are known and can provide a baseline (Post 2002).

Estuarine food webs are often complex since they combine terrestrial and marine sources of primary and secondary production (Deegan and Garritt 1997, Chanton and Lewis 2002, Winemiller et al. 2007). Food webs in estuarine habitats are often supported through a variety of primary production pathways including benthic production through submerged vegetation and microalgae, estuarine C3 and C4 plants, and pelagic production (i.e., phytoplankton). It is especially important to understand how primary producers support the estuarine food web because they additionally provide habitat, prevent erosion, and provide a means to sequester blue carbon.

The goals of this project were to 1) perform isotopic analysis on plant and animal tissue from each habitat type across sampling sites, 2) quantify the relative importance of individual producers and energy sources to the overall food web in the bay and to specific species and, 3) to evaluate the influence of habitat arrangement on trophic ecology of the Matagorda Bay Complex.

Sample Collection and Isotope Processing Methods

To accomplish our goals and in an attempt to cover the spatial extent of the bay, Matagorda Bay was divided into nine ecologically distinct regions that were sampled seasonally over multiple years (March 2020 – August 2022; Figure 143). Habitat types varied across these regions of WMB. Saltmarsh plants cover the majority of the outer edges of the bay, with few exceptions including the northeastern region surrounding Palacios Beach. Seagrasses were located most densely in the southwest and southcentral regions, with some sparser seagrass patches located within the western regions. The southeast region where the Colorado River meets Matagorda Bay was the least saline, least vegetated, and mostly mud substrata. Prior to the freeze

event of February 2021 (Winter Storm Uri), living mangroves were located along the southwest region of the bay near Port O'Connor.

Samples for stable isotope analyses were collected quarterly (Mar, Jun, Sep, Dec), with some collected opportunistically monthly (May-Dec) throughout the study duration (2020-2022), from numerous sampling locations within the regions described above.

Primary producers were collected to quantify basal isotope values of the WMB food web and included particulate organic matter (POM), benthic microalgae (BMA), seagrasses, spartina, mangrove, and macroalgae. POM was used to estimate the isotope signature of pelagic production, and BMA was collected as a proxy of benthic production (i.e., microscopic, unicellular photoautotrophs that inhabit the upper centimeters of sediment). POM was collected from sampling locations in 2 L bottles and put on ice until filtration. BMA was collected by scooping the first few centimeters of the substrata within a plastic collection container and put on ice until lab migration. A vertical migration technique via 63 μm nitex mesh was used to isolate BMA from the field sediment sample. After vertical migration, BMA was scraped and pipetted from the surface of the nitex mesh. Samples of POM and BMA were then vacuum filtered onto 47 mm precombusted (500 °C for 8 h) glass fiber filter papers (GF/F, Whatman) until filters were clogged, then rinsed and vacuumed thoroughly with DI water. Filters were then oven dried at 60 °C for 48 h (Heratherm OGS180 drying oven, ThermoScientific) to be prepared for isotope analysis.

Vegetation including seagrasses (*Halodule beaudettei*, *Ruppia maritima*, *Halophila engelmanni*), saltmarsh cordgrass (*Spartina alterniflora*; herein 'marsh grass'), black mangrove (*Avicennia germinans*), and attached macroalgae were collected in bags, and put on ice until lab processing. Vegetation samples were thoroughly rinsed in fresh water to remove any salts, sediments, and epibiota, then examined under a dissecting microscope to determine cleanliness. Marsh grass samples were divided and analyzed separately as aboveground, living green blades and belowground biomass. Cleaned pieces of vegetation were then oven dried at 60 °C for 48 h.

Primary consumers included zooplankton and micronekton (fishes and shrimps < 2 mm total length; TL) that exhibit primary consumer roles (i.e., consume detritus, macroalgae, seagrass, plankton) and exhibit relatively low mobility at their collected size and age classes (Matich et al. 2021). Zooplankton were collected via 100 μm zooplankton net and placed on ice until lab processing. To isolate zooplankton from POM, zooplankton samples were first filtered onto 63 μm nitex mesh, and thoroughly rinsed with DI water. Samples were examined under a dissecting microscope to remove any debris, then vacuum filtered onto 47 mm precombusted GF/F filters, rinsed and vacuumed with DI water, then oven dried at 60 °C for 48 h. Micronekton were collected via bag seines done in triplicates at each collection site during quarterly sampling.

Secondary consumers (micronekton; fishes, shrimps, crabs > 2 cm TL) were collected using a variety of catch methods to ensure a wide diversity of species and sizes which included bag seines, benthic sleds, gill nets (varying panels of mesh sizes 2.5 – 7.6 cm), entanglement nets (10.2 cm mesh size), cast nets, and hook and line.

Fishes < 15 cm were immediately placed on ice and brought to the lab whole for processing. Fishes > 15 cm and all elasmobranchs were measured, sexed (elasmobranchs), and biopsied in the field via a 4 mm biopsy punch, then released. Blue crabs were measured, sexed, and a single claw was removed for tissue collection before crabs were released. All shrimps were taken whole to have their abdomens removed upon processing. Muscle samples and collected whole fish were kept on ice until being catalogued and frozen at -20 °C upon returning to the lab. Shrimps > 2 cm had tail muscle excised and could be treated as individual samples, while shrimps < 2 cm had tail muscle excised and had 10 individuals pooled together as one isotope sample.

All consumer muscle samples were examined under a dissecting microscope to be cleaned and checked for the presence of bones, skin, shell, or scales, and thoroughly rinsed with DI water. Cleaned samples were then oven dried at 60 °C for 48 h then homogenized into a fine powder with an agate mortar and pestle.

After all samples (GF/F filters and solids) had been oven dried and ground (solids), they were prepared for isotope analysis. For bulk $\delta^{13}\text{C}$ and $\delta^{15}\text{N}$ isotope analyses, filters were trimmed of excess, then one half of the filter was wrapped into a 10x10 mm tin. Encapsulated GF/F samples were placed in a 48 plate well and shipped for analysis. Dried, homogenized vegetation samples were weighed to the nearest 4 mg, while dried, homogenized consumer muscle samples were weighted to the nearest 1 mg. Encapsulated solid materials were wrapped into 9x5 mm tins and placed in 96 plate wells to be shipped for analyses.

All stable isotope analyses were done through the Stable Isotopes for Biosphere Science (SIBS) Laboratory at Texas A&M University at College Station. Analysis of the stable isotopes C and N was performed using an Elemental Analyzer (Costech Analytical Technologies, Valencia, CA, USA) coupled to a Thermo Scientific Delta V Isotope Ratio Mass Spectrometer in continuous flow (He) mode (EA-IRMS; Thermo Fisher Scientific, Waltham, MA, USA). Calibration of carbon was performed using United States Geological Survey Glutamic Acid 40 and Glutamic Acid 41 as standards, as well as two in-house laboratory developed standards SIBS-pEc and SIBS-pCo. Atmospheric nitrogen was used for calibration of $\delta^{15}\text{N}$ values. Stable isotope data were presented in standard delta notation in per mil units (‰), δC , δN , or $\delta\text{S} = [(R_{\text{sample}}/R_{\text{standard}}) - 1] \times 1000$, where X is the heavy isotope, R_{sample} is the ratio of heavy to light isotope in the sample, and R_{standard} is the ratio of heavy to light isotope in the reference standard.

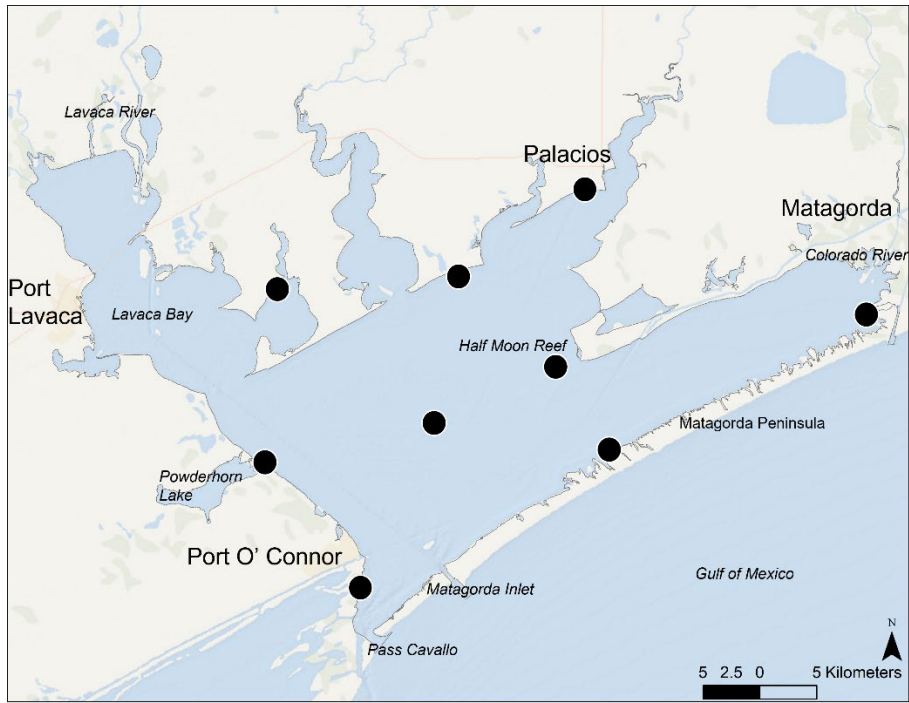


Figure 143. General sampling locations for stable isotope samples in West Matagorda Bay.

Results

We obtained a total of 144 POM, 110 BMA, 43 seagrass, 84 marsh grass, 30 macroalgae, and 6 mangrove samples (Table 32). We received a total of 132 POM and 93 BMA bulk $\delta^{13}\text{C}$ and $\delta^{15}\text{N}$ isotope values, while all other primary producers were analyzed in full (Table 32; Figure 144). Mangroves had the most depleted (mean \pm SD) $\delta^{13}\text{C}$ signature (-24.55 ± 1.59 ‰), while marsh grass (-12.74 ± 0.82 ‰) and seagrasses (-12.44 ± 1.87 ‰) had the most enriched $\delta^{13}\text{C}$ signatures. BMA (-16.97 ± 2.79 ‰) and macroalgae (-18.00 ± 3.47 ‰) had the largest variation among their signatures, with a relatively large overlap along the $\delta^{13}\text{C}$ axis between the two.

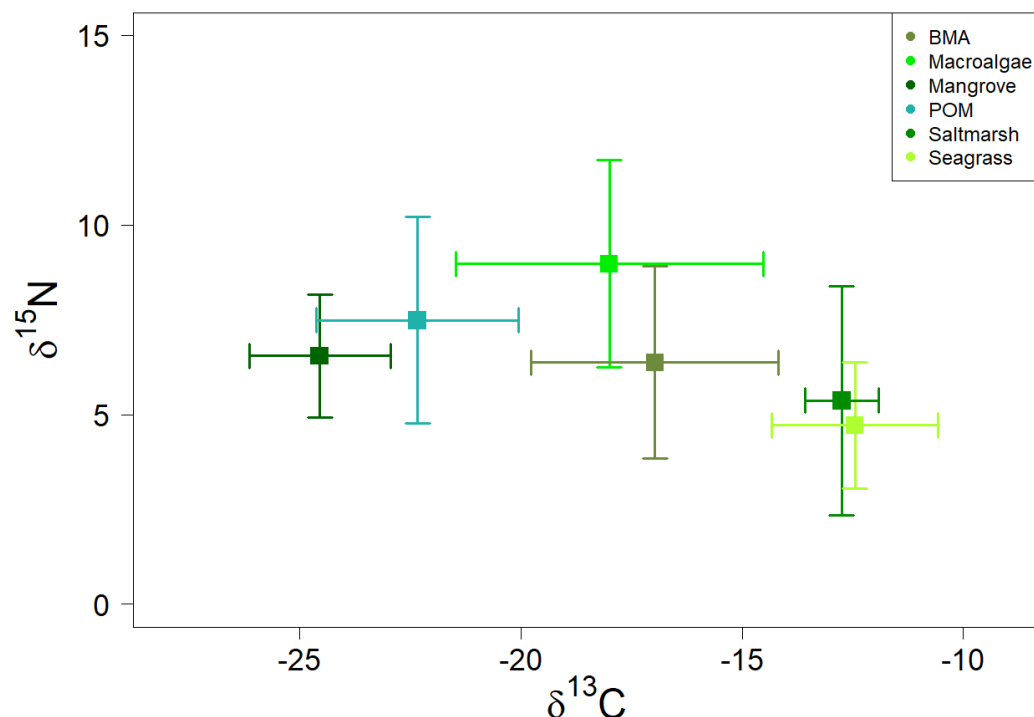


Figure 144. Isotopic biplot of primary producers collected as energy sources within the West Matagorda Bay food web.

We obtained a total of 67 zooplankton samples and have received a total of 56 isotope values. Zooplankton $\delta^{13}\text{C}$ values ranged from -27.9 to -17.52 ‰ (-22.01 ± 2.2 ‰), while $\delta^{15}\text{N}$ values ranged from 1.23 to 14.29 (8.63 ± 2.73 ‰) (Table 1; Figure 3). Zooplankton signatures overlapped with POM signatures, even though efforts were taken to remove POM signatures from the zooplankton samples, although the mean $\delta^{15}\text{N}$ for zooplankton was comparatively higher than POM.

A total of 51 bag seine collections were conducted throughout the study. From these collections, approximately 88 samples were selected for isotope analysis to quantify primary consumer isotope signatures. These samples have been processed for isotope analysis, but data has not yet been received.

We obtained a total of 947 consumers for this study, of which approximately 500 were selected for isotope analysis. Consumer selection was based on collection date and site, and sampling triplicates when applicable for improved statistical power and mixing model capabilities.

We received 356 bulk $\delta^{13}\text{C}$ and $\delta^{15}\text{N}$ isotope values for secondary consumers across 26 species (Table 32; Figure 145). Across fishes, mean $\delta^{15}\text{N}$ values ranged from 10.73 ‰ (Striped Mullet) to 18.3 ‰ (Spinner Shark). The top three trophic levels indicated by $\delta^{15}\text{N}$ values were occupied by Spinner Shark (18.3 ± 0.9 ‰), Atlantic Sharpnose Shark (17.1 ± 0.4 ‰), and Gafftopsail Catfish (17.0 ± 1.1 ‰). In contrast, the lowest three trophic levels were occupied by Striped Mullet (10.7 ± 2.34 ‰), Sheepshead (12.1 ± 1.4 ‰), and Gizzard Shad (12.6 ± 2.12 ‰). $\delta^{13}\text{C}$ values for consumers ranged from -24.0 (gizzard shad) to -12.9 (Atlantic Stingray); these values were well within the total range of primary producer $\delta^{13}\text{C}$, indicating the source endmembers were sufficiently quantified for mixing models of the Matagorda Bay food web (Figure 146). There was no significant difference between the five species of shrimps analyzed for this study, so all shrimp species are represented by a single point in the isotope biplot (Figure 4; Anova, $F_{4,14} = 0.592$, $p = 0.67$).

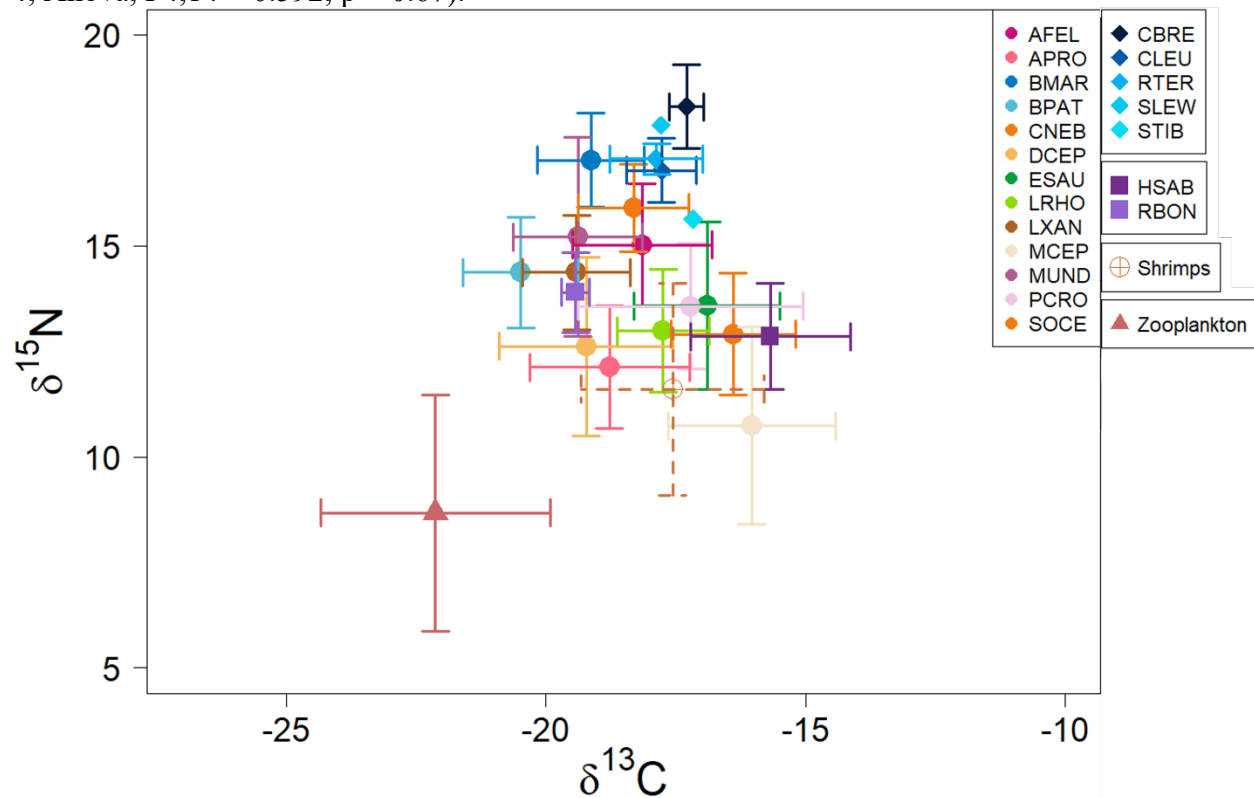


Figure 145. Isotopic biplot of primary consumers (zooplankton) and secondary consumers (micronekton) collected within Matagorda Bay. Each species is represented by a unique color, and described in the legend using a three letter code representative of their species name: Teleost fishes: AFEL, *Ariopsis felis*; APRO, *Archosargus probatocephalus*; BMAR, *Bagre marinus*; BPAT, *Brevoortia patronus*; CNEB, *Cynoscion nebulosus*; DCEP, *Dorosoma cepedianum*; ESAU, *Elops saurus*; LRHO, *Lagodon rhomboides*; LXAN, *Leiostomus xanthurus*; MCEP, *Mugil cephalus*; MUND, *Micropogonias undulatus*; PCRO, *Pogonias cromis*; SOCE, *Sciaenops ocellatus*. Sharks: CBRE, *Carcharhinus brevipinna*; CLEU, *Carcharhinus leucas*; RTER, *Rhizoprionodon terraenova*; SLEW; *Sphyrna lewini*, STIB; *Sphyrna tiburo*. Stingrays: HSAB, *Hypanus sabinus*; RBON, *Rhinoptera bonasus*. Shrimps are the pooled signature of *Panaeid* and *Palaemonetes* sp..

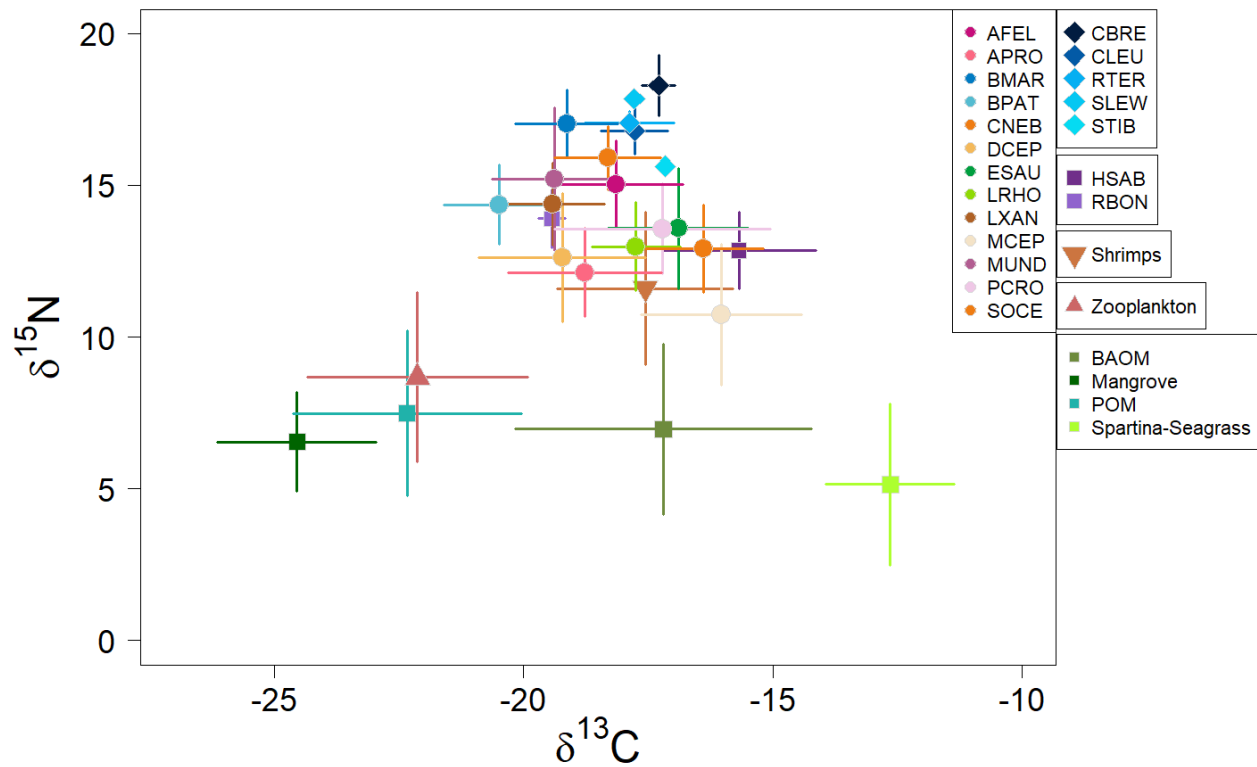


Figure 146. Isotopic biplot of primary producers (diet sources), primary consumers (zooplankton), and secondary consumers (macronekton) sampled in Matagorda Bay 2020 – 2021. Some primary producers were combined based on overlap along the $\delta^{13}\text{C}$ axis into BAOM (Benthic algal organic matter) and Spartina-Seagrass (saltmarsh and seagrasses). Teleost fish species are uniquely colored in circles, sharks are uniquely colored diamonds, stingrays are uniquely colored squares, shrimp species are combined and represented as a single upside down triangle, zooplankton are the pink triangle, and producers are uniquely colored squares in green shades.

Table 32. Collection and $SI A_{bulk}$ summary of Matagorda Bay food web.

	Code/Abbreviation	n Collected	n Selected for $SI A_{bulk}$	n $SI A_{bulk}$ data in hand	$\delta^{13}C$ range (mean \pm SD)	$\delta^{15}N$ range (mean \pm SD)	$\delta^{34}S$ range (mean \pm SD)	Size (see footnote) range (mean \pm SD) (mm)
<i>Primary Producers</i>								
Particulate Organic Matter (POM)	POM	144	144	132	-27.14 to -15.49 (-22.34 \pm 2.29)	-8.80 to 16.19 (7.48 \pm 2.72)	-	-
Benthic Microalgae (BMA)	BMA	110	110	93	-23.40 to -11.82 (-16.97 \pm 2.79)	-3.81 to 12.24 (6.37 \pm 2.53)	-	-
Seagrasses (<i>Halodule</i> , <i>Ruppia</i> , <i>Halophila</i>)	Seagrass	43	43	43	-16.86 to -9.29 (-12.45 \pm 1.87)	1.03 to 8.34 (4.72 \pm 1.66)	-	-
			18	18	-	-	-6.79 to 7.38 (2.26 \pm 4.62)	-
Saltmarsh cordgrass (<i>Spartina alterniflora</i>)	Saltmarsh	84	84	84	-14.91 to -11.09 (-12.75 \pm 0.82)	-1.12 to 11.5 (5.37 \pm 3.02)	-	-
			18	18	-	-	-9.76 to 13.89 (-0.35 \pm 7.18)	-
Macroalgae		30	30	30	-25.84 to -10.57 (-18.0 \pm 3.47)	1.43 to 14.53 (8.97 \pm 2.73)	-	-
Black mangrove (<i>Avicennia germinans</i>)		6	6	6	-26.87 to -22.66 (-24.55 \pm 1.59)	4.80 to 9.10 (6.54 \pm 1.62)	-	-
<i>Primary Consumers</i>								
Zooplankton		67	67	56	-27.29 to -17.52 (-22.01 \pm 2.20)	1.23 to 14.29 (8.63 \pm 2.73)	-	-
Blue crabs (<i>Callinectes sapidus</i>)	CSAP	52	24	3	-20.1 to -17.5 (-19.5 \pm 0.5)	9.1 to 13.0 (11.5 \pm 2.1)	-	140 to 170 (157.7 \pm 15.7)
Brown shrimp (<i>Farfantepenaeus aztecus</i>)	FAZT	20	10	4	-19.1 to -14.6 (-17.2 \pm 2.1)	8.3 to 15.3 (11.7 \pm 3.3)	-	17.7 to 35 (25.9 \pm 7.2)
Pink shrimp (<i>Farfantepenaeus duorarum</i>)	FDUO	4	4	3	-19.0 to -14.6 (-17.2 \pm 2.2)	8.6 to 13.3 (11.3 \pm 2.4)	-	21.16 to 25 (22.7 \pm 2.01)
White shrimp (<i>Litopenaeus setiferus</i>)	LSET	22	14	5	-20.9 to -15.8 (-18.6 \pm 2.3)	8.0 to 14.7 (11.9 \pm 2.9)	-	10 to 29 (17.5 \pm 7.3)
Daggerblade grass shrimp (<i>Palaemonetes pugio</i>)	PPUG	27	18	4	-17.5 to -16.3 (-16.9 \pm 0.59)	8.8 to 14.3 (11.8 \pm 2.3)	-	8.3 to 13.6 (11.04 \pm 2.2)
Marsh grass shrimp (<i>Palaemonetes vulgaris</i>)	PVUL	16	8	3	-18.5 to -16.3 (-17.5 \pm 1.1)	7.6 to 13.5 (11.0 \pm 3.1)	-	10.3 to 11.5 (10.9 \pm 6.01)
<i>Secondary Consumers (fishes and elasmobranchs)</i>								
Hardhead catfish (<i>Ariopsis felis</i>)	AFEL	147	61	59	-21.1 to -14.6 (-18.1 \pm 1.3)	12.6 to 17.9 (15.0 \pm 1.45)	-	50 to 340 (218 \pm 62.3)
Sheepshead (<i>Archosargus probatocephalus</i>)	APRO	11	11	2	-19.86 to -17.69 (-18.7 \pm 1.5)	11.1 to 13.2 (12.1 \pm 1.4)	-	217 to 247 (232 \pm 21.2)
Gafftopsail catfish (<i>Bagre marinus</i>)	BMAR	22	22	18	-21.6 to -17.5 (-19.1 \pm 1.03)	14.5 to 18.7 (17.0 \pm 1.1)	-	174 to 980 (401.2 \pm 212.5)
Gulfmenhaden (<i>Brevoortia patronus</i>)	BPAT	92	34	14	-22.1 to -17.9 (-20.5 \pm 1.1)	12.3 to 16.5 (14.3 \pm 1.3)	-	70 to 198 (139 \pm 34.1)
Spinner shark (<i>Carcharhinus brevipinna</i>)	CBRE	6	6	6	-17.8 to -16.9 (-17.3 \pm 0.3)	16.5 to 19.1 (18.3 \pm 0.9)	-	336 to 604 (409.7 \pm 98.4)
Bull shark (<i>Carcharhinus leucas</i>)	CLEU	16	15	12	-18.8 to -16.9 (-17.7 \pm 0.67)	15.6 to 18.1 (16.8 \pm 0.76)	-	670 to 1300 (962.3 \pm 178.2)
Spotted seatrout (<i>Cynoscion nebulosus</i>)	CNEB	51	37	28	-21.2 to -16.1 (-18.3 \pm 1.1)	14.0 to 17.6 (15.9 \pm 1.03)	-	78 to 640 (327 \pm 102.2)
Gizzard shad (<i>Dorosoma cepedianum</i>)	DCEP	25	19	19	-24.0 to -17.5 (-19.2 \pm 1.67)	9.8 to 16.6 (12.6 \pm 2.12)	-	191 to 307 (232.7 \pm 40.6)
Ladyfish (<i>Elops saurus</i>)	ESAU	14	14	9	-18.3 to -13.7 (-16.9 \pm 1.4)	9.9 to 15.8 (13.6 \pm 1.9)	-	215 to 485 (350.4 \pm 104.5)
Atlantic stingray (<i>Hypopus sabinus</i>)	HSAB	71	71	64	-19.5 to -12.9 (-15.6 \pm 1.53)	10.3 to 17.3 (12.9 \pm 1.3)	-	200 to 542 (307.1 \pm 58.5)
Pinfish (<i>Lagodon rhomboides</i>)	LRHO	119	52	15	-19.4 to -16.1 (-17.7 \pm 0.88)	10.9 to 15.9 (12.9 \pm 1.5)	-	60 to 183 (119 \pm 46.2)
Spot (<i>Leiostomus xanthurus</i>)	LXAN	21	14	8	-20.6 to -17.6 (-19.4 \pm 1.04)	13.1 to 17.2 (14.4 \pm 1.4)	-	152 to 550 (226.1 \pm 131.7)
Striped mullet (<i>Mugil cephalus</i>)	MCCEP	148	48	9	-18.8 to -13.6 (-16.0 \pm 1.61)	8.34 to 14.6 (10.7 \pm 2.34)	-	145 to 292 (230 \pm 55.8)
Atlantic croaker (<i>Micropogonias undulatus</i>)	MUND	23	18	16	-22.1 to -17.2 (-19.4 \pm 1.2)	10.3 to 18.3 (15.2 \pm 2.4)	-	121 to 203 (160.1 \pm 21.2)
Black drum (<i>Pogonias cromis</i>)	PCRO	27	27	18	-20.8 to -13.6 (-17.2 \pm 2.2)	11.4 to 16.5 (13.6 \pm 1.5)	-	159 to 800 (372.7 \pm 161.9)
Cownose ray (<i>Rhinoptera bonasus</i>)	RBON	3	3	3	-19.7 to -19.2 (-19.4 \pm 0.26)	12.8 to 14.7 (13.9 \pm 0.9)	-	712 to 780 (746 \pm 34)
Atlantic sharpnose shark (<i>Rhizoprionodon terraenovae</i>)	RTER	4	4	4	-18.7 to -16.9 (-17.9 \pm 0.89)	16.7 to 17.5 (17.1 \pm 0.4)	-	422 to 710 (595.3 \pm 131.9)
Scalloped hammerhead shark (<i>Sphyrna lewini</i>)	SLEW	1	1	1	-17.8	17.8	-	526
Red drum (<i>Sciaenops ocellatus</i>)	SOCE	42	39	28	-18.6 to -14.7 (-16.4 \pm 1.2)	10.1 to 15.6 (12.9 \pm 1.4)	-	145 to 542 (303.8 \pm 81.6)
Bonnethead shark (<i>Sphyrna tiburo</i>)	STIB	1	1	1	-17.2	15.6	-	690

¹Sizes were measured depending on taxa. Blue crab measurements reflect Carapace Width (CW) in mm; Shrimp measurements reflect Carapace Length (CL) in mm; Teleost fishes and shark measurements reflect Standard Length (SL) in mm; Stingray measurements reflect Disc Width (DW) in mm.

Goal 2: Quantify the relative importance of individual producers and energy sources to the overall food web in the bay and to specific species

To quantify the relative importance of individual producers and energy sources to the overall food web in Matagorda and to specific species, Bayesian stable isotope mixing models in R (package: *simmr*; Parnell (2019)) were conducted (Phillips et al. 2014). To provide the *simmr* model with the most simplified versions of production sources within the Matagorda food web, producers of ecological similarity and with high degrees of overlap specifically along the $\delta^{13}\text{C}$ axis were grouped together. The resulting sources for the *simmr* model included POM, BAOM (benthic algal organic matter: grouped BMA and macroalgae), and C4 plants (grouped marsh and seagrasses) (Figure 147A). Mangrove was removed as a source for the final model since preliminary modeling determined the overall contribution of mangrove as a source to the estuarine consumers was extremely low. Additionally, we were only able to obtain a few samples of mangrove before they died off following the hard freeze event of February 2021. Fifteen consumer species were included in the model, determined by having enough isotope values available to make a meaningful model (Figure 147A).

The mean (\pm SE) percent contributions from each source across all twelve species were $40.12 \pm 1.78\%$ for POM, $32.74 \pm 0.98\%$ for BAOM, and $27.23 \pm 0.68\%$ for C4 Plants (Table 33). POM had the highest mean (\pm SD) source contribution for gulf menhaden ($69.8 \pm 7.9\%$), whereas POM had the lowest source contribution for Atlantic stingray ($11.9 \pm 5.4\%$) (Figure 147B). In contrast, BAOM had the highest mean source contribution for striped mullet ($40.1 \pm 20.2\%$), whereas BAOM had the lowest source contribution for black drum ($56.5 \pm 21.3\%$) (Figure 147C). C4 Plant source contribution ranged from $10.7 \pm 5.3\%$ (gulf menhaden) to $45.5 \pm 7.4\%$ (red drum) (Figure 147D). While C4 Plants were not a direct source of contribution to the fifteen species included in the *simmr* model, seagrass and marsh grass signatures may be able to be used to determine a spatial context to isotope signatures since the seagrass and marsh grass is distributed along gradients within Matagorda Bay.

Table 33. Mean (\pm SD) percent source contributions to consumers of Matagorda Bay food web resulting from simmr model. Sources included particulate organic matter (POM), benthic algal organic matter (BAOM), and seagrasses and marsh grass (C4 Plants).

	% Source Contributions (mean \pm SD)		
	POM	BAOM	C4 Plants
Hardhead catfish (<i>Ariopsis felis</i>)	43.5 \pm 5.9	29.9 \pm 11.5	26.7 \pm 6.4
Gafftopsail catfish (<i>Bagre marinus</i>)	54.7 \pm 7.3	25.1 \pm 12.2	20.1 \pm 7.0
Gulf menhaden (<i>Brevoortia patronus</i>)	69.8 \pm 7.9	19.5 \pm 10.0	10.7 \pm 5.3
Spotted seatrout (<i>Cynoscion nebulosus</i>)	47.3 \pm 5.9	24.1 \pm 11.0	28.6 \pm 6.4
Gizzard shad (<i>Dorosoma cepedianum</i>)	54.0 \pm 9.3	30.9 \pm 14.7	15.1 \pm 7.6
Ladyfish (<i>Elops saurus</i>)	27.5 \pm 10.8	38.2 \pm 19.8	34.3 \pm 12.3
Pinfish (<i>Lagodon rhomboides</i>)	40.8 \pm 7.3	25.8 \pm 13.3	33.4 \pm 8.1
Spot (<i>Leiostomus xanthurus</i>)	56.2 \pm 11.2	26.5 \pm 14.9	17.3 \pm 8.2
Striped mullet (<i>Mugil cephalus</i>)	19.3 \pm 9.8	41.4 \pm 20.7	39.3 \pm 14.6
Atlantic croaker (<i>Micropogonias undulatus</i>)	56.9 \pm 8.1	26.1 \pm 12.9	17.0 \pm 7.2
Black drum (<i>Pogonias cromis</i>)	22.3 \pm 11.6	56.5 \pm 21.3	21.2 \pm 11.9
Red drum (<i>Sciaenops ocellatus</i>)	26.5 \pm 6.6	28.0 \pm 13.0	45.5 \pm 7.4
Atlantic stingray (<i>Hypanus sabinus</i>)	11.9 \pm 5.4	44.5 \pm 11.1	43.6 \pm 6.5
Bull shark (<i>Carcharhinus leucas</i>)	41.9 \pm 33.8	25.5 \pm 13.4	33.7 \pm 8.3
Shrimps (Panaeids, <i>Palaemonetes</i> sp.)	29.0 \pm 10.7	49.1 \pm 19.4	21.9 \pm 10.6

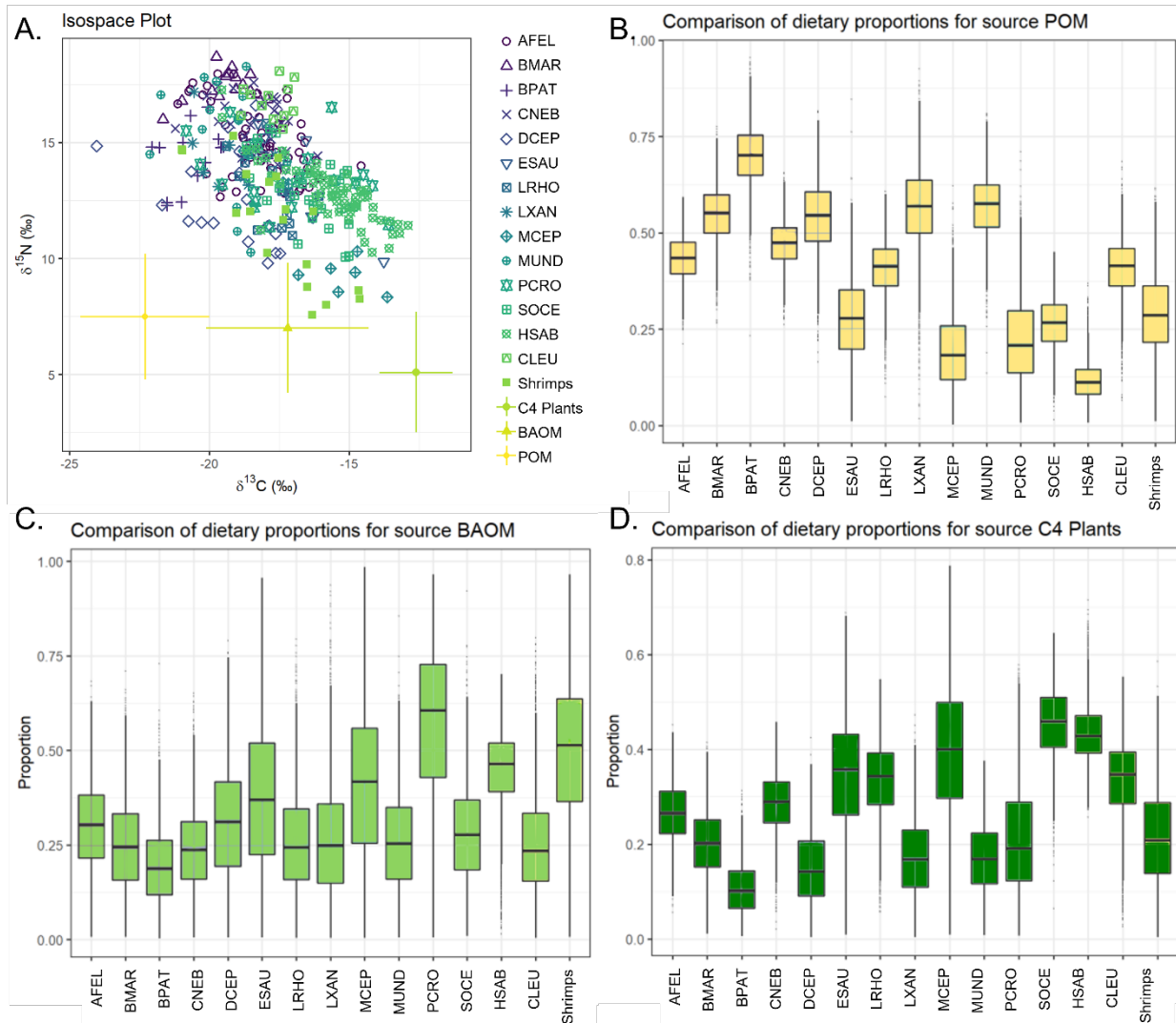


Figure 147. Results from simmr model. A) Isospace plot with grouped sources and consumer species used in final mixing model. Dietary proportions of sources B) POM, C) BAOM, and D) C4 Plants to the consumer species in the final simmr model.

Goal 3: Evaluate the influence of habitat arrangement on trophic ecology of the Matagorda Bay Complex

The influence of habitat arrangement on the trophic ecology of the Matagorda Bay Complex can be assessed directly through the use of primary producers. Spatial inverse distance weighted interpolations (IDWs) were done for POM and BMA across each season to assess spatial influences of producer values (Figure 148). POM showed a fairly strong seasonal gradient where values were more depleted near the Colorado River and Palacios, compared to more depleted areas near Powderhorn Lake in the summer. POM can directly relate to seasonal rain patterns by becoming more enriched with increasing salinity (Fry and Sherr 1989, Lebreton et al. 2016). POM was most $\delta^{13}\text{C}$ enriched during the fall. In contrast, BMA values were most depleted across the bay during the fall, and the most enriched during winter and spring. These interpolations are helpful for visualizing isotopic patterns observed in Matagorda Bay, yet they

do interpolate over space far from where samples were sometimes collected. With completed isotope data, a complex mixing model (*MixSiar*) can be done to fully understand spatial (i.e., habitat) patterns on the food web of Matagorda Bay (Parnell et al. 2010, Parnell et al. 2013).

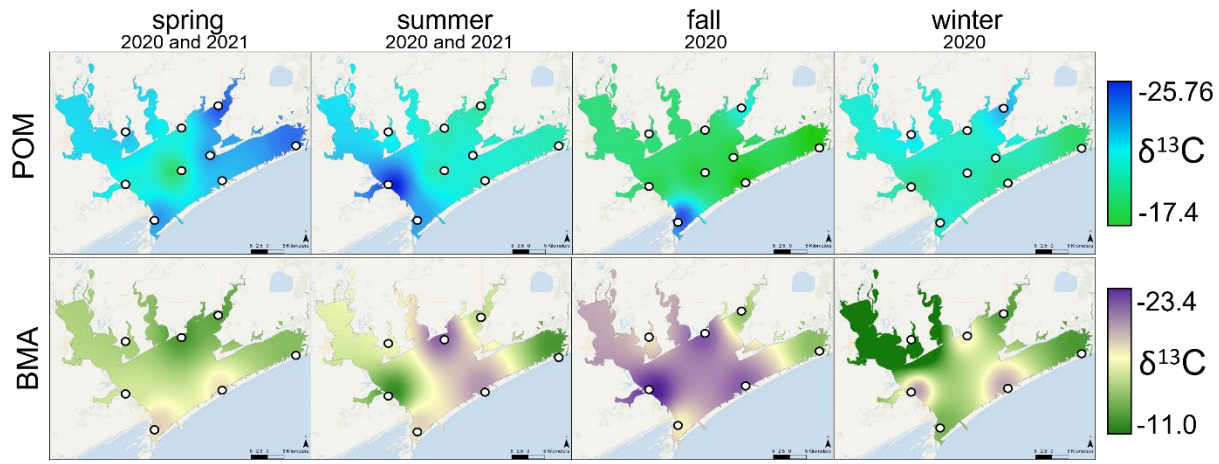


Figure 148. Inverse distance weighted (IDW) interpolations of $\delta^{13}\text{C}$ for particulate organic matter (POM) and benthic microalgae (BMA) across seasons in West Matagorda Bay. Relatively depleted values of $\delta^{13}\text{C}$ are shown in blue for POM and purple for BMA, relatively enriched values of $\delta^{13}\text{C}$ are shown in green. Sampling locations for each producer are marked by white circles.

Additionally, stable isotope analysis of sulfur ($\delta^{34}\text{S}$) has proven to be a useful tool in estuarine food web ecology studies. Previous studies have used the addition of sulfur as a third element in an attempt to determine the importance of potential food sources unable to be distinguished using a dual element approach (Moncreiff and Sullivan 2001, Connolly et al. 2004, Fry et al. 2008). Estuarine plants typically have four available sources of sulfur, so by different producers utilizing different sources of S, it allows for different signatures. Using $\delta^{34}\text{S}$ as an added tracer to the Matagorda Bay food web helps to evaluate the influence of habitat arrangement on the trophic ecology of the bay as there is a spatial gradient of seagrasses and marsh grasses within Matagorda Bay. By distinguishing different $\delta^{34}\text{S}$ values for each of these producers, this information can greatly enhance our understanding of the Matagorda Bay Complex food web.

We analyzed some preliminary data ($n = 18$), using $\delta^{34}\text{S}$ to separate seagrass and marsh grass producers in the marine based food web of Matagorda Bay (Figure 149). For $\delta^{34}\text{S}$ isotope analyses, additional vegetation samples were weighed to the nearest 5 mg. Seagrass $\delta^{34}\text{S}$ ranged from -6.79 to 7.38 ‰ (2.26 ± 4.62 ‰). Marsh grass (*Spartina*) $\delta^{34}\text{S}$ ranged from -9.76 to 13.89 (- 0.35 ± 7.18 ‰). Seagrass and marsh grass were separated by 2.61 ‰ along the $\delta^{34}\text{S}$ axis, compared to being only separated by 0.3 ‰ along the $\delta^{13}\text{C}$ axis. In general, $\delta^{34}\text{S}$ signatures for producers tend to be further apart than those for $\delta^{13}\text{C}$ and $\delta^{15}\text{N}$, and although variation within producer samples is also higher, the use of $\delta^{34}\text{S}$ is promising for thoroughly understanding the complexities of the Matagorda Bay food web. By applying $\delta^{34}\text{S}$ analysis to additional seagrass and marsh grass samples, as well as consumers of Matagorda Bay, mixing model accuracy can be improved and incorporate the spatial component that is presented by the natural distribution of these two habitat types.

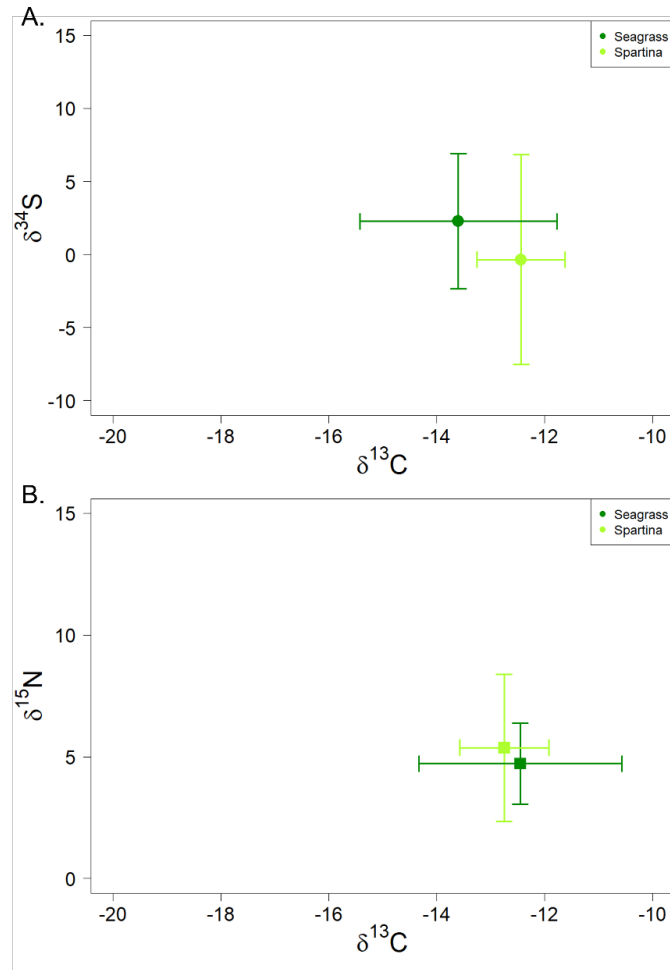


Figure 149. A) Preliminary data ($n = 18$) separating seagrass and marsh grass producer values using $\delta^{34}\text{S}$. B) Original seagrass ($n = 43$) and marsh grass ($n = 84$) producer values from Figure 139 for reference.

Continued Work

Due to the nature of isotope analyses, we will continue to update the food web contribution models presented here as we receive more data from the processing laboratories. Additionally, further work with $\delta^{34}\text{S}$ analyses will be applied to consumers of Matagorda Bay and incorporated into mixing models.

Compound specific isotope analysis of amino acids (CSIA-AA) is a recently developed technique that provides information into food web dynamics without some of the challenges associated with bulk stable isotope analysis. For instance, the $\delta^{15}\text{N}_{\text{AA}}$ “source” AAs (e.g., phenylalanine) change very little during trophic transfers, and thus reflect their “source” isotopic value. Therefore, source amino acids can provide more accurate information on the contribution of diet sources towards consumers, without collecting and quantifying that information separately. These methods have great potential to elucidate sources of production and potential sources that were not initially collected as part of the bulk stable isotope components of this study. Using a few key predators of the Matagorda Bay Complex: red drum, gafftopsail catfish, spotted seatrout, carcharhinid sharks, and Atlantic stingrays, we intend to estimate trophic positions and add refined food web ecology information to what is already presented here.

Literature Cited

- Chanton, J., and F. G. Lewis. 2002. Examination of coupling between primary and secondary production in a river-dominated estuary: Apalachicola Bay, Florida, USA. *Limnology and Oceanography* **47**:683-697.
- Connolly, R. M., M. A. Guest, A. J. Melville, and J. M. Oakes. 2004. Sulfur stable isotopes separate producers in marine food-web analysis. *Oecologia* **138**:161-167.
- Deegan, L. A., and R. H. Garritt. 1997. Evidence for spatial variability in estuarine food webs. *Marine Ecology Progress Series* **147**:31-47.
- Fry, B. 2007. Coupled N, C and S stable isotope measurements using a dual-column gas chromatography system. *Rapid Communications in Mass Spectrometry: An International Journal Devoted to the Rapid Dissemination of Up-to-the-Minute Research in Mass Spectrometry* **21**:750-756.
- Fry, B., M. Cieri, J. Hughes, C. Tobias, L. A. Deegan, and B. Peterson. 2008. Stable isotope monitoring of benthic-planktonic coupling using salt marsh fish. *Marine Ecology Progress Series* **369**:193-204.
- Fry, B., and E. B. Sherr. 1989. $\delta^{13}\text{C}$ measurements as indicators of carbon flow in marine and freshwater ecosystems. Pages 196-229 *Stable Isotopes in Ecological Research*. Springer.
- Lebreton, B., J. B. Pollack, B. Blomberg, T. A. Palmer, L. Adams, G. Guillou, and P. A. Montagna. 2016. Origin, composition and quality of suspended particulate organic matter in relation to freshwater inflow in a South Texas estuary. *Estuarine, Coastal and Shelf Science* **170**:70-82.
- Matich, P., O. N. Shipley, and O. C. Weideli. 2021. Quantifying spatial variation in isotopic baselines reveals size-based feeding in a model estuarine predator: implications for trophic studies in dynamic ecotones. *Marine Biology* **168**:1-12.
- Moncreiff, C. A., and M. J. Sullivan. 2001. Trophic importance of epiphytic algae in subtropical seagrass beds: evidence from multiple stable isotope analyses. *Marine Ecology Progress Series* **215**:93-106.
- Parnell, A. 2019. Package 'simmr'.
- Parnell, A. C., R. Inger, S. Bearhop, and A. L. Jackson. 2010. Source partitioning using stable isotopes: coping with too much variation. *PLoS One* **5**:e9672.
- Parnell, A. C., D. L. Phillips, S. Bearhop, B. X. Semmens, E. J. Ward, J. W. Moore, A. L. Jackson, J. Grey, D. J. Kelly, and R. Inger. 2013. Bayesian stable isotope mixing models. *Environmetrics* **24**:387-399.
- Peterson, B. J., and B. Fry. 1987. Stable isotopes in ecosystem studies. *Annual Review of Ecology and Systematics* **18**:293-320.
- Phillips, D. L., R. Inger, S. Bearhop, A. L. Jackson, J. W. Moore, A. C. Parnell, B. X. Semmens, and E. J. Ward. 2014. Best practices for use of stable isotope mixing models in food-web studies. *Canadian Journal of Zoology* **92**:823-835.
- Post, D. M. 2002. Using stable isotopes to estimate trophic position: models, methods, and assumptions. *Ecology* **83**:703-718.
- Winemiller, K. O., S. Akin, and S. C. Zeug. 2007. Production sources and food web structure of a temperate tidal estuary: integration of dietary and stable isotope data. *Marine Ecology Progress Series* **343**:63-76.

Habitat and Resource Use Across the Matagorda Bay Ecosystem

Overview

The estuarine environment is characterized by a diverse combination of habitat types—including oyster reefs, seagrass beds, wind-tidal flats, intertidal and subtidal soft-sediments, and marshes—that serve many important functions. Oyster reefs provide valuable ecosystem services including water filtration, shoreline stabilization, and provision of habitat for ecologically and economically important species like shrimp, crabs, and fishes (Boesch & Turner 1984, Grabowski et al. 2012, Ehrich & Harris 2015). Seagrass beds provide habitat that supports fisheries by acting as nursery grounds for juveniles (Duarte 2002, Barbier et al. 2011), and produce and store large quantities of organic carbon, with global net production estimated at $0.6 \times 10^{13} \text{ g C yr}^{-1}$ (Duarte & Chiscano 1999, Cullen-Unsworth & Unsworth 2013). Wind-tidal flats and microphytobenthos (microalgal)-dominated soft-sediments are also important contributors to the productivity of shallow estuarine systems. Microalgal species growing in the surface sediments can have higher productivity than both local macroalgal and phytoplankton production at $3.4 \times 10^9 \text{ g C yr}^{-1}$ (Pinckney & Zingmark 1993, Ansell et al. 1999). Additionally, these soft-sediment environments are home to many infaunal species that are important for wading bird and shorebird diets (Powell 1987, Congdon & Catterall 1994). Salt marshes filter water entering estuarine areas, provide habitat, and boost production of many ecologically and economically important fisheries species (Barbier et al. 2011).

Estuarine areas are increasingly exploited and threatened by anthropogenic and climate-driven stressors (i.e., habitat degradation, pollution) (Kappel 2005, Halpern et al. 2007). When habitats are degraded, the remaining ecological functions may not be diminished or lost (Ruesink et al. 2006). For instance, primary production and organic matter quality can vary greatly between habitat types (Correll 1978) and conversion of one habitat to another likely affects the fate of organic matter in food webs. Significant losses of primary producers from coastal areas have occurred at rapid pace (Kennish 2002, Airoidi & Beck 2007, Lotze et al. 2011), and consequences of these losses on ecosystem functioning are not yet fully understood. There is a need to better understand how estuarine habitats function, including flows of organic matter, and also how individual habitats contribute to overall ecosystem functioning (Elliott & Whitfield 2011).

Trophic interactions are an important aspect of understanding community dynamics through food web structure. These relationships help describe the ways in which energy is transferred between producers and their respective consumers through the flow of organic matter. However, these interactions are often complex as organisms' diets can be derived from many sources or can change based on resource availability and life history stages. The use of stable isotope compositions, especially carbon and nitrogen, have been deployed to unravel this complexity and to create more informative food webs.

Unique stable isotope compositions in primary producers are based on the origin of CO_2 (atmospheric, marine) and the used photosynthetic pathway (C4, C3, CAM). The combination of CO_2 source and photosynthetic pathway creates varied $\delta^{13}\text{C}$ values among primary producer types; C3 plants (e.g. *Batis maritima*) for instance have a much lower $\delta^{13}\text{C}$ value than seagrasses (Raven 1992, Fry 2006). While carbon isotope composition can inform the origin of organic matter in a given ecosystem, nitrogen isotope composition can provide information on trophic levels of consumers (Minagawa & Wada 1984, Post 2002). Consumers are more ^{15}N -enriched with increasing trophic levels, meaning that consumers from higher trophic levels have a higher concentration of ^{15}N . These unique stable isotope compositions can be used to narrow the

potential source of organic matter in consumer diets (Fry 2006). Ultimately the use of stable isotopes allows for higher resolution of food web mapping, based on what is assimilated by consumers, and better linkages between consumer and producer groups.

The use of stable isotopes can provide insight on the quantity and quality of organic matter, helping to better describe trophic interactions across habitat types. Stable isotopes can be used in combination with assessments of faunal community composition to help build a framework of food web interactions across different oyster reef settings.

Using Matagorda Bay as a study system, the focus of this portion of the research was to assess estuarine ecological functioning by combining information about flows of organic matter (i.e. determined using stable isotope compositions of food sources and consumers) with traditional community metrics (diversity, abundance, and biomass). Differences in primary producer biomass, quality, and distribution were assessed to determine their effects on the bay system as a whole.

Oyster Reefs

Introduction

Reefs built by the eastern oyster, *Crassostrea virginica*, support numerous ecological functions in estuarine ecosystems such as habitat provision, enhanced benthic pelagic coupling, and increased species biodiversity (Lenihan 1999, Beck et al. 2011). As ecosystem engineers, oysters increase structural complexity through reef formation (Humphries et al. 2011b, Karp et al. 2018), providing substrate for recruitment (O'Beirn et al. 2000) and refuge from predators (Soniati et al. 2004), that enhances local biodiversity (Godbold et al. 2011). Oyster reefs also release chemicals (e.g. from shells, living oysters, fouling organisms) that may act as settlement cues to facilitate recruitment (Tamburri et al. 1992, Turner et al. 1994, Smee et al. 2013). The physical structure of the reef can alter water flows and delivery of suspended organic matter to the sediments, enhancing feeding rates of reef-associated fauna (Lenihan 1999, Grabowski & Powers 2004) and reducing chlorophyll *a* and bacterial concentrations in the water column (Cressman et al. 2003).

Interactions between landscape setting and local environmental conditions can influence ecological structure and function on oyster reefs. Wind-directed dispersal and increased water flow can augment recruitment of invertebrate larvae and provide nourishment through resuspension of organic matter (Roegner & Mann 1995, Lenihan 1999). Proximity to adjacent habitat can also influence flow rates and faunal community composition on oyster reefs. Oyster reefs at marsh edges often experience slower water flow due to changes in coastline topography and attenuation of wave energy by vegetated habitat (Leonard & Croft 2006). Dampening of water movement by marsh grasses may decrease flow energies by an order of magnitude compared to areas without marsh (Leonard & Luther 1995). Oysters can have a positive feedback on this process by further reducing water velocity after their establishment which can promote sediment deposition and marsh accretion (Sharma et al. 2016, Ridge et al. 2017). Proximity to adjacent habitats can also increase reef-associated faunal abundance and diversity by increasing refugia and connectivity (Grabowski et al. 2005, Sharma et al. 2016, Gain et al. 2016).

Human activities can also influence reef structure and faunal community composition. Anthropogenic disturbance through increased boating traffic and commercial harvest can disrupt oyster settlement and negatively impact reef growth (Grizzle et al. 2002). Boat wakes erode shorelines and increase suspended sediment concentrations which can degrade oyster reef structures and affect reef diversity (Bilkovic et al. 2019). Oyster harvest in subtidal areas in the Gulf of Mexico is typically conducted using a dredge that can degrade the physical reef structure,

alter the biological community, and modify sediment biogeochemistry (Lenihan & Peterson 2004, Mercaldo-Allen & Goldberg 2011, Humphries et al. 2011b, Karp et al. 2018). Sediment resuspension from dredging activities can limit oyster recruitment (Powers et al. 2009). Reductions in reef structure due to dredging can also negatively impact reef-associated fauna density and diversity (Griffiths et al. 2006, Karp et al. 2018), and ecosystem service provision (Lenihan et al. 2001).

Severe declines in oyster reef habitat have prompted world-wide assessments of oyster population status (Kirby 2004, Jackson 2008, Beck et al. 2011, Zu Ermgassen et al. 2012), however, these assessments often consider all reefs to be the same, without consideration of differences in landscape setting and human activities. We characterized and compared subtidal oyster populations and reef fauna on open-bay reefs—isolated oyster bars oriented perpendicular to the shore in open water and open to harvest—and fringing reefs—parallel and directly adjacent to marsh habitat and closed to harvest—to determine how landscape setting influences oyster reef populations and provision of habitat for reef-resident fauna. Given the large extent of diversity of subtidal oyster reefs throughout Gulf of Mexico estuaries, increased understanding of the influence of landscape setting can help inform future management decisions.

Methods

Water quality

During each sampling event, water temperature (°C), salinity (PSU), dissolved oxygen (DO) concentration (mg l⁻¹), and pH were measured at each site using a YSI Pro DSS multiparameter Instrument (YSI ProDSS User Manual 2014). Surface sediment and suspended particulate organic matter were collected for chlorophyll *a* at all sampling sites via replicate benthic cores (2 cm deep, 38.5 cm² area) and 1L bottom water collections, respectively, during each sampling event.

In the laboratory, sediment samples were thawed and processed in the dark. Samples were sieved through a 500-µm mesh screen to eliminate macrofauna, large detrital particles, and shell hash, then freeze dried for 24-72 h and ground using a mortar and pestle. Water samples were sieved on a 250 µm mesh screen to remove large zooplankton and detritus, then filtered through pre-combusted glass fiber filters, and then freeze dried for 24 h. Chlorophyll *a* was extracted from filters and sediments overnight using a non-acidification technique and read on a Turner Trilogy fluorometer (Welschmeyer 1994; EPA method 445.0).

The effects of season and reef type on water quality and chlorophyll *a* were evaluated using two-way analysis of variance (ANOVA) tests, followed by the Westfall test for post hoc comparisons.

Faunal community

During each sampling event, four replicate 1.0 m² throw traps with 1 mm mesh sides and a modified 7.6 cm metal skirt on the bottom were pressed securely into each reef to collect fauna and ensure that no organisms could escape (Gain et al. 2016). Throw traps were deployed simultaneously at each reef to minimize disturbance. After the samplers were secured to the reef habitat, live and dead oysters were collected from a 0.5 m² subset of the enclosed area, counted, and measured for live oyster size and volume. All material was excavated to a depth of 0.1 m from a second, 0.25 m² subset of the enclosed area and thoroughly rinsed over a 500 mm mesh. All collected fauna were placed into jars with 10% buffered formalin. In the laboratory, fauna were identified to the lowest practical taxonomic level, counted, and soft tissues were weighed after drying for 24 h at 60 °C.

The effects of date and reef type on oyster density, size, and biomass, and faunal density, biomass, species richness, and Hill's N1 diversity were evaluated using two-way analysis of variance (ANOVA) tests unless noted otherwise. All data were either fourth-root or log-transformed to improve ANOVA normality assumptions. Post-hoc comparisons were performed using the Westfall test in multcomp package (Hothorn et al. 2008) where applicable. Univariate data management and analyses were performed using R Studio 4.0.0 (R Core Team 2021). Differences in biomass of reef fauna assemblages were described using non-metric multidimensional scaling analysis (nMDS; Clarke & Warwick 1994) with a Bray-Curtis similarity matrix, overlaid with results from cluster analysis of group averages. Biomass data were log transformed. Significant clusters were determined using similarity profile analysis (SIMPROF). Species that were contributing the most to dissimilarity between clusters were determined using similarity percentage analysis (SIMPER). Multivariate analyses were conducted using PRIMER v7.0 (Clarke & Gorley 2014).

Stable isotope analyses

Surface sediment organic matter (SSOM) and suspended particulate organic matter (SPOM) were collected at all sampling sites via replicate benthic cores (2 cm deep, 38.5 cm² area) and 1L bottom water collections, respectively, during each sampling event. Oysters were collected for sampling of oyster shell organic matter (OSOM). Water samples and oysters were transported to the laboratory in coolers in the dark.

In the laboratory, samples of SSOM were thawed and processed in the dark. Samples were sieved through a 500- μ m mesh screen to eliminate macrofauna, large detrital particles, and shell hash, then freeze dried for 24-72 h and ground using a mortar and pestle. Samples to be analyzed for the measurements of $\delta^{13}\text{C}$ values and % of organic carbon were decarbonated by adding 2 mol l⁻¹ HCl drop by drop until cessation of bubbling then allowed to completely dry at 65 °C on a heating block for 24-36 hours under a fume hood. These samples were then rinsed with ultrapure water, freeze-dried, and manually ground again.

Collection of OSOM was done by scrubbing the surface of lightly rinsed oyster shells into artificial seawater using a soft plastic brush. Water samples for SPOM and OSOM analyses were sieved on a 250 μ m mesh screen to remove large zooplankton and detritus, then filtered through pre-combusted glass fiber filters, and then freeze dried for 24 h. Carbonates were removed from filters for $\delta^{13}\text{C}$ and % of organic carbon measurements by contact with HCl fumes for 4 h in a vacuum-enclosed system. Nitrogen isotope compositions were determined using raw filters.

Chlorophyll *a* was extracted from filters (i.e. SPOM and OSOM) and sediments (i.e. SSOM) overnight using a non-acidification technique and read on a Turner Trilogy fluorometer (Welschmeyer 1994; EPA method 445.0).

Microphytobenthos were collected from the reef adjacent shoreline by scraping the first millimeter of sediment until a 1 L container was filled. Samples were transported in coolers (4°C) to the laboratory and Microphytobenthos were extracted using methods described by Riera & Richard (1996), modified by Herlory et al. (2007). Extracted samples were filtered on pre-combusted glass fiber filters and were processed and analyzed using the SPOM filter method outlined above.

Additional primary producers (C3 and C4 salt marsh plants) were collected from the shoreline adjacent to the oyster reefs. Leaves of the three of the most abundant C3 and C4 plants were collected, thoroughly washed stored at -20 °C, freeze-dried, and then ground to a homogenous fine powder. Nitrogen and carbon isotope compositions were determined on raw plant samples.

Fauna collected for stable isotope analysis were sieved live on a 500- μm mesh within 24 h of sample collection, separated by taxa, and placed in aquaria with artificial seawater for 24-48 hours to allow evacuation of gut contents. For each species identified, three individuals of differing size classes were reserved when possible. Soft tissues were collected from all macrofauna and mollusk shells were manually removed. All fauna samples were stored at -20°C , freeze-dried, and then ground to a homogenous fine powder. Nitrogen isotope compositions were analyzed on raw faunal samples. When samples had carbonates, they were also analyzed after decarbonation for $\delta^{13}\text{C}$ and % of organic carbon measurements. Samples were decarbonated by adding 2 mol l^{-1} HCl drop by drop until cessation of bubbling then allowed to completely dry at 65°C on a heating block for 24-36 hours under a fume hood. These samples were then rinsed with ultrapure water, freeze-dried, and manually ground again.

Appropriate amounts of each sample type were packed into tin capsules, except acidified sediment samples, which were packed in silver capsules and then packed into tin capsules to improve their combustion during the elemental analysis. Samples were prepared in Texas A&M University-Corpus Christi laboratories for stable isotope analysis before sending off for analysis of carbon and nitrogen at the University of La Rochelle Littoral, Environment and Societies Joint Research Unit stable isotope facility.

Stable isotope statistical analysis

Stable isotope data were analyzed using biplots and mixing models (SIMMR package in R) to determine and compare consumer food source uses between reef types across seasons. Consumers were grouped into guilds based on feeding strategy including: suspension, deposit, omnivore, and carnivore. Food sources used were determined across sampling periods to define important basal food sources and the flows of organic material through the communities. Consumer trophic levels (TL_i) were calculated using $\delta^{15}\text{N}$ values of some primary consumers as a baseline.

$$\text{TL}_i = 2 + \frac{(\delta^{15}\text{N}_i - \delta^{15}\text{N}_b)}{\text{TFF}}$$

where $\delta^{15}\text{N}_i$ is the $\delta^{15}\text{N}$ value of consumer (i) and $\delta^{15}\text{N}_b$ is the $\delta^{15}\text{N}$ value of the baseline. The baseline ($\delta^{15}\text{N}_b$) was calculated using the mean $\delta^{15}\text{N}$ values of the filter feeding bivalve *Crassostrea virginica* for each site and sampling period. A trophic fractionation factor (TFF) of 3.4‰ was used for $\delta^{15}\text{N}$ (Vander Zanden & Rasmussen 2001).

Stable isotope mixing models (SIMMs) were used to estimate resource contributions to consumer diets across reef types for each season. Exploratory analysis showed a significant portion of SSOM was comprised of microphytobenthos (MPB) and therefore only SSOM, SPOM, and OSOM were used in final mixing models. TFF's used in SIMMs for $\delta^{15}\text{N}$ was $2.5 \pm 2.5\text{‰}$ for primary consumers and $3.4 \pm 0.4\text{‰}$ for other consumers (Vander Zanden & Rasmussen 2001). TFF's for $\delta^{13}\text{C}$ was $0.4 \pm 1.3\text{‰}$ for all consumers (Post 2002). SIMMs were run for 10^5 iterations with a 5,000 iteration burn in. Median posterior distributions were calculated with 95% and 50% credibility intervals.

An index was developed in an effort to bridge information between community structure and functioning of the food web, to provide a more comprehensive view of the functioning of each reef type (i.e., open-bay reef and fringing reef) at each season. To better understand resource use at the community scale, an index of mean food resource contribution (MFRC) was also developed. The MFRC combines posterior distribution outputs from SIMMs for each taxon with taxon-specific biomass to determine the proportions of resources used within a community:

$$\text{MFRC}_j = \frac{\sum_{i=1}^n (\text{MPD}_{ij} \times B_i)}{\sum_{i=1}^n B_i}$$

where MPD_{ij} is the median posterior distribution of resource j for consumer i and B_i is the biomass of the consumer i in a community composed of n taxa. MFRCs were calculated for three resources: SSOM, SPOM, and OSOM, for each reef type per season.

Scheirer-Ray-Hare tests were used to compare isotope compositions of potential food sources and MFRCs between reef type and season unless indicated otherwise. Post-hoc comparisons were performed using the Dunn test with a Bonferroni adjustment when applicable.

Results & Discussion

Water quality

Water quality was similar between reef sites, with greater variation due to typical seasonal patterns rather than location (Figure 150). Average temperature and salinity were greater in summer 2020 (mean \pm standard deviation: 30.4 ± 1.0 °C, 25.2 ± 3.0) and lower in winter 2020 (17.5 ± 0.8 °C, 17.2 ± 3.4). Mean dissolved oxygen concentrations were inversely related to temperature (11.1 ± 2.4 mg L⁻¹ in winter 2020 and 6.1 ± 1.4 mg L⁻¹ in summer 2020). Sediment chlorophyll concentrations were greater at open-bay reefs ($7.0 \times 10^{-11} \pm 7.4 \times 10^{-11}$ g m⁻²) than fringing reefs ($1.4 \times 10^{-11} \pm 8.1 \times 10^{-12}$ g m⁻²), indicating more fresh organic matter was available in these reefs. This is likely due to the location of open-bay reefs, where water flow is stronger, and mixing is greater.

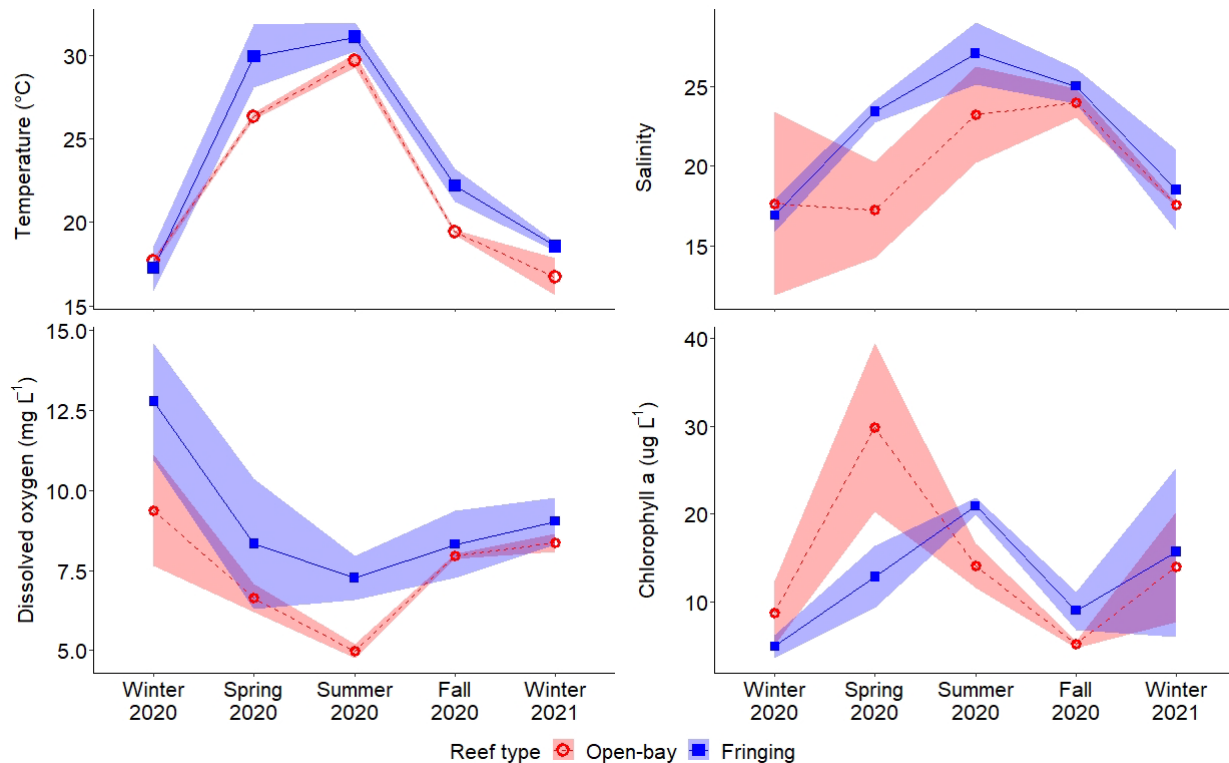


Figure 150. Temperature, salinity, dissolved oxygen, and chlorophyll a of suspended particulate organic matter (mean \pm standard deviations) in water at open-bay and fringing reefs in Matagorda Bay. Shaded areas represent standard deviations.

Reef Structure

Live oyster density was consistently higher on open-bay reefs (139 ± 153 ind. m^{-2}) than fringing reefs (23 ± 25 ind. m^{-2}) (ANOVA contrast, $p < 0.001$; Figure 151) and was lowest in summer 2020 for both reef types (ANOVA contrast, $p = 0.04$). Dead oyster shell density and volume were generally greater on open-bay reefs (1032 ± 715 ind. m^{-2} , $16.6 \times 10^{-3} \pm 11.5 \times 10^{-3}$ m^3) than fringing reefs (295 ± 284 ind. m^{-2} , $4.4 \times 10^{-3} \pm 5.9 \times 10^{-3}$ m^3) respectively (ANOVA contrast, $p = 0.007$, $p = 0.02$). This indicates there were greater amounts of live and dead shell on open-bay reefs.

Oyster size was similar between reef types and seasons, with live oyster shell heights of 76.8 ± 35.3 mm on open-bay reefs and 74.9 ± 28.3 mm on fringing reefs (ANOVA contrast, $p = 0.66$). Live oyster biomass (dry weight) was generally higher on open-bay reefs (mean 129.7 ± 214.9 g m^{-2}) than on fringing reefs (44.0 ± 53.5 g m^{-2}) (ANOVA contrast, $p \leq 0.08$) and was lowest in summer 2020 (ANOVA contrast, $p = 0.03$). These data indicate that higher oyster biomass at open-bay reefs is due to the presence of more individuals rather than larger oyster size.

Many mechanisms may affect oyster density and biomass across Matagorda Bay. Prevailing south/southeast winds and water flow may shuttle oyster larvae towards open-bay reefs in the northwest, while directing larvae away from fringing reefs in the east, resulting in higher oyster density and biomass at open-bay reefs (Turner et al. 1994, Kim et al. 2013). Increased water flow at open-bay reefs may also have enhanced oyster survivorship and growth through provision of more organic matter (Roegner & Mann 1995, Lenihan 1999). Although oyster density and biomass were higher at open-bay reefs, there was also higher variability. The patchiness of open-bay oyster reef structure may be attributed to adjacent commercial harvest, as well as to higher boating activity which can remove and displace oysters from their optimal environment (Grizzle et al. 2002).

Oyster reef size and substrate also play a role in facilitating oyster settlement. Oysters preferentially settle on hard substrates, with a particular affinity for old oyster shells (Crisp 1967, Veitch & Hidu 1971). Open-bay reefs are considerably larger, covering an area of more than 100 acres, with a greater density of dead oyster shells as well as shell hash bottom type. By contrast, fringing reefs cover less than one acre and are comprised of less densely packed shells with muddy substrate available between oyster clumps. The increased area of hard substrate at open-bay reefs may facilitate oyster settlement and higher densities of live oysters in these areas. Higher variability in cultch size may explain more variable oyster densities at open-bay reefs. The small, tightly packed shell fragments found near reef crests can reduce larval oyster settlement through reduction of interstitial space (Nestlerode et al. 2007). Additionally, greater boating activity in these areas may shift reef substrates, leading to uneven settlement and higher post-settlement loss (Grizzle et al. 2002).

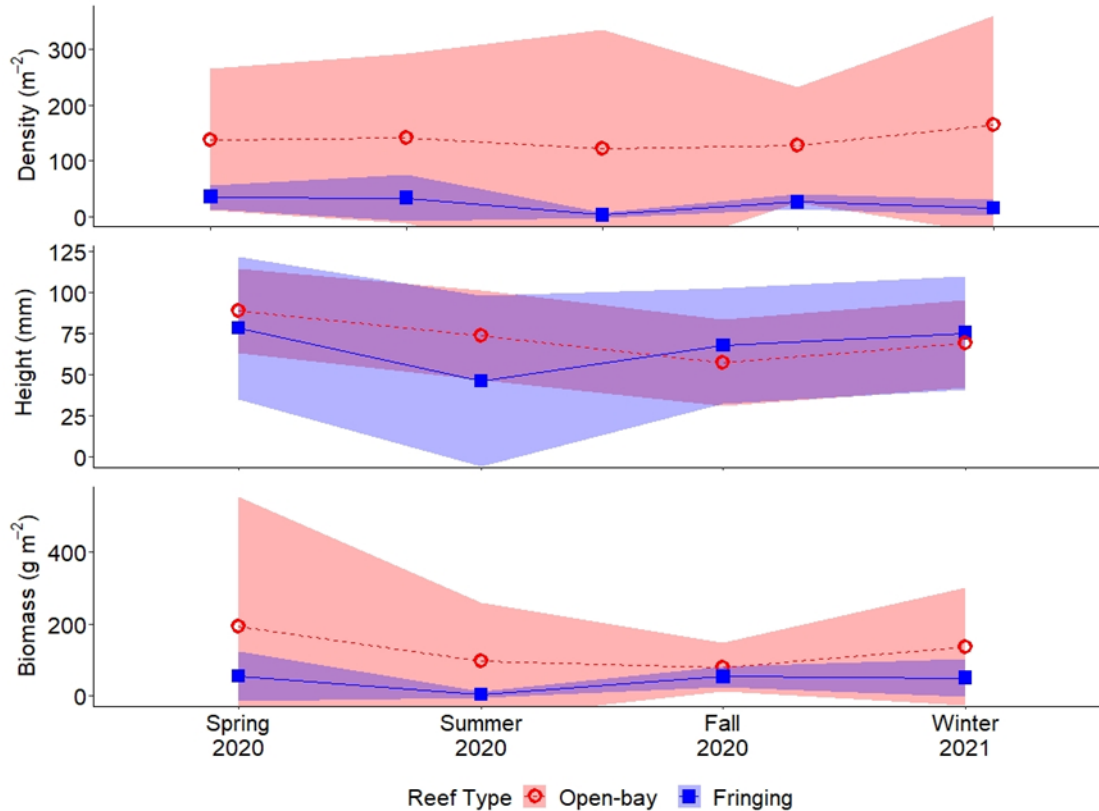


Figure 151. Density, shell height and biomass (mean \pm standard deviations) of oysters at open-bay and fringing reefs in Matagorda Bay.

Faunal Community

A total of 76 different reef faunal species, excluding oysters, were identified over the course of the study. Fringing reefs had 65 unique taxa, while open-bay reefs had 48. Fauna density was higher on fringing reefs (7027 ± 7942 ind. m⁻²) than open-bay reefs (3719 ± 3472 ind. m⁻²) (ANOVA contrast, $p = 0.004$) and lowest in fall 2020 (ANOVA contrast, $p = 0.003$; Figure 152). Fauna biomass was higher on open bay reefs (16.84 ± 18.42 g DW m⁻²) than on fringing reefs (7.47 ± 19.02 g DW m⁻²) (ANOVA contrast, $p < 0.001$) and was not distinct among seasons (ANOVA contrast, $p = 0.16$). Species diversity (per 0.25 m⁻²) was similar among reef types and stable across sampling dates (ANOVA contrasts, $p = 0.46$, $p = 0.08$; Figure 152). Species richness ranged from 4-7 species in open-bay reefs and from 3-8 species in fringing reefs.

Biomass-based faunal community composition separated into two groups with at least 59% similarity (Figure 153). The first group comprised all samples from the open-bay reef and the second group included all samples from the fringing reef. SIMPER analysis showed both open-bay reefs and fringing reef macrofauna biomass was dominated by Panopeidae crabs, accounting for 80% of total biomass in open-bay reefs and 67% of total biomass in fringing reefs. Differences in faunal community composition between reef types were characterized by higher biomass of Porcellanidae and Ampithoidae crustaceans on open bay reefs and higher biomass of Leptocheiliidae tanaid crustaceans and Eunicida polychaetes on fringing reefs.

The combination of oyster reef complexity and substrata are important factors shaping community structure and composition. Fringing reefs offer a habitat mosaic of oyster clumps with high vertical relief fixed within a soft-sediment bottom. This mixture of increased refugia and interstitial space (O'Beirn et al. 2000) and access to rich organic matter within the sediments (Castel et al. 1989), supports a higher density of infauna. This may also explain the increased presence of errant polychaetes and tanaids among fringing reefs, as access to sediment for feeding and refugia augment survival (Kneib 1992, Lejart & Hily 2011). By contrast, open-bay reefs are dominated by nekton communities, specifically panopeidae and porcellanidae crab families, which are more reliant oyster shells than soft sediments (Meyer 1994). The omnivorous and suspension feeding modes of these respective families are supported by the higher water flows and mixing in open bay reefs, since access to organic matter from the sediment is more limited in these reefs.

Many physical factors (i.e. wind, water flow, disturbance) are also important in shaping oyster reef faunal communities. Higher wind and water flows at open-bay reefs may aid recruitment (Nowell & Jumars 1984) which is particularly important for the larval stages of nekton communities. Recruitment of fringing reef infauna is less dependent on flow as life history traits of these smaller organisms are more suited to small-scale dispersal (Wetzer et al. 1997, Lundquist et al. 2006, Cole et al. 2007).

Disturbance from anthropogenic influences, such as increased boat traffic and commercial harvest may also play a role in community composition of oyster reefs. Boating activity can disturb sediments, displace bottom substrate, and remove vegetation (Grizzle et al. 2002, Donnarumma et al. 2019). Additionally, the oyster dredging that occurs on open bay reefs can decrease reef structure and increase sedimentation (Marshall 1954, Lenihan & Peterson 1998). Taken together, boating and harvest activities may reduce refugia and alter water quality. Smaller organisms that rely increased structure and stable sediments may then be unable to effectively colonize open bay reefs, leading to the dominance of larger, more motile organisms in these area.

Species richness was 139% higher on fringing reefs than open-bay reefs. This may in part be due to differences in the community structure itself, where open-bay reefs are dominated by larger nekton species, while fringing reefs have a greater community of small-bodied infauna. Larger species have been shown to more readily occupy hard, unvegetated habitat (Kornis et al. 2018) and smaller organisms are supported by habitats with increased refugia (Humphries et al. 2011a). In addition to the increased interstitial space, fringing reefs offer greater habitat heterogeneity with soft sediment, oyster reef, and adjacent saltmarsh all closely connected. The wider range of microhabitat available may also account for the increase in total richness (Grabowski et al. 2005, Gain et al. 2016), as more species can coexist by utilizing the space and resources in different ways (Godbold et al. 2011, Zeppilli et al. 2016).

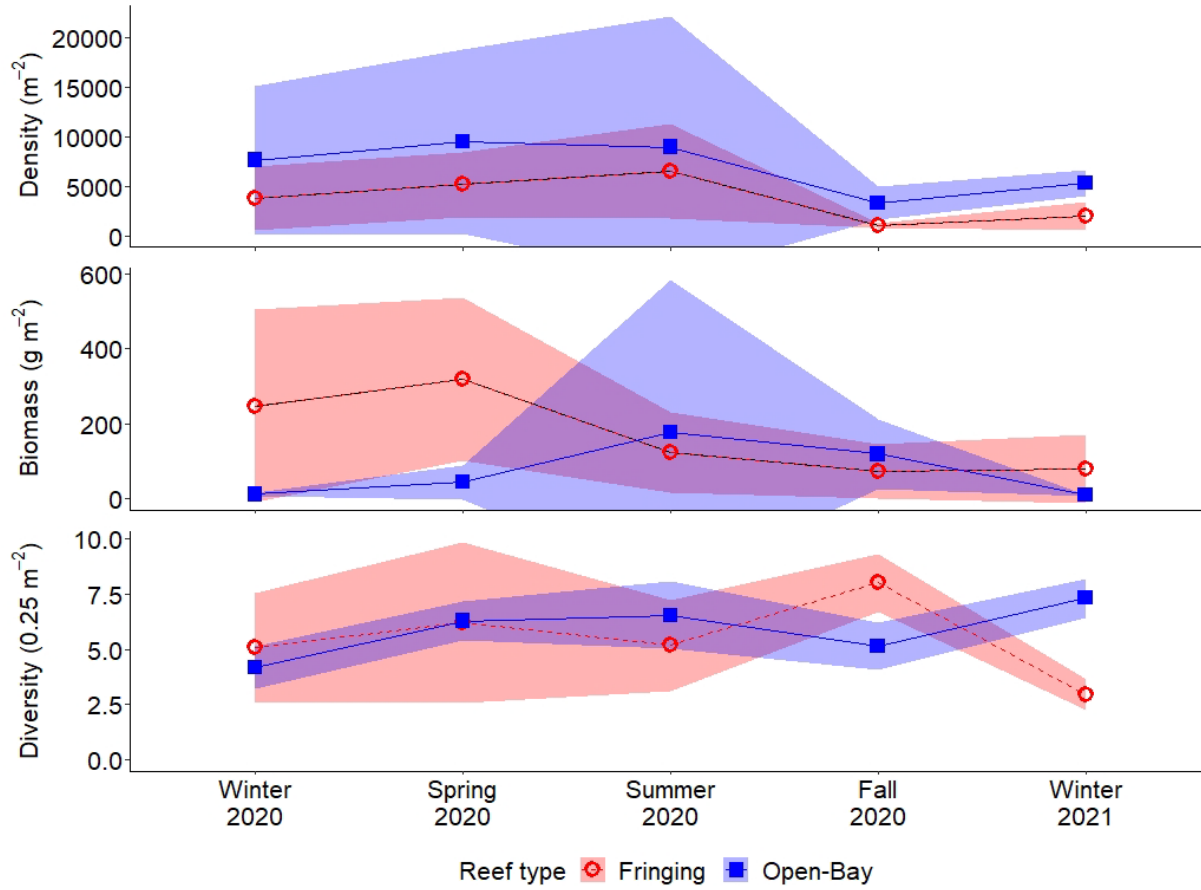


Figure 152. Density, biomass and diversity (mean \pm standard deviation) of reef fauna, excluding oysters, at open-bay and fringing reefs in Matagorda Bay.

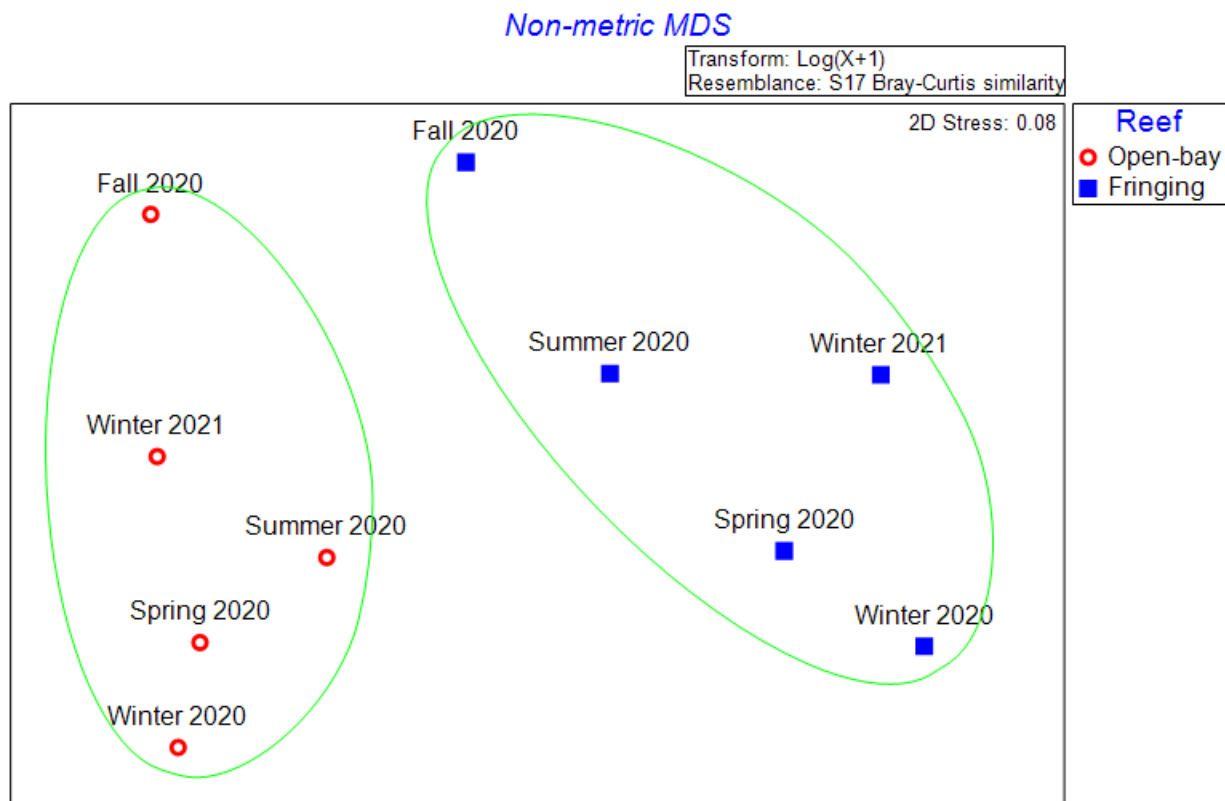


Figure 153. Biomass-based non-metric multidimensional scaling analysis with a Bray-Curtis similarity matrix of reef fauna from open-bay and fringing reefs across different sampling times in Matagorda Bay. Green lines represent grouping based on SIMPROF analysis, with at least 59% similarity between groups.

Stable isotope composition of potential food sources

The three most abundant terrestrial primary producers (*Spartina*, *Batis*, and *Salicornia*) and microphytobenthos (MPB) were collected from the shoreline adjacent to the oyster reefs. *Spartina* (mean \pm standard deviation: $-14.4\text{‰} \pm 0.6$) $\delta^{13}\text{C}$ values were higher than all other primary producers (Dunn's tests, $p < 0.05$), and MPB ($-21.5\text{‰} \pm 2.1$) $\delta^{13}\text{C}$ values were higher than *Batis* ($-28.7\text{‰} \pm 1.2$) and *Salicornia* ($-29.9\text{‰} \pm 0.5$) (Dunn's tests, $p < 0.001$). These isotope values are typical of terrestrial plants and benthic algae.

Isotope compositions of marine organic matter sources, SPOM, OSOM and SSOM were similar between open bay and fringing reefs (Figure 154). SSOM $\delta^{13}\text{C}$ values (mean \pm standard deviation: $-22.2\text{‰} \pm 1.3$) were higher than those of OSOM ($-23.7\text{‰} \pm 1.1$) and SPOM ($-25.9\text{‰} \pm 2.0$) ($p < 0.001$). OSOM had higher $\delta^{15}\text{N}$ values ($10.7\text{‰} \pm 0.8$) than SPOM ($8.9\text{‰} \pm 1.4$) and SSOM ($8.4\text{‰} \pm 0.4$) ($p < 0.001$). SSOM values may be more enriched in ^{13}C , due to the greater presence of benthic algae in the sediments.

Some seasonal differences of organic matter isotope compositions were observed: SPOM had higher $\delta^{13}\text{C}$ values in spring 2020 ($-23.8\text{‰} \pm 0.8$) than in fall 2020 ($-28.6\text{‰} \pm 0.5$) and lower $\delta^{15}\text{N}$ values in winter 2020 ($7.0\text{‰} \pm 1.0$) than in other seasons ($p < 0.001$). SSOM $\delta^{13}\text{C}$ values were higher in winter 2020 ($-21.0\text{‰} \pm 0.7$) than in summer 2020 ($-22.6\text{‰} \pm 0.7$) ($p < 0.05$). OSOM $\delta^{13}\text{C}$ values were higher in spring 2020 ($-22.3\text{‰} \pm 0.9$) than in fall 2020 and winter 2021 ($-24.5\text{‰} \pm 0.6$, and $-24.7\text{‰} \pm 0.7$, respectively) and $\delta^{15}\text{N}$ values were lower in winter 2020 than in other seasons ($p < 0.05$).

Seasonal variation among producer isotopes was observed across the sampling period, where both ^{13}C and values ^{15}N were enriched in the spring and summer compared to winter. Several studies have reported similar patterns, with the accumulation of heavier carbon isotopes attributed to changes in runoff, temperature, and light availability, which impact primary production (Cooper & DeNiro 1989, Vizzini & Mazzola 2003). Our study area had higher runoff rates in fall and winter (USGS data), which likely flushed ^{13}C -depleted terrestrial organic matter into the bay. Additionally, lower temperatures and less light availability can dampen primary production, leading to less fractionation of carbon isotopes. This is further supported by our data which show depressed chlorophyll *a* during fall and winter, suggesting lower rates of primary production. Variation of ^{15}N values is also linked with temperature, where colder periods can lead to a reduction in denitrification (Baeta et al. 2009), resulting less ^{15}N fractionation. This may account for the depletion of ^{15}N across producers during fall and winter.

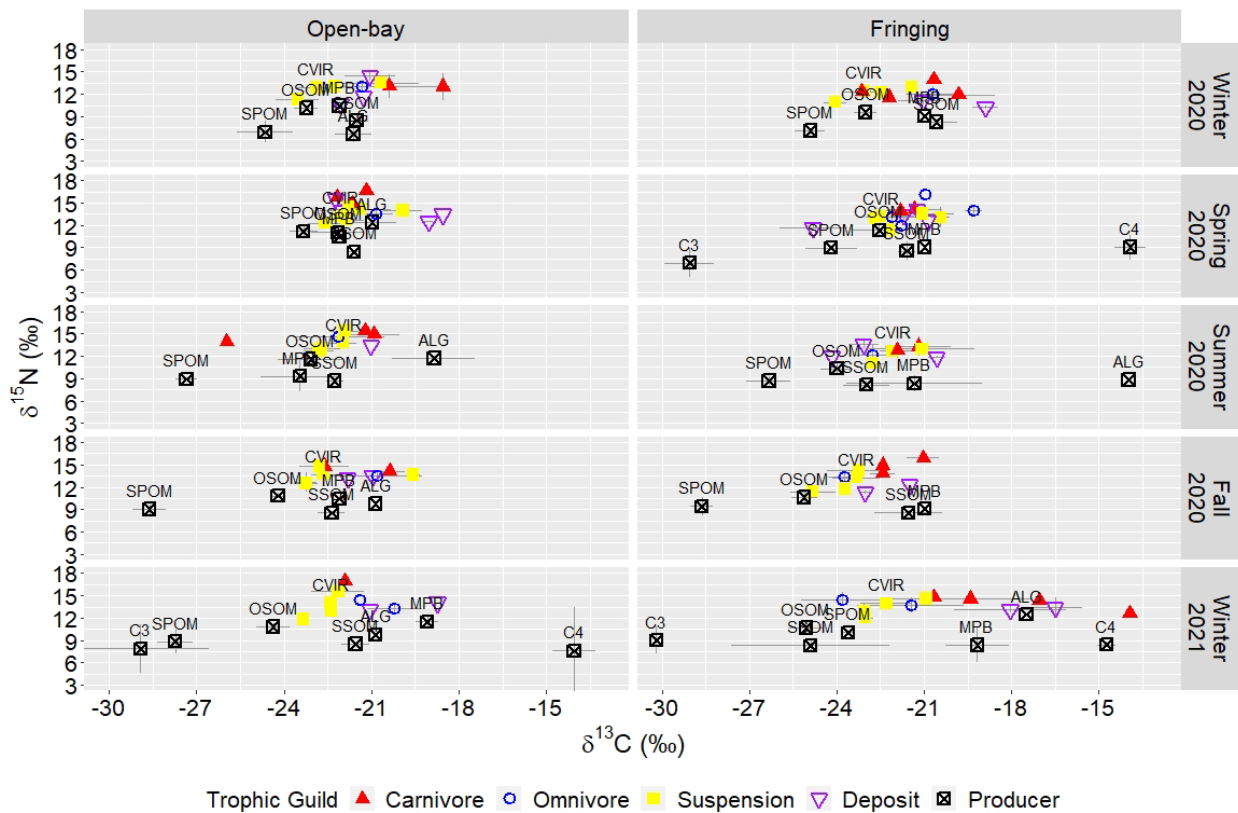


Figure 154. $\delta^{13}\text{C}$ and $\delta^{15}\text{N}$ values of trophic guilds from open-bay and fringing reefs across sampling period Winter 2020-Winter 2021.

Stable isotope composition of consumers

Isotope compositions were determined on 27 different consumer taxa collected from oyster reefs. Consumer $\delta^{13}\text{C}$ values ranged from -26.0 to -13.9‰ and $\delta^{15}\text{N}$ values ranged from 10.0 to 17.0‰. Isotope compositions for *Crassostrea virginica* were analyzed independently; other consumers were grouped and analyzed according to feeding guild (Figure 155).

C. virginica had similar $\delta^{13}\text{C}$ values across reef types, ranging from -24.2 to -21.6‰ (mean \pm standard deviation: -22.5‰ \pm 0.6) for open-bay reefs and -24.7 to -20.8‰ (-22.7‰ \pm

0.7) for fringing reefs. $\delta^{13}\text{C}$ values were seasonally elevated in spring ($-22.3\text{‰} \pm 0.4$) and summer 2020 ($-22.0\text{‰} \pm 0.3$), and lower in fall ($23.0\text{‰} \pm 0.7$) and winter 2020 ($-23.0\text{‰} \pm 0.5$) ($p < 0.05$). $\delta^{15}\text{N}$ values of oysters were higher in open-bay reefs ($13.4\text{‰} \pm 0.8$, $n = 25$) than in fringing reefs ($13.0\text{‰} \pm 0.8$) ($p < 0.05$). $\delta^{15}\text{N}$ values were lower in winter 2020 ($12.6\text{‰} \pm 0.7$) than in fall 2020 ($13.5\text{‰} \pm 0.4$) and winter 2021 ($14.0\text{‰} \pm 0.7$) ($p < 0.05$). Food source contributions were similar between the two reef types. OSOM represented the highest contribution to *C. virginica* food resources, ranging from 32 to 100% in fringing reefs and from 15 to 100% in open-bay reefs. Contributions of SPOM and of SSOM were very minor, except in spring 2020 for SPOM (0 to 44% in fringing reefs and 0.4 to 75% in open-bay reefs).

Though consumer isotopes were similar across reef type, some seasonal variation was seen across trophic guilds. Suspension feeders were enriched in ^{13}C during spring ($-21.6\text{‰} \pm 1.0$) and depleted of ^{15}N in winter ($12.4\text{‰} \pm 1.0$). This pattern mirrors producer isotope values and reflects suspension feeder diet of organic matter derived from the water. Conversely, deposit feeders and carnivores were more enriched in ^{13}C during winter months ($-18.1\text{‰} \pm 1.9$, $-18.9\text{‰} \pm 2.8$ respectively). This is contrary to our data that show generally depressed ^{13}C of producers in cooler months. This may in part be explained by a resource use shift during winter, where deposit feeders may have fed on more marine based sources of organic matter, leading to more enriched ^{13}C values. Additionally, microphytobenthos had greater enrichment of $\delta^{13}\text{C}$ during winter, suggesting deposit feeders were acquiring more of their diet from benthic algae during this time.

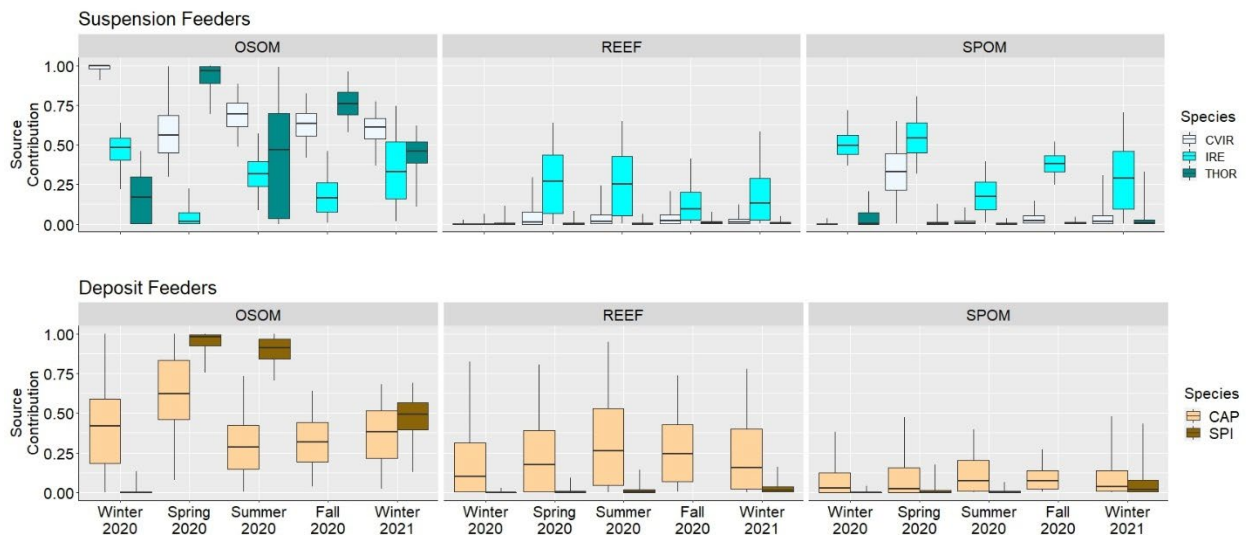


Figure 155. Outputs of stable isotope mixing models, indicating source contributions of three main pools of organic matter (OSOM, SSOM, SPOM) (mean \pm standard deviation) for A) suspension and B) deposit feeding organisms.

Mean food resource contributions

Despite significant differences in oyster reef structure, community composition, and resource availability; actualized resource use was remarkably similar among reef types. Mixing models showed oyster shell organic matter (OSOM) was the most extensively used resource among oysters. Mean food resource contributions (MFRC) also showed OSOM was the most used resource across the reef community, comprising 35 to 88% of their collective diet, while

SPOM and SSOM contributed 1 to 43% and 0 to 34%, respectively (Figure 156). This indicates oyster shells are acting as a substrate for a unique combination of organic matter, stemming from marine and terrestrial inputs.

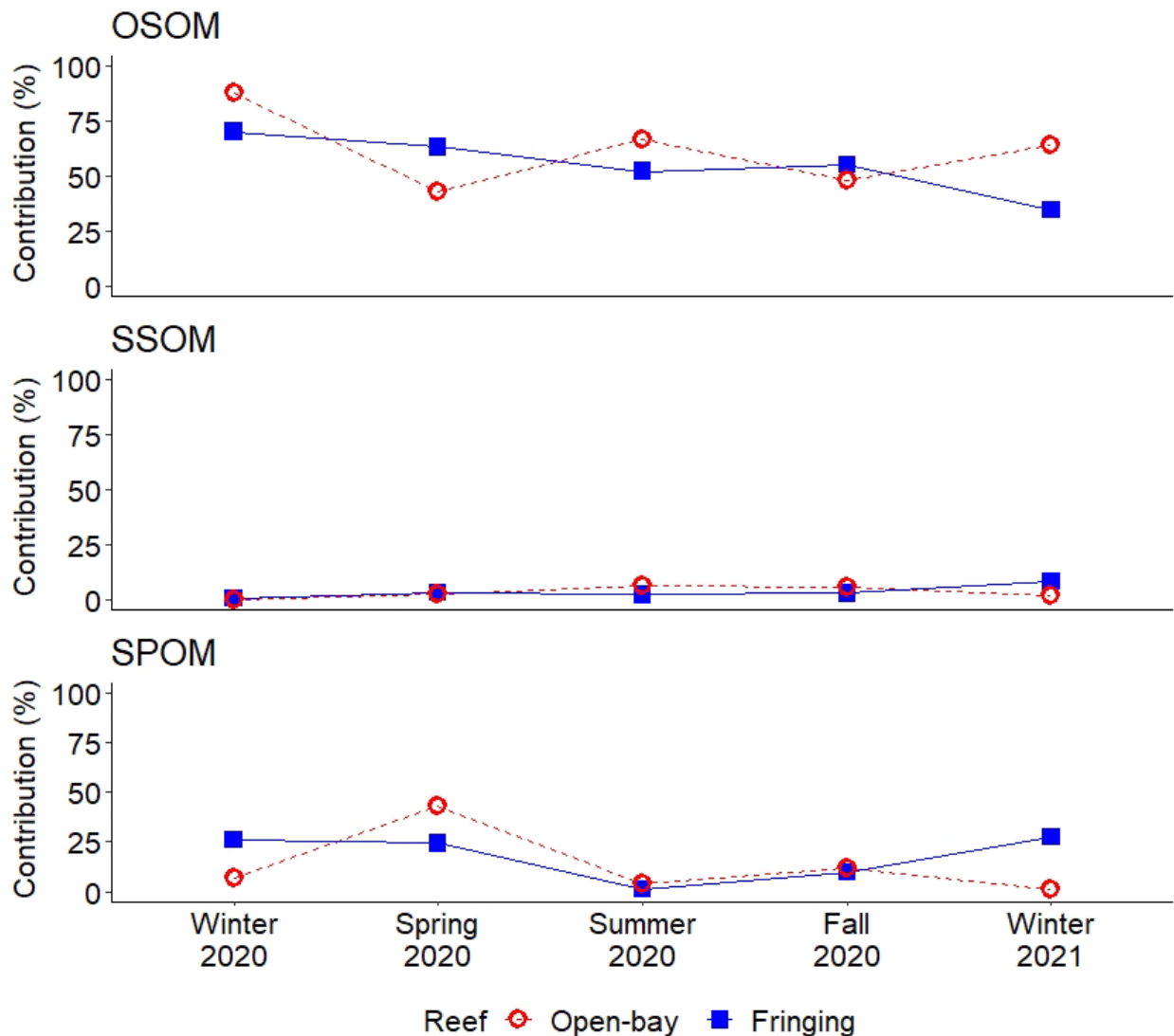


Figure 156. Mean food resource contribution (MFRC) index of three main pools of organic matter (OSOM, SSOM, SPOM) at open-bay and fringing oyster reefs in Matagorda Bay.

Wind-tidal Flats

Introduction

Wind-tidal flats are coastal soft bottom habitats characterized by harsh, changeable environmental conditions between the mean low and mean high tide, where wind—rather than tides—play a major role driving patterns of inundation and exposure (Reineck & Singh 1980). Irregular inundation and extreme temperatures limit macrophyte development and favor development of cyanobacterial mats (Tunnell & Judd 2002), which can contribute nearly as much primary productivity as seagrass meadows (Odom & Wilson 1962, Withers & Tunnell 1998). Cyanobacteria bind the sediments, provide food resources that support colonization by invertebrate communities, and contribute to the role of wind-tidal flats as significant feeding

grounds for wintering and migrating birds, including federally-designated threatened species (Embry 2020).

Irregular inundation of the tidal flats is one of the major factors that drive primary production and the conversion of biomass to higher trophic level consumers (Withers & Tunnell 1998). Both exposure and inundation are necessary for the cyanobacterial mats to proliferate; inundation nourishes the mats, and exposure allows them to grow. Tidal events also help recruit infaunal organisms to the mats, which support higher trophic level consumers like shorebirds. These communities make use of the provided fresh organic matter either through grazing or from decomposed material in the sediment (Withers & Tunnell 1998, Tunnell & Judd 2002). Despite the important role of irregular tidal flat flooding on food web dynamics, long term changes of inundation frequency place tidal flats at risk worldwide. Tidal flats are particularly vulnerable to disturbance such as sea level rise, which converts flats to shallow, submerged habitat, and to anthropogenic activities such as coastal development, dredge disposal, and marsh mitigation (Tunnell & Judd 2002, Zhang et al. 2018, Xie et al. 2018). On the global scale, approximately 16% of tidal flats have been lost in just the past three decades (Murray et al. 2019), although local losses can be much higher, up to 80% in estuaries around the world including those in Texas (Tunnell & Judd 2002) and China (Murray et al. 2014, Chen et al. 2016). These losses have important consequences for organisms including changes in infaunal recruitment and decreased foraging habitat for many overwintering birds.

The purpose of this portion of the study was to evaluate wind-tidal flats and marsh habitats for spatio-temporal changes in infaunal communities and food web interaction.

Materials and Methods

Study Area and Collection

Field sampling was conducted on wind-tidal flats along the back side of the Matagorda peninsula in spring and summer of 2021. Two wind-tidal flats with adjacent marsh habitat were used to evaluate spatio-temporal changes in faunal communities and flows of organic matter (Figure 157).

A permanent transect was established in the center of the wind-tidal flat running through the tidal flat-marsh boundary into the marsh (Figure 157C). Depth loggers were placed on a PVC marker in the marsh. A 1 m² quadrat was placed in five stations along the transect, starting in the marsh and moving towards the tidal flat. For each quadrat, a habitat survey was conducted, including assessment of percent algal mat coverage and extent of inundation across site. Photos were collected at each quadrat.

Water quality and suspended particulate organic matter were collected and processed as described the oyster sampling methodology (above). To determine benthic macrofauna community composition, five replicate 38.5 cm² core samples were taken to a depth of 5 cm within the 1 m² quadrat for each station and processed as described previously.

Three 38.5 cm² sediment cores were collected within the 1 m² quadrat for analysis of chlorophyll *a* in the sediment and stable isotopes of C and N. Cores were taken to a depth of 12 cm, with sections taken from 0-2, 2-5, and 5-12 cm. The top of each core was gently scraped to remove the algal mat. Cyanobacterial mats were thoroughly rinsed to remove sediment, before processing for stable isotopes. Sediment was processed as previously described (above) for chlorophyll *a* and stable isotope analysis.

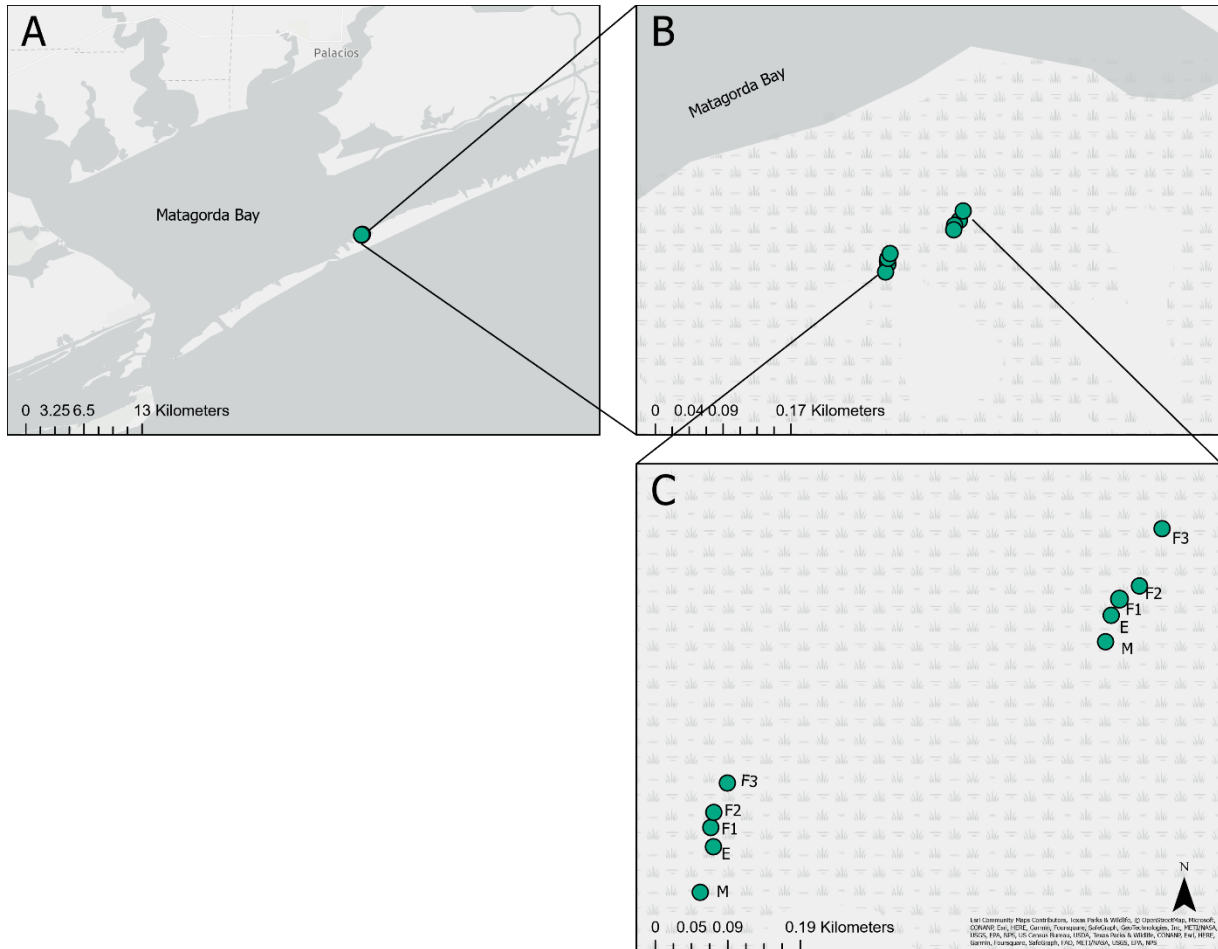


Figure 157. Map of A) Matagorda Bay with B) wind-tidal flats, and C) design for sampling microhabitats across the marsh-tidal flat complex. Marsh (M), Edge boundary (E), and Tidal Flats (F1, F2, F3).

Statistical Analysis

Data analysis was performed using RStudio 4.0.0 (R Foundation for Statistical Computing 2020). Species diversity and richness were calculated for macrofauna and infauna. Community composition was then assessed for significance using analysis of variance (ANOVA) models, followed by appropriate post-hoc testing.

Results & Discussion

Water quality

Water quality measurements were similar between tidal flat sites, with greater variation due to typical seasonal patterns rather than location (Figure 158). Average temperature and salinity were greater in summer 2021 (mean \pm standard deviation: 28.7 ± 0.4 °C, 24.6 ± 0.3) than spring 2021 (24.8 ± 4.1 °C, 15.1 ± 0.9). Mean dissolved oxygen concentrations were greater in spring 2021 (9.1 ± 4.2 mg L⁻¹) and lower in summer 2021 (3.5 ± 1.2 mg L⁻¹). Chlorophyll *a* in

the bay adjacent to tidal flats was greater spring 2021 ($26.5 \pm 5.6 \text{ ug L}^{-1}$) and lower in summer 2021 ($16.4 \pm 4.7 \text{ ug L}^{-1}$; Figure 158).

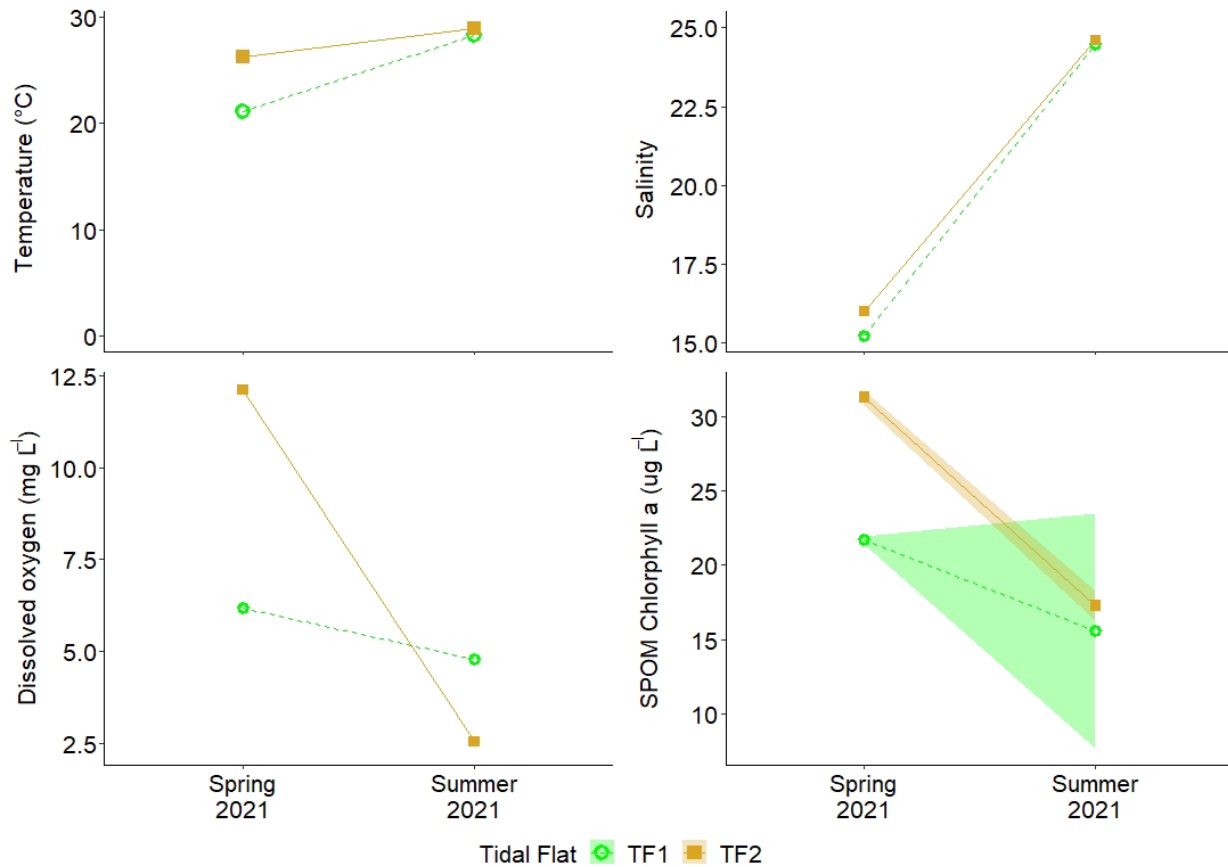


Figure 158. Temperature, salinity, dissolved oxygen, and chlorophyll a of suspended particulate organic matter (mean \pm standard deviation) in Matagorda Bay, adjacent to wind-tidal flat sites. Shaded areas represent standard deviations.

Marsh-Tidal Flat Assessment

The marsh-tidal flat complex was assessed for depth of inundation and percent coverage by algal mat (Figure 159). The marsh was more inundated ($0.13 \pm 0.13 \text{ m}$) than in the center of the tidal flat ($0.15 \pm 0.10 \text{ m}$) and were submerged deeper in spring 2021 ($0.25 \pm 0.07 \text{ m}$) than summer 2021 ($0.01 \pm 0.02 \text{ m}$). Algal mat coverage was greater in the center of the flat ($75.0 \pm 34.1 \%$) than in the marsh ($3.3 \pm 8.1 \%$) and was greater in spring 2021 ($62.5 \pm 41.7 \%$) than summer 2021 ($22.0 \pm 19.8 \%$).

Sediment chlorophyll *a* concentrations were measured across microhabitats in spring 2021 (Figure 160). Sediment chlorophyll *a* concentrations were greater in the marsh ($7.2 \pm 4.1 \text{ mg m}^{-2}$) than in the tidal flat-marsh edge boundary ($5.9 \pm 2.3 \text{ mg m}^{-2}$) and tidal flat ($2.7 \pm 1.4 \text{ mg m}^{-2}$) habitats, indicating more fresh organic matter was available in the marsh during the spring season.

In Matagorda Bay, seasonal tide changes are greater than daily fluctuations. Spring and fall are characterized by higher tides and overall water level, while summer and winter are often much lower. This likely explains the pattern of inundation seen at our tidal flat locations.

Algal mat coverage was greater in the tidal flats than in the marsh. This is expected given that moving towards the marsh boundary, space becomes increasingly more occupied by salt-marsh plants. Additionally, slightly lower algal mat coverage in summer 2021 may be explained by prolonged lack of inundation. Algal mats can more successfully proliferate when the sediment is irregularly dampened and exposed. Too much coverage can reduce light penetration and stunt growth, while prolonged exposure can also kill the algae.

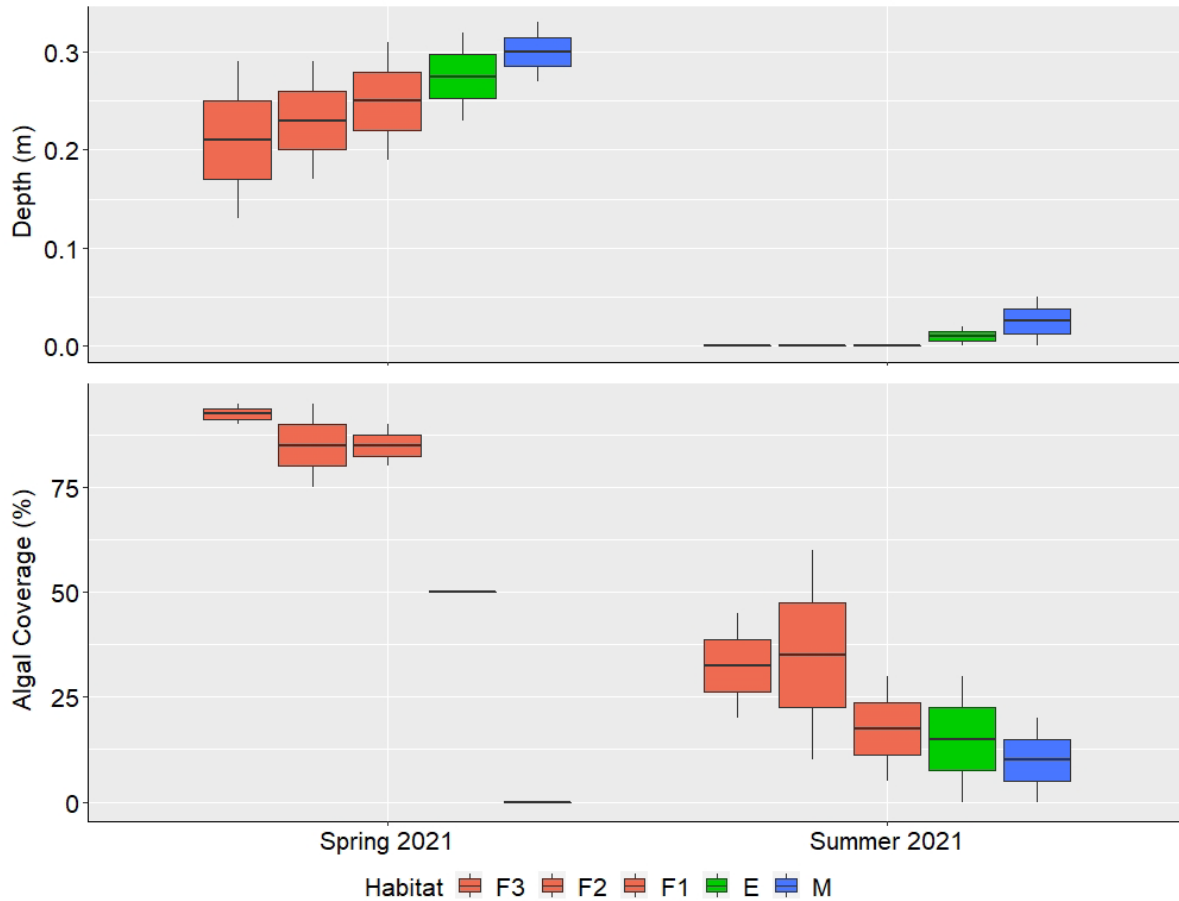


Figure 159. Average depth of inundation and percent coverage by algal mat across microhabitats of the marsh-tidal flat complex in Matagorda Bay for spring 2021 and summer 2021.

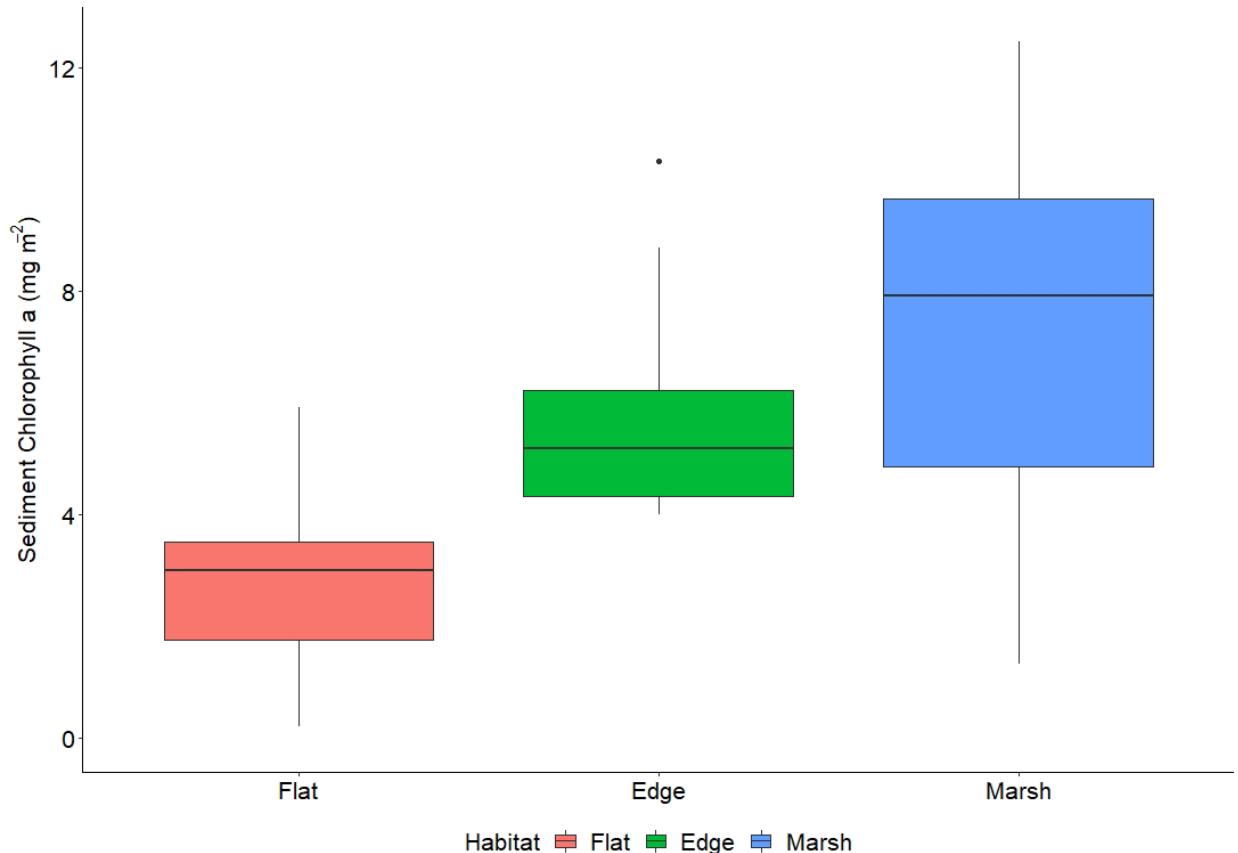


Figure 160: Sediment chlorophyll a microhabitats within the marsh-tidal flat complex in Matagorda Bay for spring 2021.

Faunal community

A total of 20 different faunal species were identified over the course of the study, with similarities across tidal flat locations. Differences in faunal richness, density, and abundance were seen across microhabitats, moving from the tidal flats into the marsh, and by season (Figure 161). Marsh habitat had 18 unique taxa, edge boundary had 7, and tidal flats had 9. Fauna density was greater in marsh ($11468 \pm 13557 \text{ ind. m}^{-2}$) than the marsh edge-tidal flat boundary ($3766 \pm 2906 \text{ ind. m}^{-2}$) or tidal flat habitat ($1879 \pm 1627 \text{ ind. m}^{-2}$). Fauna density was greater in summer 2021 ($5507 \pm 9238 \text{ ind. m}^{-2}$) than spring 2021 ($2842 \pm 4123 \text{ ind. m}^{-2}$). Fauna biomass was greater in marsh ($952.73 \pm 999.20 \text{ DW m}^{-2}$) than the marsh edge-tidal flat boundary ($528.44 \pm 400.43 \text{ DW m}^{-2}$) or tidal flat habitat ($514.24 \pm 1242.52 \text{ DW m}^{-2}$). Fauna biomass was greater in summer 2021 ($699.80 \pm 624.82 \text{ DW m}^{-2}$) than spring 2021 ($509.77 \pm 1400.44 \text{ DW m}^{-2}$). Species diversity (per 37.4 cm^2) was similar among tidal flat locations and season, but different across microhabitats. Mean species richness was greater in marsh (3 ± 1), than edge (2 ± 1) or flat (1 ± 1) habitats.

Faunal density, biomass, and diversity were higher in salt marsh habitat compared to edge boundary or tidal flat habitats and may be explained by greater structural complexity. Tidal flats are covered in cyanobacterial mats that are flush with the sediment and offer minimal protection from predation. Marshes, by contrast are filled with a variety of plants from *Spartina*, *Batis*, and *Salicornia*, all of which provide dense ground cover and refugia from predation. Many

shore and wading birds actively avoid areas of dense marsh in favor of mud or tidal flats which are more accessible. Direct access to the sediments in tidal flat-marsh edge boundary and tidal flat habitats likely enhances foraging success, even when total prey abundance is lower. Despite the importance of these tidal flat areas as secondary feeding grounds for many shore birds, these habitats are slowly disappearing. Irregular inundation is necessary for the proper maintenance of these systems, however, increasing water levels often convert these habitats to shallow subtidal or salt-marsh habitat.

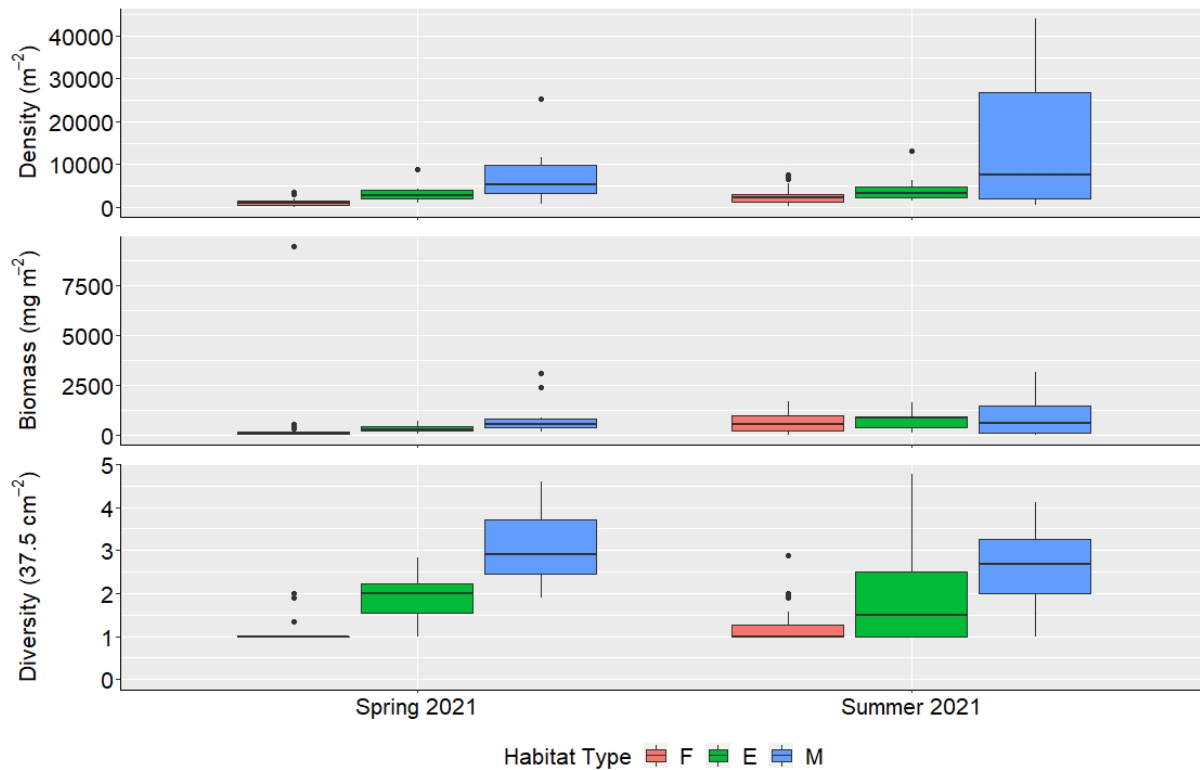


Figure 161: Density, biomass, and diversity (mean \pm standard deviation) of benthic macrofauna from the marsh-tidal flat complex in Matagorda Bay.

Ecosystem Scale Resource Use

Introduction

A major concern for many resource managers is understanding the health and productivity of ecosystems, which has become increasingly important with the rise coastal populations and adjacent land use. Of particular interest on the Texas coast is Matagorda Bay, which contains numerous intertidal and subtidal habitats including seagrass beds, oyster reefs, salt marshes, wind-tidal flats, and soft sediment habitats (Santiago et al. 2019; Ward & Armstrong 1980). These habitats in turn provide necessary resources for many commercially important and even threatened species, including sea-turtles and over-wintering birds (Metz & Landry 2016; Shaver 1994).

The Matagorda Bay ecosystem has been increasingly threatened by anthropogenic activities such as commercial and recreational fishing, expanding population growth, and increases in tourism and agriculture (Bissett et al. 2009; Brody et al. 2004; Wilber & Bass 1998). Although many studies assess the impact of human stress on individual habitats, few have aimed

to assess how these impacts will affect bay systems as a whole. This has important implications as there has been a recent rise in bay usage, with increased commercial harvest of oyster reefs, and growing demand for coastal development (Buttler et al.; Powell 2020; Robinson; Schattenberg 2019). These changes in bay usage are likely to have a direct impact not only on the local communities, but also on how resources are distributed and used across the bay.

The purpose of this study is to determine how the primary producers from different subtidal habitats contribute to food web functioning across the Matagorda Bay ecosystem as a whole. Isotope compositions of food sources produced in seagrass beds, open water, and subtidal bare bottom habitats were assessed, as were changes in use of these food resources by a suspension feeder (i.e. the oyster *Crassostrea virginica*).

Materials and methods

Study area and collection

Sampling occurred in Matagorda Bay, Texas in August 2020. Ten zones were created moving from the North (1) to the South (10) to best group data for analysis (Figure 162).

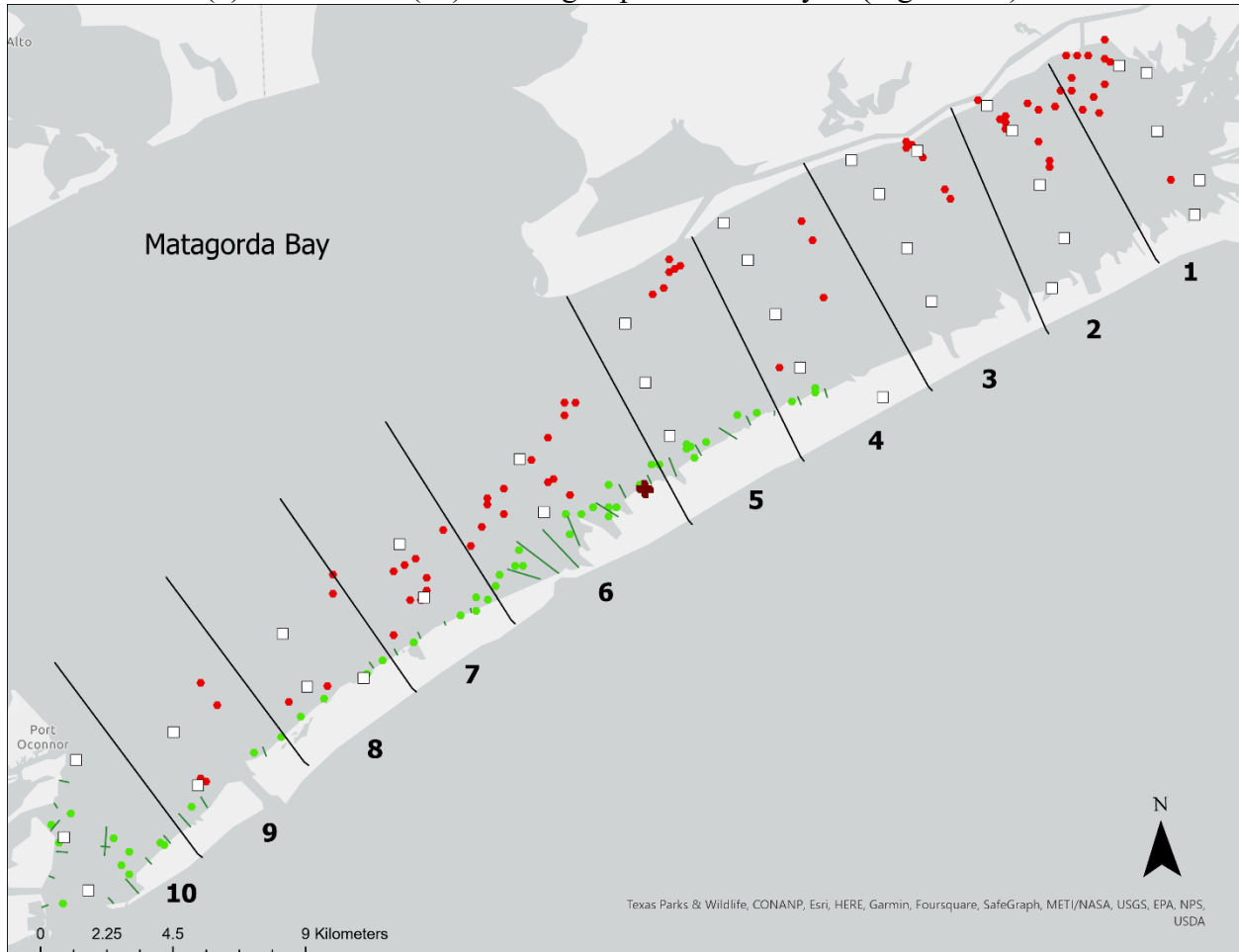


Figure 162: Map of Matagorda Bay with sampling locations split up by zones running from North (1) to South (10).

Water quality and suspended particulate organic matter were collected and processed as described above in the oyster reef methodology. Sediment was collected from benthic habitats and seagrass beds using a 38.5 cm² and a 63.6 cm² core, respectively. Cores were collected with minimal disturbance with the top 2 cm and 2 cm - 10 cm sliced and processed as described above. Microphytobenthos was extracted from additional sediment collections at sites across the bay for stable isotope analysis (Figure 162). Samples were collected and processed as described in section 0. Oysters were collected by towing a dredge across specified reefs in the bay. Three oysters of varying sizes were taken from each site and processed for stable isotope analysis as described in the previous Oyster Reef methodology.

Data from bay surveys were compiled to produce maps of chlorophyll *a* and carbon-nitrogen ratios of primary producers to provide a “snapshot” of organic matter contributions to the estuarine food web.

Statistical Analysis

Data analysis was performed using RStudio 4.0.0 (R Foundation for Statistical Computing 2020). Stable isotope data were analyzed using biplots to determine basal resources and oyster diets across the bay. Diet data were analyzed to define important basal food sources and the flow of organic material through the bay system.

Results & Discussion

Water Quality

Average temperature was similar across the bay, ranging from 28.9 ± 0.6 °C to 31 ± 1.4 °C (Figure 163). Mean salinity increased from 21.9 ± 0.0 to 34.9 ± 0.0 moving from north to south of the bay, where inflow from the Gulf of Mexico is greatest (Figure 163). There was no clear pattern of mean dissolved oxygen concentrations, with ranges from 5.9 ± 0.8 mg L⁻¹ (Zone 3) to 8.3 ± 4.2 mg L⁻¹ (Zone 10) (Figure 163). Chlorophyll *a* from particulate organic matter typically increased along the salinity gradient with ranges of 2.3 ± 0.1 ug L⁻¹ (Zone 10) to 19.2 ± 0.2 ug L⁻¹ (Zone 1) (Figure 163). Additionally, carbon-nitrogen ratios in particular organic matter were low overall, with values ranging from 9.5 (Zone 5) to 12.4 (Zone 9).

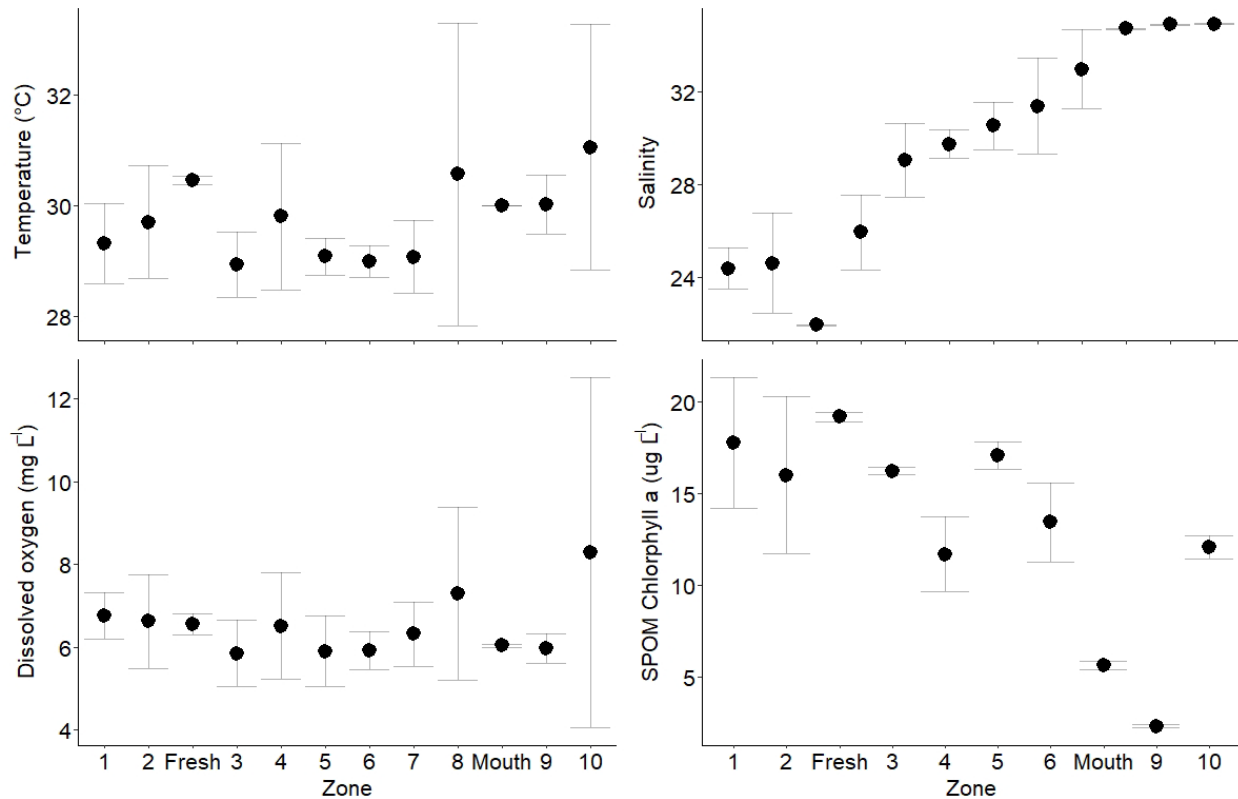


Figure 163: Temperature, salinity, dissolved oxygen, and chlorophyll *a* (mean ± standard deviation) of suspended particulate organic matter across Matagorda Bay. Zones are arranged from North (1) to South (10). Fresh indicates Intercoastal Water Way entrance to bay and Mouth indicates the mouth of the bay leading to the Gulf of Mexico.

Resource Quality

Sediment chlorophyll *a* ranged from $4.4 \pm 2.1 \text{ mg m}^{-2}$ (Zone 1) to $11.9 \pm 5.7 \text{ mg m}^{-2}$ (Zone 6). The greatest chlorophyll *a* concentrations were measured towards the middle of the bay, while the lowest chlorophyll *a* concentrations were in the furthest north reaches of the bay (Figure 164). In addition to chlorophyll *a*, carbon-nitrogen ratios were examined to determine the quality of the organic matter available. C/N ratios were fairly low overall, ranging from 9.4 (Zone 6) to 11.8 (Zone 9). Figure 165 shows lowest C/N ratios mainly along the Matagorda Peninsula. Low C/N ratios indicate high organic matter quality, suggesting the bay may be rich in fresh and usable material for animals to eat. The bulk of both chlorophyll *a* and low C/N ratios are found towards the middle of the bay (Zone 6). This may be attributed to dense stands of seagrass or patterns of inflow from the mouth of the bay.

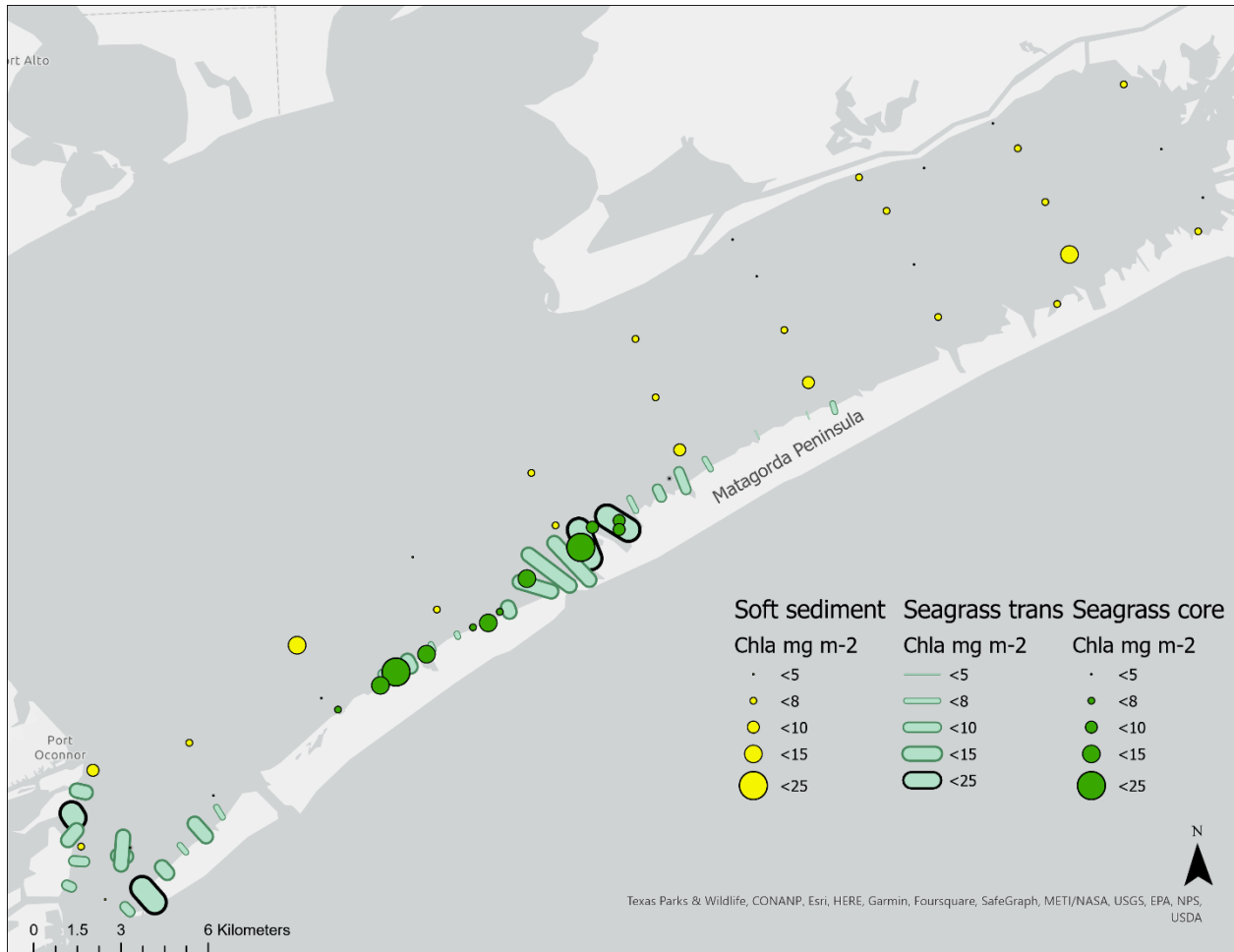


Figure 164: Map of Matagorda Bay with gradient of chlorophyll a in soft-sediments (closed yellow circles), seagrass cores (closed green circles) and transects (green bars).

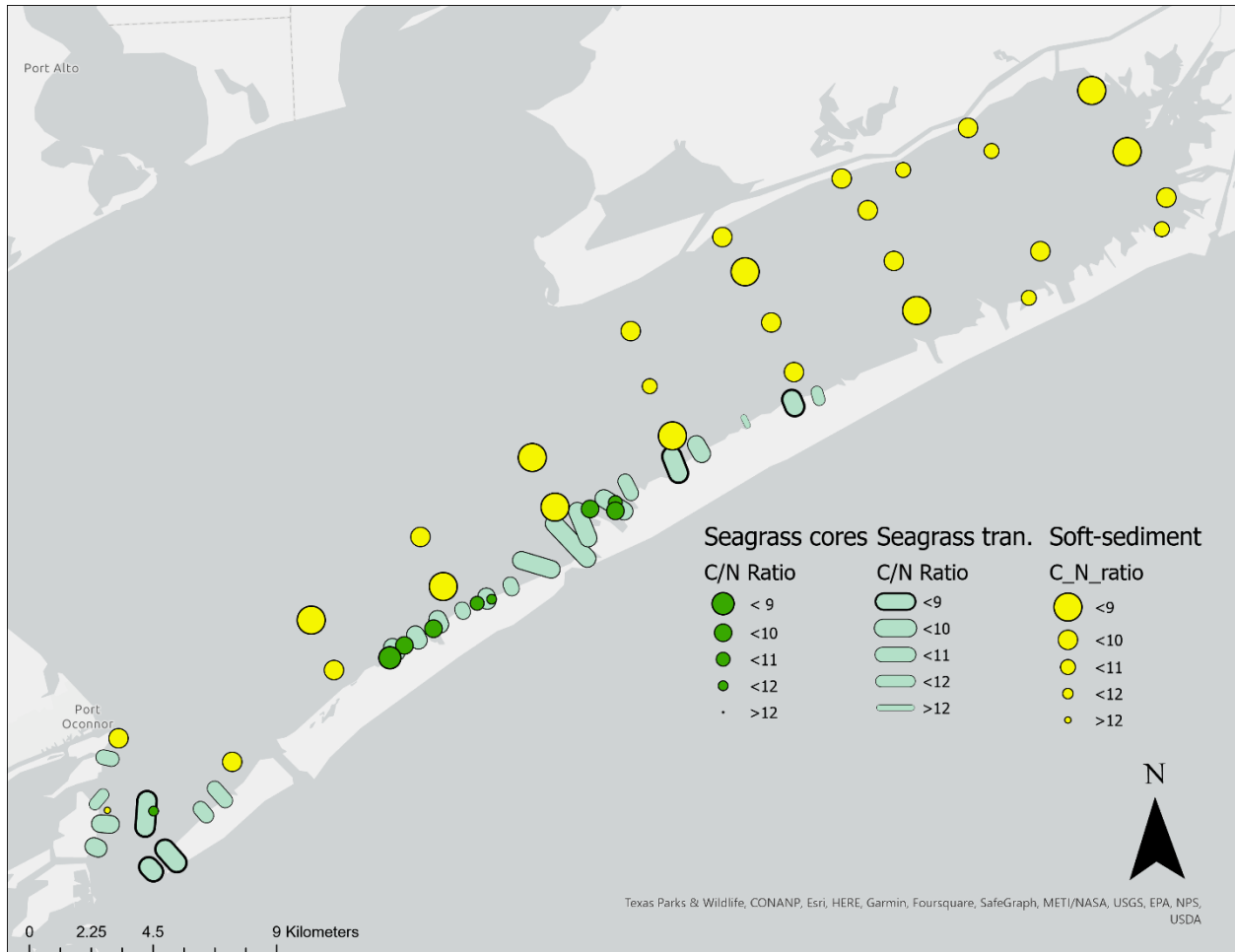


Figure 165: Map of Matagorda Bay with gradient of C/N ratios in soft-sediments (closed yellow circles), seagrass cores (closed green circles) and transects (green bars).

Assimilated Resource Use

Oysters were used as a study organism to determine how organic matter is assimilated across an ecosystem. Oyster isotope compositions were very similar across the bay with $\delta^{13}\text{C}$ values ranging from -20.9 to -22.3 ‰ and $\delta^{15}\text{N}$ values ranging from 12.1 to 14.1 ‰ (Figure 166). Biplots of oysters in relation to primary producers and pools of organic matter suggest major contributors to the oyster diet are likely OSOM, macroalgae, and benthic microalgae (Figure 166).

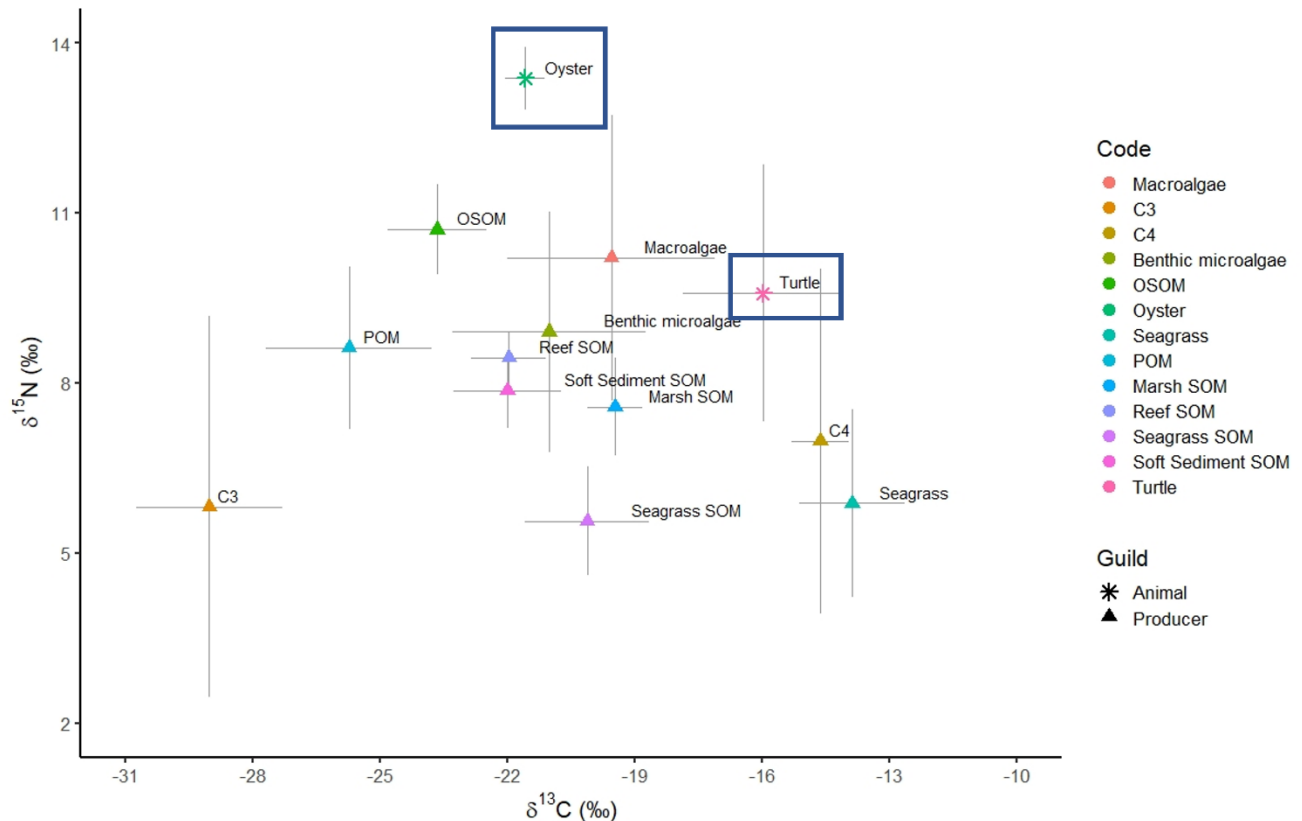


Figure 166: $\delta^{13}\text{C}$ and $\delta^{15}\text{N}$ values (mean \pm standard deviation) of producers and two consumers (*C. virginica* and *C. mydas* highlighted in boxes) from Matagorda Bay.

The consistency of *C. virginica* isotope values indicates that resource use is similar, regardless of position in the bay. This is not altogether surprising, as resource quality appears to be similar where oyster densities are greatest. Most oysters are found in polyhaline waters, with abundances decreasing as water becomes more saline. In Matagorda Bay, the best salinity conditions for oyster are limited to the mid to northern parts of bay's eastern arm. Despite the slightly higher C/N ratios of sediment and water in this portion of the bay, results still indicate that high-quality material is available for consumption.

Turtle Resource Use

Inclement cold weather conditions resulted in many green turtle fatalities along the Texas coast in February 2021. Here we use stable isotopes to examine turtle tissue samples—blood, muscle, skin, and scute—and diet for 14 individuals found in Matagorda Bay during this freeze event.

Isotope compositions of turtle blood, muscle, skin, and scute were similar between individuals (Figure 167) with $\delta^{13}\text{C}$ and $\delta^{15}\text{N}$ values less than 1‰ difference between sample types. This indicates that (1) turtle diet is likely similar year-round, and (2) any turtle tissue sample type is appropriate to determine diet.

Biplots of green turtles in relation to primary producers and pools of organic matter suggest major contributors to the turtle diet are likely sediment organic matter, seagrass and

other C4 plants (Figure 166). Known studies of turtle diet confirm green turtles mainly consume seagrass and algae. Seagrass values from Baffin Bay, Nueces, Bay, and Laguna Madre from 2014 to 2021 were added to the biplot because stable isotope data for seagrass in Matagorda Bay were not available, which likely added variability to these results. Sediment cores taken within seagrass beds of Matagorda Bay, show less enrichment of ^{13}C , further suggesting pure seagrass material may be less enriched than the substituted values.

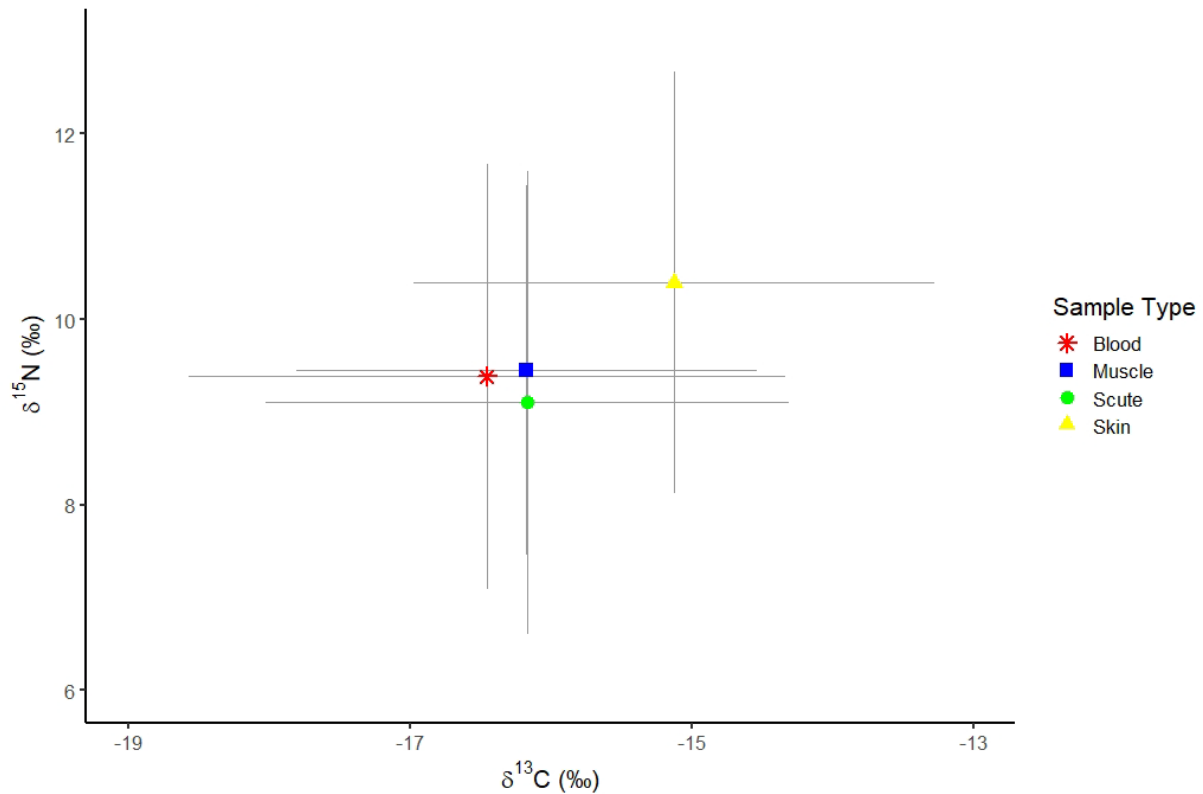


Figure 167: $\delta^{13}\text{C}$ and $\delta^{15}\text{N}$ values (mean \pm standard deviation) of *Chelonia mydas* tissue types (Blood, Muscle, Scute, Skin) from February 2021.

Literature Cited

- Airoidi L, Beck M (2007) Loss, status and trends for coastal marine habitats of Europe. *Oceanography and Marine Biology* 45:345–405.
- Ansell A, Gibson RN, Barnes M (1999) *Oceanography and marine biology, an annual review*. CRC Press.
- Armstrong NE (1987) The ecology of open-bay bottoms of Texas: A community profile. U.S. Department of the Interior, Fish and Wildlife Service, Research and Development, National Wetlands Research Center.
- Baeta A, Pinto R, Valiela I, Richard P, Niquil N, Marques JC (2009) $\Delta^{15}\text{N}$ and $\delta^{13}\text{C}$ in the Mondego estuary food web: Seasonal variation in producers and consumers. *Marine Environmental Research* 67:109–116.
- Barbier EB, Hacker SD, Kennedy C, Koch EW, Stier AC, Silliman BR (2011) The value of estuarine and coastal ecosystem services. *Ecological Monographs* 81:169–193.
- Beck MW, Brumbaugh RD, Airoidi L, Carranza A, Coen LD, Crawford C, Defeo O, Edgar GJ, Hancock B, Kay MC, Lenihan HS, Luckenbach MW, Toropova CL, Zhang G, Guo X (2011) Oyster reefs at risk and recommendations for conservation, restoration, and management. *BioScience* 61:107–116.
- Bilkovic DM, Mitchell MM, Davis J, Herman J, Andrews E, King A, Mason P, Tahvildari N, Davis J, Dixon RL (2019) Defining boat wake impacts on shoreline stability toward management and policy solutions. *Ocean & Coastal Management* 182:104945.
- Blomberg BN, Palmer TA, Montagna PA, Beseres Pollack J (2018) Habitat assessment of a restored oyster reef in South Texas. *Ecological Engineering* 122:48–61.
- Boesch DF, Turner RE (1984) Dependence of fishery species on salt marshes: the role of food and refuge. *Estuaries* 7:460–468.
- Castel J, Labourg P-J, Escaravage V, Auby I, Garcia ME (1989) Influence of seagrass beds and oyster parks on the abundance and biomass patterns of meio- and macrobenthos in tidal flats. *Estuarine, Coastal and Shelf Science* 28:71–85.
- Chen Y, Dong J, Xiao X, Zhang M, Tian B, Zhou Y, Li B, Ma Z (2016) Land claim and loss of tidal flats in the Yangtze Estuary. *Scientific Reports* 6:24018.
- Clarke K, Gorley R (2014) *PRIMER version 7: User manual/tutorial*. Plymouth Marine Laboratory, UK.

- Clarke K, Warwick R (1994) A framework for studying changes in community structure. In: *Change in marine communities: An approach to statistical analysis and interpretation*. Plymouth Marine Laboratory, UK
- Cole VJ, Chapman MG, Underwood AJ (2007) Landscapes and life-histories influence colonisation of polychaetes to intertidal biogenic habitats. *Journal of Experimental Marine Biology and Ecology* 348:191–199.
- Congdon BC, Catterall CP (1994) Factors influencing the eastern curlew's distribution and choice of foraging sites among tidal flats of Moreton Bay, South eastern Queensland. *Wildl Res* 21:507–517.
- Cooper LW, DeNiro MJ (1989) Stable carbon isotope variability in the seagrass *Posidonia oceanica*: evidence for light intensity effects. *Marine Ecology Progress Series* 50:225–229.
- Correll DL (1978) Estuarine Productivity. *BioScience* 28:646–650.
- Cressman K, Posey M, Mallin MA, Leonard L, Alphin T (2003) Effects of oyster reefs on water quality in a tidal creek estuary. *Journal of Shellfish Research* 22:753–762.
- Crisp DJ (1967) Chemical factors inducing settlement in *Crassostrea virginica* (Gmelin). *Journal of Animal Ecology* 36:329–335.
- Cullen-Unsworth L, Unsworth R (2013) Seagrass meadows, ecosystem services, and sustainability. *Environment: Science and Policy for Sustainable Development* 55:14–28.
- Donnarumma L, Di Stefano F, Appolloni L, Ferrigno F, Rendina F, A. R, Sandulli R, Russo G (2019) Recreational boating influence on *Posidonia oceanica* beds in the marine protected area “Isola di Ventotene e Santo Stefano.”
- Duarte C (2002) The future of seagrass meadows. *Environmental Conservation* 29:192–206.
- Duarte CM, Chiscano CL (1999) Seagrass biomass and production: a reassessment. *Aquatic Botany* 65:159–174.
- Ehrich MK, Harris LA (2015) A review of existing eastern oyster filtration rate models. *Ecological Modelling* 297:201–212.
- Elliott M, Whitfield AK (2011) Challenging paradigms in estuarine ecology and management. *Estuarine, Coastal and Shelf Science* 94:306–314.

- Embry P (2020) Slimy mudflat biofilms feed migratory birds-and could be threatened. <https://www.scientificamerican.com/article/slimy-mudflat-biofilms-feed-migratory-birds-and-could-be-threatened/> (accessed June 24, 2020)
- Fry B (2006) *Stable Isotope Ecology*. Springer Science & Business Media.
- Gain IE, Brewton RA, Reese Robillard MM, Johnson KD, Smee DL, Stunz GW (2016) Macrofauna using intertidal oyster reef varies in relation to position within the estuarine habitat mosaic. *Mar Biol* 164:8.
- Godbold JA, Bulling MT, Solan M (2011) Habitat structure mediates biodiversity effects on ecosystem properties. *Proceedings of the Royal Society B: Biological Sciences* 278:2510–2518.
- Grabowski JH, Brumbaugh RD, Conrad RF, Keeler AG, Opaluch JJ, Peterson CH, Piehler MF, Powers SP, Smyth AR (2012) Economic valuation of ecosystem services provided by oyster reefs. *BioScience* 62:900–909.
- Grabowski JH, Hughes AR, Kimbro DL, Dolan MA (2005) How habitat setting influences restored oyster reef communities. *Ecology* 86:1926–1935.
- Grabowski JH, Powers SP (2004) Habitat complexity mitigates trophic transfer on oyster reefs. *Marine Ecology Progress Series* 277:291–295.
- Griffiths J, Dethier MN, Newsom A, Byers JE, Meyer JJ, Oyarzun F, Lenihan H (2006) Invertebrate community responses to recreational clam digging. *Mar Biol* 149:1489–1497.
- Grizzle RE, Adams JR, Walters LJ (2002) Historical changes in intertidal oyster (*Crassostrea virginica*) reefs in a Florida Lagoon potentially related to boating activities. *Journal of Shellfish Research* 21:749–756.
- Halpern BS, Selkoe KA, Micheli F, Kappel CV (2007) Evaluating and ranking the vulnerability of global marine ecosystems to anthropogenic threats. *Conservation Biology* 21:1301–1315.
- Hothorn T, Bretz F, Westfall P (2008) Simultaneous inference in general parametric models. *Biometrical Journal* 50:346–363.
- Humphries AT, La Peyre MK, Decossas GA (2011a) The effect of structural complexity, prey density, and “predator-free space” on prey survivorship at created oyster reef mesocosms. *PLoS One* 6:e28339.

- Humphries AT, La Peyre MK, Kimball ME, Rozas LP (2011b) Testing the effect of habitat structure and complexity on nekton assemblages using experimental oyster reefs. *Journal of Experimental Marine Biology and Ecology* 409:172–179.
- Jackson JBC (2008) Ecological extinction and evolution in the brave new ocean. *Proceedings of the National Academy of Sciences* 105:11458–11465.
- Kappel CV (2005) Losing pieces of the puzzle: threats to marine, estuarine, and diadromous species. *Frontiers in Ecology and the Environment* 3:275–282.
- Karp MA, Seitz RD, Fabrizio MC (2018) Faunal communities on restored oyster reefs: effects of habitat complexity and environmental conditions. *Marine Ecology Progress Series* 590:35–51.
- Kennish MJ (2002) Environmental threats and environmental future of estuaries. *Environmental Conservation* 29:78–107.
- Kim C-K, Park K, Powers SP (2013) Establishing restoration strategy of eastern oyster via a coupled biophysical transport model. *Restoration Ecology* 21:353–362.
- Kirby MX (2004) Fishing down the coast: historical expansion and collapse of oyster fisheries along continental margins. *PNAS* 101:13096–13099.
- Kneib RT (1992) Population dynamics of the tanaid *Hargeria rapax* (Crustacea: Peracarida) in a tidal marsh. *Marine Biology* 113:437–445.
- Kornis MS, Bilkovic DM, Davias LA, Giordano S, Breitburg DL (2018) Shoreline hardening affects nekton biomass, size structure, and taxonomic diversity in nearshore waters, with responses mediated by functional species groups. *Estuaries and Coasts* 41:159–179.
- Lejart M, Hily C (2011) Differential response of benthic macrofauna to the formation of novel oyster reefs (*Crassostrea gigas*, Thunberg) on soft and rocky substrate in the intertidal of the Bay of Brest, France. *Journal of Sea Research* 65:84–93.
- Lenihan HS (1999) Physical-biological coupling on oyster reefs: how habitat structure influences individual performance. *Ecological Monographs* 69:251–275.
- Lenihan HS, Peterson CH (2004) Conserving oyster reef habitat by switching from dredging and tonging to diver-harvesting. *Fishery Bulletin* 102:298–306.
- Lenihan HS, Peterson CH (1998) How habitat degradation through fishery disturbance enhances impacts of hypoxia on oyster reefs. *Ecological Applications* 8:128–140.

- Leonard LA, Croft AL (2006) The effect of standing biomass on flow velocity and turbulence in *Spartina alterniflora* canopies. *Estuarine, Coastal and Shelf Science* 69:325–336.
- Leonard LA, Luther ME (1995) Flow hydrodynamics in tidal marsh canopies. *Limnology and Oceanography* 40:1474–1484.
- Lotze HK, Coll M, Dunne JA (2011) Historical changes in marine resources, food-web structure and ecosystem functioning in the Adriatic Sea, Mediterranean. *Ecosystems* 14:198–222.
- Lundquist CJ, Thrush SF, Hewitt JE, Halliday J, MacDonald I, Cummings VJ (2006) Spatial variability in recolonisation potential: influence of organism behaviour and hydrodynamics on the distribution of macrofaunal colonists. *Marine Ecology Progress Series* 324:67–81.
- Marshall N (1954) Changes in the physiography of oyster bars in the James River, Virginia. *Virginia Journal of Science* 5:173–181.
- Mercaldo-Allen R, Goldberg R (2011) Review of the ecological effects of dredging in the cultivation and harvest of molluscan shellfish.
- Meyer DL (1994) Habitat partitioning between the xanthid crabs *Panopeus herbstii* and *Eurypanopeus depressus* on intertidal oyster reefs (*Crassostrea virginica*) in southeastern North Carolina. *Estuaries* 17:674–679.
- Minagawa M, Wada E (1984) Stepwise enrichment of ^{15}N along food chains: Further evidence and the relation between $\delta^{15}\text{N}$ and animal age. *Geochimica et Cosmochimica Acta* 48:1135–1140.
- Murray NJ, Clemens RS, Phinn SR, Possingham HP, Fuller RA (2014) Tracking the rapid loss of tidal wetlands in the Yellow Sea. *Frontiers in Ecology and the Environment* 12:267–272.
- Murray NJ, Phinn SR, DeWitt M, Ferrari R, Johnston R, Lyons MB, Clinton N, Thau D, Fuller RA (2019) The global distribution and trajectory of tidal flats. *Nature* 565:222–225.
- Nestlerode JA, Luckenbach MW, O’Beirn FX (2007) Settlement and survival of the oyster *Crassostrea virginica* on created oyster reef habitats in Chesapeake Bay. *Restoration Ecology* 15:273–283.
- Nowell ARM, Jumars PA (1984) Flow Environments of Aquatic Benthos. *Annual Review of Ecology and Systematics* 15:303–328.

- O'Beirn F, Luckenbach M, Nestlerode JA, Coates GM (2000) Toward design criteria in constructed oyster reefs: oyster recruitment as a function of substrate type and tidal height. *Journal Of Shellfish Research* 19:387–395.
- Odom HT, Wilson RF (1962) Further studies on reaeration and metabolism of Texas Bays, 1958-1960. *Publications of the Institute of Marine Science* 8:23–55.
- Orlando SPJr, Rozsas LP, Ward GH, Klein CJ (1993) Salinity characteristics of Gulf of Mexico estuaries: Silver Spring. Strategic Environmental Assessment Division, Office of Ocean Resources Conservation and Assessment, National Oceanic and Atmospheric Administration, Silver Spring, MD.
- Pinckney JL, Zingmark RG (1993) Modeling the annual production of intertidal benthic microalgae in estuarine ecosystems. *Journal of Phycology* 29:396–407.
- Post DM (2002) Using stable isotopes to estimate trophic position: models, methods, and assumptions. *Ecology* 83:703–718.
- Powell GVN (1987) Habitat use by wading birds in a subtropical estuary: implications of hydrography. *The Auk* 104:740–749.
- R Core Team (2021) A language and environment for statistical computing. R Foundation for Statistical Computing.
- Raven JA (1992) Present and potential uses of the natural abundance of stable isotopes in plant science, with illustrations from the marine environment. *Plant, Cell & Environment* 15:1083–1091.
- Reineck H-E, Singh IB (1980) *Depositional Sedimentary Environments: With Reference to Terrigenous Clastics*, 2nd edition. Springer, Berlin.
- Ridge JT, Rodriguez AB, Fodrie FJ (2017) Salt marsh and fringing oyster reef transgression in a shallow temperate estuary: implications for restoration, conservation and blue carbon. *Estuaries and Coasts* 40:1013–1027.
- Riera P, Richard P (1996) Isotopic determination of food sources of *Crassostrea gigas* along a trophic gradient in the estuarine bay of Marennes-Oléron. *Estuarine, Coastal and Shelf Science* 42:347–360.
- Roegner GC, Mann R (1995) Early recruitment and growth of the American oyster *Crassostrea virginica* (Bivalvia: Ostreidae) with respect to tidal zonation and season. *Marine Ecology Progress Series* 117:91–101.

- Ruesink JL, Feist BE, Harvey CJ, Hong JS, Trimble AC, Wisheart LM (2006) Changes in productivity associated with four introduced species: ecosystem transformation of a 'pristine' estuary. *Marine Ecology Progress Series* 311:203–215.
- Sharma S, Goff J, Cebrian J, Ferraro C (2016) A hybrid shoreline stabilization technique: Impact of modified intertidal reefs on marsh expansion and nekton habitat in the northern Gulf of Mexico. *Ecological Engineering* 90:352–360.
- Smee DL, Overath RD, Johnson KD, Sanchez JA (2013) Intraspecific variation influences natural settlement of eastern oysters. *Oecologia* 173:947–953.
- Solis RS, Powell GL (1999) Hydrography, mixing characteristics, and residence times of Gulf of Mexico estuaries. In: *Biogeochemistry of Gulf of Mexico Estuaries*. Wiley, New York, NY
- Soniat TM, Finelli CM, Ruiz JT (2004) Vertical structure and predator refuge mediate oyster reef development and community dynamics. *Journal of Experimental Marine Biology and Ecology* 310:163–182.
- Tamburri MN, Zimmer-Faust RK, Tamplin ML (1992) Natural sources and properties of chemical inducers mediating settlement of oyster larvae: a re-examination. *Biol Bull* 183:327–338.
- Tunnell JW, Judd FW (2002) *The Laguna Madre of Texas and Tamaulipas*. Texas A&M University Press.
- Turner EJ, Zimmer-Faust RK, Palmer MA, Luckenbach M, Pentchef ND (1994) Settlement of oyster (*Crassostrea virginica*) larvae: effects of water flow and a water-soluble chemical cue. *Limnology and Oceanography* 39:1579–1593.
- Vander Zanden MJ, Rasmussen JB (2001) Variation in $\delta^{15}\text{N}$ and $\delta^{13}\text{C}$ trophic fractionation: Implications for aquatic food web studies. *Limnology and Oceanography* 46:2061–2066.
- Veitch FP, Hidu H (1971) Gregarious setting in the American oyster *Crassostrea virginica* Gmelin: I. Properties of a partially purified "Setting factor." *Chesapeake Science* 12:173–178.
- Vizzini S, Mazzola A (2003) Seasonal variations in the stable carbon and nitrogen isotope ratios ($^{13}\text{C}/^{12}\text{C}$ and $^{15}\text{N}/^{14}\text{N}$) of primary producers and consumers in a western Mediterranean coastal lagoon. *Marine Biology* 142:1009–1018.
- Welschmeyer NA (1994) Fluorometric analysis of chlorophyll a in the presence of chlorophyll b and pheopigments. *Limnology and Oceanography* 39:1985–1992.

- Wetzer R, Brusca R, Wilson G (1997) Taxonomic Atlas of the Benthic Fauna of the Santa Maria Basin and Western Santa Barbara Channel. Vol. 11 - The Crustacea, Part 2. The Isopoda, Cumacea, and Tanaidacea. Santa Barbara Museum of Natural History.
- Withers K, Tunnell JW (1998) Identification of tidal flat alterations and determination of effects on biological productivity of these habitats within the Coastal Bend. Corpus Christi Bay National Estuary Program CCBNEP.
- Xie W, He Q, Zhang K, Guo L, Wang X, Shen J (2018) Impacts of human modifications and natural variations on short-term morphological changes in estuarine tidal flats. *Estuaries and Coasts* 41:1253–1267.
- YSI ProDSS User Manual (2014) YSI Incorporated, Yellow Springs.
- Zeppilli D, Pusceddu A, Trincardi F, Danovaro R (2016) Seafloor heterogeneity influences the biodiversity–ecosystem functioning relationships in the deep sea. *Sci Rep* 6:26352.
- Zhang X, Zhang Y, Zhu L, Chi W, Yang Z, Wang B, Lv K, Wang H, Lu Z (2018) Spatial-temporal evolution of the eastern Nanhui mudflat in the Changjiang (Yangtze River) Estuary under intensified human activities. *Geomorphology* 309:38–50.
- Zu Ermgassen PSE, Spalding MD, Blake B, Coen LD, Dumbauld B, Geiger S, Grabowski JH, Grizzle R, Luckenbach M, McGraw K, Rodney W, Ruesink JL, Powers SP, Brumbaugh R (2012) Historical ecology with real numbers: past and present extent and biomass of an imperilled estuarine habitat. *Proceedings of the Royal Society B: Biological Sciences* 279:3393–3400.

Water Quality and Plankton Monitoring using Historical and Ongoing Datasets

Water Quality and Plankton Monitoring

Overview

Estuaries of the Texas coast contain highly productive aquatic habitats that support birds, fish, and shellfish. Water quality is a major determinant of the health of estuaries, and in other regions, high rates of population growth and accompanying land use change have been shown to have a detrimental impact on water quality. In Texas, the population in Texas coastal counties increased by 29% from 1997 to 2012 (Texas A&M Natural Resources Institute 2014), and projections suggest that there will be an additional 34% population increase by 2050 (Texas State Data Center, <http://txsdc.utsa.edu/Data/TPEPP/Projections/Index.aspx>). Urbanization associated with population growth is known to cause water quality degradation through enhancement of pollutant loadings (e.g., nutrients, organic matter, bacterial pathogens) (Peierls et al. 1991; Vernberg et al. 1992; Hopkinson and Vallino 1995; Handler et al. 2006). In addition, population growth and climate variability/change affects freshwater inflows and ultimately the salinity levels in estuaries through water usage and withdrawals (reviewed by Montagna et al. 2013). Studies in estuaries have noted deleterious effects on living resources and habitat from long-term declines in freshwater inflows (reviewed by Montagna et al. 2013).

Regular assessments of water quality in estuaries can help to identify areas of concern in terms of water quality change, help to understand causes of change(s), and guide management interventions. Here we quantify spatial patterns and long-term trends in the water quality of Matagorda Bay and its tributaries. While in-depth evaluation of causative factors and correlation among variables was outside the scope of this project, we discuss relevant results in the context of possible drivers and impacts, and include an assessment of locations that may need additional monitoring to identify drivers of unwanted changes.

Methods

Data Source and Acquisition

Texas Commission on Environmental Quality data were downloaded from the TCEQ Surface Water Quality Monitoring Program website for Matagorda Bay and its tributaries (Figure 168; Table 34). Stations that were monitored through 2019 were included for analysis. All data manipulation and statistical analyses were performed in R (R Core Team 2020).

Ten water quality variables were assessed in this study (Table 35). For all variables, observations at depths greater than 0.4 meters were removed, as the focus was on water quality based on surface-depth sampling. Routine monitoring was, for the most part, performed on a quarterly schedule. Observations were categorized by year and season, where Winter = D(year+1) JF, Spring = MAM, Summer = JJA, and Fall = SON. In cases where there were multiple sampling events in a single season, the average value and date for the season were calculated.

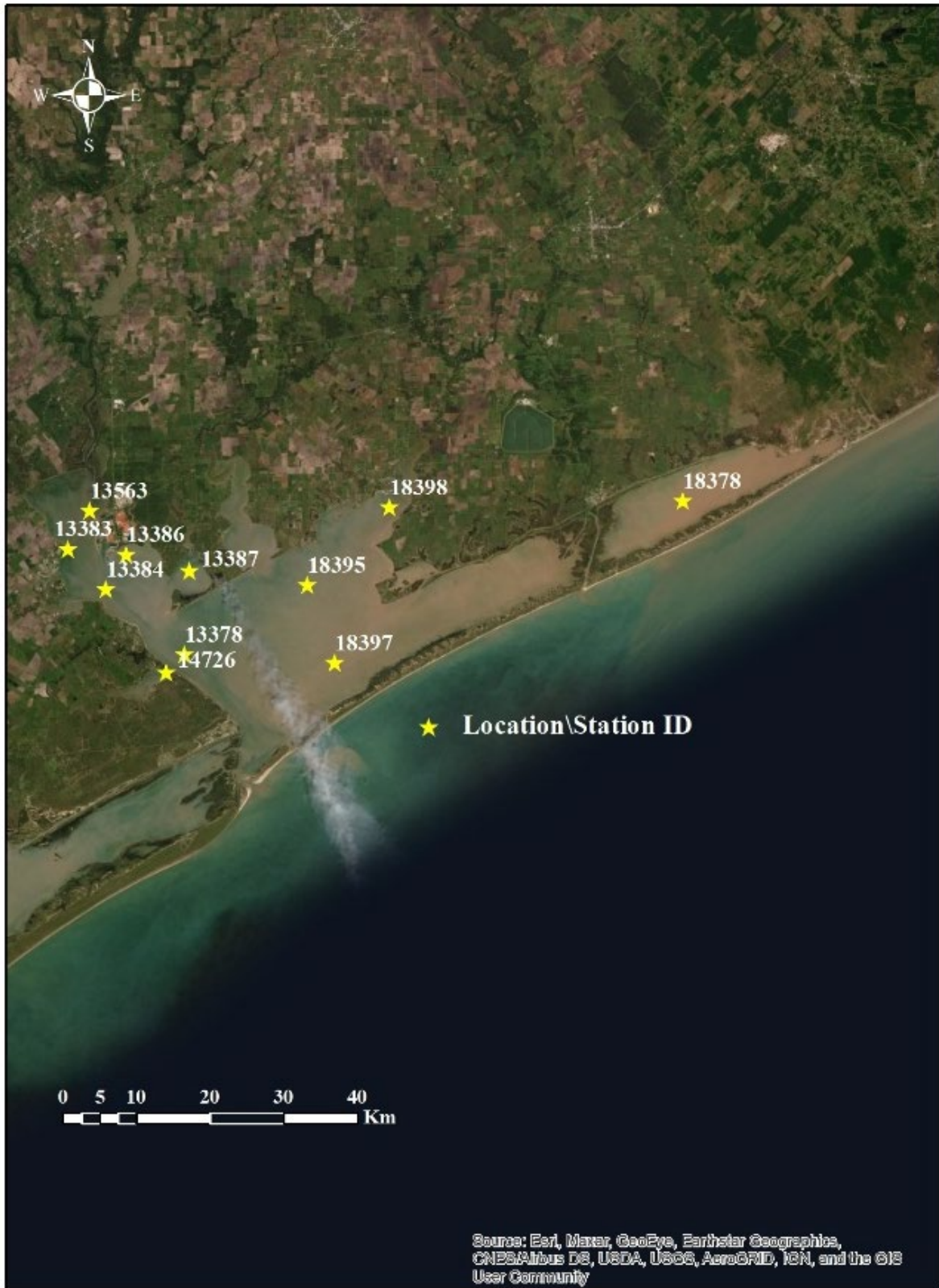


Figure 168. Map of Matagorda Bay showing the location of TCEQ sampling stations.

Table 34. Station ID for sites that were evaluated as part of this study.

Waterbody Name	Station ID
Matagorda Bay	13378
Powderhorn Lake	14726
Matagorda Bay	18395
Matagorda Bay	18397
Cox Bay	13386
East Matagorda Bay	18378
Keller Bay	13387
Lavaca Bay	13383
Lavaca Bay	13384
Lavaca Bay	13563
Tres Palacios Bay	18398

Table 35. Water quality variables assessed in this study.

Parameter Name	Units	Parameter Code	Screening Level
Chlorophyll <i>a</i> (Chl <i>a</i>)	µg/L	70953	11.6 µg/L
Nitrate + Nitrite (N+N)	mg/L	00630	0.17 mg/L
Ammonia	mg/L	00610	0.10 mg/L
Total Kjeldahl Nitrogen (TKN)	mg/L	00625	-
Dissolved Oxygen (DO)	mg/L	00300	-
pH	standard	00400	-
Total Phosphorus (TP)	mg/L	00665	0.21 mg/L
Salinity	PPT	00480	-
Water Temperature	Degrees C	00010	-
Secchi Depth	m	00078	-

Summary Statistics

Summary statistics were calculated for data collected from 2010 to 2019 (10 years). Based on the general practice of the TCEQ, censored observations (flagged by GTLT “<”) were halved prior to calculation of means. Water quality screening levels and criteria were obtained from the TCEQ Guidance for Assessing and Reporting Surface Water Quality in Texas (TCEQ 2020).

Temporal Trend Analysis

A dataset with at least 10 years of data, up to and including 2019, was required for trend analysis. Temporal trends for each variable (averaged for the year and season for the entire period of record, as described above) were computed using Kendall’s tau regression analysis (Kendall 1955) with the NADA Package in R (Lee 2020). Kendall’s tau is a nonparametric method that computes a correlation coefficient based on ranked values, where censored unedited values (i.e., not halved) are treated as ties. Trendlines were estimated using the Akritas-Theil-Sen

nonparametric line (Akritas *et al.* 2021) and the Turnbull estimate for intercept (Turnbull 1976) with a critical alpha = 0.05.

Results and Discussion

Average salinities fell within a relatively narrow range of ~18-26, with highest values observed at Matagorda Bay, Powderhorn Lake, East Matagorda Bay stations, slightly lower values observed at Cox, Keller, Tres Palacios and one Lavaca station, and lowest values observed at two upper Lavaca Bay stations (Figure 169). The Lavaca Bay stations were also subject to wide variation in salinity from near 0 to ~40. One site (13563) in Lavaca Bay displayed a long-term increase in salinity (Table 36). Average pH ranged from 8.1 to 8.3 across all stations (Figure 170). Variability was noticeable though, with values occasionally reaching <8.0 where potential harm to calcifying organisms may occur (reviewed by Gazeau *et al.* 2013). The most common causes of lower pH in estuaries include an influx of low pH water from wetlands or marshes during rainfall or degradation of algal biomass upon bloom cessation (Baumann and Smith 2018; Carstensen and Duarte 2019). Furthermore, a trend of decreasing pH was observed at two Lavaca Bay stations (13383, 13384), Cox Bay, and Keller Bay (Table 36). In contrast, increasing pH was observed in Powderhorn Lake and Tres Palacios Bay. Secchi depth, an indicator of light penetration, was generally deepest on average at the Matagorda Bay, Keller Bay and Tres Palacios stations (~0.6-0.8 m), and shallower at the Powderhorn Lake, Cox, East Matagorda Bay and Lavaca Bay sites (~0.4-0.55 m; Figure 171). A trend of increasing Secchi depth (i.e., water that was becoming more transparent) was observed at the East Matagorda Bay station (Table 36).

Average N+N concentrations were relatively low (<0.05 mg/L) compared to many other estuarine systems, although higher concentrations were periodically observed (Figure 172). Box plots of N+N from 2010-2019 in the Matagorda Bay ecosystem. One station in Lavaca Bay (13563) displayed N+N concentrations that exceeded TCEQ's screening level (0.17 mg/L) in 20.6% of samples (Table 37), which is the threshold suggesting a concern is warranted for that variable (TCEQ 2020a). Two stations in Lavaca Bay (13383, 13384), one station in Matagorda Bay (13378), Cox Bay, Keller Bay and Tres Palacios Bay all displayed a trend of decreasing N+N over time (Table 36). Average ammonia concentrations were uniformly low (<0.05 mg/L; Figure 173) and while higher concentrations were occasionally observed, no site exceeded the TCEQ screening level (0.1 mg/L) more than 11% of the time (Table 36). One station in Matagorda Bay (13378), one station in Powderhorn Lake (14726), Cox Bay, and two stations in Lavaca Bay (13383, 13384) displayed decreasing ammonia over time, while East Matagorda displayed an increasing trend (Table 37). Changes in laboratory methods and detection limits may obscure the trend analysis results however, particularly for variables such as N+N and ammonia where the majority of values were recorded as below detection limits. Thus, caution should be used for interpretation of trends for those variables. Overall, the dominant form of nitrogen was TKN, which represents the sum of ammonia and organic nitrogen. In this case, because ammonia concentrations were very low, it can be assumed that most of the TKN represents organic nitrogen. Average TKN ranged from ~0.5-1.0 mg/L (Figure 174), with highest values observed at two of the Lavaca Bay stations. Unfortunately, TCEQ does not have established screening levels for TKN, but numerous studies have now shown that organic nitrogen can be a major contributor to algal growth and may tend to favor growth of harmful algae species (Anderson *et al.* 2002; Burkholder *et al.* 2008). Considering that several studies have documented the sensitivity of algal growth in Texas estuaries to nitrogen availability

(Örnólfsson et al. 2004; Wetz et al. 2017), it is recommended that additional attention be paid to TKN from a regulatory standpoint. This is particularly pertinent given the trend of increasing TKN at two stations in Lavaca Bay (13383, 13563; Table 36). Average TP concentrations were low, ranging from ~0.05-0.13 mg/L (Figure 175), and while higher concentrations were occasionally observed, no site exceeded the TCEQ screening level (0.21 mg/L) more than 11% of the time (Table 37). Two stations in Lavaca Bay (13383, 13384), Cox Bay, and one station in Matagorda Bay (13378) displayed increasing trends in TP, while Powderhorn Lake showed a decreasing trend (Table 36).

Aside from the aforementioned direct measurements of nutrient concentrations, chlorophyll *a* and dissolved oxygen are two sensitive indicators of nutrient enrichment. Average surface dissolved oxygen concentrations varied little between stations, ranging from 7.6-8.0 mg/L (Figure 176). Low concentrations that would be potentially harmful to aquatic life (<2 mg/L) were occasionally observed at two Matagorda Bay stations (18395, 18397), one Lavaca Bay station (13384) and more frequently in Tres Palacios Bay. In addition, a decreasing trend was observed at two Lavaca Bay stations (13383, 13384), Cox Bay and Keller Bay (Table 36). Average chlorophyll *a* concentrations were low (<10 µg/L) with the exception of Tres Palacios Bay, which averaged 12.0 µg/L (Figure 177). Three stations in Lavaca Bay (13383, 13563) and Tres Palacios Bay (18398) showed evidence of attaining a TCEQ-designated concern, as chlorophyll *a* concentrations exceeded the TCEQ screening level (11.6 µg/L) on 24% (13383), 23% (13563) and 55% (18398) of sampling events (Table 37). One Lavaca Bay station (13563), one Matagorda Bay station (13378), and Powderhorn Lake showed evidence of increasing chlorophyll *a* (Table 36).

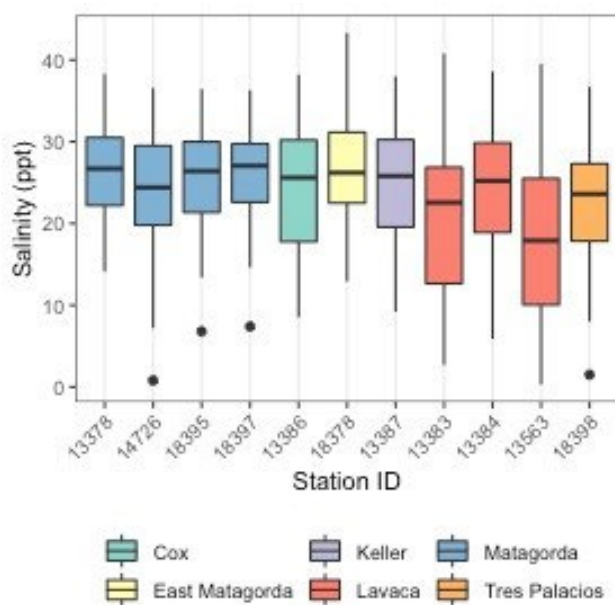


Figure 169. Box plots of salinity from 2010-2019 in the Matagorda Bay ecosystem.

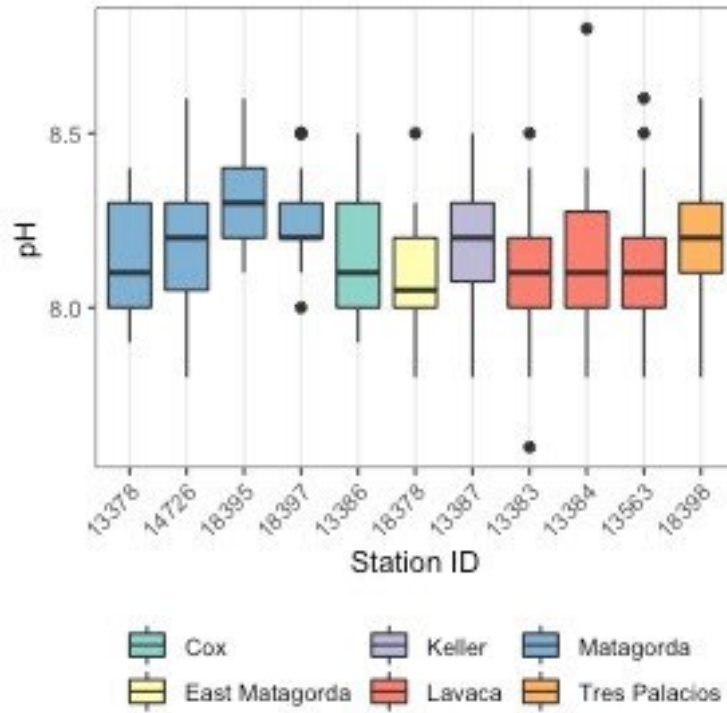


Figure 170. Box plots of pH from 2010-2019 in the Matagorda Bay ecosystem.

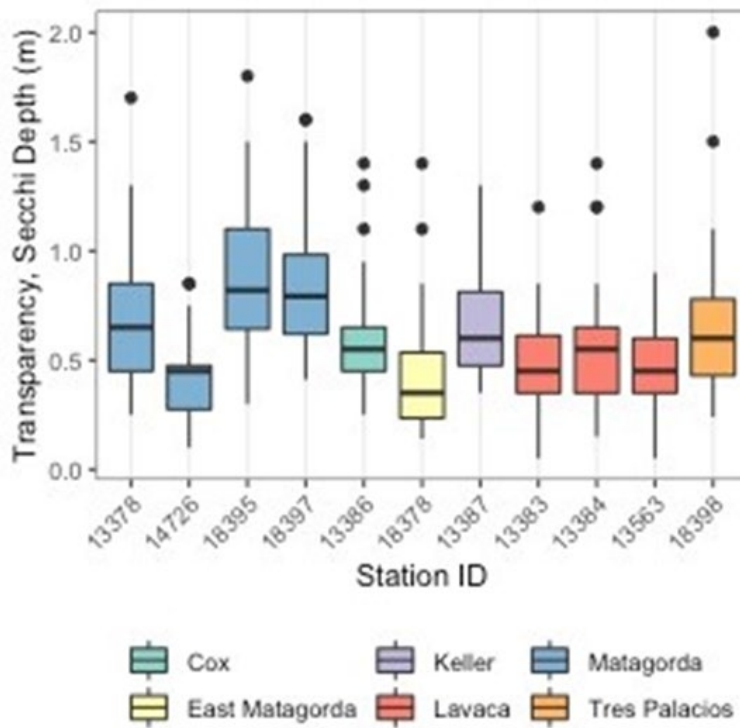


Figure 171. Box plots of Secchi depth from 2010-2019 in the Matagorda Bay ecosystem.

Table 36. Long-term trends in water quality variables. Gray shaded cells indicate variables/sites where statistically significant trends were detected. “+” indicates increasing trend, while “-” indicates decreasing trend.

Waterbody Name	Station ID	Chl <i>a</i>	N+N	Ammonia	TKN	DO	pH	TP	Salinity	Temp	Secchi
Matagorda Bay	13378	+	-	-	NS	NS	NS	+	NS	NS	NS
Powderhorn Lake	14726	+	NS	-	NS	NS	-	-	NS	NS	NS
Matagorda Bay	18395	NS	NS	NS	NS	NS	-	NS	NS	NS	NS
Matagorda Bay	18397	NS	NS	NS	NS	NS	NS	NS	NS	NS	NS
Cox Bay	13386	NS	-	-	NS	-	-	+	NS	NS	NS
East Matagorda Bay	18378	NS	NS	+	NS	NS	NS	NS	NS	NS	+
Keller Bay	13387	NS	-	NS	NS	-	-	NS	NS	NS	NS
Lavaca Bay	13383	NS	-	-	+	-	-	+	NS	NS	NS
Lavaca Bay	13384	NS	-	-	NS	-	-	+	NS	NS	NS
Lavaca Bay	13563	+	NS	NS	+	NS	NS	NS	+	NS	NS
Tres Palacios Bay	18398	NS	-	NS	NS	NS	+	NS	NS	NS	NS

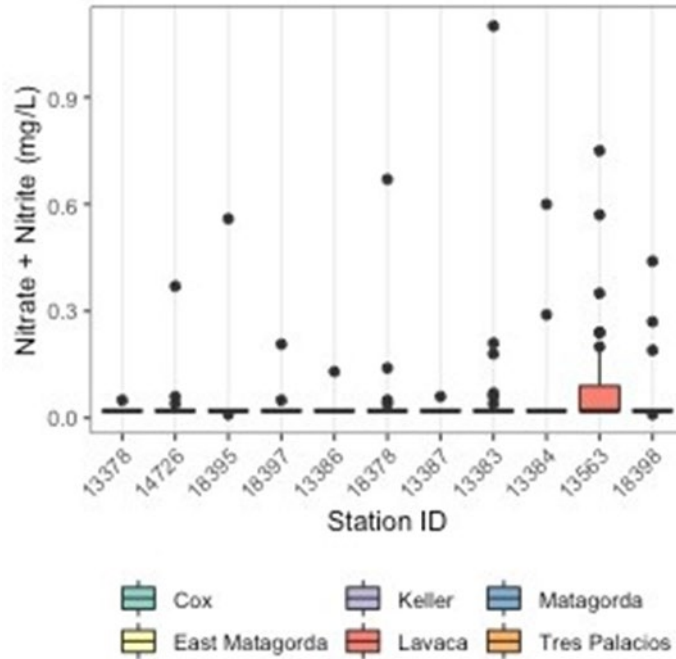


Figure 172. Box plots of N+N from 2010-2019 in the Matagorda Bay ecosystem.

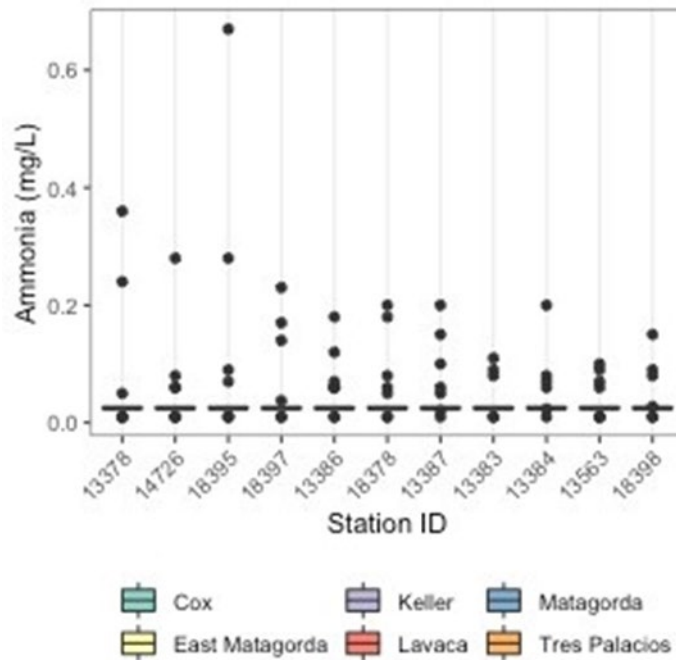


Figure 173. Box plots of ammonia from 2010-2019 in the Matagorda Bay ecosystem.

Table 37. Percent of samples from 2010-2019 that exceeded the TCEQ screening level for ammonia (0.10 mg/L), N+N (0.17 mg/L), TP (0.21 mg/L), and Chl a (11.6 µg/L). Bold text indicates where the 10-year dataset suggested potential excessive concentrations because of screening level exceedance in at least 20% of samples.

Waterbody name	Station ID	Ammonia	N+N	TP	Chl a
Matagorda	13378	6.1	0.0	3.3	9.4
Powderhorn Lake	14726	3.1	3.0	3.3	17.6
Matagorda	18395	6.5	3.1	0.0	17.2
Matagorda	18397	10.7	3.3	3.7	14.8
Cox	13386	7.1	0.0	0.0	16.7
East Matagorda	18378	0.0	0.0	10.7	2.8
Keller	13387	10.3	0.0	0.0	16.7
Lavaca	13383	3.3	9.3	3.7	24.2
Lavaca	13384	3.2	5.9	0.0	12.1
Lavaca	13563	3.0	20.6	9.7	22.9
Tres Palacios	18398	3.2	9.4	3.3	55.2

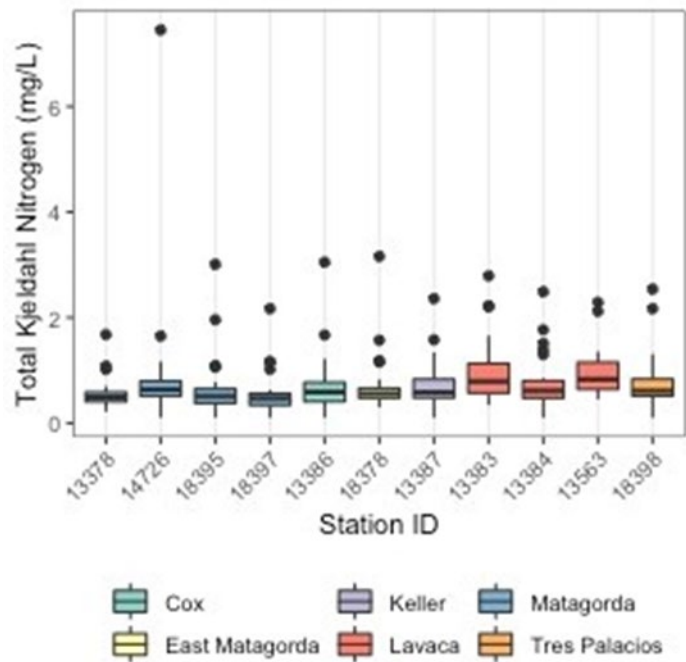


Figure 174. Box plots of TKN from 2010-2019 in the Matagorda Bay ecosystem.

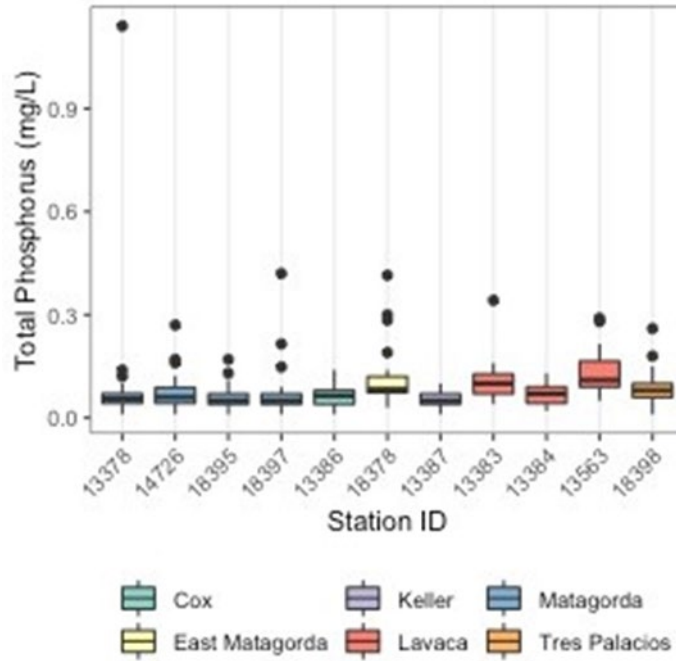


Figure 175. Box plots of TP from 2010-2019 in the Matagorda Bay ecosystem.

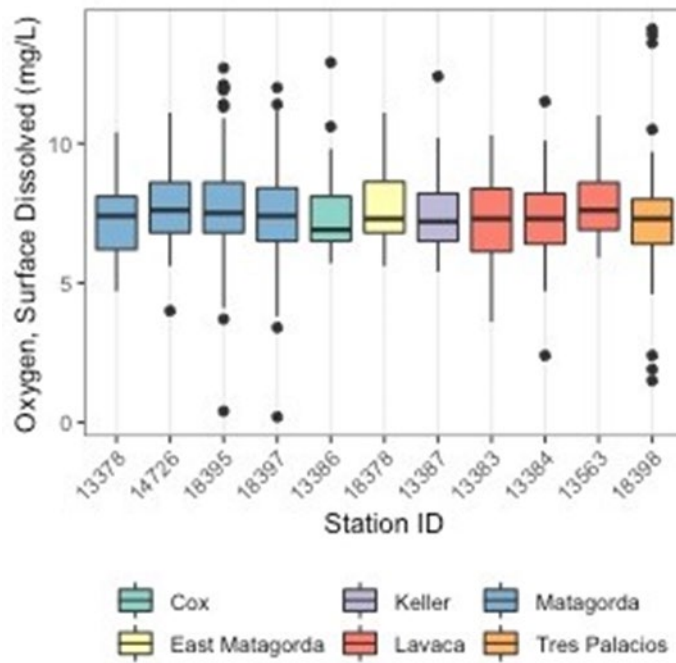


Figure 176. Box plots of DO from 2010-2019 in the Matagorda Bay ecosystem.

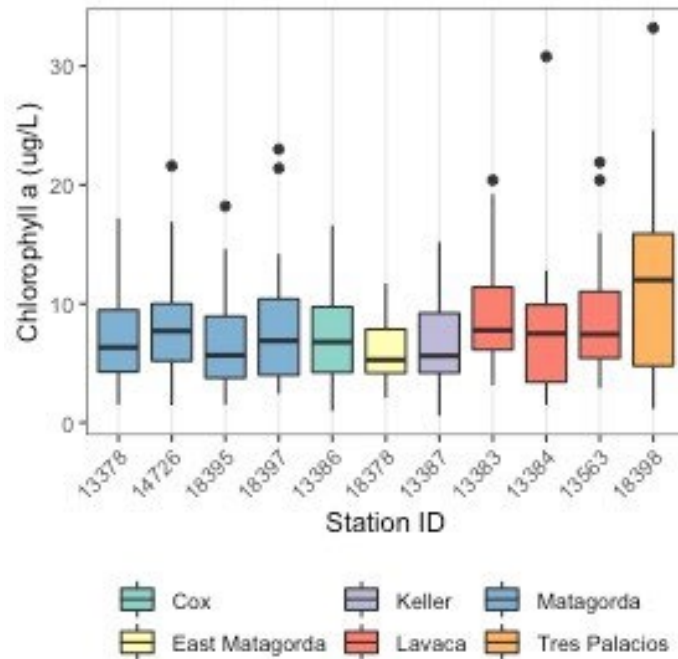


Figure 177. Box plots of Chl *a* from 2010-2019 in the Matagorda Bay ecosystem.

Summary and recommendations

Results from this analysis of water quality patterns and trends in Matagorda Bay highlight several key features. First, nutrient indicators show that, in general, the Matagorda Bay ecosystem is not currently displaying widespread symptoms of excess nutrients. Based on screening levels set forth by TCEQ, it could be argued that Lavaca Bay and Tres Palacios Bay are exceptions to this statement, as both frequently (>20% of samples collected) exceeded chlorophyll *a* screening levels. Furthermore, Lavaca Bay in particular had one or more stations displaying long-term increases in chlorophyll *a*, TKN or TP, or long-term decreases in dissolved oxygen, all of which point to an ecosystem that is under pressure from watershed nutrient sources. Additional attention clearly needs to be paid to nutrient conditions in Lavaca Bay and its feeder rivers/creeks before harm occurs to the ecosystem. Aside from water quality issues related to nutrient pollution, the other major challenge facing Texas coastal ecosystems is a long-term decline in freshwater inflow that can manifest as increasing salinity levels (Montagna et al. 2013). Adequate freshwater inflow and salinity levels are vital influences on estuarine ecosystem health (Copeland 1966; Montagna et al. 2013), as prolonged increases in salinity above historical conditions can lead to deleterious declines in upper trophic level biomass and changes in diversity (Copeland 1966; Livingston et al. 1997; Palmer and Montagna 2015). Based on the data analyzed here, only one station (near the mouth of the Lavaca River in Lavaca Bay) showed a long-term salinity increase. However, the P.I. has heard numerous stakeholder concerns about salinity in the eastern arm of West Matagorda Bay where, unfortunately, no TCEQ monitoring stations are currently active. Additional monitoring is recommended in this data poor region of Matagorda Bay to allow for a more holistic assessment of conditions in the bay.

Literature Cited

- Akritis MG, Murphy SA, and Lavalley MP. 2021. The Theil-Sen Estimator with Doubly Censored Data and Applications to Astronomy. *J Am Stat Assoc* 90: 170–7.
- Anderson DM, Glibert PM, and Burkholder JM. 2002. Harmful algal blooms and eutrophication: nutrient sources, composition, and consequences. *Estuaries* 25: 704-726
- Baumann H, and Smith EM. 2018. Quantifying metabolically driven pH and oxygen fluctuations in US nearshore habitats at diel to interannual time scales. *Estuar Coasts* 41: 1102-1117
- Burkholder JM, Glibert PM, and Skelton HM. Mixotrophy, a major mode of nutrition for harmful algal species in eutrophic waters. *Harmful Algae* 8: 77-93
- Carstensen J, and Duarte CM. 2019. Drivers of pH variability in coastal ecosystems. *Environ Sci Tech* 53: 4020-4029
- Copeland, B.J., 1966. Effects of decreased river flow on estuarine ecology. *J. Water Poll. Control Fed.* 38: 1831-1839.
- Gazeau, F., Parker, L.M., Comeau, S., Gattuso, J.P., O'Connor, W.A., Martin, S., Portner, H.O., Ross, P.M., 2013. Impacts of ocean acidification on marine shelled molluscs. *Mar. Biol.* 160: 2207-2245.
- Handler, N.B., Paytan, A., Higgins, C.P., Luthy, R.G., Boehm, A.B., 2006. Human development is linked to multiple water body impairments along the California coast. *Estuar. Coasts* 29: 860-870.
- Hopkinson, C.S., Vallino, J.J., 1995. The relationships among man's activities in watersheds and estuaries – a model of runoff effects on patterns of estuarine community metabolism. *Estuaries* 18: 598-621.
- Kendall M. 1955. Rank Correlation Methods. London: Charles Griffin and Company. Lee L. 2020. NADA: Nondetects and Data Analysis for Environmental Data. R package version 1.6-1.1.
- Livingston, R.J., Niu, X, Lewis, F.G., Woodsum, G.C., 1997. Freshwater input to a Gulf estuary: long-term control of trophic organization. *Ecol. App.* 7: 277-299
- Montagna, P. A., T. A. Palmer, and J. Beseres Pollack. 2013. Hydrological changes and estuarine dynamics, Springer New York.
- Örnólfssdóttir, E. B., S. E. Lumsden, and J. L. Pinckney. 2004. Nutrient pulsing as a regulator of phytoplankton abundance and community composition in Galveston Bay, Texas. *J Exp Mar Biol Ecol* 303: 197–220.

- Palmer, T. A., and P. A. Montagna. 2015. Impacts of droughts and low flows on estuarine water quality and benthic fauna. *Hydrobiologia* 753: 111–129.
- Peierls, B.L., Caraco, N.F., Pace, M.L., Cole, J.J., 1991. Human influence on river nitrogen. *Nature* 350: 386-387.
- R Core Team. 2020. R: A language and environment for statistical computing. Vienna, Austria: R Foundation for Statistical Computing.
- TCEQ. 2020. Draft 2020 Guidance for Assessing and Reporting Surface Water Quality in Texas. Texas Commission on Environmental Quality.
- Turnbull B. 1976. The empirical distribution function with arbitrarily grouped, censored and truncated data. *J R Stat Soc Ser B* 38: 290–5.
- Vernberg, F.J., Vernberg, W.B., Blood, E., Fortner, A., Fulton, M., McKellar, H., Michener, W., Scott, G., Siewicki, T., Elfigi, K., 1992. Impact of urbanization on high-salinity estuaries in the southeastern United States. *Neth. J. Sea Res.* 30: 239-248.
- Wetz MS, Cira E, Sterba-Boatwright B, *et al.* 2017. Exceptionally high organic nitrogen concentrations in a semi-arid South Texas estuary susceptible to brown tide blooms. *Estuar Coast Shelf Sci* 188: 27–37.

Influence of freshwater inflow from the Colorado River on nutrients and phytoplankton in Matagorda Bay

Overview

Freshwater inflow is a major driver of environmental conditions in estuaries (Gillanders and Kingsford 2002; Burford et al. 2011). In Texas, variability in the El Niño/La Niña cycle largely controls rainfall patterns (Kim et al. 2014), with El Niño characterized by increased rainfall and La Niña by dry conditions (Kim et al. 2014). Freshwater inflow is also influenced by diversions of water away from rivers into reservoirs for human use (Flemer and Champ 2006). Lastly, climate change may cause greater evaporation rates or extended drought periods, decreasing river flow (Konapala et al. 2020).

Inflow variability can affect important estuary attributes. For example, decreased inflow can increase salinity in estuaries, resulting in reduced mixing and introduction of diseases and parasites from saltier water (Longley 1994; Gillanders and Kingsford 2002). Low inflow can reduce riverine-derived nutrient loading (Longley 1994; Gillanders and Kingsford 2002), leading to decreased primary and secondary production as well as loss of fish harvests and nursery habitats (Longley 1994; Boynton and Kemp 2000; Barbosa et al. 2010; Burford et al. 2011; Barroso et al. 2018). In contrast, high inflow can expand the brackish zone and create hospitable nursery habitats for various organisms including juvenile fish, shrimp and oysters (Longley 1994). Increased river inflow can also bring a fresh supply of nutrients (Burford et al. 2011; Bruesewitz et al. 2013), and with sufficient nutrients and light, primary production can increase (Flemer and Champ 2006).

In Matagorda Bay, past drought conditions have stopped inflow completely to Matagorda Bay (Montagna et al. 2002). Freshwater decreased significantly between 1940-1950 due to drought (Longley 1994). A dry period in the 1960s also decreased inflow rates (Longley 1994). In 1993, river flow to Matagorda Bay was reduced by diversion from the Colorado River (Kim et al. 2009). However, there have been few studies on the response of phytoplankton to these low inflow periods. Phytoplankton are often the dominant primary producer in estuaries and play an essential role by forming the base of the food web. With increasing urbanization and population growth in its watershed, freshwater demand will also increase, which will likely further decrease freshwater inflow (Texas Water Development Board 2017). Because of this, it is imperative that we begin to understand how phytoplankton may respond to changes in freshwater inflow to Matagorda Bay. In this study, monthly sampling was conducted in Matagorda Bay for 24 months to assess phytoplankton biomass and community structure in varying environmental conditions, including changing freshwater input. Three hypotheses were tested: 1) Chlorophyll *a* (Chl *a*) and phytoplankton biovolume will correlate with freshwater inflow, 2) Chl *a* maximum will be at the site closest to the Colorado River, and 3) the phytoplankton community will be dominated by functional groups that prefer brackish, nutrient-rich conditions.

Site Description

The Matagorda Bay system is located on the central Texas coast and has the second largest surface area of Texas estuaries (Figure 178). The system is lagoonal, mostly isolated from the Gulf of Mexico, and comprised of a main bay (Matagorda Bay) and several subsystems including Lavaca Bay and East Matagorda Bay (Ward and Armstrong 1980). The mean depth of Matagorda Bay is 2.8 meters, and the residence time is about 2.5 months (Ward and Armstrong 1980; Armstrong 1982; Palmer et al. 2011). Depending on the declination of the moon, the tidal range can be semi-diurnal at about 0.2 meters (minimum declination) or diurnal at about 0.8

meters (at maximum declination) (Ward and Armstrong 1980). Circulation in the bay is also influenced by wind-driven wave action, mainly from south to southeastern winds of the Gulf of Mexico that keep the bay well-mixed (Ward and Armstrong 1980). For this study, sampling locations were in the main bay, which receives freshwater input from the Colorado River. Six sites (A1, MAD, A2, A4, A6, A9) were chosen along a river inflow gradient (Figure 178).

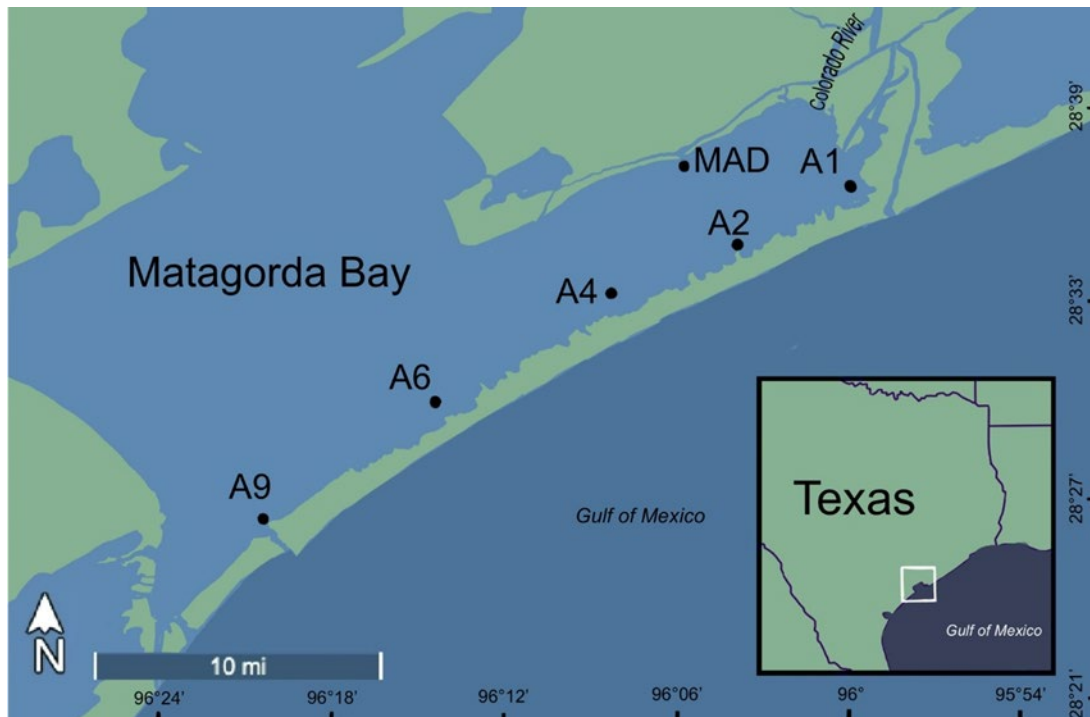


Figure 178. Map of sample sites in Matagorda Bay.

Methods

Sampling

From November 2019 to October 2021, monthly sampling was conducted in Matagorda Bay, excluding March 2020 due to COVID precautions. At each site, water was collected at 10 cm below the surface in brown HDPE bottles and stored on ice for nutrient and Chl *a* analysis. Additional samples were kept at ambient water temperature for phytoplankton enumeration. Light attenuation was measured with a Secchi disk. Salinity, pH, dissolved oxygen (DO; mg L⁻¹), and temperature (°C) were recorded at 0.5 m increments, starting at 0.1 cm below the surface with a YSI multiparameter sonde. Colorado River inflow data were obtained from USGS at gauge 08162501. Freshwater inflow was recorded based on a seven-day average leading up to and including the sampling date, based on Roelke et al. (2017), for the best reflection of the relationship between freshwater input and phytoplankton growth.

Biogeochemical Analyses

Chilled water samples were filtered through 25 mm GF/F filters for nutrient analysis and stored in a -20 °C freezer. Samples were thawed to room temperature and then analyzed on a Seal QuAAtro autoanalyzer. Standard curves with five different concentrations were run daily at the beginning of each run. Fresh standards were made prior to each run by diluting a primary standard with low nutrient surface seawater. Deionized water (DIW) was used as a blank, and

DIW blanks were run at the beginning and end of each run, as well as after every 8-10 samples to correct for baseline shifts. Method detection limits were 0.02 μM for nitrate plus nitrite (N+N) and ammonium (NH_4^+), and $< 0.01 \mu\text{M}$ for orthophosphate (PO_4^{3-}) and silicate (SiO_4). Dissolved inorganic nitrogen (DIN) was calculated as the sum of NH_4^+ and N+N.

Phytoplankton Analyses

Chl *a* was obtained by filtering 25 mL of chilled sample water through Whatman 25 mm GF/F filters that were stored in a -20°C freezer until extracted. To extract Chl *a*, filters were placed in tubes with 10 mL of 90% HPLC grade acetone for 16-24 hours. Then for analysis, a Turner Trilogy fluorometer was used to read Chl *a* using a non-acidified method (Welschmeyer 1994; EPA method 445.0).

To determine microplankton abundance, 60 mL of sample from the bottle stored at ambient temperature was preserved with 1 mL acid Lugol's solution. Between 1-10 mL of sample was settled in an Utermohl chamber for 1 hour per mL before counting on an Olympus 1X-71 inverted microscope at 20x magnification. To calculate biovolume, formulas from Hillebrand et al. (1999) and Sun and Liu (2003) were used based on the geometric shape of the genus, using average cell measurements from counts. Sun and Liu (2003) formulas were used if there was a conflict between the two paper's formulas. If no third dimension of a cell was visible, this dimension was estimated based on relationships observed from cells for which all dimensions could be obtained.

Sample water (4 mL) was fixed with 80 μL glutaraldehyde for flow cytometric analysis and stored at -20°C until analysis. Samples were thawed in the dark at room temperature then filtered through 20 μm Nytex mesh. Picoplankton were enumerated with an Accuri C6 Plus flow cytometer. The detection limit for picoplankton was 1040 cells mL^{-1} and values below the detection limit were treated as zeros.

Statistical Analyses

Kendall's tau was used to determine correlations between Chl *a*, phytoplankton biovolume, or functional group biovolume and environmental variables at each site. The Kruskal-Wallis test with a post-hoc Dunn test was used to determine differences between non-normal environmental variables. All previous analyses and figures were generated in R 4.1.2 or Microsoft Excel. Principal components analysis and figure generation was performed in PRIMER-E Ltd. ANOVA was only used for data that met assumptions (normal).

Results

Environmental factors

The mean Colorado River discharge was $276 \text{ m}^3 \text{ s}^{-1}$. The lowest discharge was $33 \text{ m}^3 \text{ s}^{-1}$ (August 2020) and the highest discharge was $2940 \text{ m}^3 \text{ s}^{-1}$ (May 2021; Figure 179). Mean salinity ranged from 5.7 in May 2021 during the peak flow of $2940 \text{ m}^3 \text{ s}^{-1}$, to 29.2 in August 2020 (Figure 180). There was an increasing salinity gradient for sites with distance from the river mouth (Figure 181). Median salinities at the three sites closest to the river mouth (A1, MAD and A2) were significantly lower than the three sites farther away (A4, A6 and A9; $p < 0.001$, Table 38). There was distinct seasonality in surface temperature, with highest average temperatures observed in August 2020 and July 2021 (30.3°C and 29.7°C respectively; Figure 182) and lowest temperatures in November of 2019 and December 2020 (15.9°C and 14.8°C respectively; Figure 182). Mean Secchi depth was less than 1 m for all sites over the duration of the study (Figure 183). Secchi depth at the sites closest to the river mouth were consistently shallower than the sites farther away (Figure 184). A1 and MAD had significantly shallower

Secchi depths than A4, A6 and A9 ($p < 0.01$, Table 38). There was no significant difference in Secchi depth with different amounts of discharge ($p = 0.153$).

Mean N+N concentration was $< 20 \mu\text{M}$ for the duration of the study and reached two maximums in the winter season (January 2020, $14.5 \mu\text{M}$ and December 2020, $16.7 \mu\text{M}$; Figure 185). A1, MAD and A2 had significantly higher median N+N concentrations than A4, A6 and A9 ($p < 0.01$; Table 38). N+N had a significant negative linear relationship with increasing distance from the river ($p < 0.01$; Figure 186) and temperature ($p = 0.05$; Figure 187). Mean ammonium concentration was $< 9 \mu\text{M}$ for the duration of the study and reached two maximums, $5.2 \mu\text{M}$ in January 2021 and $6.9 \mu\text{M}$ in April 2021 (Figure 188). Ammonium had a significant negative linear relationship with increasing distance from the river ($p = 0.01$; Figure 189). There was no significant difference in median ammonium between sites (Table 38).

The mean orthophosphate concentration for all six sites across sampling dates was $1.7 \mu\text{M}$, and the maximum orthophosphate concentration ($3.4 \mu\text{M}$) occurred on the same sampling date as the maximum discharge (May 2021; Figure 190). Orthophosphate had a significant negative linear relationship with increasing distance from the river mouth ($p < 0.01$; Figure 191). Median orthophosphate was significantly higher at A1 compared to all other sites, and A9 had a significantly lower median orthophosphate than A1, MAD and A2 (Table 38). Orthophosphate had a significant positive linear relationship with discharge ($p = 0.01$; Figure 192). The system is consistently nitrogen-limited, based on nutrient ratios ($\text{DIN}:\text{PO}_4 < 16$; Figure 193).

Silicate concentration ranged from $6.2 \mu\text{M}$ to $133.9 \mu\text{M}$ and the mean silicate concentration across sites was $56.0 \mu\text{M}$ (Figure 194). Mean silicate concentration was relatively low at the beginning of the study (November 2019) through April 2020, increased through November 2020, and decreased until March 2021. After March 2021, silicate concentration increased and peaked in May 2021. Silicate had a significant negative linear relationship with increasing distance from the river mouth ($p < 0.01$; Figure 195). Silicate had a significant positive linear relationship with both discharge ($p < 0.01$) and temperature ($p = 0.01$; Figure 196; Figure 197). Potential silicate limitation ($\text{Si}:\text{DIN} < 1$) only occurred on two dates, January (0.72) and February (0.69) of 2020 (data not shown).

Principal components analysis yielded a PC1 characterized by salinity, with most nutrients inversely related to salinity, and a PC2 characterized by temperature and Chl *a* inversely related to DO (Figure 198). PC1 explained 34.1% of variation, and PC2 23.0% variation. Winter and spring separated from the other two seasons on PC1 and were characterized by higher nutrient concentrations and lower salinity (Figure 198). PC2 shows that summer and fall had higher temperatures and lower DO generally (Figure 198). The only spatial difference seen in the PCA by site is a separation of A1, which had higher nutrient concentrations and lower salinity (Figure 199).

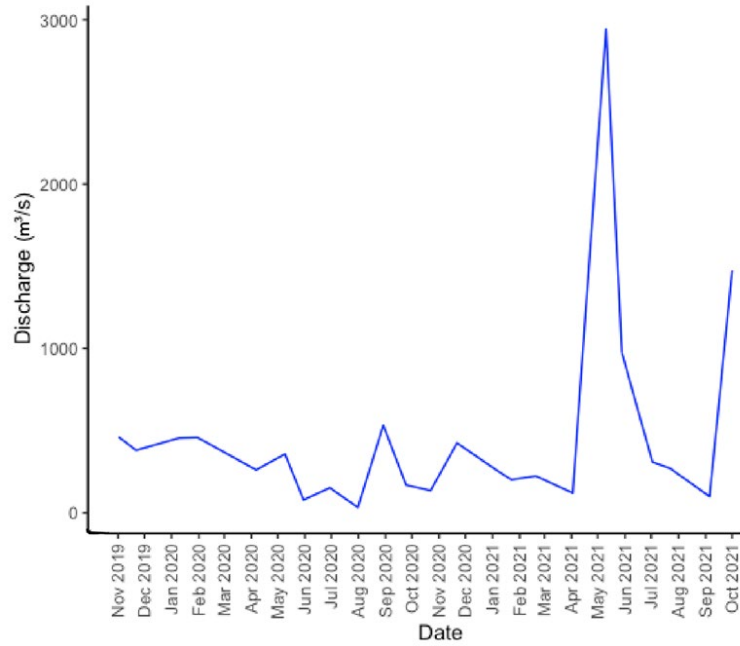


Figure 179. Average weekly discharge from Colorado River up to sampling dates.

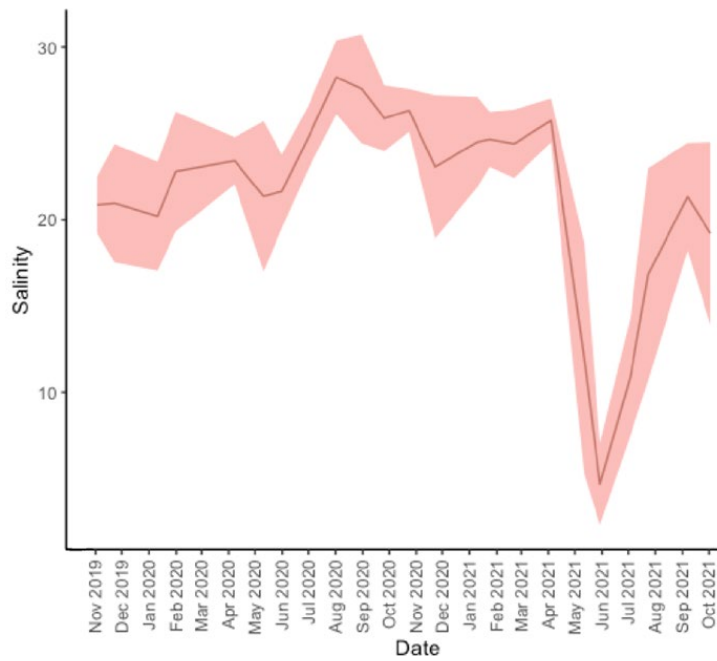


Figure 180. Mean salinity from November 2019-October 2021 (shade is 95% confidence interval).

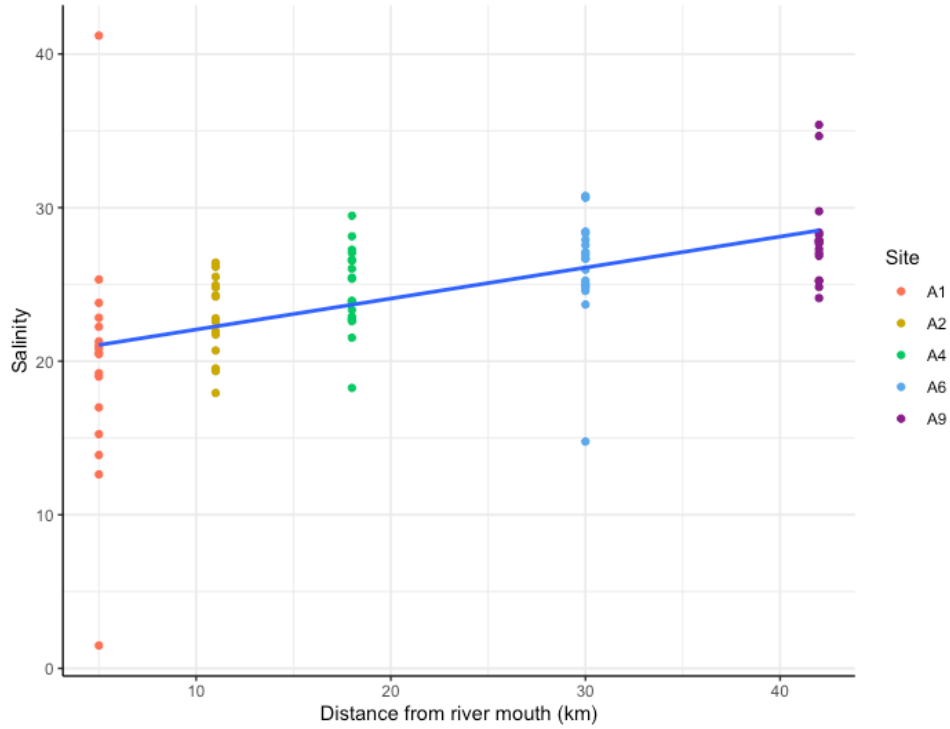


Figure 181. Salinity gradient from river mouth.

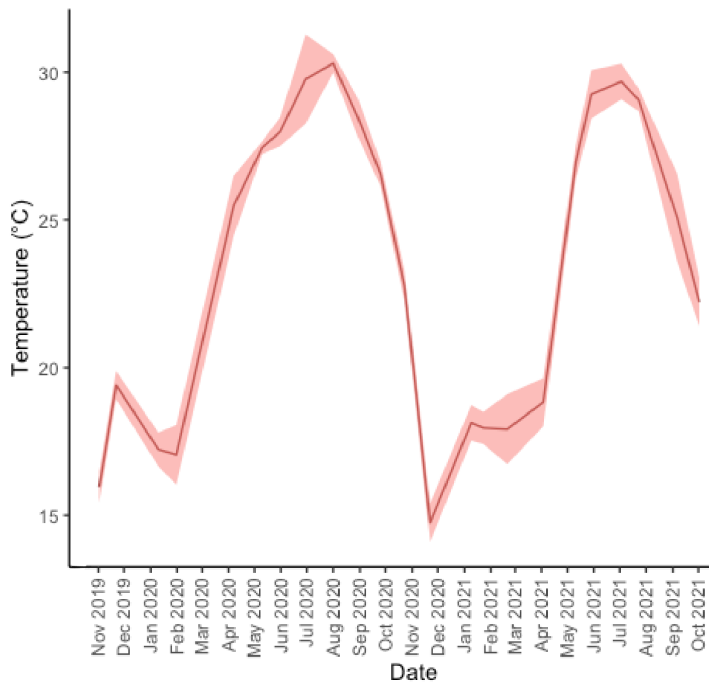


Figure 182. Mean temperature from November 2019-October 2021 (shade is 95% confidence interval).

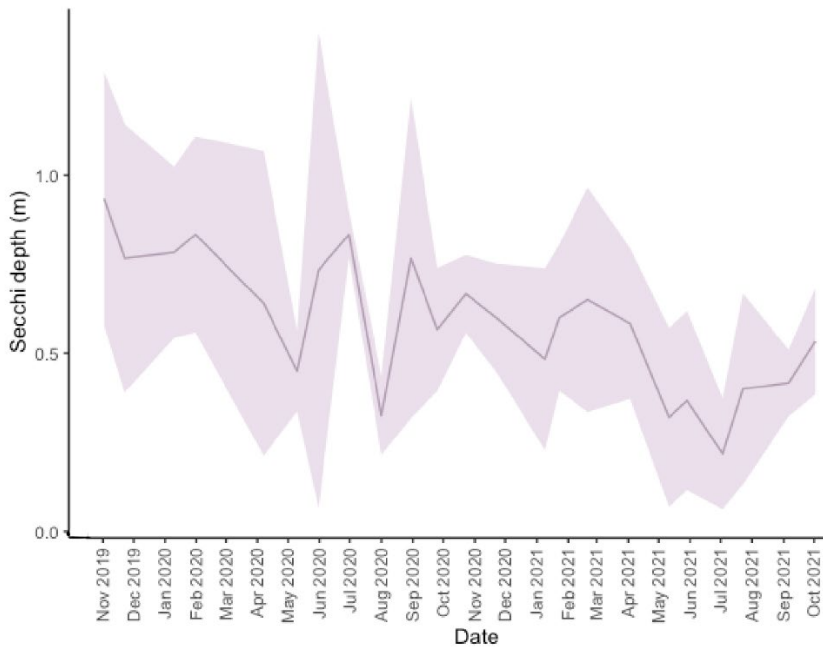


Figure 183. Mean Secchi depth from November 2019-October 2021 (shade is 95% confidence interval).

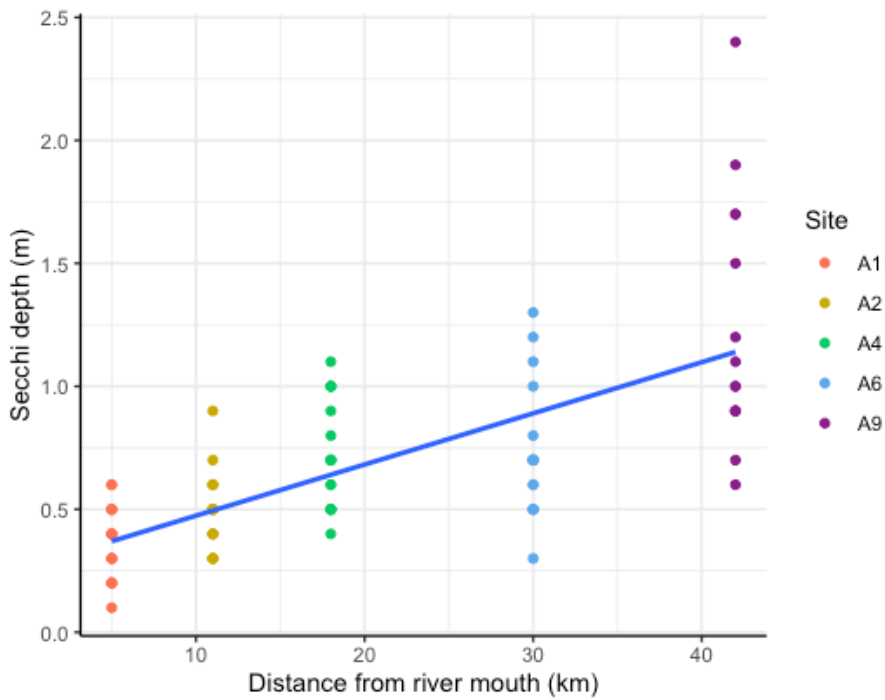


Figure 184. Secchi depth gradient from river mouth.

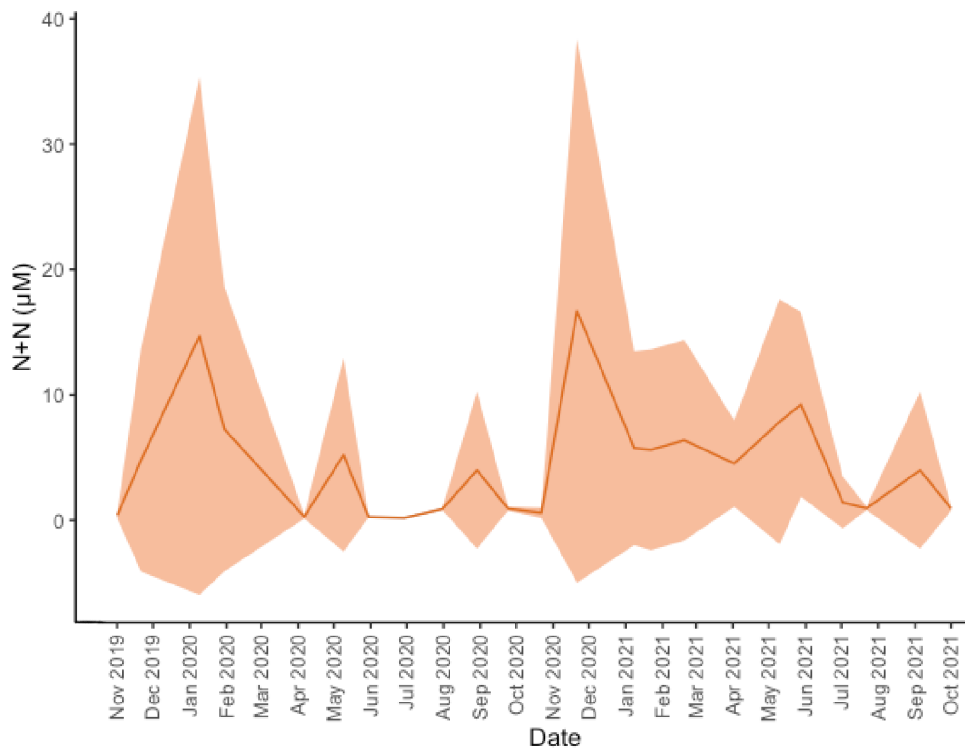


Figure 185. Mean N+N from November 2019-October 2021 (shade is 95% confidence interval).

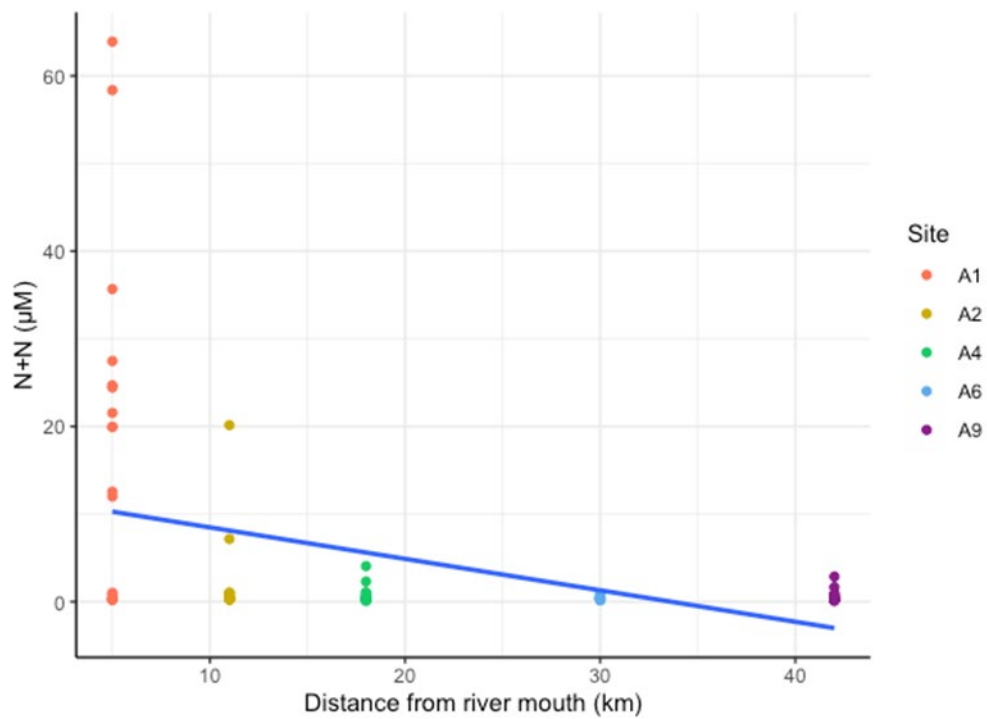


Figure 186. N+N gradient moving away from river mouth.

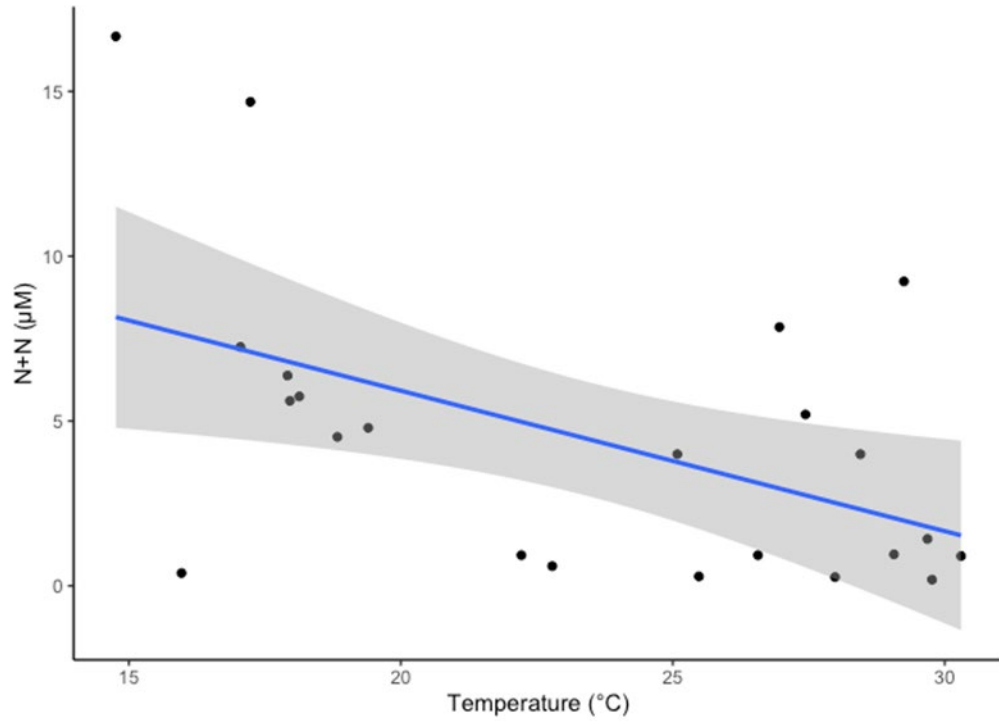


Figure 187. Mean N+N versus mean temperature for all dates.

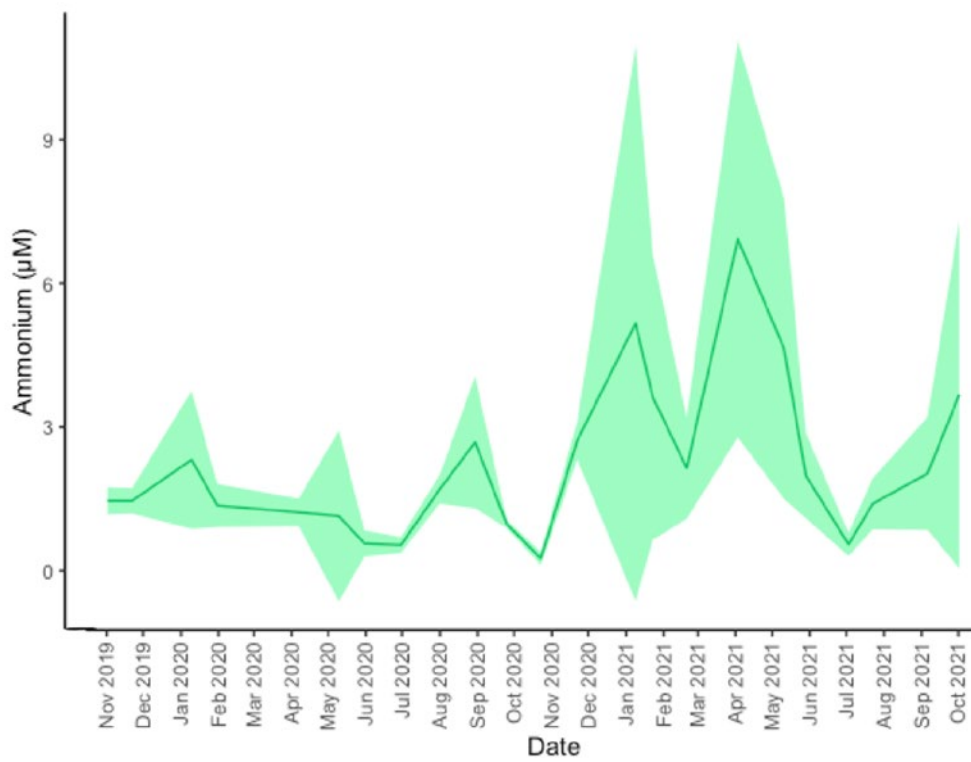


Figure 188. Mean ammonium from November 2019-October 2021 (shade is 95% confidence interval).

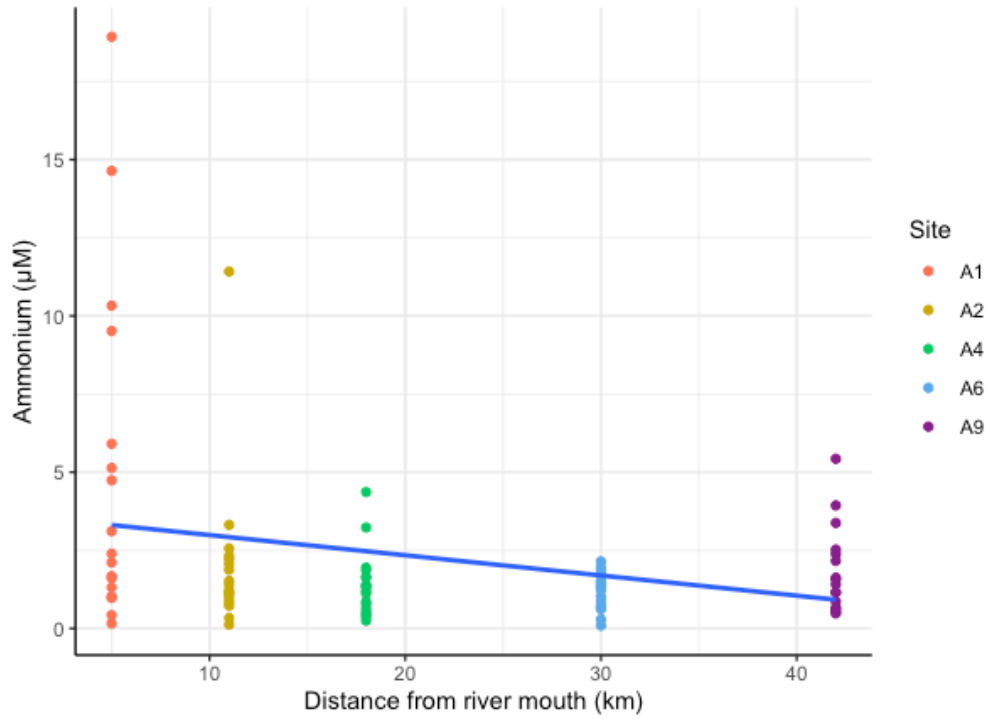


Figure 189. Ammonium gradient moving away from river mouth.

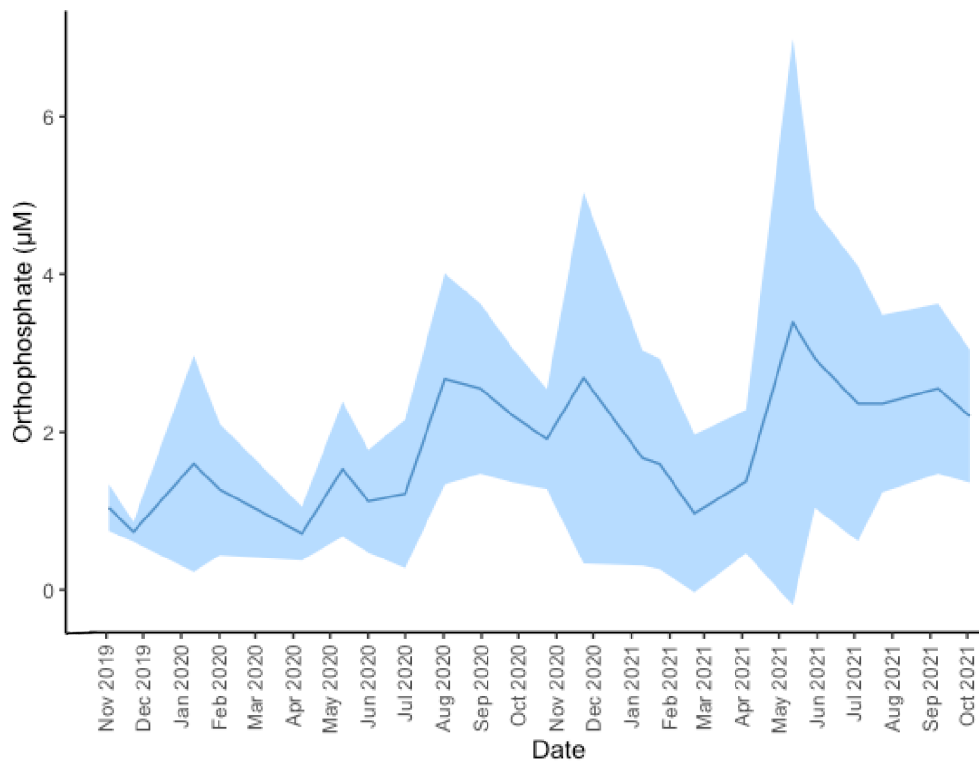


Figure 190. Mean orthophosphate from November 2019-October 2021 (shade is 95% confidence interval).

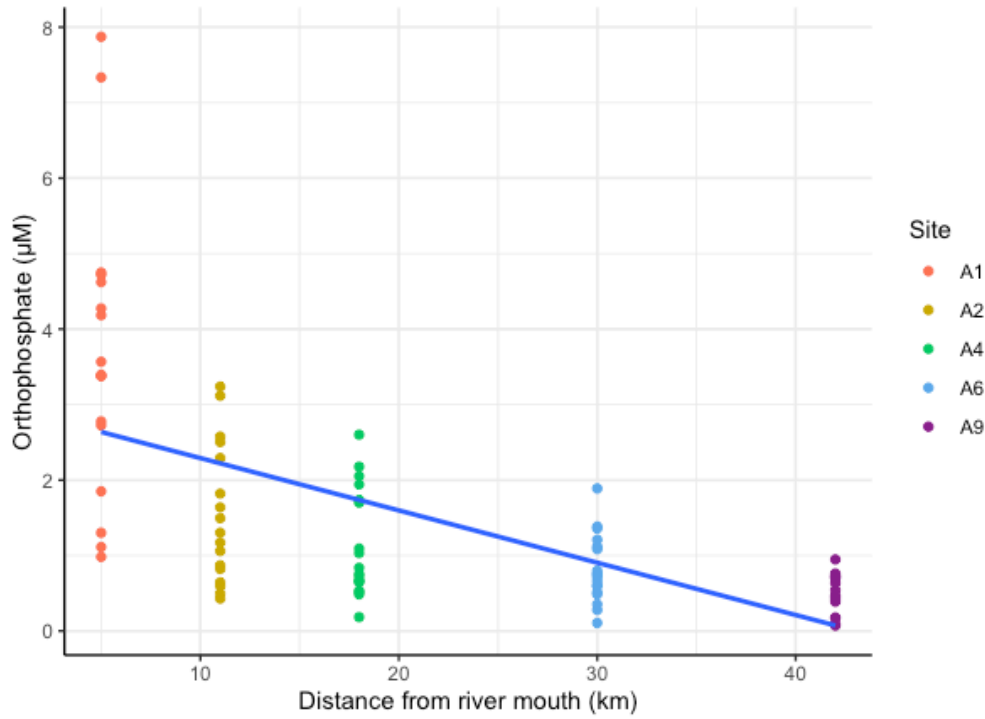


Figure 191. Orthophosphate gradient across sites moving away from river mouth.

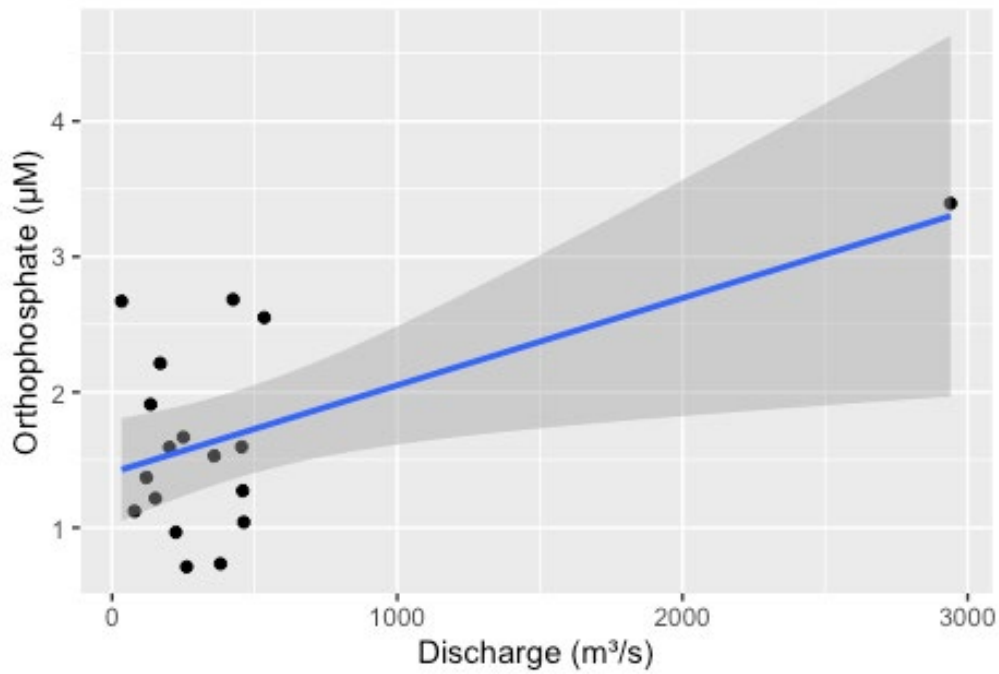


Figure 192. Mean orthophosphate versus discharge for all dates.

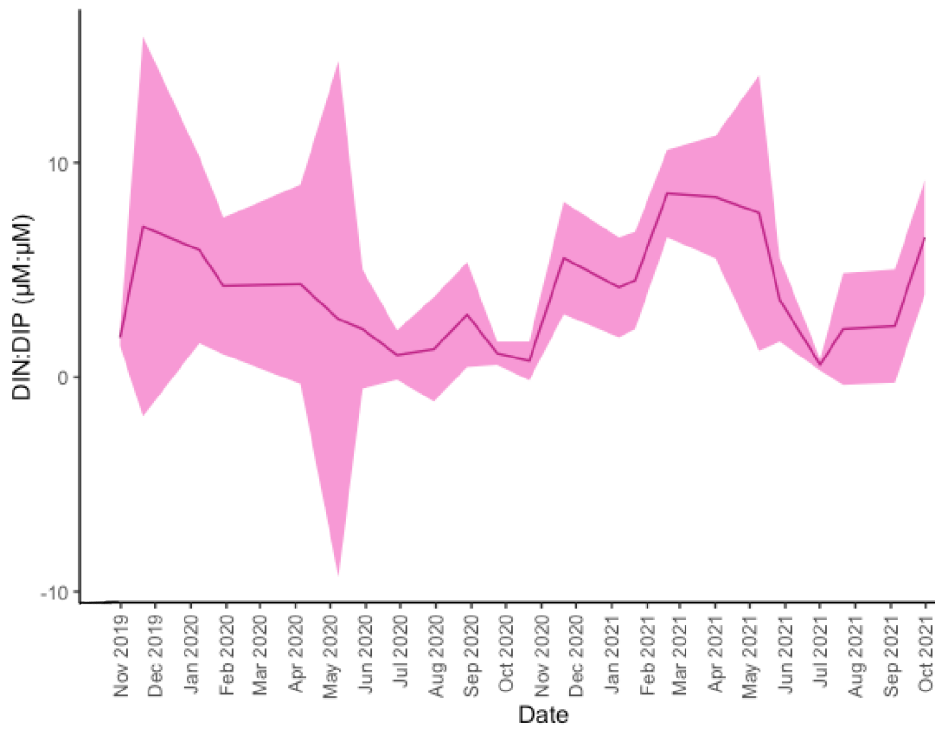


Figure 193. Mean DIN:DIP ratio from November 2019-October 2021 (shade is 95% confidence interval).

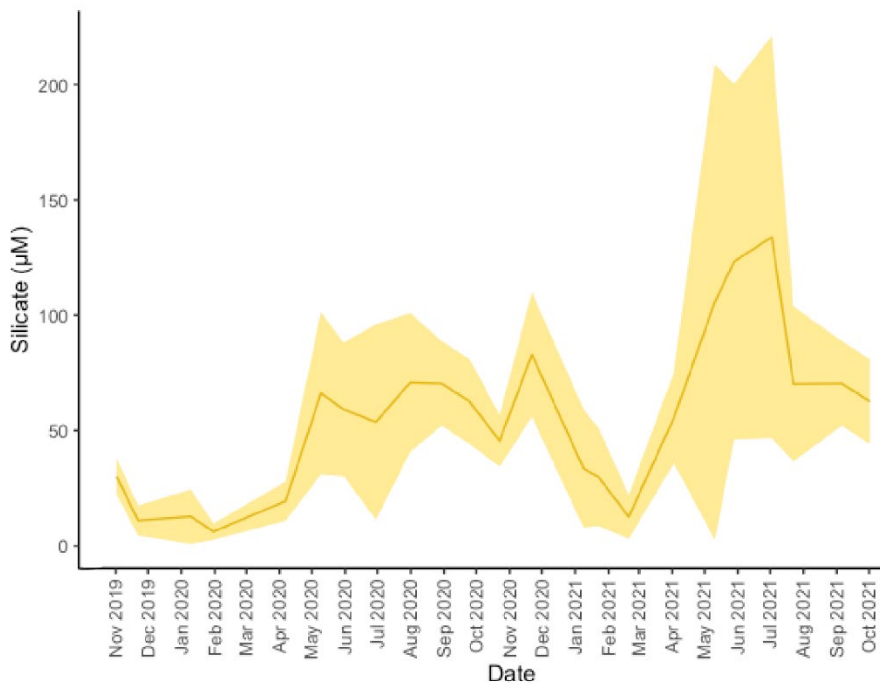


Figure 194. Mean silicate from November 2019-October 2021 (shade is 95% confidence interval).

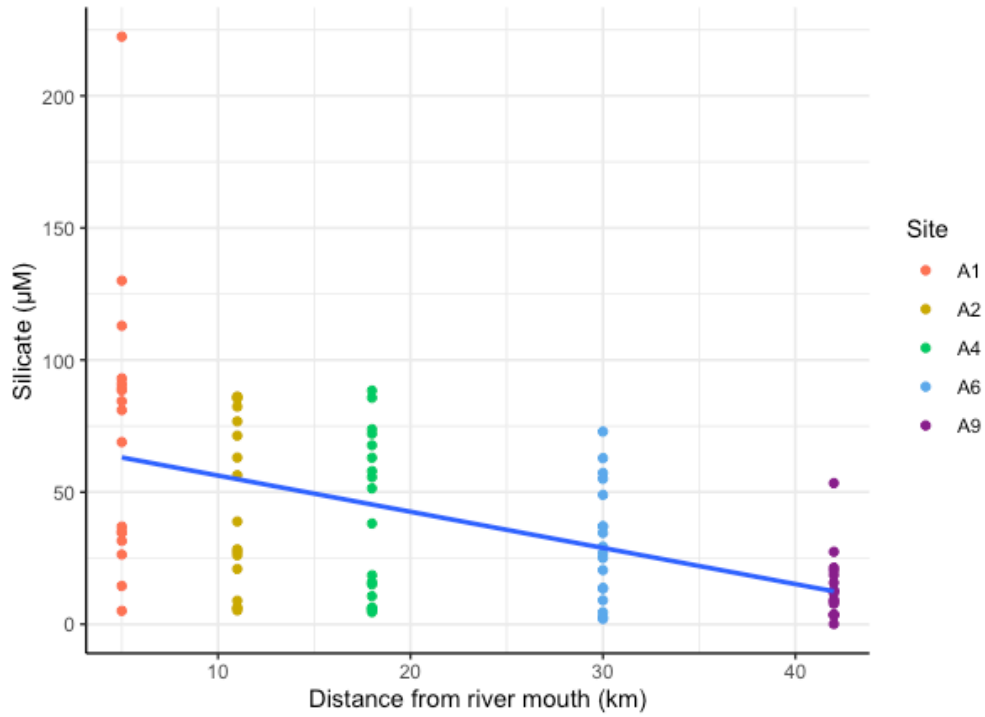


Figure 195. Silicate gradient across sites moving away from river mouth.

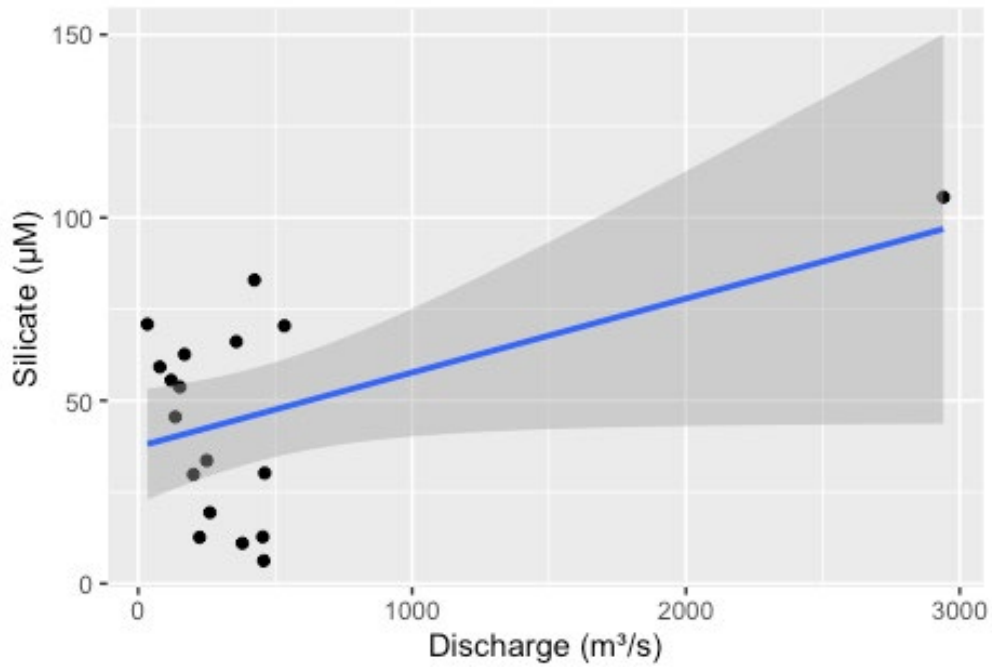


Figure 196. Mean silicate versus discharge for all dates.

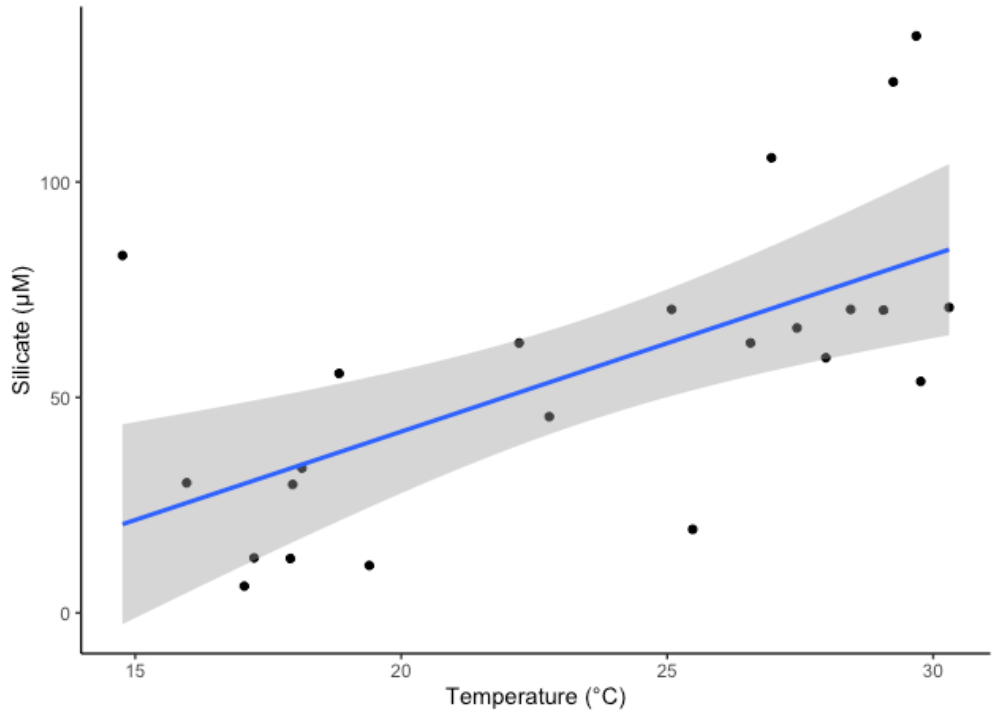


Figure 197. Mean silicate versus mean temperature for all sites and dates.

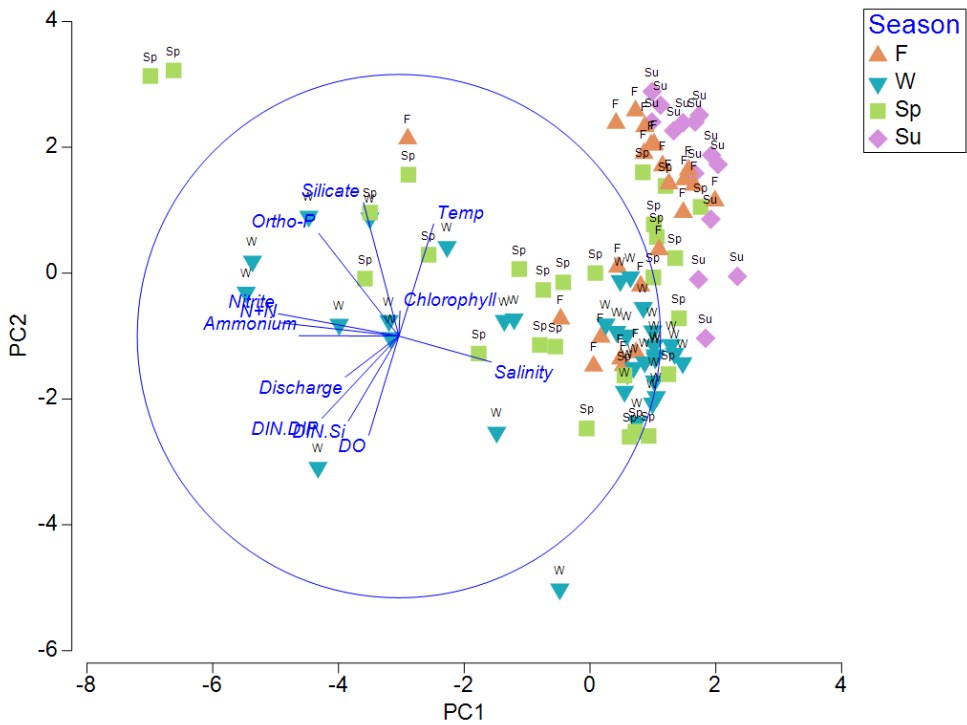


Figure 198. PCA by season.

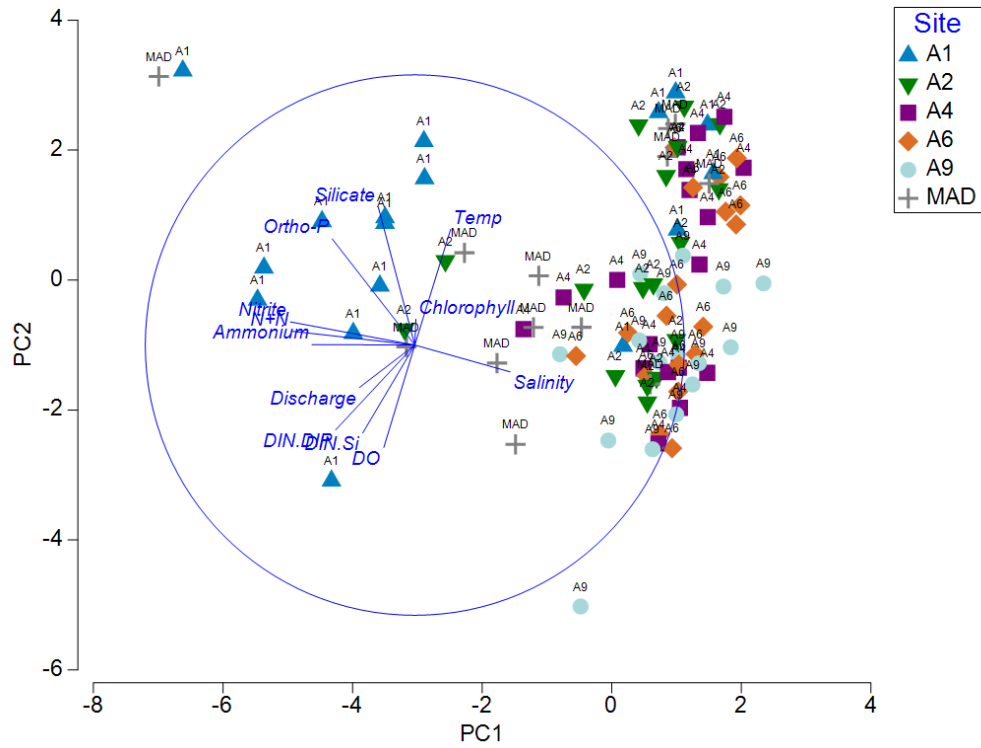


Figure 199. PCA by site.

Table 38. Kruskal-Wallis test for environmental factors and each site (adjusted p-values for multiple comparisons with Dunn Test). Shared letters/colors signify no significant difference between two sites.

Site	A1	MAD	A2	A4	A6	A9				
Chlorophyll (mg/L)	a	a	a	a	a	b				
N+N (μM)	a	a	a	b	b	b				
Orthophosphate (μM)	a	a	d	b	d	b	c	b	c	c
Salinity	a	a	b	a	b	b	c	c	d	d
Ammonium (μM)	a	a	a	a	a	a				
Silicate (μM)	a	a	a	b	a	b	c	b	c	c
DIN:DIP (μM)	a	b	a	b	a	b	b	a	b	a
DIN:Si (μM)	a	a	a	a	a	a				
Secchi depth (m)	a	a	a	b	b	c	b	c	c	
Total biovolume (microns/mL)	a	a	a	a	a	a				
Diatom biovolume (microns/mL)	a	a	a	a	a	a				
Euglenoid biovolume (microns/mL)	a	a	a	a	a	a				
Dinoflagellate biovolume (microns/mL)	a	a	b	a	b	b	a	b	a	b

Table 31. continued

Site	A1		MAD		A2		A4		A6		A9	
Cryptophyte biovolume (microns/mL)	a		a		a		a		a		a	
Picocyanobacteria (cells/mL)	a		a		a		a		a		a	
Picoeukaryotes (cells/mL)	a	b	b	c	a	a	c	a	c	b		

Chl a and biovolume

The mean Chl a concentration across all sites was 16.0 µg/L, with a minimum of 5.7 µg/L and maximum of 38.4 µg/L (Figure 200). The Chl a maximum occurred at the site closest to the river mouth in December 2019. Chl a concentration had a significant negative linear relationship with distance from river mouth ($p < 0.01$; Figure 201). A9, the site farthest from the river mouth, had a significantly lower median Chl a than all other sites except A6 ($p < 0.001$; Table 38). Chl a was strongly ($\tau > \pm 0.3$) negatively correlated with salinity ($p < 0.01$) and Secchi depth (m) ($p < 0.01$; Table 39), and weakly positively correlated ($\tau < 0.3$) with orthophosphate ($p = 0.02$), silicate ($p = 0.05$), temperature ($p = 0.02$) and total biovolume ($p < 0.01$, Table 39).

While Chl a concentrations were significantly lower at one site (A9), total biovolume did not significantly differ between any sites ($p = 0.6$; Table 38). There were also no significant differences in the biovolume of diatoms ($p = 0.74$), euglenoids ($p = 0.12$), or cryptophytes ($p = 0.51$) between sites (Table 38). Dinoflagellates were significantly lower at A4 compared to A1 ($p = 0.02$, Table 38). Chl a and total biovolume were also not significantly correlated ($p = 0.14$; Table 39). For example, while there was a Chl a maximum (125.6 µg/L) at site A1 in December 2019, this did not correspond with a biovolume maximum (not shown). In November 2020, the opposite pattern occurred, with a biovolume maximum ($5.4 \times 10^6 \mu\text{m}^3/\text{mL}$) but no corresponding Chl a maximum (data not shown).

Diatom biovolume had a positive correlation ($\tau = 0.13$, $p = 0.05$) with salinity and a negative correlation with ammonium ($\tau = -0.28$, $p < 0.01$; Table 40). Cryptophyte biovolume had a negative correlation with salinity ($\tau = -0.30$, $p < 0.001$) and temperature ($\tau = -0.43$, $p < 0.001$), as well as a positive correlation with discharge ($\tau = 0.25$, $p < 0.001$; Table 40). Dinoflagellate biovolume was positively correlated with temperature ($\tau = 0.15$, $p = 0.03$) and salinity ($\tau = 0.20$, $p < 0.01$) and negatively correlated with N+N ($\tau = -0.18$; $p < 0.01$) and ammonium ($\tau = -0.20$, $p < 0.01$). Picocyanobacteria were negatively correlated with ammonium ($\tau = -0.22$, $p < 0.01$) and N+N ($\tau = -0.21$, $p < 0.01$) and positively correlated with salinity ($\tau = 0.14$, $p = 0.04$) and temperature ($\tau = 0.27$, $p < 0.01$; Table 40). Picoeukaryotes were negatively correlated with N+N ($\tau = -0.14$, $p = 0.04$) and positively correlated with temperature ($\tau = 0.33$, $p < 0.01$; Table 40). Total biovolume was negatively correlated with ammonium ($p < 0.01$) and positively correlated with temperature ($p = 0.03$).

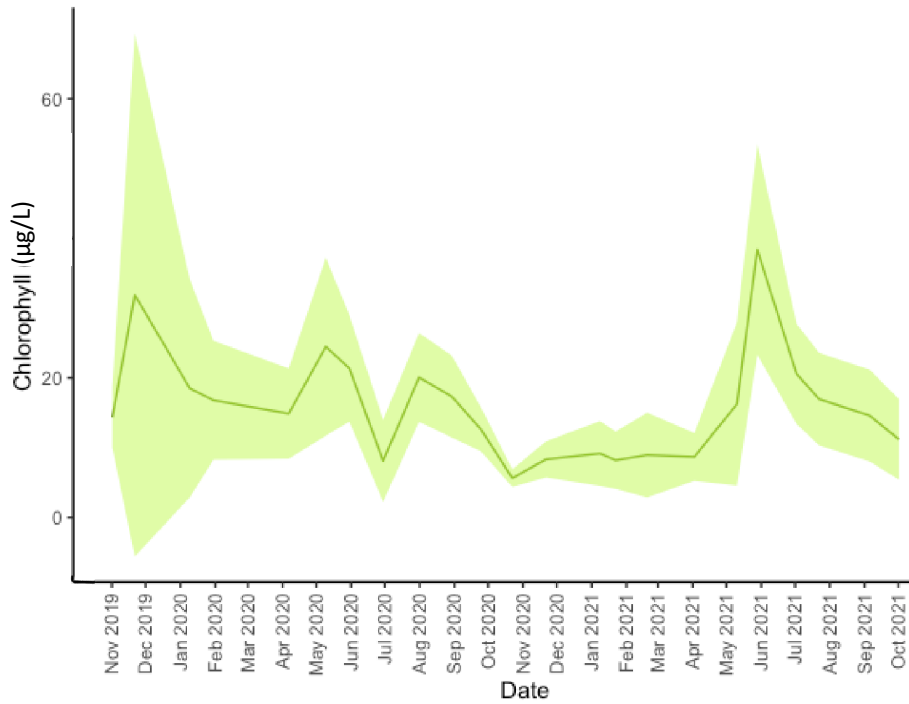


Figure 200. Mean chlorophyll (a) concentration from November 2019-October 2021 (shade is 95% confidence interval).

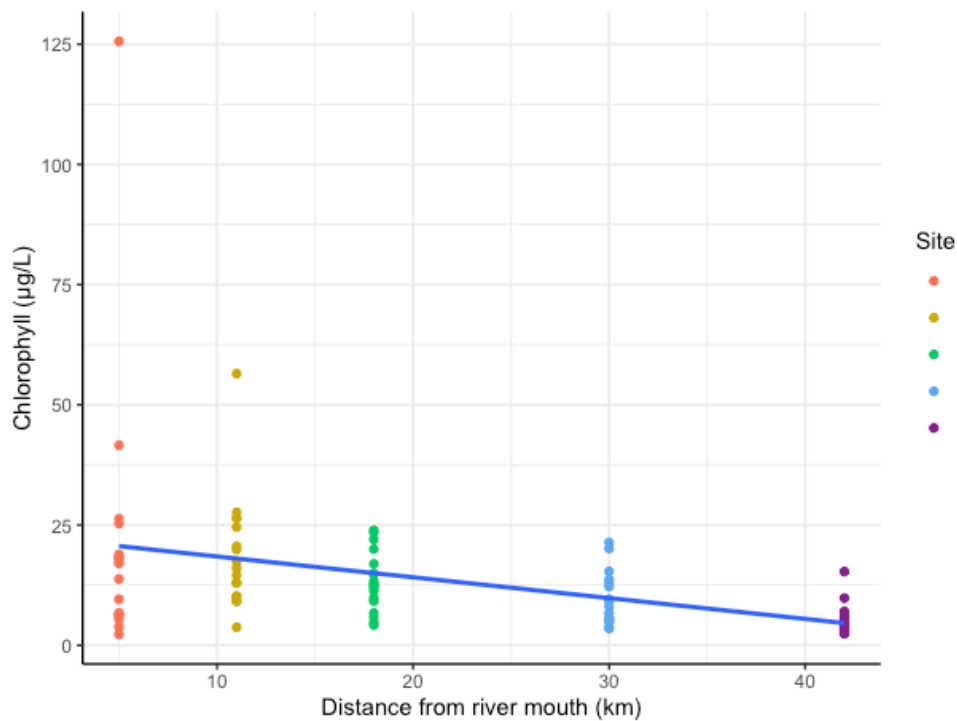


Figure 201. Chlorophyll gradient moving away from river mouth.

Table 39. Kendall's tau correlation results between chlorophyll and environmental variables, as well as biovolume for all sites. Highlighted variables indicate significant correlations ($\alpha=0.05$).

	Chlorophyll	
	p-value	tau
Salinity	<0.01	-0.40
Ammonium (μM)	0.27	-0.08
N+N (μM)	0.73	-0.02
PO ₄ (μM)	0.02	0.17
Silicate (μM)	0.05	0.14
DO (μM)	0.81	-0.01
Temperature ($^{\circ}\text{C}$)	<0.01	0.22
Discharge (m/s)	0.08	0.11
Secchi depth (m)	<0.01	-0.34
Total biovolume (microns ³ /mL)	<0.01	0.23

Table 40. Kendall's tau correlation results between phytoplankton total and functional group biovolume and environmental variables. Highlighted variables indicate significant correlations ($\alpha=0.05$).

	Cryptophyte		Euglenoid		Diatom		Dinoflagellate		Picocyanobacteria		picoeukaryotes		Total biovolume	
	tau	p-value	tau	p-value	tau	p-value	tau	p-value	tau	p-value	tau	p-value	tau	p-value
Salinity	-0.26	<0.001	-0.04	0.61	0.13	0.05	0.20	0.004	0.14	0.04	<0.01	0.89	0.08	0.25
Ammonium	0.13	0.06	0.09	0.17	-0.28	<0.01	-0.20	0.004	-0.22	<0.01	0.13	0.06	-0.27	<0.01
N+N	0.02	0.78	0.02	0.73	-0.06	0.38	-0.18	0.009	-0.21	<0.01	-0.14	0.04	-0.07	0.31
PO ₄	-0.05	0.47	-0.05	0.47	0.05	0.42	-0.05	0.44	0.02	0.75	0.10	0.14	0.11	0.10
Silicate	-0.13	0.06	-0.05	0.48	0.02	0.77	-0.04	0.57	<0.01	0.97	0.11	0.12	0.03	0.64
Temp	-0.42	<0.001	-0.11	0.09	0.09	0.17	0.15	0.03	0.27	<0.01	0.33	<0.01	0.15	0.03
Discharge	0.25	<0.001	0.06	0.41	-0.01	0.94	-0.01	0.89	0.09	0.22	0.04	0.59	0.03	0.63
Secchi depth	0.06	0.42	0.07	0.37	0.12	0.11	0.09	0.20	0.09	0.20	-0.12	0.11	0.05	0.47

Phytoplankton community composition

The study area is a diatom-dominated system, with diatoms comprising of 55% of total biovolume for the entire sampling period, followed by picoeukaryotes (25%), euglenoids (12%), dinoflagellates (6%), and picocyanobacteria (2%). Chlorophytes and cryptophytes contributed negligible biovolume compared to other functional groups. Diatom biovolume increased beginning in the fall of 2020 at sites A1 and A2 (Figure 202, Figure 203). Diatom biomass at A4, A6 and A9 was more constant over time (Figure 204-Figure 206). The minimum mean total biovolume of all sites occurred at MAD ($7.96 \times 10^6 \mu\text{m}^3/\text{mL}$; Figure 207). Euglenoid biovolumes generally peaked during December 2019 and March 2021 when present at a site. Mean total microplankton biovolume for each site ranged between approximately $8\text{-}10 \times 10^6 \mu\text{m}^3/\text{mL}$. Picocyanobacteria biovolume was very low compared to other functional groups and after September 2020 decreased to below the detection limit until May 2021. Picoeukaryotes generally increased from the beginning of the study to a maximum of $2.65 \times 10^7 \mu\text{m}^3/\text{mL}$ in April 2020 at site A2 (Figure 203). Picoeukaryote biovolume then decreased between April 2020 and June 2020, and then increased for a second maximum of $1.48 \times 10^7 \mu\text{m}^3/\text{mL}$ in September 2020 again at site A2. Like picocyanobacteria, picoeukaryote biovolume decreased to almost zero after this September 2020 peak. Picoeukaryote biovolume significantly decreased moving away from the river mouth ($p < 0.01$; data not shown).

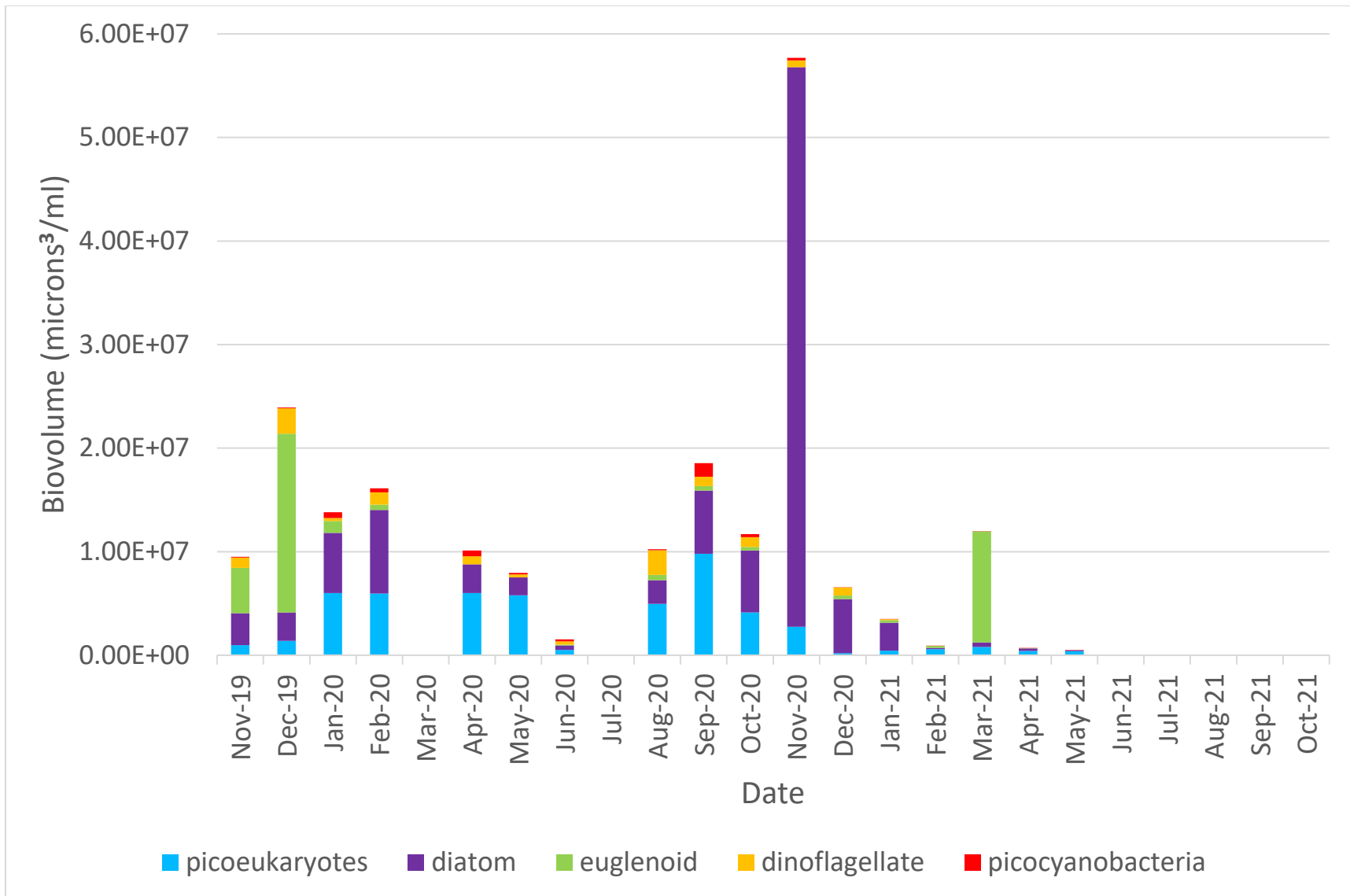


Figure 202. Site A1 functional group biovolume over time.

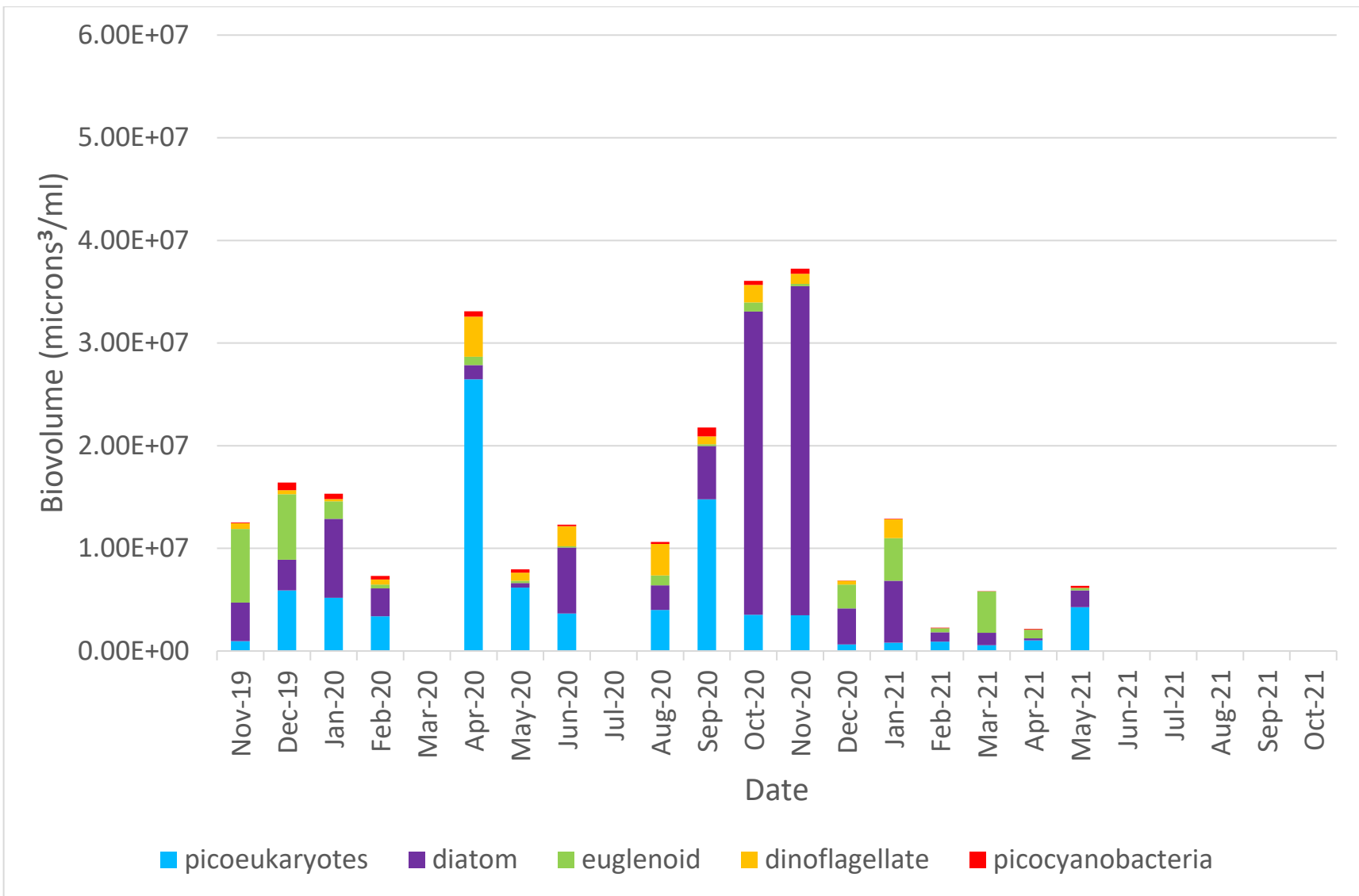


Figure 203. Site A2 functional group biovolume over time.

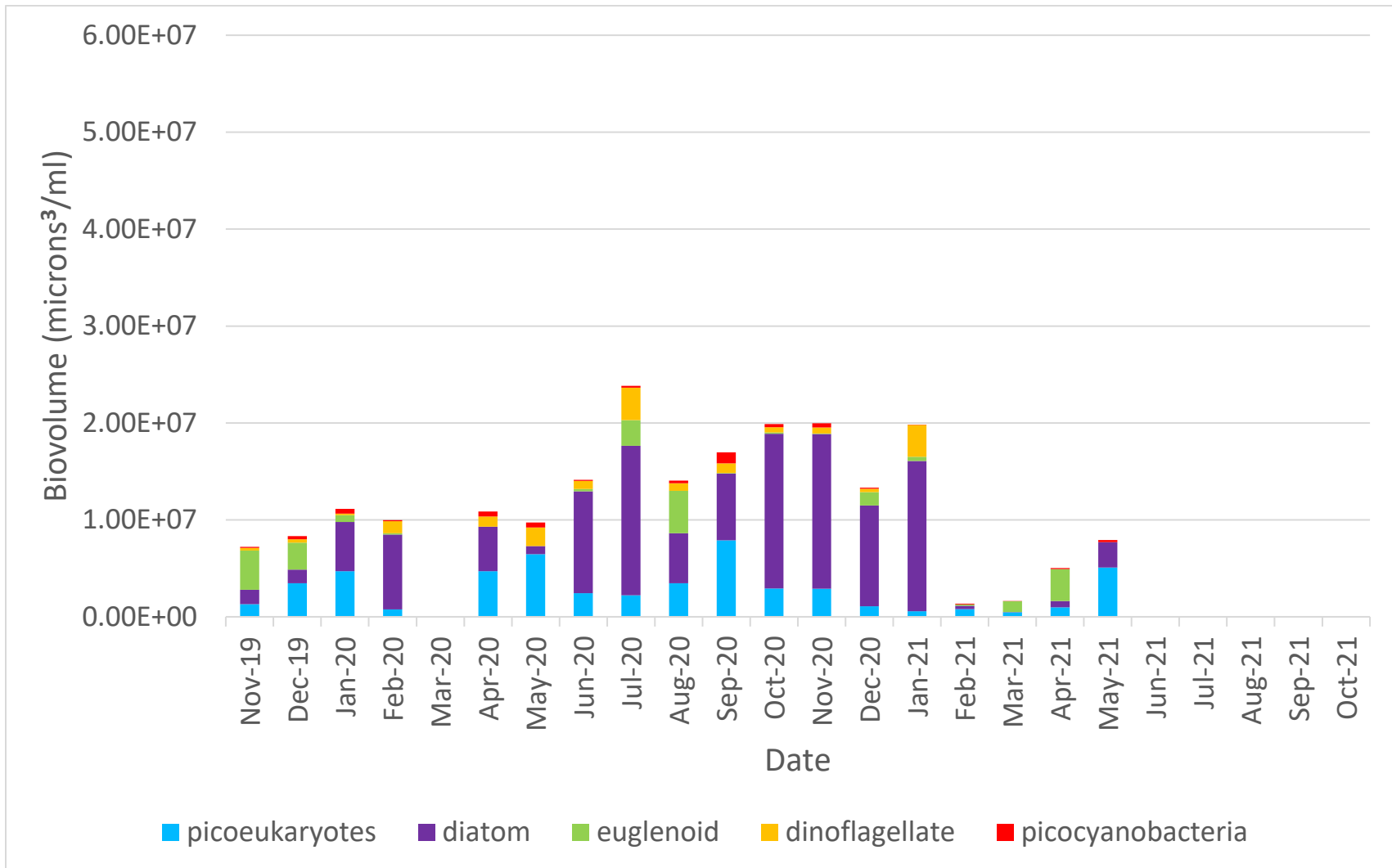


Figure 204. Site A4 functional group biovolume over time.

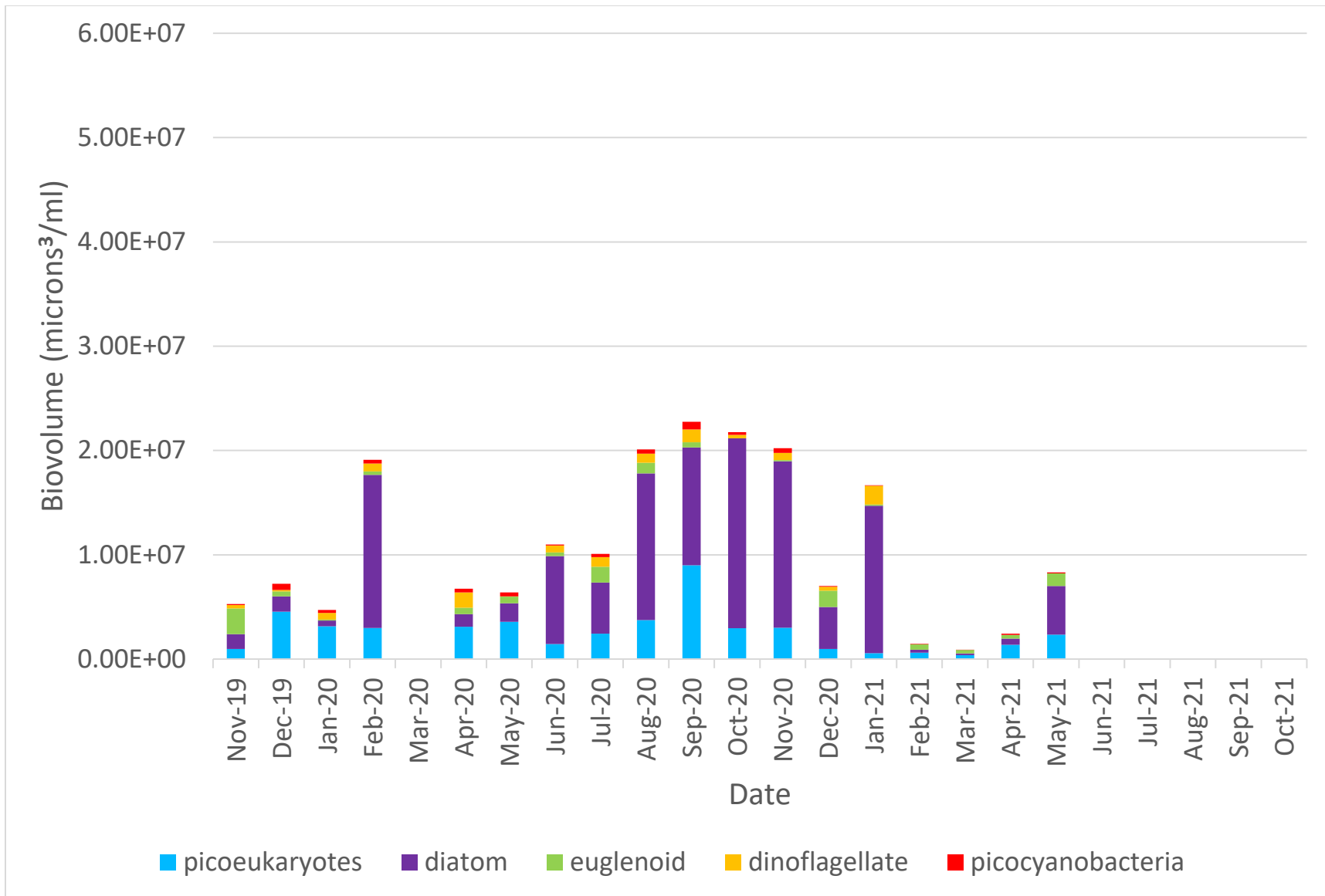


Figure 205. Site A6 functional group biovolume over time.

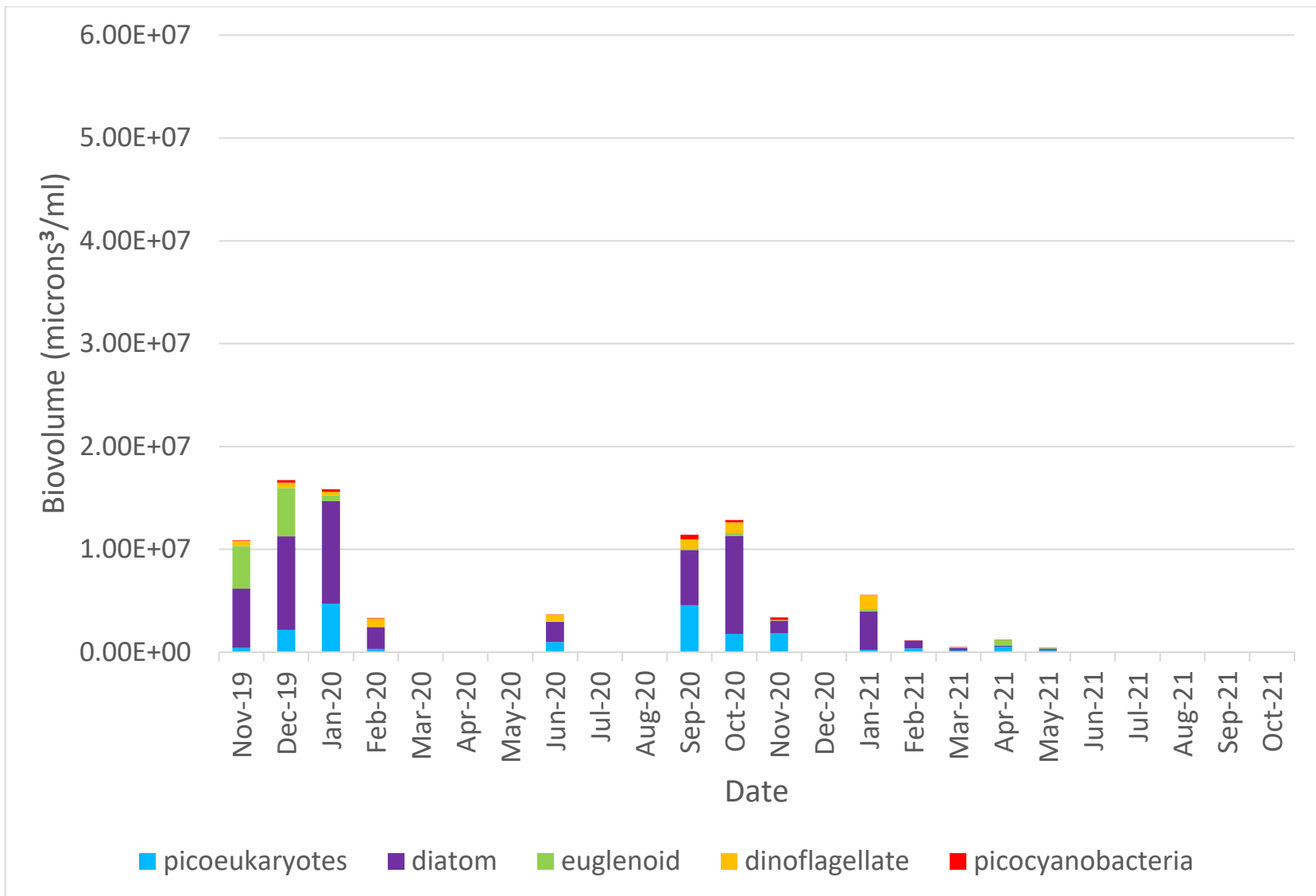


Figure 206. Site A9 functional group biovolume over time.

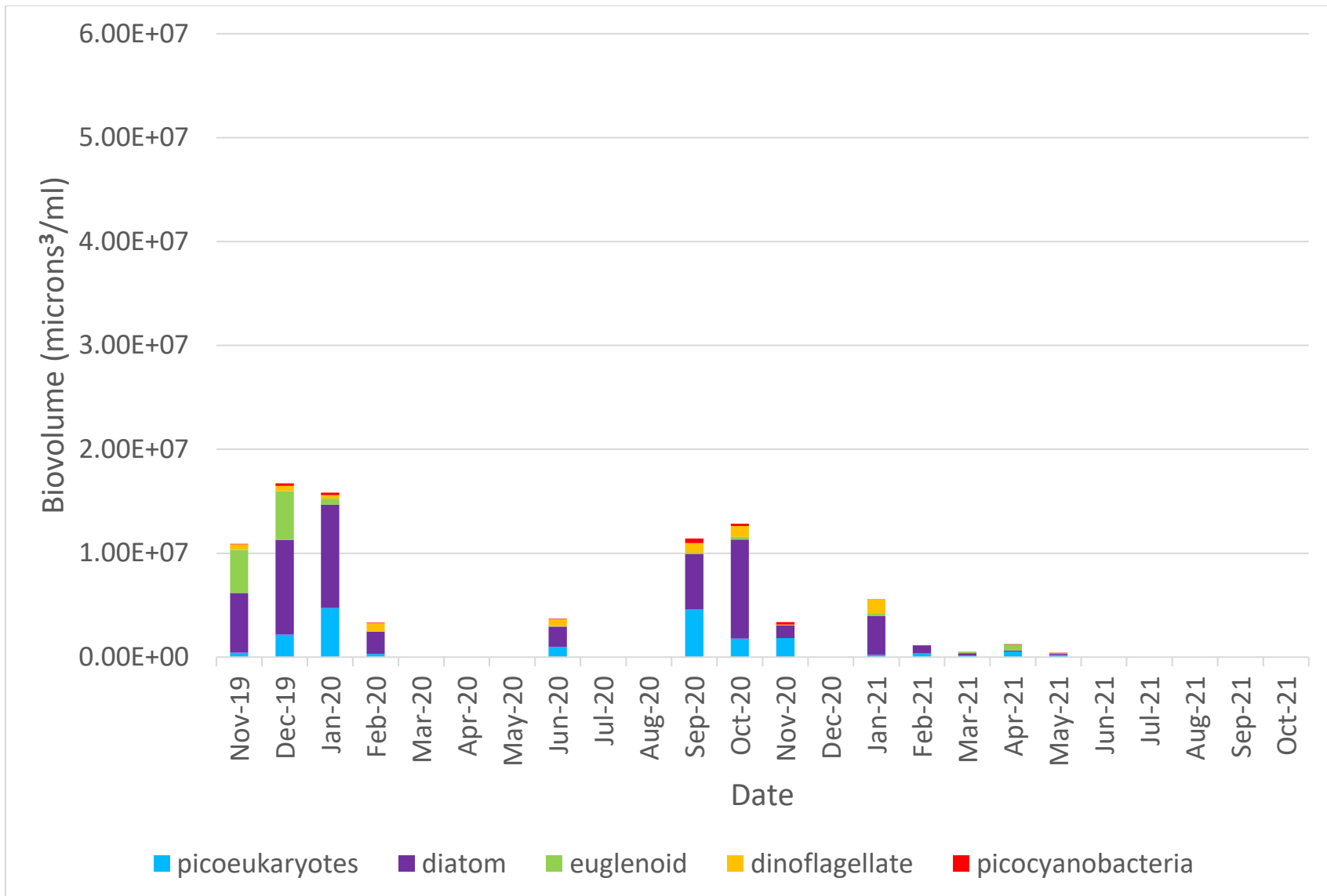


Figure 207. Site MAD functional group biovolume over time.

Harmful algae

Several genera present in samples were potential harmful algal bloom formers (HABs). Dinoflagellate potential HABs included *Heterocapsa*, *Prorocentrum*, *Akashiwo*, *Gonyaulax*, *Cochlodinium*, *Karenia*, *Oxyphysis oxytoxoides* and *Dinophysis*. *Dinophysis* was present during three sampling dates of this study: January 2020, February 2020 and April 2020. *Dinophysis* concentration was strongly positively correlated only with N+N ($\tau=0.42$, $p=0.04$) and strongly negatively correlated Si:DIN ($\tau=-0.48$, $p=0.03$; Table 41).

Table 41. Kendall's tau correlation results between HAB biomass/Dinophysis and environmental variables. Highlighted variables indicate significant correlations ($\alpha=0.05$).

	<i>Dinophysis</i>	
	tau	p-value
Salinity	0.20	0.33
Ammonium (μM)	0.05	0.82
N+N (μM)	0.42	0.04
PO ₄ (μM)	0.02	0.94
Silicate	0.39	0.06
DIN:DIP	0.20	0.33
Si:DIN	-0.48	0.03
Temperature	-0.23	0.12
Discharge	0.32	0.12

Discussion

Phytoplankton are important components of the estuarine food web because of their role as primary producers (Field et al. 1998). Altered freshwater inflow has influenced phytoplankton communities in estuaries across the world (Cloern et al. 1983; Barroso et al. 2018). Freshwater inflow is projected to be further altered in the future due to anthropogenic uses (e.g., agriculture and consumption) and climate change (e.g., changes in frequency or intensity of rainfall, storms and warming). Thus it is important to understand how environmental changes, including shifts in freshwater inflow, may alter phytoplankton communities because of effects on water quality, estuarine ecology and economically important species at higher trophic levels. To elucidate the influence that freshwater inflow has on environmental conditions and phytoplankton in Matagorda Bay, this study quantified relevant variables over a 24 month period. Freshwater inflow influenced the spatiotemporal patterns of nutrients, Chl *a* and biovolume. On average, the highest nutrient concentrations, Chl *a* and phytoplankton biovolume were observed at a site closest to the river mouth. During the study, diatoms were consistently the dominant functional group in terms of biovolume. A harmful dinoflagellate, *Dinophysis sp.*, was observed for several months, although not at bloom levels. This study exemplifies the need for more frequent and long-term monitoring to investigate conditions associated with blooms and *Dinophysis* presence.

Nutrient patterns

Freshwater inflow, distance from the river mouth, and seasonality affected the concentration and distribution of nutrients within Matagorda Bay. All nutrients measured (N+N, ammonium, orthophosphate and silicate) were highest near the river mouth and decreased in sites farther away from the mouth, a spatial pattern that indicates the river is an important source of nutrients to the estuary. High riverine inflow is known to increase total phosphorous in Matagorda Bay (Longley et al. 1994), and here the maximum orthophosphate concentration co-occurred with maximum riverine discharge in May 2021. Matagorda Bay historically has low dissolved inorganic nitrogen (DIN), and only the area closest to the river mouth sees a marked increase in nitrogen from river discharge (Longley et al. 1994). DIN limitation, as noted by $\text{DIN:PO}_4 < 16$, was observed for the duration of this study, and the highest DIN concentration was also found near the mouth of the river. Silicate had a significant positive relationship with discharge, indicating the Colorado River was an important source, and studies have shown rivers are a significant source of silicate to coasts worldwide (Frings 2017). Temperature changes associated with seasonality can also affect nutrient availability in the water column. Increasing temperature has been correlated to increasing silicate solubility, which may explain the significant positive linear relationship between silicate concentration and temperature observed in this study (Varkouhi and Wells 2020).

Chl a patterns

Chl *a* concentrations were influenced by spatiotemporal factors such as proximity to the river mouth and inflow rate. High Chl *a* has been observed in other estuaries near river mouths, and often has a negative relationship to salinity (Cloern et al. 1983; Masotti et al. 2018). Here the highest mean Chl *a* concentration was observed at site A1 (21.3 $\mu\text{g/L}$), and the maximum single recording of Chl *a* was also at site A1 (125.6 $\mu\text{g/L}$). Higher Chl *a* concentration may be due to the higher concentration of nutrients near the river mouth, as observed in Masotti et al. (2018). Chl *a* was negatively correlated with Secchi depth in this study, indicating that algal biomass was an important contributor to light attenuation in this system. This could have implications for bottom-dwelling organisms by shading them, perhaps decreasing benthic primary production (Dunton 1994). Because riverine inflow appears related to Chl *a* concentration in Matagorda

Bay, potential future decreases to inflow could have an impact on the food web by decreasing water column primary production but perhaps increasing light availability to benthic producers (Dunton 1994).

Biovolume patterns

Although Chl *a* was higher at sites near the river mouth, there was no significant difference in total biovolume between sites. Total biovolume homogeneity across the estuary may be due to zooplankton grazers acting as a top-down control on phytoplankton (Cloern and Dufford 2005; Buyukates and Roelke 2005). While there was a weak ($\tau < 0.3$) correlation between total biovolume and Chl *a*, there were several instances of a mismatch between maximums of one and not the other. The general lack of relationship between Chl *a* and biovolume maximums is not surprising, as other authors have found this as well (Felip and Catalan 2000; Lancelot and Muylaert 2011; Alvarez-Fernandez and Riegman 2014). For example, there was a Chl *a* maximum in December 2019 without a corresponding biovolume maximum, possibly due to increased Chl *a* per cell. Conversely, a November 2020 biovolume maximum did not correspond to a Chl *a* maximum. Variability in the amount of chlorophyll per cell can be due to a variety of factors including species composition, light and nutrient availability (Falkowski 1980; Langdon 1987; Geider et al. 1997). Boyer et al. (2009) observed Chl *a* content in fresh algae mass to vary from 0.1 to 9.6% of biomass, exemplifying that it can vary widely within cells. This study underscores the necessity of multiple measures of phytoplankton biomass to characterize the communities more accurately in estuaries.

Across the 24 months, the highest average total biovolume occurred in November 2020 at site A1, which corresponded with a Nitzschioid diatom bloom. This bloom occurred after a period of decreased discharge, which may have increased residence time and allowed the bloom to develop in the presence of ample nutrient supply (Ketchum 1954). Conversely, a bloom of the diatom genus *Leptocylindrus* corresponded with maximum inflow in May 2021 and was located at site A6. Another study observed a *Leptocylindrus* bloom following an extreme inflow increase to a temperate estuary (Bate and Adams 2000). The high inflow at the time of the bloom may have pushed phytoplankton farther into the estuary, and fueled production through increased nutrient availability, as shown by simultaneous increases in N+N, orthophosphate and silicate in May 2021 (Burford et al. 2011; Bruesewitz et al. 2013). Other studies have shown that the location of the Chl *a* maxima moves downstream after periods of elevated inflow (Pennock 1985; Paerl et al. 2014). The high inflow was sufficient to affect the distribution of the bloom, but not enough to flush cells out of the estuary. In short, the blooms in this study exemplify that different taxon proliferate under different conditions.

Phytoplankton community composition

Matagorda Bay's high wind action and prevalence of river-derived nutrients likely contributed to diatoms dominating over other phytoplankton functional groups in this system (Longley 1994; Smayda 1997). Carrick et al. (1993) observed a two-fold increase in diatom biomass during increased wind speed in a shallow Florida lake, potentially due to resuspension of benthic diatoms and decreased light limitation. A diatom bloom was also observed in the oligotrophic, subtropical Gulf of Eilat when wind speeds increased from 3 m s⁻¹ to 10 m s⁻¹ (Iluz et al. 2009). In several estuarine studies, biovolume was dominated by diatoms when the wind speeds were between >3 and 9 m s⁻¹ (Arfi and Bouvy 1995; de Jonge and van Beusekom 1995; Fejes et al. 2005). The mean monthly wind speed for this study in Matagorda Bay was 7.4 m s⁻¹, which likely explains why diatoms dominated biovolume. Diatom biovolume also had a positive correlation with salinity, indicating that this functional group was successful not only near the

river mouth, but throughout the estuary. Upwelling favorable winds in the northwestern Gulf of Mexico promote diatom success over other functional groups, and these diatoms may be advected into the more saline parts of the estuary, such as site A9 (Anglès et al. 2019). A ship channel between another Texas subtropical estuary (Aransas Bay) and the Gulf of Mexico sampled had a community comprised mostly of diatoms, so the Gulf of Mexico is a possible source of diatoms to Texas estuaries (Reyna et al. 2017). Also, blooms observed in another wind-driven estuary on the Texas coast (Galveston Bay) were diatom-dominated (Roelke et al. 2013). The ratio of Si:DIN remaining above 1 for the majority of the study period could have also contributed to diatom success over dinoflagellates or other functional groups (Longley et al. 1994).

Picoeukaryotes were prevalent during the summer and their biovolume correlated with water temperature ($p < 0.01$). Stawiarski et al. (2016) found that picoplankton generally increase with increasing temperatures until they reach the optimal temperature for their species. Temperature was beginning to increase in March 2020, and this correlates with a picoeukaryote cells/mL maximum in April 2020. Temperature reached a maximum for summer 2020 in August, and picoeukaryotes again peaked in September 2020. Picoeukaryotes had a negative correlation with N+N ($p = 0.04$), which may be due to depletion of this nutrient as picoeukaryote cells increase in number. Picocyanobacteria also a positive correlation with temperature ($p < 0.01$), a phenomenon observed in other studies as well (Paerl 2014; Smucker et al. 2021). Picocyanobacteria biovolume had a weak positive correlation with salinity, and one study found highest growth of subtropical cyanobacteria at salinities between 16 and 25 (Rai and Rajashekar 2016), which is similar to the range of the salinities in which most cells occurred in our study (15-30). Picocyanobacteria had a negative correlation with both nitrogen forms measured (ammonium and N+N), suggesting potential uptake of both in support of growth (Olofsoon et al. 2019; Aldunate et al. 2020).

Dinophysis

Blooms of the toxic dinoflagellate, *Dinophysis* sp., have resulted in closure of shellfish harvesting seven times since 2008 in Matagorda Bay (Campbell et al., 2010, Harred and Campbell 2014). In this study, *Dinophysis* was present in January, February and April 2020, corresponding with the window of temperature (~11-19°C) in which past blooms have occurred in the Gulf of Mexico (Harred and Campbell 2014). Its presence corresponded with a period of lower inflow, and this as well as other studies (Swanson et al. 2010) did not find a correlation between *Dinophysis* and salinity. *Dinophysis* has bloomed in the Gulf of Mexico in salinity ranging from 28 to 33, while in our study salinity was lower (20-23) during *Dinophysis* presence, which may be why *Dinophysis* never reached bloom levels. The occurrence of *Dinophysis* during low inflow conditions further suggests that either the availability of recycled nutrients was sufficient or there was a month-long lag between elevated inflow/nutrients and *Dinophysis* presence. The potential for silicate limitation that was observed in January and February 2020, as indicated by Si:DIN < 1, may explain this *Dinophysis* success over diatoms, considering dinoflagellates are not silicate limited (Flynn and Martin-Jézéquel 2000). Because the ratio of Si:DIN increased ten-fold between February 2020 and April 2020, silicate limitation may have ceased and thus diatoms outcompeted *Dinophysis*, causing the decline of the dinoflagellate. The ratio of Si:DIN never fell below 1 again, and this may partially explain why *Dinophysis* was not abundant after April 2020.

Future implications and recommendations

Texas' population is rapidly growing and is projected to increase by more than 70 percent from 2020-2070 (Texas Water Development Board 2017). With this growth, water demand is projected to increase by 17%, introducing possible effects on aquatic ecosystems (Texas Water Development Board 2017). In addition, projections indicate that an increase in drought severity may occur (Nielsen-Gammon et al. 2021). During these times, evaporation will likely further decrease freshwater inflow (Konapala et al. 2020). These decreases in freshwater inflow could result in a decrease in phytoplankton biovolume due to decreases in nutrient inputs (Wetz et al. 2011, Philips et al. 2012). Decreased freshwater inflow may conversely increase phytoplankton biovolume closest to the river mouth, possibly due to increased residence time, as we saw a diatom bloom and *Dinophysis* presence during periods of decreased discharge in this study (Flemer and Champ 2006). Increased residence time is especially concerning for harmful dinoflagellates as extended residence times allow this slow-growing functional group time to reproduce (Murrell et al. 2002). These opposing responses from different taxa to the same environmental changes again highlights the necessity of researching bloom causes on a taxa-by-taxa basis.

To better elucidate mechanistic linkages between freshwater inflow and phytoplankton in Matagorda Bay, future studies could employ experimental or modeling approaches to better discern the role of nutrients and flushing. While more frequent sampling was not possible in this study, future studies may also consider daily sampling upon detection of a potential HAB species, such as *Dinophysis*, because phytoplankton biovolume and communities can change on this shorter time scale (Cloern et al. 2014). More frequent sampling could give a clearer understanding of influential environmental factors on blooms.

Literature Cited

- Alvarez-Fernandez, S. and R. Riegman. 2014. Chlorophyll in North Sea coastal and offshore waters does not reflect long term trends of phytoplankton biomass. *J. Sea Res.* 91: 35-44.
- Aldunate, M., C. Henríquez-Castillo, Q. Ji, J. Lueders-Dumont, M. R. Mulholland, B. B. Ward, P. von Dassow, and O. Ulloa. 2020. Nitrogen assimilation in picocyanobacterial inhabiting the oxygen-deficient waters of the eastern tropical North and South Pacific. *Limn. and Oceanogr.* 65: 437-453.
- Anglès, S., A. Jordi, D. W. Henrichs, and L. Campbell. 2019. Influence of coastal upwelling and river discharge on the phytoplankton community composition in the northwestern Gulf of Mexico. *Prog. Oceanogr.* 173: 26-36.
- Arfi, R., M. Bouvy. 1995. Size, composition and distribution of particles related to wind induced resuspension in a shallow tropical lagoon, *J. Plankt. Res.* 17: 557-574.
- Armstrong, N. E. 1982. Responses of Texas estuaries to freshwater inflows. In: V. S. Kennedy [ed.], *Estuarine comparisons*. Academic Press.
- Barbosa, A. B., R. B. Domingues, H. M. Galvão. 2010. Environmental forcing of phytoplankton in a Mediterranean estuary (Guadiana Estuary, South-western Iberia): A decadal study of anthropogenic and climatic influences. *Estuar. Coasts.* 33:324-341.
- Barroso, H. dS., T. C. L. Tavares, M. dO. Soares, T. M. Garcia, B. Rozendo, A. S. C. Vieira, P. B. Viana, T. M. Pontes, T. J. T. Ferreira, J. P. Filho, C. A. F. Schettini, S. T. Santaella. 2018. Intra-annual variability of phytoplankton biomass and nutrients in a tropical estuary during a severe drought. *Estuar. Coast. Shelf Sci.* 213: 283-293.
- Bate, G., and J. Adams. 2000. The effects of a single freshwater release into Kromme Estuary. *Water S. A.* 26: 329-332.
- Boyer, J.N., Kelble, C.R., Ortner, P.B., Rudnick, D.T., 2009. Phytoplankton bloom status: Chlorophyll a biomass as an indicator of water quality condition in the southern estuaries of Florida, USA. *Ecol. Indic.* 9: S56–S67.
- Boynton, W. R., and W. M. Kemp. 2000. Influence of river flow and nutrient loads on selected ecosystem processes—A synthesis of Chesapeake Bay data. In: Hobbie, J.E. (Ed.), *Estuarine Science—A Synthetic Approach to Research and Practice*. Island Press, Washington, DC, 269–298.

- Bruesewitz, D. A., W. S. Gardner, R. F. Mooney, L. Pollard, and E.J. Buskey. 2013. Estuarine ecosystem function response to flood and drought in a shallow, semiarid estuary: Nitrogen cycling and ecosystem metabolism. *Limnol. Oceanogr.* 58: 2293–2309.
- Burford M. A., A. T. Revill, D. W. Palmer, L. Clementson, B. J. Robson, and I. T. Webster. 2011. River regulation alters drivers of primary productivity along a tropical river-estuary system. *Mar. Freshw. Res.* 62: 141-151.
- Buyukates, Y. and D. Roelke. 2005. Influence of pulsed inflows and nutrient loading on zooplankton and phytoplankton community structure and biomass in microcosm experiments using estuarine assemblages. *Hydrobiologica* 548: 233-249.
- Campbell, L., R. J. Olsen, A. Abraham, D. W. Henrichs, C. J. Hyatt, and E. J. Buskey. 2010. First harmful *Dinophysis* (dinophyceae, dinophysiales) bloom in the U.S. is revealed by automated imaging flow cytometry. *J. Phycol.* 46: 66-75.
- Carrick, H. J., F. J. Aldridge, and C. L. Schelske. 1993. Wind influences phytoplankton biomass and composition in a shallow, productive lake. *Limnol. Oceanogr.* 38: 1179-1192.
- Cloern, J. E., A. E. Alpine, B. E. Cole, R. L. J. Wong, J. F. Arthur, and M. D. Ball. 1983. River discharge controls phytoplankton dynamics in the Northern San Francisco Bay Estuary. *Estuar. Coast. Shelf Sci.* 16: 415–429.
- Cloern, J. E., and R. Dufford. 2005. Phytoplankton community ecology: Principles applied in San Francisco Bay. *Mar. Ecol. Prog. Ser.* 285: 11–25.
- Cloern, J. E., S. Q. Foster, and A. E. Kleckner. 2014. Phytoplankton primary production in the world's estuarine-coastal ecosystems. *Biogeosci.* 11: 2477-2501.
- Dunton, K. 1994. Seasonal growth of the subtropical seagrass *Halodule wrightii* in relation to continuous measurements of underwater irradiance. *Mar. Bio.* 120: 479-489.
- Falkowski, P. G. 1980. Light-shade adaptation in marine phytoplankton. *Plant Physio.* 66: 592-595.
- Fejes, E., D. Roelke, G. Gable, J. Hellman, K. McInnes, and D. Zuberer. 2005. Microalgal productivity, community composition, and pelagic food web dynamics in a subtropical, turbid salt marsh isolated from freshwater inflow. *Estuaries.* 28: 96–107.
- Felip, M. and J. Catalan. 2000. The relationship between phytoplankton biovolume and chlorophyll in a deep oligotrophic lake: decoupling in their spatial and temporal maxima. *J. Plankt. Res.* 22: 91-106.

- Field C. B., M. J. Behrenfeld, J. T. Randerson, P. Falkowski. Primary production of the biosphere: integrating terrestrial and oceanic components. 1998. *Science* 281:237-40.
- Flemer, D. A., and M. A. Champ. 2006. What is the future fate of estuaries given nutrient over-enrichment, freshwater diversion and low flows? *Mar. Poll. Bull.* 52: 247-258.
- Flynn, K. J. and V. Martin-Jézéquel. 2000. Modelling Si–N-limited growth of diatoms. *J. Plankton Res.* 22: 447-472.
- Frings, P., 2017. Revisiting the dissolution of biogenic Si in marine sediments: a key term in the ocean Si budget. *Acta Geochim.* 36: 429-432.
- Iluz, D., G. Dishon, E. Capuzzo, E. Meeder, R. Astoreca, V. Montecino, P. Znachor, D. Ediger, and J. Marra. 2009. Short-term variability in primary productivity during a wind-driven diatom bloom in the Gulf of Eilat (Aqaba). *Aquat. Microb. Ecol.* 56: 205-215.
- Geider, R. J., H. L. MacIntyre, and T. M. Kana. 1997. Dynamic model of phytoplankton growth and acclimation: responses of the balanced growth rate and the chlorophyll a: carbon ratio to light, nutrient-limitation and temperature. *Mar. Ecol. Prog. Ser.* 148: 187-200.
- Gillanders, B. M., and M. Kingsford. 2002. Impact of changes in flow of freshwater on estuarine and open coastal habitats and the associated organisms. *Oceanogr. Mar. Bio.* 40: 233-309.
- Harred, L. B., and L. Campbell. 2014. Predicting harmful algal blooms: a case study with *Dinophysis ovum* in the Gulf of Mexico. *J. Plankt. Res.* 36: 1434-1445.
- Hillebrand, H., C.-D. Durselen, D. Kirschtel, U. Pollinger, and T. Zohary. 1999. Biovolume calculation for pelagic and benthic macroalgae. *J. Phycol.* 35: 403–424.
- Iluz, D., G. Dishon, E. Capuzzo, E. Meeder, R. Astoreca, V. Montecino, P. Znachor, D. Ediger, J. Marra. 2009. Short-term variability in primary productivity during a wind-driven diatom bloom in the Gulf of Eilat (Aqaba). *Aquat. Microb. Ecol.* 56: 205-215
- de Jonge, V. N., and J. E. E. van Beusekom. 1995. Wind- and tide-induced resuspension of sediment and microphytobenthos from tidal flats in the Ems estuary. *Limnol. Oceanogr.* 40: 766-778.
- Ketchum, B. H. 1954. Relation between circulation and planktonic populations in estuaries. *Ecology* 35: 191-200.

- Kim, H., and P. A. Montagna. 2009. Implications of Colorado river (Texas, USA) freshwater inflow to benthic ecosystem dynamics: A modeling study. *Estuar. Coast. Shelf Sci.* 83: 491-504.
- Kim, H., S. Son, P. Montagna, B. Spiering, and J. Nam. 2014. Linkage between freshwater inflow and primary productivity in Texas estuaries: downscaling effects of climate variability. *J. Coast. Res.* 68: 65-73.
- Konapala, G., A. K. Mishra, Y. Wada and M. E. Mann. 2020. Climate change will affect global water availability through compounding changes in seasonal precipitation and evaporation. *Nat. Com.* 11: 1-10.
- Lancelot, C., and K. Muylaert. 2011. Trends in estuarine phytoplankton ecology. *Estuar. Coast. Shelf Sci.* 7: 5-15.
- Langdon, C. 1987. On the causes of interspecific differences in the growth-irradiance relationship for phytoplankton. Part I. A comparative study of the growth-irradiance relationship of three marine phytoplankton species: *Skeletonema costatum*, *Olisthodiscus luteus* and *Gonyaulax tamarensis*. *J. Plankton Res.* 9: 459-482.
- Longley, W. L. 1994. Freshwater inflows to Texas bays and estuaries: ecological relationships and methods for determination of needs. Texas Water Development Board and Texas Parks and Wildlife Department.
- Masotti, I., P. Aparicio-Rizzo, M. A. Yevenes, R. Garreaud, L. Belmar, L. Fariás. 2018. The influence of river discharge on nutrient export and phytoplankton biomass off the Central Chile coast (33°–37°S): seasonal cycle and interannual variability. *Front. Mar. Sci.* 5: 1-12.
- Montagna, P. A., M. Alber, P. Doering, and M. S. Connor. 2002. Freshwater inflow: science, policy, management. *Estuaries* 25: 1243–1245.
- Murrell, M. C., R. S. Stanley, E. M. Lores, G. T. DiDonato, and D. A. Flemer. 2002. Linkage between microzooplankton grazing and phytoplankton growth in a Gulf of Mexico estuary. *Estuaries* 25: 19–29.
- Nielsen-Gammon, J., J. Escobedo, C. Ott, J. Dedrick, and A. Van Fleet. 2021. Assessment of historic and future trends of extreme weather in Texas, 1900-2036. Texas A&M University, Office of the Texas State Climatologist.
- Olofsson, M., E. K. Robertson, L. Edler, L. Arneborg, M. J. Whitehouse, H. Ploug. 2019. Nitrate and ammonium fluxes to diatoms and dinoflagellates at a single cell level in mixed field communities in the sea. *Sci. Rep.* 9: 1-12.

- Paerl, H. W., N. S. Hall, B. L. Peierls and K. L. Rossignol. 2014. Evolving paradigms and challenges in estuarine and coastal eutrophication dynamics in a culturally and climatically stressed world. *Estuar. Coasts*. 37: 243-258.
- Palmer, T. A., P. A. Montagna, J. Beseres Pollack, R. D. Kalke, H. R. DeYoe. 2011. The role of freshwater inflow in lagoons, rivers, and bays. *Hydrobiologia*. 667: 49-67.
- Pennock, J. R. 1985. Chlorophyll distributions in the Delaware estuary: regulation by light-limitation. *Estuar. Coast. Shelf Sci*. 21: 711-725.
- Phlips, E. J., S. Badylak, J. Hart, D. Haunert, J. Lockwood, K. O'Donnell, D. Sun, P. Viveros and M. Yilmaz. Climatic influences on autochthonous and allochthonous phytoplankton blooms in a subtropical estuary, St. Lucie Estuary, Florida, USA. *Estuar. Coasts*. 35: 335-352.
- Rai, S. V., and M. Rajashekhar. 2016. Effect of pH, salinity and temperature on the growth of six species of cyanobacteria isolated from Arabian sea coast of Karnataka. *International Journal of Biosciences and Technology*. 9: 1-6.
- Reyna, N. E., A. K. Hardison, Z. Liu. 2017. Influence of major storm events on the quantity and composition of particulate organic matter and the phytoplankton community in a subtropical estuary, Texas. *Front. Mar. Sci*. 4: 1-14.
- Roelke, D. L., H. Li, N. J. Hayden, C. J. Miller, S. E. Davids, A. Quigg and Y. Buyukates. 2013. Co-occurring and opposing freshwater inflow effects on phytoplankton biomass, productivity and community composition of Galveston Bay, USA. *Mar. Ecol. Prog. Ser*. 477: 61-76.
- Roelke, D. L., H. Li, C. J. Miller-DeBoer, G. M. Gable, and S E. Davis. 2017. Regional shifts in phytoplankton succession and primary productivity in the San Antonio Bay System (USA) in response to diminished freshwater inflows. *Mar. Freshw. Res*. 68: 131-145.
- Smayda, T. J. 1997, b. Harmful algal blooms: their ecophysiology and general relevance to phytoplankton blooms in the sea. *Limnol. Oceanogr*. 42: 1137-1153.
- Smucker, N. J., J. J. Beaulieu, C. T. Nietch, and J. L. Young. 2021. Increasingly severe cyanobacterial blooms and deep water hypoxia coincide with warming water temperatures in reservoirs. *Glob Chang Biol*. 11 :2507-2519.
- Stawiarski, B., E. T. Buitenhuis, and C. Le Quéré. 2016. The physiological response of picophytoplankton to temperature and its model representation. *Front. Mar. Sci*. 3. doi: [10.3389/fmars.2016.00164](https://doi.org/10.3389/fmars.2016.00164)

- Sun, J., and D. Liu. 2003. Geometric models for calculating cell biovolume and surface area for phytoplankton. *J. Plankt. Res.* 25: 1331–1346.
- Swanson, K. M., L. J. Flewelling, M. Byrd, A. Nunez, T. A. Villareal. 2010. The 2008 Texas *Dinophysis ovum* bloom: distribution and toxicity. *Harmful algae* 9: 190-199.
- Texas Water Development Board. 2017. Chapter 5: Future population and water demand. Water for Texas.
- Varkouhi, S. and J. Wells. 2020. The relation between temperature and silica benthic exchange rates and implications for near-seabed formation of diagenetic opal. *Results in Geophysical Sciences*. 1: 1-14. doi: 10.1016/j.ringsps.2020.100002
- Ward., G and Armstrong, N.E. 1980. Matagorda Bay, Texas: its hydrography, ecology, and fishery resources. No. FWS/OBS-81/52. Washington, D.C.: Fish and Wildlife Service, U.S. Department of the Interior.
- Welschmeyer, N. A. 1994. Fluorometric analysis of chlorophyll a in the presence of chlorophyll b and pheopigments. *Limnol. Oceanogr.* 39: 1985-1992.
- Wetz, M. S., E. A. Hutchinson, R. S. Lunetta, H. W. Paerl, and J. C. Taylor. 2011. Severe droughts reduce estuarine primary productivity with cascading effects on higher trophic levels. *Limnol. Oceanogr.* 56: 627-638.

Moving Forward

Project Findings Summary

There is wide consensus in the scientific community that to conserve natural resources, managers must take an ecosystem-based management approach. This assessment of West Matagorda Bay was unique in that it was the first study to integrate a broad ecosystem-based management approach to fully gain an in-depth understanding of the fundamental underlying ecological processes and stressors that interact to support a resilient ecosystem. The data presented here help identify and prioritize areas for protecting and sustaining marine populations within this estuarine complex.

To address those needs, we assembled an expert team consisting of world-class sea turtle biologists and marine ecologists to meet the needs of this research effort. The overall goal of this project was to inform the development of effective restoration and conservation strategies for endangered sea turtles by implementing a multi-disciplinary ecosystem assessment for West Matagorda Bay. To accomplish this goal, the team addressed a set of key research objectives to address the overall goal of informing the development of effective restoration and conservation strategies for endangered sea turtles and birds by implementing a multi-disciplinary ecosystem assessment of West Matagorda Bay.

Key Deliverables and Takeaways:

Habitat Mapping – We develop detailed habitat maps forming the basis of the study. As the primary function of an estuary relies on an understanding of these foundational habitats, this mapping allows assessments and visualization of biological and physical characteristics of the estuary on a spatial and temporal basis. These delineations showed how key areas support the species of interest situated within the habitat mosaic but also how they will be affected by flooding events and any potential sea rise in the future.

- Having these comprehensive baseline maps allowed for a detailed evaluation of the West Matagorda Bay project area that included an assessment of the abundance, community composition, distribution, seasonality, and habitat trends.
- Land cover dynamics were assessed over numerous time scales (past, present, and future) to gain a better understanding of West Matagorda Bay. These allowed for documentation of habitat changes since the mid-1800's along with modeling of local coastal habitat changes predicted under two sea-level rise (SLR) scenarios and further characterized vulnerable habitat locations as future management priority areas.
- The intertidal and bordering uplands of the Matagorda Bay system were mapped using state-of-the-art high-resolution multispectral satellite imagery. The imagery was combined with topographic lidar data with similar spatial resolution plus earlier land classification data with a 30-m pixel scale in a novel processing routine that classifies intertidal and marginal upland environments.

- Georeferencing of historical maps and vertical aerial photographs plus information from prior studies of coastal change reveal the morphodynamics of the Colorado River Delta, Matagorda Peninsula, and the eastern portion of Matagorda Island during the last 170 years. Matagorda Peninsula and Island are barrier features, which protect Matagorda Bay from high-energy conditions as well as host habitats themselves. From 1850 to 2020, the combined intertidal and upland areas experienced a net decrease in area from 97 to 78 km², a 20% reduction in size. The Colorado River Delta, on the other hand, increased in size from about 2 km² to 23 km², adding valuable marsh habitat to the bay.
- Matagorda Bay is experiencing Sea Level Rise (SLR) making bay margin environments susceptible to changes in habitat types. Results from the Sea Level Affecting Marshes Model (SLAMM) were compiled and assessed for the intertidal and bordering uplands of the Colorado Delta, Matagorda Peninsula, and the eastern portion Matagorda Island. All areas are projected to increase in open water in both 0.5- and 1.5-m SLR scenarios by the year 2100. Most notably, the majority of the Colorado River Delta marsh is projected to convert to tidal flats under the 0.5-m scenario and to open water in the 1.5-m scenario. Matagorda Peninsula and Island are expected to experience a decrease in estuarine marsh in both scenarios.
- SLR land cover change modeling results, storm surge vulnerability maps, and a detailed topographic model developed from lidar data were combined in a habitat vulnerability map for the entire intertidal and bordering upland margin of the Matagorda Bay system. The map shows areas of present and future critical habitats that provide valuable ecosystem functions. For the 0.5 m SLR scenario, 239 km² of current marsh, beaches, dunes, and tidal flats are expected to remain as critical habitat, 166 km² of non-critical habitat are expected to become critical habitat, and 72 km² are expected to become open water under the 0.5 m GMSLR scenario. However, under the 1.5 m SLR scenario, only 112 km² of current marsh, beaches, dunes, flats are expected to remain as critical habitat, 226 km² are expected to become critical habitat, and 212 km² are expected to become open water. Under the 1.5 m scenario, basically all present-day marsh and flat areas are converted to open water while presently stable upland habitat is converted to critical habitat. This emphasizes the importance of preserving upland environments susceptible to transitioning to critical habitats as sea level rises and storms persist.

Sea Turtle Movement – We established an extensive animal tracking component for key species of interest, allowing an understanding of distribution, migration, and movement patterns for these animals of interest. We showed how the bay supports endangered species, promotes/enhances recovery, and developed long-term scientific recommendations for sustaining and enhancing their populations. This first-of-its-kind study provides an in-depth understanding of the ecosystem that supports threatened and endangered sea turtles. In this ecosystem-based approach, we developed effective management and conservation strategies that can be used to identify and prioritize areas to protect for sea turtles within the estuarine complex by describing their distribution, seasonal habitat use, and migration patterns along the Gulf of Mexico

including drivers for these movement patterns. Finally, we provided data on the ecological roles of sea turtles in this estuarine complex, the health of the sea turtles, and the ecosystem processes that impact these marine reptiles.

- Texas bays and estuaries provide one of the most important developmental habitats for green turtles in the northwestern Gulf of Mexico. Our study confirms that Matagorda Bay provides important developmental feeding and resting areas for green turtles, with populations increasing since the 1990's, and extends the range of critical habitat for the species further north than previously documented.
- Most of the green turtles we tracked with satellite and acoustic transmitters remained resident in Matagorda Bay; however, we also found connectivity with other Texas bays and the Gulf of Mexico and Mexican waters.
- The high use areas we identified in this study, including the seagrass beds and the jetties in west Matagorda Bay, require special management consideration or protections for immature and juvenile green turtles that use these areas daily to feed, rest, develop, and grow. We recommend prioritizing areas of high seagrass diversity for the protection of green turtle foraging habitat.
- We also recommend managing the seagrass beds present to maintain their abundance and diversity of seagrass species critical to green turtles in Matagorda Bay.
- We also recommend special consideration of the jetties in the Matagorda Ship Channel due to the high number of sea turtles sighted and the multiple species observed there.
- Changing ambient and water temperatures, particularly below 15°C, are drivers of green turtle movements within and outside Matagorda Bay. Targeted search and rescue efforts for cold-stunned turtles should begin when water temperatures decline below 10°C.

Biological Sampling – Benthic habitats (including seagrasses, oyster reefs, and open bay bottom) throughout the project area support thriving and diverse ecological communities. This study demonstrated that recruitment to and use of seagrass and saltmarsh habitats by post-settlement nekton in Matagorda Bay was linked to biological and physicochemical properties of the estuary during settlement and early life periods. For the avian component, we observed a bird community typical of a Texas Gulf Coast estuarine ecosystem. Seasonal marsh vegetation sampling within the bay demonstrated the high degree of temporal and spatial variation in estuarine saltmarsh communities, differing both across and within study sites.

- This study provides insights for management of this important Texas estuary by identifying conditions related to high abundance and diversity of post-settlement fishes, which are known to influence population and ecosystem resilience.
- Seagrass and saltmarshes are major components of estuarine habitats in Matagorda Bay, and these structured habitats serve as nurseries for a wide range of fishes.
- Seagrass consistently had higher abundances of post-settlement fishes than saltmarsh, and the density of fishes in both habitats differed by season and year.

- Diverse assemblages were present in both seagrass and saltmarsh habitat and both diversity measures evaluated at the family level (taxonomic richness and Shannon diversity) differed significantly between seasons and years.
- Community structure differed significantly between seagrass and saltmarsh habitat driven primarily by families of fishes that use these nursery habitats seasonally (drum and croaker, flounder, mojarra, and pipefishes) and highly abundant resident taxa that occur throughout the year (gobies, porgies, and killifishes).
- Density, richness, and diversity of juvenile fishes in Matagorda Bay were related primarily to three factors: habitat type (seagrass vs. saltmarsh), dissolved oxygen, and distance to tidal pass.
- Species in the family Sciaenidae revealed species-specific differences in habitat use, with staggered entry into Matagorda Bay nurseries to presumably limit temporal overlap and potential competition.
- The study confirmed and documented the unique ecological nuances with respect to diversity and abundance of marsh vegetative communities and coastal bird assemblages between the barrier island sites and the more inland marsh locations.
- We observed multiple species of rail inhabiting the lower marsh habitats, an abundance of tern, heron, and wading bird species utilizing the marsh fringe, and large flocks of shorebirds foraging and roosting on the tidal flats.
- Overall, the ecological diversity of organisms varies both spatially and temporally and is largely driven by the interactive effects of a myriad of environmental factors.

Trophic Ecology and Food Web Analyses – We showed that the Matagorda Bay food web is robust and supports a wide diversity of consumers through different sources of primary production.

- Particulate organic matter (POM) has the largest source contribution, indicating the open water habitat of the bay is likely important for fostering plankton communities and sustaining planktivore feeders. While seagrasses and marsh habitat sources are reflected among the consumers, it is likely that they are not large diet source contributors themselves and instead support productive and necessary nursery habitat for the food web.
- Due to the heterogeneity of the Matagorda Bay system, the food web is best understood by analyzing across different spatial scales and regions throughout the bay.
- Many planktivorous consumers are important prey to the larger bodied, piscivorous predators of the system, enhancing the importance of POM as a key contributor to the Matagorda Bay food web.
- Benthic production is also an important contributor to omnivores and detritivores but varies over space and time.

- Preserving valuable habitat (seagrasses and marsh habitat) and the flow dynamics that exist within the Matagorda Bay system is critical to having a resilient food web in the face of continued anthropogenic and environmental changes.

Habitat and Resource Use across the Matagorda Bay Ecosystem – We showed that Matagorda Bay is a highly dynamic and rapidly changing ecosystem due to its location at the land-sea interface and unique combination of terrestrial and marine influences.

- Large nutrient inputs from the watershed and organic matter contributions support many key ecosystem functions.
- These functions are maintained by a variety of habitats including seagrass beds, oyster reefs, wind-tidal flats, saltmarshes, and soft-sediment communities.
- These results also demonstrate that habitat setting can impact resource quality and use across the entire bay ecosystem. For example, isolated open-bay reefs have greater overall oyster abundance than marsh-fringing reefs. Taken together, these findings indicate that habitat setting plays a significant role in oyster reef structure and functioning.
- The wind-tidal flats of this system are important for binding sediments, cycling nutrients, recruiting fauna, and serving as feeding grounds for wintering and migrating birds.

Water Quality and Plankton Monitoring – Water quality is a key determinant of ecosystem health. Other components of the study showed that Matagorda Bay and its tributaries generally support highly productive aquatic habitats for birds, fish, and shellfish, which can be attributed in part to good water quality. However, changing watershed land use, increasing populations and development, and climate variability/change can negatively affect water quality, and there are indications that water quality in the ecosystem is not as healthy as it was in previous years.

- Regular assessment of water quality status and trends are important for supporting management and decision making around estuarine ecosystem health.
- Additional attention is recommended to studying nutrient conditions in Lavaca Bay and its feeder rivers/creeks before harm occurs to the ecosystem.
- This study also underscores the impact of long-term alterations to freshwater inflow and salinity levels in estuaries of the central Texas coast.
- Additionally, our plankton community studies highlight the essential role that the Colorado River plays in the Matagorda Bay ecosystem.

Recommendations for Future Management:

Together this work focused on two key overall deliverables to be met. Specifically, these were:

(1) Recommendations for mitigation and restoration activities that will address impacts of flooding and sea rise for Species of Interest; and

(2) Identification of priority areas in need of protection, where the implementation of mitigation and restoration activities would be feasible and beneficial.

First, our baseline mapping allowed for determination of the status of habitat types and coverages within the estuary, and we have provided detailed habitat maps. Our intense fine-scale mapping studies allowed us to assess habitat changes from the mid-1800's to present. This coupled with modeling of local coastal habitat changes allowed for creating predictable land-use changes under two sea-level rise (SLR) scenarios. This enables further characterization of vulnerable habitat locations as prioritization of future area in need of protection, management, or restoration.

As is common with estuaries, the ecological diversity of organisms varies both spatially and temporally and is largely driven by the interactive effects of a myriad of environmental and ecological factors. This underscores the need for more ecosystem-level studies such as this. These dynamics are captured in the overall Matagorda Bay Ecological Assessment Report. The ecological interconnectivity in estuaries such as Matagorda Bay speak to the productivity of the Bay, but also presents challenges on how to address potential ecological change over time with respect to flooding and sea level rise. Briefly:

- A variety of restoration strategies have been designed and implemented within similar systems, with varying degrees of practicality and effect. In addition, the allocation of resources to one strategy over another depends on overall project goals (i.e., managing for diversity vs. managing for a single species). This report specifically addresses these needs and prioritizes areas in most need of protection.
- The flow from the Colorado River is important in establishing the prominent estuarine gradient within Matagorda Bay, preserving valuable habitat (seagrasses and marsh habitat), is critical to having a stable diverse food web and is a major driver for the estuarine complex.
- This study provides insights for management of this important Texas estuary by identifying conditions related to high abundance and diversity of post-settlement nekton, which are known to influence population and ecosystem resilience. These parameters were driven by the availability of key habitats, and particular attention to those habitat types is clearly warranted for future conservation.
- Results from our study suggest that estuarine vegetation habitats such as seagrasses and salt marshes support the highest abundance and species diversities for birds. Moreover, among avian species observed, Eastern Black Rail are more closely associated with marsh habitats.
- Increases in oyster bed foraging habitat would be beneficial for the American oystercatcher and other shorebirds by creating habitat, forage, and shoreline protection.

- The creation of temporary rookery islands could benefit colonial waterbirds and provide refuge for migrants. The expansion of coastal wetlands and estuarine plant species inland with potential sea level rise, supplemented with freshwater sources, could enhance existing marsh, waterfowl and crane species.
- Restoration and mitigation opportunities are numerous within the project area, and it is imperative that this expansive database and maps be thoroughly examined and considered a priori, and the desired ecological goals be clearly articulated to maximize success in future development and implementation.
- The wind-tidal flats of this system are important for binding sediments, cycling nutrients, recruiting fauna, and supporting wind-tidal flat importance as feeding grounds for wintering and migrating birds. However, long-term changes in inundation frequency place tidal flats at risk worldwide. This work characterized how seasonal inundation and spatial changes across the marsh-tidal flat complex affect community composition and resource quality. Seasonal differences in resource quality and community structure likely impact ecological functioning of tidal flats, where changes in infauna recruitment may have important consequences for foraging organisms, such as shorebirds.
- Additional attention to nutrient conditions is recommended in Lavaca Bay and its feeder rivers/creeks to monitor any potential impacts to the ecosystem.
- Only one water quality station, located near the mouth of the Lavaca River in Lavaca Bay, showed a long-term salinity increase. However, numerous stakeholder concerns have been raised about salinity in the eastern arm of West Matagorda Bay where, unfortunately, no TCEQ monitoring stations are currently active. Additional monitoring is recommended in this data poor region of Matagorda Bay to allow for a more holistic assessment of conditions in the bay.
- Phytoplankton are important primary producers in estuaries and represent a link between freshwater inflow and higher order consumers (fish, shellfish). They are also sensitive indicators of environmental variability and change. Estuaries of the Texas coast, such as Matagorda Bay, are vulnerable to long-term decreases in freshwater inflow due to increasing upstream human freshwater needs as well as climate change. Thus, it is critical to understand how phytoplankton communities respond to freshwater inflow variability in order to project how future inflow changes may affect estuarine ecosystem functioning and health.

In summary, data generated from an ecosystem-based approach such as this study will be crucial to developing effective restoration and conservation strategies, and it can be used to identify and prioritize areas for long-term protection of endangered species such as turtles, coastal birds, and many other species. While this work is extensive, it also sets the stage for future research and other studies that will further contribute toward understanding how the Matagorda Bay Ecosystem functions. Moreover, this study generated key baseline information that will be essential to gauge progress and make predictions about and assess future changes in the Matagorda Bay System.